

# **Titanium-Catalyzed Deoxygenation of Alcohols and Valorization of Biomass**

## **Dissertation**

der Mathematisch-Naturwissenschaftlichen Fakultät  
der Eberhard Karls Universität Tübingen  
zur Erlangung des Grades eines  
Doktors der Naturwissenschaften  
(Dr. rer. nat.)

vorgelegt von  
Alexandru Căciuleanu  
aus Braşov/Rumänien

Tübingen  
2024

Gedruckt mit Genehmigung der Mathematisch-Naturwissenschaftlichen Fakultät der Eberhard Karls  
Universität Tübingen.

Tag der mündlichen Qualifikation:

24.09.2024

Dekan:

Prof. Dr. Thilo Stehle

1. Berichterstatter/-in:

Prof. Dr. Ivana Fleischer

2. Berichterstatter/-in:

Prof. Dr. Florian Beuerle

The experimental work discussed in this thesis was performed from October 2019 to January 2023 at the University of Tübingen under supervision of Prof. Dr. Ivana Fleischer.

## Table of contents

1.	General Introduction .....	1
1.1.	Overview on Deoxygenation Reactions.....	1
1.1.1.	Common Protocols for the Deoxygenation of Carbonyls.....	1
1.1.2.	Protocols for the Deoxygenation of Alcohols and Bioactive Molecules.....	3
1.1.2.1.	Two-step Deoxygenation Procedures.....	3
1.1.2.2.	Direct Deoxygenation Procedures .....	11
1.2.	Lignin Valorisation through Deoxygenation Procedures.....	15
1.3.	References.....	18
2.	H-donors in Deoxygenation Reactions.....	19
2.1.	Formic Acid .....	19
2.2.	Hydrosilanes .....	20
2.3.	Hantzsch Esters.....	23
2.4.	References.....	29
3.	Aims of this Work.....	31
4.	Optimization of Pd-Catalysed Transfer Hydrogenolysis .....	32
4.1.	Overview on Pd-Catalysed Deoxygenation of Alcohols .....	32
4.2.	General Motivation .....	40
4.3.	Optimization and Screening.....	40
4.3.1.	Solvent Screening.....	41
4.3.2.	Further Optimization Experiments .....	43
4.3.3.	Ligand Screening.....	46
4.3.4.	Influence of Water-content over Reactivity .....	49
4.4.	Conclusions.....	50
4.5.	References.....	51
5.	Co-Catalysed Deoxygenation of Benzylic Alcohols.....	52
5.1.	General Motivation .....	52
5.2.	Overview on the Applications of Co-Pincer Complexes .....	52
5.3.	Results and Discussions for Co-Catalysed Deoxygenation .....	60
5.3.1.	Initial Conditions and Ligand Screening.....	60
5.3.2.	Additive Screening .....	63
5.4.	References.....	65
6.	Co/Ti- and Ti-Catalysed Deoxygenation of Benzylic Alcohols.....	67



6.1.	Overview on Ti-catalysed Deoxygenation of Alcohols.....	67
6.1.1.	Introduction in Organotitanium Chemistry .....	67
6.1.2.	Ti-Catalysed Deoxygenation of Alcohols .....	71
6.2.	Co/Ti Co-Catalysed Deoxygenation .....	78
6.2.1.	Preliminary Investigations .....	78
6.2.2.	Conditions Screening.....	79
6.3.	Results and Discussions for Ti-Catalysed Deoxygenation .....	83
6.3.1.	Preliminary Conditions Screening.....	83
6.3.2.	Hantzsch Esters and Ammonium Borane as Reducing Agents .....	85
6.3.3.	Silane and Reaction Parameters Optimization .....	91
6.3.4.	Substrates Screening.....	102
6.3.5.	Unsuccessful Substrates .....	105
6.3.6.	Deoxygenation-Dehalogenation Reaction.....	107
6.3.7.	Deoxygenation-Hydrogenation Reaction .....	108
6.3.8.	Selectivity Reactions .....	111
6.3.9.	Miscellaneous Substrates.....	111
6.3.10.	Deoxygenation of Lignin Building Blocks and Model Substrates .....	113
6.3.11.	Mechanistic Studies.....	117
6.4.	Conclusions and Outlook on Co- and Ti-catalysed Deoxygenation Procedures .....	122
6.5.	References.....	123
7.	Summary/Zusammenfassung .....	126
8.	Experimental Part.....	130
8.1.	General Information.....	130
8.2.	Chromatography and Analytical Techniques.....	130
8.3.	General Experimental Procedures for Deoxygenation of Benzylic Alcohols.....	131
8.4.	Other General Experimental Procedures.....	133
8.5.	Analytical Data for Isolated Deoxygenation Products.....	134
8.6.	Analytical Data for Non-isolated Deoxygenation Products.....	164
8.7.	Analytical Data for Benzyl Alcohols .....	180
8.8.	Analytical Data for Synthesis of Hantzsch Esters .....	196
8.9.	Miscellaneous Products and Analytical Data.....	202
8.10.	Calibration Data for GC-FID Analysis .....	221
8.11.	References.....	222

9.	Appendix.....	223
9.1.	List of Abbreviations .....	223
9.2.	Acknowledgements.....	225

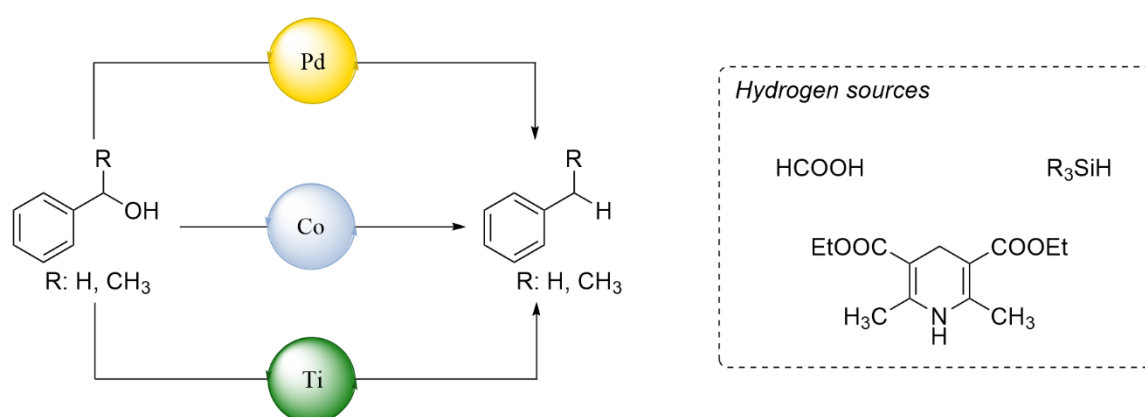
## 1. General Introduction

This thesis contains 4 sections and covers the development of deoxygenation reactions of benzylic alcohols catalysed by homogenous Pd-, Co- and Ti-based systems (Scheme 1.1).

In the first section various literature-available deoxygenation procedures will be discussed in order to better understand the evolution and applications of these methodologies. Moreover, the H-donation capabilities of hydrosilane, formic acid and Hantzsch esters will be presented.

In the second section multiple heterogenous Pd-catalysed deoxygenation methods will be presented together with the optimization attempts conducted for the Pd-catalysed homogenous deoxygenation procedure developed by Ciszek and Fleischer.

The third and fourth section contain the work on the development of new homogenous Co- and Ti-catalysed deoxygenations methods in which formic acid, hydrosilanes and Hantzsch esters were utilized as H-donors.



**Scheme 1.1.** General deoxygenation protocols.

### 1.1. Overview on Deoxygenation Reactions

Deoxygenation reactions constitute one of the most important tools in organic chemistry. These transformations imply the cleavage of a C-O, P-O or S-O bond and, in most cases, the formation of a new C-H bond. In this chapter, various procedures for the deoxygenation of alcohols and the classification thereof will be presented, but first, for a better comprehension of these approaches, standard methodologies for the deoxygenation of carbonyl compounds will be discussed. Additionally, selected examples of applications of deoxygenation reactions, namely the late-stage functionalization of bioactive molecules and the valorisation of biomass, will be presented.

#### 1.1.1. Common Protocols for the Deoxygenation of Carbonyls

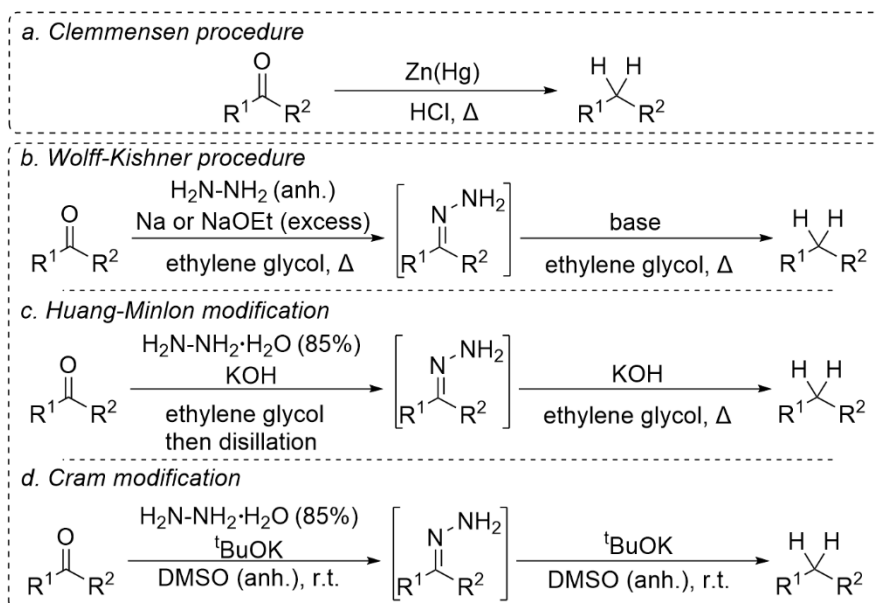
The most common procedures for the deoxygenation of carbonyl compounds are the Clemmensen deoxygenation and the Wolff-Kishner (W-K) reduction. Both these original methods were reported early in the 20<sup>th</sup> century and are considered to be complementary to each other due to the substrate tolerance towards acidic and alkaline conditions. Meanwhile, multiple procedures derived from these two deoxygenation methodologies were published in order to render the initial approaches better suited for both laboratory and industrial-scale applications. Lately, the modified Wolff-Kishner procedures were also used as an intermediate step in the deoxygenation of alcohols.

The Clemmensen reduction was published by E. Clemmensen in 1913 (Scheme 1.2 - a).<sup>1,2</sup> This method utilizes a zinc-mercury amalgam dissolved in a concentrated HCl solution for the deoxygenation of aldehydes and ketones. Although this system is very efficient for the reduction of

aromatic carbonyls, substrates, which are unstable under harsh acidic conditions, are unsuitable for this protocol.

The Wolff-Kishner deoxygenation procedure was developed through the independent studies of N. Kishner in 1911 and L. Wolff in 1912 (Scheme 1.2 - b).<sup>3,4</sup> In this procedure anhydrous hydrazine and an excess of metallic Na or sodium ethoxide were dissolved in high-boiling solvents like ethylene glycol. The excess of sodium was needed to control the amount of *in situ* generated water, thus, the formation of sodium hydroxide. This reaction proceeds through a base-catalysed condensation of the ketone with hydrazine and the generation of the hydrazone intermediate. The deprotonation of the intermediate and the subsequent thermal decomposition of the hydrazone at approximately 200 °C led to the formation of the corresponding alkane. Due to the harsh basic and thermal reaction conditions, this method could be applied on a limited number of substrates. Additionally, very long reaction times were needed under these initial conditions. Thus, various alternatives of this procedure were developed, from which the Huang-Minlon modification and the Cram modification are worth mentioning in the frame of this thesis.

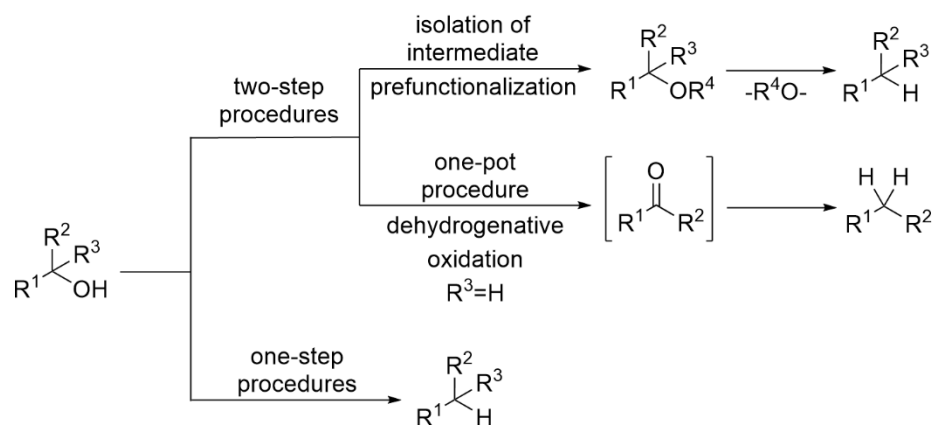
The variation developed by Huang-Minlon was published in 1946 (Scheme 1.2 - c).<sup>5</sup> A “two-step” reaction procedure was proposed, in which the reaction mixture should be heated to 190-200 °C only after the KOH-catalysed condensation step is considered complete and the water and excess hydrazine are distilled off. Thus, the utilization of hydrated hydrazone was possible, and the addition of Na excess was unnecessary. Additionally, the reaction time was reduced from 50–100 h to 3 h. This alternative to the W-K reduction was later applied in multiple industrial-scale processes.<sup>6,7</sup> In 1962, Cram *et al.* reported a low-temperature alternative to the Wolff-Kishner reduction (Scheme 1.2 - d).<sup>8</sup> By using this protocol, the deoxygenation of carbonyls yielded high amounts of alkane even at room temperature. This was achieved by the slow addition of the hydrazine in a <sup>t</sup>BuOK/DMSO solution. Following these modifications, the Wolff-Kishner reduction became one of the most popular procedures for the deoxygenation of carbonyls.



**Scheme 1.2.** Standard procedures for the deoxygenation of carbonyls; (a) Clemmensen reduction;<sup>1</sup> (b) Wolff-Kishner reduction;<sup>3,4</sup> (c) Huang-Minlon modification of W-K;<sup>5</sup> (d) Cram modification of W-K.<sup>8</sup>

### 1.1.2. Protocols for the Deoxygenation of Alcohols and Bioactive Molecules

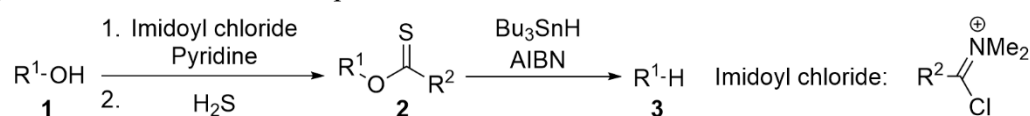
Lately, more thermal, catalytical procedures for the deoxygenation of alcohols were developed. These methodologies can be classified in two categories, based on the number of steps needed for the C-O bond cleavage (Scheme 1.3). The first and more established category is based on two-step procedures, which can further be divided into two categories depending on the reaction intermediates. The majority of two-step deoxygenation procedures include a prefunctionalization of the starting material, namely the transformation of the hydroxyl groups into better leaving groups like ethers, thionoesters or phosphites. Although these procedures are usually attractive due to the mild reaction conditions, they have the major drawback of generating large amounts of waste, which, in some cases, is highly toxic. The other approach for two-step procedures involves the generation of the corresponding carbonyl compound *via* a dehydrogenative oxidation of the alcohol, followed by an *in situ* Wolff-Kishner-type reduction. These procedures were developed more recently and have the advantage of being more compliant with the green chemistry principles compared to the deoxygenations involving prefunctionalization, due to the unharmed by-products, namely N<sub>2</sub> and water. However, the main disadvantage of these procedures is that they can be applied only for the transformation of primary and secondary alcohols. The second category are the single-step deoxygenation reactions, which are more desirable due to the atom-economy, but more difficult to achieve because of the bond high dissociation (BDE) energy of the C-OH bond.



**Scheme 1.3.** Classification of methodologies for the deoxygenation of alcohols.

#### 1.1.2.1. Two-step Deoxygenation Procedures

One of the most popular homogenous procedures utilized for the deoxygenation of alcohols (1) and generation of the corresponding alkane is the Barton-McCombie (B-M) protocol (Scheme 1.4).<sup>9</sup> In this reaction, 1.5 equivalents of tributyltin (Bu<sub>3</sub>SnH) and azobisisobutyronitrile (AIBN) as radical initiator are employed. The process proceeds through the functionalization of the hydroxy group with imidoyl chloride and hydrogen sulphide (H<sub>2</sub>S) to give the corresponding thionoester (2) or xanthate derivative. This intermediate is susceptible to a radical attack at the S-atom from the *in situ* generated Bu<sub>3</sub>Sn•, followed by a rearrangement and the expulsion of the alkyl radical, which further abstracts hydrogen atom to form the desired product.



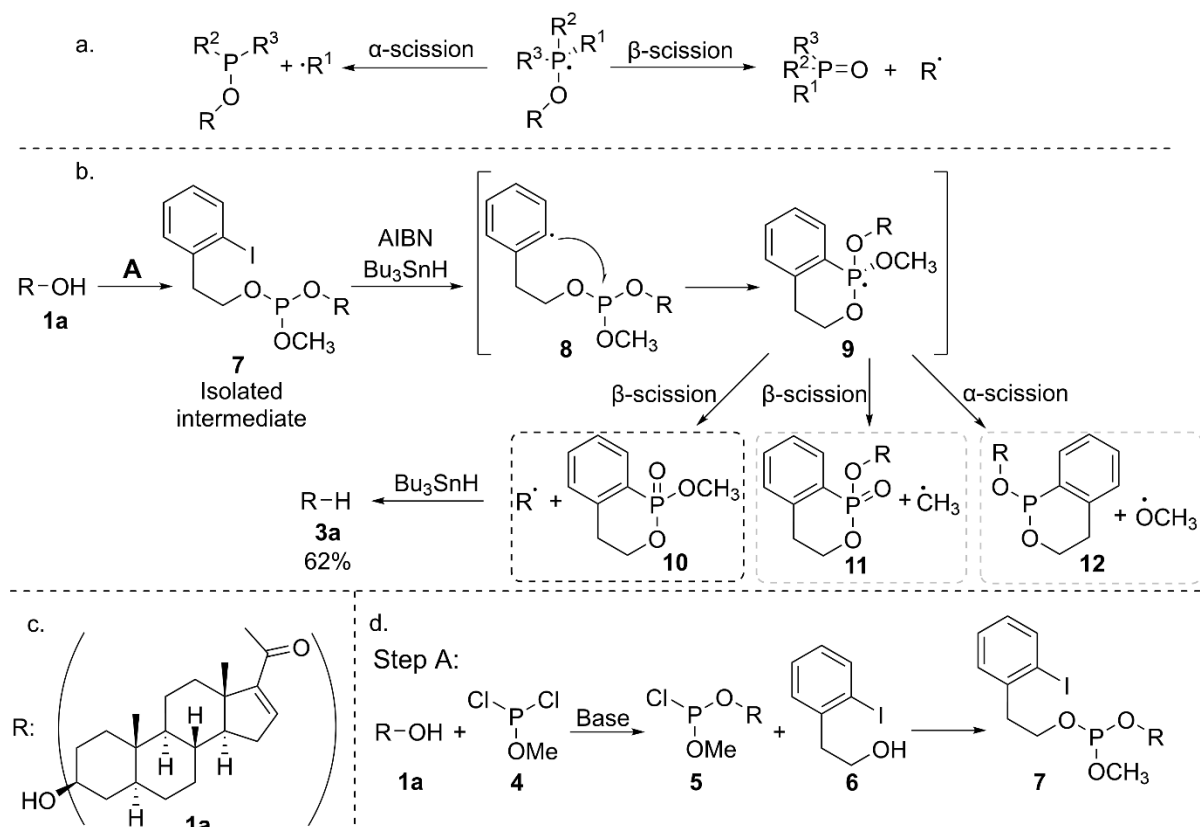
**Scheme 1.4.** General reaction scheme of the Barton-McCombie reaction.<sup>9</sup>

Although effective in deoxygenating compounds bearing multiple functionalities beside the alcoholic moieties,<sup>10</sup> like cholesterol derivatives and sugars,<sup>11</sup> the Barton-McCombie reaction has some major disadvantages, like the generation of unwanted side-products, regeneration of the alcohol, the use and formation of toxic tin-compounds and poor atom-economy.<sup>10</sup> Additionally, this procedure is best-suited for sterically hindered secondary alcohols, due to the increased stability of the reaction intermediates. Consequently, a range of procedures were developed over time in order to undermine these drawbacks and make the deoxygenation reactions suitable for a wider range of applications. Thus, the main goals of these studies was to broaden the substrate scope of the transformation, reduce the quantity of tin-compounds or eliminate them completely by substituting them with low amounts of a benign catalyst and to avoid the necessity of prefunctionalization.<sup>12</sup>

Another approach for the deoxygenation of alcohols *via* prefunctionalization is the prior formation of phosphorus-containing intermediates in a phosphitylation-deoxygenation reaction sequence. The first example of a procedure which follows this sequence was published by Ireland *et al.* in 1972.<sup>13</sup> This procedure utilized harsh reaction conditions, in which alcohols were first transformed into the corresponding phosphorodiamidites and then deoxygenated by a lithium-ethylamine solution. An improved version of the Ireland protocol was developed by Zhang and Koreeda in 2004 (Scheme 1.5).<sup>14</sup> The main difference between the two approaches was that in the latter the deoxygenation step was achieved *via* the B-M protocol. Both these procedures were based on the capability of trivalent phosphines to generate relatively stable radical species upon inter- or intramolecular radical addition. This type of P-based species can further undergo  $\alpha$ -scission, which leads to the substitution at the P-atom and generation of a new trivalent species, or  $\beta$ -scission *via* a O-R bond cleavage, followed by the oxidation to the corresponding phosphonate and the generation of an alkyl radical (Scheme 1.5 - a).<sup>15</sup> The  $\beta$ -scission pathway is favoured by the bulkier substituents at the P-atom.

The route envisioned for the deoxygenation of steroids bearing alcoholic moieties is presented in scheme 1.4 - b and c. First, the formation of isolated intermediate **7** was achieved by the base-catalysed reaction of the alcoholic substrate **1a** with methyl dichlorophosphite (CH<sub>3</sub>OPCl<sub>2</sub>, **4**), followed by the addition of 2-(2-iodophenyl)ethanol (**6**) to the previously generated product **5** (Scheme 1.4 - d). It was presumed that the aryl-containing substituent at the P-atom would inhibit the  $\alpha$ -scission pathway and that by grafting the iodo-substituent on the aromatic ring, the intramolecular radical addition would be possible. Indeed, upon treatment of **7** with the radical initiator AIBN and the H-donor, the formation of radical compound **8** was observed, which leads to the generation of **9** *via* an intermolecular radical addition. Subsequent generation of **10** through a  $\beta$ -scission, upon the addition of tributyltin hydride, leads to the formation of the desired product **3a**, in a 62% yield with no traces of  $\alpha$ -scission product being detected. Unfortunately, side-product **11** was also produced in considerable amounts in this example. This side-reaction was suppressed when the deoxygenation of more sterically inaccessible aliphatic primary and secondary alcohols was attempted. Moreover, when aliphatic tertiary alcohols were submitted to the reaction, no side-product was detected in the reaction mixture. This procedure was effective on cholesterol derivatives and sugars.

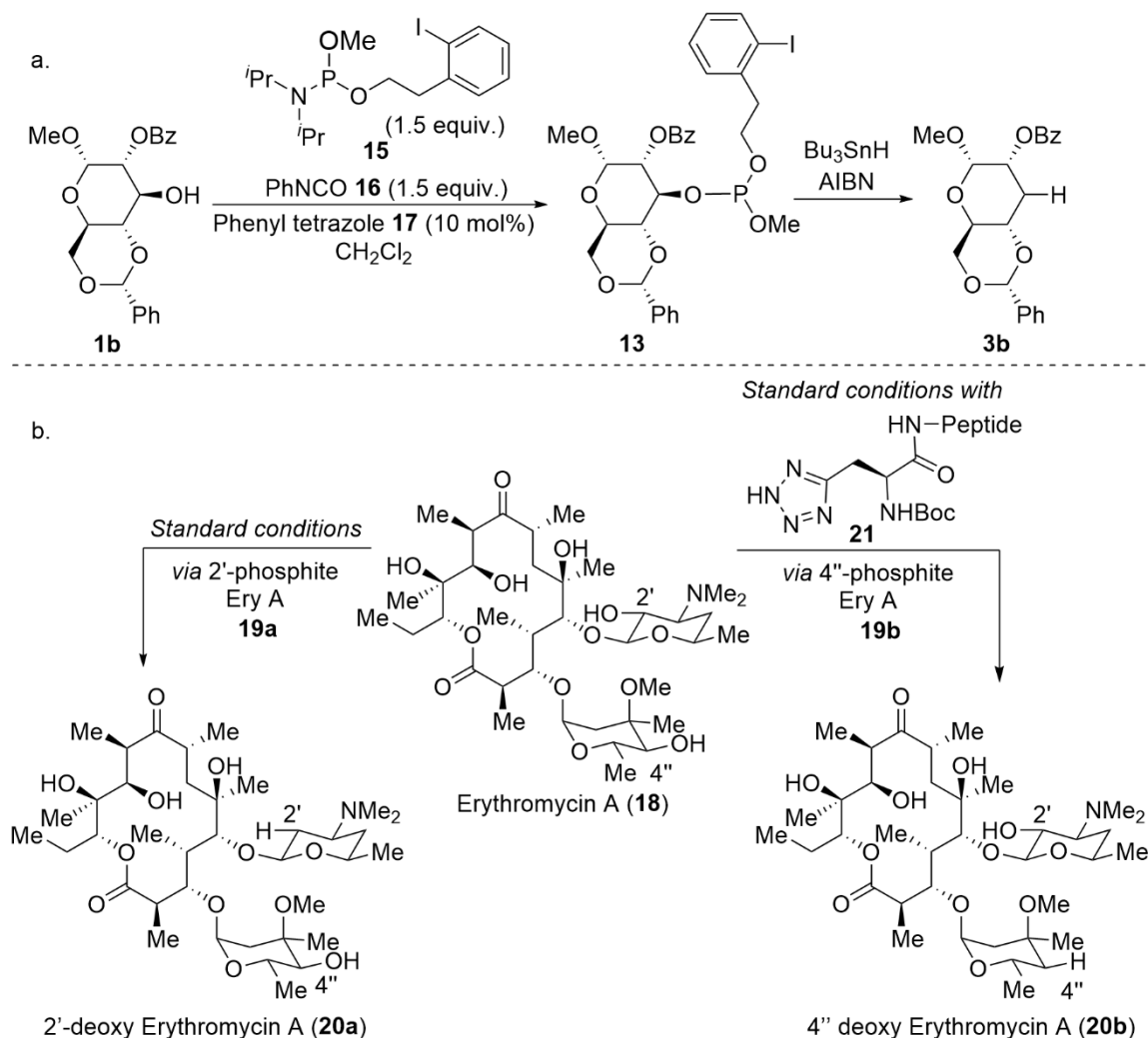
The main advantages of this procedure, compared to the classical Barton-McCombie deoxygenation, is the increased stability of the reaction intermediates, the possibility of deoxygenating even more sterically hindered substrates and the facile isolation of the desired products. However, this method is unattractive for many applications due to the employment of the highly reactive chlorophosphites.



**Scheme 1.5.** Deoxygenation procedure developed by Zhang and Koreeda; (a) possible scission pathways; (b) proposed mechanism for the deoxygenation of compound **1a**; (c) Complete structure of steroid **1a**; (d) General scheme for the generation of the reaction intermediate **7**.<sup>14</sup>

In an attempt to overcome the main disadvantage of the previously described procedure, Jordan and Miller reported in 2012 a similar methodology for the deoxygenation of alcohols but instead of using chlorophosphites as precursors, the group decided to use phosphoramidite **15** (Figure 1.6 - a).<sup>16</sup> These compounds are far less reactive than the chlorophosphites and, due to the *i*Pr substituents, **15** is not susceptible to hydrolysis or oxidation. Additionally, phenyl tetrazole (**17**) or tetrazoles bearing a peptide backbone, for example compound **21**, were used as the catalyst for the first step of the procedure with the goal of enhancing the regioselectivity of the transformation. The main problem that the group encountered during the development of the deoxygenation procedure was the difficult purification of the phosphitylation product when low-molecular-weight alcohols were subjected to the transformation. This phenomenon occurred due to the *in situ* formed urea generated from the side-reaction between the free amine liberated from phosphoramidite **15** and the amine scavenger phenyl isocyanate (**16**). This drawback was overcome by applying the Barton-McCombie conditions to the reaction mixture from the first step after only basic work-up. This was possible mainly when the deoxygenation of more sterically hindered substrates was attempted. Following the successful development of the deoxygenation procedure, a regioselective reduction of the hydroxylic sites of unprotected Erythromycin A (Ery A)(**18**) was endeavoured (Figure 1.6 - b). By utilizing the standard procedure, the main product of the transformation was 2'-deoxy Erythromycin A (**20a**), *via* 2'-phosphite Ery A (**19a**), due to the higher reactivity of the -OH group from this position. In order to selectively deoxygenate the 4''-hydroxy group, the phosphorylation catalyst was modified by substituting the phenyl ring with a peptide backbone. Indeed, by utilizing the tetrazole-based catalyst **21**, intermediate **19b** was formed and

then 4''-deoxy Erythromycin A (**20b**) was selectively obtained with a global yield of 60%. However, this procedure should be considered a complementary, and not a substituting, regioselective protocol to the Barton-McCombie deoxygenation due to the higher yield of 2'-deoxy Erythromycin A obtained through the B-M procedure.



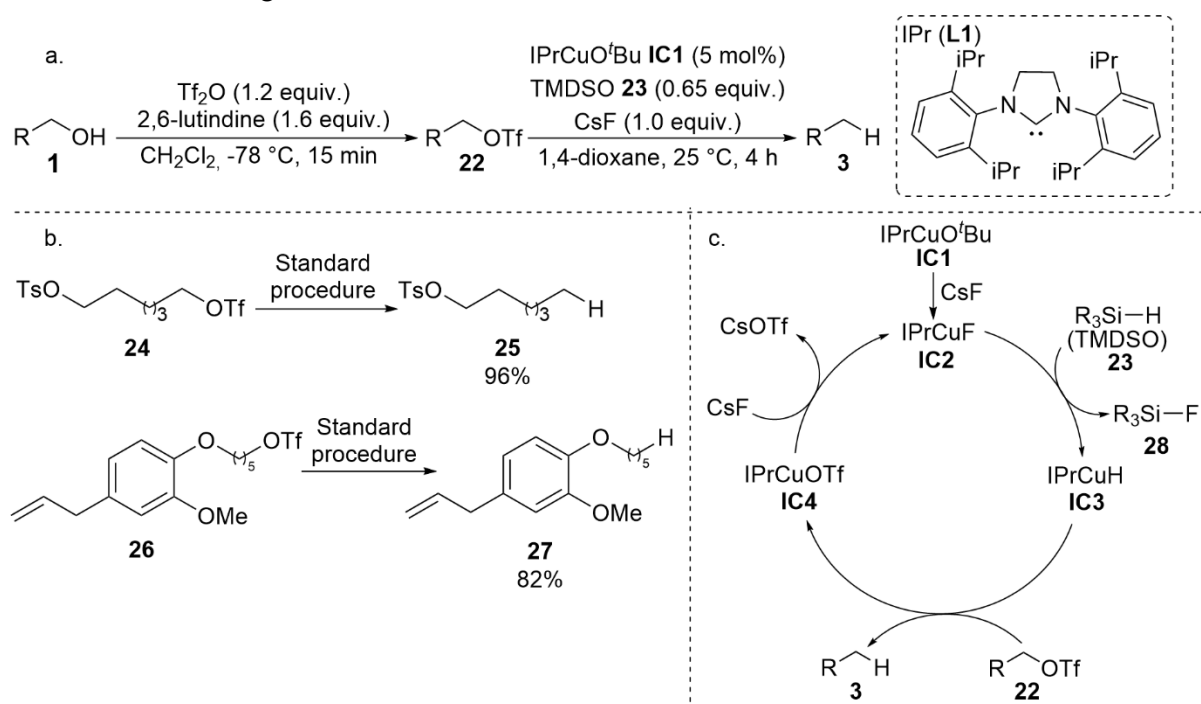
**Scheme 1.6.** Deoxygenation procedure developed by Jordan and Miller; (a) proposed mechanism for the deoxygenation of compound **1b**; (b) regioselective deoxygenation pathways of Ery A (**18**).<sup>16</sup>

A more recent example of a catalytic deoxygenation of aliphatic alcohols, which proceeds through the prefunctionalization of the hydroxyl group, was reported in 2013 by Dang *et al.*<sup>17</sup> In this procedure, the -OH group is initially transformed into a sulfonate ester, followed by the C-O bond cleavage and the generation of the corresponding alkane (Scheme 1.7 – a). The second step of this procedure was catalysed by a Cu/NHC system with silane as H-donors and a fluorine source. Previously, this system proved to be very effective for the hydrogenation of alkenes and later proved its capabilities in transforming secondary aliphatic iodides into the corresponding alkanes. During the optimization screenings, it was observed that the most-suitable sulfonate ester group is the triflate, which could be deoxygenated in an almost quantitative yield. Due to the mild reaction conditions, tosylates and nosylates were completely unreactive in this catalytic system, thus enabling the selectivity of the transformation. The utilization of triflates as reaction intermediates proved to be beneficial, because of the accessibility of triflates **22** from primary aliphatic alcohols, which are usually more difficult to



reduce through prefunctionalization procedure compared to their secondary and tertiary counterparts. The corresponding triflates were obtained *via* a slightly modified method as lower temperature and the use of 2,6-lutidine instead of pyridine enhanced the selectivity of the transformation and simplified the purification of the desired product. The most effective H-donor in this catalytic system was found to be 1,1,3,3-tetramethyldisiloxane (TMDSO, **23**) while, surprisingly, other hydrosilanes did not yield any traces of the desired product. This deoxygenation reaction showed a high degree of chemoselectivity as, during the process, only the triflate group was reduced, even in substrates bearing other reducible functionalities on the aromatic ring, like nitrile, halides or alkenyl. Additionally, substrates bearing both tosyl and triflate groups **24** as well as substrates containing terminal double bonds and triflate groups **26** were selectively deoxygenated at the triflate site to generate product **25** and **27**, respectively, in very high yield (Scheme 1.7 – b). Furthermore, the bulkiness of the NHC-ligand **L1** played a major role in the successful formation of the desired product.

Both radical clock and radical scavenger experiments indicated that this reaction follows an ionic pathway, (Scheme 1.7 – c). First, the precatalyst **IC1** reacts with Caesium fluoride (CsF) to form complex **IC2**. The halogenated Cu complex **IC2** reacts with the silane, generating the active Cu-H species **IC3**. Subsequently, the transfer hydrogenolysis leads to the C-O bond cleavage of **22**, the formation of the desired product **3** and the generation of complex **IC4**. The regeneration of the complex **IC2** is achieved through the reaction of **IC4** with caesium fluoride.

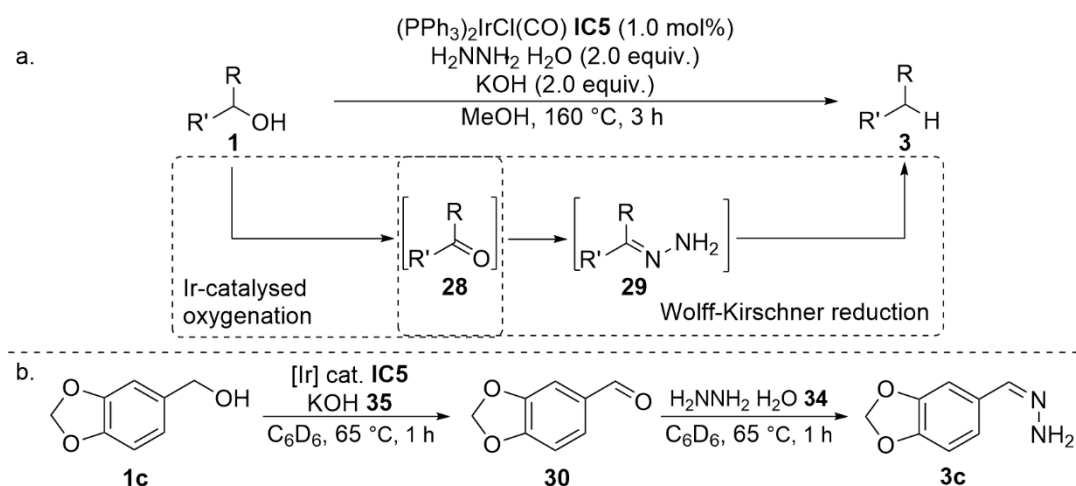


**Scheme 1.7.** (a) Deoxygenation reaction developed by Dang *et al.*; (b) examples of chemoselective transformations; (c) proposed mechanism of the deoxygenation procedure.<sup>17</sup>

In 2013, Hunag *et al.* developed an Ir-catalysed one-pot, two-step deoxygenation system, whose main step is a prior oxidation of the alcohol followed by a Wolff-Kirschner deoxygenation reaction, which was described in detail in chapter 1.1.1.<sup>18</sup> This is the first example of an alcohol deoxygenation procedure, which utilizes the superior reactivity of carbonyl compounds towards deoxygenation, instead of transforming the hydroxyl group into a better leaving group (Scheme 1.8). During the optimization experiments, multiple Ir-based catalysts were tested, among which Vaska's complex **IC5** proved to be

the most efficient one for this transformation. The utilization of a polar, protic solvent improved the transformation, as MeOH led to the highest yield of alkane. Surprisingly, water was also suitable for this procedure, but even in thoroughly optimized conditions, the yield of the desired product did not exceed 50%. The choice and quantity of base were also investigated. Although triethylamine or cesium carbonate showed some degree of effectiveness, 2 equivalents of potassium hydroxide were best suited for the reaction. This result was convenient as KOH is one of the most used bases in the Wolff-Kishner reduction. The amount of base needed for the formation of the alkane in a quantitative yield hints that both steps of the procedure might be facilitated by the basic media. Other important parameters, which positively influenced the outcome of the reaction, were increased temperature, higher concentration and a shorter reaction time. Thus, a variety of primary benzylic alcohols were deoxygenated with this procedure, yielding excellent amounts of the desired products despite some exceptions. A substrate bearing a methoxy group in the *ortho* position led to a substantial decrease in yield compared to its *para*- and *meta*-substituted counterparts due to the chelation effect on the catalyst's metallic centre. Additionally, a considerable decrease in alkane yield was observed for secondary benzylic alcohols, substrates bearing multiple hydroxy groups and aliphatic substrates. The primary aliphatic alcohols were also reduced by this catalytic system but in significantly lower yields than their benzylic counterparts.

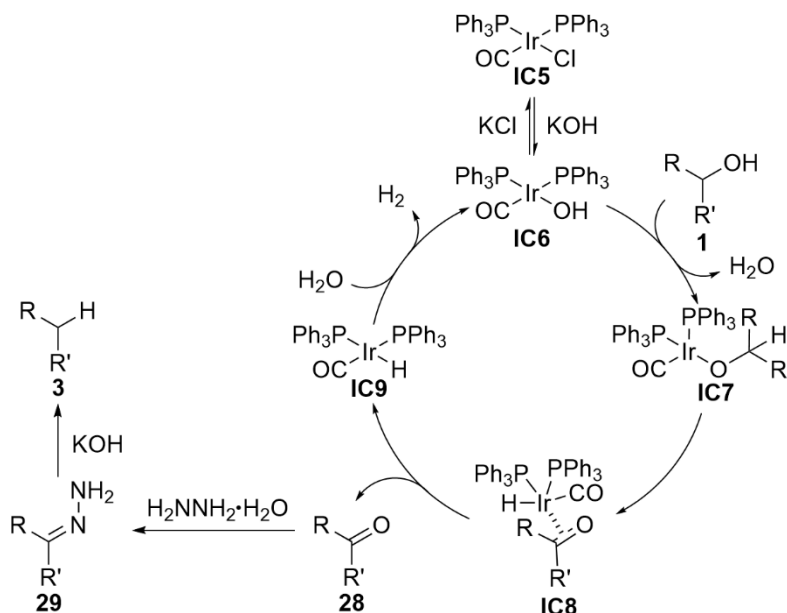
The mechanistic experiments revealed more information about the reaction pathway. As expected, tertiary benzylic alcohols could not be deoxygenated *via* this method, due to the absence of the  $\beta$ -hydrogen atom. The formation of the carbonyl intermediate **28** was evidenced by treating alcohol **1c** only with the Ir-catalyst **IC5** and one equivalent of KOH in deuterated benzene (Scheme 1.8 - b). Interestingly, without the addition of a base, no conversion was observed. Subsequently, the addition of hydrazine to this reaction mixture led to the generation of the hydrazone **29**, which is the specific intermediate in the Wolff-Kishner reduction.



**Scheme 1.8.** (a) deoxygenation methodology developed by Huang *et al.*; (b) investigations on the reaction intermediates.<sup>18</sup>

Competition reactions between alcohols and olefins showed that the system is capable of catalysing both the deoxygenation reaction and the hydrogenation of both intramolecular and intermolecular double bonds, but the two processes do not negatively interfere with each other. Thus, a mechanistic pathway was postulated (Scheme 1.9). First, Vaska's complex (**IC5**) reacts with the base to form complex **IC6**. The hydroxy group is then substituted by the alcohol **1** to generate complex **IC7**

which, *via* a  $\beta$ -H elimination, leads to the formation of **IC8**. The dissociation of **IC8** leads to the formation iridium hydride **IC9** and to the expulsion of the carbonyl intermediate **28**, which is further transformed through a Wolff-Kishner reduction into the corresponding hydrazone **29** and then to the desired alkane **3**. Subsequently, the regeneration of the iridium hydroxide **IC6** takes place through the hydroxylation of complex **IC9**.

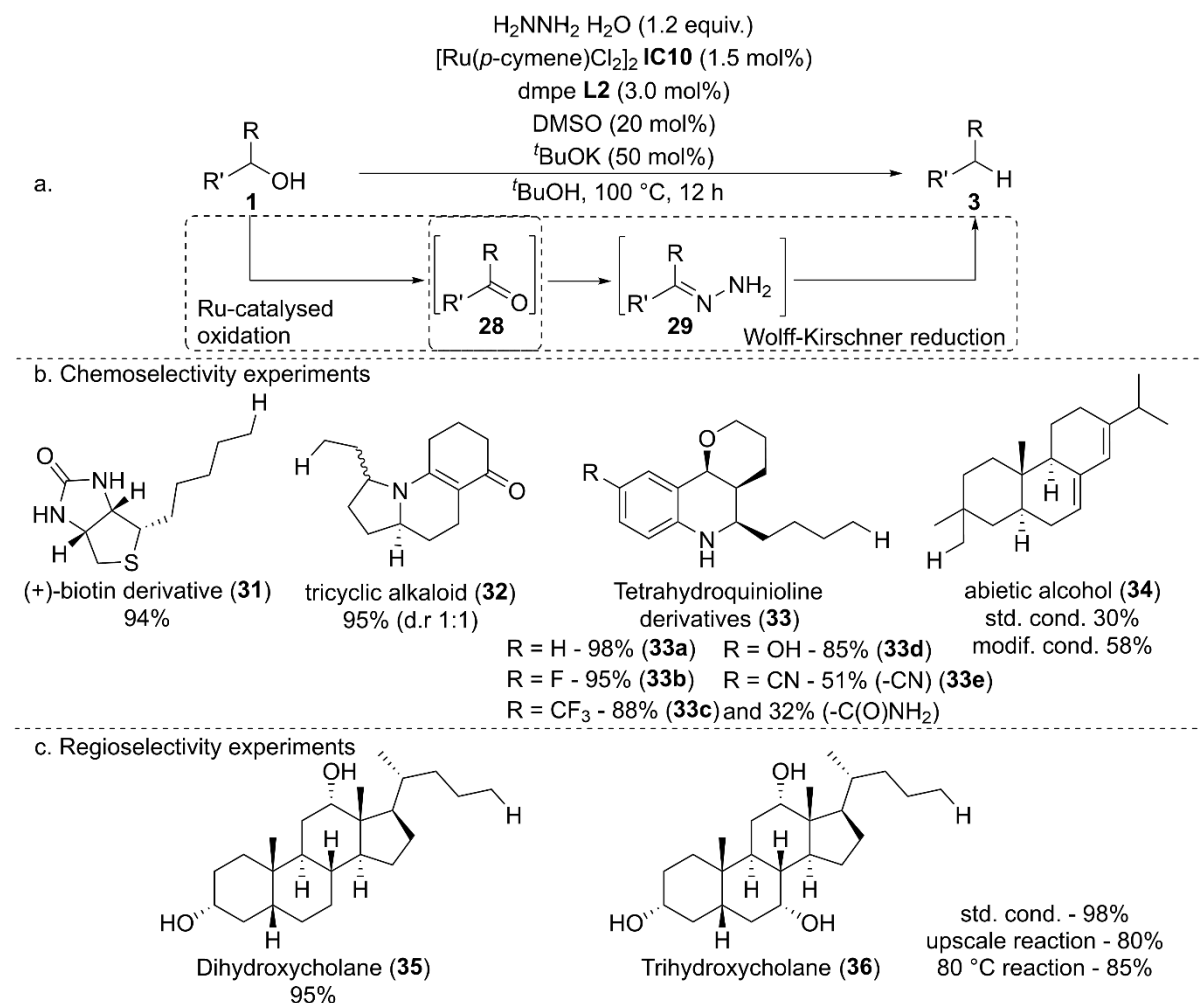


**Scheme 1.9.** Proposed mechanism for the deoxygenation methodology developed by Huang *et al.*<sup>18</sup>

In 2016, the same group published an improved version of this one-pot methodology, reporting a chemoselective Ru-catalysed deoxygenation reaction, which addressed the reactivity problem of primary aliphatic substrates, as well as the thermal and high concentration concerns (Scheme 1.10 – a).<sup>19</sup> In order to lower the reaction temperature, established low-temperature Wolff-Kishner procedures were analysed.<sup>8</sup> Thus, *tert*-butanol (*t*BuOH) was chosen as additive for the preliminary reactions, which were conducted in DMSO. Unfortunately, under these conditions no Ru- or Ir-based catalyst gave any satisfactory results. To overcome this setback, the amounts of *t*BuOH and DMSO were reversed. Therefore, *tert*-butanol was employed as solvent and DMSO as additive in order not to saturate the coordination sites of the catalyst. Indeed, this led to improved yields at only 80 °C by using ruthenium-based catalysts with bidentate phosphine ligands, like 1,2-bis(dimethylphosphino)ethane (dmpe) (**L2**). In this modified system, inorganic bases proved to be efficient for the deoxygenation of alcohols, but potassium *tert*-butoxide (*t*BuOK) was able to promote the transformation to quantitative yields even in substoichiometric amounts at 100 °C. Under these conditions, primary aliphatic and benzylic alcohols were deoxygenated in excellent yields.

Besides, multiple functionalities were tolerated by the catalytic system, like thioethers, amino groups, internal double and triple bonds, and phenolic hydroxyl groups. Even highly functionalized biotin derivative **31** was deoxygenated in an almost quantitative yield without the disruption of thiophene or ureido groups (Scheme 1.10 - b). These results laid the foundation for the investigations of chemoselectivity. The limitation of this catalytic system regarding the substrate scope were compounds bearing a methoxy group in the *ortho*-position and substrates containing functionalities, which are liable to strong basic conditions, like amides and esters.

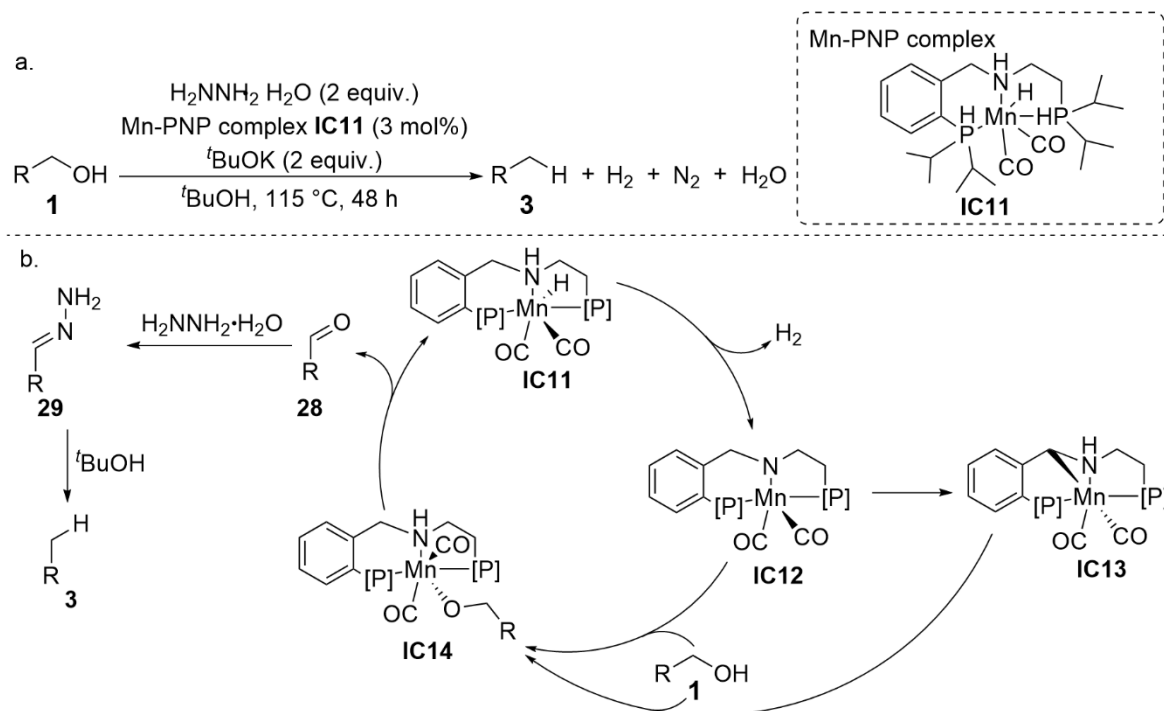
Hence, the chemoselectivity and regioselectivity of the catalytic system were tested on various complex bioactive molecules (Scheme 1.10 – b and c). By using the standard Ru-based system, tricyclic heterocycle alkaloid (**32**) and tetrahydroquinoline-based molecules (**33a-e**) were chemoselectively deoxygenated in excellent yields. The nitrile/substituted compound **33e** led to moderate yield due to the basic conditions, under which it underwent partial hydrolysis to the corresponding amide. In the case of **32**, a complete selectivity towards the reduction of the alcoholic moiety was observed, but, due to the basic reaction conditions, the epimerization on the pyrrolidine ring occurred. In contrast, tetrahydroquinoline derivatives (**33a-e**) retained the stereochemistry throughout the process and without affecting other functional groups present in the molecule. For the deoxygenation of abietic alcohol (**34**), bearing a conjugated double bond system, an increased amount of catalyst, ligand and hydrazine and a prolonged reaction time had to be used in order to obtain satisfactory yields, due to the steric hindrance. Thus, based on the steric bias, the regioselectivity of the system was tested. For these experiments, multiple alcohols bearing a steroidal backbone were chosen. Remarkably, in both deoxycholic alcohol (**35**) and trihydroxycholane (**36**) the primary alcoholic moiety was selectively reduced in exceptional yields, without the need of using protecting groups for the secondary and tertiary -OH groups. In the case of **36**, both the upscaled reaction and the reaction conducted at 80 °C yielded the desired product in very good amounts (80% and 85%, respectively).



**Scheme 1.10.** (a) Deoxygenation reaction developed by Dai *et al.*; (b) chemoselective reductions of bioactive molecules; (c) regioselective reductions of steroids.<sup>19</sup>

Inspired by this pioneering work, Bauer *et al.* reported in 2017 a procedure for the deoxygenation of primary benzylic and aliphatic alcohols, which utilizes the same oxidation-Wolff-Kishner reduction approach, catalysed by an Mn-PNP-complex. (Scheme 1.11 – a).<sup>20</sup> The main advantage of this procedure is the use of a non-precious metal-based catalyst for the oxidative step, which is more cost effective than both the Ir- and Ru-based catalysts. Besides, the reaction can be conducted without a base, albeit with lower yields. For the second step of the procedure, conditions related to a low-temperature variant of the Wolff-Kishner deoxygenation were employed. The most effective Mn-PNP complex for this purpose was complex **IC11**, which was previously used in the N-formylation of amines.<sup>21</sup> The best-performing base proved to be <sup>t</sup>BuOK with the optimal loading of 2 equivalents. By using the optimized reaction conditions, a number of primary benzylic and aliphatic substrates bearing various functional groups, like methoxy, amino, pyridinyl or trifluoromethyl substituents, were successfully deoxygenated. Due to the low reactivity towards secondary alcohols, an intermolecular competitive experiment was conducted, which led to the almost exclusive deoxygenation of the primary-alcohol substrate.

Based on the mechanistic studies and available literature a reaction pathway was proposed (Scheme 1.11 – b). <sup>t</sup>BuOH facilitates the elimination of molecular hydrogen from complex **IC11**, this leading to the generation of **IC12**. This complex can undergo intramolecular C-H bond activation to form **IC13**. Both **IC12** and **IC13** complexes can lead to the formation of complex **IC14** via an oxidative addition. The decomposition of **IC14** is followed by the regeneration of the compound **IC11** and the liberation of the aldehyde, which is further transformed into the desired alkane via the hydrazone intermediate.



**Scheme 1.11.** (a) deoxygenation reaction developed by Bauer *et al.*; (b) proposed mechanism of the deoxygenation procedure.<sup>20</sup>

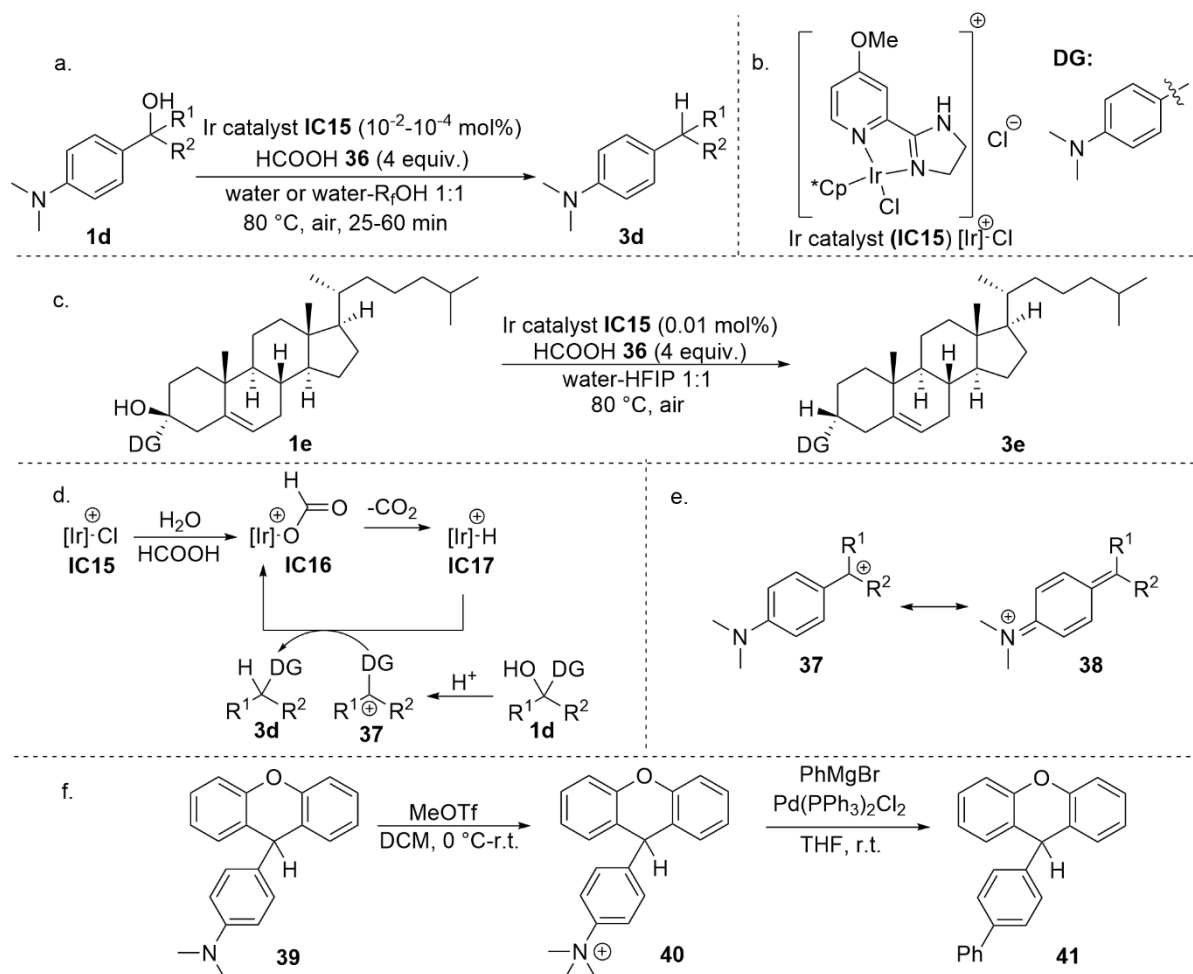
### 1.1.2.2. Direct Deoxygenation Procedures

Recently, new homogenous catalytic procedures for the direct deoxygenation of benzylic alcohols emerged. Different precious and non-precious metal based catalysts proved their capabilities

for this type of deoxygenation procedures, mainly Ir-, Ni- and Ti-based catalysts. The Ti-based procedures will be extensively discussed in chapter 6.1.

A prominent example of a regioselective direct deoxygenation procedure was published in 2018 by Yang *et al.*<sup>22</sup> This reaction was conducted in water, at 80 °C, in air, using an Ir-based catalyst (**IC15**) and formic acid (**36**) as H-donor and promotor through the induced low pH value (Scheme 1.12 – a). The high yields and site-selectivity of the transformation were achieved by introducing a directing group (DG) into the alcoholic substrate, which should act as an activating entity for the geminal hydroxy group. For this role, multiple aromatic amines were screened, mostly secondary ones. During these experiments, *para*-substituted phenyls proved to be more efficient than their *ortho* and *meta* counterparts at promoting the deoxygenation of secondary benzylic alcohols. Additionally, increasing the steric hindrance at the N-atom further inhibited the activation of the -OH group, leading to a decrease in yield. Therefore, 4-(*N,N*-dimethylamino)phenyl moiety was chosen as being the optimal directing group for this transformation. The negative influence of the N-substituents' bulkiness over the yields of the desired product was smaller on primary benzylic alcohols, thus almost quantitative yields of the corresponding alkane were obtained with various directing groups. Secondary alcohols, bearing aromatic moieties beside the directing group, were deoxygenated in very high yields regardless of the molecular backbone or substituents grafted on the aromatic ring. When the aromatic moiety was substituted by an aliphatic chain, trifluoroethanol (R<sub>f</sub>OH) or hexafluoroisopropanol (HFIP) had to be added to the reaction mixture in order to obtain satisfactory results. The same positive effect of fluoroalkanols on the transformation was also observed for the deoxygenation of tertiary alcohols. The regioselectivity of the method was demonstrated, as no reduction of alcoholic moieties was observed without the directing group present in the  $\alpha$ -position. For example, bioactive molecule **1e** was successfully deoxygenated to **3e** via a prior introduction of the directing group. The reactions on steroids showed excellent stereoselectivity with only one diastereomer being isolated in all cases (Scheme 1.12 – c). Based on the deuterium labelling experiments and previous <sup>1</sup>H-NMR investigations, a mechanistic pathway was proposed (Scheme 1.12 – d). First, the formylation of the Ir-catalyst **IC15** takes place with the generation of complex **IC16**. In parallel, the alcohol is protonated, and the carbocation **37** is produced after the elimination of water. Carbocation **37** can be stabilized by either the directive group (**38**) or by the fluoroalkanols, depending on the substrate (Scheme 1.11 – e). Following the CO<sub>2</sub> liberation, the presumed active species **IC17** is formed. The iridium hydride **IC17** further reacts with the carbocation **37**, leading to the formation of the desired product and the regeneration of active complex **IC16** through an oxidative addition of another deprotonated formic acid (**36**) molecule.

Although very efficient, this method has two main drawbacks, namely the cost-effectiveness, due to the employment of a Ir-based catalyst and the necessity of the amine as a directive functionality in the  $\alpha$ -position. Yang *et al.* addressed the latter problem by proposing further functionalization pathways of the amine group by applying a Kumada coupling procedure on the deoxygenation product (Scheme 1.11 – e). This procedure led to the generation of compound **41** in excellent yields starting from compound **39**, rendering this procedure more attractive for synthetic applications.

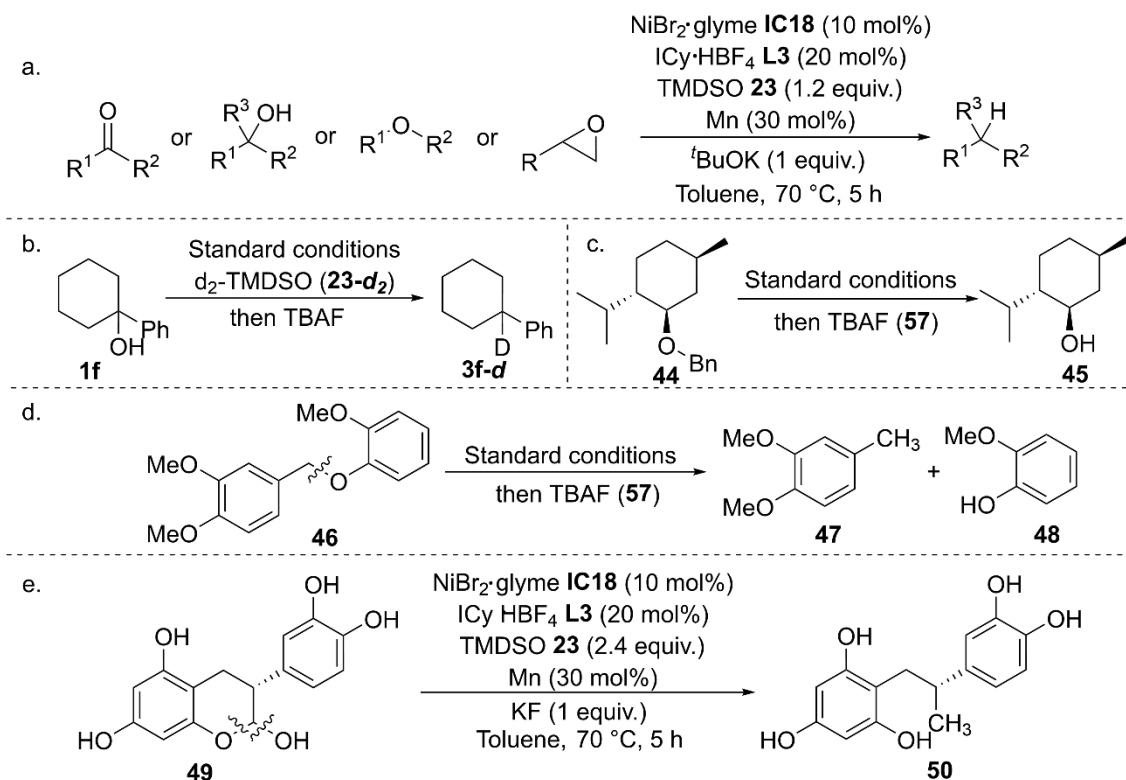


**Scheme 1.12.** (a) deoxygenation reaction developed by Yang *et al.*; (b) Ir-based precatalyst **IC15** and the directing group (DG); (c) diastereoselective deoxygenation of alcohol **1e**; (d) proposed mechanism of the deoxygenation procedure; (e) stabilizing mechanism of the carbocation; (f) late-stage functionalization of the directing group.<sup>22</sup>

Another direct deoxygenation procedure was developed by Cook and coworkers in 2021 (Scheme 1.13 - a).<sup>23</sup> This versatile procedure was successfully applied for the deoxygenation of alcohols, carbonyls, ethers, and epoxides. This protocol utilizes a homogenous Ni/NHC catalytic system and hydrosilanes as H-donors. TMDSO (**23**) proved to be more efficient as a hydrogen donor than other hydrosilanes. For the formation of the presumed active species, a basic additive is needed to deprotonate the NHC ligand ICy•HBF<sub>4</sub> (**L3**) and furnish the Ni-complex, and Mn is employed as the reducing agent for the Ni<sup>2+</sup> to Ni<sup>0</sup> process. First, this catalytic system was optimized for the deoxygenation of ketones. During these studies, it was remarked that when the Ni-precatalyst **IC18** was not added to the reaction mixture, no alkane was obtained. However, the complete consumption of the starting material was observed, and noticeable amounts of the corresponding alcohol were detected. In order to examine the reactivity of the potential alcoholic intermediate, it was directly subjected to the transformation. Indeed, this reaction resulted in a high yield of the corresponding alkane. Thus, it was hypothesised that, first, a Brønsted base-catalysed reduction of the substrate takes place before the *in situ* formed alcohol is further reduced to the alkane by the Ni/NHC catalyst. The subsequent substrate screening revealed that this catalytic system was capable of deoxygenating primary, secondary and tertiary benzylic and

aliphatic alcohols in good to excellent yields. The existence of a  $\pi$ -system in the vicinity of the reactive site and the decrease in steric impediments were both beneficial for this transformation. The same reactivity pattern was observed when aldehydes and ketones were subjected to the transformation, leading to similarly high yields. Under the same conditions, silyl ethers, ethers, and epoxides were deoxygenated in high yields.

Hence, the applicability of this catalytic system in various fields was investigated. By using deuterated TMDSO (**23-d<sub>2</sub>**) for the deoxygenation of alcohol **1f**, the newly formed C-D bond in the alkane (**3f-d**) was selectively observed at the site of the former C-O bond, proving that this procedure can be applied in isotopic labelling (Scheme 1.13 - b). When tetra-*n*-butylammonium fluoride (TBAF) was added in the reaction mixture, selective O-Bn bond cleavage of the benzyl-protected alcohol (**44**) was also observed (Scheme 1.13 - c). This result led to the conclusion that this catalytic system can be used for the degradation of lignin- (**46**) and tannin-model substrates (**49**). Indeed, when these substrates were subjected to the transformation, the selective cleavage of the alcoholic and ethereal C(sp<sup>3</sup>)-O bond was obtained (Scheme 1.13 - d and e).



**Scheme 1.13.** (a) deoxygenation reaction developed by Cook *et al.*; (b) Isotopic labelling experiments; (c) Deprotection reaction; (d) deoxygenation of lignin model substrates; (e) deoxygenation of tannin model compound.<sup>23</sup>

During the kinetic isotope effect experiments, it was observed that by exchanging the TMDSO (**23**) with its deuterated counterpart, the reduction rate decreased considerably, indicating that the H-transfer from the catalyst to the alcohol proceeds prior or at the rate-determining step. Moreover, through these experiments, a possible elimination-hydrogenation pathway was excluded, because styrene was not transformed into ethylbenzene under standard conditions, and by submitting a deuterated homobenzylic alcohol to the reaction, the deuterium distribution remained constant in the obtained product. A mechanism proceeding through a carbocation was dismissed because no



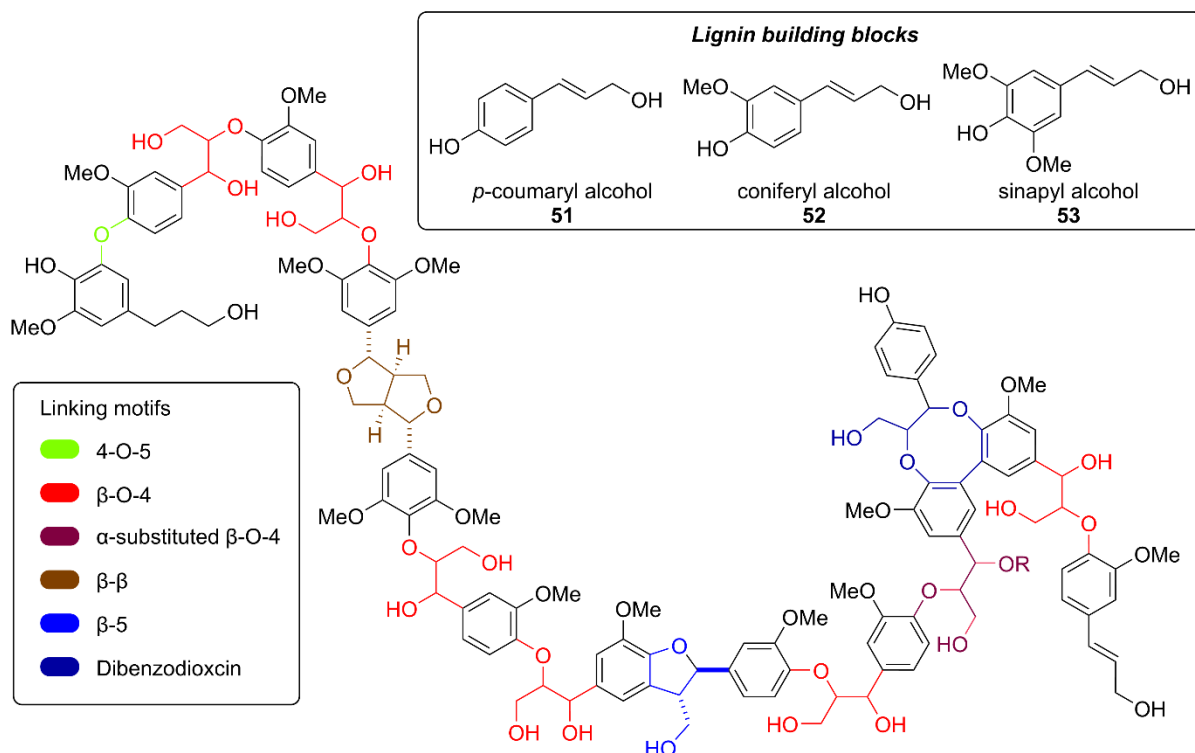
rearrangement was detected. *Via* radical clock experiments a possible radical mechanism was also dismissed. Albeit these extensive mechanistic investigations, the reaction pathway of this versatile transformation has not been fully elucidated to this date.

## 1.2. Lignin Valorisation through Deoxygenation Procedures

Beside the utilization in late-stage functionalization of bioactive molecules, deoxygenation reactions are used for the valorisation of biomass, especially lignin, and its transformation into biofuels and industrial-valuable compounds.<sup>24-27</sup> The most efficient approach towards the valorisation of lignin implies the preliminary depolymerization of this biomass through chemical or biological strategies.<sup>28, 29</sup> The depolymerisation step is followed by a selective hydrodeoxygenation procedure during which, through the cleavage of the hydroxylic and phenolic C-O bonds, benzene, toluene, styrene and other high valuable aromatic hydrocarbons are generated.<sup>27</sup>

Lignin is one of the most prominent biopolymer in nature, accounting for up to 30% of biomass.<sup>30</sup> In plants it has both a structural as well as a physiological role by conferring rigidity to the cells and by facilitating water transport throughout the plants.<sup>31</sup> In industry, the largest quantities of lignin are produced as a by-product by the pulping industry during the wood deconstruction procedures and isolation of cellulose from lignocellulosic biomass.<sup>31, 32</sup> Until recently, lignin was regarded only as a residue of these processes and burnt in order to energetically sustain the pulping process.<sup>26</sup>

Due to the desire of the chemical industry to find new alternatives to fossil raw materials, valorisation procedures of this biopolymer were developed.<sup>33</sup> The attractiveness of lignin for the chemical industry relies on its molecular complexity which can lead to the generation of a large variety of aromatic compounds. This characteristic is derived from the pathway through which lignin is formed in nature, namely through the radical coupling of monolignols: *p*-coumaryl alcohol (**51**), coniferyl alcohol (**52**) and sinapyl alcohol (**53**). From the combination of these three lignin building blocks, various linking motifs are generated, some of the most common being highlighted in figure 1.1.



**Figure 1.1.** Lignin with highlighted linking motifs and lignin building blocks.<sup>34</sup>

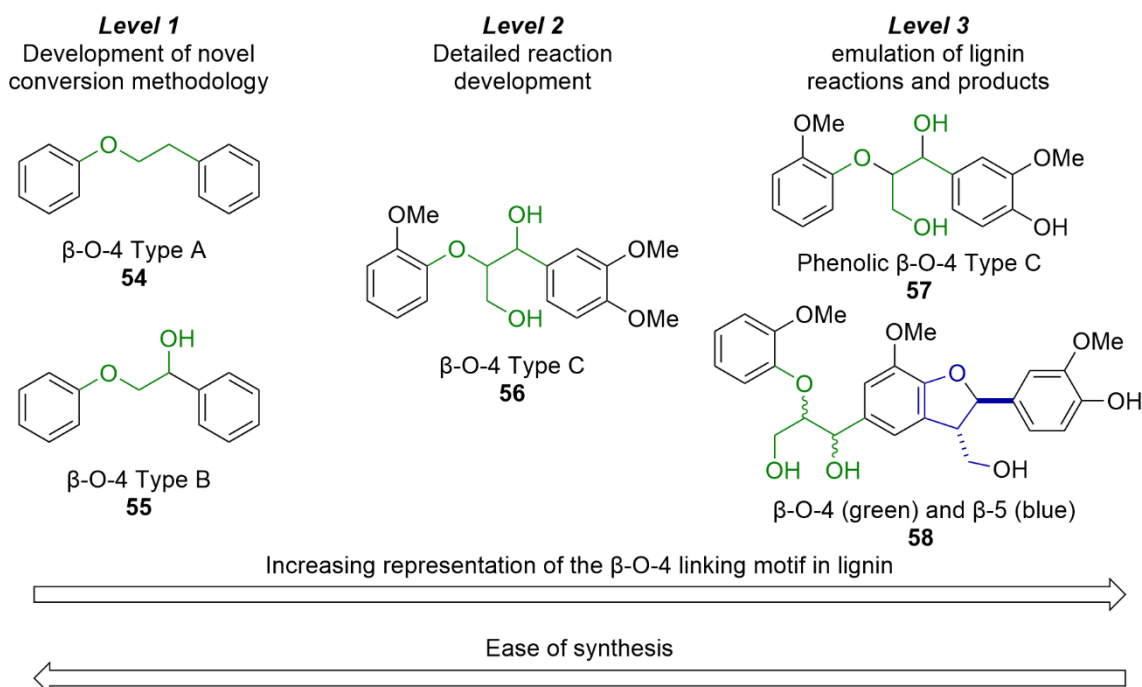
The types of linkage and the percentage of each subunit present in the lignin sample heavily varies between plant species, age, and environmental factors. The most common linkage motif, regardless of the type of wood from which lignin is extracted, is the  $\beta$ -O-4 motif (Table 1.1). Additionally, the separation process of lignin from lignocellulosic biomass induces more complexity to the structure due to the chemical treatment.

**Table 1.1.** Abundancies of common linking motifs in softwood, hardwood, and grasses.<sup>34</sup>

Lignin	$\beta$ -O-4 (%)	$\beta$ -5 (%)	$\beta$ - $\beta$ (%)	5-5 <sup>[a]</sup> (%)	4-O-5 (%)
Softwood	45-55	9-12	2-6	5-7	2
Hardwood	60-62	3-11	3-12	<1	2
Grasses	74-84	5-11	1-7	n.d.	n.d.

n.d. – not determined; [a] In the form of dibenzodioxocin.

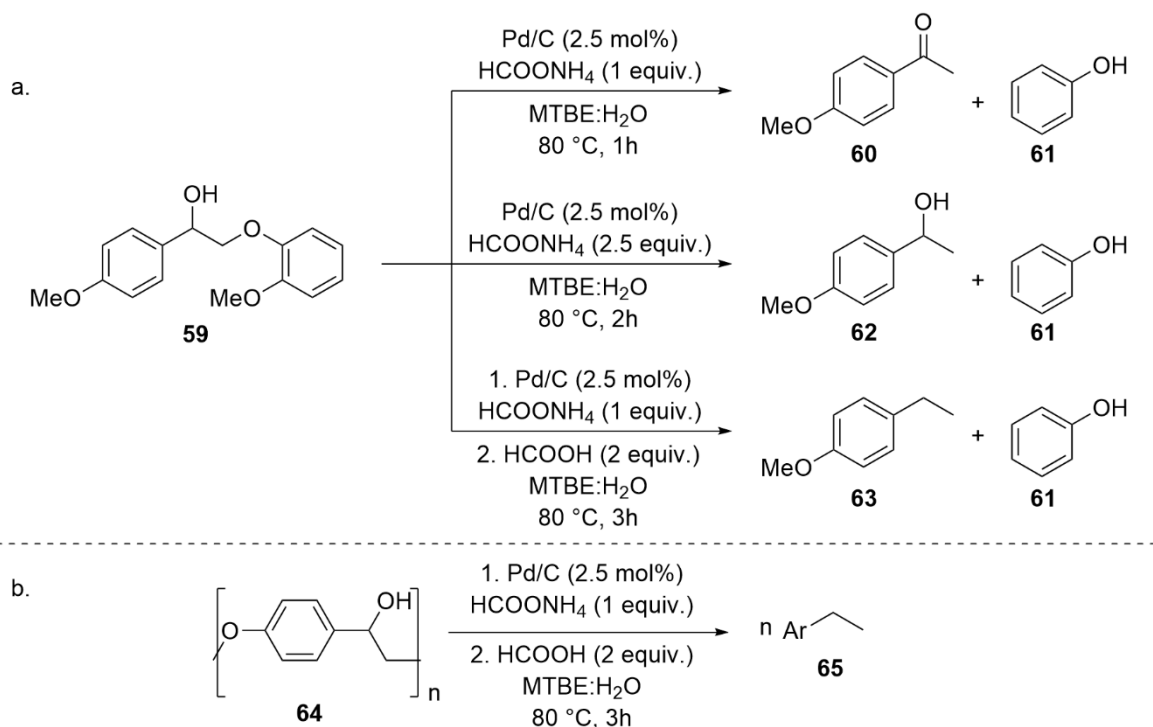
The high molecular mass and the large variety of C-C and C-O bonds which can be found in the structure on lignin also represents the main challenges in the development of a robust catalytic valorisation strategy of this biopolymer. Therefore, up to this date, in most small-scale lignin valorisation methodologies, model systems were extensively utilized in this research field. This strategy eliminates the solvation problems which arise from the high molecular mass of lignin and also facilitates the development of specific procedures for various motifs. In 2020, the group of Deuss classified the model systems containing the  $\beta$ -O-4 motif into three categories based on the molecular complexity of the model substrate (Figure 1.2).<sup>34</sup>



**Figure 1.2.** Deuss classification of model substrates' molecular complexity.<sup>34</sup>

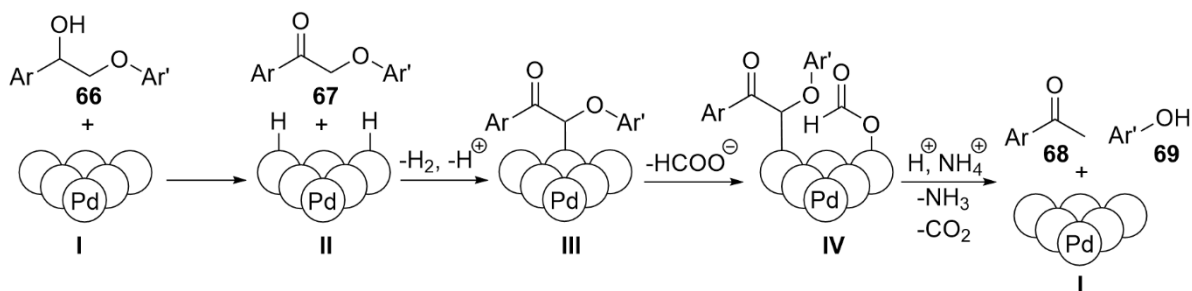
An example of a deoxygenation procedure which was further used in the valorisation of lignin was developed Samec's group.<sup>35, 36</sup> In this transfer hydrogenolysis procedure, a Pd/C-HCOOH catalytic

system was utilized for the cleavage of the  $\beta$ -O-4' linkage motif (Scheme 1.14). Additionally, a base was needed in the reaction system in order to inhibit the competing disproportionation reaction. Interestingly, depending on the amount of base used in this reaction and a delayed addition of formic acid (**36**), model substrate **59** was selectively transformed into the corresponding ketone **60**, alcohol **62** or alkane **63**, beside phenol (**60**). Moreover, this catalytic system was capable of efficient depolymerisation of artificial lignin model polymer **64** and degraded 73% of the  $\beta$ -O-4' units of organosolv lignin from *Pinus Sylvestris*.



**Scheme 1.14.** (a) Possible reaction pathways depending on the reaction conditions; (b) depolymerization of compound **64**.<sup>35</sup>

The mechanistic studies indicated that the reaction pathway proceeds through the dissociative chemisorption of substrate **66** to Pd complex **I**, followed by the formation of ketone **67** and the absorption of hydrogen on the metallic surface to generate complex **II**. The enol tautomer of ketone **67** is absorbed on the Pd surface to generate complex **III**. Following the absorption of a formate ion to Pd, complex **IV** is generated. Subsequently, the decomposition of complex **IV** leads to the generation of the desired deoxygenated product.



**Scheme 1.15.** The mechanism for the deoxygenation of lignin model substrates.<sup>35</sup>

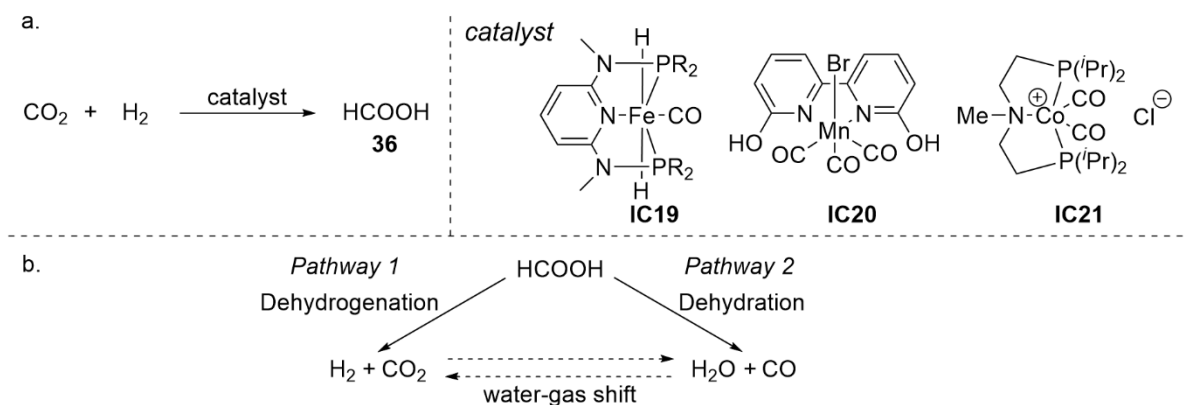
**1.3. References**

1. E. Clemmensen, *Ber. Dtsch. Chem. Ges.*, 1913, **46**, 1837-1843.
2. E. Clemmensen, *Ber. Dtsch. Chem. Ges.*, 1914, **47**, 51-63.
3. N. Kishner, *J. Russ. Phys. Chem. Soc.*, 1911, **43**, 582-595.
4. L. Wolff, *Liebigs Ann. Chem.*, 1912, **394**, 86-108.
5. M. Huang, *J. Am. Chem. Soc.*, 1946, **68**, 2487-2488.
6. J. T. Kuethe, K. G. Childers, Z. Peng, M. Journet, G. R. Humphrey, T. Vickery, D. Bachert and T. T. Lam, *Org. Process Res. Dev.*, 2009, **13**, 576-580.
7. D. Znidar, A. O’Kearney-McMullan, R. Munday, C. Wiles, P. Poechlauer, C. Schmoelzer, D. Dallinger and C. O. Kappe, *Org. Process Res. Dev.*, 2019, **23**, 2445-2455.
8. D. J. Cram and M. R. V. Sahyun, *J. Am. Chem. Soc.*, 1962, **84**, 1734-1735.
9. D. H. R. Barton and S. W. McCombie, *J. Chem. Soc., Perkin trans. 1*, 1975, 1574-1585.
10. D. Crich and L. Quintero, *Chem. Rev.*, 1989, **89**, 1413-1432.
11. D. H. R. Barton and W. B. Motherwell, *Pure Appl. Chem.*, 1981, **53**, 15-31.
12. L. Chenneberg and C. Ollivier, *CHIMIA*, 2016, **70**, 67.
13. R. E. Ireland, D. C. Muchmore and U. Hengartner, *J. Am. Chem. Soc.*, 1972, **94**, 5098-5100.
14. L. Zhang and M. Koreeda, *J. Am. Chem. Soc.*, 2004, **126**, 13190-13191.
15. W. G. Bentrude, J. H. Hargis, N. A. Johnson, T. B. Min, P. E. Rusek, Jr., H.-W. Tan and R. A. Wielesek, *J. Am. Chem. Soc.*, 1976, **98**, 5348-5357.
16. P. A. Jordan and S. J. Miller, *Angew. Chem. Int. Ed.*, 2012, **51**, 2907-2911.
17. H. Dang, N. Cox and G. Lalic, *Angew. Chem. Int. Ed.*, 2014, **53**, 752-756.
18. J.-L. Huang, X.-J. Dai and C.-J. Li, *Eur. J. Org. Chem.*, 2013, **2013**, 6496-6500.
19. X.-J. Dai and C.-J. Li, *J. Am. Chem. Soc.*, 2016, **138**, 5433-5440.
20. J. O. Bauer, S. Chakraborty and D. Milstein, *ACS Catal.*, 2017, **7**, 4462-4466.
21. S. Chakraborty, U. Gellrich, Y. Diskin-Posner, G. Leitus, L. Avram and D. Milstein, *Angew. Chem. Int. Ed.*, 2017, **56**, 4229-4233.
22. S. Yang, W. Tang, Z. Yang and J. Xu, *ACS Catal.*, 2018, **8**, 9320-9326.
23. A. Cook, H. MacLean, P. St. Onge and S. G. Newman, *ACS Catal.*, 2021, **11**, 13337-13347.
24. F. G. Calvo-Flores, J. A. Dobado, J. Isac-García and F. J. Martín-Martínez, in *Lignin and Lignans as Renewable Raw Materials*, 2015, pp. 9-48.
25. D. S. Argyropoulos and S. B. Menachem, in *Biopolymers from Renewable Resources*, ed. D. L. Kaplan, Springer Berlin Heidelberg, Berlin, Heidelberg, 1998, pp. 292-322.
26. L. Monsigny, E. Feghali, J.-C. Berthet and T. Cantat, *Green Chem.*, 2018, **20**, 1981-1986.
27. J. G. Tillou, C. J. Ezeorah, J. J. Kuchta, S. C. D. Dissanayake Mudiyansele, J. D. Sitter and A. K. Vannucci, *RSC Sustain.*, 2023, **1**, 1608-1633.
28. L. Jiang, C.-G. Wang, P. L. Chee, C. Qu, A. Z. Fok, F. H. Yong, Z. L. Ong and D. Kai, *Sustainable Energy Fuels*, 2023, **7**, 2953-2973.
29. Z. Sun, B. Fridrich, A. de Santi, S. Elangovan and K. Barta, *Chemical Reviews*, 2018, **118**, 614-678.
30. J. Zakzeski, P. C. A. Bruijninx, A. L. Jongerius and B. M. Weckhuysen, *Chem. Rev.*, 2010, **110**, 3552-3599.
31. M. Graglia, N. Kanna and D. Esposito, *ChemBioEng Rev.*, 2015, **2**, 377-392.
32. I. Haq, P. Mazumder and A. S. Kalamdhad, *Bioresour. Technol.*, 2020, **312**, 123636.
33. L. Alves de Souza, P. Magalhães de Souza, G. Tozzi Wurzler, V. Teixeira da Silva, D. A. Azevedo, R. Wojcieszak and F. Bellot Noronha, *ACS Sustain. Chem. Eng.*, 2023, **11**, 67-77.
34. C. W. Lahive, P. C. J. Kamer, C. S. Lancefield and P. J. Deuss, *ChemSusChem*, 2020, **13**, 4238-4265.
35. M. V. Galkin, S. Sawadjoon, V. Rohde, M. Dawange and J. S. M. Samec, *ChemCatChem*, 2014, **6**, 179-184.
36. M. V. Galkin and J. S. M. Samec, *ChemSusChem*, 2014, **7**, 2154-2158.

## 2. H-donors in Deoxygenation Reactions

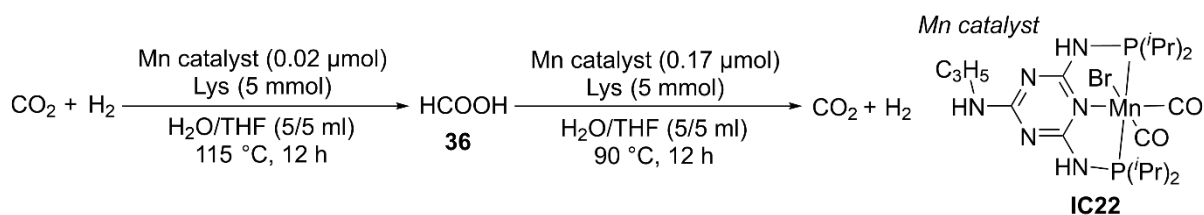
### 2.1. Formic Acid

Formic acid (**36**) is one of the most used molecules in synthetic chemistry and it represents a promising alternative to H<sub>2</sub> as energy carrier.<sup>1</sup> This wide applicability derives from a series of characteristics. The selling price of formic acid (**36**) is low compared to other hydrogen sources (32.4 Euro/100 mL – Sigma Aldrich) due to the fact that HCOOH (**36**) can be obtained through the hydrogenation of CO<sub>2</sub>, even with non-precious metal based homogenous catalysts, thus increasing the recyclability of HCOOH (**36**) (Scheme 2.1 - a).<sup>2-6</sup> Additionally, emerging large scale production strategies of formic acid (**36**) in biorefineries is very cost effective, one example being the process of oxidizing sugars with hydrogen peroxide.<sup>7</sup> From the safety perspective, the safe handling and transportation due to low flammability, non-toxicity, and biodegradability of HCOOH (**36**) make it suitable for green applications.<sup>8</sup> Another important advantage of formic acid (**36**) is its versatility, as it can act as an acid, formyl moiety, and as a reducing agent through decomposition. There are two established decomposition pathways of formic acid, which are dependent on the catalyst used for the process (Scheme 2.1 - b).<sup>8</sup> Therefore, HCOOH (**36**) can act as both hydrogen and carbon source.



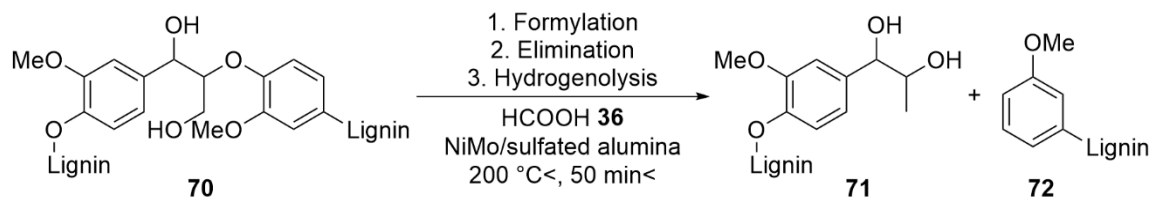
**Scheme 2.1.** (a) Hydrogenation of CO<sub>2</sub> to formic acid and non-precious metal based catalyst;<sup>2-6</sup> (b) Decomposition pathways of formic acid.<sup>8</sup>

Most of the decomposition processes, which follow pathway 1, rely on heterogeneous catalysts due to their superior TOF and recyclability (Scheme 2.1 - b).<sup>9,10</sup> However, in recent years more efficient homogeneous procedures were developed, based on both precious and non-precious metals.<sup>10-16</sup> In a recent report from 2022, the Beller's group developed a Mn-based homogenous catalyst capable of both the dehydrogenation of formic acid (**36**), and the hydrogenation of CO<sub>2</sub> in the presence of lysine (Scheme 2.2).<sup>17</sup> Remarkably, this Mn-Lys catalytic system could be reused in both processes up to 10 times without a notable yield drop, thus proving that homogenous catalytic processes can be as efficient as the established heterogenous methods.



**Scheme 2.2.** Hydrogenation-dehydrogenation procedure developed by the group of Beller.<sup>17</sup>

The versatility of formic acid (**36**) was further proven in a lignin degrading process. In 2017, the group of Barth used a NiMo catalyst for the degradation of lignin into bio-oil by using, among others, formic acid (**36**) as hydrogen donor (Scheme 2.3).<sup>18</sup> Interestingly, the mechanistic studies concluded that the activity of formic acid is not owed to pathway 1, but to a formylation-elimination-hydrogenolysis reaction sequence.



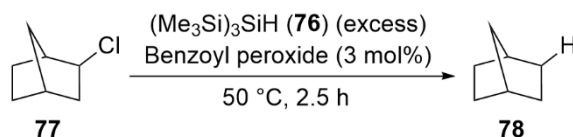
**Scheme 2.3.** Lignin degrading process developed by Barth's group.<sup>18</sup>

Due to its remarkable properties, H-donation capabilities, and synthetic applications in deoxygenation procedures, as it was stated in chapter 1.1 and 1.2 and will be further described in chapter 4.1, formic acid was found suitable for Pd- and Co-catalysed deoxygenation procedures developed during these studies.

## 2.2. Hydrosilanes

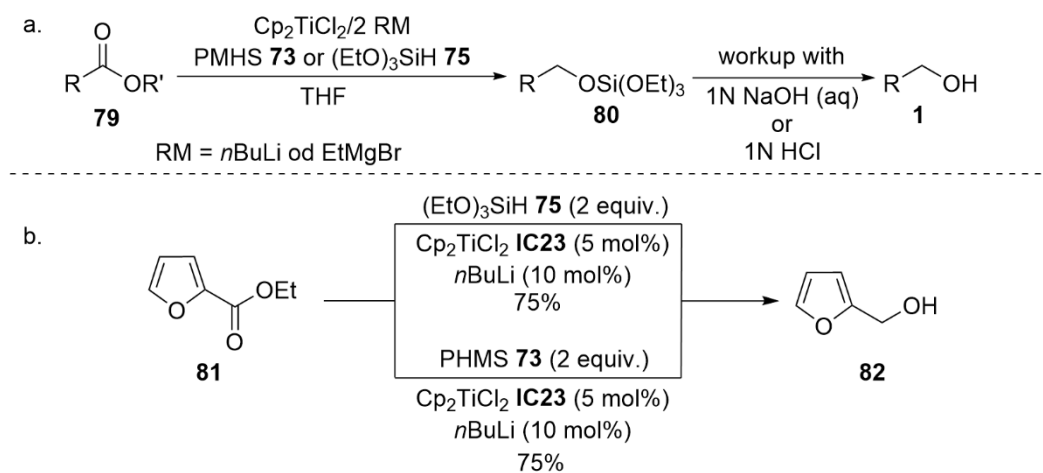
In the last 50 years, the scope of reactions in which hydrosilanes served as H-donors expanded exponentially, due to the versatility of this compound class. In contrast to other H-donors, hydrosilanes possess the ability to donate a hydrogen atom through both radical and ionic pathways.<sup>19</sup> Therefore, hydrosilanes can substitute both highly toxic reagents, like tributyltin hydride, or highly pyrophoric H-donors like lithium aluminium hydride (LiAlH) or sodium borohydride (NaBH<sub>4</sub>).<sup>19</sup> Additionally, the derivatization possibilities of the hydrosilanes with various functional groups impact the strength of the Si-H bond, thus, enabling more synthetic applications for which this compound class is suitable. Other important characteristics which increase the attractiveness of hydrosilanes, are the low toxicity, the high stability towards decomposition, and the fact that their utilization in synthetic applications complies with most green chemistry regulations.<sup>20</sup> Some of the silanes which proved to be efficient reducing agents in the transformations of oxygen-containing substrates were tetramethyldisiloxane (TMDSO, **23**), its polymeric counterpart polymethylhydrosiloxane (PMHS, **73**), triethylsilane (Et<sub>3</sub>SiH, **74**), triethoxysilane (EtO<sub>3</sub>SiH, **75**) and methyldiethoxysilane (Me(EtO)<sub>2</sub>SiH, **76**), each having its advantages and disadvantages which made them suitable for different applications.

The first application in which hydrosilanes were utilized as H-donor was reported by Chatgililoglu *et al.* in 1988 (Scheme 2.4).<sup>21</sup> In this procedure alkyl and aryl halides were dehalogenated to the corresponding hydrocarbon by using tris(trimethylsilyl)silane (**76**) as a free radical reducing agent. Previously, the same group showed that by exchanging the Si atom substituents, the BDE of the Si-H bond could be lowered.<sup>22</sup> The utilization of triethylsilane (**74**) in this methodology did not lead to any satisfactory results. However, when the ethyl moiety was substituted with TMS units the BDE of the Si-H bond was lowered from 90 kcal/mol to 79 kcal/mol, hence, the hydrogen donating capabilities were enabled.<sup>23</sup> The radical pathway of the transformation was highlighted by the inhibition of the reactivity upon the addition of the 2,6-di-tert-butyl-4-methylphenol (BHT) radical scavenger and through radical clock experiments with 5-hexenyl. Although this methodology was not suitable for reducing oxygen-containing substrates, it showed that through careful derivatization, hydrosilanes could be utilized in hydrogen transfer procedures.



**Scheme 2.4.** Dehalogenation procedure developed by Chatgililoglu *et al.*<sup>21</sup>

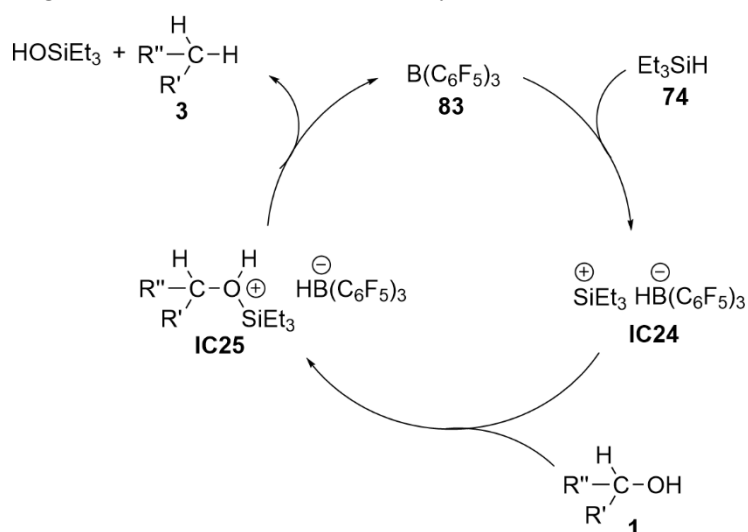
Following the results of Chatgililoglu *et al.* Buchwald's group developed between 1991 and 1995 multiple procedures for the reduction of esters to the corresponding primary alcohols (Scheme 2.5).<sup>24,25</sup> In the first methodology, a titanocene hydride catalyst, generated through the reaction between titanocene dichloride ( $\text{Cp}_2\text{TiCl}_2$ , **IC23**) and  $n\text{BuLi}$  or  $\text{EtMgBr}$ , was utilized together with two equivalents of triethoxysilane (**75**) as reducing agent (Scheme 2.5 - a). Although this procedure proved to be very efficient for the reduction of esters, safety concerns regarding the usage of triethoxysilane (**75**) made this method less attractive for large-scale applications.<sup>26</sup> Through the disproportion of triethoxysilane (**75**) highly pyrophoric  $\text{SiH}_4$  was generated. The investigations conducted by Buchwald did not completely elucidate the pathway through which this side-reaction takes place, but it was indicated that this unwanted process is catalysed by the Ti species present in the reaction mixture. Beside the disproportion reactions, the vapours of methoxy and ethoxy hydrosilanes can cause blindness and death through inhalation.<sup>27</sup> Therefore, a second procedure was developed in which the stable PMHS (**73**) was employed as reducing agent (Scheme 2.5 - b).<sup>25</sup> The main advantages of the utilization of this silicon-based reducing agent is its non-hazardous character towards human health, the stability towards oxidation and water, and the facile separation from the crude reaction mixture.<sup>28</sup> The yields of the desired compounds produced through this method was similar to the ones obtained through the triethoxysilane procedure. The exact mechanistic pathway through which the reduction of esters proceeds was not extensively investigated.



**Scheme 2.5.** Ti-catalyzed methods for the deoxygenation of esters developed by Buchwald's group.<sup>24, 25</sup>

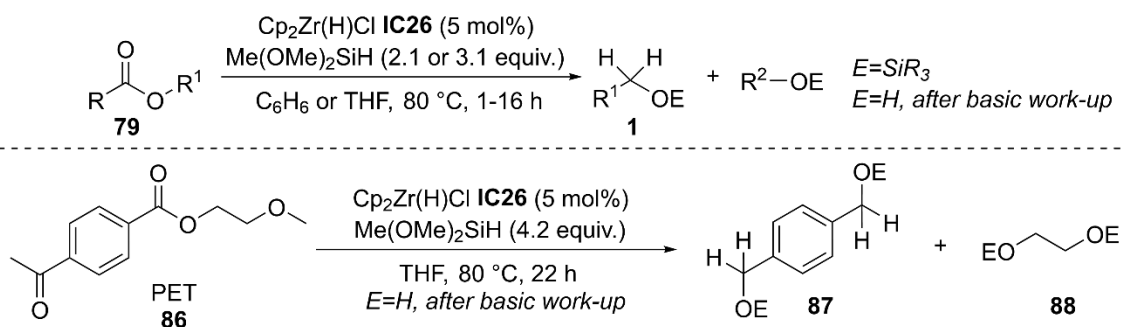
In 2000, Gevorgyan *et al.* developed a protocol for the deoxygenation of alcohols and ethers to the corresponding alkane, by using 3 equivalents of  $\text{Et}_3\text{SiH}$  (**74**) as H-donor and catalytic amounts of Lewis acid, namely  $\text{B}(\text{C}_6\text{F}_5)_3$  (**83**) (Scheme 2.6).<sup>29</sup> The most promising results were obtained for the primary alcohols and ethers, while tertiary substrates could not be transformed into the desired products. The mechanistic studies showed that the reaction proceeds through an ionic  $\text{S}_{\text{N}}1$  mechanism, as it is described in scheme 2.6. First, ate-complex **IC24** is formed through the reaction between  $\text{B}(\text{C}_6\text{F}_5)_3$  (**83**) and triethylsilane **74**. The Si-cation of complex **IC24** reversibly coordinates to the silyl ether to form

oxonium complex **IC25** which through decomposition would lead to the formation of the desired product **3** and to the regeneration of the Lewis acid catalyst **83**.



**Scheme 2.6.** Proposed mechanism for the deoxygenation procedure developed by Gevorgyan *et al.*<sup>29</sup>

Another recent example of a deoxygenation method in which hydrosilanes were utilized as H-donor was reported by Cantat's group (Scheme 2.7).<sup>30</sup> In this methodology the Zr-based Schwartz's reagent **IC26** was used as catalyst and methyldimethoxysilane (**84**) as reducing agent for the reduction of benzylic esters to their corresponding alcohols, after the basic work-up with 10 wt% NaOH of the resulted reaction mixture (Scheme 2.7 - a). Although triethoxysilane (**75**) proved to be efficient in this catalytic system, due to the higher amount needed for a quantitative transformation, 5 equivalents instead of 2 equivalents with  $\text{Me}(\text{MeO})_2\text{SiH}$  (**84**), and due to the safety concerns,  $(\text{EtO})_3\text{SiH}$  (**75**) was discarded as a suitable H-donor. Additionally, beside its utility for the deoxygenation of various benzylic esters, this system proved its efficiency for the depolymerisation of commonly used polyesters, for example polylactic acid (PLA, **85**) or polyethylene terephthalate (PET, **86**) (Scheme 2.7 - b). The mechanistic studies showed that the addition of the hydrosilanes was indispensable for the complete transformation of the starting material into the desired product.

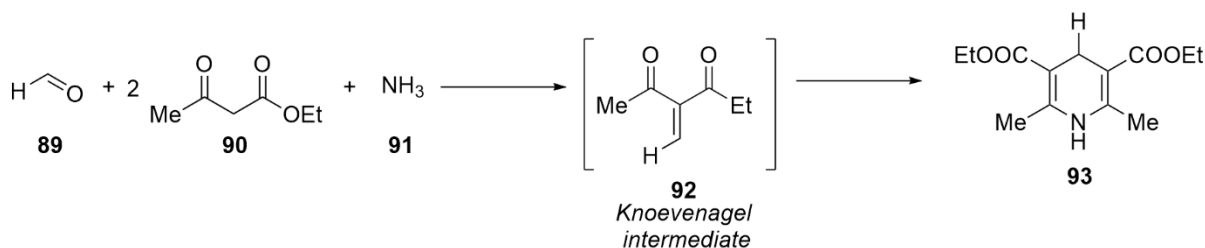


**Scheme 2.7.** Zr-catalysed deoxygenation methodology of esters and polymers developed Cantat's group.<sup>30</sup>



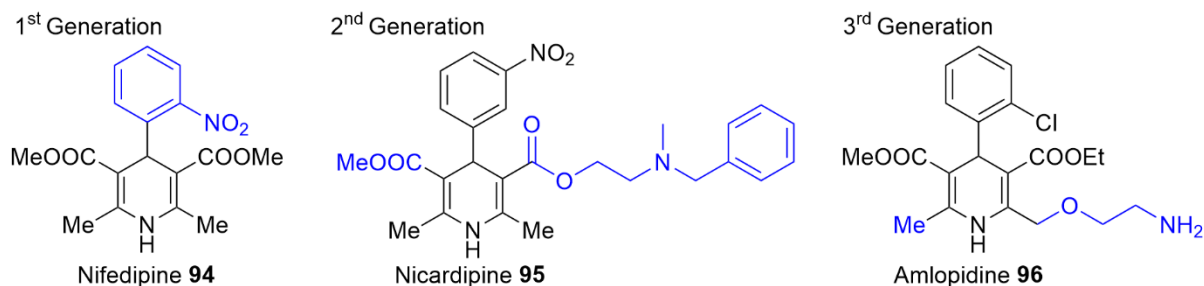
### 2.3. Hantzsch Esters

1,4-Dihydropyridines (1,4-DHP) were first synthesised in 1882 by Arthur Rudolf Hantzsch, therefore compound **93** received the simple name of “Hantzsch ester” (HEH).<sup>31, 32</sup> The synthesis of the Hantzsch ester involves a multi-component one-pot reaction and is based on the condensation of a carbonyl compound with 2 equivalents of a  $\beta$ -ketoester in the presence of ammonia or an ammonium salt (Scheme 2.8).<sup>33</sup> The key mechanistic step of this synthesis is the formation of intermediate **92** *via* a Knoevenagel condensation. Although the Hantzsch ester was utilized as a mild reducing agent for the first time in 1939 by Mumm and Diederichsen,<sup>34</sup> the structure of this compounds was established only in 1955 by Berson and Brown.<sup>35</sup> Later studies showed that structurally Hantzsch ester resembles the part of the reduced nicotinamide adenine dinucleotide (NADH) capable of transferring hydrogen atoms in living organisms.<sup>32</sup> Therefore, studies on the biological activity and medicinal applications of Hantzsch ester and its derivatives were conducted.



**Scheme 2.8.** Original synthesis of Hantzsch esters.<sup>31, 33</sup>

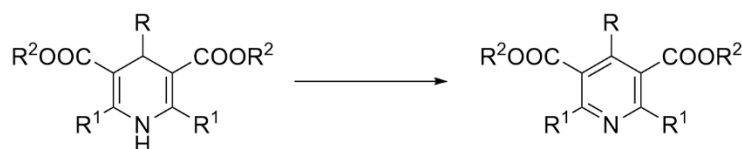
1,4-DHP derivatives proved to be efficient calcium channels blockers (CCB) and are nowadays widely used for the treatment of hypertension, coronary spasm, hypertrophic cardiomyopathy, and other heart conditions.<sup>36, 37</sup> The mechanism of action of these pharmaceutical compounds consists in promoting the vasodilatation of the peripheral arteries, thus leading to a decrease in blood pressure, and the vasodilatation of the coronary artery, hence leading to an increase in blood flow.<sup>36, 38</sup> These effects are a consequence of the interaction between the 1,4-DHP derivatives and the L-type voltage-gated calcium channels in the vascular smooth muscle.<sup>36</sup> During the last 75 years many new biologically active 1,4-DHPs were developed.<sup>39</sup> The first Hantzsch ester, which was approved for pharmaceutical use in Germany, was nifedipine **94** under the commercial name of Adalat in 1975. This product was developed at Bayer AG by Bossert and Vater.<sup>40, 41</sup> The evolution of this calcium antagonist class was possible due to the easy derivatization of the 1,4-DHP backbone. Based on their structure and efficiency, the derivatives can be categorized into three generations (Figure 2.1).<sup>39</sup> The first generation of biologically active 1,4-DHPs are symmetric achiral molecules, which bear different derivatised aromatic moieties at position 4.<sup>41</sup> The second generation of 1,4-DHPs are chiral derivatives, which contain different substituents in positions 3 and 5, for example Nicardipine **95**. Due to the different pharmacological activity of the two enantiomers, strategies for the generation of enantiomerically pure products were developed. The most used procedure is the resolution of the racemic monocarboxylic acids, usually *via* the formation of diastereomeric salts, their separation of the diastereomeric and subsequent selective removal of the esterifying group.<sup>41</sup> The third generation of Hantzsch esters bears a second desymmetrization site in positions 2 and 6 and also exhibits a greater lipophilicity compared to the previous generations. These modifications lead to a distinctive and more stable pharmacokinetic profile.<sup>39, 42</sup> The facile modification possibilities of the structure of 1,4-dihydropyridines unravelled new capabilities not only in the pharmacological field but also for the synthetic applications.



**Figure 2.1.** Examples of Hantzsch esters generations with pharmaceutical applications.<sup>39-42</sup>

Hantzsch esters proved to be efficient reducing agents in both thermal and photochemical reactions. In both cases, the driving force of the H-atom transfer capability of Hantzsch esters is based on the oxidation of the 1,4-DHP moiety into an aromatic pyridine ring (Scheme 2.9).<sup>43</sup> The studies on the hydrogen transfer mechanism of the Hantzsch esters started in 1955 by using deuterated Hantzsch esters derivatives and it was determined that the transfer occurs from C4 (Scheme 2.9 - a). Later, it was discovered that this transfer occurs directly from the Hantzsch ester to the substrate and that the solvent is not involved in the process.<sup>44</sup> In 1999, Zhu *et al.* reported a study on the H-atom transfer mechanisms in thermal and photochemical reactions.<sup>45</sup> This study showed that in both types of transformations the H-atom in position 4 is donated faster compared to the H connected to the nitrogen atom. Under thermal conditions, the deuterium labelling experiments showed that by using 4-*d*<sub>2</sub>-HEH the deuterium atoms were found in the final product (Scheme 2.9 - b). However, the utilization of *N-d*-HEH didn't lead to the formation of the deuterated product. Additionally, the kinetic studies conducted with both 4-*d*<sub>2</sub>-HEH and *N-d*-HEH showed that the C<sub>4</sub>-H cleavage occurs in the rate-determining step of the transformation. The same conclusions were also drawn from the photochemical reactions (Scheme 2.9 - c).

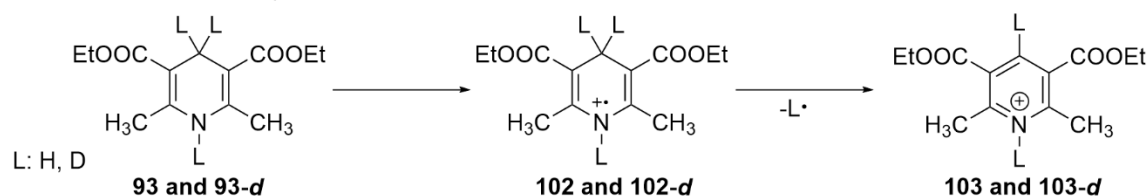
a. Hantzsch esters oxidation



b. Donation mechanism in thermal reactions



c. Donation mechanism in photochemical reactions

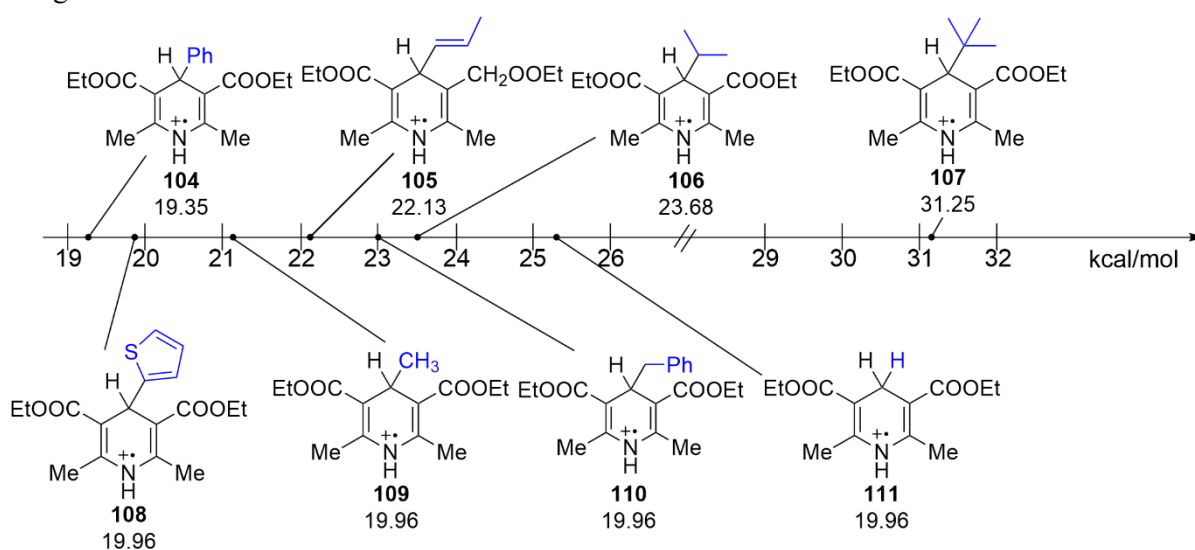


**Scheme 2.9.** Donation mechanisms of the Hantzsch esters.<sup>45</sup>

The main difference between the two types of transformations is the mechanism through which the H-atom is transferred from C4. In the case of thermal reactions, the H-atom is donated through a

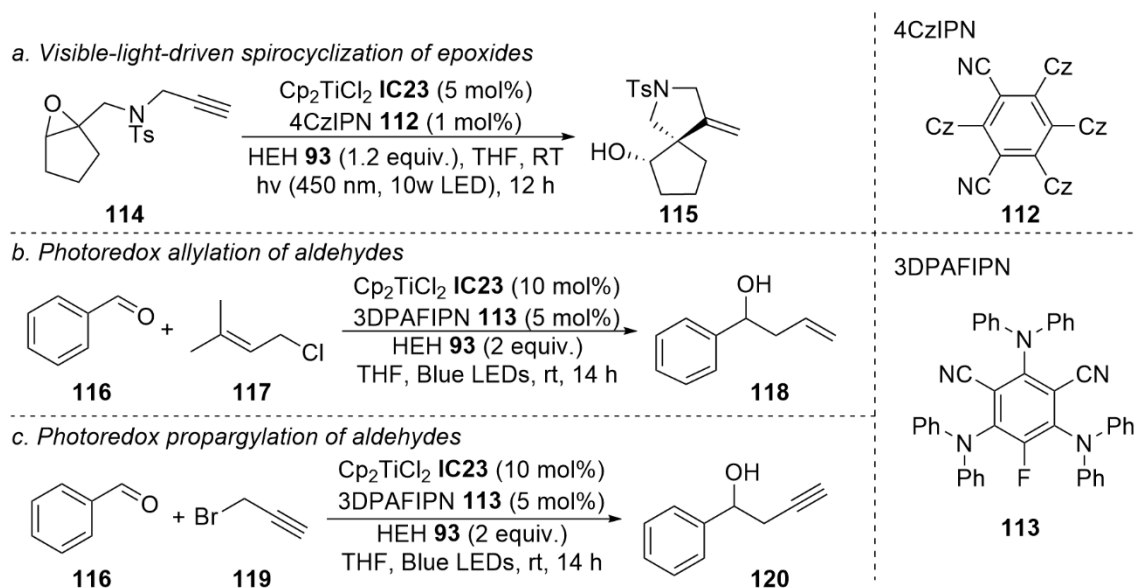
hydride-transfer mechanism while under photochemical conditions the hydrogen atom is transferred *via* a sequential electron-HAT mechanism.

The derivatization of the Hantzsch ester at position 4 can modify its hydrogen transfer capabilities. In 2021, Shen *et al.* reported a quantitative estimation of the hydrogen atom donating properties of various Hantzsch esters radical cations bearing alkyl and aryl moieties at C4.<sup>46</sup> First, this study showed that the donation of the H-radical cannot occur spontaneously as the process is thermodynamically unfavourable. However, no facile correlation between the electronic and steric properties of the substituent and the Gibbs Free Energy Change of the C-H bond cleavage could be attributed. Some examples of the tested Hantzsch ester derivatives and their  $\Delta G_{HD}^0(XRH^+)$  are displayed in figure 2.2.



**Figure 2.2.**  $\Delta G_{HD}^0(XRH^+)$  of various Hantzsch esters radical cations.<sup>46</sup>

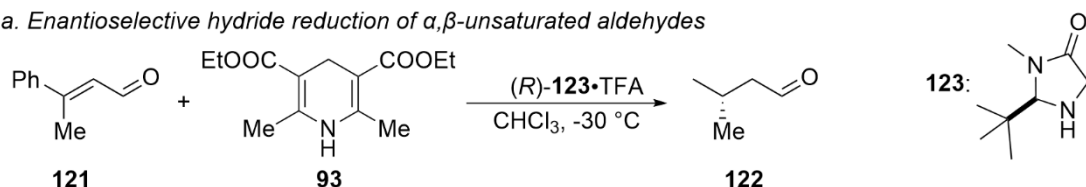
During the last decade, Hantzsch esters were preponderantly used in photochemical transfer hydrogenations. Although there are many examples of HEH-mediated reactions, in the frame of this thesis only some recent examples will be briefly mentioned, namely procedures, in which Ti-species were used as catalyst (Scheme 2.10). In 2020, Lin *et al.* published a visible-light-driven spirocyclization of epoxides methodology, which implied the utilization of a dual  $Cp_2TiCl_2$  (**IC23**)-4CzIPN (**112**) precatalytic system and Hantzsch ester as organic reductant (Scheme 2.10 - a).<sup>47</sup> The mechanistic studies showed that the generation of the catalytically active  $Ti^{3+}$  proceeds through the reaction with the excited  $Ir^{3+}$ -species. The newly generated  $Ir^{4+}$  species is then reduced by the Hantzsch ester to produce the  $HEH^+$  (**102**). Following this reaction, the BDE of C4-H is lowered to 31.4 kcal/mol, thus the  $Ti^{3+}$ -catalysed hydrogen atom transfer from the Hantzsch ester to the substrate can occur. Recently, the group of Cozzi reported two other examples of  $Cp_2TiCl$ -catalysed photoredox transformations, in which  $HEH$  (**93**) was used as H-donor, namely a Barbier-type allylation procedure and a propargylation of aldehydes methodology (Scheme 2.10 - b and c).<sup>48, 49</sup> In both cases 3DPAFIPN (**113**) was used as photocatalyst for the oxidation of the Hantzsch ester and the generation of  $HEH^+$  (**102**). Additionally, similarly to the procedure developed by Lin *et al.*, in both reactions the  $Ti^{3+}$ -catalysed H atom transfer occurs only after the *in situ* generation of the  $HEH$  radical species (**102**) in the photocatalytic cycle. Beside the H-donor capabilities, Hantzsch esters derivatized at position 4 were shown to donate an alkyl or aryl moiety to different substrates under photochemical conditions.<sup>50</sup>

Scheme 2.10. Photocatalytic reactions with Hantzsch ester as reducing agent.<sup>47-49</sup>

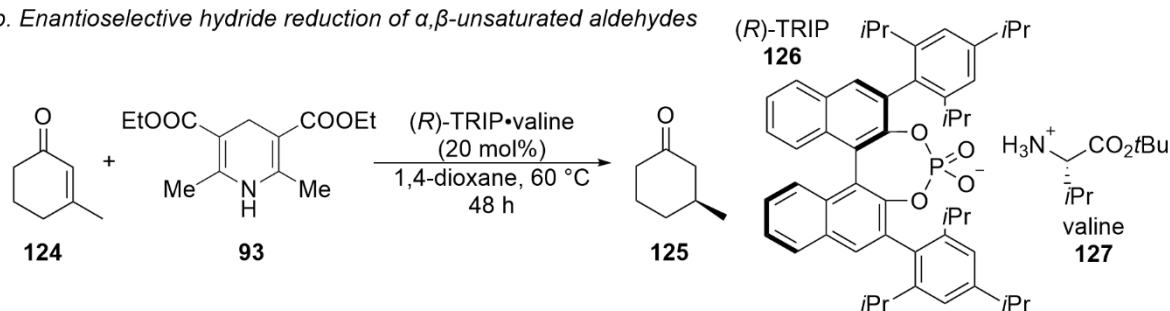
Hantzsch esters were also successfully utilized in multiple organocatalytic procedures and some of the pioneering works on this topic are presented herein (Scheme 2.11). In 2004, the group of MacMillan published an imidazolidinium **123** catalysed procedure for the enantioselective reduction of  $\alpha,\beta$ -unsaturated aldehydes (Scheme 2.11 - a).<sup>51</sup> During the initial screenings, Hantzsch ester **93** proved to be more efficient for the H-atom transfer compared to NADH or *N*-benzylnicotinamide in terms of both yield and enantiomeric excess. Through this protocol both *E*- and *Z*-conformers of olefin **121** were transformed into the corresponding (*S*)-enantiomer **122**, regardless of the purity of the starting material and the steric impediments of the substrate. Complementary to the work of MacMillan, Martin and List published in 2006 a protocol for the enantioselective hydrogenation of  $\alpha,\beta$ -unsaturated ketones (Scheme 2.11 - b).<sup>52</sup> Similarly to the method developed by MacMillan, this procedure uses Hantzsch ester **93** as an organic reducing agent. In this case, the catalytic system was composed of protonated valine ester **127** and a chiral phosphoric acid, namely (*R*)-Trip (**126**) as counterion. It enabled the transformation of enone **124** into the corresponding alkyl ketone **125** in quantitative yields and with very high enantioselectivities. It was presumed that the catalytic efficiency of this system is based on the *in situ* formation of a three-component complex between the chiral phosphoric acid, the valine derivative and the Hantzsch ester, which is stabilized through hydrogen bonding. Recently, Chen *et al.* published an organocatalysed procedure for the deoxygenation of tertiary propargylic alcohols and the formation of the corresponding alkyne (Scheme 2.11 - c).<sup>53</sup> Similarly to the previously described organocatalytic methodologies, Hantzsch ester was employed in this reaction as an/the organic reductant, while (*R*)-TRIP (**126**) proved to be the most efficient organocatalyst for this application. During the optimization process, a balance between high yields and a satisfactory enantiomeric excess was difficult to achieve. It was presumed that this transformation proceeds through a (*R*)-TRIP-HEH-substrate tricomponent transition state and that the basicity of the *in situ* formed pyridine derivative was interfering with the enantiomeric control of the transformation. Thus, an additive screening was conducted in order to discover a suitable Brønsted acid for this application and *p*-fluorophenylboronic acid was found to be the most effective, leading to a 95% yield and a 79% *ee*. In order to further increase the enantioselectivity of the reaction, the ethyl moiety from the ester groups of the Hantzsch ester were

substituted by a benzyl group and indeed the enantiomeric excess was increased to 91%. The control reactions revealed that the *in situ* formed pyridine derivative negatively affects only the first step of the transformation, although the oxidation of the Hantzsch ester occurs only in the second step of the reaction. Thus, a sequential addition strategy was adopted, and this change led to the deoxygenation of the alcohol **128** in quantitative yield and 93% *ee*, without the addition of the boronic acid. Similarly to the presumption of Martin and List, the mechanistic studies indicated the second part of the transformation proceeds through the formation of a cone-shaped three-component complex stabilized via hydrogen bonding.

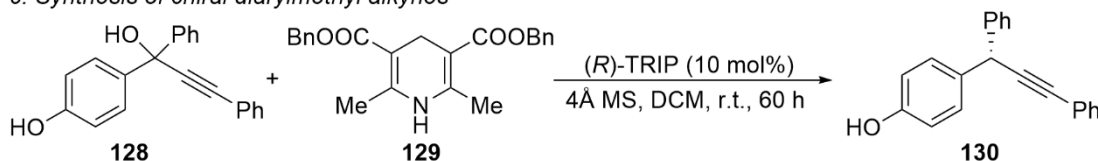
a. Enantioselective hydride reduction of  $\alpha,\beta$ -unsaturated aldehydes



b. Enantioselective hydride reduction of  $\alpha,\beta$ -unsaturated aldehydes

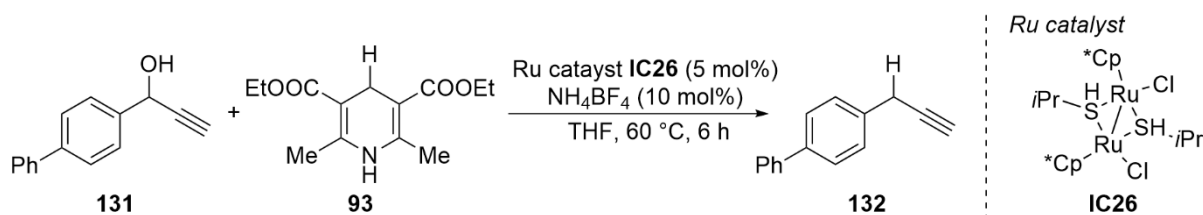


c. Synthesis of chiral diarylmethyl alkynes



Scheme 2.11. Organocatalytic reactions with Hantzsch ester as H-donor.<sup>51-53</sup>

1,4-Dihydropyridines proved to be efficient organic reducing agents in multiple synthetic applications based on thermal metal-catalysed procedures, for example in the hydrogenation of C=C, C=O and C=N bonds, in condensation reactions and in aminations. Recently, a Ru-catalysed procedure for the deoxygenation of propargylic alcohols bearing terminal alkyne moieties was reported by Ding *et al.*<sup>54</sup> Previously, Ding *et al* published a Ru-catalysed deoxygenation protocol, in which triethylsilane was used as H-donor. The deuterium-labelling experiments conducted by using deuterated Hantzsch ester **93-*d*<sub>2</sub>** led to the formation of **132-*d*** in quantitative yield and with 98% deuterium incorporation at the propargylic position. Furthermore, the utilization of a 1:1 mixture between **93** and **93-*d*<sub>2</sub>** led to the formation of a 7:3 mixture of **132** and **132-*d***, hinting towards a possible involvement of the hydrogen transfer in the rate-determining step.



Scheme 2.12. Ru-catalysed deoxygenation of allylic alcohols.<sup>54</sup>

In conclusion, Hantzsch esters were successfully used in a wide variety of transformations involving hydrogen atom transfers. HEH proved to be a very versatile mild organic reducing agent in photocatalytic, organocatalytic and in metal-catalysed procedures. Additionally, Hantzsch ester was capable of substituting other organic reducing agents, like hydrosilanes in deoxygenation reactions. Hence, the utilization of Hantzsch ester was chosen for the Ti-catalysed deoxygenation procedure as a safer and greener alternative to the triethoxysilane.

## 2.4. References

1. J. Eppinger and K.-W. Huang, *ACS Energy Lett.*, 2017, **2**, 188-195.
2. F. Bertini, M. Glatz, N. Gorgas, B. Stöger, M. Peruzzini, L. F. Veiros, K. Kirchner and L. Gonsalvi, *Chem. Sci.*, 2017, **8**, 5024-5029.
3. A. Dubey, L. Nencini, R. R. Fayzullin, C. Nervi and J. R. Khusnutdinova, *ACS Catal.*, 2017, **7**, 3864-3868.
4. A. Glüer and S. Schneider, *J. Organomet. Chem.*, 2018, **861**, 159-173.
5. A. Z. Spentzos, C. L. Barnes and W. H. Bernskoetter, *Inorg. Chem.*, 2016, **55**, 8225-8233.
6. F. Bertini, N. Gorgas, B. Stöger, M. Peruzzini, L. F. Veiros, K. Kirchner and L. Gonsalvi, *ACS Catal.*, 2016, **6**, 2889-2893.
7. M. Achour, D. Álvarez-Hernández, E. Ruiz-López, C. Megías-Sayago, F. Ammari, S. Ivanova and M. Á. Centeno, *Tetrahedron Green Chem.*, 2023, **2**, 100020.
8. X. Liu, S. Li, Y. Liu and Y. Cao, *Chinese J. Catal.*, 2015, **36**, 1461-1475.
9. L. Li, X. Chen, C. Zhang, G. Zhang and Z. Liu, *ACS Omega*, 2022, **7**, 14944-14951.
10. A. Wang, P. He, J. Wu, N. Chen, C. Pan, E. Shi, H. Jia, T. Hu, K. He, Q. Cai and R. Shen, *Energy Fuels*, 2023, **37**, 17075-17093.
11. N. H. Anderson, J. Boncella and A. M. Tondreau, *Chem. - Eur. J.*, 2019, **25**, 10557-10560.
12. A. M. Tondreau and J. M. Boncella, *Organometallics*, 2016, **35**, 2049-2052.
13. E. A. Bielinski, P. O. Lagaditis, Y. Zhang, B. Q. Mercado, C. Würtele, W. H. Bernskoetter, N. Hazari and S. Schneider, *J. Am. Chem. Soc.*, 2014, **136**, 10234-10237.
14. T. Zell, B. Butschke, Y. Ben-David and D. Milstein, *Chem. - Eur. J.*, 2013, **19**, 8068-8072.
15. A. Boddien, B. Loges, F. Gärtner, C. Torborg, K. Fumino, H. Junge, R. Ludwig and M. Beller, *J. Am. Chem. Soc.*, 2010, **132**, 8924-8934.
16. S. Enthaler, *ChemSusChem*, 2008, **1**, 801-804.
17. D. Wei, R. Sang, P. Sponholz, H. Junge and M. Beller, *Nat. Energy*, 2022, **7**, 438-447.
18. M. Oregui-Bengoechea, I. Gandarias, P. L. Arias and T. Barth, *ChemSusChem*, 2017, **10**, 754-766.
19. B. Arkles and G. Larson, *Silicon Compounds: Silanes & Silicones*, 2013.
20. K. Kuciński and G. Hreczycho, *Green Chem.*, 2020, **22**, 5210-5224.
21. C. Chatgililoglu, D. Griller and M. Lesage, *J. Org. Chem.*, 1988, **53**, 3641-3642.
22. C. Chatgililoglu, K. U. Ingold and J. C. Scaiano, *J. Am. Chem. Soc.*, 1982, **104**, 5119-5123.
23. C. Chatgililoglu, C. Ferreri, Y. Landais and V. I. Timokhin, *Chem. Rev.*, 2018, **118**, 6516-6572.
24. S. C. Berk, K. A. Kreutzer and S. L. Buchwald, *J. Am. Chem. Soc.*, 1991, **113**, 5093-5095.
25. K. J. Barr, S. C. Berk and S. L. Buchwald, *J. Org. Chem.*, 1994, **59**, 4323-4326.
26. S. L. Buchwald, *Chem. Eng. News*, 1993, **71**, 2-3.
27. A. S. Wells, *Org. Process Res. Dev.*, 2010, **14**, 484-484.
28. J. Pesti and G. L. Larson, *Org. Process Res. Dev.*, 2016, **20**, 1164-1181.
29. V. Gevorgyan, M. Rubin, S. Benson, J.-X. Liu and Y. Yamamoto, *J. Org. Chem.*, 2000, **65**, 6179-6186.
30. M. Kobylarski, L. J. Donnelly, J.-C. Berthet and T. Cantat, *Green Chem.*, 2022, **24**, 6810-6815.
31. A. Hantzsch, *Ber. Dtsch. Chem. Ges.*, 1881, **14**, 1637-1638.
32. U. Eisner and J. Kuthan, *Chem. Rev.*, 1972, **72**, 1-42.
33. M. Rueping, J. Dufour and F. R. Schoepke, *Green Chem.*, 2011, **13**, 1084-1105.
34. O. Mumm and J. Diederichsen, *Liebigs Ann. Chem.*, 1939, **538**, 195-236.
35. J. A. Berson and E. Brown, *J. Am. Chem. Soc.*, 1955, **77**, 447-450.
36. R. G. McKeever and R. J. Hamilton, in *StatPearls*, 2023.
37. F. Picard, N. Sayah, V. Spagnoli, J. Adjedj and O. Varenne, *Arch. Cardiovasc. Dis.*, 2019, **112**, 44-55.
38. B. Williams, G. Mancina, W. Spiering, E. Agabiti Rosei, M. Azizi, M. Burnier, D. L. Clement, A. Coca, G. de Simone, A. Dominiczak, T. Kahan, F. Mahfoud, J. Redon, L. Ruilope, A. Zanchetti, M. Kerins, S. E. Kjeldsen, R. Kreutz, S. Laurent, G. Y. H. Lip, R. McManus, K. Narkiewicz, F. Ruschitzka, R. E. Schmieder, E. Shlyakhto, C. Tsioufis, V. Aboyans, I. Desormais and E. S. C. S. D. Group, *Eur. Heart J.*, 2018, **39**, 3021-3104.
39. V. K. Sharma and S. K. Singh, *RSC Adv.*, 2017, **7**, 2682-2732.

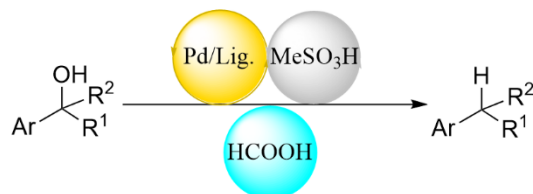
40. F. Bossert and W. Vater, *Naturwissenschaften*, 1971, **58**, 578-578.
41. S. Goldmann and J. Stoltefuss, *Angew. Chem. Int. Ed.*, 1991, **30**, 1559-1578.
42. A. L. Wang, C. Iadecola and G. Wang, *J. Geriatr. Cardiol.*, 2017, **14**, 67-72.
43. S. G. Ouellet, A. M. Walji and D. W. C. Macmillan, *Acc. Chem. Res.*, 2007, **40**, 1327-1339.
44. R. Abeles and F. H. Westheimer, *J. Am. Chem. Soc.*, 1958, **80**, 5459-5460.
45. X.-Q. Zhu, Y.-C. Liu and J.-P. Cheng, *J. Org. Chem.*, 1999, **64**, 8980-8981.
46. G.-B. Shen, L. Xie, Y.-X. Wang, T.-Y. Gong, B.-Y. Wang, Y.-H. Hu, Y.-H. Fu and M. Yan, *ACS Omega*, 2021, **6**, 23621-23629.
47. S. Lin, Y. Chen, F. Li, C. Shi and L. Shi, *Chem. Sci.*, 2020, **11**, 839-844.
48. A. Gualandi, F. Calogero, M. Mazzarini, S. Guazzi, A. Fermi, G. Bergamini and P. G. Cozzi, *ACS Catal.*, 2020, **10**, 3857-3863.
49. F. Calogero, A. Gualandi, M. D. Matteo, S. Potenti, A. Fermi, G. Bergamini and P. G. Cozzi, *J. Org. Chem.*, 2021, **86**, 7002-7009.
50. F. Gu, W. Huang, X. Liu, W. Chen and X. Cheng, *Adv Synth Catal.*, 2018, **360**, 925-931.
51. S. G. Ouellet, J. B. Tuttle and D. W. C. MacMillan, *J. Am. Chem. Soc.*, 2005, **127**, 32-33.
52. N. J. A. Martin and B. List, *J. Am. Chem. Soc.*, 2006, **128**, 13368-13369.
53. M. Chen and J. Sun, *Angew. Chem. Int. Ed.*, 2017, **56**, 11966-11970.
54. H. Ding, K. Sakata, S. Kuriyama and Y. Nishibayashi, *Organometallics*, 2020, **39**, 2130-2134.



### 3. Aims of this Work

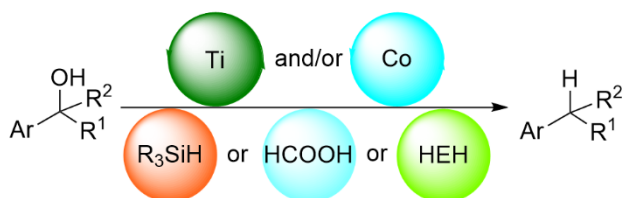
As it was presented in the introduction chapters, deoxygenation reaction of alcohols has applications in various fields, the most important being in the transformation of biomass in industrial-valuable compounds. Most of the methods used in large-scale applications are heterogenous and based on precious metals. Only recently homogenous procedures were developed and unfortunately their limitations make them still unattractive for industrial applications. The work which will be presented in this thesis focuses on the optimization and development of atom-economical homogeneous deoxygenation procedures catalysed by both precious and non-precious metals.

In the first part of this work the optimization of the Pd-catalysed transfer hydrogenolysis procedure previously developed by B. Cizsek in the Group of Prof. I. Fleischer was conducted (Scheme 3.1).<sup>1</sup> Starting from the already obtained knowledge, the aim of this work was to get a better understanding of the mechanism of this transformation. First, the influence of various physical parameters over the system was investigated in order to make the reaction more efficient. Additionally, a ligand and solvent screening was conducted so that the selectivity of the transformation increased.



**Scheme 3.1.** Pd-catalysed deoxygenation procedure developed by Cizsek and Fleischer.<sup>1</sup>

The second and most consistent part of this thesis is represented by the development of a new 3d-metal catalysed deoxygenation procedure. Due to their oxophilic character, attempts with both Ti- and Co-based catalysts were conducted. Only recently non-precious metal catalysed deoxygenation methods were reported in the literature. The major challenge of these procedures is the need of a catalyst regenerating agent. Therefore, one of the major focus points of this pursuit was the screening of various reducing agents which can fulfil a dual role, both in the hydrogen donation step and in the regeneration of the catalyst in order to increase the atom-economical character of the process. In addition to this, a high functional group tolerance would make this procedure suitable for lignin degradation. Furthermore, mechanistical studies could bring more insight on the reaction pathway which could facilitate the upscaling of this methodology.



**Scheme 3.2.** Newly developed Ti- and Co-catalysed deoxygenation procedures.

## 4. Optimization of Pd-Catalysed Transfer Hydrogenolysis

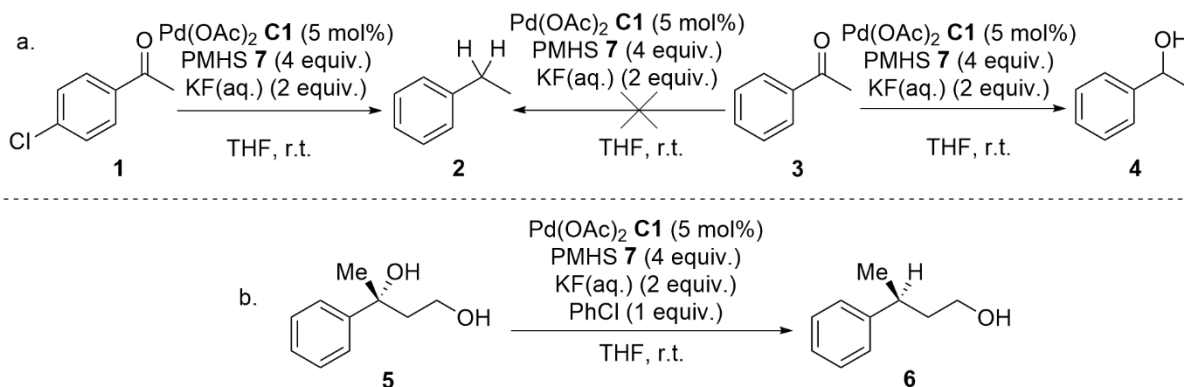
### 4.1. Overview on Pd-Catalysed Deoxygenation of Alcohols

Complementary to the deoxygenation methods previously described, Pd-catalysed deoxygenation procedures are a well-established tool in organic chemistry due to the wide variety of O-containing functional groups, which can be reduced to the corresponding alkanes. Therefore, Pd-based procedures are widely used in the valorisation of biomass (Chapter 1.2). A large part of the reported methodologies for the deoxygenation of alcohols use heterogeneous catalysts for this transformation, in particular Pd/C, and hydrogen gas as H-donor.<sup>2</sup> The main advantage of Pd/C-catalysed reductions of benzylic alcohols, compared to other charcoal deposited noble metals catalysts, like Rh/C, Ru/C or Pt/C, is the selectivity of the transformation, which arises from its tolerance towards aromatic rings.<sup>3</sup> Still, this classical heterogenous approach has some drawbacks, like cost efficiency. Although being cheap, atom-efficient, and readily available, H<sub>2</sub> leads to poor selectivity and is difficult to handle due to its flammability. Additionally, special equipment is required due to high pressures and high temperatures necessary for these transformations.<sup>4</sup> The reduction of alcohols comes with further complications, compared to the reduction of other O-containing functional groups, as in most cases, the hydroxyl group has to be converted into a better leaving group first, due to the high BDE of the alcoholic C-O bond and unfavourable thermodynamics.<sup>5</sup> In consequence, new heterogenous and homogenous procedures were developed, in which different Pd-based catalysts were used and alternative H-donors were investigated.

In 2011, Rahaim and Maleczka reported a Pd-polymethylhydrosiloxane (PMHS, **7**) catalysed deoxygenation procedure of benzylic ketones and alcohols in presence of fluoride ions (Scheme 4.1).<sup>6</sup> This system was already studied in the 80s and 90s, when it was reported that the polymeric structure of PHMS enhanced the catalytic activity of Pd and the selectivity of various reductions.<sup>7, 8</sup> Chauhan *et al.* explained this phenomenon as a consequence of the formation and dispersion of Pd-nanoclusters in the structure of siloxane.<sup>9</sup> The studies concluded that the siloxane acts both as H-donor and stabilizing and regeneration agent for the metallic nanoclusters.<sup>9, 10</sup> The better stability of the Pd-nanoclusters towards oxygen and humidity induced by PHMS enables to conduct the reactions under air and to enhance recyclability of the system.<sup>9</sup>

During their previous studies on the hydrodehalogenation of chloroarenes, Rahaim and Maleczka observed that, besides the desired reaction, the benzylic carbonyl group of **1** was completely reduced to **2**.<sup>11</sup> Further investigation showed, that without the *p*-Cl substituent, the reduction of **3** yielded only benzylic alcohol **4** (Scheme 4.1 - a). The addition of chlorobenzene, chloroanisole or trimethylsilyl chloride to the catalytic system enabled the deoxygenation of non-halogenated benzyl ketones and alcohols. It is worth mentioning that this reaction is regio- and stereospecific as only the benzylic C-OH was reduced, and the product retained the initial configuration of the molecule with 81% *ee* (Scheme 4.1 - b). Additionally, benzyl protected alcohols were reduced to the corresponding alkanes in presence of chlorobenzene.

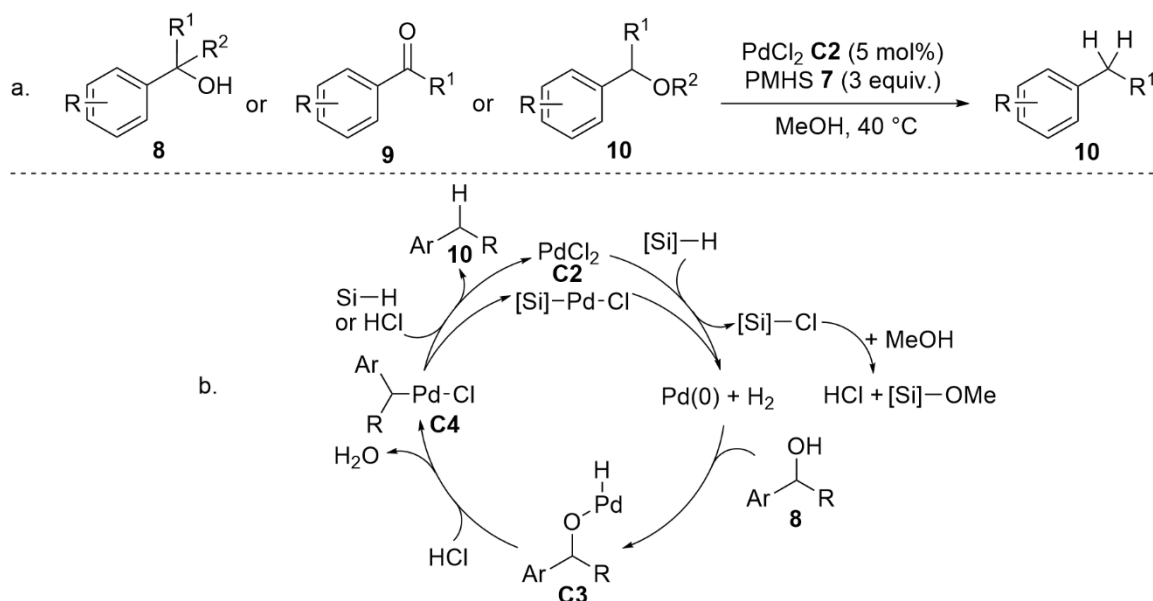
Preliminary mechanistic studies suggested that the transformation is dependent of the rate at which HCl is generated during the reaction. It was proposed that the acid is formed following the disproportionation of the *in situ* produced Ar-Pd-Cl complex in presence of PMHS (**7**) and water. This hypothesis might explain the suppression of the catalytic system when neutralizing additives are added and the low tolerance towards substrates bearing basic nitrogen atoms.



**Scheme 4.1.** Pd-PMHS-catalysed deoxygenation of benzyl alcohols with aqueous KF solution; (a) in the absence of Cl anions; (b) with Cl-containing additive.<sup>6</sup>

Following the studies conducted in the group of Maleczka, Wang *et al.* developed a fluoride-free Pd-PMHS-catalysed deoxygenation procedure of benzylic alcohols, ketones and ethers (Scheme 4.2 - a).<sup>12</sup> They achieved this by using an excess of PMHS in MeOH and by exchanging the Pd-source from Pd(OAc)<sub>2</sub> to PdCl<sub>2</sub>. This system was successfully applied to both primary and secondary benzylic alcohols and, similarly to the report of Maleczka, this catalytic system was able to also deoxygenate benzylic ketones and ethers. Both electron-donating and electron-withdrawing groups were tolerated by the catalytic system, but partial reduction of nitro- and halide functionalities was observed.

Based on the observations made during the screenings and mechanistic investigations, a catalytic cycle was proposed (Scheme 4.2 - b). After the PMHS-facilitated reduction of PdCl<sub>2</sub> (**C2**) to Pd(0), an oxidative addition of the alcohol occurred. During this step, HCl is generated from the reaction of the *in situ* formed Si-Cl species with the solvent. The acid is further involved in the key step of the catalytic cycle, namely the formation of a Bn-Pd-Cl complex. This hypothesis was supported by the outcome of the deuteration-labelling experiments. The final step of the catalytic cycle is the reductive elimination to the deoxygenated product, of which the reduction pathway and generated Pd-based species are yet to be discovered.

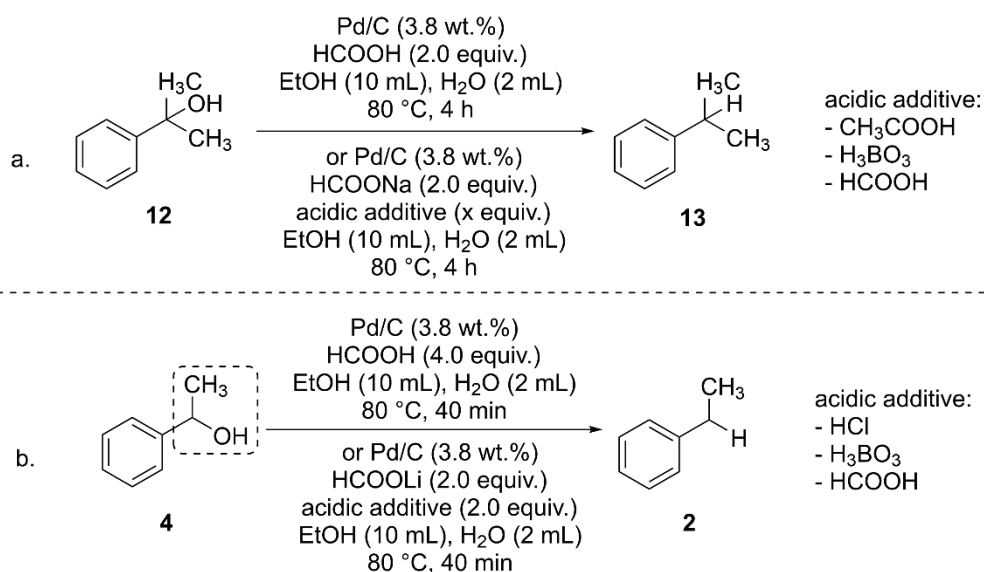


**Scheme 4.2.** Pd-PMHS-catalysed deoxygenation of benzyl alcohols in methanol (a) model reactions with alcohols, ketones or esters; (b) proposed mechanism.<sup>12</sup>

These reports show the extraordinary reductive capabilities of the Pd-PMHS system in alcohol deoxygenation reactions. Both studies disclosed the determining role of the *in situ* generated HCl in such catalytic systems. Unfortunately, some drawbacks such as the lack of chemoselectivity, and multiple reductions of other functional groups could not be resolved in these systems. Consequently, various methodologies were developed by using different hydrogen donors.

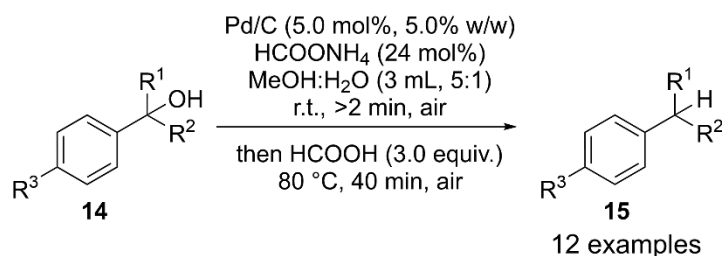
The utilization of formic acid (**11**) as a hydrogen source comes with some advantages as it was stated in chapter 2.1, the most important one being the convenient side-products, their recyclability and the facile work-up.<sup>13, 14</sup> Liu and co-workers reported a Pd/C-catalysed transfer hydrogenolysis of 2-phenyl-2-propanol (**12**) using HCOOH (**11**) as H-donor (Scheme 4.3 - a).<sup>15</sup> During their studies, the H-donor capabilities of multiple formate salts were tested but all of them proved to be less efficient for this transformation than formic acid. Adding an acidic additive to formate salts or using stoichiometric mixtures between salts and formic acid evidenced an improvement of the transfer hydrogenolysis, but the yields did not exceed 44% of the desired product. These results are contrary to the ones obtained in the transfer hydrogenolysis of aryl chlorides<sup>16, 17</sup> and benzyl esters.<sup>18</sup> Based on mechanistic studies, it was concluded that the low pH value of the reaction medium, when formic acid is employed as hydrogen donor, enhances the deoxygenation capabilities of the catalytic system. This phenomenon might indicate that the transformation depends on the dissociation of HCOOH (**11**) into H<sup>+</sup> and HCOO<sup>-</sup>.

Similar conclusions concerning H-donors were stated by Feng *et al.* when they applied the same Pd/C-HCOOH catalytic system on the deoxygenation of secondary benzylic alcohols (Scheme 4.3b).<sup>19</sup> Again, the usage of formic acid instead of formate salts proved to be beneficial for the transformation in terms of both reactivity and selectivity as it hindered the formation of acetophenone (**3**), which was observed when using formate salts. Interestingly, when no H-donor was added to the reaction mixture, low amounts of ethylbenzene (**2**) were obtained. Similarly, to the report of Liu *et al.*,<sup>15</sup> the addition of HCOOH as acidic additive to formate salts led to the formation of higher amounts of ethylbenzene (**2**). Additionally, a higher excess of formic acid relatively to the amount of substrate enhanced the conversion and yield. Another important parameter, which was examined during these studies was the role of the water content in the reaction. The results showed that adding up to 2 mL of water to the reaction mixture facilitated the transformation of  $\alpha$ -methylbenzyl alcohol (**4**) into ethylbenzene (**2**). A further increase of the water content led to a decrease in selectivity and the formation of acetophenone (**3**). Moreover, the ionic dissociation of formic acid is crucial for the deoxygenation of secondary benzylic alcohols. In both reports, it was hypothesised, that the dissociative chemisorption of HCOO<sup>-</sup> ions on the Pd-surface take place while the hydroxyl group is transformed into -OH<sub>2</sub><sup>+</sup>. Consequently, the C-O bond cleaves while Pd-H and CO<sub>2</sub> is generated on the catalyst surface. When no H-donor is present, the alcohol itself acts as the H-donor.



**Scheme 4.3.** Pd-HCOOH-catalysed deoxygenation of benzylic alcohols; (a) Procedure by Liu *et al.*;<sup>15</sup> (b) Procedure reported by Feng *et al.*<sup>19</sup>

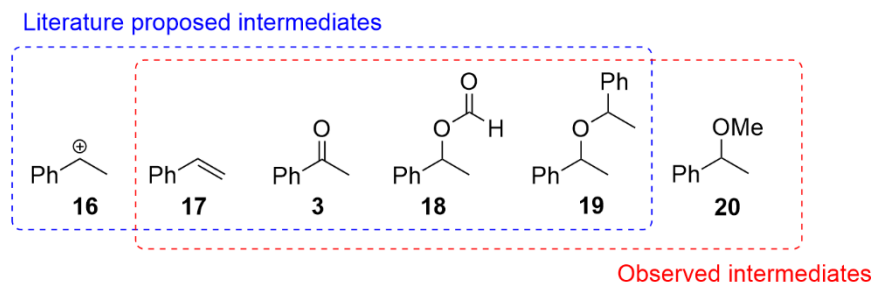
In 2013, the group of Samec introduced another Pd/C-HCOOH catalytic system for the deoxygenation of benzylic alcohols (Scheme 4.4).<sup>20</sup> Later, this procedure was applied in the valorisation of lignin, as discussed in chapter 1.2 (Schemes 1.14 and 1.15).<sup>21, 22</sup> When using 1-phenylethanol (**4**) as substrate, the formation of acetophenone (**3**) was observed in a 1:1 mixture with ethylbenzene (**2**). By substituting formic acid with various formate salts, the desired reaction was completely suppressed. However, when catalytic amounts of base were added as activation agent for the Pd catalyst, for instance ammonium formate or triethylamine, the Pd/C-HCOOH system demonstrated its capabilities towards the deoxygenation of 1-phenylethanol (**4**), and ethylbenzene (**2**) was obtained in quantitative yield. Similarly, to the previously described procedures, the presence of small amounts of water proved to be beneficial for the desired reaction. It was assumed that water increased the formate salt solubility and, hence, inhibited the formation of acetophenone (**3**) through a disproportionation reaction. The disproportionation pathway would imply the initial oxidation of the alcohol to a carbonyl compound and the generation of molecular hydrogen. The substrate screening revealed that beside secondary benzylic alcohols, primary and tertiary benzylic alcohols were suitable for the deoxygenation. Thus, a pathway involving the formation of a carbenium ion, or a dehydrogenation reaction were dismissed. In-depth mechanistic studies were endeavoured to determine the mechanism.



**Scheme 4.4.** General reaction of Pd-HCOOH-catalysed deoxygenation of benzylic alcohols *via* the procedure developed by the group of Samec.<sup>20</sup>

During the optimization and substrate screening, potential intermediates were detected. (Figure 4.1, red box). Some of these compounds were already described in the literature as possible

intermediates in deoxygenation reactions, which used similar catalytic systems (Figure 4.1, blue rectangle).<sup>18, 19, 23, 24</sup> In order to determine, which of these could act as intermediates in this reaction, their initial conversion rates in this system were compared with the initial consumption rate of 1-Phenylethanol (**4**). Both styrene (**17**) and acetophenone (**3**) gave higher rates at  $t=0$  s while the others showed lower initial rates relative to the alcohol.

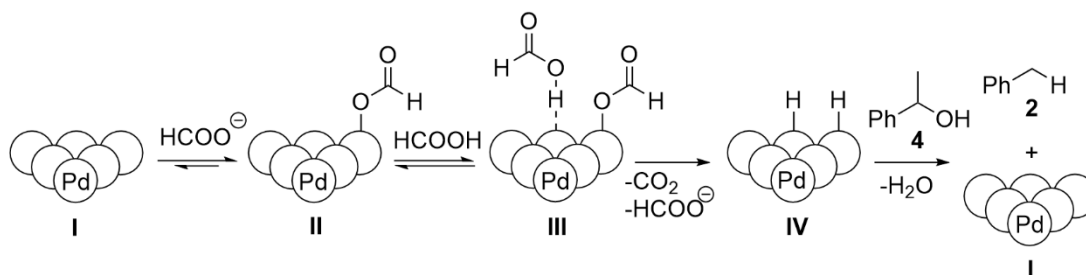


**Figure 4.1.** Literature proposed intermediates for deoxygenation of benzylic alcohols (blue rectangle) and possible intermediates observed during the studies (red rectangle).<sup>20</sup>

Subsequently, reaction order studies were conducted. No dependency between the concentration and initial rate was observed when the amount of alcohol or base varied. The independence of the reaction order in correlation to the concentration of alcohol shows that the cleavage of the C-O bond is not the rate-limiting step of the reaction, while lower or higher concentrations of base favours the formation of side-product through other pathways. Both the H-donor and the catalyst gave first-order dependencies ensuing that the hydrogen transfer between the formic acid and the Pd catalyst is involved in the rate-determining step. This step was further investigated *via* the deuterium kinetic isotope effect of the hydrogen transfer. The substitution of the “hydride” H-atom with deuterium resulted in a notable decrease in reaction rate, while employing HCOOD (**11-*hd***) led to the opposite effect on the reaction rate, with  $k_H/k_D$  of  $0.62 \pm 0.11$ . These results strengthened the conclusion that the hydride transfer between the formic acid (**11**) and Pd is the rate-determining step of the reaction.

Based on the mechanistic investigations and observations made during the screening, multiple reaction pathways were discarded. A disproportion of tertiary alcohol could not take place. Additionally, such a pathway could not occur as no dependence of the reaction rate on the alcohol concentration was observed. Ester and ether were not observed under optimized conditions and their initial reactions rates are much lower comparing to the alcohol. Therefore, it is unlikely that these compounds are intermediates in this transformation. Consequently, elimination pathway and carbocation formation is improbable as primary substrates were transformed in good yields to the desired product.

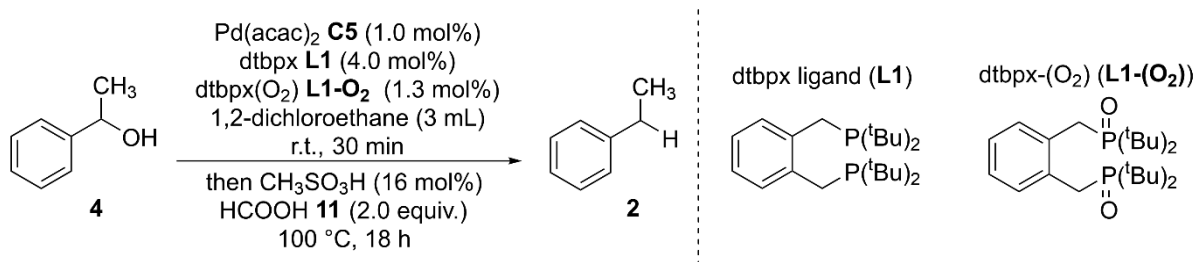
After the extensive mechanistic experiments, the Samec group proposed a mechanism, which starts with the formation of the formate anion and its adsorption on the catalyst generating a formate-palladium species **II** (Scheme 4.5). The latter is further protonated with a formic acid molecule to form complex **III**. Subsequently, a hydrogen chemisorption takes place with the generation of **IV**, which is catalytically active towards the deoxygenation of benzylic alcohols.



**Scheme 4.5.** The mechanism for heterogeneous deoxygenation of benzylic alcohols proposed by the group of Samec.<sup>20</sup>

In 2018, the Fleischer group reported the first homogeneous Pd-catalysed transfer hydrogenolysis of benzylic alcohols.<sup>1, 25</sup> This procedure uses a Pd- $\alpha,\alpha'$ -bis(di-*tert*-butylphosphino)-ortho-xylene (dtbpx, **L1**) complex, formic acid (**11**) as hydrogen donor and methanesulfonic acid (**21**) as co-catalyst and it was conducted in dichloroethane (DCE) at 100 °C for 18 h (Scheme 4.6). The inspiration for this system was a catalytic methodology based on Pd salts, bidentate phosphine ligand and acid co-catalyst which was previously established in the same group for the thiocarbonylation of vinyl arenes.<sup>26</sup>

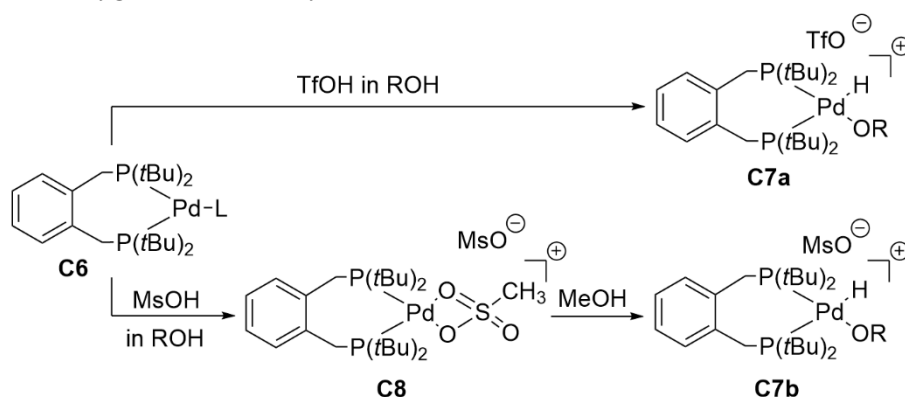
They found that with  $\alpha,\alpha'$ -bis(di-*tert*-butylphosphino)-ortho-xylene (dtbpx, **L1**) (Scheme 4.6) as ligand, both Pd<sup>0</sup> and Pd<sup>2+</sup> precatalysts led to satisfying yields of the desired product, with Pd(acac)<sub>2</sub> (**C5**) being the most efficient one. In contrast, Pd/C yielded only traces of ethylbenzene (**2**) and a significant amount of styrene (**17**).



**Scheme 4.6.** General reaction for homogeneous Pd-catalysed deoxygenation of benzylic alcohols with HCOOH as H-donor.<sup>1, 25</sup>

Subsequently, the group conducted a ligand screening. Multiple mono- and bidentate ligands were submitted to the reaction but only dtbpx (**L1**) proved to be capable of facilitating desired catalytic activity while all the other tested ligands led to the formation of high amounts of styrene (**17**). Dtbpx (**L1**) was first synthesised by Moulton in 1976, while the first Pd-dtbpx complex was reported by Crascall *et al.* in 1992.<sup>27</sup> Afterwards, Clegg and Eastham used this complex in the industrial process of obtaining methyl propanoate *via* methoxycarbonylation of ethane which is part of the Lucite alpha process.<sup>28, 29</sup> During the development of this industrial process, it was proven that the catalytic capabilities of the system can be influenced by the properties of the ligand like high electron density and steric factors induced by the *t*Bu groups.<sup>30</sup> The pathway through which this catalyst is capable of donating a H-atom heavily depends on the acidic co-catalyst chosen for the particular system and solvent (Scheme 4.7). The direct formation of the palladium hydride **C7a** can be achieved in presence of alcohols susceptible to  $\beta$ -hydride oxidation and in presence of weak coordinating anions provided by the catalyst. An exception was found, when utilizing methanesulfonic acid, where a cationic Pd complex

**C8** is generated before the Pd-H **C7b** can be obtained *in situ*.<sup>31</sup> This kind of reactivity proved to be optimal for the deoxygenation of benzylic alcohols.



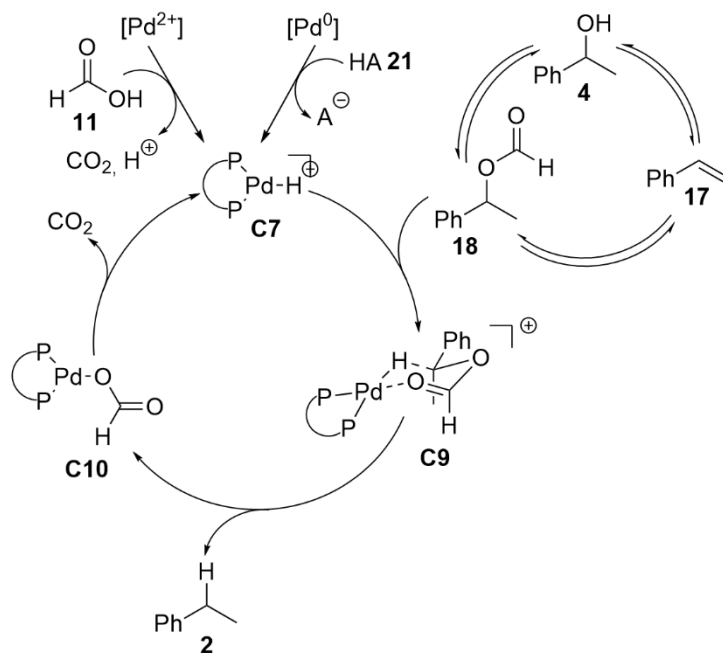
**Scheme 4.7.** Pathways for generation of palladium hydride species with and without methanesulfonic acid.

Another important aspect of the catalytic activity of the Pd-dtbpx complex in this transformation is the presence of the oxidized form of the ligand. Ciszek showed that a 3:1 ratio between dtbpx (**L1**) and dtbpx(O<sub>2</sub>) (**L1-O<sub>2</sub>**) is optimal for suppressing the formation of side-products during the reaction. Although the reason behind this positive effect was not fully elucidated, as dtbpx(O<sub>2</sub>) (**L1-O<sub>2</sub>**) alone proved to be catalytically inactive for this reaction, it was hypothesised that the oxidized form could prevent the conglomeration or decomposition of the Pd-based catalyst (Scheme 4.6).<sup>1</sup>

Regarding mechanistic experiments, kinetic studies showed that there was no induction period in formation of the desired product hinting towards a homogenous catalysis. This hypothesis was further supported by qualitative poisoning experiments, as both mercury and dibenzo[*a,e*]cyclooctatetraene (DCT) completely quenched the reaction. To further exclude Pd nanoparticles as active catalyst, they were employed in the reaction and yielded only traces of the desired product. Interestingly, after the addition of dtbpx and methanesulfonic acid in the reaction mixture, ethylbenzene (**2**) was obtained in 66% yield leading to the conclusion that palladium nanoparticles can serve as reservoir for the generation of the catalytically active homogenous species. Thus, a so-called *cocktail catalysis* was suspected.<sup>25</sup>

Based on these results, a mechanism for the deoxygenation of benzylic alcohols was proposed (Scheme 4.8).<sup>1</sup> First, the generation of the cationic Pd-H complex **C7a** is facilitated either by the formic acid or the acidic co-catalyst. Simultaneously, the alcohol is transformed into the corresponding formate **18**, which further coordinates through the carbonyl group to Pd, leading to the formation of six-membered distorted chair-like complex **C9**. The hydrogen transfer from Pd leads to the generation of the desired product **2** and complex **C10**. After CO<sub>2</sub> release, the catalytically active species **C7a** is regenerated.

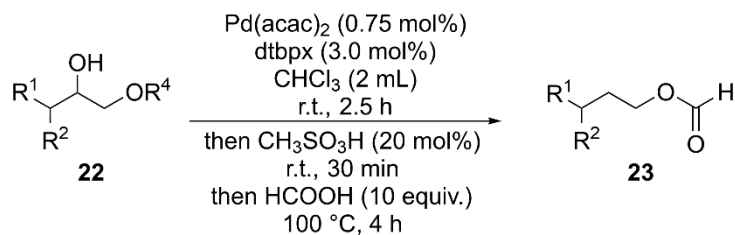




**Scheme 4.8.** Proposed mechanism for the homogenous Pd-catalysed deoxygenation of benzylic alcohols with HCOOH as H-donor.<sup>1</sup>

Although this system proved to be very capable in the transfer hydrogenolysis of benzylic alcohols, it still possesses some drawbacks, the main one being the limitation in ligand alternatives and the necessity of controlling the ratio between the ligand and its oxidated form. Finding another ligand capable of generating an active catalyst could enhance the selectivity of the reaction. Additionally, relatively high Pd loading, and the utilization of halogenated solvent make this procedure less attractive.

Following the obtained results in the Pd-catalysed deoxygenation of benzylic alcohols, Schmidt *et al.* applied a modified version of this catalytic system for the reductive rearrangement of glycol derivatives and the production of terminal formic esters (Scheme 4.9).<sup>32</sup> As it was described in chapter 1.2, these substrates are used as lignin model substrates due to their structural resemblance with the constituent motifs of this feedstock. The optimisation studies revealed that, beside the nature of the Pd source, ligand and co-catalyst, the exact stoichiometry plays an important role in this transformation. Furthermore, the addition order has a major impact on the outcome of the reaction. Analogous to the deoxygenation of benzylic alcohols, dtbpx (**L1**) proved to be the only ligand capable of generating a catalytically active complex for this purpose. The catalytic system showed a very high tolerance towards various substituents attached to the ethereal oxygen atoms. Moreover, a number of modifications of the aromatic backbone and its substitution with aliphatic chains did not suppress the reactivity. Subsequently, the mechanistic studies showed that this transformation proceeds through a [1,2]-hydrogen shift.



**Scheme 4.9.** General reaction for the reductive rearrangement of glycol derivatives.

#### 4.2. General Motivation

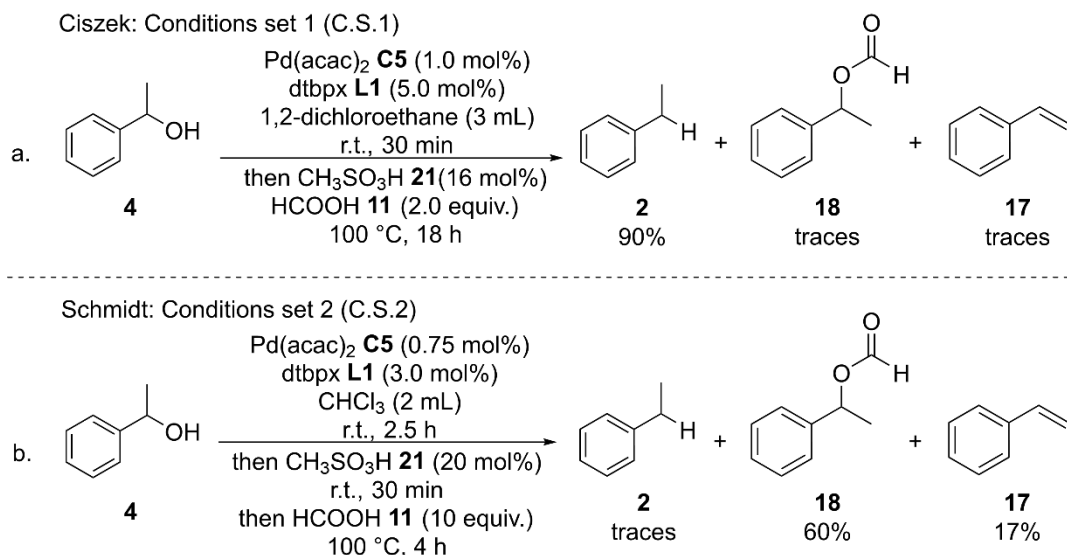
Based on the results of B. Ciszek and I. Fleischer regarding the deoxygenation of benzylic alcohols, the main goal of this project was the further optimization of the reaction conditions.<sup>1</sup> This project should lead to an increase of product yield on a broader substrate scope, better understanding of the reaction mechanism, more economically and environmentally efficient reaction conditions and increased chemo-, stereo- and regioselectivity. These goals could be achieved by reducing the Pd-catalyst loading, by uncovering more ligands capable of forming active species with the precatalyst and by substituting the halogenated solvent with “greener” alternatives. Enhancing these properties would yield a more attractive transformation for both laboratory and industrial application. Additionally, the fields in which this system could be used would extend to the synthesis and functionalization of biologically active compounds and the valorisation of lignin.

A procedure that would be suitable for the aims of this optimization project, in view of low Pd-catalyst and ligand loading, are the reaction conditions developed by Schmidt *et al.*, which were applied in the reductive rearrangement of glycol derivatives.<sup>32</sup> Furthermore, the optimal stoichiometry for this reaction will be investigated.

Additionally, a ligand screening will be conducted, which could widen the catalytic capabilities of the system. In order to obtain the desired selectivity properties, multiple phosphine-based ligands will be investigated, as a follow-up on Ciszek’s ligand screening. Moreover, avoiding the necessity to employ both dtbpx (**L1**) and dtbpx(O<sub>2</sub>) (**L1-O<sub>2</sub>**) is desired. Subsequently, the influence of the *in situ* generated water and the water from external sources (e.g., solvent moisture) will be studied.

#### 4.3. Optimization and Screening

Initially, the reaction was reproduced applying the exact conditions described by Ciszek *et al.* (Scheme 4.10 - a). The only deviation from the standard procedure was the exclusive utilization of 5 mol% dtbpx (**L1**). The result was mostly in accordance with the published data, as the desired product was obtained in 90% yield instead of quantitative yield.<sup>1</sup> The small difference in yield might arise from the elimination of the oxidized form of dtbpx (**L1**) from the catalytic system. Beside the desired product, small amounts of formate **18**, styrene (**17**) and higher-mass products were detected *via* GC-MS (Figure 4.2 - pg. 43). The formation of these high molecular mass compounds was observed throughout the optimization and ligand screening, but they were never isolated as they were considered to be only side-products and not possible intermediates. Product **24** was presumably generated through an acid-catalysed dehydrative coupling reaction while formation pathway of compound **25** is still unknown (Figure 4.2).<sup>33</sup> Subsequently, the exact conditions developed for the reductive rearrangement of glycol derivatives were applied, with the goal of deoxygenating secondary benzylic alcohols (Scheme 4.10 - b). This procedure did not lead to satisfying results as only traces of ethylbenzene (**2**) were obtained, whereas formate **18** and styrene (**17**) were produced in significant amounts. In conclusion, a thorough adaptation of C.S.2 conditions to the needs of the deoxygenation reaction had to be performed.



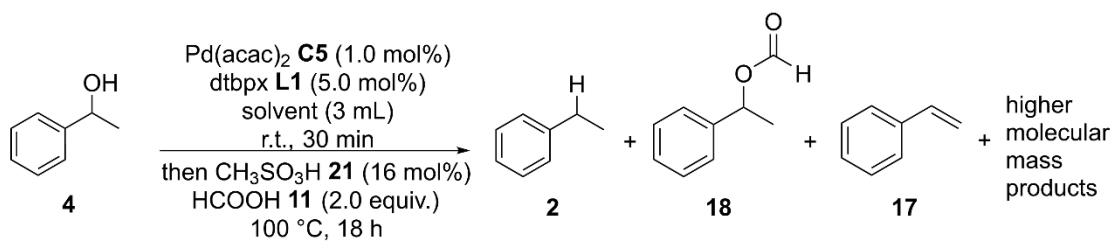
**Scheme 4.10.** Preliminary reactions for deoxygenation of benzyl alcohols (a) Procedure developed by Ciszek *et al.* (C.S.1);<sup>1</sup> (b) Procedure developed by Schmidt *et al.* (C.S.2).<sup>32</sup>

#### 4.3.1. Solvent Screening

Using the C.S.1 conditions, a solvent screening was carried out, in order to gain more insight into its role in the catalytic reaction. All solvents were dried and degassed prior use. Firstly, other halogenated solvents than DCE were tested (Table 4.1 - Entry 1). Conducting the reaction in chloroform led to a slight decrease in the yield of the desired product **2** to 87% showing that this solvent is suitable for the transformation and that a decrease in polarity and boiling point does not significantly affect the reaction (Table 4.1 - Entry 2). In both of these reactions (Table 4.1 - Entries 1 and 2), only traces of styrene (**17**) and formate **18** have been detected in the crude reaction mixture. When dichloromethane was chosen as a solvent for the reaction, a noticeable decrease in yield was observed to 52% (Table 4.1 Entry 3). A possible reason could be its volatility, due to which the reaction was only carried out at 80 °C.

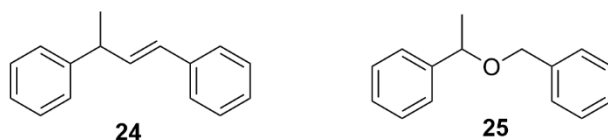
Further decreasing the polarity by using toluene as solvent led to diminished yield of ethylbenzene (**2**) (15%) (Table 4.1 - Entry 4). In this case, products with high molecular mass were detected *via* GC-FID (Figure 4.2). This outcome could be explained by the poor coordinating properties of toluene or by the poor solubility of the components. The importance of solvent coordination and solubility was further emphasised by carrying out the reactions in THF and ethyl acetate, which led to the formation of 61% and 77% yield of **2**, respectively, although the reaction in THF was conducted at 80 °C (Table 4.1 – Entries 5 and 6).

Interestingly, the reactions in MeOH and EtOH completely suppressed the desired transformation (Table 4.1 – Entries 7 and 8). This result was surprising as alcoholic media should enhance the formation of Pd-H, which is presumably the catalytically active species.<sup>31</sup> A possible explanation for this phenomenon might be a competitive esterification reaction between the alcohols and the HCOOH in the acidic media. Unfortunately, due to their volatility, neither methyl- nor ethyl formate **18** was detected *via* GC-FID.

**Table 4.1.** Solvent screening for the deoxygenation of 1-Phenylethanol (**4**).


Entry <sup>[a]</sup>	Solvent	Yield of <b>2</b> (%) <sup>[b]</sup>	Yield of <b>18</b> (%) <sup>[b]</sup>	Yield of <b>17</b> (%) <sup>[c]</sup>
1	DCE (standard reaction)	93	traces	-
2	CHCl <sub>3</sub>	87	traces	traces
3 <sup>[c]</sup>	CH <sub>2</sub> Cl <sub>2</sub>	52	8	28
4	Toluene	15	17	-
5 <sup>[c]</sup>	THF	61	traces	14
6	EtOAc	77	traces	traces
7 <sup>[c]</sup>	MeOH	-	64	traces
8	EtOH	-	64	traces

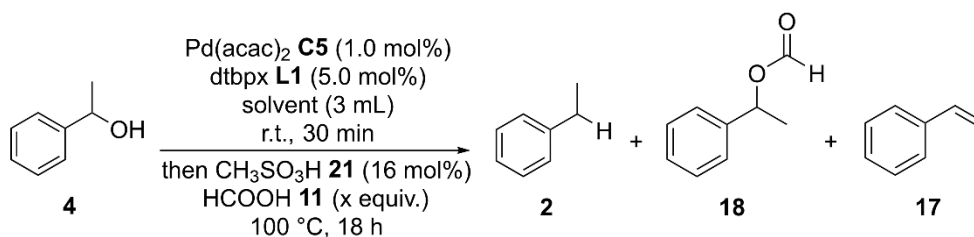
[a] Standard reaction conditions: 1-phenylethanol (0.120 mL, 1.00 mmol, 1.00 equiv.), Pd(acac)<sub>2</sub> (3.05 mg, 0.01 mmol, 1.00 mol%) and dtbpx (21.0 mg, 0.05 mmol, 5.00 mol%) in solvent (3 mL), stirred for 30 min. at r.t., then MeSO<sub>3</sub>H (0.01 mL, 0.16 mmol, 0.16 equiv.) and HCOOH (0.08 mL, 3.00 mmol, 3.00 equiv.) stirred for 18 h at 100 °C in a Schlenk pressure tube. [b] Yields were determined *via* quantitative GC-FID using *n*-pentadecane as internal standard. [c] Reaction conducted at 80 °C.

**Figure 4.2.** Examples of higher molecular mass products detected *via* GC-MS.

In order to observe if the solvent plays a role in the disproportionation of formic acid and therefore enhances the reactivity, chloroform, 1,2-dichloroethane and ethyl acetate were selected for reactions, in which the amount of HCOOH (**11**) was varied compared to the standard conditions (Table 4.2). Analysing the obtained results, a trend was observed. When using the C.S.1 procedure for the reaction, the addition of 5 equivalents of formic acid had an unfavourable effect on the formation of ethylbenzene (**2**) (Table 4.2 – Entries 1, 4 and 7). Doubling the amount of formic acid (**11**) to 10 equivalents led to an almost complete quenching of the desired reaction (Table 4.2 – Entries 2, 5 and 8). However, in all cases higher amounts of formate **18** and styrene (**17**) were obtained compared to the standard C.S.1 reaction. These outcomes were unexpected, as more formic acid should facilitate both the formation of Pd-H and the functionalization of the alcohol.<sup>1</sup> Intrigued by these results, the procedure was modified, and the addition of formic acid was delayed by 20 minutes. Remarkably, this had a positive impact towards the generation of ethylbenzene (**2**) even by using 10 equivalents of formic acid (**11**), however, the yields were still lower comparing to the results obtained with standard C.S.1 conditions (Table 4.2 - Entries 3, 6 and 9).

Following the results of the solvent screening, it was concluded that, both chlorinated and coordinating solvents are suitable for this transformation. These results hint that, under optimized conditions, the solvent could substitute dtbpx(O<sub>2</sub>) (**L1-O<sub>2</sub>**) in the stabilizing role of the catalytically active species. A plausible explanation for the poor yields obtained whilst varying the amount of formic acid (**11**) was the possible interference of the formic acid with the generation of the six-member-ring intermediate **C9**, thus leading to the deactivation of the palladium catalyst (Chapter 4.1 - Scheme 4.6). This hypothesis would explain the higher yields of formate **18** and styrene (**17**).

**Table 4.2.** Variable formic acid loading experiments in different solvents.



Entry <sup>[a]</sup>	Solvent	Formic acid (equiv.)	Yield of <b>2</b> (%) <sup>[b]</sup>	Yield of <b>18</b> (%) <sup>[b]</sup>	Yield of <b>17</b> (%) <sup>[b]</sup>
1	CHCl <sub>3</sub>	5	49	27	17
2	CHCl <sub>3</sub>	10	14	51	32
3 <sup>[c]</sup>	CHCl <sub>3</sub>	10	51	25	11
4	DCE	5	60	25	9
5	DCE	10	17	58	28
6 <sup>[c]</sup>	DCE	10	62	17	traces
7	EtOAc	5	9	36	-
8	EtOAc	10	-	43	traces
9 <sup>[c]</sup>	EtOAc	10	37	29	-

[a] Standard reaction conditions: 1-phenylethanol (0.120 mL, 1.00 mmol, 1.00 equiv.), Pd(acac)<sub>2</sub> (3.05 mg, 0.01 mmol, 1.00 mol%) and dtbpx (21.0 mg, 0.05 mmol, 5.00 mol%) in solvent (3 mL), stirred for 30 min. at r.t., then MeSO<sub>3</sub>H (0.01 mL, 0.16 mmol, 0.16 equiv.) and HCOOH (x equiv.) stirred for 18 h at 100 °C in a Schlenk pressure tube. [b] Yields were determined *via* quantitative GC-FID using *n*-pentadecane as internal standard. [c] Reactions with 20 min added before the addition of formic acid.

#### 4.3.2. Further Optimization Experiments

Based on the insights gained during the solvent screening, the optimization of the C.S.2 procedure for the deoxygenation reaction started with the optimization of addition- and reaction time. The prolongation of the reaction time from 4 h to 18 h increased the yield of ethylbenzene (**2**) to 34%. A furtherance in reaction time to 48 h did not lead to a perceptible improvement, resulting in only 36% yield of the desired compound. Therefore, the 18 h reaction time was further used for the optimization reactions.

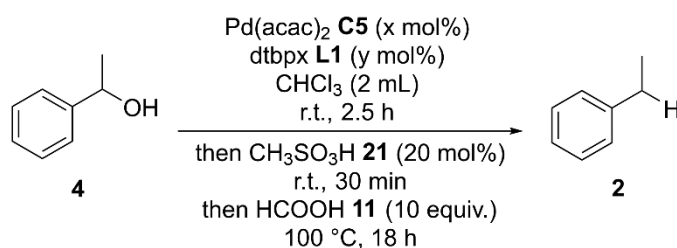
The simultaneous addition of reaction components completely deactivated the catalytic process, as only formate **18** was formed in high amount and traces of styrene (**17**) were observed *via* GC-FID.

A further 30 minutes extension of the addition time between the reaction components did not lead to higher yields of the desired product. Thus, the addition order and time were maintained during the optimization process, according to the C.S.2 methodology.

Another parameter of interest during the optimization process was the catalyst loading and the ratio between the metal catalyst and the ligand loading. The ratio between Pd/ligand/acid can have a major impact on the reaction's outcome.<sup>32</sup> Due to the exclusion of dtbpx(O<sub>2</sub>) (**L1-O<sub>2</sub>**) the standard loading ratio for the process was considered 1:5 Pd:dtbpx. During this screening, the yields of formate **18** and styrene (**17**) were not measured (Table 4.3).

Increasing the Pd-loading from 0.75 mol% to 1 mol% and utilizing it in a 1:5 Pd/ligand ratio, led to a raise of ethylbenzene (**2**) yield to 62% (Table 4.3 – Entries 1 and 5). Subsequently, when the 1:4 ratio was used, in relation to 1 mol% of metal precatalyst, 47% yield of ethylbenzene (**2**) was obtained (Table 4.3 – Entry 2). Decreasing the amount of **L1** further led to an observable drop in the yield of ethylbenzene (**2**) to 15% (Table 4.3 – Entry 3). In order to get a better insight about the importance of the amount of ligand present in the reaction, 1 mol% of Pd was submitted with 8 mol% of ligand. This reaction yielded 65% of ethylbenzene (**2**), leading to the conclusion that, from the cost-efficiency perspective, the optimal Pd/ligand ratio is 1:5 (Table 4.3 – Entry 4). These results showed that the main factor in the formation of the desired product is the amount of precatalyst. Although it is unclear, if the ligand plays a role in both formation of the active species and preventing the formation and precipitation of nanoparticles from solution, it was shown that, in order to have a satisfying transformation, a minimum four time greater ligand loading, compared to precatalyst loading, is necessary. In contrast, a substantial uplift in the amount of ligand causes the transformation to become cost inefficient.

**Table 4.3.** Catalyst-ligand ratio investigations.



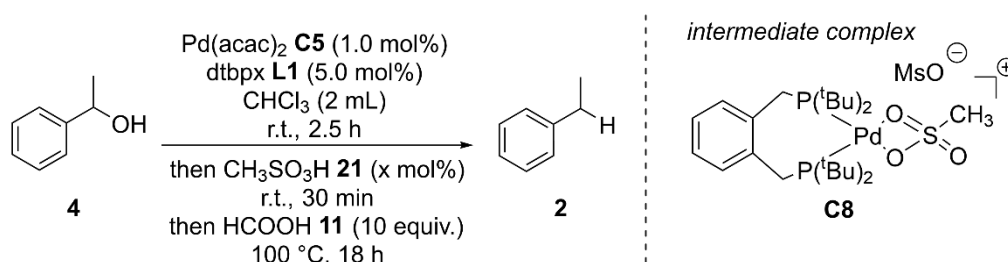
Entry <sup>[a]</sup>	Catalyst loading (mol%)	Ligand loading (mol%)	Yield of <b>2</b> (%) <sup>[b]</sup>
1 <sup>[c]</sup>	1	5	62
2	1	4	47
3	1	3	15
4	1	8	65
5 <sup>[d]</sup>	0.75	3	34

[a] Standard reaction conditions: 1-phenylethanol (0.120 mL, 1.00 mmol, 1.00 equiv.), Pd(acac)<sub>2</sub> (2.28 mg, 0.075 mmol, 0.75 mol%) and dtbpx (11.8 mg, 0.03 mmol, 3.00 mol%) in chloroform (2 mL), stirred for 2.5 h at r.t., then MeSO<sub>3</sub>H (0.013 mL, 0.20 mmol, 0.20 equiv.) stirred for 30 min. at r.t., then HCOOH (0.19 mL, 10.0 mmol, 10.0 equiv.) stirred for 18 h at 100 °C in a Schlenk pressure tube. [b] Yields were determined *via* quantitative GC-FID using *n*-pentadecane as internal standard. [c] Standard conditions for C.S.1 [d] Standard conditions for C.S.2

Following the conclusions, regarding the importance of the Pd/ligand ratio, the investigation for the optimal co-catalyst loading was pursued. Based on previously performed acidic co-catalyst screenings in the group of Fleischer, methanesulfonic acid (**21**) was chosen as being the most suitable option.<sup>1,32</sup> During this screening, 1 mol% of Pd precatalyst and 5 mol% of dtbpx (**L1**) were used. When no Brønsted acid was present in the reaction, no ethylbenzene (**2**) was detected in the crude reaction mixture (Table 4.4 - Entry 1). 10 mol% of MeSO<sub>3</sub>H (**21**) already led to the formation of the desired product in 21% yield (Table 4.4 – Entry 2). A further raise in co-catalyst loading to 16 mol% increased the yield of ethylbenzene (**2**) to 51% (Table 4.4 – Entry 3). Using MeSO<sub>3</sub>H (**21**) in 20 mol%, which is considered the upper limit for a catalyst loading, led to an even higher yield of 65% (Table 4.4 – Entry 4). Therefore, this amount of co-catalyst was further used during the ligand screening.

Based on these results and on the studies of Ciszek, it was concluded that the coordination of the mesylate is beneficial for the generation of the active species, through the formation of intermediate complex **C8**. Additionally, the co-catalyst may be responsible for hindering the formation of the proposed inactive heterogenous species. Beside the positive interaction with the metal-based catalyst, methanesulfonic acid might play a role in the formation of the formate **18**.

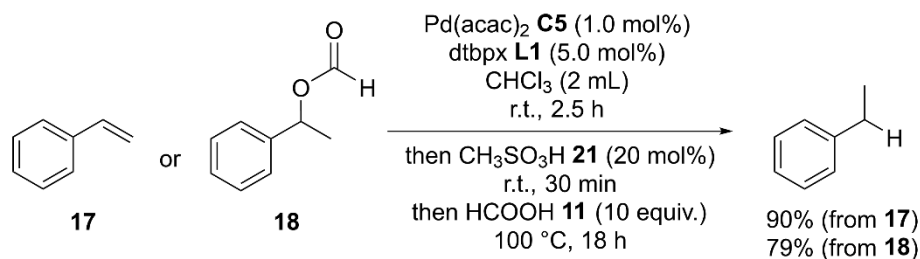
**Table 4.4.** Methanesulfonic acid amount variation.



Entry <sup>[a]</sup>	MeSO <sub>3</sub> H loading (mol%)	Yield (%) <sup>[c]</sup>
1 <sup>[b]</sup>	No additive	-
2	10	21
3	16	51
4	20	65

[a] Standard reaction conditions: 1-phenylethanol (0.120 mL, 1.00 mmol, 1.00 equiv.), Pd(acac)<sub>2</sub> (3.05 mg, 0.01 mmol, 1.00 mol%) and dtbpx (21.0 mg, 0.05 mmol, 5.00 mol%) in chloroform (2 mL), stirred for 2.5 h at r.t., then MeSO<sub>3</sub>H (0.013 mL, 0.20 mmol, 0.20 equiv.) stirred for 30 min. at r.t., then HCOOH (0.19 mL, 10.0 mmol, 10.0 equiv.) stirred for 18 h at 100 °C in a Schlenk pressure tube. [b] Yields were determined *via* quantitative GC-FID using *n*-pentadecane as internal standard.

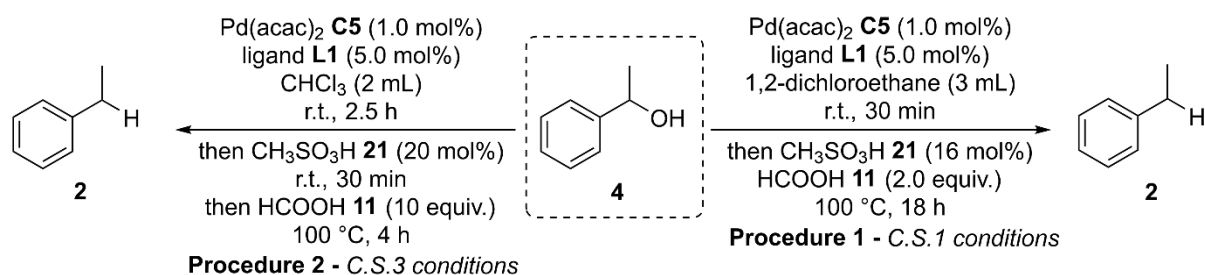
Before pursuing the ligand screening, both possible intermediates, formate **18** and styrene (**17**), were examined in the reaction conditions established during this study (Scheme 4.11). Compound **18**, which is the more plausible intermediate in the deoxygenation reaction, led to the generation of ethylbenzene (**2**) in 79% yield and styrene afforded ethylbenzene (**2**) in 90% yield. These results hint that these reaction conditions are more capable regarding hydrogenation reactions than for deoxygenations. Due to the numerous studies of Pd-catalysed hydrogenations, further investigations into the hydrogenation were not pursued.



**Scheme 4.11.** Reactivity investigations of possible intermediates.

### 4.3.3. Ligand Screening

Consequently, a ligand screening was conducted using both C.S.1 procedure and the new reaction conditions C.S.3, developed during this study (Scheme 4.12). As it was previously mentioned, finding a new ligand capable of generating an active catalytic species with the Pd-precatalyst is of great interest, as it would enable the reactivity to a broader scope of substrates, would improve the chemoselectivity, could generate stereoselectivity and would bring more information about the reaction pathway. This screening is a continuation of the ligand studies already reported by Ciszek in his thesis and beside **L1**, only **L5** and **L13** were tested again (Figure 4.3 and Figure 4.4, respectively).



**Scheme 4.12.** Ligand screening procedures; (right) Procedure 1 - C.S.1 conditions; (left) Procedure 2 - C.S.3 conditions.

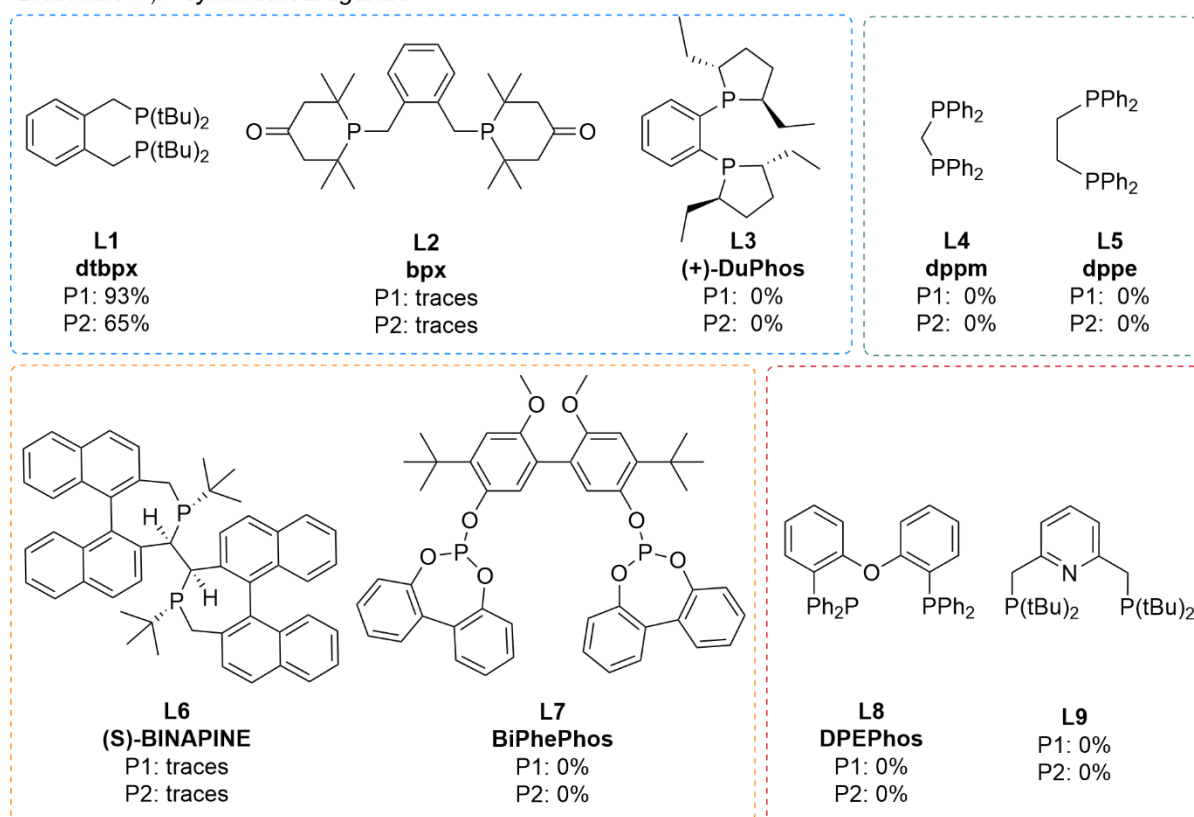
First, the capabilities of bidentate symmetrical P,P-ligands to generate active catalyst for the deoxygenation were investigated. Ligands bearing the same backbone as **L1** were suggested as possible alternatives for dtbpx (**L1**) (Figure 4.3 - blue rectangle). Based on the available literature reports the most promising ligand that could substitute dtbpx (**L1**) in this transformation, was **L2**. In 2017, Nobbs *et al.* published a bpx-Pd catalysed procedure for the isomerizing methoxycarbonylation of alkanes.<sup>34</sup> This system showed improved catalytic activity and turnover number comparing to dtbpx-Pd complex, which is the benchmark catalyst for this transformation. It was hypothesised, that the reason behind the effectiveness of the bpx-Pd catalyst was structural resemblance of the ligand with dtbpx (**L1**) and the similar bite angle, of approximately 100°, which was observed for both **L1** and **L2** in Pd-complexes. However, the electronic properties between the two ligands differ, as the s-donating character is lower, and the  $\pi$ -accepting character is higher for the P-atom in bpx (**L2**) compared to dtbpx (**L1**). This phenomenon is a consequence of the smaller C-P-C angle in **L2** than in **L1**. Additionally, based on the rhodium studies, it was concluded, that bpx (**L2**) can enhance the electrophilic character of the metal centre compared to dtbpx (**L1**). Subsequently, the studies showed that the basic character of bpx (**L2**) is weaker than for the standard ligand **L1**.

Therefore, the synthesis of bpx (**L2**) was carried out. Although the generation of **L2** was proven *via*  $^{31}\text{P}$ -NMR spectroscopy of the crude mixture, the purification procedure was partially unsuccessful



as solvent and phorone were still present in considerable amounts in the final mixture. The unpurified ligand was submitted in both catalytical reactions, but the desired product was observed only in traces in the crude reaction mixtures of both procedures. Although these results were unsatisfying, due to the impurities and solvent traces, which were still present in the ligand, the catalytic activity of **L2** could not fully investigated. Therefore, bpx (**L2**) should not be excluded as a possible replacement for dtbpx (**L1**) for this deoxygenation procedure. Next, the electron rich (+)-DuPhos (**L3**), was tested in the deoxygenation reaction but no product was observed in either procedure. However, large amounts of high molar mass products were detected *via* GC-MS. Next, the catalytic activity of ligands bearing aliphatic backbones was investigated (Figure 4.3 - green rectangle). These reactions showed a very poor conversion of the benzylic alcohols; therefore, no ethylbenzene (**2**) was generated. A possible explanation for this phenomenon is the small bite angle of both **L4** and **L5** ligands at 72° and 78°, respectively.<sup>35, 36</sup> Unfortunately, exchanging the aliphatic backbone with rigid motifs did not afford the desired product in significant amounts (Figure 4.3 - orange rectangle). **L6**, containing chiral P-atoms, led to the formation of ethylbenzene (**2**) in traces, when applying both procedures, but the yields were too low to examine the stereoselectivity of the reaction. The electron-deficient ligand **L7**, bearing bulky P-atom substituents showed no satisfactory catalytical activity as almost no conversion of the starting material was detected. Based on this result it was concluded that an electron-rich ligand is needed for a successful transformation of 1-phenylethanol (**4**) to ethylbenzene (**2**).

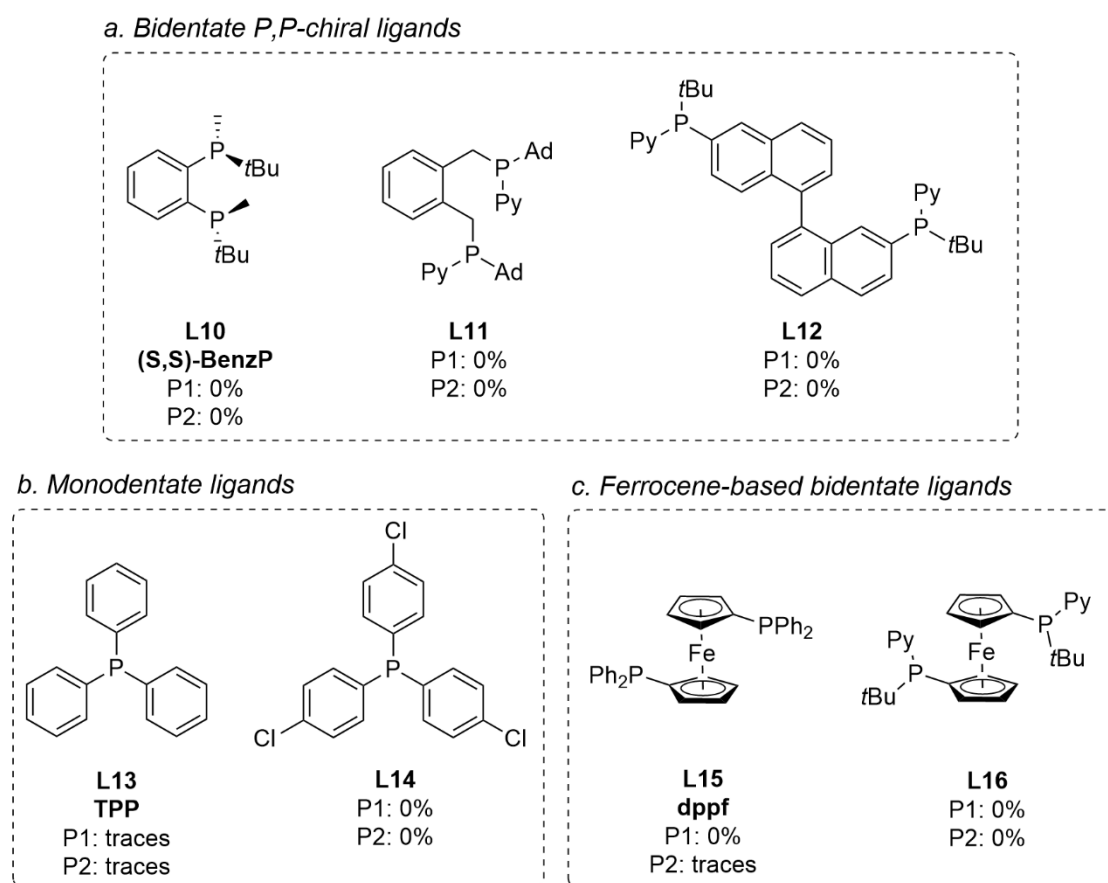
#### Bidentate P,P-symmetrical ligands



**Figure 4.3.** P-symmetrical ligands. blue rectangle - ligands with similar structure as dtbpx; green rectangle - ligands with aliphatic backbones; orange rectangle - ligands with rigid backbones; red rectangle - tridentate ligands.

Subsequently, the catalytic activity of tridentate POP- and PNP-type ligands, **L8** and **L9**, was examined (Figure 4.3 - red rectangle). Following these reactions, no traces of the ethylbenzene (**2**) were detected *via* GC-MS however, while large amounts of compound **23** were produced. The failure of the desired transformation could be a consequence coordination sites saturation or of the rigidity of the formed Pd complex.

Ligands bearing chiral P-atoms were investigated as possible alternatives for dtbpx (**L1**) (Figure 4.4 - a). Analogously to **L3**, no formation of ethylbenzene (**2**) was observed when **L10** was employed. Following this result, it was concluded, that the bridging methylene group between the backbone and the P-atoms is essential for the transformation, due to the increased structural flexibility induced by its presence. **L11** and **L12** bearing pyridine and adamantyl or tertbutyl substituents at the P-atom inhibited the generation of the desired product, possibly due to the basic moieties which can neutralize the acidic reaction medium.<sup>37</sup> However, this moiety favoured the formation of significant amounts of compound **18**. Triphenylphosphine (**L13**) led to the formation of ethylbenzene (**2**) in traces in both procedures. The introduction of three *para*-Cl substituents in the ligand structure completely suppressed the reactivity of the catalytic system (Figure 4.4 - b). The two ferrocene-based ligands, **L15** and **L16**, tested in the reaction did not afford ethylbenzene (**2**) in significant amounts, as traces were only detected when **L15** was submitted in procedure 2 (Figure 4.4 - c).



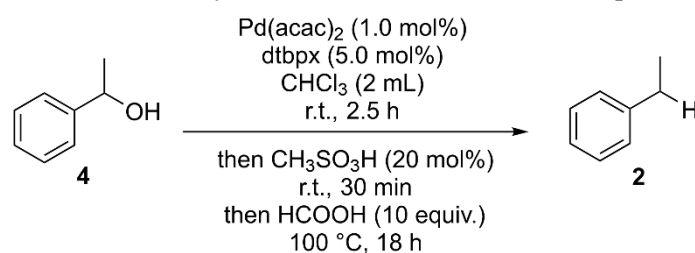
**Figure 4.4.** (a) bidentate P,P-chiral ligands; (b) monodentate ligands; (c) ferrocene-based ligands.

#### 4.3.4. Influence of Water-content over Reactivity

During the optimization reactions, it was observed that the use of non-distilled, or non-degassed solvents led to a complete inhibition of the desired transformation (Table 4.5 – Entries 1 and 2). These results hint towards a homogenous active catalytical species, as heterogenous Pd-HCOOH procedures reported in the literature were operated under air and, in those methodologies, the addition of small amounts of water enhanced the deoxygenation reaction. Beside the pre-existing water content in the solvent, the decomposition of formic acid leads to the *in situ* generation of water. This process might inhibit the formation of ethylbenzene (**2**) through the deactivation of the homogenous, catalytic active species. Therefore, multiple experiments were performed, in which 3 Å molecular sieves were added to the reaction mixture, by using the conditions from C.S.3 procedure. Additionally, an investigation of the water influence on the ligand capabilities of generating catalytically active species was conducted.

The reaction performed by using the C.S.3 system in CHCl<sub>3</sub> with molecular sieves, showed a slight increase in yield, from 62% to 69% (Table 4.5 – Entry 3). Unfortunately, by using the same conditions and exchanging **L1** with **L11**, **L12** and **L16**, no traces of ethylbenzene (**2**) were detected in the crude reaction mixtures (Table 4.5 – Entries 4 to 6). However, in comparison to the reaction conducted during the ligand screening, only small amounts of formate **18** were detected *via* GC-FID and GC-MS. Instead, higher amounts of styrene (**17**) were observed in the reaction mixtures.

**Table 4.5.** Water influence on reactivity and the formation of the active species.



Entry <sup>[a]</sup>	Deviation	Ligand	Yield (%) <sup>[c]</sup>
1 <sup>[b]</sup>	Undistilled solvent	<b>L1</b>	-
2	Undegassed solvent	<b>L1</b>	-
3	3 Å MS	<b>L1</b>	69
4	3 Å MS	<b>L11</b>	-
5	3 Å MS	<b>L12</b>	-
6	3 Å MS	<b>L16</b>	-

[a] Standard reaction conditions: 1-phenylethanol (0.120 mL, 1.00 mmol, 1.00 equiv.), Pd(acac)<sub>2</sub> (3.05 mg, 0.01 mmol, 1.00 mol%) and dtbpx (21.0 mg, 0.05 mmol, 5.00 mol%) in chloroform (2 mL), stirred for 2.5 h at r.t., then MeSO<sub>3</sub>H (0.013 mL, 0.20 mmol, 0.20 equiv.) stirred for 30 min. at r.t., then HCOOH (0.19 mL, 10.0 mmol, 10.0 equiv.) stirred for 18 h at 100 °C in a Schlenk pressure tube. [b] Yields were determined *via* quantitative GC-FID using *n*-pentadecane as internal standard.

#### 4.4. Conclusions

In conclusion, optimization studies for the Pd-catalysed deoxygenation procedure were conducted. These were followed by ligand screening and investigation of the water influence over the catalytic process. Unfortunately, the aims of the optimization experiments were only partially achieved, as the system developed during this studies underperformed in comparison to the procedure reported by Ciszek and Fleischer. Two possible reasons behind this unfavourable outcome might be: the exclusion of the oxidized form of dtbpx (**L1-O<sub>2</sub>**) from the catalytic system or the interaction of the formic acid excess with the catalytically active species.

During the ligand screening, phosphines bearing different electronic and structural properties were investigated. None of the tested ligands, except dtbpx (**L1**), afforded the desired product in satisfactory yields, however, some information on the desirable ligand characteristics were gathered. It was concluded that a viable ligand for the formation of a catalytically active species for the deoxygenation reaction should possess a rigid backbone, a high degree of coordination flexibility through the methylene bridges, high electron-density on the P-atoms and bulky P-substituents, which should not interact with the acidic reaction medium. Due to the structural, electronic properties and weak basic character, bpx (**L2**) should be still considered as a possible candidate in replacing dtbpx (**L1**), but the purification procedure must be optimized before further investigations should be carried out.

The experiments conducted on the influence of water in the reaction mixture showed that the water content has a negative effect on the desired transformation. Consequently, the higher amount of water generated when using 10 equivalents of formic acid can also be a possible explanation for the lower yields of ethylbenzene (**2**), but more investigations have to be performed in order to gain a better understanding of its role.

Future studies should continue the pursuit of finding alternative ligands for dtbpx (**L1**), in order to get a better understanding on the mechanistic pathway of the Pd-catalysed deoxygenation and to enhance both the yields and the selectivity of the reaction.

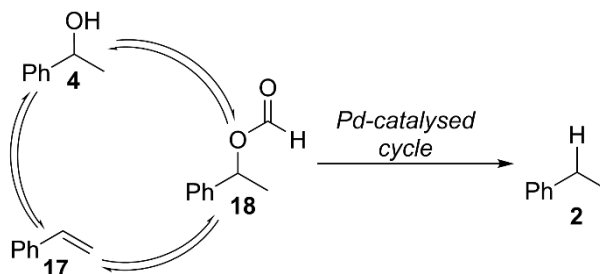
**4.5. References**

1. B. Ciszek and I. Fleischer, *Chem. Eur. J.*, 2018, **24**, 12259-12263.
2. J. M. Herrmann and B. König, *Eur. J. Org. Chem.*, 2013, **2013**, 7017-7027.
3. V. S. Ranade and R. Prins, *Chem. Eur. J.*, 2000, **6**, 313-320.
4. A. Volkov, K. P. J. Gustafson, C.-W. Tai, O. Verho, J.-E. Bäckvall and H. Adolfsson, *Angew. Chem. Int. Ed.*, 2015, **54**, 5122-5126.
5. D. Cao, Z. Chen, L. Lv, H. Zeng, Y. Peng and C.-J. Li, *iScience*, 2020, **23**.
6. R. J. Rahaim, Jr. and R. E. Maleczka, Jr., *Org. Lett.*, 2011, **13**, 584-587.
7. L. A. Fowley, D. Michos, X.-L. Luo and R. H. Crabtree, *Tetrahedron Lett.*, 1993, **34**, 3075-3078.
8. E. Keinan and N. Greenspoon, *J. Org. Chem.*, 1983, **48**, 3545-3548.
9. B. P. S. Chauhan, J. S. Rathore and T. Bando, *J. Am. Chem. Soc.*, 2004, **126**, 8493-8500.
10. B. P. S. Chauhan, J. S. Rathore, M. Chauhan and A. Krawicz, *J. Am. Chem. Soc.*, 2003, **125**, 2876-2877.
11. R. J. Rahaim and R. E. Maleczka, *Tetrahedron Lett.*, 2002, **43**, 8823-8826.
12. H. Wang, L. Li, X.-F. Bai, J.-Y. Shang, K.-F. Yang and L.-W. Xu, *Adv. Synth. Catal.*, 2013, **355**, 341-347.
13. Q.-Y. Bi, J.-D. Lin, Y.-M. Liu, H.-Y. He, F.-Q. Huang and Y. Cao, *Angew. Chem. Int. Ed.*, 2016, **55**, 11849-11853.
14. X. Liu, S. Li, Y. Liu and Y. Cao, *Chinese J. Catal.*, 2015, **36**, 1461-1475.
15. X. Liu, G. Lu, Y. Guo, Y. Guo, Y. Wang and X. Wang, *J. Mol. Catal. A: Chem.*, 2006, **252**, 176-180.
16. Y. Ben-David, M. Gozin, M. Portnoy and D. Milstein, *J. Mol. Catal. A*, 1992, **73**, 173-180.
17. S. Rajagopal and A. F. Spatola, *J. Org. Chem.*, 1995, **60**, 1347-1355.
18. S. Rajagopal and A. F. Spatola, *Appl. Catal. A: Gen.*, 1997, **152**, 69-81.
19. J. Feng, C. Yang, D. Zhang, J. Wang, H. Fu, H. Chen and X. Li, *Appl. Catal. A: Gen.*, 2009, **354**, 38-43.
20. S. Sawadjoon, A. Lundstedt and J. S. M. Samec, *ACS Catal.*, 2013, **3**, 635-642.
21. M. V. Galkin, S. Sawadjoon, V. Rohde, M. Dawange and J. S. M. Samec, *ChemCatChem*, 2014, **6**, 179-184.
22. M. V. Galkin and J. S. M. Samec, *ChemSusChem*, 2014, **7**, 2154-2158.
23. B.-S. Kwak, T.-J. Kim and S.-I. Lee, *Appl. Catal. A: Gen.*, 2003, **238**, 141-148.
24. K. J. Miller and M. M. Abu-Omar, *Eur. J. Org. Chem.*, 2003, **2003**, 1294-1299.
25. B. Ciszek, Doktors der Naturwissenschaften, Eberhard Karls Universität Tübingen, 2019.
26. V. Hirschbeck, P. H. Gehrtz and I. Fleischer, *J. Am. Chem. Soc.*, 2016, **138**, 16794-16799.
27. L. E. Craswell and J. L. Spencer, *J. Chem. Soc., Dalton Trans.*, 1992, **24**, 3445-3452.
28. J. Vondran, M. R. L. Furst, G. R. Eastham, T. Seidensticker and D. J. Cole-Hamilton, *Chem. Rev.*, 2021, **121**, 6610-6653.
29. B. Harris, *Ingenia*, 2010, **45**, 18-23.
30. W. Clegg, M. R. J. Elsegood, G. R. Eastham, R. P. Tooze, X. Lan Wang and K. Whiston, *Chem. comm.*, 1999, **18**, 1877-1878.
31. W. Clegg, G. R. Eastham, M. R. J. Elsegood, B. T. Heaton, J. A. Iggo, R. P. Tooze, R. Whyman and S. Zacchini, *J. Chem. Soc., Dalton Trans.*, 2002, **17**, 3300-3308.
32. T. A. Schmidt, B. Ciszek, P. Kathe and I. Fleischer, *Chem. Eur. J.*, 2020, **26**, 3641-3646.
33. M. Bödl and I. Fleischer, *Eur. J. Org. Chem.*, 2019, **2019**, 5856-5861.
34. J. D. Nobbs, C. H. Low, L. P. Stubbs, C. Wang, E. Drent and M. van Meurs, *Organometallics*, 2017, **36**, 391-398.
35. S. M. Mansell, *Dalton Trans.*, 2017, **46**, 15157-15174.
36. P. W. N. M. van Leeuwen, P. C. J. Kamer and J. N. H. Reek, *Pure Appl. Chem.*, 1999, **71**, 1443-1452.
37. R. Sang, P. Kucmierczyk, K. Dong, R. Franke, H. Neumann, R. Jackstell and M. Beller, *J. Am. Chem. Soc.*, 2018, **140**, 5217-5223.

## 5. Co-Catalysed Deoxygenation of Benzylic Alcohols

### 5.1. General Motivation

Due to the limited success in optimizing the Pd-catalysed procedure, the development of a new method for the deoxygenation of benzylic alcohols was endeavoured. Based on the observations made during the previous project and on the catalytic cycle proposed by Ciszek and Fleischer, the equilibrium reaction between the alcohol **4**, formate **18** and styrene (**17**) was again thoroughly analysed (Scheme 5.1).<sup>1</sup> In the case of the previously described protocol, it was hypothesised that the alcohol had to be first transformed, *via* esterification, into the corresponding formate **18** in order to obtain the desired alkane. These considerations were based on the successful deoxygenation of primary benzylic alcohols in quantitative yields and on the Pd-catalysed transformation of formate **18** into the corresponding alkane without the further addition of formic acid (**11**). Although an elimination-hydrogenation pathway could not be completely excluded, due to the successful Pd-catalysed hydrogenation of styrene, it was assumed that this mechanism plays only a secondary role in the overall deoxygenation procedure.



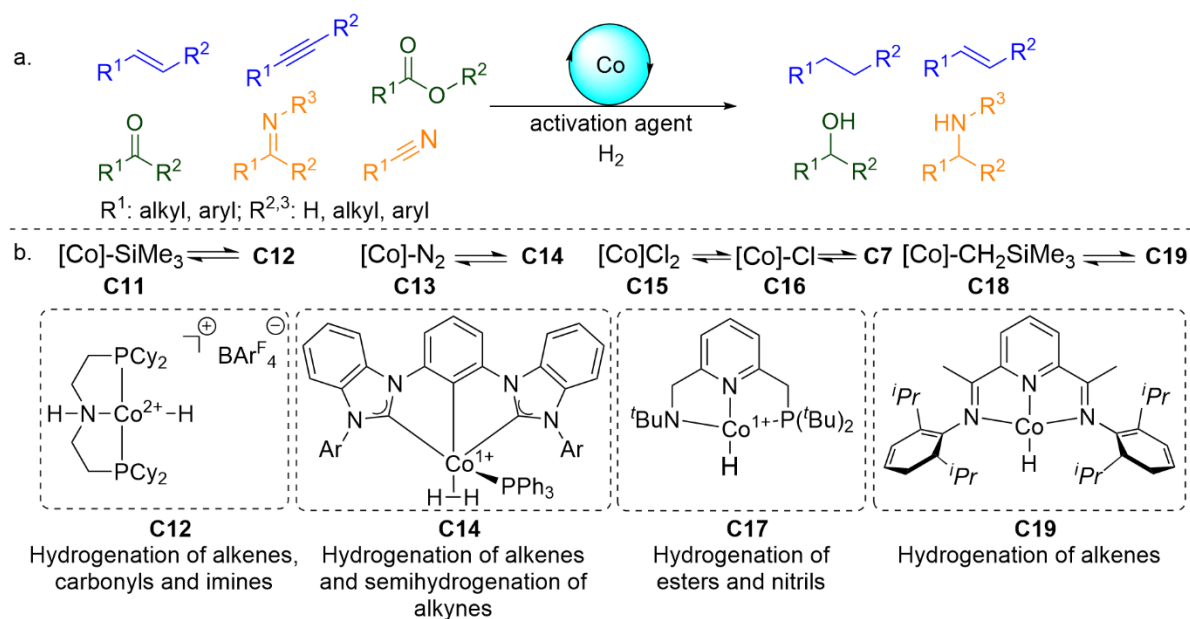
**Scheme 5.1.** Equilibrium reaction between 1-phenylethanol (**4**), 1-phenylethyl formate (**18**) and styrene (**17**).

Thus, the focus of the search for a new catalytic system was on the ability of the active species to transform either of the previously detected intermediates into compounds with a saturated hydrocarbon sidechain. Other aspects, which were taken into consideration, were the cost-effectiveness and the commercial availability of the metal sources and ligands. Therefore, 3d-metal-based catalysts seemed to be the best suitable candidates for this process. Although, to the best of our knowledge, no thermal Co-catalysed deoxygenation procedure was published to this date, Co-PNP catalysts proved to be a very attractive candidate for this role due to their hydrogenation capabilities and facile *in situ* formation. Additionally, it was reported that these complexes can also lead to the generation of molecular hydrogen through the oxidation of formic acid (**11**). These properties of the Co-based complexes will be extensively discussed in chapter 5.2.

### 5.2. Overview on the Applications of Co-Pincer Complexes

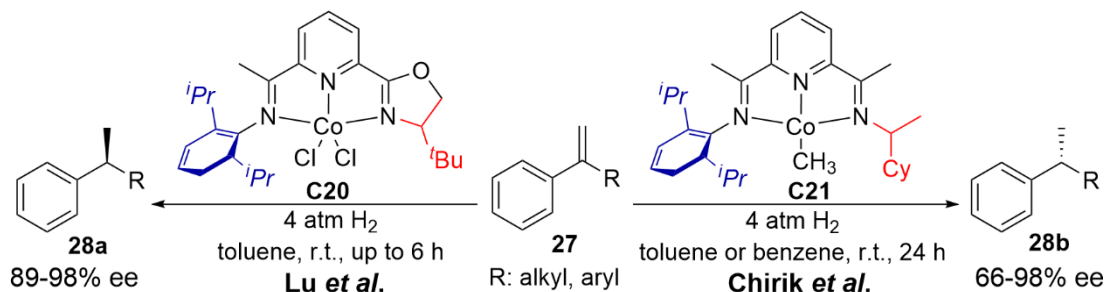
Over the last two decades, the activity of Co-pincer complexes was extensively studied in various hydride transfer reactions, especially in homogeneously catalysed hydrogenations of alkenes, alkynes, carbonyls, esters, imines and nitriles (Scheme 5.2 - a).<sup>2</sup> The more established route for the hydrogenation of alkenes is the inner-sphere mechanism, which implies the insertion, and subsequent elimination of the olefin from the metal centre. In 2012, Hanson *et al.* reported a comprehensive homogenous catalytic procedure for the reduction of alkenes, carbonyls and imines based on the anionic Co-complex **C11** (Scheme 5.2 - b).<sup>3</sup> The mechanistic investigation hinted towards the *in situ* formation

of the corresponding  $\text{Co}^{2+}$ -H **C12**. Therefore, it was concluded that the versatility of this method was a consequence of the  $2+$  oxidation state of the active species. More often, the Co-catalysed hydrogenation procedures rely on the *in situ* reduction of the  $\text{Co}^{2+}$ -precatalyst, with the newly generated  $\text{Co}^{1+}$  complex acting as the catalytically active species. Some of the most prominent examples of this kind of transformations were developed by groups of Fout, Milstein and Budzelaar. In 2016, Fout's group published their work on the hydrogenation of alkenes and the selective semihydrogenation of alkynes and later, in 2019, they reported the Co-catalysed selective hydrogenation of  $\alpha,\beta$ -unsaturated alkenes (Scheme 5.2 - b).<sup>4,6</sup> All these catalytical hydrogenations were mediated by the same Co-CCC pincer type complex **C14**. For the hydrogenation of alkenes, the proposed mechanism proceeds through a  $\text{Co}^{1+}/\text{Co}^{3+}$  pathway. The major steps of the proposed mechanism are the formation of the dihydrogen complex **C14** from the reaction of complex **C13** with  $\text{H}_2$ , the substitution of the phosphine ligand by the olefin coordination, the oxidative addition of  $\text{H}_2$  to the metal centre and the subsequent hydrogenation of the alkene. The Co-catalysed semihydrogenation of internal alkynes exhibited excellent selectivity towards the formation of the *E*-isomer. However, the addition of the *ex situ* generated **C14** led to the exclusive formation of the *Z*-alkene. Thus, after conducting extensive mechanistic studies it was concluded that this reaction proceeds through a hydrogenation-isomerization sequence, both steps being facilitated by **C14**. Co-NNPyridine complex **C15** was utilized as a precatalyst by the Milstein's group in the exhaustive homogenous hydrogenation of esters and nitriles (Scheme 5.2 - b). In both transformations, **C15** had to be reduced to a catalytically active  $\text{Co}^{1+}$  species by a sodium triethylborohydride ( $\text{NaBHET}_3$ ) (**26**)/base system. Depending on the amount of  $\text{NaBHET}_3$  (**26**) added to the reaction mixture, different  $\text{Co}^{1+}$  complexes could be selectively obtained *in situ*. For the generation of Co-complex **C16**, active for the complete hydrogenation of nitriles, 1 equivalent of borohydride **26** was needed, while 2 equivalents of **7** were required for the generation of the cobalt hydride **C17**. These observations were in accordance with the results published by Chirik *et al.* regarding the *in situ* reduction of Co-PNP complexes and the generation of the corresponding  $\text{Co}^{1+}$  species.<sup>7</sup> One of the first Co-pincer hydrogenation procedures of alkenes was developed by Budzelaar's group (Scheme 5.2 - b). The approach for this transformation was the use of a strong  $\pi$ -acceptor ligand that would stabilize the low-spin  $\text{Co}^{1+}$  species but still allow its oxidation to a  $\text{Co}^{3+}$  state. Indeed, square-planar  $\text{Co}^{2+}$  complex **C18** generated the  $\text{Co}^{1+}$  hydride **C19** upon addition of molecular hydrogen. In order to verify the ability of **C18** to generate a  $\text{Co}^{3+}$  species, **C18** was treated with  $\text{NaCN}$  and, indeed, the corresponding  $\text{Co}^{3+}$  was obtained. Thus, **C18** proved its potential activity in a  $\text{Co}^{1+}/\text{Co}^{3+}$  redox cycle.



**Scheme 5.2.** (a) Co-catalysed hydrogenations; (b) Examples of Co-complexes used in hydrogenation reactions.<sup>3-5, 8</sup>

Inspired by the pioneering work of Budzelaar, Chirik's and Lu's groups independently developed two enantioselective procedures for the hydrogenation of alkenes (Scheme 5.3).<sup>9, 10</sup> This could be achieved by the desymmetrization of the pincer ligands, namely by introducing both a chiral and protecting element into the ligand structure.

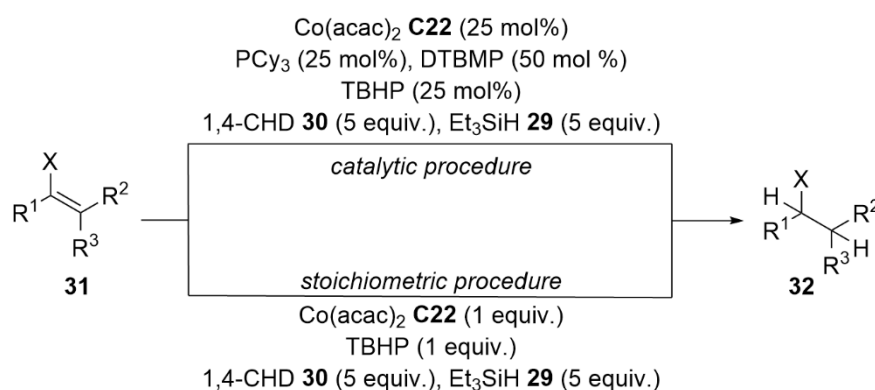


**Scheme 5.3.** Stereoselective hydrogenation of alkenes with asymmetric Co-NNN pincer ligands; (blue) protecting moiety.<sup>9, 10</sup>

A widely used approach for the derivatization of alkenes is the metal hydride hydrogen atom transfer (MH HAT). Beside hydrogenation, this mechanism enables the a wide variety of other functionalizations, for example isomerizations, couplings, hydrohalogenations or hydrations.<sup>11</sup> These reactions proceed through an outer-sphere mechanism and facilitate the generation of alkyl radicals during the process. Both an oxidative and a reductive turnover are possible in these transformations, thus taking advantage of  $\text{Co}^{2+}/\text{Co}^{3+}$  or  $\text{Co}^{2+}/\text{Co}^{1+}$  redox processes, respectively.<sup>12</sup> The main advantages of these procedures are the mild conditions and the enhanced chemoselectivity.<sup>13</sup> The Co-mediated hydrogenation protocols of alkenes through MH HAT pathway were extensively studied in the second half of the 20<sup>th</sup> century.<sup>14-19</sup> These reactions were conducted with stoichiometric amounts of added or *in situ* generated cobalt tetracarbonyl hydride.<sup>20</sup>



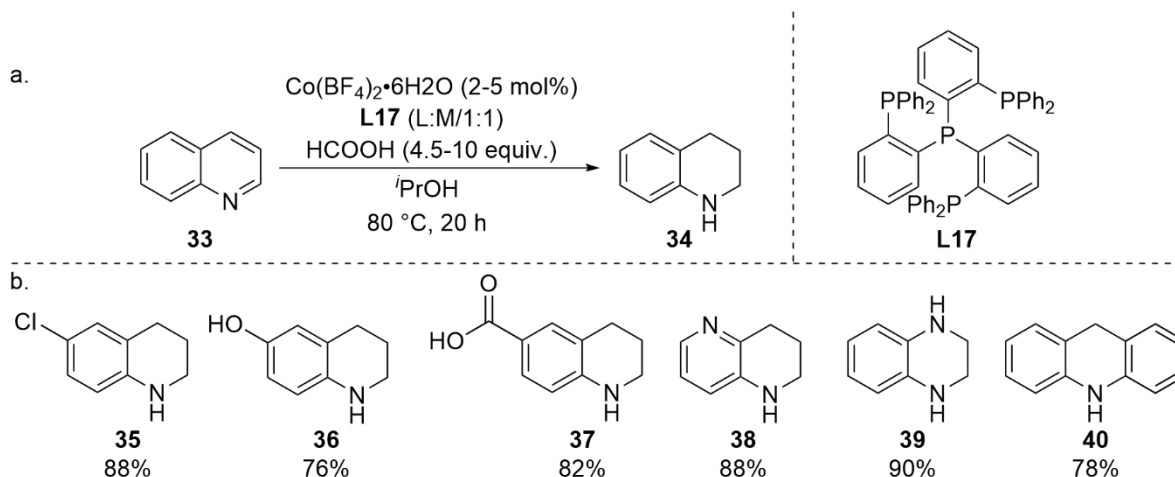
One example of a more recent advancement in the MH HAT chemistry was the study of King *et al.* on Co-mediated selective hydrogenation of alkenyl halides (Scheme 5.4).<sup>21</sup> For this purpose, two protocols were developed, both utilizing  $\text{Co}(\text{acac})_2$  (**C22**) as precatalyst, *t*-butylhydroperoxide as activator and a combination of triethylsilane (**29**) and 1,4-cyclohexadiene (**30**) as reductants. For the catalytic hydrogenation of terminal olefins, tricyclohexylphosphine (**L1**) and 2,6-di-*t*-butyl-4-methylpyridine (**12**) were also added to the reaction mixture. For the hydrogenation of tri- and tetrasubstituted olefins stoichiometric amounts of  $\text{Co}(\text{acac})_2$  (**C22**) were employed for the desired transformation in satisfactory yields. During the deuteration experiments, it was observed that each reducing agent selectively donates a H-atom to one of the positions, triethylsilane (**29**) to the terminal C-atom and 1,4-cyclohexadiene (**30**) to the internal C-atom. Additionally, **30** acts as a radical trap for the *in situ* generated alkyl radical. Based on the mechanistic studies and observations it was presumed that the mechanism of this transformation relies on a  $\text{Co}^{2+}/\text{Co}^{3+}\text{-H}$  redox cycle.



**Scheme 5.4.** MH HAT catalytic and stoichiometric procedures for the hydrogenation of alkenyl halides.<sup>21</sup>

As it was discussed, most of the Co-catalysed hydrogenation procedures use molecular hydrogen as H-source due its availability and atom-efficiency. In 2017, Cabrero-Antonino *et al.* reported a Co-catalysed procedure for the hydrogenation of quinolines, in which formic acid (**11**) was utilized as hydrogen donor (Scheme 5.5 - a).<sup>22</sup> As it was stated in chapter 2.3., the main advantages of using formic acid (**11**) in transfer hydrogenation procedures are the safety, stability, avoidance of high-pressure setups and, in ideal conditions, the generation of only benign side-products, namely  $\text{CO}_2$ .<sup>23</sup> Following the initial screenings, it was concluded that  $\text{Co}(\text{BF}_4)_2 \cdot 6\text{H}_2\text{O}$  (**C23**), ligand **L17** and formic acid (**11**) in isopropanol afforded the highest yield of the desired product. The addition of water, acidic or alkaline additives or the exchange of the H-source led to a complete inhibition of the reactivity. The control reactions showed that without the addition of the metal catalyst or  $\text{HCOOH}$  (**5**), the desired transformation could not take place, thus hinting towards an exclusive hydrogen donation pathway from the formic acid (**11**) and not from the solvent. Additionally, it was observed that only Co-complex **C23** was able to form a catalytically active species for this transformation. Some of the more commonly used  $\text{Co}^{2+}$ - and  $\text{Co}^{3+}$ -sources, like  $\text{CoCl}_2$  (**C24**),  $\text{CoBr}_2$  (**C25**) or  $\text{Co}(\text{acac})_3$  (**C26**) did not lead to the conversion of the starting material. The subsequent ligand screening showed that the only suitable phosphine for this application was the tetradentate ligand **L17**, while bi- and tridentate ligands did not exhibit the desired reactivity. Alongside the *in situ* formed active catalyst, the *ex situ* formed complex  $[\text{CoF}(\text{L1})]^+[\text{BF}_4]^-$  (**C27**) also facilitated the generation of tetrahydroquinoline **34** from quinoline **33**. Besides isopropanol, other protic solvents were also able to enhance the activity of the catalytic system.

Interestingly, toluene could also be used as solvent in this reaction, albeit with an almost 30% decrease in yield. Under optimized conditions, a wide range of quinolines were selectively hydrogenated, while both electron-withdrawing and electron-donating functionalities, like halide **35**, phenol **36** or carboxyl **37** were tolerated by the catalytic system (Scheme 5.5 - b). Remarkably, other N-heterocycles, like 1,5-naphtridine (**38**), quinoxaline (**39**) and acridine (**40**), were also hydrogenated through this Co-HCOOH procedure at a higher temperature. The nature of the catalyst was investigated *via* poisoning experiments. The addition of different quantities of mercury into the reaction mixture did not negatively affect the yields in the case of hydroquinolines. Hence, it was indicated that this reaction was catalysed by a homogenous system.



**Scheme 5.5.** (a) Co-catalysed hydrogenation of quinolines with formic acid; (b) Examples of hydrogenation products.<sup>22</sup>

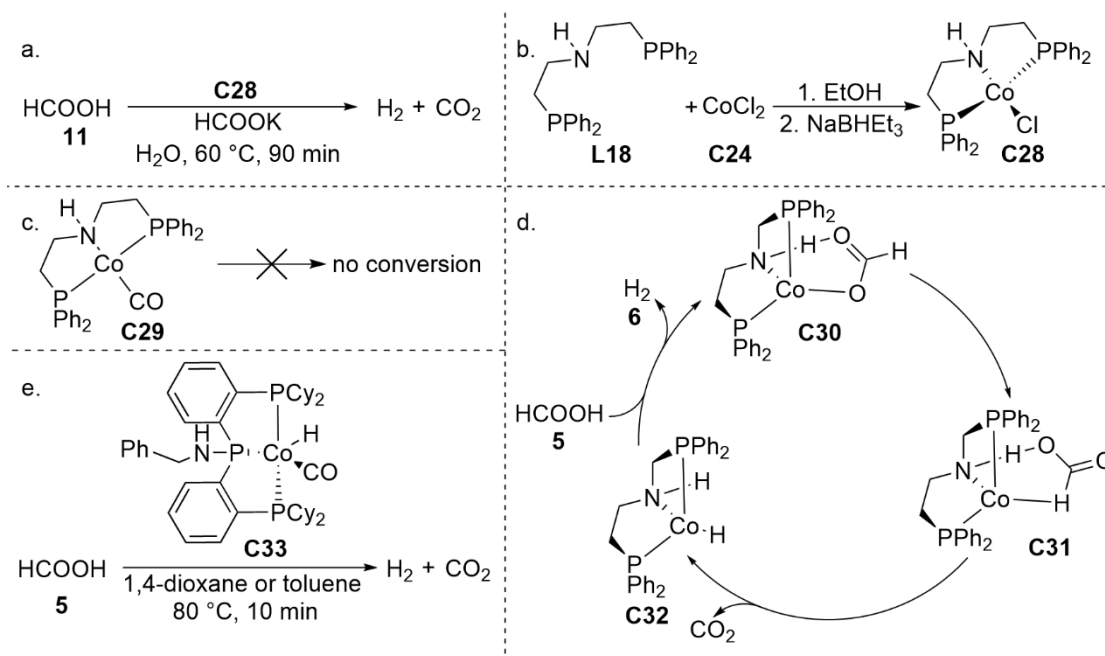
Subsequently, Beller's group reported a Co-PNP-based procedure for *in situ* generation of H<sub>2</sub> (**5**) through the dehydrogenation of formic acid (**11**) in aqueous solution (Scheme 5.6 - a).<sup>24</sup> The screening for a suitable Co-complex, which would be able to dehydrogenate formic acid (**11**), started with the employment of various Co<sup>2+</sup> species, but none of the examined compounds exhibited the desired reactivity. Next, *ex situ* prepared Co<sup>1+</sup>-complexes were tested in potassium formate (HCOOK) aqueous solution and, remarkably, complex **C28** was able to decompose formic acid (**11**) in almost quantitative yields (Scheme 5.6 - b). The presence of the HCOOK proved to be essential for the generation of H<sub>2</sub>. In order to make this procedure more attractive from the compounds handling perspective, the *in situ* generation of complex **C28** was attempted. The addition of one equivalent of NaBHET<sub>3</sub> (**26**) as reducing agent in the reaction mixture was insufficient for a satisfactory transformation, due to the incomplete reduction of the Co<sup>2+</sup> precatalyst. Instead, increasing the amount of H<sub>2</sub> to 3 equivalents led to the desired catalytical activity of the Co-based system.

The kinetic isotope effect investigations showed that the decarboxylation is involved in the rate-determining step. Additionally, the inactivity of complex **C29** suggested that the carbon monoxide, which could be generated through a dehydration pathway, acts as a poisoning agent for the active Co-species (Scheme 5.6 - c).

The proposed reaction mechanism begins with a substitution of the Cl with a formic acid (**11**) molecule to form complex **C30** (Scheme 5.6 - d). The rearrangement leads to the activation of the C-H bond in complex **C31**, which after dissociation leads to the release of CO<sub>2</sub> (**13**) and the generation of

Co-H species **C32**. Following the coordination of another HCOOH molecule (**11**) to complex **C22**, H<sub>2</sub> is liberated and the regeneration of complex **C20** occurs.

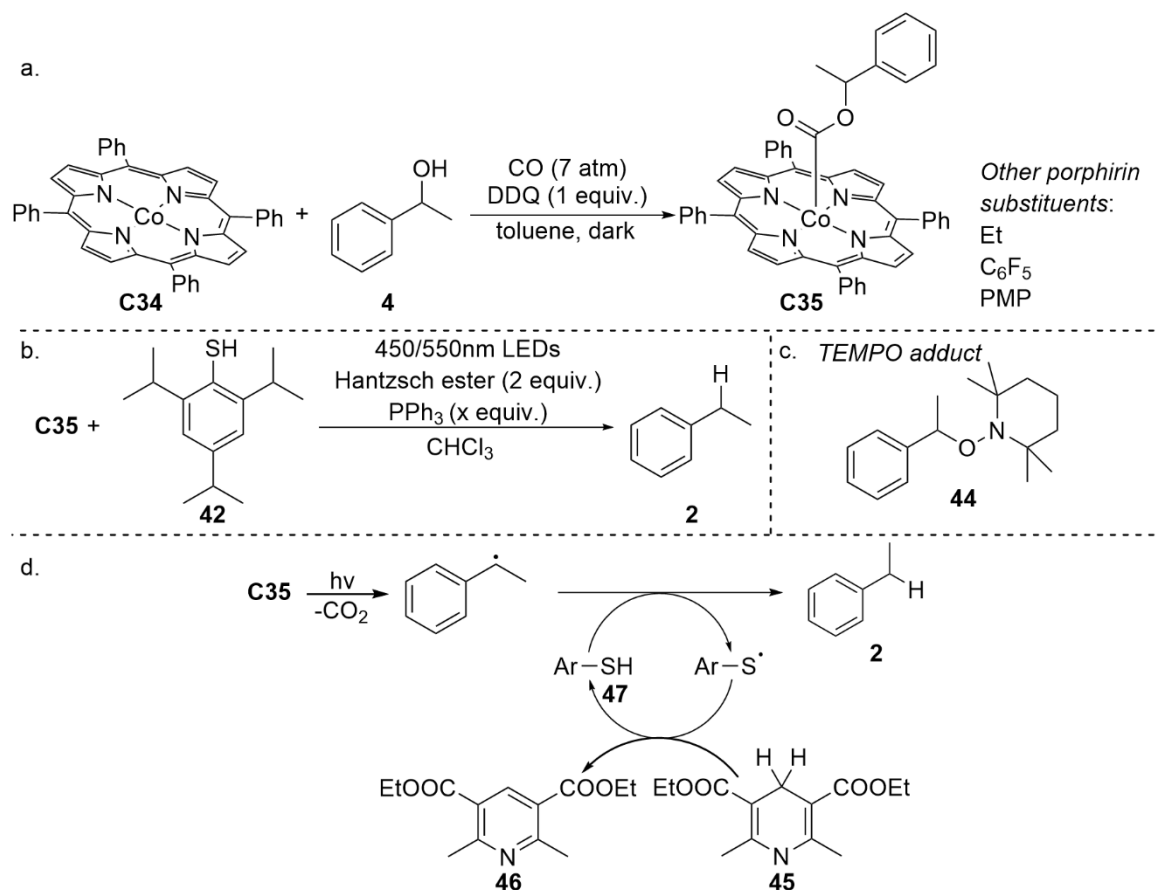
The ensuing report of Lentz *et al.* in 2021 presented another method for the dehydrogenation of formic acid (**11**) in toluene and dioxane by using a Co-PPP complex **C33** (Scheme 5.6 - e).<sup>25</sup> Thus, Co-pincer complexes proved to be efficient catalysts for the *in situ* generation of molecular hydrogen from formic acid (**11**) in various reaction environments.



**Scheme 5.6.** (a) Co-catalysed dehydrogenation of HCOOH in aqueous media; (b) *Ex situ* synthesis of **C18**; (c) CO poisoning experiment; (d) Proposed catalytic cycle for the dehydrogenation of formic acid in aqueous media; (e) Co-catalysed dehydrogenation of HCOOH in organic media.<sup>24</sup>

As it was stated in the previous chapter, no Co-catalysed thermal procedure for the deoxygenation of alcohols to the corresponding alkanes was reported to this date. The only instance, in which the Co-catalysed deoxygenation was observed, was during the studies of Ebisawa *et al.* on the enantioselective hydrofunctionalization of alkenes.<sup>26</sup> In this reaction the deoxygenation of 2,2,2-trifluoroethanol (**41**) was essential for the high enantioselectivity of the procedure. However, a photochemical Co-catalysed method for the deoxygenation of benzylic alcohols was developed by Chambers *et al.*<sup>27</sup> The envisioned route for the C-O bond cleavage starts with the carbonylation of the alcohol **4** followed by the reaction of the *in situ* formed formate with Co-porphyrin complex **C34** to generate the corresponding Co-porphyrin-alkoxycarbonyl complex **C35** under strong oxidative conditions. Subsequently, the carbon-centred radical is formed, and, through a photocatalysed hydrogen transfer, ethylbenzene (**2**) is obtained (Scheme 5.7 - a and b). For the generation of the Co-porphyrin-alkoxycarbonyl complex **C35**, 7 atm of CO and a 1:5 ratio between 2,3-dichloro-5,6-dicyano-1,4-benzoquinone (DDQ) and alcohol proved to be optimal. The investigations on the dissociation of the Co-C bond were conducted by adding TEMPO (**26**) as a radical trap into the reaction and by irradiating the mixture with a high intensity LED lamp with emission peaks at 450 and 550 nm. Indeed, this protocol led to the liberation of CO<sub>2</sub> and the formation of the TEMPO adduct (**27**) in very good yields, regardless of the substituents grafted on the porphyrin (Scheme 5.7 - c). Remarkably, only a small amount of Co-porphyrin complex **C35** was degraded following the transformation, therefore proving

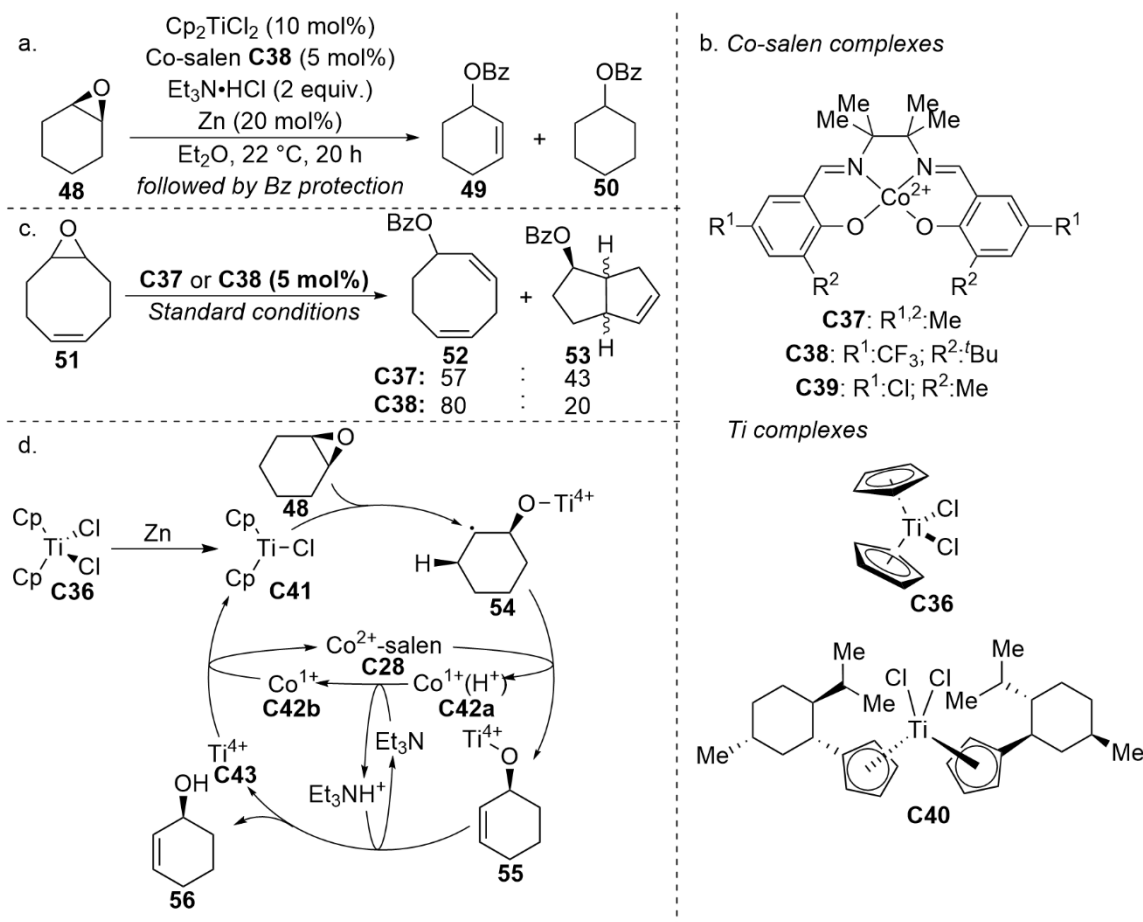
the recyclability of the catalyst. Neither thiophenol **42** nor Hantzsch ester **45** were able to effectively donate a H-atom solely to the generated benzyl radical. Instead, a thiophenol/Hantzsch ester dual system afforded ethylbenzene (**2**) in 94% yield, as thiophenol **42** acted as a H-donor and Hantzsch ester **45** as a regeneration agent and inhibiting agent for the dimerization of the thiophenol **42** (Scheme 5.7 - d).



**Scheme 5.7.** (a) Synthesis of Co-porphyrin-alcoxycarbonyl complex **C35**; (b) Photocatalytic generation of ethylbenzene (**2**); (c) Radical trap product **44**; (d) Proposed mechanism for the photocatalytic process.<sup>27</sup>

In 2019, Ye and co-workers reported a bimetallic-catalysed procedure for the isomerization of epoxides to allylic alcohols (Scheme 5.8 - a).<sup>28</sup> This protocol uses the homolytic epoxides ring-opening potential of Ti<sup>3+</sup> species in synergy with the hydrogen atom transfer capabilities of Co-salen complexes. Following the initial investigation on the reaction components it was concluded that by using Cp<sub>2</sub>TiCl<sub>2</sub> (**C36**) and the electron-deficient Co-salen complex **C38**, together with Zn as a metal reductant and Et<sub>3</sub>N•HCl, the desired allylic alcohol **49** was obtained in quantitative yields (Scheme 5.8 - b). The control reactions showed that, without the Co-catalyst, saturated compound **50** was exclusively obtained. Additionally, excluding the Et<sub>3</sub>N•HCl or Zn from the reaction mixture led to no conversion of the substrate. In order to get a better understanding about the role of the ligand substituents, a radical rearrangement experiment on compound **51** was conducted (Scheme 5.8 - c). It was observed that the utilization of the more electron-rich Co-complex **C37** facilitated the formation of the bicyclic compound **53** in higher yields, through an intramolecular cyclization. Consequently, the electron-rich complexes prove to be less efficient for the cleavage of the  $\gamma$ -C-H bond. Additionally, by exchanging

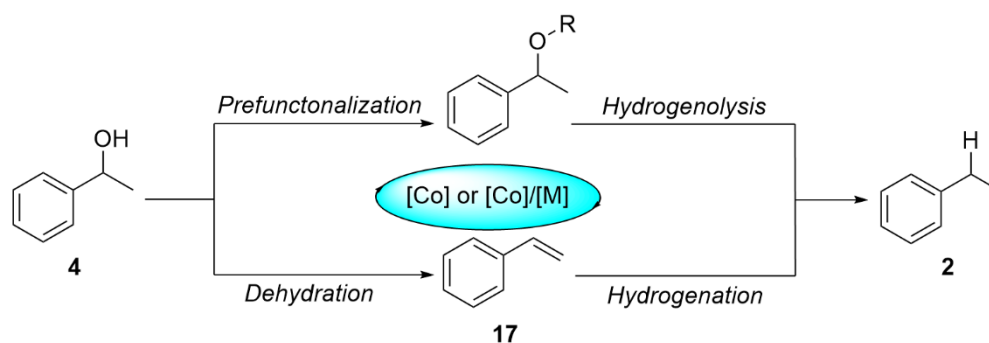
the Ti-complex **C36** for **C40** and optimizing the steric and electronic properties of the Co-salen complex **C39** an enantioselective variant of this transformation was elaborated (Scheme 5.8 - b).



**Scheme 5.8.** (a) Co- and Ti-catalysed isomerization of epoxides to allylic alcohols; (b) Co-salen complexes; (c) Radical rearrangement experiment; (d) Ti-complexes; (e) Proposed mechanism for the isomerization of epoxides.<sup>28</sup>

Based on the observations made during the development of this protocol, a catalytic cycle was envisioned (Scheme 5.8 - d). First, the Ti<sup>3+</sup> species **C41** reacts with the substrate **48** to generate intermediate **54**. The formation of a  $\beta$ -C-centred radical in compound **54** causes the weakening of the  $\gamma$ -C-H bond, therefore Co-complex **C38** is able to extract the H-atom leading to the formation of **C42a**. The exact mechanism of this transfer was not uncovered but it can proceed either through a HAT-process or *via* a proton-coupled electron transfer. Then, the Et<sub>3</sub>N·HCl facilitated proton transfer to Ti<sup>4+</sup> species from **55** affording the desired allyl alcohol **56**. Et<sub>3</sub>N·HCl is regenerated through the proton transfer between **C42a** and triethylamine. Subsequently, the regeneration of both catalysts proceeds through the single electron transfer between Ti<sup>4+</sup> species **C43** and the Co<sup>1+</sup>-complex **C42b**.

Therefore, we acknowledge the potential of Co-complexes for a deoxygenation reaction, *via* a mono- or bimetallic system (Scheme 5.9). The first possible reaction pathway proceeds through a prefunctionalization of the alcoholic substrate followed by a hydrogenolysis process. The second envisioned route implies the dehydration of the benzylic alcohol and a subsequent hydrogenation of the *in situ* generated alkene.

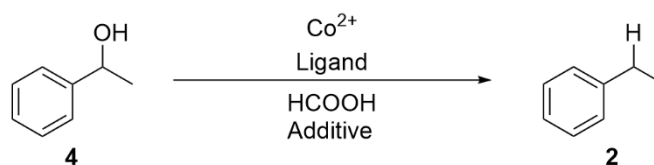


Scheme 5.9. Proposed routes for the Co-catalysed deoxygenation of alcohols.

### 5.3. Results and Discussions for Co-Catalysed Deoxygenation

#### 5.3.1. Initial Conditions and Ligand Screening

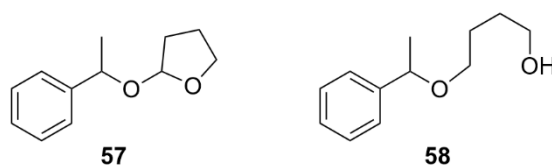
The first route envisioned for the deoxygenation of alcohols was based on a redox-neutral  $\text{Co}^{2+}$ -catalysed system and employed formic acid (**11**) as H-donor (Scheme 5.10). During these preliminary investigations, the capability of various ligands and additives to enhance the desired reactivity was tested.



Scheme 5.10. General reaction of the  $\text{Co}^{2+}$ -based approach.

The pursuit of finding a catalytic system capable of yielding the desired alkane (**2**) started with a preliminary ligand screening. The main categories of ligands tested for this transformation were N-based ligands, P-based bidentate ligands, pincer PNP and POP ligands, monodentate P-ligands and salen (Figure 5.2). The results of these investigations are displayed in table 5.1. For these studies  $\text{CoCl}_2$  (**C24**) was used as the Co-source and 1-phenylethanol (**4**) was selected as the model substrate. Additionally, different solvents at reflux were used during these studies in order to observe their influence over the reactivity.

Throughout these investigations, the formation of various higher molecular mass products was observed *via* GC-MS, analogous to the optimization of the Pd-catalysed deoxygenation presented in chapter 4.3 (Figure 5.1). Beside the products also detected during the previously described Pd-catalysed procedure, compounds **57** and **58** were detected in significant amounts in the crude reaction mixture. The formation of both closed (**57**) and open (**58**) THF adducts might occur *via* a  $\text{Co}^{2+}$  catalysed process, similar to the one described by Iqbal.<sup>29</sup> This procedure would imply the *in situ* formation of a vinyl ether, but the mechanism through which the dehydrogenation of tetrahydrofuran proceeds was not clarified. These compounds were only considered side-products and not possible intermediates of the process; hence, they were not isolated or further analysed.



**Figure 5.1.** THF adducts detected *via* GC-MS during the development of the Co-catalysed deoxygenation.

The reactions with bidentate ligands **L19** and **L20** did not afford ethylbenzene (**4**), instead, both formate **18** and styrene (**17**) were produced (Table 5.1. – Entries 1-3). The formation of high amounts of **18** was anticipated as in 2005 Velusamy *et al.* reported a  $\text{Co}^{2+}$ -catalysed procedure for the acetylation of alcohols.<sup>30</sup> Reactions with **L19** were conducted under both air and argon (Table 5.1. – Entries 1 and 2). The conversion of the starting material was considerably higher under inert conditions, but most of the alcohol **4** was transformed into higher molecular mass products (Table 5.1. – Entry 2). Another difference between the two reactions was that the reaction conducted under Ar afforded more styrene (**17**) than formate **18**, instead, the reaction in air afforded exclusively 1-phenylethyl formate (**18**). Both reactions conducted under Ar with bidentate N-based ligands **L19** and **L20** showed similar conversions, regardless of the solvent used, THF or toluene (Table 5.1. – Entries 2 and 3).

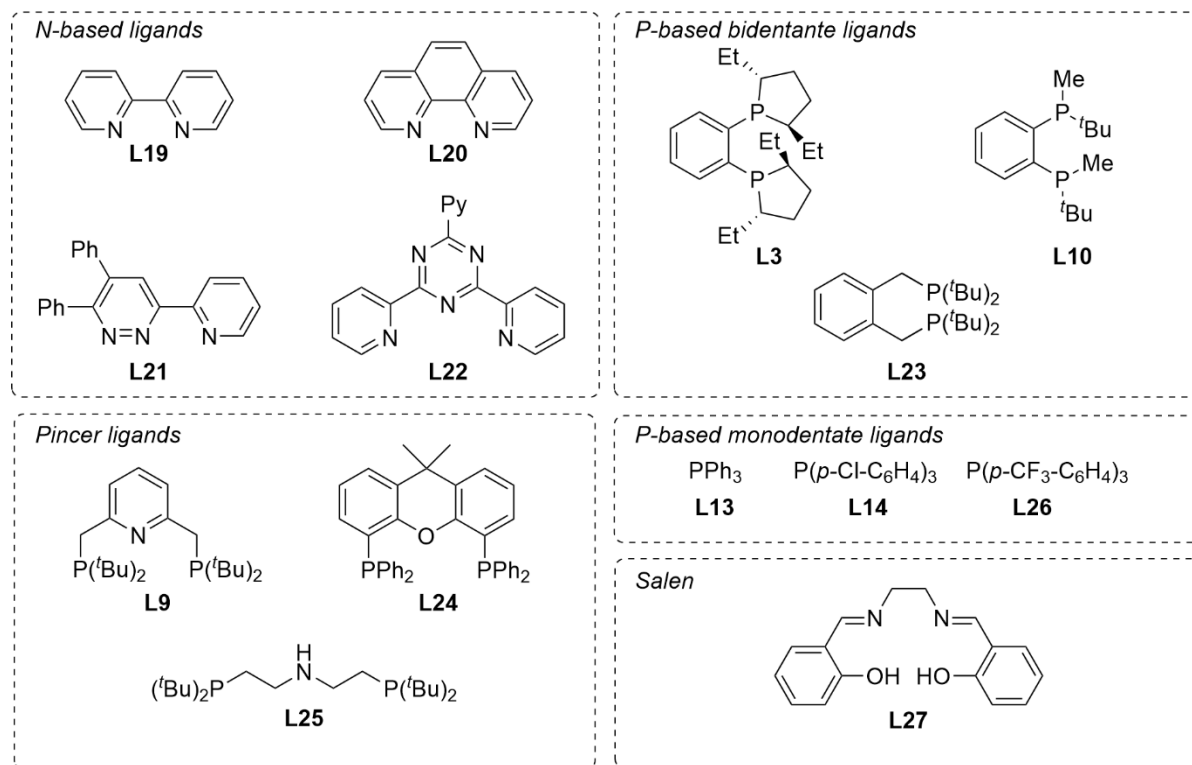
In the reactions with ligand **L21**, traces of ethylbenzene (**4**) were detected (Table 5.1. – Entries 4 and 5). These results were unexpected as no synthesis or application for a  $\text{Co}^{2+}$ -**L21** complex was reported in the literature up to this date. Analogous to the reactions with **L19** and **L20**, both reactions with **L21** gave comparable conversions regardless of the used solvent, however the reaction conducted in toluene led to the formation of higher quantities of both formate **18** and styrene (**3**) (Table 5.1. – Entries 4 and 5). This phenomenon might occur due to the higher reaction temperature. Unfortunately, the reaction, in which **L22** was employed, converted only 34% of the starting material and only small amounts of formate **18** could be detected beside the higher molecular mass compounds (Table 5.1. – Entry 6).

Then, P-based bidentate ligands were subjected to the reaction (Table 5.1. – Entries 7-10). This class of ligands was previously employed in various Co-catalysed reactions, for example in the asymmetric hydrogenation of enamides<sup>31</sup> or hydrogenation of  $\text{CO}_2$ .<sup>32</sup> Unfortunately, none of the ligands **L3**, **L10** and **L23** were able to generate a catalytically active  $\text{Co}^{2+}$ -complex for the desired transformation, instead, these complexes proved to be very efficient at catalysing the formation of formate **18**. The high conversions and formation of substantial amounts of formate **18** in all reactions in which the activity of bidentate P-based ligands was tested, strengthened the hypothesis that the higher reaction temperatures might be beneficial for the desired transformation by inhibiting the generation of higher molecular mass compounds (Table 5.1. – Entries 7-10).

As it was mentioned in the previous chapter, Co-pincer complexes were successfully employed in both  $\text{Co}^{1+}$  and  $\text{Co}^{2+}$ -catalysed transformations. Additionally, **L9** was used as precatalysts in Co-catalysed reduction of esters reported by Junge *et al.*<sup>33</sup> In reactions conducted in toluene, both PNP- (**L9** and **L25**) and POP-pincer (**L24**) ligands were able to afford the desired alkane **2** in traces. (Table 5.1. – Entries 11, 12 and 14). Beside ethylbenzene (**2**), the utilization of **L9** and **L25** led to the formation of formate **18** in good yields while **L24** facilitated the formation of the higher molecular mass products in both  $\text{CHCl}_3$  and toluene (Table 5.1. – Entries 11-14).

Subsequently, the capabilities of monodentate P-based ligands were examined. Triphenylphosphine (**L13**) afforded ethylbenzene (**2**) in traces (Table 5.1. – Entry 15). The

derivatization of the triphenylphosphine ligand in the *p*-position with Cl- and CF<sub>3</sub>-substituents completely inhibited the formation of the desired alkane **2** (Table 5.1. – Entries 16 and 17). Instead, both **L14** and **L26** afforded formate **18** and styrene (**17**) in good yields. The last ligand tested in this preliminary study was salen (Table 5.1. – Entry 18). Unfortunately, **L27** also facilitated the formation of only traces of ethylbenzene (**2**).



**Figure 5.2.** Ligands tested in the preliminary investigations.

In conclusion, unactivated Co<sup>2+</sup>-complexes proved to be inefficient for the deoxygenation of benzylic alcohols. The most promising ligands tested were **L21**, the pincer ligands **L9**, **L24** and **L25**, triphenylphosphine **L13** and salen **L27**. Additionally, it was concluded that toluene was the best suited solvent for these transformations, however, due to the low yields obtained, the role of the solvent could not be comprehensively investigated.

**Table 5.1.** Initial ligand screening

Entry <sup>[a]</sup>	Ligand	Solvent	Conversion (%) <sup>[b]</sup>	Yield of <b>2</b> (%) <sup>[b]</sup>	Yield of <b>18</b> (%) <sup>[b]</sup>	Yield of <b>17</b> (%) <sup>[b]</sup>
1 <sup>[c]</sup>	<b>L19</b>	THF	53	-	50	-
2	<b>L19</b>	THF	92	-	16	22



3	<b>L20</b>	Toluene	95	-	58	traces
4	<b>L21</b>	THF	71	traces	11	traces
5	<b>L21</b>	Toluene	74	traces	19	6
6	<b>L22</b>	THF	34	-	5	-
7	<b>L3</b>	CHCl <sub>3</sub>	80	-	46	11
8	<b>L10</b>	CHCl <sub>3</sub>	75	-	37	9
9	<b>L23</b>	CHCl <sub>3</sub>	89	-	71	-
10	<b>L23</b>	Toluene	86	-	65	traces
11	<b>L9</b>	Toluene	92	traces	66	-
12	<b>L24</b>	CHCl <sub>3</sub>	79	-	5	10
13	<b>L24</b>	Toluene	90	traces	35	5
14	<b>L25</b>	Toluene	85	traces	42	-
15	<b>L13</b>	Toluene	70	traces	43	traces
16	<b>L14</b>	THF	74	-	31	35
17	<b>L26</b>	Toluene	89	-	39	29
18	<b>L27</b>	THF	90	traces	19	-

[a] Standard reaction conditions: In a Schlenk pressure tube anhydrous CoCl<sub>2</sub> (26,0 mg, 0.20 mmol, 20.0 mol%), Ligand (0.20 mmol, 20.0 mol%) and 1-phenylethanol (0.120 mL, 1.00 mmol, 1.00 equiv.) in solvent (3 mL) stirred for 30 min. at r.t., then HCOOH (0.38 mL, 10.0 mmol, 10.0 equiv.) stirred for 18 h at reflux; [b] Yields were determined *via* quantitative GC-FID using *n*-pentadecane as internal standard; [c] Reaction conducted under air.

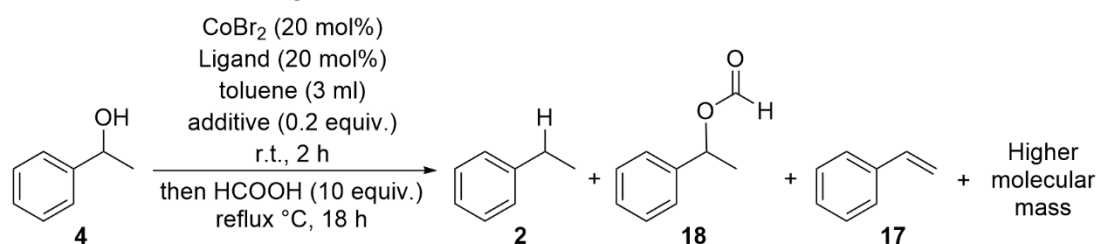
### 5.3.2. Additive Screening

Hence, the addition of various additives was considered in order to obtain the desired product **2**. First, it was hypothesised that that addition of an acidic co-catalyst would facilitate the transformation of 1-phenylalcohol (**4**) into formate **18** and styrene (**17**). This step would be followed either by the Co<sup>2+</sup>-catalysed C-O bond cleavage or by the hydrogenation of the intermediate. Thus, 0.2 equivalents of methanesulfonic acid (**21**) were added to the reaction mixture. Unfortunately, none of the acidic co-catalysed reactions afforded the desired product **2** (Table 5.2. – Entries 1-4). When bidentate P-based ligands **L3** and **L10** were employed to the reaction, both the enhancement of formate **18** generation and the inhibition of side-reactions were observed (Table 5.2. – Entries 1 and 2). In the reaction with POP-pincer ligand **L24** a slight increase in yield of both 1-phenylethyl formate (**18**) and styrene (**17**) occurred (Table 5.2. – Entry 3). Interestingly, the addition of molecular sieves into the reaction mixture with ligand **L24** led to 45% yield of styrene (**17**), the highest detected during these initial screenings (Table 5.2. – Entry 4).

Due to the limited success of the Co<sup>2+</sup>-catalysed procedures, the *in situ* generation of a Co<sup>1+</sup> complex was endeavoured. Thus, the reducing capabilities of various additives was tested. First, a Zn/MeOH system was employed for the reduction of the Co<sup>2+</sup> complex with PNP-ligands **L9** and **L25** (Table 5.2. – Entries 5 and 6) but none of the reactions led to the formation of ethylbenzene (**2**). This reducing system was previously utilized by Friedfeld and co-workers for the Co-catalysed asymmetric

hydrogenation of enamides.<sup>31</sup> Next, the reducing capacities of sodium borohydride (**59**) with and without formic acid (**11**) was investigated (Table 5.2. – Entries 7-10). NaBH<sub>4</sub> (**59**) was previously employed by Fringuelli *et al.* for the Co<sup>2+</sup>-catalysed hydrogenation of olefines and azides.<sup>34, 35</sup> Regardless of the employed ligand, **L9** or **L24**, the reactions without formic acid (**11**) showed very low conversion of the starting material **4**, 14% and 26%, respectively (Table 5.1. – Entries 8 and 10). By using both formic acid (**11**) and NaBH<sub>4</sub> (**59**) the conversion increased to 60% and 70% but no ethylbenzene (**2**) was detected in the final reaction mixtures. Subsequently, inspired by the previously discussed system developed by Beller *et al.*, NaBHET<sub>3</sub> (**26**) was also subjected to the reaction as reducing agent but also in this case no ethylbenzene (**2**) was generated (Table 5.2. – Entry 11).<sup>24</sup>

**Table 5.2.** Additive screening



Entry [a]	Additive	Ligand	Conversion (%) <sup>[b]</sup>	Yield of <b>2</b> (%) <sup>[b]</sup>	Yield of <b>18</b> (%) <sup>[b]</sup>	Yield of <b>17</b> (%) <sup>[b]</sup>
1	MeSO <sub>3</sub> H	<b>L3</b>	97	-	80	8
2	MeSO <sub>3</sub> H	<b>L10</b>	95	-	63	5
3	MeSO <sub>3</sub> H	<b>L24</b>	90	-	11	18
4	MeSO <sub>3</sub> H and M.S. (3Å)	<b>L24</b>	90	-	8	45
5	Zn/MeOH	<b>L9</b>	92	-	46	traces
6	Zn/MeOH	<b>L25</b>	96	-	75	traces
7 <sup>[c],[d]</sup>	NaBH <sub>4</sub>	<b>L9</b>	14	-	-	-
8 <sup>[c]</sup>	NaBH <sub>4</sub>	<b>L9</b>	60	-	44	traces
9 <sup>[c],[d]</sup>	NaBH <sub>4</sub>	<b>L24</b>	26	-	7	traces
10 <sup>[c]</sup>	NaBH <sub>4</sub>	<b>L24</b>	75	traces	61	traces
11 <sup>[d]</sup>	NaBHET <sub>3</sub>	<b>L9</b>	87	-	46	21

[a] Standard reaction conditions: In a Schlenk pressure tube anhydrous CoBr<sub>2</sub> (43.6 mg, 0.20 mmol, 20.0 mol%), Ligand (0.20 mmol, 20.0 mol%), additive (0.20 mmol, 20.0 mol%) and 1-phenylethanol (0.120 mL, 1.00 mmol, 1.00 equiv.) in toluene (3 mL) stirred for 30 min. at r.t., then HCOOH (0.38 mL, 10.0 mmol, 10.0 equiv.) stirred for 18 h at reflux; [b] Yields were determined *via* quantitative GC-FID using *n*-pentadecane as internal standard; [c] Reaction in THF; [d] Without HCOOH.

Thus, based on these preliminary results, it was concluded that Co<sup>1+</sup> or Co<sup>2+</sup> complexes are not able to solely catalyse the deoxygenation of benzylic alcohols. As a result, a bimetallic strategy was envisioned and, based upon the literature reports discussed in chapter 6.1, titanium was chosen a suitable, versatile candidate.

**5.4. References**

1. B. Ciszek and I. Fleischer, *Chem. Eur. J.*, 2018, **24**, 12259-12263.
2. W. Ai, R. Zhong, X. Liu and Q. Liu, *Chem. Rev.*, 2019, **119**, 2876-2953.
3. G. Zhang, B. L. Scott and S. K. Hanson, *Angew. Chem. Int. Ed.*, 2012, **51**, 12102-12106.
4. K. Tokmic, C. R. Markus, L. Zhu and A. R. Fout, *J. Am. Chem. Soc.*, 2016, **138**, 11907-11913.
5. K. Tokmic and A. R. Fout, *J. Am. Chem. Soc.*, 2016, **138**, 13700-13705.
6. S. R. Muhammad, J. W. Nugent, K. Tokmic, L. Zhu, J. Mahmoud and A. R. Fout, *Organometallics*, 2019, **38**, 3132-3138.
7. S. P. Semproni, C. C. Hojilla Atienza and P. J. Chirik, *Chem. Sci.*, 2014, **5**, 1956-1960.
8. Q. Knijnenburg, A. D. Horton, H. v. d. Heijden, T. M. Kooistra, D. G. H. Hetterscheid, J. M. M. Smits, B. d. Bruin, P. H. M. Budzelaar and A. W. Gal, *J. Mol. Catal. A Chem.*, 2005, **232**, 151-159.
9. J. Chen, C. Chen, C. Ji and Z. Lu, *Org. Lett.*, 2016, **18**, 1594-1597.
10. S. Monfette, Z. R. Turner, S. P. Semproni and P. J. Chirik, *J. Am. Chem. Soc.*, 2012, **134**, 4561-4564.
11. S. W. M. Crossley, C. Obradors, R. M. Martinez and R. A. Shenvi, *Chem. Rev.*, 2016, **116**, 8912-9000.
12. V. van der Puyl, R. O. McCourt and R. A. Shenvi, *Tetrahedron Lett.*, 2021, **72**, 153047.
13. S. A. Green, S. W. M. Crossley, J. L. M. Matos, S. Vásquez-Céspedes, S. L. Shevick and R. A. Shenvi, *Acc. Chem. Res.*, 2018, **51**, 2628-2640.
14. S. Friedman, S. Metlin, A. Svedi and I. Wender, *J. Org. Chem.*, 1959, **24**, 1287-1289.
15. J. Kwiatek, I. L. Mador and J. K. Seyler, *J. Am. Chem. Soc.*, 1962, **84**, 304-305.
16. J. A. Roth and M. Orchin, *J. Organomet. Chem.*, 1979, **182**, 299-311.
17. T. E. Nalesnik, J. H. Freudenberger and M. Orchin, *J. Mol. Catal.*, 1982, **16**, 43-49.
18. J. A. Roth, P. Wiseman and L. Ruzsala, *J. Organomet. Chem.*, 1982, **240**, 271-275.
19. F. Ungvary and L. Marko, *Organometallics*, 1982, **1**, 1120-1125.
20. M. F. Mirbach, *Inorganica Chim. Acta*, 1984, **88**, 209-211.
21. S. M. King, X. Ma and S. B. Herzon, *J. Am. Chem. Soc.*, 2014, **136**, 6884-6887.
22. J. R. Cabrero-Antonino, R. Adam, K. Junge, R. Jackstell and M. Beller, *Catal. Sci. Technol.*, 2017, **7**, 1981-1985.
23. Q.-Y. Bi, J.-D. Lin, Y.-M. Liu, H.-Y. He, F.-Q. Huang and Y. Cao, *Angew. Chem. Int. Ed.*, 2016, **55**, 11849-11853.
24. W. Zhou, Z. Wei, A. Spannenberg, H. Jiao, K. Junge, H. Junge and M. Beller, *Chem. Eur. J.*, 2019, **25**, 8459-8464.
25. N. Lentz, A. Aloisi, P. Thuéry, E. Nicolas and T. Cantat, *Organometallics*, 2021, **40**, 565-569.
26. K. Ebisawa, K. Izumi, Y. Ooka, H. Kato, S. Kanazawa, S. Komatsu, E. Nishi and H. Shigehisa, *J. Am. Chem. Soc.*, 2020, **142**, 13481-13490.
27. D. R. Chambers, A. Juneau, C. T. Ludwig, M. Frenette and D. B. C. Martin, *Organometallics*, 2019, **38**, 4570-4577.
28. K.-Y. Ye, T. McCallum and S. Lin, *J. Am. Chem. Soc.*, 2019, **141**, 9548-9554.
29. J. Iqbal, R. R. Srivastava, K. B. Gupta and M. A. Khan, *Synth. Commun.*, 1989, **19**, 901-906.
30. S. Velusamy, S. Borpuzari and T. Punniyamurthy, *Tetrahedron*, 2005, **61**, 2011-2015.
31. M. R. Friedfeld, H. Zhong, R. T. Ruck, M. Shevlin and P. J. Chirik, *Science*, 2018, **360**, 888-893.
32. M. S. Jeletic, M. L. Helm, E. B. Hulley, M. T. Mock, A. M. Appel and J. C. Linehan, *ACS Catal.*, 2014, **4**, 3755-3762.
33. K. Junge, B. Wendt, A. Cingolani, A. Spannenberg, Z. Wei, H. Jiao and M. Beller, *Chem. Eur. J.*, 2018, **24**, 1046-1052.
34. F. Fringuelli, F. Pizzo and L. Vaccaro, *Synthesis*, 2000, **2000**, 646-650.
35. F. J. Lundevall, V. Elumalai, A. Drageset, C. Totland and H.-R. Bjørsvik, *Eur. J. Org. Chem.*, 2018, **2018**, 3416-3425.

Parts of chapter 6.3 are reproduced from A. Căciuleanu, F. Vöhringer and I. Fleischer *Organic Chemistry Frontiers*, 2023,10, 2927-2935, DOI: 10.1039/D3QO00623A with permission from the Chinese Chemical Society (CCS), Shanghai Institute of Organic Chemistry (SIOC), and the Royal Society of Chemistry; schemes, tables, figures and text may differ from this publication and additional results are included.

### Author contribution:

The author of this thesis conducted the preliminary studies, the optimization reaction conditions, performed synthesis of starting materials and substrate screening as well as data collection and analysis of NMR, IR, GC-MS results. The author compiled the results and drafted the article manuscript. Felix Vöhringer conducted synthesis of starting materials and substrate screening under the supervision of the author of this thesis during its internship in the laboratory of Prof. Dr. Ivana Fleischer. Parts of the GC-MS and NMR measurements were performed by the MS and NMR department of the University of Tübingen.

Parts of chapter 6.3.2 are included in the Bachelor Theses of Tim Heumesser, which was initiated and closely supervised by the author of this thesis.

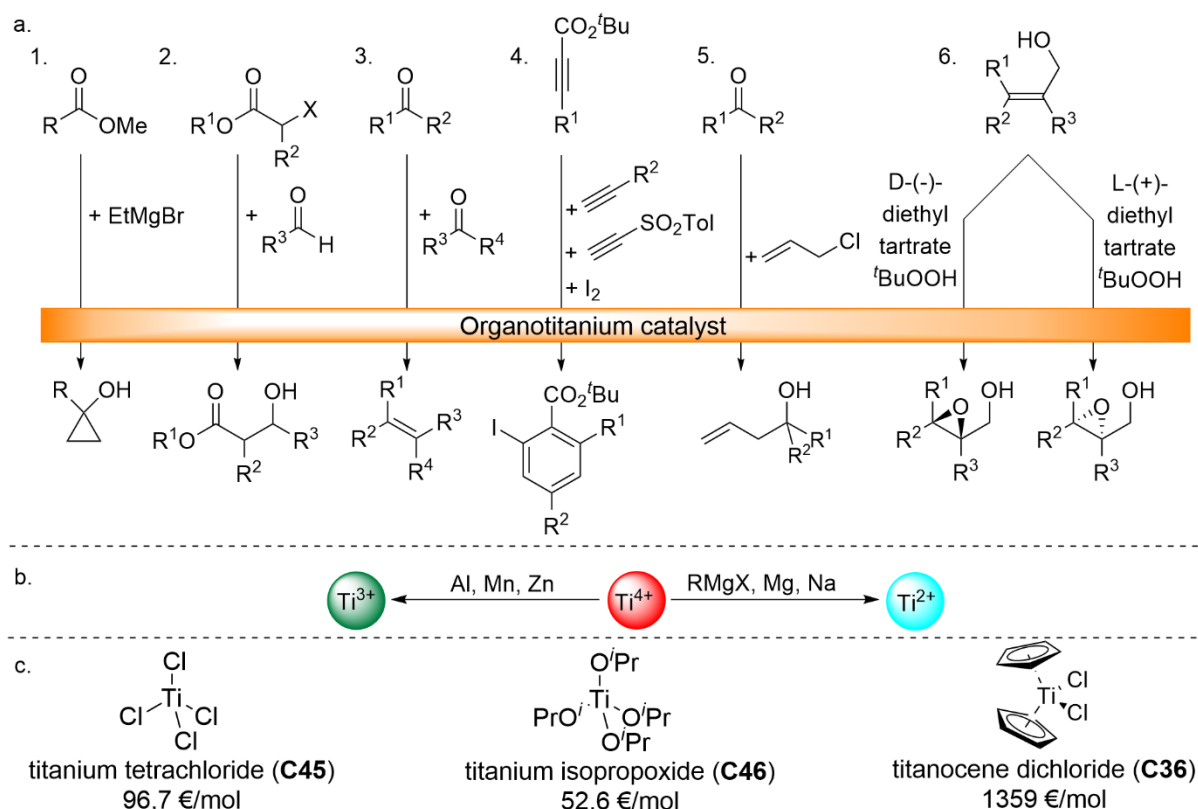
Parts of the optimization screenings from the Bachelor Theses are included herein and were conducted by the respective student. For this, interpretations and data analysis were performed by the author of this thesis and the experimental work was closely supervised. Parts of the GC-MS measurements were performed by the MS department of the University of Tübingen.

## 6. Co/Ti- and Ti-Catalysed Deoxygenation of Benzylic Alcohols

### 6.1. Overview on Ti-catalysed Deoxygenation of Alcohols

#### 6.1.1. Introduction in Organotitanium Chemistry

Organotitanium chemistry developed rapidly in the 1950s mainly because of the discovery of the Ziegler-Natta catalyst and its usage in the polymerization of olefins at industrial scale.<sup>1-3</sup> Since then, various Ti-catalysed transformations were reported. A selection is shown in scheme 6.1 - a.<sup>4-6</sup> Moreover, organotitanium reagents were extensively used in the generation of multiple natural products.<sup>7-9</sup> The versatility of the titanium complexes relies on their strong Lewis acid-character and on the facile *in situ* reduction of the stable  $Ti^{4+}$  species to  $Ti^{3+}$  and  $Ti^{2+}$  compounds.<sup>5</sup> This reduction process can be made in a controlled manner depending on the utilized reducing agent, therefore enabling the catalytic activity of organotitanium species in various radical transformations (Scheme 6.1 - b). The most common  $Ti^{4+}$  compounds used in synthesis as catalyst or precatalysts are titanium tetrachloride ( $TiCl_4$ ) (**C45**), titanium isopropoxide ( $Ti(O^iPr)_4$ ) (**C46**) and titanocene dichloride ( $Cp_2TiCl_2$ ) (**C36**) (Scheme 6.1 - c). Due to their oxophilicity, Ti-based catalysts proved to be very potent for the transformation of various substrates bearing oxo-functionalities, the reaction pathway being dictated by the oxidation state of the Ti-complex. Other characteristics, which make this compound class being very attractive are the cost-effectiveness and accessibility, as Ti is the second most abundant transition metal in Earth's crust. Additionally, the generation of non-toxic by-products is an advantage, as most Ti complexes easily degrade through oxidation to  $TiO_2$ .<sup>10</sup>

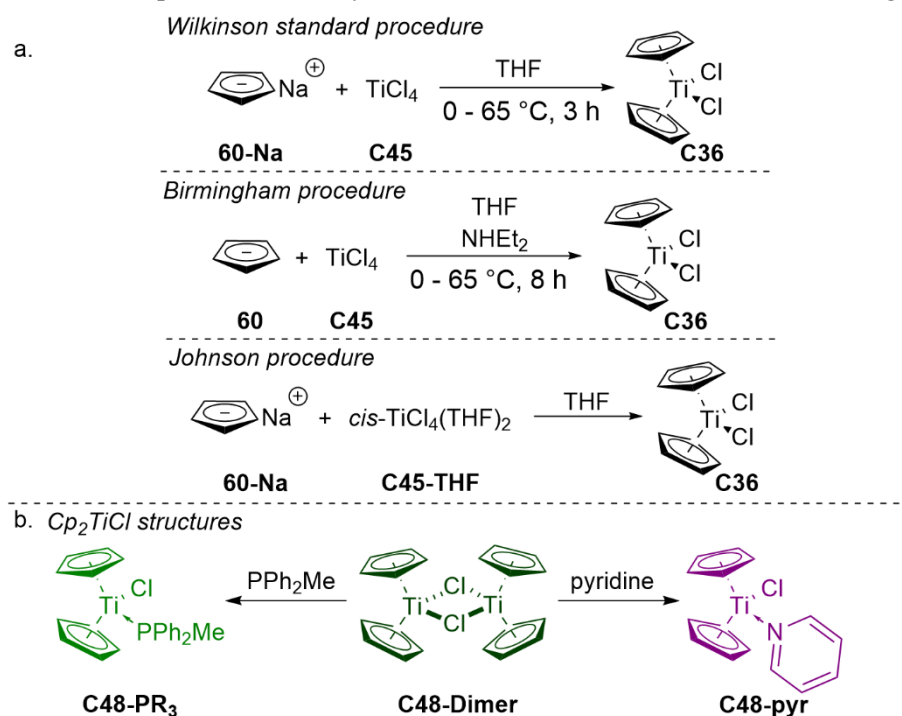


**Scheme 6.1.** (a) Examples of transformations catalysed by organotitanium species: 1. Kulinkovich reaction;<sup>11</sup> 2. Reformatsky reaction;<sup>12</sup> 3. McMurry coupling;<sup>13</sup> 4. Metal-catalysed Reppe reaction;<sup>14</sup> 5. Barbier-type reaction;<sup>15</sup> 6. Sharpless epoxidation;<sup>16</sup> (b) Generation of low-valent Ti species;

(c) Commonly utilized  $\text{Ti}^{4+}$  compounds; prices are adapted from <https://www.sigmaaldrich.com/> 16.10.2023.

As it was previously mentioned, titanocene dichloride (**C36**) emerged as one of the most valuable organotitanium complexes for synthetic applications, in both stoichiometric and catalytic amounts. Although it is more expensive than other commonly used Ti sources, its bench-top stability and facile handling can counterbalance the economic drawback (Scheme 6.1 - c). Furthermore,  $\text{Cp}_2\text{TiCl}_2$  (**C36**) is compliant to most of the green chemistry principles described by Anastas and Warner in 1998 and Winterton in 2001.<sup>17-19</sup> Later,  $\text{Cp}_2\text{TiCl}_2$ -derivatives were synthesised in order to fine-tune its electronic and steric properties. Along with titanocene dichloride (**C36**), (pentamethylcyclopentadienyl)titanium trichloride ( $\text{Cp}^*\text{TiCl}_3$ ) (**C47**) was also used in the deoxygenation procedures developed after 2010. These procedures will be extensively discussed in chapter 6.1.2.

The first synthesis of titanocene dichloride (**C36**) was reported by Wilkinson and Birmingham in 1954 and consists of the slow addition of the freshly prepared cyclopentadienyl sodium (**60-Na**) solution over a titanium tetrachloride (**C45**) solution in THF at  $0^\circ\text{C}$  under vigorous stirring.<sup>20</sup> This robust synthetic procedure is still considered as the standard method for obtaining  $\text{Cp}_2\text{TiCl}_2$  (**C36**) (Scheme 6.2 - a). Later, several variations of this method were developed, but with only minor changes compared to the standard procedure (Scheme 6.2 - a). In 1972, Green and Lucas reduced  $\text{Cp}_2\text{TiCl}_2$  (**C36**) to  $\text{Cp}_2\text{TiCl}$  (**C48**) with Zn powder and characterized for the first time the structures, which  $\text{Cp}_2\text{TiCl}$  (**C48**) adopts in solid state and in solution. During this study, the  $\text{Cp}_2\text{TiCl}$  (**C48**) solution was treated with various amines and phosphines and the formed complexes were isolated and analysed through electron spin resonance spectroscopy (ESR) (Scheme 6.2 - b). These measurements revealed that the added N- and P-compounds were able to stabilise the monomeric structure of the  $\text{Ti}^{3+}$  complex through the lone electron pair. Additionally, colorimetric observations were made during this study.



**Scheme 6.2.** (a) Standard procedure for the generation of  $\text{Cp}_2\text{TiCl}_2$  and its variations;<sup>20</sup> (b)  $\text{Cp}_2\text{TiCl}$  structures in solution and colorimetric observation.<sup>21, 22</sup>

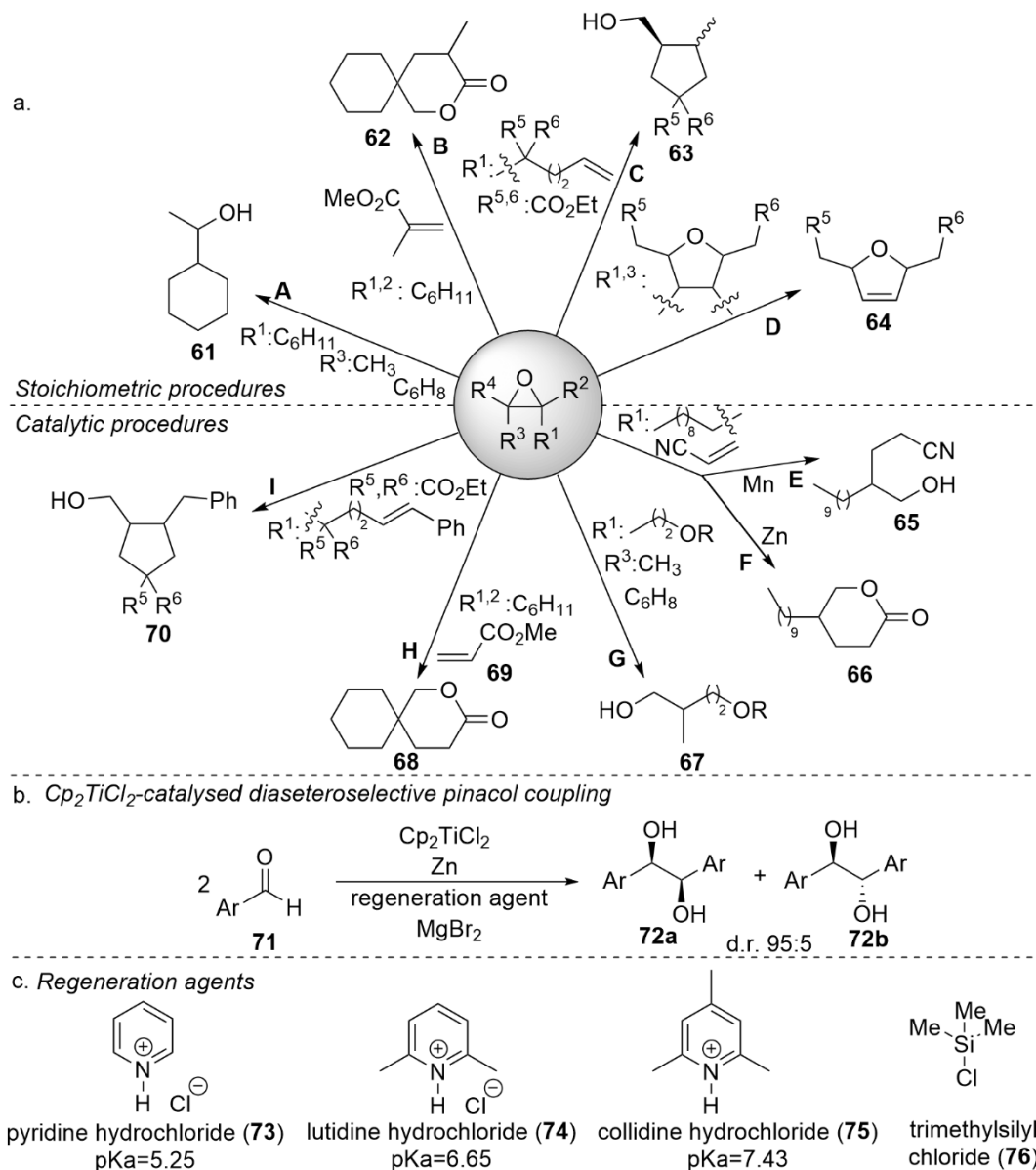
In 1988, Nugent and RajanBabu reported the first  $\text{Cp}_2\text{TiCl}_2$ -mediated transformation, namely the cyclization of epoxy olefins, which showed a high degree of chemo- and regioselectivity (Scheme 6.3 – a, A).<sup>23</sup> Based on the observations made during this study, it was presumed that the reaction follows a radical pathway. In the first step,  $\text{Cp}_2\text{TiCl}_2$  (**C36**) is reduced by Zn to a  $\text{Cp}_2\text{TiCl}$  (**C48**) radical species giving the characteristic green colour of  $\text{Ti}^{3+}$  in solution. Due to this procedure,  $\text{Cp}_2\text{TiCl}$  (**C48**) is also known as Nugent-RajanBabu reagent. Upon addition of the epoxide, the solution turns red hinting towards a reoxidation process of the organotitanium complex and the subsequent generation of the alkyl radical, which further undergoes cyclisation. Although in this protocol 2 equivalents of (**C36**) are needed for formation of the desired product in satisfactory yields, this report provides important information about the capabilities of  $\text{Cp}_2\text{TiCl}$  (**C48**) in single electron transfer processes.<sup>24</sup>

Consequently, Nugent and RajanBabu continued the pursuit of gaining more understanding about the radical generation process and further developed protocols for the regioselective reduction of epoxides, the intermolecular addition of epoxides to activated olefins and deoxygenation of the epoxides with the formation of the corresponding alkene.<sup>24-26</sup> However, the main disadvantage of these  $\text{Cp}_2\text{TiCl}_2$ -based (**C36**) procedures persisted, namely the requirement for stoichiometric amounts of organotitanium reagent (Scheme 6.3 - a, A-D).

This drawback was overcome by Gansäuer *et al.* during their studies on the cyclization of epoxy olefins (Scheme 6.3 – a, I).<sup>27</sup> Remarkably, this protocol led to the same chemo- and regioselectivity as the previously described stoichiometric procedures.<sup>28, 29</sup> In the initial steps of the process development, it was hypothesised that the addition of a Brønsted acid would lead to the protonation of the Ti-bound oxygen atom, thus lowering the Ti-O BDE, and subsequently to the regeneration of the  $\text{Ti}^{3+}$  species. This acid should be strong enough to protonate the O-atom but not strong enough to open the epoxide ring, to react with the metallic reducing agent or to deactivate the catalytically active species. Following the preliminary screenings, it was concluded that the best suited regeneration agent would be 2,4,6-trimethylpyridine (collidine) hydrochloride (**75**), due to its pKa. A later, exhaustive study on the regeneration agents suitable for  $\text{Cp}_2\text{TiCl}$ -catalysed transformations showed that the optimal pKa value of the acid should be between 5.25 (pKa value of pyridine hydrochloride **73**) and 12.5, which is 3 units lower than the pKa value of methanol (pKa value 15.5). The lower value was chosen because pyridine can act as a mild acid in chloroform and open the epoxide ring. Thus, beside collidine hydrochloride, lutidine hydrochloride (**74**) was also suitable as regeneration additive (Scheme 6.3 – c).

Another important information extracted during these studies was the distinct behaviour of Zn and Mn in these catalytic systems. For the intramolecular cyclization, Mn proved to be more efficient in generating the Ti-based active species and inhibiting the generation of chlorinated side-products. In contrast, in the intermolecular reaction between an epoxide and methyl acrylate (**69**), Mn was not able to produce the desired product, thus Zn was better suited for the transformation (Scheme 6.3 - a, H). This difference in reactivity between the two reducing metals is the result of the different Lewis acid-character of the resulted metal chlorides,  $\text{MnCl}_2$  being a weaker Lewis acid compared to  $\text{ZnCl}_2$ . Therefore, the latter is able to complex the *in situ* generated methanol, thus preventing the deactivation of the Ti catalyst. Interestingly, the addition of  $\text{ZnCl}_2$  to the reaction with Mn enhanced its reduction capabilities and the reaction yielded the desired product in similar yield as the Zn reaction. The beneficial role of zinc chloride for the cyclization reactions was also observed when methyl acrylate (**69**) was exchanged with other activated olefins like acrylonitrile (Scheme 6.3 - a, E and ).<sup>30</sup> Later, the group expanded the field of applications for the  $\text{Cp}_2\text{TiCl}_2$ -Mn catalytic system by applying it for the

diastereoselective pinacol coupling (Scheme 6.3 - b).<sup>31</sup> Analogous to the previously described transformations, collidine hydrochloride (**75**) proved to be the most efficient regeneration agent from the perspective of diastereoselectivity. In contrast to other reported intermolecular protocols, Mn was better suited than Zn as stoichiometric reductant in this reaction due to the inability of manganese to promote any side-reactions. The disadvantage of this procedure was the narrow scope of aldehydes, which could be transformed through this method. This was later overcome by using chlorotrimethylsilane (TMSCl) (**76**) as regenerating agent, albeit with considerably lower diastereoselectivity.<sup>32</sup>

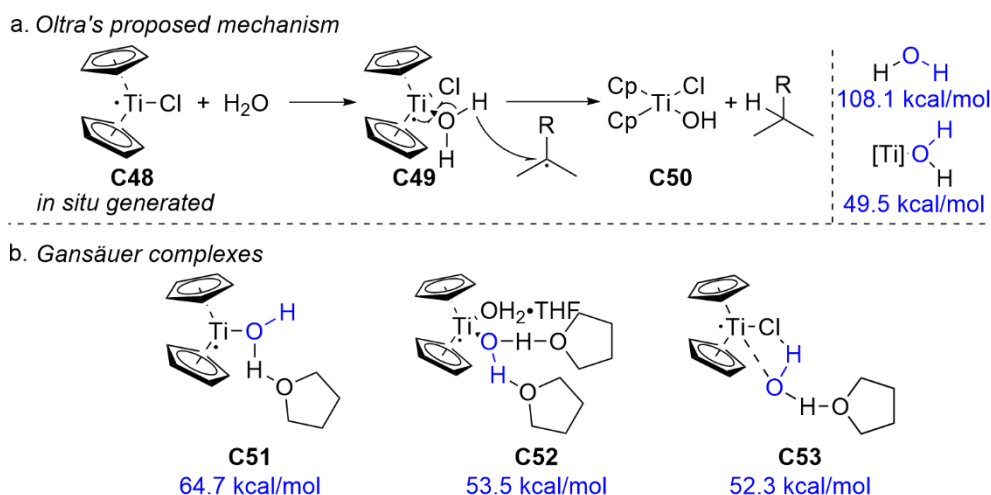


**Scheme 6.3.** (a) Stoichiometric (SP) procedures developed by Nugent and RajanBabu and catalytic procedures (CP) developed by Gansäuer mediated by  $Cp_2TiCl_2$ ;<sup>23-28, 31</sup> (b) Diastereoselective  $Cp_2TiCl_2$ -catalysed pinacol coupling;<sup>31, 32</sup> (c) Regeneration agents and their corresponding pKa values.<sup>28</sup>

Another report worth mentioning in the frame of this thesis is the work of the group of Doris on the  $Cp_2TiCl_2$ -mediated selective reduction of  $\alpha,\beta$ -unsaturated ketones.<sup>33</sup> In order to selectively hydrogenate the C-C double bond the reaction was conducted in a THF/MeOH solvent mixture. The experiments conducted with deuterated methanol showed a deuterium incorporation of >90% in both  $\alpha$



and  $\beta$  position, thus concluding that  $\text{Cp}_2\text{TiCl}$  (**C48**) was able to enhance the H-donor capabilities of the co-solvent. The capabilities of the low-valent  $\text{Ti}^{3+}$  species to promote the hydrogen donation was also observed by Barrero *et al.* during their studies radical cyclization of epoxygermacrolides.<sup>34</sup> In this case,  $\text{Cp}_2\text{TiCl}$  (**C48**) facilitated the hydrogen atom transfer from water to a C-centred radical, this being the first instance in which such a transfer was accomplished. This phenomenon was later extensively studied by the groups of Oltra and Gansäuer (Scheme 6.4). The experimental and theoretical investigations of Oltra hinted towards a mechanism that involves the generation of complex **C49**, followed by the homolytic dissociation of the O-H bond and generation of complex **C50** (Scheme 6.4 - a). The computational experiments showed that this bond cleavage is possible due to the decrease in bond dissociation energy (BDE), from 108.1 kcal/mol to 49.4 kcal/mol, following the coordination of water to the  $\text{Ti}^{3+}$  complex.<sup>35</sup> In addition, Gansäuer *et al.* proposed other possible HAT-active Ti-species complexes like **C51**, **C52** and **C53** (Scheme 6.4 - b).<sup>36</sup>



**Scheme 6.4.** (a) Hydrogen transfer mechanism for  $\text{Ti}^{3+}$ /water system proposed by Oltra's group;<sup>35</sup> (b) HAT-active complexes proposed by Gansäuer.<sup>36</sup>

### 6.1.2. Ti-Catalysed Deoxygenation of Alcohols

In 2010, Barrero's group published a Ti-mediated procedure for the deoxygenation of alcohols and diols (Scheme 6.5).<sup>37</sup> This methodology employed a stoichiometric amount of the complex **C36** and manganese as a reducing agent in THF. Tetrahydrofuran was chosen as solvent in this transformation due to its stabilizing properties towards radical Ti species. The hypothesis that this system would be able to facilitate the cleavage of the alcoholic C-O bond was based on the previously presented studies of Cuerva *et al.* on the H-donation capabilities of water *via* the formation of an intermediate complex **C49**.<sup>35</sup>

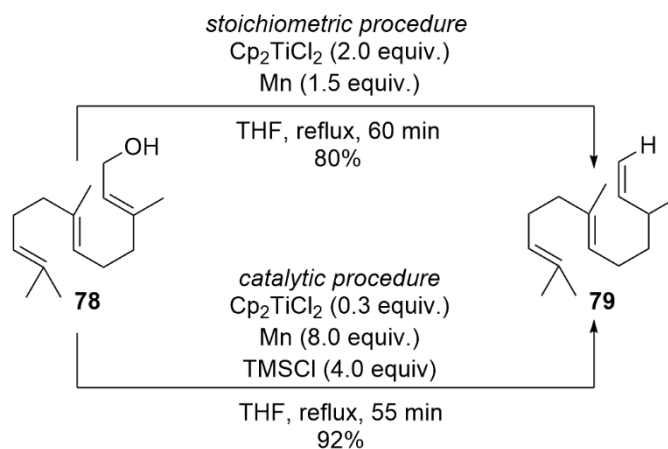
In order to prove that a C-O bond cleavage would be also possible for Ti-complexed alcohols, a DFT calculation was conducted. These computational studies showed that the C-O bond dissociation energy decreased significantly due to complexation for all tested alcohols compared to their noncomplexed counterparts (Table 6.1). Additionally, the benzylic and allylic positions would be most favoured for the homolytic cleavage of the C-O bond as shown in the lower BDEs (Table 6.1 – Entries 1 and 2).

**Table 6.1** Examples of bond dissociation energies for complexed<sup>37</sup> and noncomplexed alcohols.<sup>38, 39</sup>

Entry <sup>[a]</sup>	Alcohols	C-O BDE for uncomplexed alcohols (kcal/mol)	C-O BDE for complexed alcohols (kcal/mol)
1	Allyl alcohol	80.1	30.0
2	Benzyl alcohol	82.6	31.7
3	<i>n</i> -propanol	94.4	41.7
4	Phenol	112.4	52.3

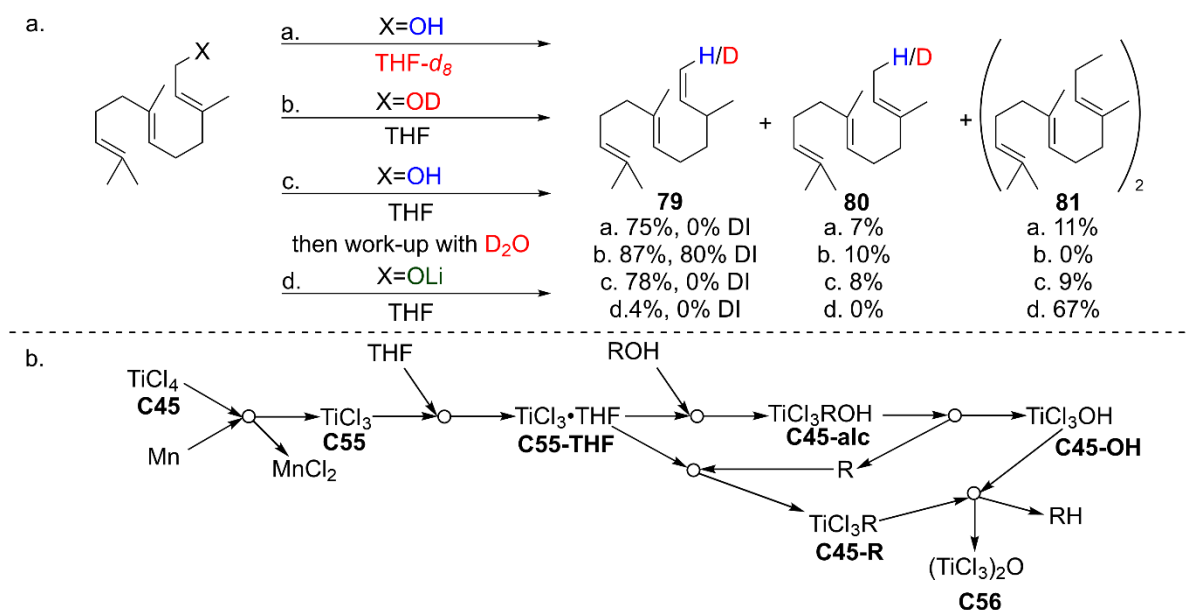
Thus, 2.1 equivalents of Ti precatalyst and 8 equivalents of Mn in THF under reflux conditions were able to deoxygenate benzyl alcohol (**4a**) to toluene (**2a**) in 93% yield. By halving the amount of Cp<sub>2</sub>TiCl<sub>2</sub> (**C36**), toluene (**2a**) was afforded in 47% yield. This result hinted towards the formation of a benzyl-Ti complex during the reaction. Further optimization of the reaction conditions showed that a 1:1.5 ratio between the Ti precatalyst and the reducing agent is optimal for this transformation. These reactions conditions were successfully used for the deoxygenation of various benzylic and allylic alcohols. Moreover, the system tolerated other easily reducible functionalities like carbonyls and double bonds, thus exhibiting a high degree of chemoselectivity. Due to the higher BDE of C(sp<sup>3</sup>)-O in aliphatic alcohols, solvents with higher boiling points were utilized for their deoxygenation. Nevertheless, a 1:1 mixture between the corresponding alkane and alkene was obtained showing the limited activity of the system on non-activated alcohols. By using the standard stoichiometry, aliphatic and aromatic 1,2-diols were transformed into the corresponding olefin. It was presumed that this reaction proceeds through a sequential cleavage of the C-O bonds, hence, leading to the radical formation of the double bond.

Following the results obtained by using the stoichiometric procedure for the deoxygenation of alcohols, a catalytic approach for this transformation was endeavoured. In order to achieve this goal, the regeneration of the catalytically active Ti<sup>3+</sup> was needed. It was proposed that TMSCl (**76**) could facilitate this process by inhibiting the formation of the Cp<sub>2</sub>Ti=O (**C54**) species through the formation of hexamethyldisiloxane (**77**). Indeed, the utilization of 30 mol% of Cp<sub>2</sub>TiCl<sub>2</sub> (**C36**), 8 equiv. of Mn and 4 equiv. of TMSCl (**76**), farnesol (**78**) was transformed into the desired product (**79**) in 92% yield. This catalytic procedure was later successfully applied for the deoxygenation of diols.

**Scheme 6.5.** Stoichiometric and catalytic procedures for the deoxygenation of alcohols developed by Barrero *et al.*<sup>37</sup>

Another contribution by Barrero is an exhaustive mechanistic study from 2015 on the stoichiometric deoxygenation procedure.<sup>40</sup> First, deuterium labelling experiments were performed on farnesol (**78**) as model substrate (Scheme 6.6 – a). No deuterated product was observed when THF-*d*<sub>8</sub> was used in the reaction nor when deuterated water was added during the reaction work-up. Instead, substituting the hydroxy group with an -OD moiety (**78-d**<sub>1</sub>), the corresponding deuterated alkane was afforded in very high yield and with 80% deuterium incorporation, hinting that the H-atom in the new C-H bond is provided by the hydroxy group. Additionally, a high regioselectivity of the deuteration process on allylic compounds was observed as the terminal olefin was almost exclusively formed. These results are in contrast to the ones obtained by using the Barton-McCombie conditions, which led to the formation of a 1:1 mixture between the two olefins **79** and **80**. Thus, a possible hydrogen atom transfer (HAT) pathway was dismissed for this reaction, and it was hypothesised that the Ti<sup>3+</sup> species acts in this reaction as a Lewis acid. Another argument for a -OH donation pathway was the formation of the farnesol dimer (**81**) as major product, when the hydrogen atom was substituted with Li in the starting material. All the conclusions taken from the experiments conducted on the allylic alcohols were confirmed when a benzylic substrate was submitted to the reaction.

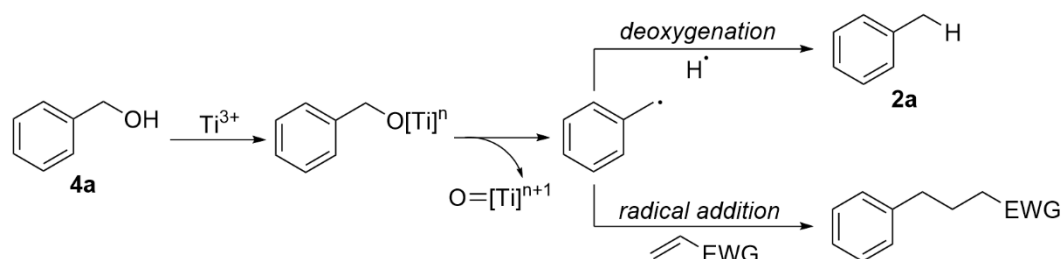
Furthermore, a kinetic modelling simulation for the stoichiometric process was conducted (Scheme 6.6 - b). For this calculations TiCl<sub>4</sub> (**C45**) was used as Ti source for simplifying the calculation. To see if such this simulation is still conclusive for this transformation, other reaction models were tested in a similar way and the results between Cp<sub>2</sub>TiCl<sub>2</sub> (**C36**) models and TiCl<sub>4</sub> (**C45**) models were analogous. Hence, the most energetically favourable pathway was discovered by calculating the reaction rates of each plausible individual step of the reaction. First, the Ti<sup>4+</sup> (**C45**) species is reduced by Mn to generate Ti<sup>3+</sup> (**C55**) to which a THF molecule coordinates generating **C55-THF**. The solvent molecule is substituted by the alcohol, which forms a complex **C45-alc** from which, through decomposing, an alkyl radical is generated. A competition between the dimerization of the radical and its reaction with another Ti<sup>3+</sup>•THF (**C55-THF**) occurs, the latter being favoured and generating TiCl<sub>3</sub>R (**C45-R**). Subsequently, the desired alkane is formed by the reaction between complex **C45-R** and TiCl<sub>3</sub>OH (**C45-OH**) and the generation of the Ti-O-Ti (**C56**) species.



**Scheme 6.6.** (a) Deuteration experiments for the deoxygenation procedure reported by Barrero's group; (b) Reaction pathway based on the kinetic modelling simulation made with Copasi.<sup>40</sup>

By simulating the transformation of different alcohols through the most plausible calculated route and comparing the results with the experimental yields, a correlation between the final data was observed, thus confirming the utility of the kinetic modelling simulation.

In 2018, Suga *et al.* reported a methodology for the generation of benzyl radicals by using a straightforward  $Ti^{4+}/Mn$  system (Scheme 6.7).<sup>41</sup> Based on this protocol both a deoxygenation and a Giese-type radical conjugated addition of electron-deficient olefins were developed. One major advantage of this protocol is that by changing the Ti additive the reaction will proceed selectively through one of the above mentioned pathways. Hence, the utilization of  $Cp_2TiCl_2$  (**C36**) will lead to the generation of the deoxygenation product, while  $TiCl_4$ (collidine) will facilitate the Giese-type addition. During the initial optimization stages of the deoxygenation reaction, a competitive polymerisation process of the benzyl radicals was observed. This undesired side-reaction was completely inhibited by the usage of 2.1 equivalents of  $Cp_2TiCl_2$  (**C36**), thus yielding the deoxygenation product in an excellent yield of 82%.

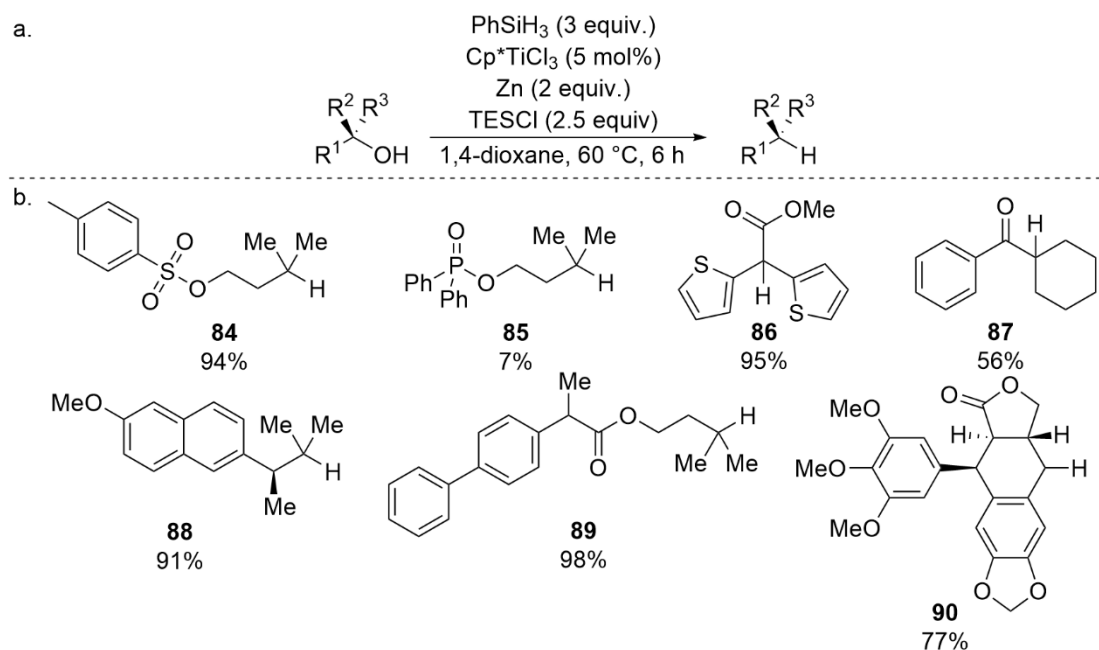


**Scheme 6.7.** Benzyl radical generation methodology reported by Suga *et al.*<sup>41</sup>

The increased interest for direct deoxygenation procedures led to the development of new  $Ti$ -catalysed procedures for the deoxygenation of alcohols. Recently, Lin and co-workers reported a regioselective deoxygenation protocol for tertiary alcohols (Scheme 6.8 - a).<sup>42</sup> This transformation utilized  $Cp^*TiCl_3$  (**C47**) in catalytic amounts,  $Zn$  as reducing agent, phenylsilane ( $PhSiH_3$ ) (**82**) as  $H$ -donor and triethylsilylchloride ( $TESCl$ ) (**83**) as regenerating agent for the catalyst. During the optimization experiments, it was observed that, beside the electronic properties, the steric hindrance of the metal catalyst plays a major role in this transformation. Thus,  $Cp^*TiCl_3$  (**C47**) catalysed the reaction in excellent yield of 89%, while less-sterically hindered cyclopentadienyltitanium trichloride ( $CpTiCl_3$ ) (**C57**) afforded the desired product only in 7% yield and  $Cp_2TiCl_2$  (**C36**) in 59% yield. Interestingly, the use of  $Mn$  instead of  $Zn$  in this catalytic process inhibited the conversion of the alcohol completely. The control reactions showed that in the absence of the  $Ti$ -catalyst, reducing agent or regeneration agent, the desired transformation was not possible. However, the reaction conducted without phenylsilane (**82**) led to the generation of corresponding alkane in 71% yield. Besides, a considerable amount of various olefins was detected in the reaction mixture. This result showed that, beside the  $H$ -donor capabilities, phenylsilane (**82**) is also responsible for inhibiting possible side-reactions. Additionally, it hinted towards the existence of a background  $H$ -transfer process from another reaction component. Further, the optimized reaction conditions were applied for the deoxygenation of tertiary aliphatic alcohols bearing different backbones and functionalities (Scheme 6.8 - b). Remarkably, sulfone, phosphate and heterocycle moieties were tolerated by the system, yielding the deoxygenated product in very good yields. When the method was applied for the transformation of alcohols bearing  $\alpha$ -carbonyl groups, the reduction of the latter was also observed as a minor side-reaction. Secondary benzylic alcohols were

also deoxygenated by this catalytic system, albeit with decreased yields. Subsequently, this procedure was employed for the reduction of alcoholic moieties in bioactive molecules. Hence, (*S*)-naproxen (**88**), flurbiprofen-derivatives (**89**) and podophyllotoxin (**90**) were successfully deoxygenated in very good and excellent yields. The limitation of this method is represented by the ring-opening of epoxy groups, the complexation of nitril groups and the cleavage of the C-X bond in aliphatic halides.

The regioselectivity of the procedure was examined by applying the system for the deoxygenation of various diols. In all cases, primary and unactivated secondary -OH groups were unreactive under these reaction conditions, thus, proving the selectivity of the system towards tertiary and activated secondary alcoholic moieties.

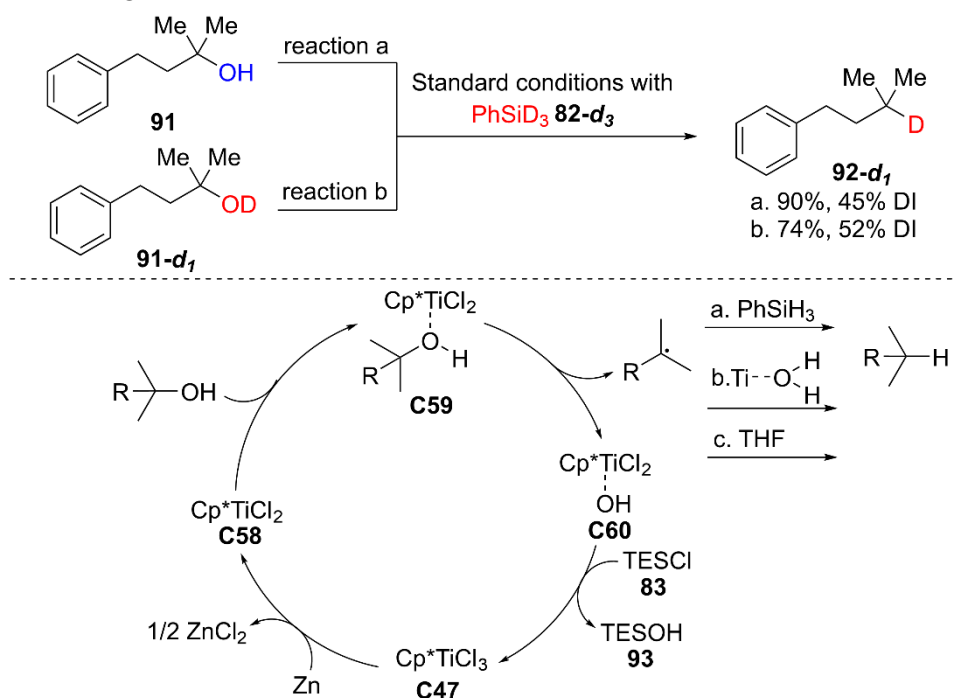


**Scheme 6.8.** (a) General reaction of the deoxygenation procedure developed by Lin *et al.*; (b) Substrate scope of the Ti-catalysed deoxygenation method.<sup>42</sup>

When phenylsilane (**82**) was substituted by its deuterated counterpart (**82-*d*<sub>3</sub>**), the desired product was obtained with only 45% deuterium incorporation (DI) (Scheme 6.9 - a). This result hinted towards the importance of the background hydrogen transfer process. In order to get more insight about this unexpected HAT-process, multiple experiments were conducted on deuterated substrate (**91-*d*<sub>1</sub>**) and by using different deuterated reaction components. Surprisingly, employing **82-*d*<sub>3</sub>** for the transformation of **91-*d*<sub>1</sub>** led to a deuterium incorporation of only 52% in **92-*d*<sub>1</sub>**. Therefore, a possible hydrogen donation pathway similar to the one proposed by the group of Barrero was discarded. The involvement of the regeneration agent or the *in situ* generated water in the background hydrogen atom transfer mechanism was tested but it was considered improbable because the employment of deuterated water and fresh TESCl (**83**) led to very low DI. In conclusion, it was hypothesised that a solvent H-donation pathway or an intramolecular hydrogen transfer might be involved in this process, but this presumption was not further investigated.

Based on the results of the deuterium labelling studies, a reaction mechanism was proposed (Scheme 6.9 - b). First, the titanium precatalyst **C47** was reduced to the corresponding  $\text{Ti}^{3+}$  species **C58**, which further reacted with the alcohol to generate complex **C59**. The cleavage of species **C59** led to the formation of Ti-OH complex **C60** and an alkyl or aryl radical, which generated the desired alkane,

via one of the possible H-donation pathways. Subsequently, complex **C60** led to the regeneration of the precatalyst **C47** through the reaction with the chlorosilane **83**.



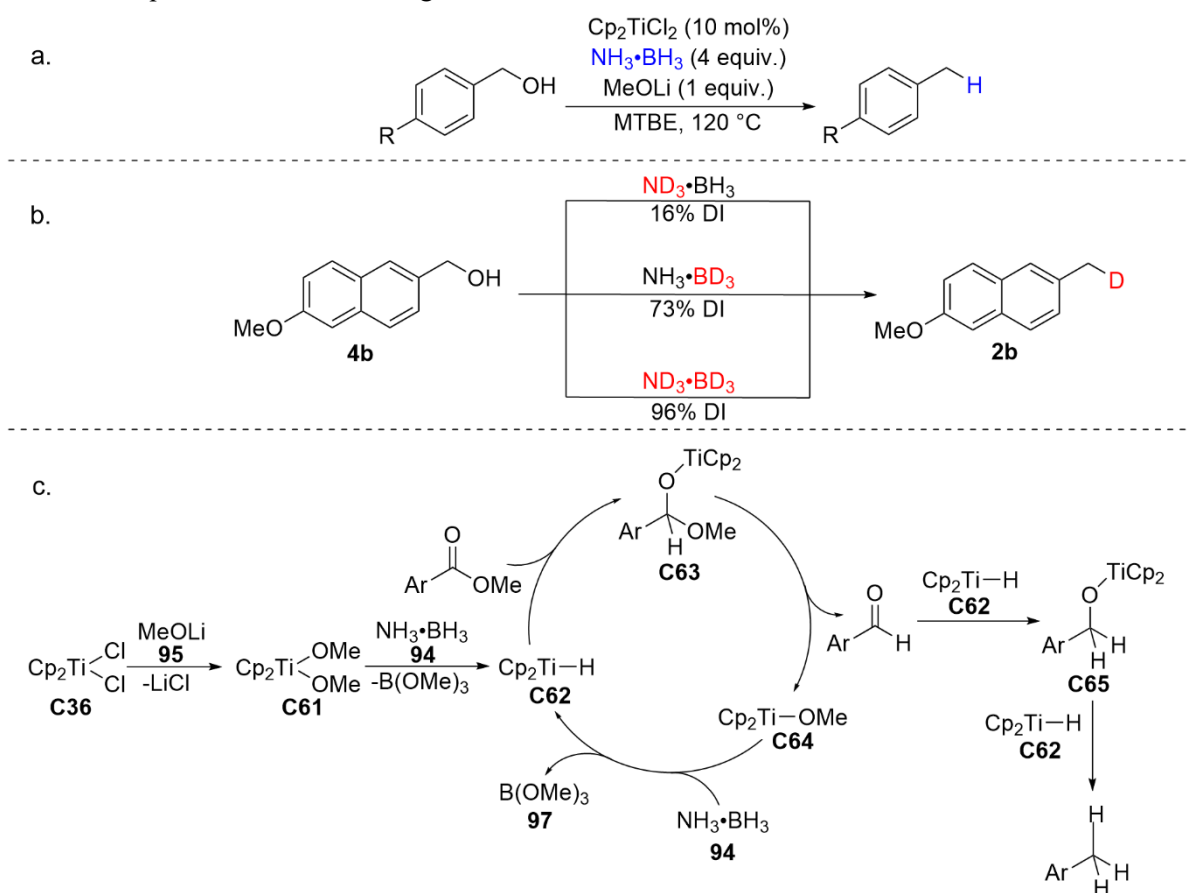
**Scheme 6.9.** (a) Deuteration experiments conducted by Lin *et al.*; (b) Proposed mechanism for the Ti-catalysed deoxygenation.<sup>42</sup>

Also in 2022, Han *et al.* reported an exhaustive reduction procedure for benzylic oxo-compounds (Scheme 6.10 - a).<sup>43</sup> The main goal of this study was the development of a direct deoxygenation method of esters and carboxylic acids to the corresponding alkanes. Later, the same procedure was applied also for the deoxygenation of carbonyls and alcohols. This methodology utilizes a  $\text{Ti}^{4+}$  as precatalyst, ammonium borane (**94**) as hydrogen donor and a base as activating agent. Interestingly, no metallic reductant was needed for the successful deoxygenation of any of the tested substrate classes. The optimization studies showed that both the use of a titanium precatalyst and the base are essential for the deoxygenation.  $\text{Cp}_2\text{TiCl}_2$  (**C36**) showed the highest reactivity towards the desired transformation, thus leading to the formation of the corresponding alkanes in quantitative yields. Multiple bases were tested in the catalytic system from which lithium methoxide (**95**) proved to be the most effective. After testing the optimal reaction conditions on the complete reduction of esters, the procedure was used for the deoxygenation of benzylic alcohols. Both electron-neutral and electron-rich alcohols were transformed into the corresponding alkanes in very good yields through this method.

The preliminary mechanistic studies focused on the investigation of possible intermediates. First, benzyl methyl ether (**96**) was subjected to the transformation, but this reaction yielded only traces of the desired product, thus, discarding the involvement of an ethereal intermediate in the reaction pathway. By stopping the reduction of esters before completion, traces of alcohol were detected. Moreover, the addition of pyrrolidine as trapping agent in the same reaction led to the formation of the corresponding amine, hence, pointing out the *in situ* formation of aldehydes during the transformation. Following the evolution of the reaction *via*  $^{11}\text{B}$ -NMR, the formation of  $\text{B}(\text{OMe})_3$  (**97**) and  $\text{B}(\text{O}^i\text{Bu})_3$  (**98**) was detected. The specific colour change of the solution from orange to dark green hinted towards the

formation of a  $\text{Ti}^{3+}$  active species. This observation was endorsed through ESR spectroscopy. Interestingly, by using deuterated ammonium borane  $\text{ND}_3\cdot\text{BD}_3$  (**94-dd**) a new signal appeared in the EPR spectra and the hyperfine splitting of  $^{49}\text{Ti}$  was observed. This result suggests a possible formation of a Ti-H complex. Further isotope-labelling experiments showed that the deuterium incorporation was significantly higher when  $\text{NH}_3\cdot\text{BD}_3$  (**94-hd**) was employed compared to  $\text{ND}_3\cdot\text{BH}_3$  (**94-dh**) (Scheme 6.10 - b).

Therefore, a possible mechanism for the exhaustive reduction of esters was projected (Scheme 6.10 - c). First, the precatalyst (**C36**) reacts with  $\text{MeOLi}$  (**95**) to generate complex **C61**, which further leads to the formation of the catalytic active complex **C62**. Then, the substrate inserts to the titanium hydride species **C62** generating complex **C63**, which undergoes  $\beta$ -O elimination. Subsequently, intermediate aldehyde and complex **C64** are formed. The latter reacts with ammonium borane **94** to regenerate the active species **C62**. The *in situ* generated aldehyde undergoes a similar reduction sequence like the ester to generate the desired alkane.



**Scheme 6.10.** Deoxygenation procedure developed by Han *et al.* (a) General reaction for the deoxygenation of benzylic alcohols; (b) Deuteration experiments; (c) Proposed mechanism for the exhaustive deoxygenation of esters.<sup>43</sup>

Thus, titanocene dichloride (**C36**) was considered a suitable candidate for enhancing the catalytic activity of the previously developed Co- based system for the catalytic deoxygenation of benzylic alcohols.

## 6.2. Co/Ti Co-Catalysed Deoxygenation

### 6.2.1. Preliminary Investigations

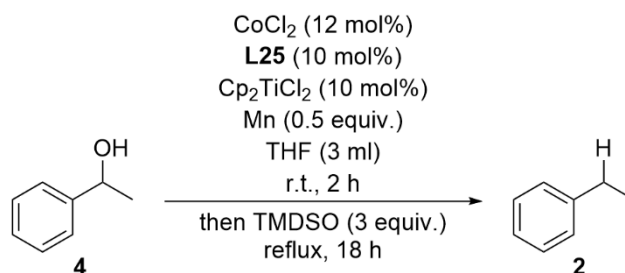
The preliminary studies on the deoxygenation of benzylic alcohols by using a bimetallic Co/Ti system started with the selection of a suitable  $Ti^{4+}$  species and metallic reducing agent. Based on the previously presented literature reports and on handling considerations,  $Cp_2TiCl_2$  (**C36**) was considered the most suitable candidate for this purpose.<sup>44</sup> In these reactions, Mn was employed as metallic reductant in the standard procedure due to the inefficiency of Zn in the Co-catalysed experiments described in chapter 5.3. The choice of PNP-ligands **L9** and **L25** and  $CoCl_2$  (**C24**) for these preliminary investigations was based on both literature reports and facile *ex situ* synthesis of the corresponding  $Co^{1+}$  complex. Additionally, the ability of salen **L27** to generate a catalytically active complex with cobalt was investigated. Due to the incompatibility of formic acid (**11**) with the Ti source, another potential H-donor had to be chosen, thus, TMDSO (**98**) was employed during these studies. A possible side-reaction that might occur from the utilization of  $Co^{1+}$  complexes and silanes is the hydrosilylation of the olefin intermediate **3**. Although the side-reaction between THF and the alcoholic substrate was observed throughout the investigations presented in chapter 5.3, anhydrous, degassed THF was chosen as the standard solvent for this procedure due the literature reports, which suggest that tetrahydrofuran is the best suitable solvent for the generation of  $Ti^{3+}$  species.

The initial conditions screening started with a one-pot reaction, in which all components were stirred in THF for 18 h (Table 6.2. – Entry 1). Remarkably, this procedure led to 87% conversion of the starting material and afforded ethylbenzene (**2**) in a 53% yield. Although this result was encouraging, the analysis of the crude reaction mixture *via* GC-MS showed the formation of various high molecular mass side-products. Thus, a two-pot procedure was attempted in order to reduce the number and amount of side-products. This approach implies the addition of a separately prepared Co-ligand complex solution over the  $Ti^{3+}$  complex mixture, followed by overnight stirring at reflux. First, both solutions were prepared in THF and this procedure resulted in a 56% yield of ethylbenzene (**2**) and a 93% conversion (Table 6.2. – Entry 2). The preparation of the Ti solution in toluene led to a decrease in both conversion and yield of alkane (Table 6.2. – Entry 3). The decrease was even more substantial when both solutions were prepared in toluene, despite the final reaction temperature being elevated from 80 °C to 110 °C (Table 6.2. – Entry 4). These experiments strengthened the hypothesis that THF would be the best suitable solvent for this protocol, albeit the reaction temperature is lower. Although the two-pot procedure in THF afforded a higher amount of ethylbenzene (**2**) compared to the one-pot reaction, the yield difference between the two was considered insufficient to overcome the handling disadvantages. Hence, the one-pot procedure was chosen for further experiments. Next, ligand **L25** was substituted by pyridine-based ligand **L9**, but the Co-**L9** complex proved to be less efficient in this transformation than the Co-**L25** complex (Table 6.2. – Entry 5). Instead, by substituting **L25** with salen **L27**, only traces of ethylbenzene (**2**) were generated beside considerable amounts of higher molecular mass compounds (Table 6.2. – Entry 6). The control reaction without the addition of a ligand, showed a very high conversion of the alcohol but did not afford any amount of ethylbenzene **2** (Table 6.2. – Entry 7). In order to inhibit the potential  $CoCl_2$ -catalysed side-reactions, an excess of ligand was added to the reaction mixture, but a 10% yield drop was observed compared to the standard procedure (Table 6.2. – Entry 8). The utilization of not degassed or undistilled THF as a solvent completely inhibited the formation of the desired product **2** (Table 6.2. – Entries 9 and 10). The addition of 3Å molecular sieves to the reaction led to a only 12% yield of **2**, instead high quantities of styrene were observed in the final mixture (Table 6.2. – Entry 11). The utilization of Zn instead of Mn in this



procedure lowered the ethylbenzene (**2**) yield to 16% and without the addition of the metallic reductant no desired product **2** was detected (Table 6.2. – Entries 12 and 13). In conclusion, 1,1,3,3-Tetramethyldisiloxane TMDSO (**98**) proved its H-donor capabilities in this protocol and **L25** was the most efficient ligand from the ones which were tested during this study. Additionally, the *in situ* generation of the Co catalyst is desired for this transformation. In order to further increase the yield of the desired alkane additional optimization reactions were conducted.

**Table 6.2.** Preliminary conditions screening of the Co/Ti-catalysed deoxygenation



Entry <sup>[a]</sup>	Deviation	Conversion (%) <sup>[b]</sup>	Yield (%) <sup>[b]</sup>
1	one pot	87	53
2	Two solutions THF	93	56
3	Two solutions Co – THF, Ti - toluene	67	49
4	Two solutions both tol.	31	20
5	<b>L9</b> instead of <b>L25</b>	80	48
6	<b>L27</b> instead of <b>L25</b>	63	traces
7	Without ligand	80	-
8	15 mol% <b>L25</b>	86	43
9	Not degassed solvent	19	-
10	Undistilled solvent	-	-
11	3 Å M.S.	90	12
12	Zn instead of Mn	40	16
13	Without reducing agent	67	-

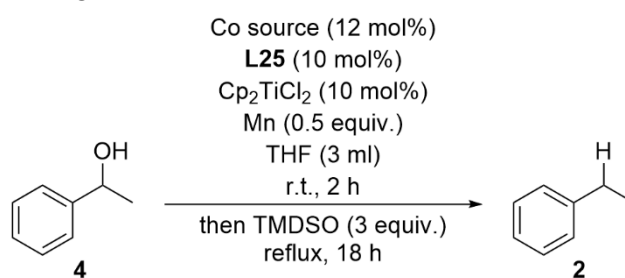
[a] Standard reaction conditions: In a Schlenk pressure tube anhydrous  $\text{CoCl}_2$  (15.6 mg, 0.12 mmol, 12.0 mol%), ligand **L25** (0.036 mL 0.20 mmol, 20.0 mol%), additive (0.20 mmol, 20.0 mol%),  $\text{Cp}_2\text{TiCl}_2$  (24.9 mg, 0.10 mmol, 10.0 mol%), Mn (27.5 mg, 0.50 mmol, 0.50 equiv.) and 1-phenylethanol (0.120 mL, 1.00 mmol, 1.00 equiv.) in THF (3 mL) stirred for 30 min. at r.t., then TMDSO (0.53 mL, 3.00 mmol, 3.00 equiv.) stirred for 18 h at reflux; [b] Yields were determined *via* quantitative GC-FID using *n*-pentadecane as internal standard;

### 6.2.2. Conditions Screening

Following the initial condition optimization, a Co source screening was conducted. For this transformation, the activity of  $\text{CoCl}_2$  (**C24**),  $\text{CoBr}_2$  (**C25**) and  $\text{Co}(\text{acac})_2$  (**C22**) was investigated. All three Co sources were submitted to the reaction solely or together with LiCl. Lithium chloride increases the solubility of both the Co salt and metallic reductant, therefore it can facilitate the formation of the

Co-active species. The addition of LiCl to the reaction with CoCl<sub>2</sub> (**C24**) led to a slightly higher conversion than the standard reaction but the yield of ethylbenzene (**2**) dropped considerably from 53% to 27% (Table 6.3. – Entry 2). This phenomenon was not further investigated, thus, it could not be fully explained. Interestingly, cobalt bromide (**C25**) was the most efficient Co source for this application (Table 6.3. – Entry 3). Moreover, the addition of LiCl to the reaction resulted in only a 2% yield decrease (Table 6.3. – Entry 4). The utilization of Co(acac)<sub>2</sub> (**C22**) inhibited almost completely the desired reaction pathway, both with and without the additive (Table 6.3. – Entries 5 and 6). Therefore, it was concluded that the most efficient cobalt source for this transformation is CoBr<sub>2</sub> (**C25**).

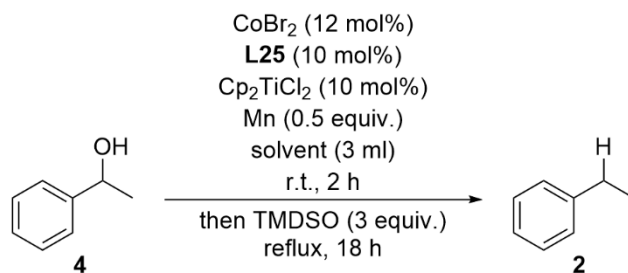
**Table 6.3.** Co source screening



Entry <sup>[a]</sup>	Co source	Conversion (%) <sup>[b]</sup>	Yield (%) <sup>[b]</sup>
1	CoCl <sub>2</sub>	87	53
2 <sup>[c]</sup>	CoCl <sub>2</sub>	90	27
3	CoBr <sub>2</sub>	98	57
4 <sup>[c]</sup>	CoBr <sub>2</sub>	92	55
5	Co(acac) <sub>2</sub>	41	traces
6 <sup>[c]</sup>	Co(acac) <sub>2</sub>	90	traces

[a] Standard reaction conditions: In a Schlenk pressure tube anhydrous Co source (0.12 mmol, 12.0 mol%), ligand **L25** (0.036 mL 0.20 mmol, 20.0 mol%), Cp<sub>2</sub>TiCl<sub>2</sub> (24.9 mg, 0.10 mmol, 10.0 mol%), Mn (27.5 mg, 0.50 mmol, 0.50 equiv.) and 1-phenylethanol (0.120 mL, 1.00 mmol, 1.00 equiv.) in THF (3 mL) stirred for 30 min. at r.t., then TMSO (0.53 mL, 3.00 mmol, 3.00 equiv.) stirred for 18 h at reflux; [b] Yields were determined *via* quantitative GC-FID using *n*-pentadecane as internal standard; [c] Reaction with 0.5 equiv. LiCl as additive

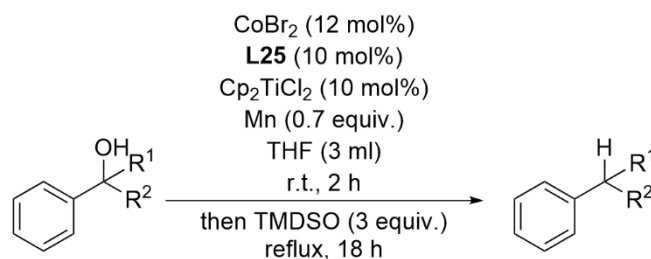
Next, a solvent screening was conducted. Due to the use of many reaction components, which can lead to unwanted side-reactions, the range of suitable solvents was narrowed. Tetrahydrofuran proved to be the most efficient solvent for this transformation, although the possible reaction temperature was the lowest throughout this screening (Table 6.4. – Entry 1). Unfortunately, in toluene the conversion decreased substantially from 98% to 53%, therefore, only a 20% yield of ethylbenzene (**2**) was obtained (Table 6.4. – Entry 2). In order to take advantage of the positive effect of THF on the transformation and to conduct the reaction at higher temperatures, a 1:1 mixture of THF and toluene was utilized (Table 6.4. – Entry 3). Indeed, the conversion of alcohol **4** was almost quantitative but the yield of compound **2** was 21% lower compared to the THF reaction. Lastly, 1,4-dioxane was used as solvent for this transformation (Table 6.4. – Entry 4). This solvent would be compliant with the previously stated high temperature principle and could also stabilize the *in situ* generated species similar to THF. However, this reaction afforded only a 15% yield of the desired product, despite the 98% conversion. Thus, THF was further utilized as the standard solvent during these investigations.

**Table 6.4.** Solvent screening

Entry <sup>[a]</sup>	Solvent	Temperature (°C) <sup>[c]</sup>	Conversion (%) <sup>[b]</sup>	Yield (%) <sup>[b]</sup>
1	THF	70	98	57
2	Toluene	120	53	20
3	THF:Toluene 1:1	110	96	36
4	1,4-dioxane	110	98	15

[a] Standard reaction conditions: In a Schlenk pressure tube anhydrous  $\text{CoBr}_2$  (26.2 mg, 0.12 mmol, 12.0 mol%), ligand **L25** (0.036 mL 0.20 mmol, 20.0 mol%),  $\text{Cp}_2\text{TiCl}_2$  (24.9 mg, 0.10 mmol, 10.0 mol%), Mn (27.5 mg, 0.50 mmol, 0.50 equiv.) and 1-phenylethanol (0.120 mL, 1.00 mmol, 1.00 equiv.) in solvent (3 mL) stirred for 30 min. at r.t., then TMSO (0.53 mL, 3.00 mmol, 3.00 equiv.) stirred for 18 h at reflux; [b] Yields were determined *via* quantitative GC-FID using *n*-pentadecane as internal standard; [c] Setup temperature;

Additionally, a preliminary substrate screening was made. Primary, secondary, and tertiary benzylic alcohols were tested. Benzyl alcohol (**4a**) was almost completely converted but afforded only 41% toluene (**2a**) (Table 6.5. – Entry 1). 57% of the secondary alcohol **4** was deoxygenated to compound **2**, while 2-phenylpropan-2-ol (**4b**) could not be transformed in cumene (**2b**, Table 6.5. - Entries 2 and 3). Hence, the deoxygenation of 1-phenylethanol (**4c**) was attempted during future studies.

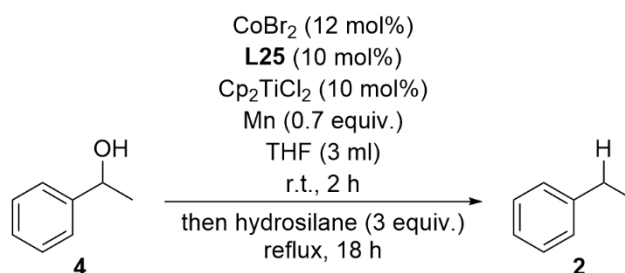
**Table 6.5.** Preliminary substrate screening

Entry <sup>[a]</sup>	Co source	Conversion (%) <sup>[b]</sup>	Yield (%) <sup>[b]</sup>
1	benzyl alcohol	96	41
2	1-phenylalcohol	98	57
3	2-phenylpropan-2-ol	60	-

[a] Standard reaction conditions: In a Schlenk pressure tube anhydrous  $\text{CoBr}_2$  (26.2 mg, 0.12 mmol, 12.0 mol%), ligand **L25** (0.036 mL 0.20 mmol, 20.0 mol%),  $\text{Cp}_2\text{TiCl}_2$  (24.9 mg, 0.10 mmol, 10.0 mol%), Mn (27.5 mg, 0.50 mmol, 0.50 equiv.) and alcohol (1.00 mmol, 1.00 equiv.) in THF (3 mL) stirred for 30 min. at r.t., then TMSO (0.53 mL, 3.00 mmol, 3.00 equiv.) stirred for 18 h at reflux; [b] Yields were determined *via* quantitative GC-FID using *n*-pentadecane as internal standard;

Another studied factor in this reaction was the nature of the silane. TMDSO (**98**) was extensively used during the development of the Co/Ti-based deoxygenation procedure due to its availability, low-toxicity, and H-donation properties but the resulting ethylbenzene yield did not exceed 57%. In this investigation, TMDSO (**98**) showed a 55% yield and a conversion of 96% (Table 6.6. – Entry 1). Thus, the H-donor capabilities of other hydrosilanes were tested. Phenylsilane (**82**) and diphenylsilane (**99**) led to low conversions and to very low yields of **2**, 6% and 8% respectively (Table 6.6. – Entries 2 and 3). Alkoxysilanes, namely triethoxysilane (**100**), were also used in deoxygenation reactions, for example in the reduction of amides.<sup>45</sup> Remarkably, the reaction with triethoxysilane (**100**) led to a 84% yield of ethylbenzene (**2**) and a complete conversion of the alcohol **4** (Table 6.6. – Entry 4).

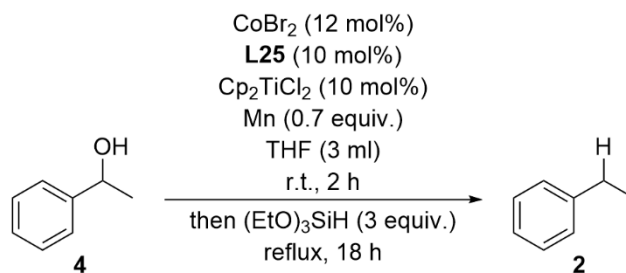
**Table 6.6.** Silane screening



Entry <sup>[a]</sup>	Solvent	Conversion (%) <sup>[b]</sup>	Yield (%) <sup>[b]</sup>
1	TMDSO	96	55
2	Phenylsilane	33	6
3	Diphenylsilane	54	8
4	Triethoxysilane	98	84

[a] Standard reaction conditions: In a Schlenk pressure tube anhydrous  $\text{CoBr}_2$  (26.2 mg, 0.12 mmol, 12.0 mol%), ligand **L25** (0.036 mL 0.20 mmol, 20.0 mol%),  $\text{Cp}_2\text{TiCl}_2$  (24.9 mg, 0.10 mmol, 10.0 mol%), Mn (27.5 mg, 0.50 mmol, 0.50 equiv.) and 1-phenylethanol (0.120 mL, 1.00 mmol, 1.00 equiv.) in THF (3 mL) stirred for 30 min. at r.t., then silane (3.00 mmol, 3.00 equiv.) stirred for 18 h at reflux; [b] Yields were determined *via* quantitative GC-FID using *n*-pentadecane as internal standard;

Following the results obtained during the hydrosilane screening, several control reactions were conducted. Without the addition of the Ti catalyst, no ethylbenzene was detected in the crude reaction mixture (Table 6.7. – Entry 1). Rather, the formation of high quantities of the corresponding silylether (**4-se**) was observed. Without the metallic reductant, traces of **2** were generated while the omission of the H-donor completely inhibited the transformation (Table 6.7. – Entries 2 and 3). Instead, the elimination of the Co source and the ligand led to the formation of ethylbenzene in a 62% yield (Table 6.7. – Entry 1). Thus, it was concluded that Co is not needed for the successful transformation of the benzylic alcohols into the corresponding alkanes.

**Table 6.7.** Control reactions.

Entry <sup>[a]</sup>	Deviation	Conversion (%) <sup>[b]</sup>	Yield (%) <sup>[b]</sup>
1	Without Ti	89	-
2	Without Mn	11	3
3	Without $(\text{EtO})_3\text{SiH}$	-	-
4	Without Co and ligand	94	62

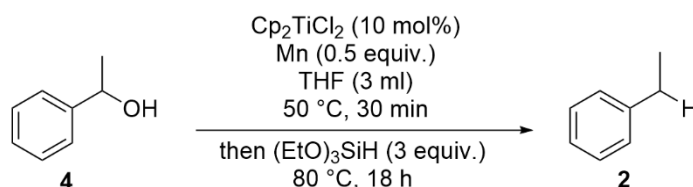
[a] Standard reaction conditions: In a Schlenk pressure tube anhydrous  $\text{CoBr}_2$  (26.2 mg, 0.12 mmol, 12.0 mol%), ligand **L25** (0.036 mL 0.20 mmol, 20.0 mol%),  $\text{Cp}_2\text{TiCl}_2$  (24.9 mg, 0.10 mmol, 10.0 mol%),  $\text{Mn}$  (27.5 mg, 0.50 mmol, 0.50 equiv.) and 1-phenylethanol (0.120 mL, 1.00 mmol, 1.00 equiv.) in THF (3 mL) stirred for 30 min. at r.t., then triethoxysilane (0.55 mL, 3.00 mmol, 3.00 equiv.) stirred for 18 h at reflux; [b] Yields were determined *via* quantitative GC-FID using *n*-pentadecane as internal standard;

In summary, the results obtained during the development of the Co/Ti-based deoxygenation protocol hinted that a Ti-catalysed deoxygenation procedure would be possible with triethoxysilane (**100**) as H-donor and Mn as metallic reductant. The development and results of these studies will be extensively discussed in chapter 6.3.

### 6.3. Results and Discussions for Ti-Catalysed Deoxygenation

#### 6.3.1. Preliminary Conditions Screening

Following the conducted control reactions on the Co/Ti co-catalysed reactions, it was observed that by using triethoxysilane (**100**) as H-donor species, the Ti catalyst proved to be capable of catalysing the reaction in higher yields than by using a bimetallic system (Table 6.8 – Entry 4). Thus, this finding was investigated in more detail (Table 6.8). The results showed that the Ti complex is necessary for the transformation, and it hinted that the catalytically active species is  $\text{Ti}^{3+}$ -based, therefore leading to the conclusion that a radical reaction pathway is plausible. It was also observed that the alkoxy silane species has a limited reduction capability but is insufficient to solely reduce  $\text{Cp}_2\text{TiCl}_2$  (**C36**).

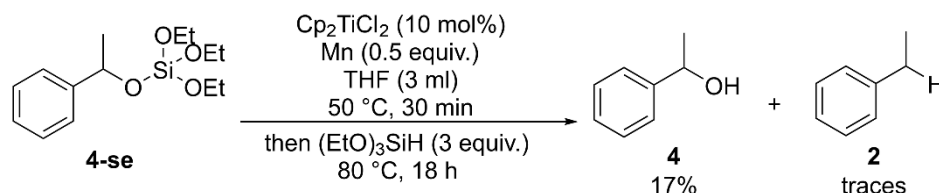
**Table 6.8.** Control reactions on Ti-based catalytic system.

Entry <sup>[a]</sup>	Deviation	Yield (%) <sup>[b]</sup>
1	Standard conditions	62
2	Without $(\text{EtO})_3\text{SiH}$	-

3	Without Cp <sub>2</sub> TiCl <sub>2</sub>	-
4	Without Mn	3

[a] Standard reaction conditions: 1-phenylethanol (0.120 mL, 1.00 mmol, 1.00 equiv.), Cp<sub>2</sub>TiCl<sub>2</sub> (24.9 mg, 0.10 mmol, 10.0 mol%), Mn (54.9 mg, 1.00 mmol, 1.00 equiv.) in THF (3 mL), stirred for 30 min at 50 °C, then (EtO)<sub>3</sub>SiH (0.55 mL, 3.00 mmol, 3.00 equiv.), 18 h, 80 °C in a Schlenk pressure tube. [b] Yields were determined *via* quantitative GC-FID using *n*-pentadecane as internal standard.

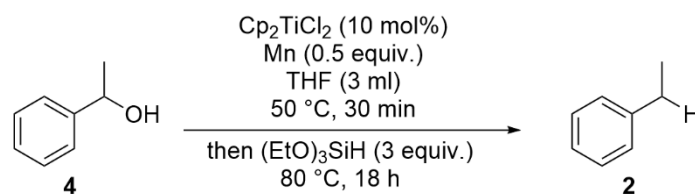
Another remark that must be made is that, beside disiloxane **98**, the main side-product of the reaction remained the corresponding silyl ether even after discarding the Co-cocatalyst. In the interest of finding the driving force behind this side reaction and the potential role of this compound as an intermediate in the reaction mechanism, silyl ether **4-se** has been used as starting material (Scheme 6.11). This reaction yielded only traces of the desired deoxygenated product and led to the regeneration of alcohol **4** in 17% yield. This result hints that the silyl ether **4-se** is not an intermediate in the catalytic process and that its formation is due to a competitive side-reaction. Additionally, this conclusion was later strengthened during reaction time optimization as no dependency between the formation of the silyl ether and the desired product was determined (Chapter 6.3.3).



**Scheme 6.11.** Silyl ether **4-se** as starting material.

Next, a preliminary solvent screening was conducted (Table 6.9). THF and 2-MeTHF afforded similar yields of ethylbenzene (**2**) (Table 6.9 - Entry 1 and 2). Instead, the reaction conducted in toluene did not lead to the formation of the desired product at all. Therefore, THF was chosen as the standard solvent for the reaction, mainly because of its availability and the temperature limitations imposed by using (EtO)<sub>3</sub>SiH (**101**) as H-donor.<sup>46</sup> The role of the solvent in the catalytic system was analysed in-depth after the extensive silane screening described in Chapter 6.3.3.

**Table 6.9.** Preliminary solvent screening.

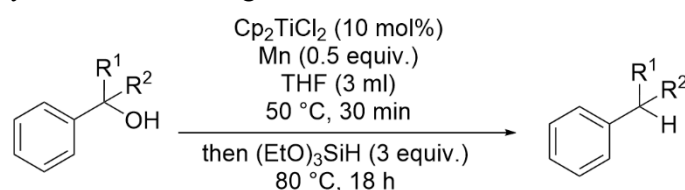


Entry <sup>[a]</sup>	Solvent	Yield (%) <sup>[b]</sup>
1	THF	62
2	2-MeTHF	65
3	Toluene	-

[a] Standard reaction conditions: 1-phenylethanol (0.120 mL, 1.00 mmol, 1.00 equiv.), Cp<sub>2</sub>TiCl<sub>2</sub> (24.9 mg, 0.10 mmol, 10.0 mol%), Mn (54.9 mg, 1.00 mmol, 1.00 equiv.) in THF (3 mL), stirred for 30 min at 50 °C, then (EtO)<sub>3</sub>SiH (0.55 mL, 3.00 mmol, 3.00 equiv.), 18 h, 80 °C in a Schlenk pressure tube. [b] Yields were determined *via* quantitative GC-FID using *n*-pentadecane as internal standard.

A preliminary substrate screening was conducted in order to determine, which benzylic alcohol would be best suited as standard substrate for this transformation (Table 6.10). Benzyl alcohol (**4a**) afforded the highest amount of the corresponding saturated hydrocarbon in 71% yield (Table 6.10 - Entry 1). 1-Phenylethanol (**4**) afforded 60% yield of ethylbenzene during the screening (Table 6.10 - Entry 2). Although this yield was considered unsuitable for a standard substrate, the encouraging factor is the reproducibility of the reaction, the yield dropping only 2% compared to the first attempts (Table 6.10 – Entry 1). The tertiary benzylic alcohol **4b** led to a poor yield of only 14% of cumene (**2b**) (Table 6.10 - Entry 3). In all three cases, the most important side-product was the corresponding silyl ether. In conclusion, primary alcohols were found to optimal for this transformation. This conclusion is somehow surprising as it does not follow the radical stability order, instead, it hints towards a negative effect of the steric hindrance on the catalytic process.

**Table 6.10** Preliminary substrate screening.



Entry <sup>[a]</sup>	Substrate	R <sup>1</sup>	R <sup>2</sup>	Yield (%) <sup>[b]</sup>
1	<b>4a</b>	H	H	68
2	<b>4</b>	CH <sub>3</sub>	H	60
3	<b>4b</b>	CH <sub>3</sub>	CH <sub>3</sub>	14

[a] Standard reaction conditions: benzylic alcohol (1.00 mmol, 1.00 equiv.),  $\text{Cp}_2\text{TiCl}_2$  (24.9 mg, 0.10 mmol, 10.0 mol%), Mn (54.9 mg, 1.00 mmol, 1.00 equiv.) in THF (3 mL), stirred for 30 min at 50 °C, then  $(\text{EtO})_3\text{SiH}$  (0.55 mL, 3.00 mmol, 3.00 equiv.), 18 h, 80 °C in a Schlenk pressure tube. [b] Yields were determined *via* quantitative GC-FID using *n*-pentadecane as internal standard.

Although encouraging, more investigations on the reactivity of this catalytic system had to be conducted. The most important drawbacks of this method were: unsatisfactory yields, the disability of conducting the reaction at higher temperatures and the toxicity and flammability of the triethoxysilane (**100**), which made it difficult to handle and also hindered the potential for the upscaling of this method, especially in a Ti-based catalytic system.<sup>47</sup> Therefore, the pursuit of developing a Ti-catalysed deoxygenation of benzylic alcohols continued with the aim of finding other reducing agents capable to donate a H-atom in this setup and with the further optimization of the reaction conditions.

### 6.3.2. Hantzsch Esters and Ammonium Borane as Reducing Agents

The first compound class that was taken in consideration as an alternative for triethoxysilane (**100**) were ammonium boranes. These compounds are safe-to-handle and are capable of storing and donating hydrogen at temperatures around 90 °C.<sup>48</sup> In order to find out if ammonium boranes were suited for this kind of transformations, the commercially available  $\text{H}_3\text{N}\cdot\text{BH}_3$  (**101**) was first submitted to the reaction (Table 6.11). In contrast to the previous reaction conditions, the Ti loading, reaction temperature and the activation time were increased so that the transformation is not limited by these parameters. Unfortunately, the primary and the secondary substrate yielded the desired product only in very small amounts (Table 6.11 – Entry 1 and 2). Nevertheless, the tertiary substrate did not afford

any trace of the desired product at all (Table 6.11 – Entry 3). The inactivity of  $\text{H}_3\text{N}\cdot\text{BH}_3$  (**101**) in this setup was further proven by the poor conversion compared to the hydrosilane reaction. Thus, ammonium borane was discarded as a possible replacement for the triethoxysilane (**100**) in the Ti-catalysed system.

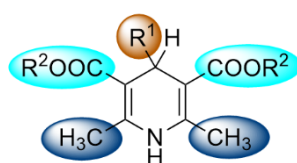
**Table 6.11.** Ammonium borane reactions.



Entry <sup>[a]</sup>	Substrate	R <sup>1</sup>	R <sup>2</sup>	Conversion (%) <sup>[b]</sup>	Yield (%) <sup>[b]</sup>
1	1a	H	H	13	traces
2	1ac	CH <sub>3</sub>	H	12	traces
3	1ag	CH <sub>3</sub>	CH <sub>3</sub>	5	-

[a] Standard reaction conditions: benzylic alcohol (1.00 mmol, 1.00 equiv.),  $\text{Cp}_2\text{TiCl}_2$  (37.3 mg, 0.15 mmol 15.0 mol%), Mn (54.9 mg, 1.00 mmol, 1.00 equiv.) in THF (3 mL), stirred for 2 h at 50 °C, then  $\text{H}_3\text{NBH}_3$  (92.6 mg, 3.00 mmol, 3.00 equiv.), 18 h, 80 °C in a Schlenk pressure tube. [b] Yields were determined *via* quantitative GC-FID using *n*-pentadecane as internal standard.

The search for a suitable H-donor continued by submitting Hantzsch esters (HEH, **45**) in the catalytic reaction. These compounds proved to be a useful reduction agent in both thermal and photochemical transfer hydrogenation reactions. As it was described in literature, this is possible due to the several hydrogen donation mechanisms (see Chapter 2.3).<sup>49</sup> Another property of Hantzsch esters is the possibility to fine-tune the H donation. Different substituents in the marked segments of the molecule can induce different reactivity and selectivity (Figure 6.1).<sup>50, 51</sup> Additionally, Hantzsch esters are considered as one of the most environmentally friendly reducing agents as they resemble  $\text{NADH}^+$  and do not produce toxic waste.



**Figure 6.1** Hantzsch ester tuneable sites.

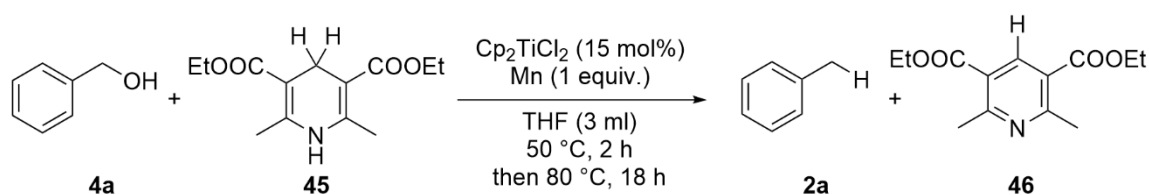
Hantzsch ester **45** was first utilized as H-donor for the deoxygenation of benzyl alcohol (**4a**). For this transformation 15 mol%  $\text{Cp}_2\text{TiCl}_2$  (**C36**) and 1 equivalent of Mn were employed in 3 ml THF. Similarly to the preliminary investigations conducted with triethoxysilane (**100**), before the addition of the 2.2 equivalents of HEH (**45**) into the reaction mixture, an activation time was considered in order to generate the catalytically active  $\text{Ti}^{3+}$  species. Interestingly, this reaction led to the formation of toluene in 58% yield. Based on this encouraging result, various conditions were screened (Table 6.12 – Entry 1).

First, the role of the concentration was investigated (Table 6.12 – Entries 2 and 3). It was observed that the yield of toluene (**2a**) increased with raising the concentration of the reaction mixture.



Lowering the amount of **45** to 1.5 equivalents or of precatalyst **C36** to 10 mol% led to a substantial decrease in yield (Table 6.12 – Entries 4 and 5). The presence of a small water content in the initial reaction mixture completely inhibited the transformation (Table 6.12 – Entry 6). The utilization of Zn instead of Mn as metallic reducing agent partially suppressed the generation of the desired product as only 18% yield of toluene (**2a**) was obtained (Table 6.12 – Entry 7). Meanwhile, no toluene (**2a**) was detected in the final reaction mixture when the reductant was eliminated from the reaction mixture (Table 6.12 – Entry 8). Subsequently, the importance of the reaction time was examined but a reaction time of 2 h proved to be insufficient for a satisfactory transformation of benzyl alcohol (**4a**). Lastly, the deoxygenation of 2-naphthalenemethanol (**4c**) was attempted and this reaction yielded 2-methylnaphthalene (**2c**) in a 67% yield. Thus, 2-naphthalenemethanol was chosen as the standard substrate for the future investigations (Table 6.12 – Entries 9 and 10).

**Table 6.12.** General optimization reactions.



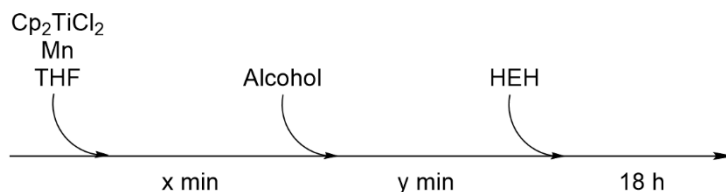
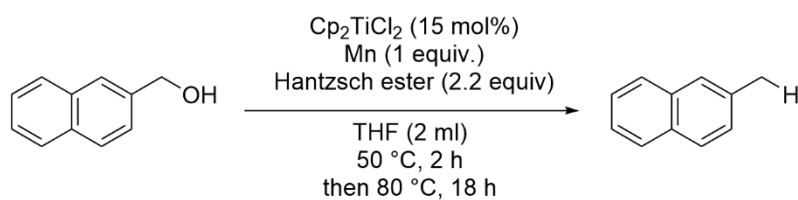
Entry <sup>[a]</sup>	Deviation	Yield (%) <sup>[b]</sup>
1	Standard conditions	58
2	4 mL instead of 3 mL	60
3	2 mL instead of 3 mL	65
4	1.5 equiv. HEH	38
5	10 mol% Cp <sub>2</sub> TiCl <sub>2</sub>	50
6	Not distilled THF	-
7	Zn instead of Mn	18
8	No Mn	-
9	2 h reaction time	12
10	2-naphthalenemethanol	67

[a] Standard reaction conditions: benzyl alcohol (0.104 mL, 1.00 mmol, 1.00 equiv.), Cp<sub>2</sub>TiCl<sub>2</sub> (37.3 mg, 0.15 mmol, 15.0 mol%), Mn (54.9 mg, 1.00 mmol, 1.00 equiv.) in THF (3 mL), stirred for 2 h at 50 °C, then HEH (557 mg, 2.20 mmol, 2.20 equiv.), 18 h, 80 °C in a Schlenk pressure tube. [b] Yields were determined *via* quantitative GC-FID using *n*-pentadecane as internal standard.

The importance of the activation times of the reaction components was studied, while the addition order remained constant. As it was previously presented, the standard procedure led to the generation of 2-methylnaphthalene (**2c**) in 67% yield (Table 6.13 – Entry 1). Prolonging the time between the addition of the alcohol and the Hantzsch ester **45** to 120 minutes lowered the obtained yield of **2c** to 62% (Table 6.13 – Entry 2). The same negative effect was also observed when the Ti precatalyst **C36** and the Mn were solely stirred for 120 minutes at 50 °C and the alcohol and the HEH **45** were added either simultaneously or for another 120 minutes each (Table 6.13 – Entries 3 and 4). The highest yield of **2c**, 70%, was obtained when the Ti complex, Mn and the alcohol were added together and

stirred for 2 h before the Hantzsch ester **45** was added to the reaction mixture (Table 5.5.6 – Entry 5). Therefore, this was considered the optimal addition order for this transformation.

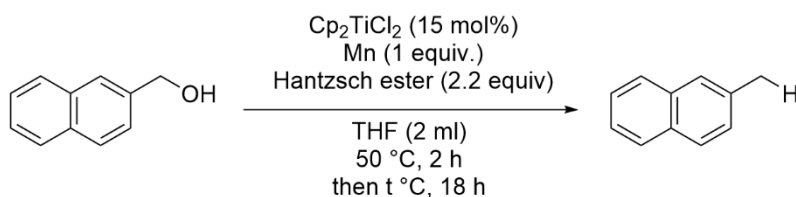
**Table 6.13.** Activation and addition time screening.



Entry <sup>[a]</sup>	x (min)	y (min)	Yield (%) <sup>[b]</sup>
1	30	60	67
2	30	120	62
3	120	0	60
4	120	120	63
5	0	120	70

[a] Standard reaction conditions: 2-naphthalenemethanol (158 mg, 1.00 mmol, 1.00 equiv.),  $\text{Cp}_2\text{TiCl}_2$  (37.3 mg, 0.15 mmol, 15.0 mol%), Mn (54.9 mg, 1.00 mmol, 1.00 equiv.) in THF (3 mL), stirred for 2 h at 50 °C, then HEH (557 mg, 2.20 mmol, 2.20 equiv.), 18 h, 80 °C in a Schlenk pressure tube. [b] Yields were determined *via* quantitative GC-FID using *n*-pentadecane as internal standard.

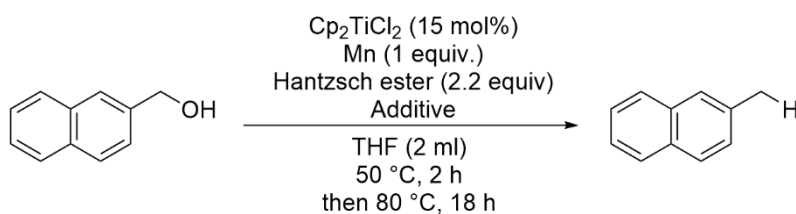
During the condition screening it was observed that a higher reaction temperature facilitated the formation of the desired compound **2c**. Below 70 °C only small amounts of the deoxygenation product were detected (Table 6.14 – Entries 1 and 2). The reaction conducted at 70 °C yielded 2-methylnaphthalene of (**2c**) in 27% yield, while at 80 °C **2c** was obtained in a 70% yield. Although a clear trend was observed, no reaction at higher temperature was conducted due to safety concerns (Table 6.14 - Entries 3 and 4). It was hypothesised that the beneficial role of a higher temperature both facilitated the cleavage of the C-H bond from the Hantzsch ester and improved the solubility of the reaction components.

**Table 6.14.** Reaction temperature screening.

Entry <sup>[a]</sup>	Temperature (°C)	Yield (%) <sup>[b]</sup>
1	50	6
2	60	8
3	70	27
4	80	70

[a] Standard reaction conditions: 2-naphthalenemethanol (158 mg, 1.00 mmol, 1.00 equiv.),  $\text{Cp}_2\text{TiCl}_2$  (37.3 mg, 0.15 mmol, 15.0 mol%), Mn (54.9 mg, 1.00 mmol, 1.00 equiv.) in THF (3 mL), stirred for 2 h at 50 °C, then HEH (557 mg, 2.20 mmol, 2.20 equiv.), 18 h, t °C in a Schlenk pressure tube. [b] Yields were determined *via* quantitative GC-FID using *n*-pentadecane as internal standard.

In order to further improve the reaction yield, an additive screening was conducted. Unfortunately,  $\text{TMSCl}$  (**76**) and triethylamine hydrochloride (**102**) completely inhibited the generation of the desired product **2c** (Table 6.15 – Entries 2 and 3). The addition of manganese chloride or lithium chloride, which should further improve the solubility of the Mn, did not lead to the desired outcome as lower yields of **2c** were obtained compared to the standard procedure (Table 6.15 – Entries 4, 5 and 6). Based on the available literature, different P-based additives were also submitted to the reactions. Diphenylphosphate (**103**) led to comparable results with the standard procedures (Table 6.15 – Entry 7). However, Diphenylchlorophosphate (**104**) quenched the reactivity of the catalytic system and BINOL (**105**) led to a decreased yield of **2c**, even with the addition of other additives like LiCl or molecular sieves (Table 6.15 – Entries 8, 9, 10 and 11). In order to determine if the potentially *in situ* generated water negatively affected the reactivity, molecular sieves were added. Unfortunately, only small amounts of 2-methylnaphthalene (**2c**) were generated (Table 6.15 – Entries 12 and 13). A combined HEH/ammonium borane H-donor system was examined, but the yield was lower compared to the standard procedure (Table 6.15 – Entry 14).

**Table 6.15.** Additives screening.

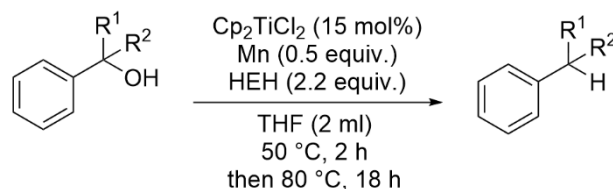
Entry <sup>[a]</sup>	Additives	Yield (%) <sup>[b]</sup>
1	none	70
2	$\text{TMSCl}$	-
3	$\text{Et}_3\text{N} \cdot \text{HCl}$	-
4	$\text{MnCl}_2$	21

5	LiCl	35
6	1.2 equiv. LiCl	37
7	Diphenylphosphate	66
8	Diphenylchlorophosphate	-
9	0.1 equiv BINOL	17
10	0.1 equiv BINOL + 4 Å molecular sieves	32
11	0.1 equiv BINOL + LiCl	25
12	4 Å molecular sieves	9
13	4 Å molecular sieves + LiCl	11
14	H <sub>3</sub> N · BH <sub>3</sub>	49

[a] Standard reaction conditions: 2-naphtalenemethanol (158 mg, 1.00 mmol, 1.00 equiv.), Cp<sub>2</sub>TiCl<sub>2</sub> (37.3 mg, 0.15 mmol, 15.0 mol%), Mn (54.9 mg, 1.00 mmol, 1.00 equiv.) and additive (1.00 mmol, 1.00 equiv.) in THF (3 mL), stirred for 2 h at 50 °C, then HEH (557 mg, 2.20 mmol, 2.20 equiv.), 18 h, 80 °C in a Schlenk pressure tube. [b] Yields were determined *via* quantitative GC-FID using *n*-pentadecane as internal standard.

Following the conditions from optimization reactions, a preliminary substrate screening was conducted (Table 6.16). Primary alcohol 4-tertbutyl benzyl alcohol (**4a**) proved to be the most reactive in these catalytic conditions. The utilization of 1-phenylethanol (**4**) led to the formation of the corresponding deoxygenated product **2** in only a 21% yield. Subsequently, tertiary alcohol **4b** yielded the desired product **2b** in only a 9% yield. Thus, primary benzylic alcohols remained used as standard substrates for this deoxygenation protocol.

**Table 6.16.** Preliminary substrate screening.

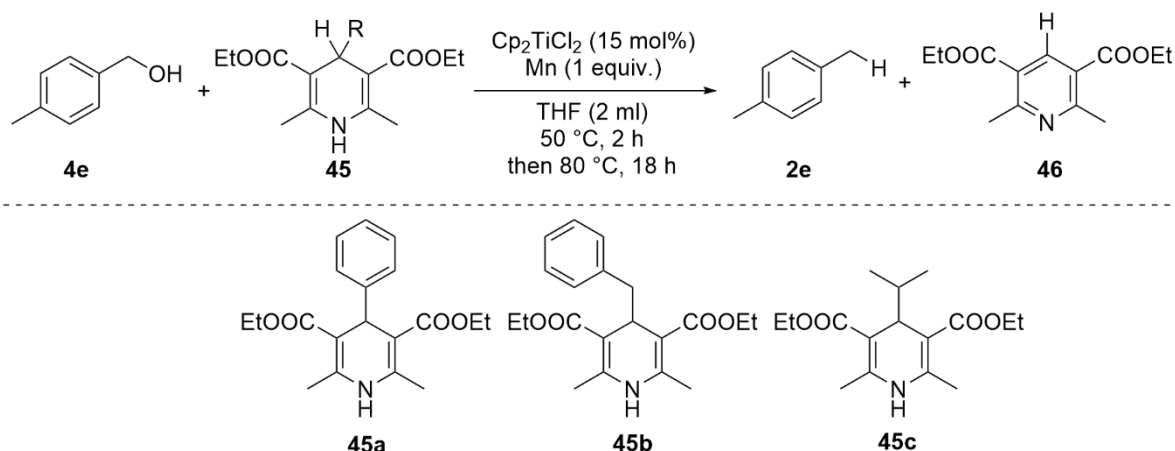


Entry <sup>[a]</sup>	Substrate	Yield (%) <sup>[b]</sup>
1	4-tertbutyl benzyl alcohol	67
2	1-phenylethanol	21
3	2-phenylpropan-2-ol	9

[a] Standard reaction conditions: benzyl alcohol (0.104 mL, 1.00 mmol, 1.00 equiv.), Cp<sub>2</sub>TiCl<sub>2</sub> (37.3 mg, 15 mol%), Mn (54.9 mg, 1.00 mmol, 1.00 equiv.) in THF (3 mL), stirred for 2 h at 50 °C, then HEH (557 mg, 2.2 mmol, 2.2 equiv.), 18 h, 80 °C in a Schlenk pressure tube. [b] Yields were determined *via* quantitative GC-FID using *n*-pentadecane as internal standard.

Subsequently, the hydrogen transfer capability of C4-derivatised Hantzsch (**45a-c**) esters was tested. Additionally, the transfer of an aryl or alkyl moiety to the alcoholic substrate was attempted. Unfortunately, none of the reactions led to the formation of the deoxygenation nor derivatization product. However, it could be determined *via* GC-MS, that beside the aromatization of the Hantzsch ester and formation of pyridine derivatives **46a-c**, the pyridine derivative **46** was formed in significant

amounts. The rerunning of these reactions did not reveal more information about the reaction pathway. The presumption of these experiments was that benzene and toluene could be formed from the Hantzsch esters under these conditions, but this type of reactivity was not further investigated.

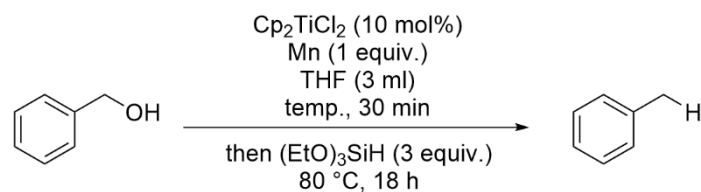


**Scheme 6.12.** Hantzsch esters derivatives screening.

In conclusion, Hantzsch ester **45** proved to be a good reducing agent under these conditions. However, no further improvement could be made on the reaction conditions in order to achieve quantitative yields. Thus, the decision was made to further utilize hydrosilanes as H-donors for the Ti-catalyzed deoxygenation procedure.

### 6.3.3. Silane and Reaction Parameters Optimization

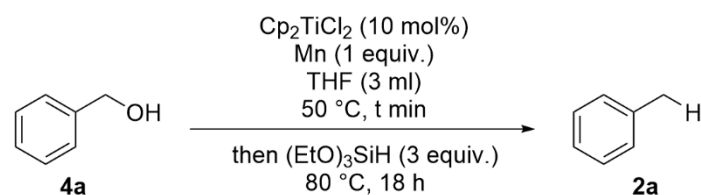
Based on the results obtained during the development of the Co- and Co/Ti-catalyzed deoxygenation procedure and the preliminary results presented in Chapter 6.3.1, an extensive parameter optimization was conducted. Inspired by the mechanistic studies conducted by Ukaji *et al.*<sup>41</sup> this process started by investigating the importance of the optimal values for activation time and temperature. After numerous mechanistic investigations, they concluded that the rate-limiting step in their transformation is the formation of a  $\text{Ti}^{3+}$ -alcohol complex, which can further undergo the radical conjugate addition of electro-deficient olefines. Additionally, the observations made during the previous development of non-precious metal-based catalytic systems hinted towards a beneficial role of an increased temperature and activation time for the desired transformation (Chapter 6.3.2). The obtained results of these reactions are presented in tables 6.13 and 6.14. First, the activation temperature was investigated. Analogously to the Co/Ti-catalysed deoxygenation, the highest yield was obtained by stirring the reaction at 50 °C before adding triethoxysilane (**100**) (Table 6.17 – Entry 1). A 10 °C decrease compared to the standard activation temperature (50 °C) resulted in a significant drop in yield from 68% to 47% (Table 6.17 – Entry 2). Conducting the substrate activation at room temperature afforded only traces of the desired product and prolonging the activation time at this temperature afforded toluene (**2a**) only in 25% yield (Table 6.17 – Entry 3 and 4). These experiments showed that the temperature plays a crucial role in this transformation.

**Table 6.17.** Activation temperature screening.

Entry <sup>[a]</sup>	Temperature (°C)	Yield (%) <sup>[c]</sup>
1	50 (standard condition)	68
2	40	47
3	r.t.	traces
4	r.t. <sup>[b]</sup>	25

[a] Standard reaction conditions: benzyl alcohol (0.104 mL, 1.00 mmol, 1.00 equiv.),  $\text{Cp}_2\text{TiCl}_2$  (25.0 mg, 10 mol%),  $\text{Mn}$  (54.9 mg, 1.00 mmol, 1.00 equiv.) in THF (2 mL), stirred for 2 h at t °C, then  $(\text{EtO})_3\text{SiH}$  (0.59 mL, 3.00 mmol, 3.00 equiv.), 18 h, 80 °C in a Schlenk pressure tube. [b] 2 h activation time [c] Yields were determined *via* quantitative GC-FID by using *n*-pentadecane as internal standard.

By adding all the reagents at the same time, no desired product was observed, only silyl ether **4a-se** (Table 6.18 – Entry 1). Then, the standard activation time of 30 min was doubled resulting in a slight increase in yield from 68% to 71% (Table 6.18 – Entry 3). Therefore, the silane addition was further deferred by 120 and 150 minutes (Table 6.18 – Entry 4 and 5). After 120 min activation time, a significant increase in toluene (**2a**) yield (82% vs. 68%) was determined. This yield remained mostly constant when prolonging the activation time by 30 minutes. Interestingly, a further increase in the activation time seemed to have a negative impact on the catalytic process as toluene (**2a**) was obtained in only 33% yield after 4 h activation time (Table 6.18 – Entry 6). As a conclusion, a 120 min activation time was found as being optimal for the catalytic process, thus it was further utilized in the development of the To-catalysed deoxygenation process.

**Table 6.18.** Activation time screening.

Entry <sup>[a]</sup>	Time (min)	Yield (%) <sup>[b]</sup>
1	-	-
2	30	68
3	60	71
4	120	82
5	150	81

6	240	33
[a] Standard reaction conditions: benzyl alcohol (0.104 mL, 1.00 mmol, 1.00 equiv.), Cp <sub>2</sub> TiCl <sub>2</sub> (24.9 mg, 0.10 mmol, 10.0 mol%), Mn (54.9 mg, 1.00 mmol, 1.00 equiv.) in THF (2 mL), stirred for t min at 50 °C, then (EtO) <sub>3</sub> SiH (0.55 mL, 3.00 mmol, 3.00 equiv.), 18 h, 80 °C in a Schlenk pressure tube. [b] 2 h activation time [c] Yields were determined <i>via</i> quantitative GC-FID using <i>n</i> -pentadecane as internal standard.		

During these investigations, it was observed that the pressure inside the reaction vessel is a major factor for a successful transformation. By sealing the reaction vessel immediately after adding the silane, without further purging the system with inert gas, the system provided the highest amount of toluene (**2a**). This experimental detail was kept in the methodology throughout the rest of the screening.

A comprehensive silane screening was conducted (Table 6.19). Except the standard reaction with triethoxysilane (**100**), 2-MeTHF was used as standard solvent for all screened silanes. Since 2-MeTHF and the other silanes could withstand higher temperatures without any safety concerns this decision was made because of the beneficial role of the increased temperatures on the desired transformation. First, triethylsilane (**29**) was tested in the reaction as this hydrosilane was reported in the literature as being a capable H-donor in Lewis acid-based stoichiometric systems (Table 6.19 - Entry 1).<sup>52, 53</sup> Unfortunately, this reaction afforded only silyl ether **4a-se**. This outcome was surprising as the theoretical BDE of the Si-H bond in Et<sub>3</sub>SiH (**29**) is lower than in (EtO)<sub>3</sub>SiH (**100**), 92.8 kcal/mol and 95.0 kcal/mol respectively.<sup>54</sup>

Next, inspired by the work of Shenvi *et al.*<sup>55</sup>, hydrosilanes bearing phenyl substituents PhSiH<sub>3</sub> (**82**) and Ph<sub>2</sub>SiH<sub>2</sub> (**99**) were submitted to the reaction (Table 6.19 - Entries 2 and 3). Beside the wide variety of hydrogenations in which this type of silanes are utilized,<sup>56,57</sup> other arguments for using these hydrosilanes were the lower BDE of the Si-H bonds compared to the alkyl-substituted silanes<sup>54</sup> and the multiple hydrogen donation sites. Unfortunately, both yields of 18% and 4% respectively were considered unsatisfactory.

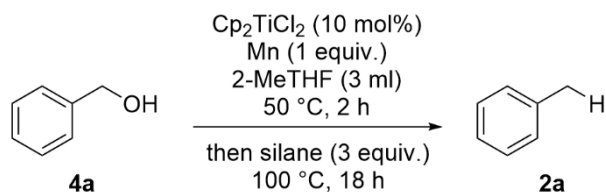
After a further analysis of the commercially available hydrosilanes, TMS<sub>3</sub>SiH (**106**) and TMSO<sub>3</sub>SiH (**107**) were chosen as suitable candidates for the H-donor role (Table 6.19 - Entry 4 and 5). As it was stated in Chapter 2.1, tris(trimethylsilyl)silane (**106**) was used in different radical reactions as a substitute for the tributyltin hydride, especially in alternatives of the Barton-McCombie deoxygenation<sup>58</sup>. Although the Si-H BDE in TMS<sub>3</sub>SiH (**106**) is low, 83.7 ± 1.0 kcal/mol, compared to other hydrosilanes, TMSO<sub>3</sub>SiH (**107**) yielded toluene in 57%, more than double compared to tris(trimethylsilyl)silane (**106**) which afforded only 26% yield.

This outcome hinted that the BDE may not be the most important factor in finding an efficient H-donor and regeneration agent for this transformation. A possible explanation for the obtained yields during the preliminary investigations and silane screening could be the Lewis acidity of the silanes, which increases with the presence of multiple Si-O bonds. This hypothesis was also presented by Cantat *et al.*<sup>59</sup> in their reported catalytic selective reduction of amides. It is presumed that the increased Lewis acidity does not influence the H-donating capability of the silanes, instead it facilitates the catalyst regeneration process. A negative consequence resulting from having three alkoxy groups attached to the Si center is the possible generation of SiH<sub>4</sub> due to the liability of the Si-O bond in Ti<sup>3+</sup> catalyzed procedures.<sup>60</sup>

Based on this outcome, 1,1,3,3-tetramethyldisiloxane, the standard silane for the Co and Ti/Co catalyzed systems was again submitted to the deoxygenation procedure (Table 5.5.12 - Entry 6). Unfortunately, the reaction afforded toluene (**2a**) in only 37% yield leading to the conclusion that TMDSO (**98**) is unsuitable for this methodology.

Thus, the silane screening continued and Me(EtO)<sub>2</sub>SiH (**108**) was submitted to the catalytic process (Table 6.19 - Entry 7). The structure of this hydrosilane is a compromise between high reactivity and safety, due to the existence of the Si-C bond which is much more stable in this type of catalytic system compared to triethoxy-substituted hydrosilane (Table 6.19 - Entry 8). This reaction yielded the desired product in 96% and, therefore, was chosen as the most suitable H-donor for this transformation.

**Table 6.19.** Silane screening.

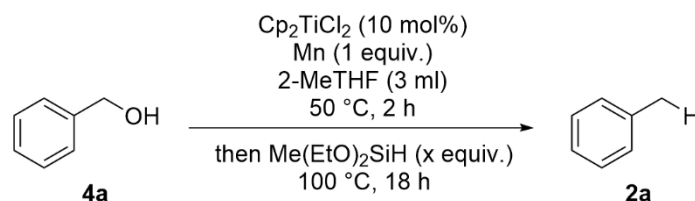


Entry <sup>[a]</sup>	Silane	Yield (%) <sup>[c]</sup>
1	Et <sub>3</sub> SiH	-
2	PhSiH <sub>3</sub>	18
3	Ph <sub>2</sub> SiH <sub>2</sub>	4
4	TMS <sub>3</sub> SiH	26
5	TMSO <sub>3</sub> SiH	57
6	[(CH <sub>3</sub> ) <sub>2</sub> SiH] <sub>2</sub> O	37
7	Me(EtO) <sub>2</sub> SiH	96
8 <sup>b</sup>	(EtO) <sub>3</sub> SiH (standard conditions)	99

[a] Reaction conditions: benzyl alcohol (0.104 mL, 1.00 mmol, 1.00 equiv.), Cp<sub>2</sub>TiCl<sub>2</sub> (24.9 mg, 0.10 mmol, 10.0 mol%), Mn (54.9 mg, 1.00 mmol, 1.00 equiv.) in 2-MeTHF (2 mL), stirred for 2 h at 50 °C, then silane (3.00 mmol, 3.00 equiv.), 18 h, 100 °C in a Schlenk pressure tube. [b] Reaction at 80 °C. [c] Yields were determined *via* quantitative GC-FID using *n*-pentadecane as internal standard.

Following the silane screening, the optimal silane loading was investigated. Both decreasing and increasing the silane quantity in the reaction led to lower toluene (**2a**) yields due to different reasons. On the one hand, when adding 2.2 equivalents of silane the conversion dropped from >95% to 72% resulting in only 53% yield of toluene (**2a**) (Table 6.20 - Entry 1). On the other hand, when 4 equivalents were added, the yield also decreased significantly to 62% due to the formation of higher quantities of silyl ether (Table 6.20 - Entry 2).

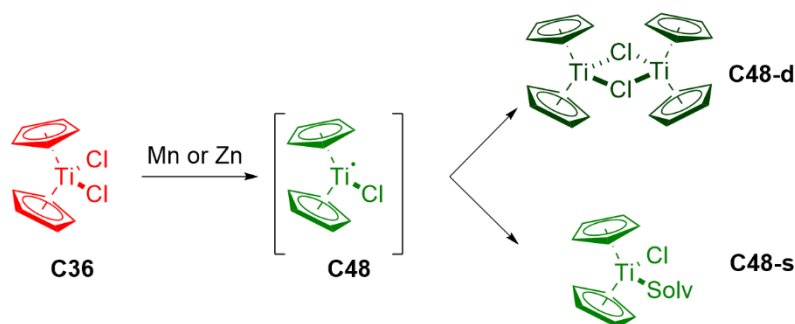


**Table 6.20.** Silane loading screening.

Entry <sup>[a]</sup>	Deviation	Conversion (%) <sup>b</sup>	Yield (%) <sup>b</sup>
1	2.2 equiv. Me(EtO) <sub>2</sub> SiH	72	53
2	4 equiv. Me(EtO) <sub>2</sub> SiH	99	62

[a] Reaction conditions: benzyl alcohol (0.104 mL, 1.00 mmol, 1.00 equiv.), Cp<sub>2</sub>TiCl<sub>2</sub> (24.9 mg, 0.10 mmol, 10.0 mol%), Mn (54.9 mg, 1.00 mmol, 1.00 equiv.) in 2-MeTHF (2 mL), stirred for 2 h at 50 °C, then silane (x equiv.), 18 h, 100 °C in a Schlenk pressure tube. [b] Yields were determined *via* quantitative GC-FID using *n*-pentadecane as internal standard.

Choosing the right solvent for the reaction is crucial as it plays a major role for both the desired transformation and reduction process of the Ti<sup>4+</sup> precatalyst.<sup>34</sup> The main three factors that determine if a solvent is good for the transformation are: solubility of the precatalyst and reducing agent, boiling point and vapour pressure as well as the capacity of stabilizing the Ti<sup>3+</sup> generated species.<sup>61</sup> There are studies, which were conducted on the reduction Ti<sup>4+</sup> species to Ti<sup>3+</sup> or Ti<sup>2+</sup> by using different kind of reducing agents<sup>6</sup> as it was described in chapter 6.1.1. Most of these studies also focus on the colorimetry of the reduction and on the stabilizing capacity of a certain solvent over the *in situ* generated catalyst.<sup>62</sup> Following the studies of Green *et al.* on the structure of Cp<sub>2</sub>TiCl, this topic became of interest after it was discovered that different arrangements of Ti<sup>3+</sup> species are possible in solution as it is presented in Scheme 6.13.<sup>24, 61, 63</sup> After the reduction of the Cp<sub>2</sub>TiCl<sub>2</sub> (C36) with Mn or Zn, C48 can dimerize by forming halogen bonding (C36-d) or it can be stabilized in a monomeric form by the coordination of a solvent molecule to the metallic centre (C48-s). During the reduction step a colour change can be observed from red to green. Consequently, the colour of C48-s can change on a large spectrum due to the influence of the solvent coordination.

**Scheme 6.13.** Cp<sub>2</sub>TiCl structures in solution.

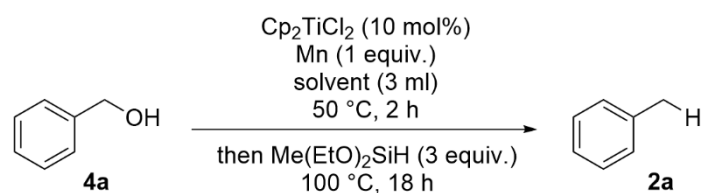
Up to this date it is not clear which species is the active one in Ti<sup>3+</sup> catalysed reactions but in most transformations, THF was selected as being the best suited solvent. Although the kinetic and mechanistic studies show that a dimeric species would be more catalytically active, in reality the reactivities of both forms contribute almost equally in Ti<sup>3+</sup>-based systems.<sup>64</sup> This can be explained by the effective coordination of the solvent through the electron pair from the oxygen atom into a titanium empty orbital leading to the formation of species C48-s.

Therefore, a solvent screening was conducted (Table 6.21). Based on the available literature and the observations made during the preliminary optimization studies, the first selected solvent was THF. This reaction was conducted at 80 °C due to safety concerns which arise from the low boiling point and the exponentially escalating vapour pressure of THF.<sup>65</sup> These initial reaction conditions proved to be promising as they led to a quantitative conversion and a satisfactory yield of the desired product (Table 6.21 - Entry 1). As it was observed in all the non-precious metal catalysed reactions conducted during this work, the corresponding silyl ether was still produced in significant quantities. When conducting the reaction in THF at lower temperature by 10 °C than the initial reaction the yields dropped drastically from 82% to 13% (Table 6.21 - Entry 2). These results led to the conclusion that higher temperature may enhance the desired transformation. Thus, higher boiling point solvents were conducted. First, toluene was chosen, and the reaction was conducted at 100 °C but no desired product, in this case ethylbenzene **2**, was observed in the obtained reaction mixture (Table 6.21 - Entry 3). This result was surprising as toluene is described as a suitable solvent for Ti-based catalytic systems.<sup>34</sup> The possible reasons why the transformation was unsuccessful may be either the poor solubility of the reducing agent in the solvent and therefore the generation of the Ti<sup>3+</sup> active species did not take place or the poor stabilizing capacity of toluene of the monomeric species **C48-s**. Another possible explanation of the inactivity of the catalytic system in toluene might be the formation of bimetallic complexes analogous to the Ti-Zn complex [Ti(C<sub>5</sub>H<sub>5</sub>)Cl]<sub>2</sub>ZnCl<sub>2</sub> which was prepared in toluene by Salzmann in 1968.<sup>66</sup> During the reaction, the solution kept the red colouring hinting toward a poor *in situ* generation of the Ti<sup>3+</sup> species.

In order to test this hypothesis, the reaction was then conducted in a 1:1 toluene:THF mixture at 80 °C (Table 6.21 - Entry 4). Following this procedure, 16% of the desired product was obtained leading to the conclusion that the main focus in choosing the solvent should be on its donating capability. This conclusion was again confirmed as also the reaction in chloroform did not lead to the formation of the desired product even at 100 °C (Table 6.21 - Entry 5). Surprisingly, the reaction conducted in 1,4-dioxane and at 100 °C was unsuccessful as well (Table 6.21 - Entry 6). After analysing the reaction procedure, the conclusion was that the solvent might still contain a small amount of stabilizer, which could negatively affect the transformation.

In the last stage of the solvent screening, 2-MeTHF was subjected to the reaction. This solvent has the advantages that it has a higher boiling point compared to THF, similar stabilizing properties, a lower miscibility with water and it is also considered to be an environmentally friendly solvent.<sup>67</sup> The reaction in 2-MeTHF at 80 °C already showed a slightly improved yield than the procedure with THF (Table 6.21 - Entry 7) and the reaction at 100 °C showed a 96% yield (Table 6.21 - Entry 8). Therefore, 2-MeTHF was selected as solvent for further optimization steps and substrate screenings.

**Table 6.21.** Solvent screening.

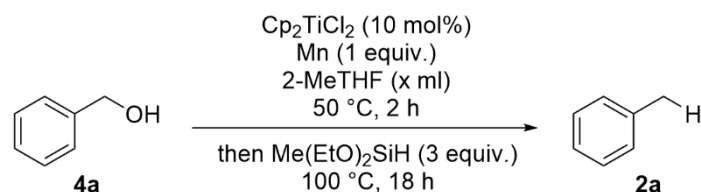


Entry <sup>[a]</sup>	Solvent	Yield (%) <sup>[d]</sup>
1 <sup>[b]</sup>	THF	82
2 <sup>[c]</sup>	THF	13
3 <sup>[c]</sup>	Toluene	-
4 <sup>[b]</sup>	THF:Toluene 1:1	16
5	CHCl <sub>3</sub>	-
6	Dioxane	-
7 <sup>[b]</sup>	2-MeTHF	85
8	2-MeTHF	96

[a] Reaction conditions: benzyl alcohol (0.104 mL, 1.00 mmol, 1.00 equiv.), Cp<sub>2</sub>TiCl<sub>2</sub> (24.9 mg, 0.10 mmol, 10.0 mol%), Mn (54.9 mg, 1.00 mmol, 1.00 equiv.) in solvent (2 mL), stirred for 2 h at 50 °C, then (EtO)<sub>2</sub>MeSiH (0.48 mL, 3.00 mmol, 3.00 equiv.), 18 h, 100 °C in a Schlenk pressure tube. [b] Reaction at 80 °C. [c] Reaction at 70 °C. [d] Yields were determined *via* quantitative GC-FID using *n*-pentadecane as internal standard. [e] the reaction was conducted on 1-phenylethanol.

Additionally, the optimal concentration of the reaction mixture was investigated (Table 6.22). It was observed that lowering the solvent volume had a beneficial role on the transformation. Increasing the concentration from 0.25 M to 0.5 M led to the formation of the desired product in 96% yield (Table 6.22 - Entry 2). This result hints that the dimeric Ti-structure is more catalytically active as higher concentrations favour the formation of this structure.<sup>64</sup> In contrast, concentrating the solution even further disabled the transformation completely as not even traces of toluene (**2a**) were detected (Table 6.22 - Entry 1). It was presumed that this outcome was a consequence of stirring problems and poor solubility of the reagents.

**Table 6.22.** Concentration screening.



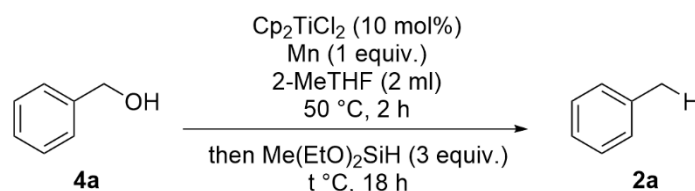
Entry <sup>[a]</sup>	Concentration (M)	Yield (%) <sup>[b]</sup>
1	1	-
2	0.5	96
3	0.33	85
4	0.25	79

[a] Standard reaction conditions: benzyl alcohol (0.104 mL, 1.00 mmol, 1.00 equiv.), Cp<sub>2</sub>TiCl<sub>2</sub> (24.9 mg, 0.10 mmol, 10.0 mol%), Mn (54.9 mg, 1.00 mmol, 1.00 equiv.) in 2-MeTHF (x mL), stirred for 2 h at 50 °C, then (EtO)<sub>2</sub>MeSiH (0.48 mL, 3.00 mmol, 3.00 equiv.), 18 h, 100 °C in a Schlenk pressure tube. [b] Yields were determined *via* quantitative GC-FID using *n*-pentadecane as internal standard.

To make this reaction more efficient, the next examined parameter was the reaction temperature (Table 6.23). Although the goal of this process was to successfully conduct the reaction at room temperature, the first tested temperature was 50 °C, the same as the activation temperature, which was investigated previously (Table 6.23 - Entry 1). At this temperature, the reaction did not afford any desired product and a 10 °C rise was insufficient as well for the catalytic methodology to transform benzyl alcohol (**4a**) into toluene (**2a**) (Table 6.23 - Entry 2).

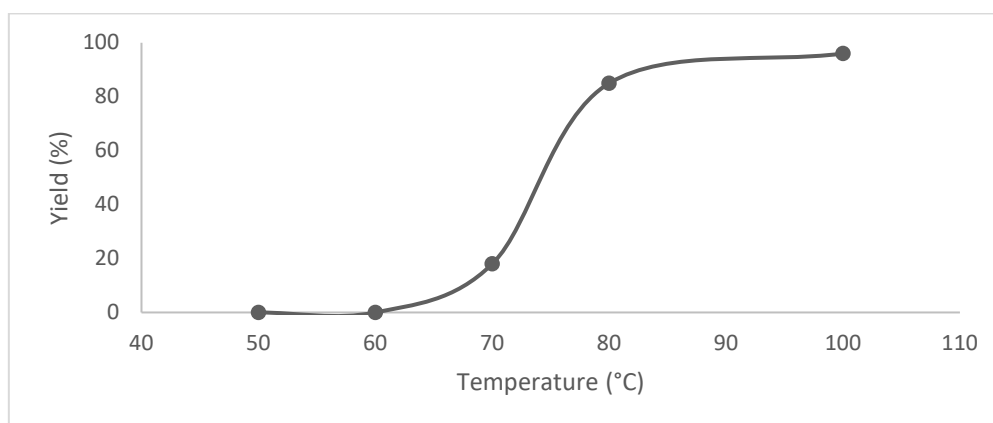
Toluene (**2a**) was first detected when the reaction was conducted at 70 °C, but the yield was not encouraging at only 17% (Table 5.5.16 - Entry 3). As presented in Figure 5.5.5, a major difference was observed when the reaction was submitted at 80 °C as the yield of the desired product increased to 85% (Table 5.5.16 - Entry 4). Although this reaction in 2-MeTHF already proved to be more efficient compared to the reaction conducted in THF at the same temperature, the 3% yield difference was insufficient to change the standard procedure. Therefore, all the further reactions were stirred at 100 °C for 18 h after the addition of the hydrosilane.

**Table 6.23.** Temperature screening.



Entry <sup>[a]</sup>	Temperature (°C)	Yield (%) <sup>[b]</sup>
1	50	-
2	60	-
3	70	18
4	80	85
5	100	96

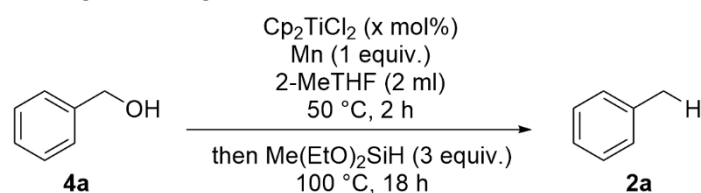
[a] Reaction conditions: benzyl alcohol (0.104 mL, 1.00 mmol, 1.00 equiv.),  $\text{Cp}_2\text{TiCl}_2$  (24.9 mg, 0.10 mmol, 10.0 mol%),  $\text{Mn}$  (54.9 mg, 1.00 mmol, 1.00 equiv.) in 2-MeTHF (2 mL), stirred for 2 h at 50 °C, then  $(\text{EtO})_2\text{MeSiH}$  (0.48 mL, 3.00 mmol, 3.00 equiv.), 18 h in a Schlenk pressure tube. [b] Yields were determined *via* quantitative GC-FID using *n*-pentadecane as internal standard.



**Figure 6.1.** Graphical representation of the reactivity dependency regarding reaction temperature.

Lowering the catalyst loading was also attempted as this would make the reaction more attractive for both laboratory and large-scale applications (Table 6.24). A lower catalyst loading of 5 mol% respective 8 mol%  $\text{Cp}_2\text{TiCl}_2$  (**C36**) (Table 6.24 - Entry 1 and 2) proved to be insufficient to afford the desired product in quantitative yield. By adding more titanium catalyst into the system, the reaction did not improve significantly in terms of toluene (**2a**) yield or reaction time (Table 6.24 – Entry 5 and 6). Later in the development of this catalytic system 12 mol% Ti-catalyst were also submitted to the transformation of 2-phenylethanol (**4**). Surprisingly, this reaction afforded only 79% yield of ethylbenzene (**2**), comparable to the standard reaction conditions of 10 mol% (Table 6.24 – Entry 4 and 7). In conclusion, 10 mol% was considered the optimal amount of Ti-catalyst to be used for this transformation.

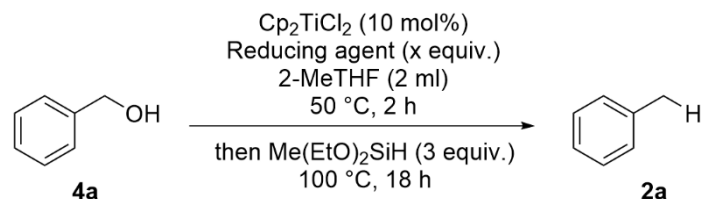
**Table 6.24.** Catalyst loading screening.



Entry <sup>[a]</sup>	Ti loading (mol%)	Yield (%) <sup>[d]</sup>
1	5	77
2	8	81
3	10 (standard condition)	96
4 <sup>[c]</sup>	10	78
5	12	97
6 <sup>[b]</sup>	12	31
7 <sup>[c]</sup>	12	79

[a] Standard reaction conditions: benzyl alcohol (0.104 mL, 1.00 mmol, 1.00 equiv.),  $\text{Cp}_2\text{TiCl}_2$  (24.9 mg, 0.10 mmol, 10.0 mol%), Mn (54.9 mg, 1.00 mmol, 1.00 equiv.) in 2-MeTHF (2 mL), stirred for 2 h at 50 °C, then  $(\text{EtO})_2\text{MeSiH}$  (0.48 mL, 3.00 mmol, 3.00 equiv.), 18 h, 100 °C in a Schlenk pressure tube. [b] 4 h reaction time [c] 2-phenylethanol instead of benzyl alcohol [d] Yields were determined *via* quantitative GC-FID using *n*-pentadecane as internal standard.

The optimization of the catalytic reaction continued with the investigation of the reducing agent and the amount needed for the reduction of  $\text{Ti}^{4+}$  to  $\text{Ti}^{3+}$ . First, 0.5 equivalents Mn were submitted in the reaction and led to 89% yield of toluene (**2a**) (Table 6.25 - Entry 1). When replacing Mn with 0.5 equivalents Zn the yield dropped 52% (Table 6.25 - Entry 2). Therefore, Mn was chosen as reducing agent for the catalytic system. The difference between the reactivity of Mn and Zn might appear due to the corresponding chlorides formed during the reactions as  $\text{MnCl}_2$  can to some degree release  $\text{Cl}^-$  ions back in the solution but this phenomenon was not further investigated.<sup>61</sup>

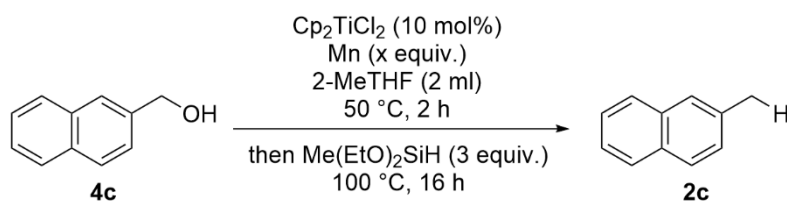
**Table 6.25.** Manganese loading screening.

Entry <sup>[a]</sup>	Reducing agent	Loading (equiv.)	Yield (%) <sup>[b]</sup>
1	Mn	0.5	89
2	Zn	0.5	52
3	Mn	1	95
4	Mn	1.5	65

[a] Standard reaction conditions: benzyl alcohol (0.104 mL, 1.00 mmol, 1.00 equiv.),  $\text{Cp}_2\text{TiCl}_2$  (24.9 mg, 0.10 mmol, 10.0 mol%), Reducing agent (x equiv.) in 2-MeTHF (2 mL), stirred for 2 h at 50 °C, then  $(\text{EtO})_2\text{MeSiH}$  (0.48 mL, 3.00 mmol, 3.00 equiv.), 18 h, 100 °C in a Schlenk pressure tube. [b] Yields were determined *via* quantitative GC-FID using *n*-pentadecane as internal standard.

The results obtained on the transformation of benzylic alcohols with 0.5 equivalents of Mn were unsuccessful to reproduce on wide range of substrates, among others 2-methylnaphthalene (**2c**) was afforded in only 76% yield in these conditions (Table 6.26 - Entry 1). Thus, the amount of Mn was increased to 1 and 1.5 equivalents.

Using 1 equivalent of Mn led to the formation of 2-methylnaphthalene (**2c**) in 95% yield (Table 6.26 - Entry 2). The positive effect over the reactivity was also observed in the conversion of benzyl alcohol (**4a**) into toluene (**2a**) as the yield rose from 89% to 95% (Table 6.26 - Entry 3). Conversely, higher amount of Mn led to a significant yield drop for both substrates (Table 6.26 - Entry 4 and Table 6.26 - Entry 3). Hence, 1 equivalent of Mn was considered as the optimal amount of reducing agent.

**Table 6.26.** Variation of manganese loading.

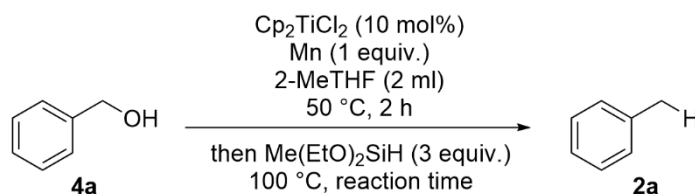
Entry <sup>[a]</sup>	Mn loading (equiv.)	Yield (%) <sup>[b]</sup>
1	0.5	76
2	1	95
3	1.5	54

[a] Standard reaction conditions: 2-naphthalenemethanol (158 mg, 1.00 mmol, 1.00 equiv.),  $\text{Cp}_2\text{TiCl}_2$  (24.9 mg, 0.10 mmol, 10.0 mol%), Mn (x equiv.) in 2-MeTHF (2 mL), stirred for 2 h at 50 °C, then  $(\text{EtO})_2\text{MeSiH}$  (0.48 mL, 3.00 mmol, 3.00 equiv.), 18 h, 100 °C in a Schlenk pressure tube. [b] Yields were determined *via* quantitative GC-FID using *n*-pentadecane as internal standard.

The reaction was originally conducted overnight in order to obtain a complete transformation (Table 6.27 - Entry 6) but in the desire to make the reaction more efficient, a reaction time optimization was conducted. Up to 4 hours reaction time the conversions were unsatisfactory, resulting in very low yields of toluene (**2a**) (Table 6.27 - Entry 1 to 4). After 8 hours, both conversion and yield increased significantly, but the reaction still did not reach the standard reaction time (Table 6.27 - Entry 5). Extending the reaction time to 48 hours a quantitative conversion was achieved but unfortunately, quantitative yield was not obtained (Table 6.27 - Entry 8).

Another element which was investigated during this screening was the importance of the pressure build-up in the reaction vessel after the silane addition. In the experiment with a reaction time of 16 hours, it was essential not to release the pressure by purging the reaction with inert gas as the yield difference between the two procedures was about 19% (Table 6.27 - Entry 6 and 7). Instead, the importance of this empirical detail faded as the reaction time was prolonged to 48 hours (Table 6.27 - Entry 8 and 9). A possible explanation for this observation is that the system needs more than 18 h to compensate for the loss of the pressure, which was created in the reaction vessel immediately after the addition of the silane, by opening the inert gas valve of the Schlenk flask. In conclusion, the reaction was further conducted for 18 h in an immediately sealed reaction vessel.

**Table 6.27.** Reaction time optimization.



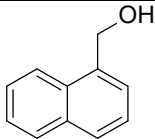
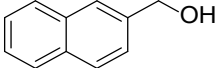
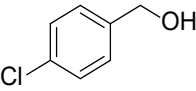
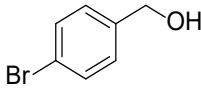
Entry <sup>[a]</sup>	Reaction Time (h)	Conversion (%) <sup>[c]</sup>	Yield (%) <sup>[c]</sup>
1	0.5	6	4
2	1	13	9
3	2	20	15
4	4	38	28
5	8	80	68
6	18	quantitative	96
7	18 <sup>[b]</sup>	quantitative	77
8	48	quantitative	92
9	48 <sup>[b]</sup>	quantitative	90

[a] Reaction conditions: benzyl alcohol (0.104 mL, 1.00 mmol, 1.00 equiv.),  $\text{Cp}_2\text{TiCl}_2$  (24.9 mg, 0.10 mmol, 10.0 mol%), Mn (54.9 mg, 1.00 mmol, 1.00 equiv.) in 2-MeTHF (2 mL), stirred for 2 h at 50 °C, then  $(\text{EtO})_2\text{MeSiH}$  (0.48 mL, 3.00 mmol, 3.00 equiv.), t h, 100 °C in a Schlenk pressure tube. [b] with pressure release before 100 °C. [c] Yields were determined *via* quantitative GC-FID using *n*-pentadecane as internal standard.

The last investigated parameter of this screening was the importance of the activation time on multiple substrates by using the final standard conditions for the catalytic systems. This proved again

to have a crucial role in generating the desired deoxygenation product (Table 6.28) on both naphthalene and halogenated substrates.

**Table 6.28.** Activation time with optimized parameters.

Substrate				
Yield (%) with 30 minutes activation <sup>[b]</sup>	56	68	47	26
Yield (%) with 2 hours activation <sup>[b]</sup>	96	95	93	73

[a] Reaction conditions: benzylic alcohol (0.104 mL, 1.00 mmol, 1.00 equiv.), Cp<sub>2</sub>TiCl<sub>2</sub> (24.9 mg, 0.10 mmol, 10.0 mol%), Mn (54.9 mg, 1.00 mmol, 1.00 equiv.) in 2-MeTHF (2 mL), stirred for 2 h at 50 °C, then (EtO)<sub>2</sub>MeSiH (0.48 mL, 3.00 mmol, 3.00 equiv.), t h, 100 °C in a Schlenk pressure tube. [b] Yields were determined *via* quantitative GC-FID using *n*-pentadecane as internal standard.

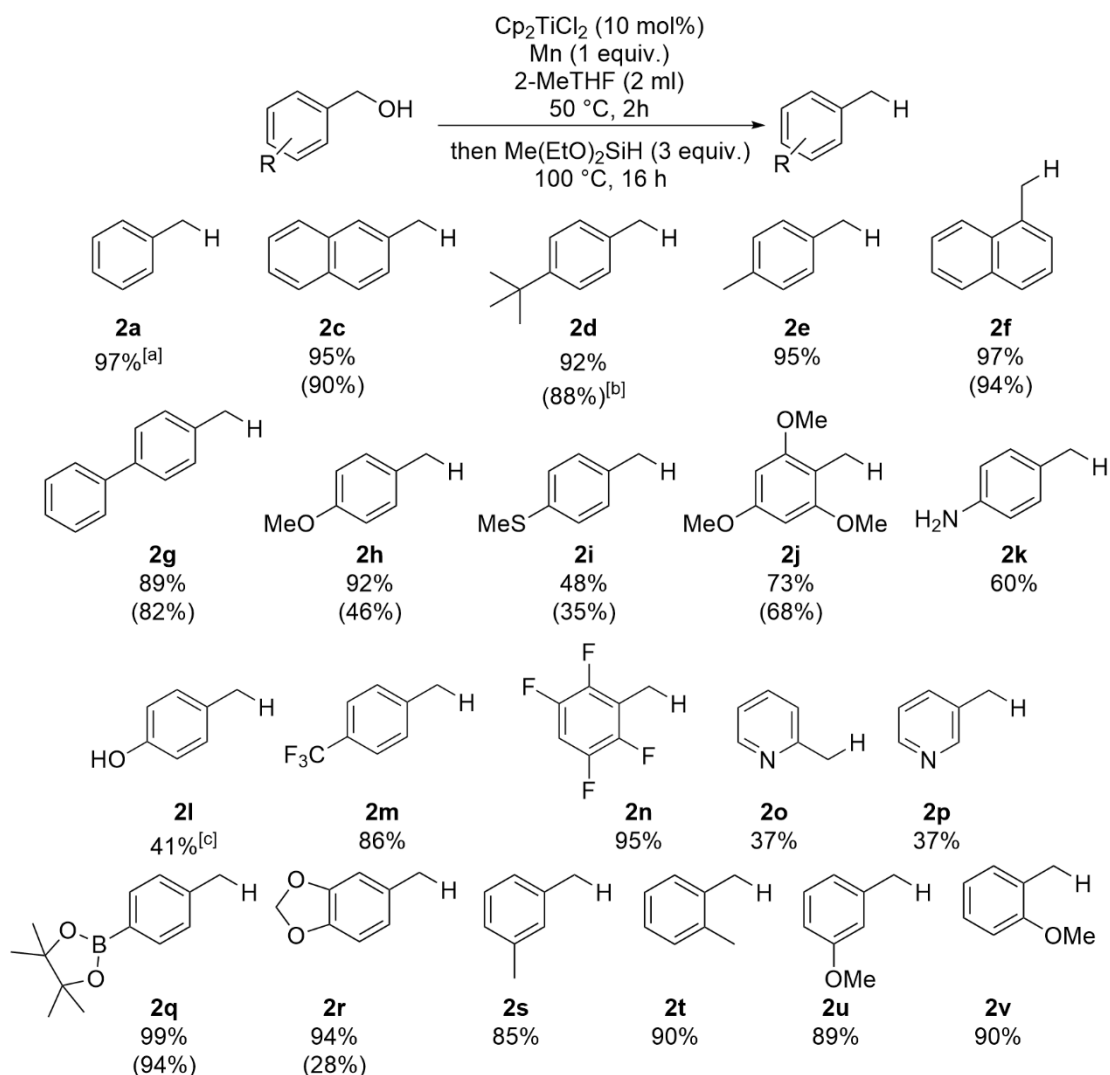
In conclusion, after an extensive optimization procedure, the standard conditions of the Ti-catalyzed deoxygenation were determined, and this procedure was submitted for the transformation of a wide variety of substrates.

#### 6.3.4. Substrates Screening

After optimizing the reaction parameters, a substrate screening was conducted. The first compounds which were submitted to the reaction were functionalized primary benzylic alcohols (Figure 6.2). Both  $\alpha$ - and  $\beta$ -methyl-naphthalenes (**2c** and **2f**) were obtained in yields above 95%. The substrates containing alkyl and aryl substituents in *para* position (**4d**, **4e** and **4g**) led to high GC-yields of the desired products (**2d**, **2e** and **2g**). Excellent results were also obtained when the benzyl backbone was replaced by naphthyl moiety.

Subsequently, more challenging substrates bearing electron-donating functional groups were submitted to the reaction. The first example of this category is 4-methoxybenzyl alcohol (**4h**) which was transformed into **2h** in excellent yield. However, the isolated yield dropped to only 46% due to the volatility of the product. Exchanging the -OMe group with -SMe (**2i**) led to a major yield drop with only 48% GC-yield. Based on the available literature, the presumption for this unsatisfying result could be the formation of a Ti-S complex which is unsuitable for the catalyst regeneration process under these conditions, but this possible poisoning process was not further investigated.<sup>68</sup> Then, the more demanding triethoxy-substituted substrate **4j** was subjected to the reaction. Although the yield dropped compared to the mono-substituted counterpart it was hypothesized that this outcome is not a consequence of the more electron-rich aromatic moiety but of the steric impediments implied by the two *ortho* substituents. Another challenging substrate containing an electron-donating functional group, which was tested in the catalytic system, was **4k** containing an amino group. In comparison to the other mono substituted substrates from this category, **4k** was converted to **2k** in only 60% yield. The reason for this result is the possible partial poisoning of the catalyst by the coordination of the N-atom to the Ti-center, which might form an insoluble complex.

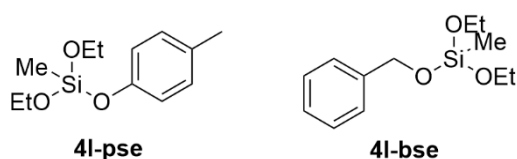




Reaction conditions: benzylic alcohol (0.104 mL, 1.00 mmol, 1.00 equiv.),  $\text{Cp}_2\text{TiCl}_2$  (24.9 mg, 0.10 mmol, 10.0 mol%), Mn (54.9 mg, 1.00 mmol, 1.00 equiv.) in 2-MeTHF (2 mL), stirred for 2 h at 50 °C, then  $(\text{EtO})_2\text{MeSiH}$  (0.48 mL, 3.00 mmol, 3.00 equiv.), t h, 100 °C in a Schlenk pressure tube. [a] GC-yields [b] number in brackets displays isolated yield [c] after deprotection.

**Figure 6.2.** Primary benzylic alcohols scope.

The pursue continued by submitting **4l** to the reaction. The analysis of the crude reaction mixture after 18 h contained only traces of the desired product. Instead, a good amount of a corresponding silyl ether was detected in the GC-MS chromatogram. Due to existence of two sites where a silyl ether could be formed a deprotection reaction was conducted by treating the mixture with 5 mL 1 M HCl solution in order to differentiate between the two possible products **4l-pse** and **4l-bse** (Figure 6.3).



**Figure 6.3.** Possible silyl ethers of substrate **4l**.

Surprisingly, **2i** was the main product of the deprotection reaction, due to the regeneration of the phenolic group. Although the GC-yield was only 41% this result was considered satisfying due to the difficulty of the transformation.

After investigating the influence of the electron-donating functional groups, the focus turned to substrates containing electron-withdrawing functional groups. The first tested substrate was **4m** which surprisingly led to the formation of **2m** in a very satisfying GC-yield of 86%. This encouraging result showed that the catalytic procedure can also tolerate substrates containing electron-poor aromatic systems. The tetrafluoro-substituted compound **4n** was transformed in almost quantitative yield to the desired product **2n**. Both these results strengthen the conclusion regarding the system tolerance toward a wide range of functional groups.

Moreover, substrates bearing heterocyclic backbones were submitted to the reaction. The preliminary attempts of transforming substrates bearing pyridinyl backbone into the desired products were unsuccessful. It was observed that a black tar was formed in the vessel during the addition of the reagents and this compound were not solubilized even at high temperatures. The presumption was that the pyridinyl moiety strongly coordinates to the metallic centre of the catalyst deactivating it. The synthesis of this Cp<sub>2</sub>TiCl-pyr complex in THF was previously characterized by Green.<sup>63</sup> Therefore, the addition order was changed for these reactions and the substrate was slowly added to the mixture only after the reduction process of the Ti-catalyst was complete. Despite these changes, the obtained yields of **2o** and **2p** were not satisfactory at only 37% for both reactions.

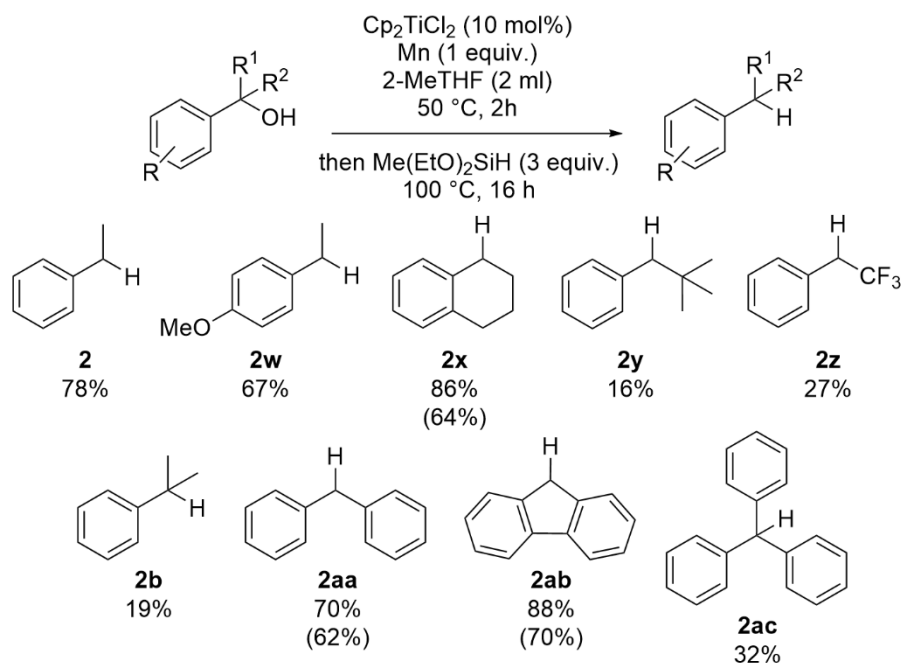
Furthermore, substrates bearing reactive functional groups were submitted to the reaction. Surprisingly, product **2q** was obtained in quantitative yield as the boronic ester moiety was not destroyed during the process. In addition, the piperonyl backbone **4r** was well tolerated by the catalytic system as it led to a 94% GC-yield of the desired product **2r**. This reaction is of great importance as it shows that ketones and aldehydes can be tolerated as well by the system in a protected form. The acidic work-up conditions led to the cleavage of the ketal moiety and the isolated yield dropped to only 28%. Although encouraging, this result showed that alternative quenching procedures should be developed when the molecular complexity of the substrates increases.

In order to investigate the influence of the substituents in *ortho* and *meta* positions, alcohols **4s**, **4t**, **4u** and **4v** were subjected to the reaction. The alkyl containing products **2s** and **2t** were obtained in high yields of 85% and 90%, respectively. Surprisingly, both **4u** and **4v** were also transformed into the desired product in satisfying yields despite higher steric impediments of **4v**.

2-Phenylethanol (**4**) was tested first, and the reaction led to promising results. (Figure 6.4) In an attempt to broaden the substrate scope, the reactivity of secondary and tertiary benzylic alcohols was also evaluated. The role of *p*-substituents was then investigated in *p*-methoxy substituted substrate **4w**. Although the yield dropped compared to **2**, the outcome of this reaction was analogous to those obtained in case of primary benzylic alcohols. By adding more rigidity to the backbone, **4x** led to an increased GC-yield of 86%. When steric impediment was increased by exchanging the methyl group with a tertbutyl group, the yield drops significantly from 78% in case of **2** to 16% in case of **2y**.

Then, the  $\alpha$ -aryl substituted substrates were submitted to the catalytic procedure. From the deoxygenation of 2-phenylpropan-2-ol (**4b**) cumene (**2b**) was obtained in 19% yield. Both **4aa** and **4ab** led to good yields of **2aa** and **2ab** (70% and 88%). It was observed that also in this case the increased rigidity of the molecule has a positive effect on the transformation. The positive influence of  $\alpha$ -aryl substituents was also seen after implementing different tertiary benzylic alcohols. The introduction of an electron-withdrawing group in the  $\alpha$ -position had a strong negative influence on the transformation

as well, as **2ac** was obtained in only 27% yield. Although **1ad** is sterically hindered, **2ak** was obtained in 32% yield due to the positive effect of the phenyl substituents in  $\alpha$ -position.



**Figure 6.4.** Secondary and tertiary benzylic alcohols scope.

In conclusion, this catalytic system proved to be effective in deoxygenating a high number of benzylic alcohols containing electron-donating and electron-withdrawing substituents grafted on the aromatic backbone. The deoxygenation of substrates bearing substituents in  $\alpha$ -position was also partially successful.

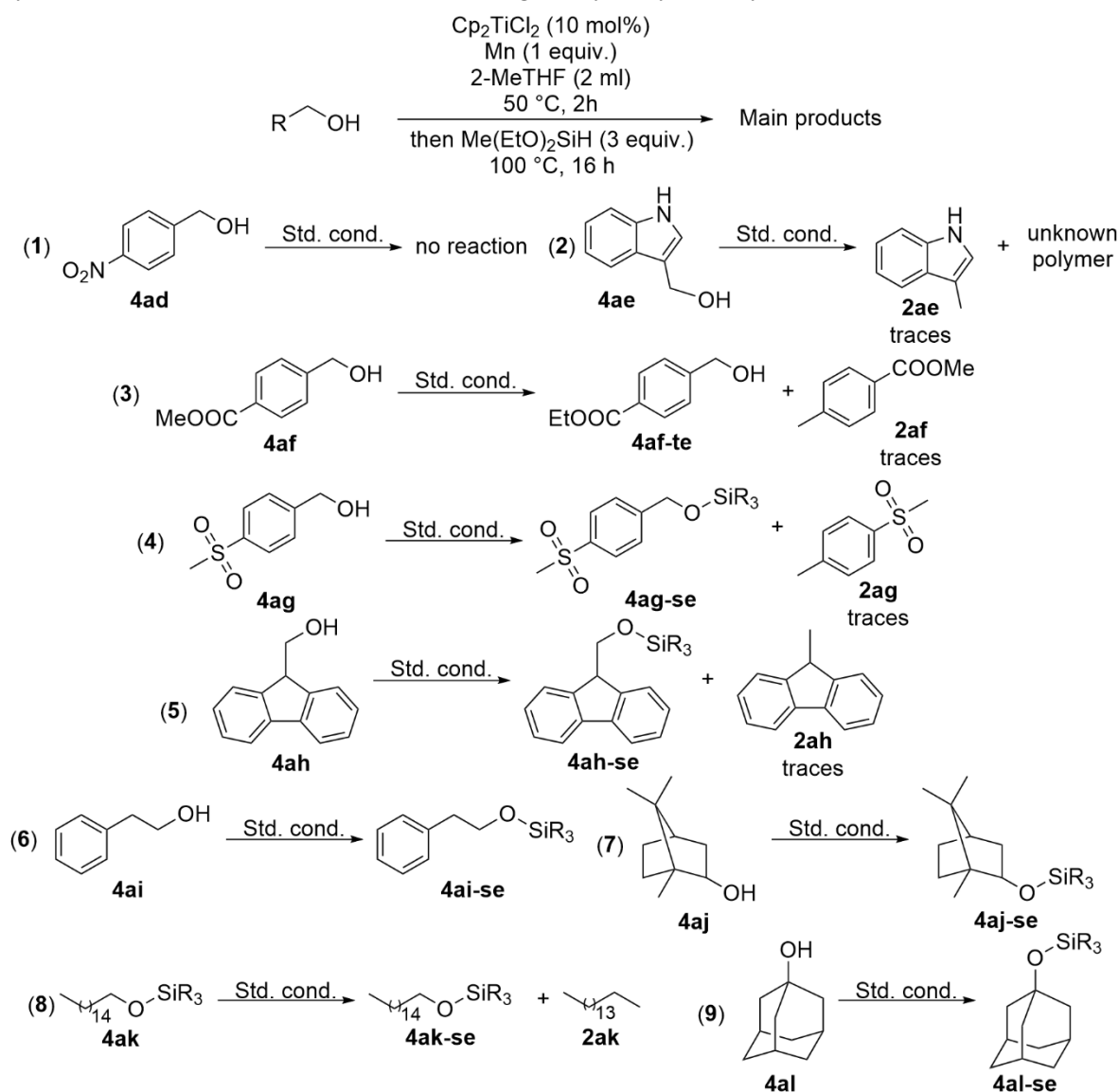
### 6.3.5. Unsuccessful Substrates

Although this process was successful for a wide range of substituted benzylic alcohols, some functionalities were not tolerated by the developed system. Substrate **4ad** containing a nitro group only afforded the protected alcohol (Scheme 6.14 – Reaction 1). The product formation was completely inhibited, and surprisingly, a reduction of the nitro group was not observed *via* GC-analysis. The presumption regarding this unsuccessful reaction was that a catalyst poisoning process occurred through a strong coordination of the  $\text{NO}_2$  group on the metallic centre followed by the formation of a catalytically inactive species.

Only traces of the desired product Skatole (**2ae**) were detected, when indole-3-carbinol (**4ae**) was submitted to the reaction (Scheme 6.14 – Reaction 2). No ring-opened, hydrogenated, or protected products were observed but surprisingly the conversion was >95%. During the reaction the formation of a black tar was observed. Due to the lack of viable products in the GC chromatogram, the presumption was that an indol-based polymer formed in the reaction mixture. Another transformation, which was considered unsuccessful, was the deoxygenation of substrate **4af** (Scheme 6.14 – Reaction 3). This transformation yielded only a small amount of **2af** and only traces of product implying the reduction of the ester group. Instead, the main peak observed was assigned to the transesterification product **2af-te**. This transformation is not surprising as report documented it in similar catalytic procedures.<sup>69</sup> The same hypothesis as for reaction (1) was stated also for the transformation of

substrate **4ag** bearing an  $-\text{SO}_2\text{Me}$  group in *para* position (Scheme 6.14 – Reaction 4). In this case, traces of the desired product were detected on the chromatogram, but the main product was also in this case the corresponding silyl ether. Summarizing all the results obtained from reactions conducted on substrates containing nitrogen and sulfur-based functional groups, the conclusion was that the catalytic system is not well suited for this kind of transformations as the reactivity in this environment decreases significantly.

Alcohols containing the  $-\text{OH}$  group in homobenzylic position **4ah** and **4ai** led to unsatisfactory results as no desired product was detected (Scheme 6.14 – Reaction 5 and 6). Another limitation of this catalytic process is the transformation of aliphatic alcohols into saturated hydrocarbons as only the silyl-protected alcohols were obtained under these reaction conditions (Scheme 6.14 – Reaction 7, 8 and 9). The only exception was substrate **4ak**, which afforded **2ak** in 12% yield. The reproducibility of this reaction turned out to be difficult, and a possible explanation for the initially successful reaction of substrate **4ak** could be a precious metal contamination. Therefore, the conclusion was that this catalytic system is unreactive towards substrates bearing the hydroxyl moiety linked to an unreactive C-atom.

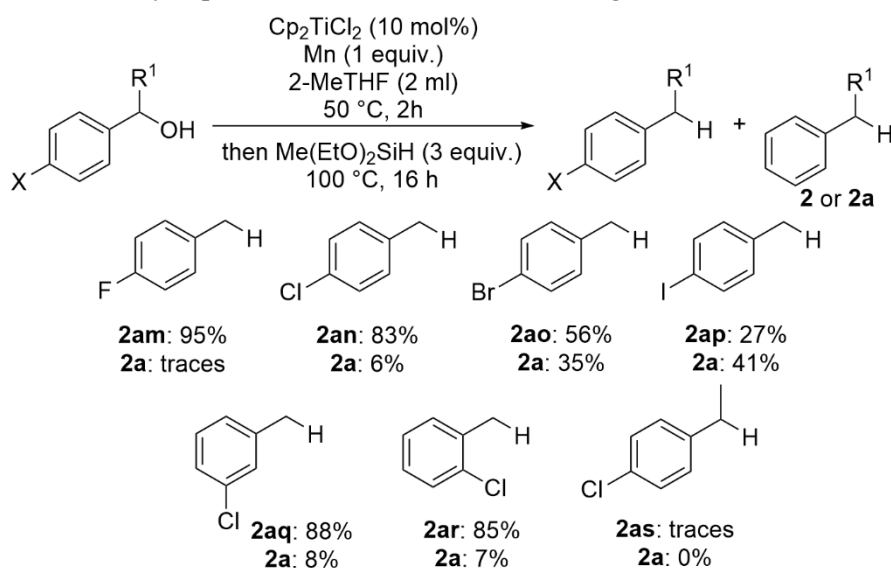


**Scheme 6.14.** List of unsuccessful substrates.

### 6.3.6. Deoxygenation-Dehalogenation Reaction

Following the previously obtained results, the substrate screening continued by submitting halogenated aromatic alcohols in the catalytic reaction (Figure 6.5). The first substrates tested were **2an** and **2ao**. Both of them underwent deoxygenation process in good yields and after analysing the chromatograms of the crude reaction mixtures, it was observed that also the characteristic peak for toluene (**2a**) appeared beside those for the desired product. Also, the presumption that there might be a reverse correlation between the desired yield and toluene (**2a**) yield (Figure 6.6) was suggested. Intrigued by these results, the chromatograms were further analysed in order to discover if also the characteristic peaks for the non-deoxygenated dehalogenated peaks were detected. Surprisingly, no traces of benzyl alcohol (**4a**) were observed in either of the mixtures. Next, fluoro- and iodo-containing **2am** and **2ap** substrates were submitted to the reaction. Substrate **4a** was transformed in **2am** in quantitative yield and only traces of toluene (**2a**) were detected.

On the contrary, substrate **4ap** led to the formation of **2ap** in only 27% yield and toluene (**2a**) was the main product of this transformation with 41% yield. Similarly, benzyl alcohol (**4a**) could not be traced in the chromatograms. Furthermore, the influence of the position of the halogen substituent on the aromatic system was investigated. The results showed that this does not have any major impact over the transformations as both **2aq** and **2ar** were obtained in almost same yield as **2an** and also the toluene (**2a**) yield remained constant. Surprisingly, the secondary benzylic alcohol **4as** with chlorine in *para*-position led to traces of product **2as** and not even traces of toluene (**2a**) were observed. This outcome could not be fully explained and was not further investigated.

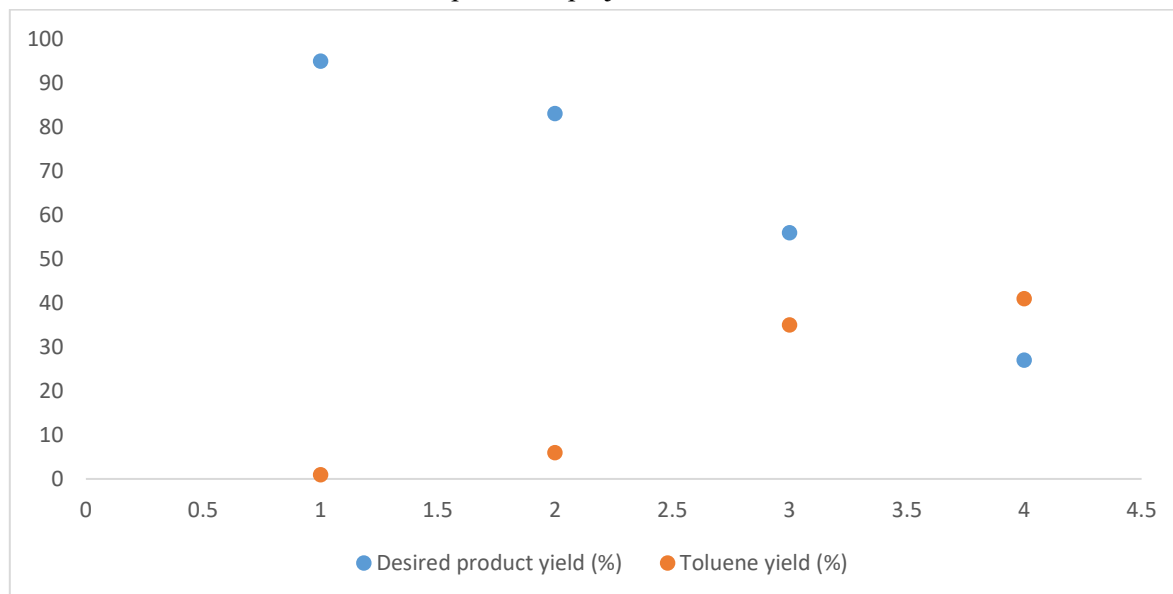


**Figure 6.5.** *p*-halogenated benzylic alcohols scope and the yield of the corresponding unsaturated products and toluene.

In order to reduce the amount of deoxygenated-dehalogenated product, the reaction time in the reduction of 4-chlorobenzyl alcohol was reduced to 8 hours. Unfortunately, beside the lower conversion and yield of the desired product, the ratio between 4-chlorotoluene and toluene (**2a**) remained constant compared to the standard reaction, 28% **2ao** and 2% **2a**).

The hypothesis, which was formulated after analyzing these results, was that the substrates first undergo the deoxygenation reaction and only then the dehalogenation reaction takes place. This theory was mostly supported by the fact that benzyl alcohol (**4a**) was not detected in any crude reaction

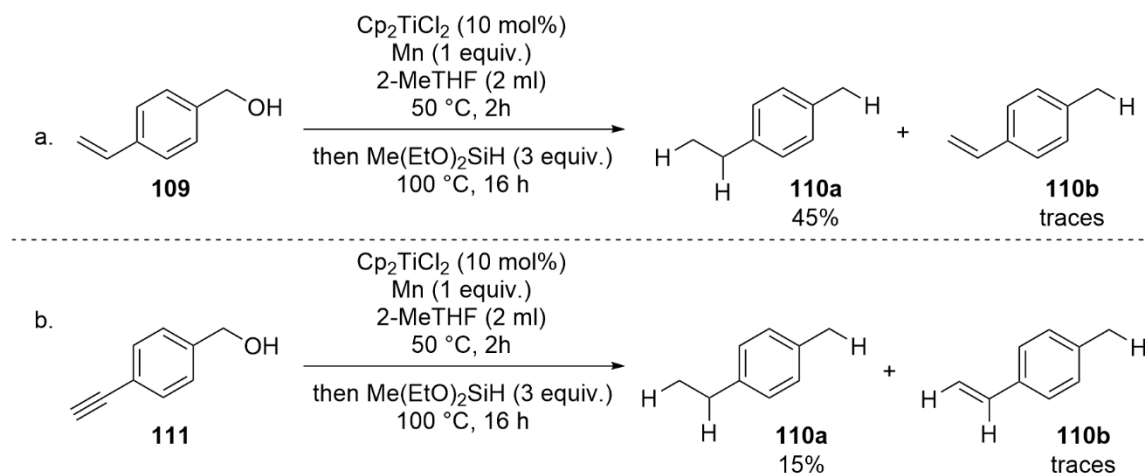
mixture. Also, it is important to state that this deoxygenation-dehalogenation sequence is maintained regardless of the halogen substituent. Further investigations into the dehalogenation mechanism were not conducted as it was outside the scope of this project.



**Figure 6.6.** *p*-Halogenated product (blue) and toluene yields trend (red).

### 6.3.7. Deoxygenation-Hydrogenation Reaction

The reactivity of substrates bearing unsaturated moieties in *para*- and  $\alpha$ -positions were also evaluated in the reaction under standard conditions. The hydrogenation capabilities of the Ti/H systems is well known and studied.<sup>70-72</sup> The aim of these reactions was to investigate a possible competition between these two transformations and to perceive, which one is preferred, deoxygenation or hydrogenation (Scheme 6.15).



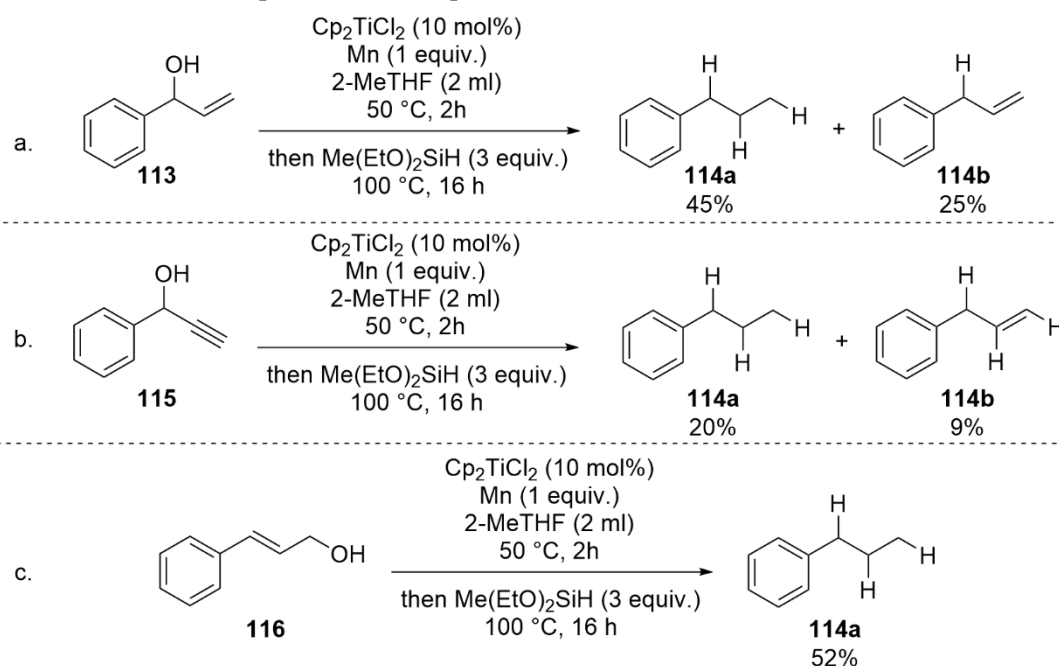
**Scheme 6.15.** Reduction of benzylic alcohols with *p*-unsaturated moiety. (a) Reduction of (4-vinylphenyl)methanol; (b) Reduction of (4-ethynylphenyl)methanol.

First, *p*-vinyl (**109**) and alkynyl (**111**) substrates were submitted to the standard reaction conditions. It was observed that both of these reactions afforded only the deoxygenated products, with **110a** as the major product regardless of starting material. The difference in yield between the two could be explained by the same hydrosilane amount used during the screening. Interestingly, 4-ethyl benzyl

alcohol (**112**) was detected in neither reaction mixture. Therefore, the conclusion was that the reduction of the double and triple bond did not occur solely without a prior deoxygenation of the substrate.

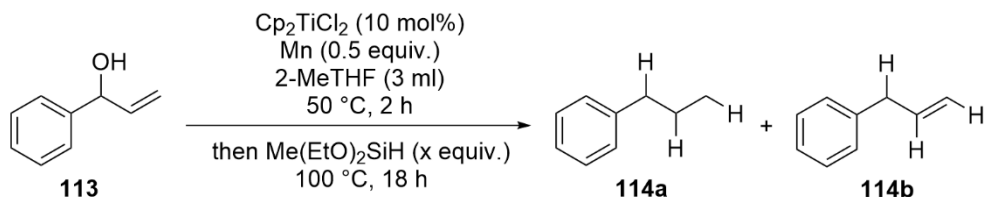
Consequently, the reactivity of substrates bearing unsaturated substituents in  $\alpha$ -positions was tested (Scheme 6.16). In case of vinyl containing substrate (**113**), the yield of the deoxygenation-hydrogenated product was similar compared to the *para*-substituted (Scheme 6.16 - a). In contrast, the yield of the only deoxygenated product **114b** was significantly higher (28%). This showed that an unsaturated substituent in the vicinity of the C-O bond has a strong positive effect on the deoxygenation process. This conclusion was further strengthened by the transformation of **115** (Scheme 6.16 - b). Both deoxygenated and deoxygenated-hydrogenated products were afforded in higher yields of 20% respectively 9%. Additionally, the non-deoxygenated hydrogenated products could not be detected in these reactions.

Intrigued by the previous results, the role of internal double bonds in the deoxygenation process was investigated. Surprisingly, when cinnamyl alcohol (**116**), which contains the -OH group in the allylic position, was submitted to the reaction, propylbenzene (**114a**) was obtained in good yield (Scheme 6.16 - c). This is the first example in this work of a deoxygenation reaction in which the hydroxy group is not in the benzylic position. In the crude reaction mixture traces of allyl benzene were detected. This discovery strengthens the theory that the transformation of alcohols containing unsaturated bonds follows a deoxygenation-hydrogenation pathway. This sequence is analogously to the one observed in the results presented in chapter 6.3.6.



**Scheme 6.16.** Reduction of  $\alpha$ -unsaturated benzylic alcohols. (a) Reduction of 1-phenyl-2-propen-1-ol; (b) Reduction of  $\alpha$ -ethynylbenzenemethanol; (c) Reduction of cinnamyl alcohol.

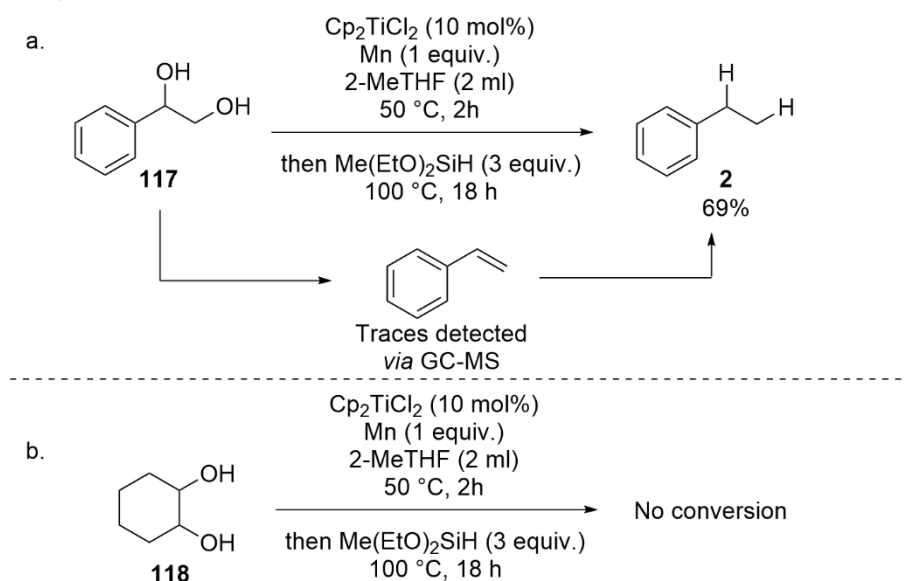
In order to increase the yield of both deoxygenation and hydrogenation, an optimization of the amount of silane was attempted (Table 6.29). Surprisingly, the changes in yield when the amount of hydrosilane were decreased or increased were not as significant as expected (Table 6.29 – Entry 1 and 3). Therefore, these experiments show that the Ti catalyst was the limiting factor in the formation of the desired deoxygenated-hydrogenated product and not the H-donor.

**Table 6.29.** Influence of hydrosilane equivalents on the deoxygenation-hydrogenation reaction of **113**.

Entry	Silane (equiv.) <sup>[a]</sup>	Yield <b>11a</b> <sup>[b]</sup>	Yield <b>11b</b> <sup>[b]</sup>
1	2	43	27
2	3	45	28
3	4	54	24

[a] Standard reaction conditions: benzyl alcohol (0.104 mL, 1.00 mmol, 1.00 equiv.),  $\text{Cp}_2\text{TiCl}_2$  (24.9 mg, 0.10 mmol, 10.0 mol%), Mn (54.9 mg, 1.00 mmol, 1.00 equiv.) in 2-MeTHF (2 mL), stirred for 2 h at 50 °C, then  $(\text{EtO})_2\text{MeSiH}$  (x equiv.), 18 h, 100 °C in a Schlenk pressure tube. [b] Yields were determined *via* quantitative GC-FID using *n*-pentadecane as internal standard.

Next, the capability of the catalytic system to reduce 1,2-diols was tested (Scheme 6.17). Interestingly, compound **117** was transformed into ethyl benzene in good yield (Scheme 6.17 - a). The pathway of this unexpected transformation was clarified as small quantities of styrene were detected *via* GC-MS. The hypothesis behind this process relies on the cleavage of the C-O bond in the benzylic position followed by a radical elimination process. Succeeding the deoxydehydration, the formed olefin gets hydrogenated affording ethyl benzene. Disappointingly, cyclohexyl diol **118** did not afford any deoxygenation product strengthening the conclusion that in order to have a radical elimination process, first, the deoxygenation has to take place, and this is possible only from benzylic or allylic positions (Scheme 6.17 - b).

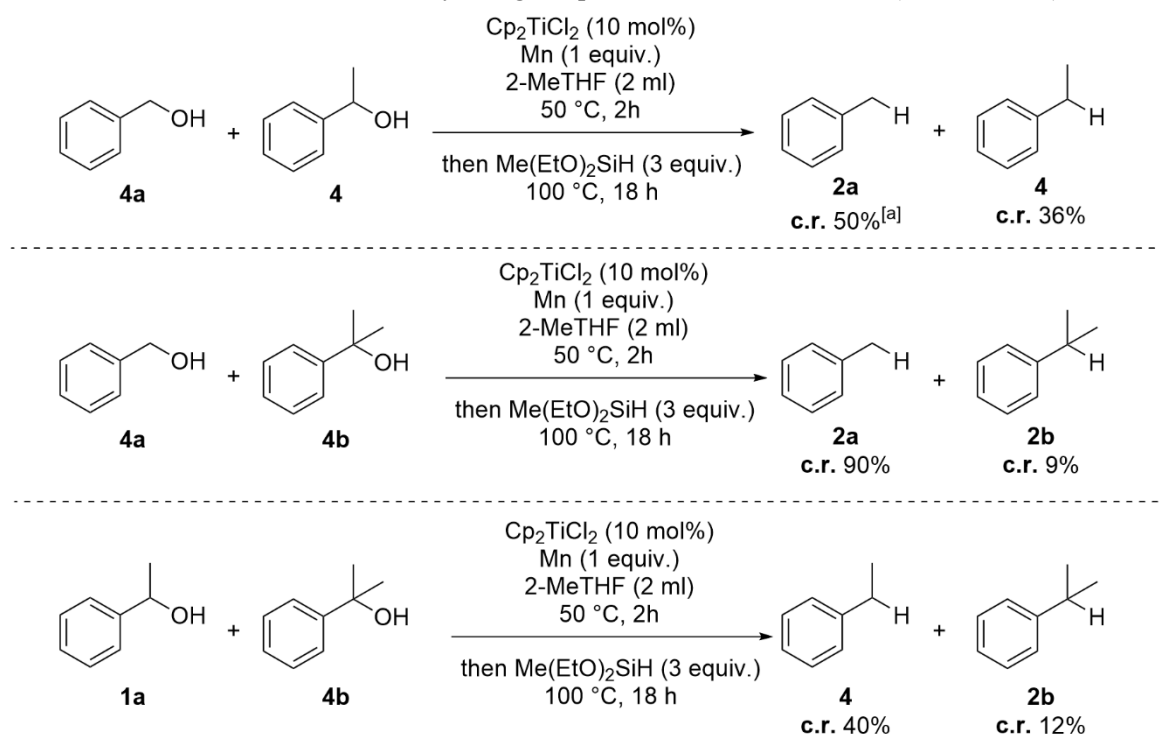
**Scheme 6.17.** Reactivity of diols. (a) Reduction of 1-Phenyl-1,2-ethanediol and possible reaction pathway; (b) Reduction of cyclohexyl diol.



Thus, unsaturated benzylic alcohols were successfully transformed into the desired deoxygenated products. Although the hydrogenation played a significant role during these reactions, the interference was not considered negative as both deoxygenated and deoxygenated-hydrogenated products are used in industrial applications.<sup>73-76</sup>

### 6.3.8. Selectivity Reactions

After analysing the results obtained during the substrate screening, a series of reactions were performed in order to investigate the selectivity of the catalytic system for primary benzylic alcohols over secondary and tertiary alcohols. For this study, intermolecular competitive reactions were conducted under standard conditions by using 1 equivalent of each substrate (Scheme 6.18).

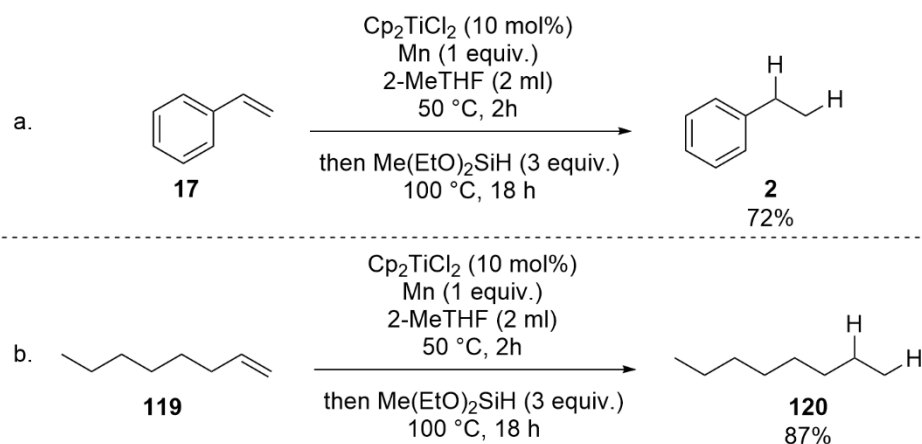


**Scheme 6.18.** Selectivity reactions. (a) Reduction of primary and secondary benzylic alcohols; (b) Reduction of primary and tertiary benzylic alcohols; (c) Reduction of secondary and tertiary benzylic alcohols; [a] c.r. – competitive reaction.

Unfortunately, throughout the whole investigation no clear selectivity was detected. In all cases, the yield dropped according to the reaction conditions but the ratio between the products remained constant compared to the reactions of single substrates. Thus, the catalytic system was considered non-selective for different alcoholic C-O connectivity patterns.

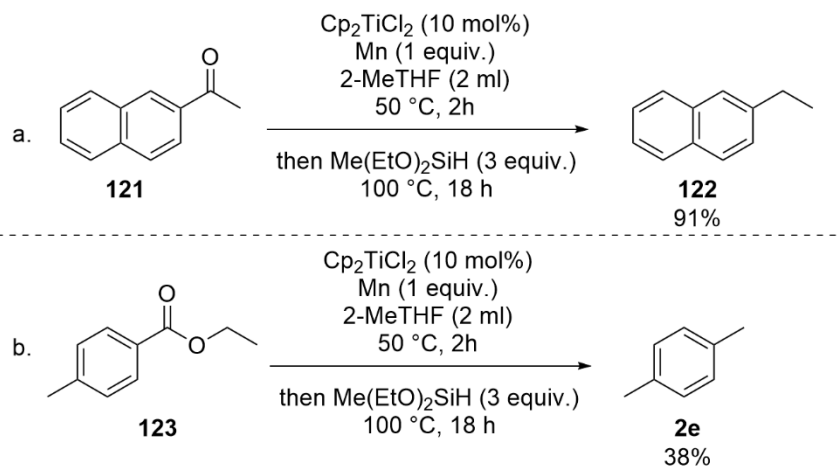
### 6.3.9. Miscellaneous Substrates

After screening a number of benzylic alcohols, the catalytic system was applied on substrates containing different functionalities (Schemes 6.19, 6.20 and 6.21). Taking in account the previous results, the reactivity of unsaturated hydrocarbons was investigated in the first step. Both styrene (**17**) and 1-octene (**119**) were transformed in high yields into the desired product, in correspondence to the available literature (Scheme 6.19 – a and b).<sup>77</sup> Additionally, no hydrosilylation products were observed in the GC-MS chromatogram.



**Scheme 6.19.** Reduction of olefins. (a) Reduction of styrene; (b) Reduction of 1-octene.

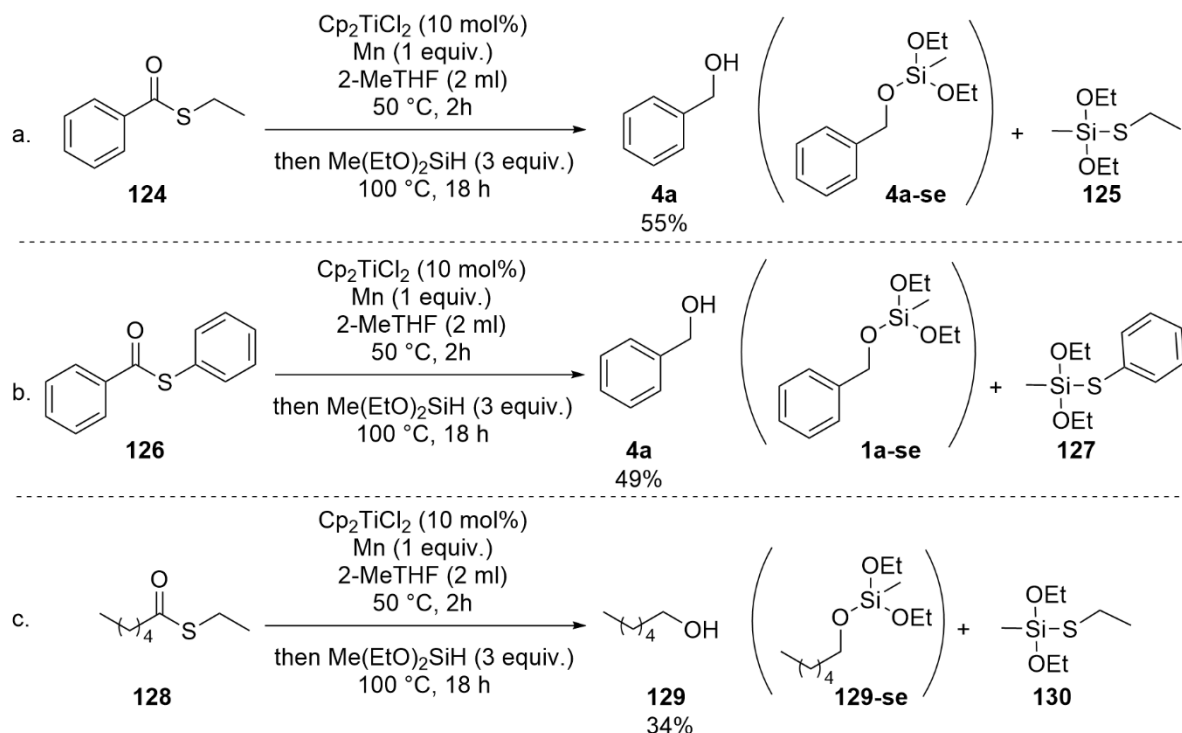
Then, 2-acetylnaphthalene (**121**) was subjected to the reaction (Scheme 6.20 – a). To our delight the transformation afforded 2-ethylnaphthalene (**122**) in 91% yield by using the standard reaction conditions. Encouraged by this result, the reactivity of esters was tested as well (Scheme 6.20 – b). Surprisingly, instead of obtaining the transesterification product analogue to the unsuccessful transformation of substrate **4ag**, *p*-xylol (**2e**) was obtained. For this reaction a low yield was expected as for a complete transformation more H-donor equivalents would be needed, thus, a 38% yield was considered satisfying.



**Scheme 6.20.** Reduction of miscellaneous substrates. (a) Reduction of 2-acetylnaphthalene; (b) Reduction of ethyl 4-methylbenzoate.

In order to gain a broader understanding about the catalytic system, also thioesters were applied in the reaction (Scheme 6.21). Interestingly, only traces of toluene (**2a**) were detected during the GC-analysis for the transformation of **124** (Scheme 6.21 - a). Instead, the main product of the reaction was the protected alcohol **4a-se**, which afforded benzyl alcohol (**4a**) in 55% yield after deprotection. Intrigued by these results, thioesters **126** and **128** were also employed. *S*-Phenyl thiobenzoate (**126**) led to the formation of benzyl alcohol (**4a**) in 49% yield after deprotection and aliphatic thioester *S*-ethyl thiohexanoate (**128**) was reduced as well to the corresponding alcohol in 34% yield (Scheme 6.21 – b and c). The difference in reactivity between esters and thioesters was unanticipated. The reactivity of the thioesters in this catalytic system should be further investigated as this kind of transformation is not

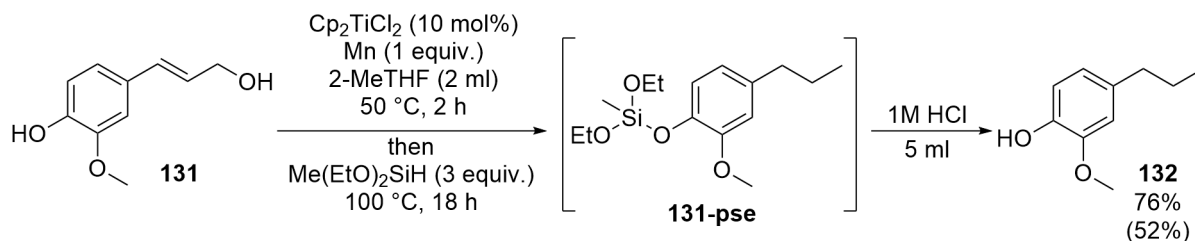
well documented in the available literature. Additionally, a more in-depth analysis should be considered regarding the difference of products between the esters and thioesters.



**Scheme 6.21.** Reactions on thioesters. (a) Reduction of *S*-ethyl thiobenzoate; (b) Reduction of *S*-phenyl thiobenzoate; (c) Reduction of *S*-ethyl thiohexanoate.

### 6.3.10. Deoxygenation of Lignin Building Blocks and Model Substrates

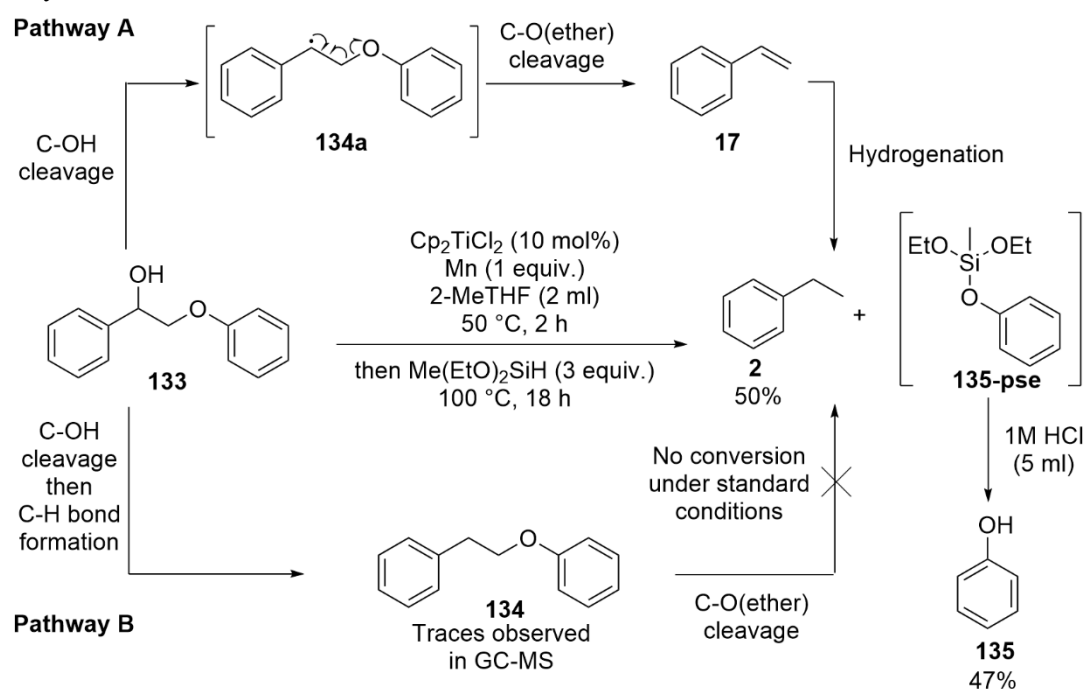
Following the optimization of the reaction conditions and the investigations of the tolerance and reactivity of the catalytic system toward a wide variety of functional groups, the applicability of this procedure on the transformation of lignin building blocks and lignin model substrates was tested. In addition, this deoxygenation methodology was applied in late-stage defunctionalisation of bioactive compounds. First, the catalytic system was applied to transform coniferyl alcohol (**131**) into an industrial-valuable product (Scheme 6.22). As it was presented in chapter 1.2, this compound is one of the three starting materials of the biosynthesis of lignin.<sup>78</sup> Despite the higher molecular complexity compared with previously deoxygenated cinnamyl alcohol (**116**), the reaction afforded the analogous product in higher yield after undergoing the acidic deprotection procedure of the phenolic -OH. Due to the previous results, the formation of compound 4-propylgvanicol (**132**) was unsurprising, instead, the yield was higher than expected. This transformation also strengthened the conclusion that the phenolic hydroxy groups are unreactive towards the deoxygenation procedure.



**Scheme 6.22.** Transformation of coniferyl alcohol.

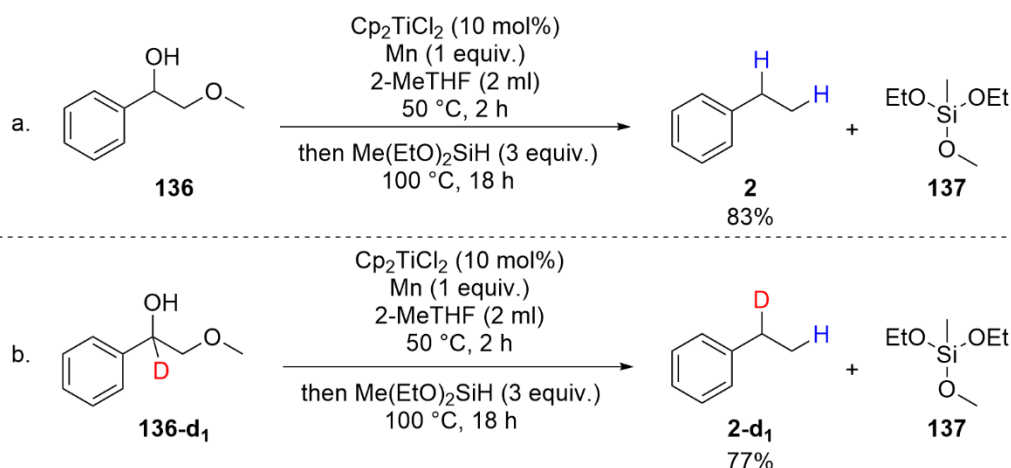
Subsequently, lignin model substrates were submitted to the deoxygenation procedure. The most common lignin constituent motif is the  $\beta$ -O-4 linkage,<sup>79</sup> which can be found in compound **133**. This compound was chosen because it does not bear any functional groups on the aromatic systems which could interfere with the reactivity of the system on the  $\beta$ -O-4 motif (Scheme 6.23).

Beside the cleavage of the C-OH bond; the cleavage of the ether bond was observed as well. Therefore,  $\alpha$ -(phenoxyethyl)benzenemethanol (**133**) afforded ethylbenzene in 50% yield and phenol (**135**) in 47% yield after deprotection. GC chromatogram of the crude reaction mixture showed traces of compound **134**. In order to obtain more information about the reaction pathway, compound **134** was submitted to the standard reaction conditions, but no conversion was observed, hinting that (2-phenoxyethyl)benzene (**134**) is not an intermediate in the reaction mechanism but a side-product. Considering the outcome of this reaction and the information gathered during the screenings, pathway B was discarded, and another possible reaction mechanism was elaborated (Pathway A). First, the cleavage of C-OH bond leads to the formation of the radical intermediate **134a** followed by the radical cleavage of the C-O(ether). The formed styrene (**17**) undergoes hydrogenation affording ethylbenzene in good yield.



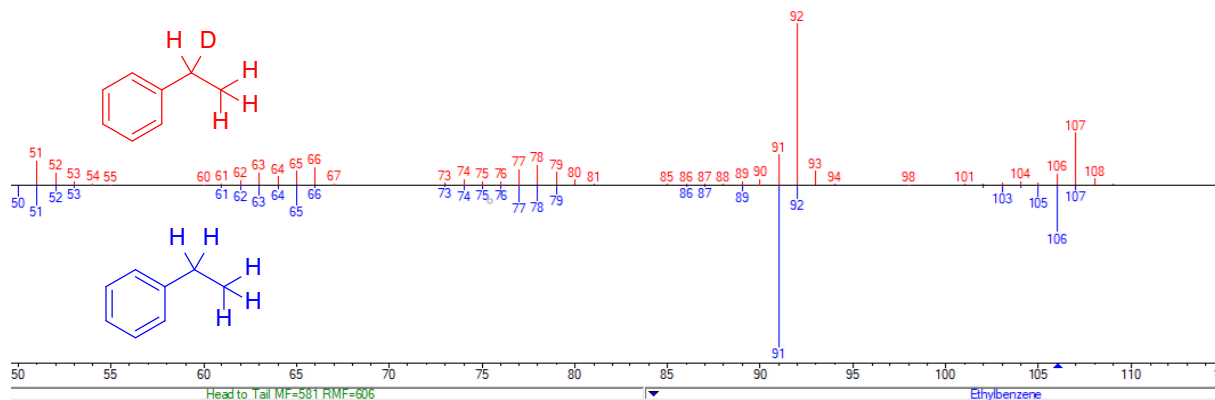
**Scheme 6.23.** Transformation of  $\alpha$ -(phenoxyethyl)benzenemethanol. Pathway A. (2-phenoxyethyl)benzene; Pathway B. Radical cleavage-hydrogenation pathway.

In order to get more insight into the proposed mechanism,  $\alpha$ -(methoxymethyl)benzenemethanol (**136**) was submitted in the catalytic system (Scheme 6.24 - a). By exchanging the phenyl moiety with a methyl group, ethylbenzene was afforded in an excellent yield of 83%. Additionally, silane **137** was detected. Following this result, deuteration labelling experiments on  $\alpha$ -(methoxymethyl)benzenemethanol derivative **136-d<sub>1</sub>** were conducted (Scheme 6.24 - b). Substrate **136-d<sub>1</sub>** afforded deuterated ethylbenzene (**2-d<sub>1</sub>**) in 77% yield.



**Scheme 6.24.** Transformation of (a)  $\alpha$ -(methoxymethyl)benzenemethanol; (b) deuterated  $\alpha$ -(methoxymethyl)benzenemethanol (b).

Its generation was proved by comparing the chromatogram obtained from the reaction product with a standard ethylbenzene chromatogram (Figure 6.7). However, the product of this reaction was not isolated due to its volatility. Therefore, the connectivity of the deuterium atom was investigated *via* GC-MS. By analysing the fragmentation pattern of **2-d<sub>1</sub>**, it can be observed that both molecular and base peaks are shifted by 1 *m/z* compared to the standard ethylbenzene fragmentation. Additionally, the base peak at 92 *m/z* can be attributed to a deuterated tropylium ion, leading to the conclusion that the initial C-D bond was not cleaved during the reaction. Based on this result, a semipinacol rearrangement or 1,2-H-shift were discarded as possible reaction pathways.

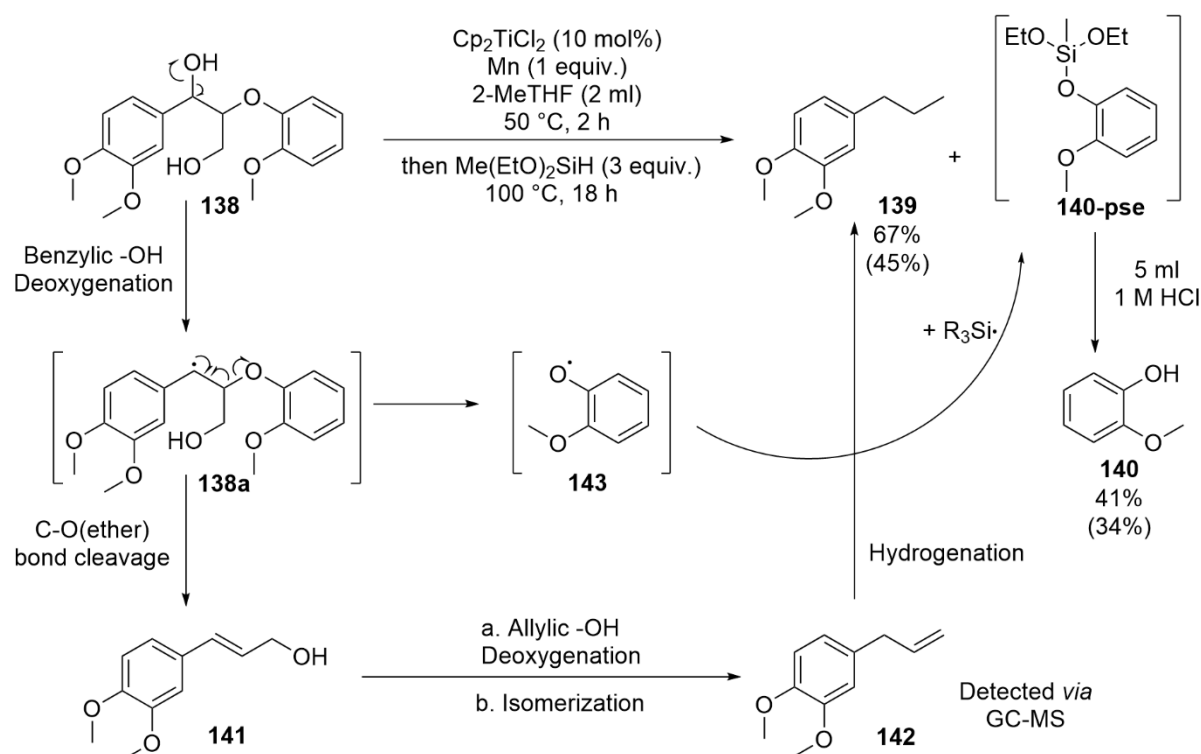


**Figure 6.7.** Comparison between obtained chromatogram for ethylbenzene-d<sub>1</sub> (red) and standard ethylbenzene chromatogram (blue).

Encouraged by the outcome of the reaction and the preliminary mechanistic studies, a more complex lignin building block was used in the reaction. Beside the specific  $\beta$ -O-4 linkage, Adlerol (**138**) contains a  $\gamma$ -carbinol unit which significantly raises the molecular complexity (Scheme 6.25). To our delight, the transformation afforded 4-propylveratrole (**139**) in 67% yield and Guanicol (**140**) in 41% yield after deprotection. In the GC-MS chromatogram, traces of methyleugenol (**142**) were detected.

This transformation was somehow surprising but based on the GC analysis and the former observations, a reaction pathway can be proposed (Scheme 6.25). The transformation starts with the homolytic cleavage of the C-OH bond followed by the breakage of ether bond and the generation of

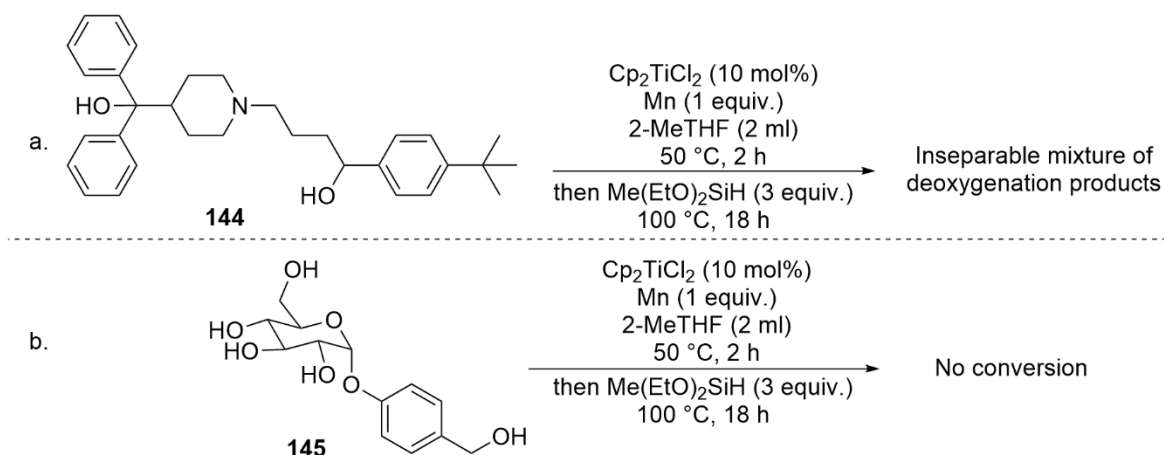
compound **141** and phenol radical **143**, which can further react with the *in situ* generated silyl radical. Analogously to the previously conducted reactions, compound **141** underwent deoxygenation and isomerization affording intermediate **142** and after the hydrogenation of the double bond product **139** was obtained.



**Scheme 6.25.** Transformation of Adlerol (**138**) and proposed mechanism.

Subsequently, a late stage defunctionalisation of pharmaceuticals was attempted (Scheme 6.26). Terfenadine (**144**) is an antihistamine which was used in allergic rhinitis treatment until 1998 when it was removed due to its side-effects (e.g. Arrhythmia).<sup>80</sup> Instead, Terfenadine (**144**) and its derivatives presented antimicrobial activity against *Staphylococcus aureus*.<sup>81</sup> Thus, a selective deoxygenation methodology for this piperidine-based motif would facilitate further application screening (Scheme 6.26 - a). However, the reaction afforded an inseparable mixture of mono and di-deoxygenated products. Analogously to the reactions conducted in chapter 5.5.8, the catalytic system was unable to selectively cleave the secondary C-OH bond.

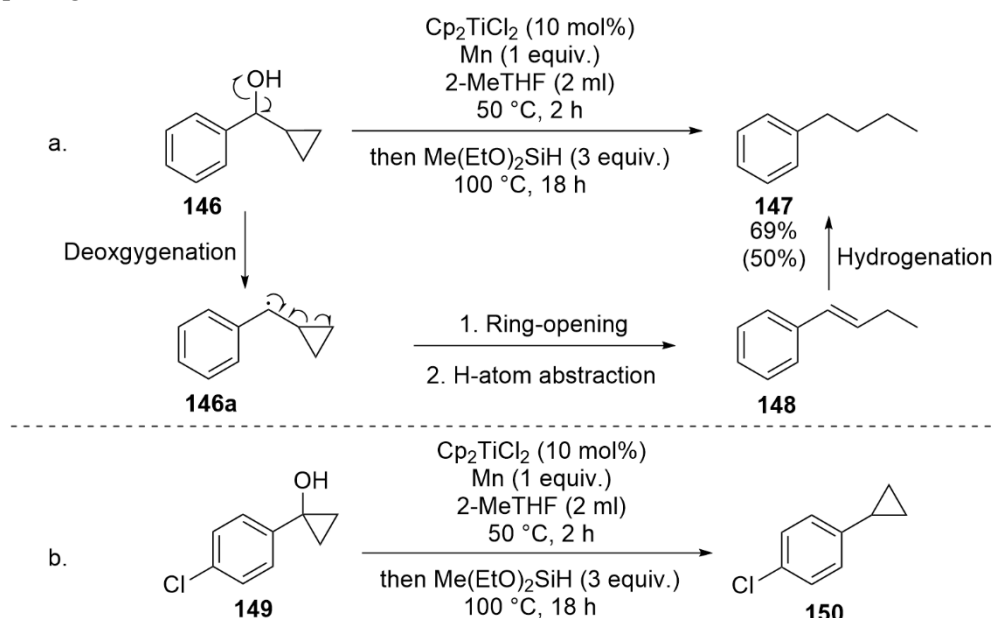
Another biologically active compound, which was subjected to the catalytic system was Gastrodin (**145**) (Scheme 6.26 - b).<sup>82</sup> The reaction was unsuccessful as no conversion under the standard reaction conditions was observed, presumably due to the low solubility of the substrate in 2-MeTHF. Another plausible reason for the failure of this reaction was the glucoside backbone which might be intolerable by the catalytic system due to the possible formation of silyl ethers.



**Scheme 6.26.** Transformation of Terfenadine (a) and Gastrodin (b).

### 6.3.11. Mechanistic Studies

Next, mechanistic studies of the deoxygenation of simple benzylic alcohols were performed. In order to get a better understanding about the reaction pathway, radical clock experiments were conducted (Scheme 6.27). The results obtained from this kind of reactions can hint towards a radical or ionic mechanism<sup>83</sup> of the reaction. For these reactions, alcohols bearing cyclopropyl moieties were selected (Scheme 6.27 - a). First, the reactivity of substrate **146** was investigated. This reaction afforded saturated compound **147** in 69% GC yield (50% isolated yield). This type of reactivity is unusual for a radical ring-opening reaction as an unsaturated sidechain was expected. The explanation for such a product would be that the unsaturated hydrocarbon chain was further hydrogenated after the ring-opening.



**Scheme 6.27.** (a) Radical clock reactions. Reduction of  $\alpha$ -cyclopropylbenzyl alcohol and possible reaction pathway; (b) Reduction of 1-(4-chlorophenyl)cyclopropanol.

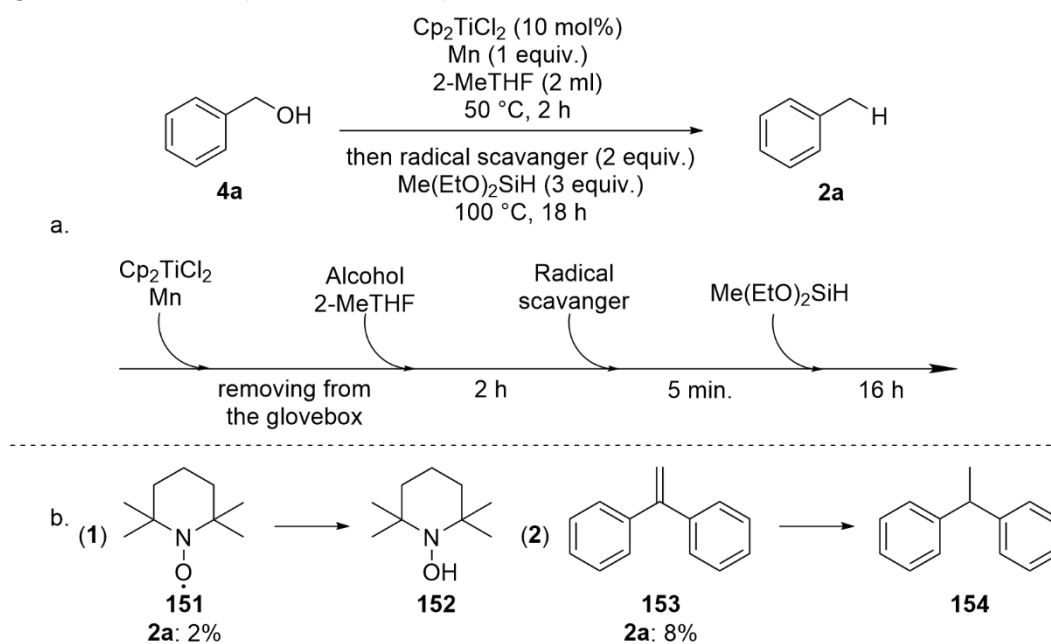
Following this result, compound **149** was also subjected in the catalytic procedure (Scheme 6.27 - b). Changing the position of the cyclopropyl fragment from homobenzylic to benzylic leads also to a change in the mechanistic path of the ring opening. Therefore, in contrast to the substrate **146**,

which is sensitive to radical deoxygenation pathways, the benzylic cyclopropyl moiety is more susceptible to ring-opening reactions following ionic mechanism, due to the increased radical stability induced by the aromatic moiety.<sup>84, 85</sup>

As only traces of product **150** were detected *via* GC-MS, beside the main product which was the corresponding silyl ether, the conclusion was the same as in the case of the first radical clock reaction, namely that the deoxygenation reaction proceeds through a radical mechanism. Due to the competitive hydrogenation, no reverse radical clock reaction was conducted.

In order to further strengthen the conclusion that this reaction follows a radical mechanism, radical trapping experiments were conducted. The aim of these reactions was to quench the reactivity of the catalytic systems and to obtain an adduct of the radical scavenger. For these experiments both O- and C-based radical scavengers were added to the reaction. Based on the previously made observations, two different sequences of addition of radical trapping reagent were elaborated for these experiments.

In the first methodology, the radical scavenger was added after the activation time elapsed (Scheme 6.28 - a) to avoid an interference with the *in situ* formation of the Ti<sup>3+</sup>-alcohol complex and thereby quenching the Ti-based catalyst. For these procedures, two different radical scavenger namely (2,2,6,6-tetramethylpiperidin-1-yl)oxidanyl (TEMPO) (**151**) and 1,1-diphenylethylene (**153**) were used. Although, in both cases the deoxygenation of benzyl alcohol (**4a**) was suppressed, no traces of the expected radical adducts were observed and instead only products of the hydrogenation of scavengers were detected (Scheme 6.28 - b).

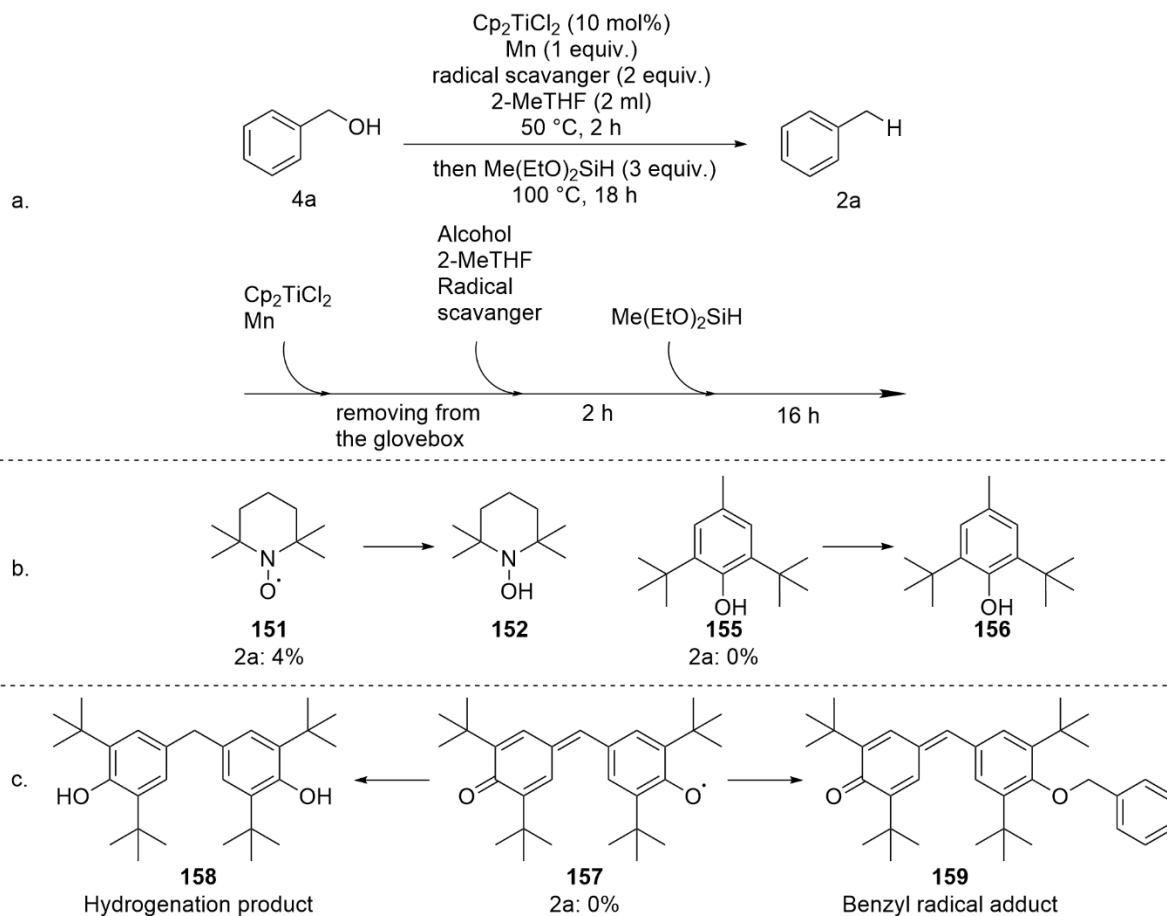


**Scheme 6.28.** First radical scavengers methodology. (a) Reaction and addition order scheme; (b) transformation of TEMPO and 1,1-diphenylethylene.

In the second procedure, the order of addition was changed as both the alcohol and the radical scavenger were submitted to the reaction at the same time (Scheme 6.29). This time TEMPO (**151**), dibutylhydroxytoluene (BHT, **155**) and Galvinoxyl (**157**) were used for trapping radical species. TEMPO (**151**) and BHT (**155**) afforded similar results as the reactions conducted under the first procedure (Scheme 6.29 - b). In contrast, the application of Galvinoxyl (**157**) led to the inhibition of the deoxygenation reaction and to the formation of the hydrogenation product **158** and benzyl radical adduct



**159** (Scheme 6.29 - c). Compound **159** was observed *via* GC-MS because the different Galvinoxyl derivatives were inseparable *via* column chromatography, but it confirms the hints toward a radical reaction pathway.

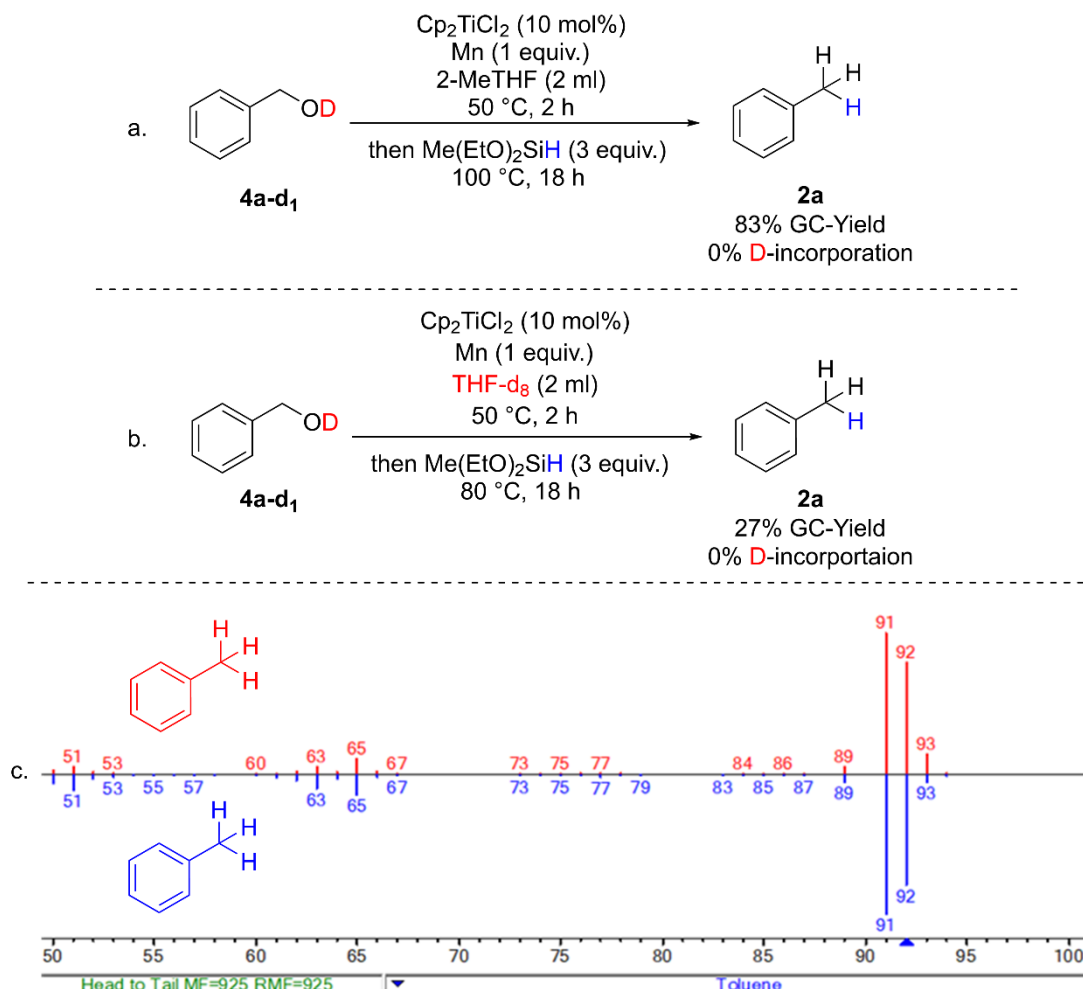


**Scheme 6.29.** Second radical scavengers methodology. (a) Reaction and addition order scheme; (b) transformation of TEMPO and BHT; (c) transformation of Galvinoxyl.

Lastly, deuterium labelling experiments were carried out (Scheme 6.30). Due to the commercial unavailability of deuterated methyldiethoxysilane and the difficult synthesis of this compound, an alternative methodology had to be developed. Based on the available literature, the source of the hydrogen atom in the newly formed C-H bond could be the hydrosilane, the hydroxyl group<sup>40</sup> or, following a transposition reaction, the methylene group.<sup>86</sup> Therefore, the strategy was to conduct the reactions with benzylic alcohols containing deuterium on different connectivities and by using Me(EtO)<sub>2</sub>SiH (**108**) as the only possible hydrogen source. Additionally, for the sake of completeness, the H-donating capabilities of the solvent were investigated, due to a corresponding hypotheses presented in the literature.<sup>86</sup> Therefore, the reactions were conducted in both deuterated and non-deuterated solvents. Due to the volatility of the products, both yields and deuterium incorporation were determined *via* GC-MS.

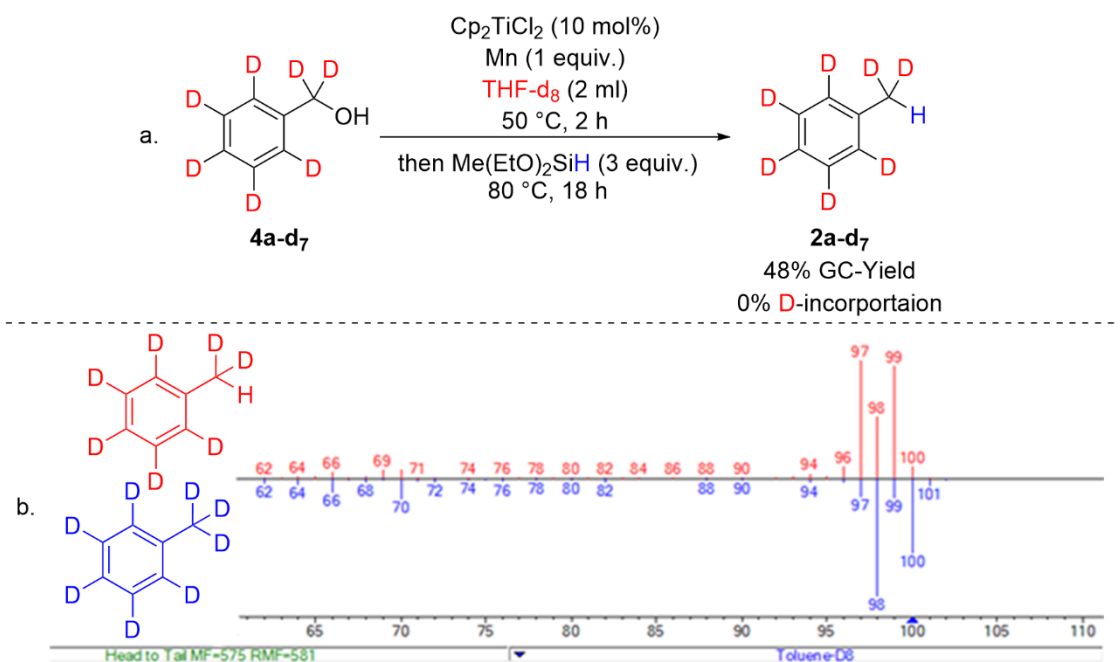
Starting from the report of Barrero *et al.*<sup>40</sup>, alcohol **4a-d<sub>1</sub>** bearing an -OD group was subjected to the standard conditions (Scheme 6.30 - a). This reaction afforded toluene (**2a**) in 83% yield and no deuterium incorporation was observed. The same result, regarding the deuterium content in the final product, was obtained when the reaction was conducted in THF-d<sub>8</sub> at 80 °C (Scheme 6.30 - b). In this case, the significant drop in yield was attributed to the lower reaction temperature. The deuterium

incorporation was determined by comparing the chromatogram of the obtained product with the standard toluene chromatogram from the NIST database (Scheme 6.30 - c).<sup>87</sup>



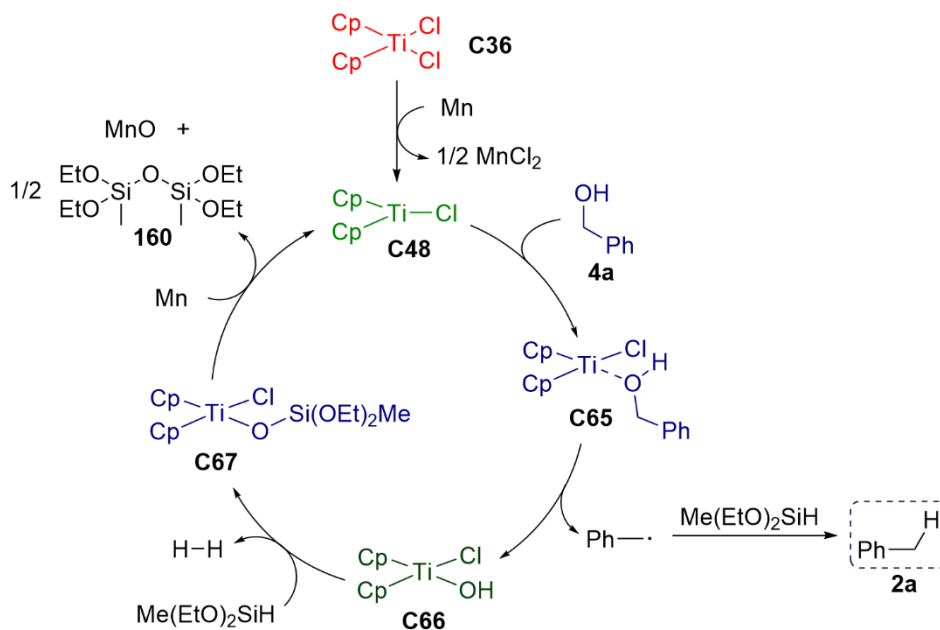
**Scheme 6.30.** Deuteration experiments with benzyl alcohol-OD under standard conditions.

When heptadeuterated benzyl alcohol **4a-d<sub>7</sub>** was subjected to the transformation in THF-d<sub>8</sub>, only toluene-d<sub>7</sub> (**2a-d<sub>7</sub>**) was obtained (Scheme 6.31 - a). This outcome was determined by the poor overlap observed by compared the fragmentation obtained in the GC-MS chromatogram with the standard toluene-d<sub>8</sub> (**2a-d<sub>8</sub>**) fragmentation (Scheme 6.31 - b). These results indicate that it is highly improbable that the solvent, the hydroxyl group, or the methylene group acts as a hydrogen donor in this catalytic system and that the only plausible hydrogen donor is the hydrosilane.



**Scheme 6.31.** Deuterations experiments with benzyl alcohol-d<sub>7</sub> in THF-d<sub>8</sub> and the chromatogram comparison: Obtained chromatogram (red) and standard chromatogram for toluene-d<sub>8</sub> (blue).

Based on all the information gathered during the extensive screenings and mechanistic studies, a reaction mechanism for the deoxygenation of benzylic alcohols can be proposed (Scheme 6.32). First, Cp<sub>2</sub>TiCl<sub>2</sub> (**C36**) is reduced by Mn forming the catalytically active Ti<sup>3+</sup> species which further reacts with the alcohol to afford complex **C65**. This species undergoes the homolytic cleavage of the C-O bond, affording complex **C66** and the benzyl radical which subtracts an H-atom from the hydrosilane. Complex **C66** further reacts with a second hydrosilane molecule generating H<sub>2</sub> and complex **C67**. This species can be reduced by Mn completing the catalyst regeneration process and producing the detected disiloxane **160**.



**Scheme 6.32.** Proposed mechanism.

#### 6.4. Conclusions and Outlook on Co- and Ti-catalysed Deoxygenation Procedures

The development of new Co-, Co/Ti- and Ti-catalysed deoxygenation procedures was attempted. The ligand and additive screenings conducted during the development of the Co-catalysed methodology led almost exclusively to the generation of 1-phenylethyl formate (**18**) and styrene (1-phenylethyl formate), and only in isolated cases to traces of the desired alkane.

Although the Co/Ti-catalysed method led to more promising results, especially after the introduction of triethoxysilane, the control reactions showed that Ti was capable to solely catalyse the desired transformation.

Thus, the development of a new homogenous Ti-based catalysed deoxygenation procedure of benzylic alcohols was accomplished. This catalytic system uses one equivalent of Mn as metal reductant and 3 equivalents Me(EtO)<sub>2</sub>SiH as hydrogen donor. Although triethoxysilane proved to be efficient in this system, it was discarded due to safety concerns.

During the screening of various parameters, it was concluded that an increased temperature and reaction time were beneficial for the generation of the desired products. Besides prolonging the reaction time, the activation period in which the catalytically active Ti<sup>3+</sup> species was formed proved to be crucial for the outcome of the reaction. Additionally, the pressure build up that was observed immediately after the addition of the hydrogen donor has a positive effect on the reaction.

The presented methodology was efficient over a wide range of benzylic alcohols, especially for the deoxygenation of primary benzylic substrates. Moreover, various non-participating functional groups, protecting groups and heterocyclic backbones were tolerated by this catalytic system. Beside hydrosilanes, Hantzsch esters could be used as hydrogen donors in this methodology, albeit with lower yields. The attempts to generate new C-C bonds by using the Ti-HEH catalytic system did not lead to satisfactory results.

In addition to its suitability for the deoxygenation of benzylic alcohols, this methodology proved to be efficient for the reduction of various other compound classes like diols, ketones, esters and thioesters. Furthermore, this catalytic procedure was able to promote sequential deoxygenation-dehalogenation and deoxygenation-hydrogenation reactions. Hence, this synthetic approach can replace two-step procedures with a one-pot reaction.

The applicability of this Ti-catalysed deoxygenation procedure in the degradation process of low and medium complexity lignin model substrates and lignin building-blocks was also demonstrated. This process led to the generation of industrially valuable molecules like phenol or guaiacol. Consequently, further experiments on higher complexity lignin model substrates should be conducted.

The mechanistic studies revealed that this reaction follows a radical pathway. This was proven through radical scavenger experiments and radical clock experiments. Moreover, the hydrogen donation mechanism was highlighted through deuteration experiments.

The main drawback of this system is the lack of selectivity towards the deoxygenation of primary, secondary, and tertiary benzylic alcohols. This was demonstrated through the results obtained in competitive reactions and during the late-stage functionalization reactions.

Regarding the perspectives, the mechanisms through which the Ti-catalysed deoxygenation of diols, ketones, esters and thioesters occurs should be further investigated in order to increase the synthetic applicability of this catalytic system. In addition, the hydrogen donation capability of more silanes could be screened and a Ti precatalyst screening could be conducted in order to increase the selectivity of this method.

**6.5. References**

1. K. Ziegler, E. Holzkamp, H. Breil and H. Martin, *Angew. Chem.*, 1955, **67**, 541-547.
2. G. Natta, *Angew. Chem.*, 1956, **68**, 393-403.
3. R. A. Collins, A. F. Russell and P. Mountford, *Appl. Petrochem. Res.*, 2015, **5**, 153-171.
4. T. McCallum, X. Wu and S. Lin, *J. Org. Chem.*, 2019, **84**, 14369-14380.
5. X. Wu, Y. Chang and S. Lin, *Chem*, 2022, **8**, 1805-1821.
6. F. Sato, H. Urabe and S. Okamoto, *Chem. Rev.*, 2000, **100**, 2835-2886.
7. N. A. Petasis, S. P. Lu, E. I. Bzowej, D. K. Fu, J. P. Staszewski, I. Akritopoulou-Zanze, M. A. Patane and Y. H. Hu, *Pure Appl. Chem.*, 1996, **68**, 667-670.
8. S. P. Morcillo, D. Miguel, A. G. Campaña, L. Álvarez de Cienfuegos, J. Justicia and J. M. Cuerva, *Org. Chem. Front.*, 2014, **1**, 15-33.
9. D. J. Ramón and M. Yus, *Chem. Rev.*, 2006, **106**, 2126-2208.
10. Z. W. Davis-Gilbert and I. A. Tonks, *Dalton Trans.*, 2017, **46**, 11522-11528.
11. O. G. Kulinkovich, S. V. Sviridov, D. A. Vasilevskii and T. S. Pritytskaya, *Zh. Org. Khim.*, 1989, **25**, 2244.
12. R. E. Estévez, M. Paradas, A. Millán, T. Jiménez, R. Robles, J. M. Cuerva and J. E. Oltra, *J. Org. Chem.*, 2008, **73**, 1616-1619.
13. J. E. McMurry and M. P. Fleming, *J. Am. Chem. Soc.*, 1974, **96**, 4708-4709.
14. D. Suzuki, H. Urabe and F. Sato, *J. Am. Chem. Soc.*, 2001, **123**, 7925-7926.
15. R. E. Estévez, J. Justicia, B. Bazdí, N. Fuentes, M. Paradas, D. Choquesillo-Lazarte, J. M. García-Ruiz, R. Robles, A. Gansäuer, J. M. Cuerva and J. E. Oltra, *Chem. Eur. J.*, 2009, **15**, 2774-2791.
16. T. Katsuki and K. B. Sharpless, *J. Am. Chem. Soc.*, 1980, **102**, 5974-5976.
17. P. Anastas and J. C. Warner, *Green Chemistry: Theory and Practice*, Oxford University Press: Oxford, 1998.
18. N. Winterton, *Green Chem.*, 2001, **3**, G73-G81.
19. M. Castro Rodríguez, I. Rodríguez García, R. N. Rodríguez Maecker, L. Pozo Morales, J. E. Oltra and A. Rosales Martínez, *Org. Process Res. Dev.*, 2017, **21**, 911-923.
20. G. Wilkinson and J. M. Birmingham, *J. Am. Chem. Soc.*, 1954, **76**, 4281-4284.
21. J. M. Birmingham, in *Adv. Organomet. Chem.*, eds. F. G. A. Stone and R. West, Academic Press, 1965, vol. 2, pp. 365-413.
22. S. E. Johnson, T. A. Bell and J. K. West, *J. Chem. Educ.*, 2022, **99**, 2121-2128.
23. W. A. Nugent and T. V. RajanBabu, *J. Am. Chem. Soc.*, 1988, **110**, 8561-8562.
24. T. V. RajanBabu and W. A. Nugent, *J. Am. Chem. Soc.*, 1994, **116**, 986-997.
25. T. V. RajanBabu and W. A. Nugent, *J. Am. Chem. Soc.*, 1989, **111**, 4525-4527.
26. T. V. RajanBabu, W. A. Nugent and M. S. Beattie, *J. Am. Chem. Soc.*, 1990, **112**, 6408-6409.
27. A. Gansäuer, M. Pierobon and H. Bluhm, *Angew. Chem. Int. Ed.*, 1998, **37**, 101-103.
28. A. Gansäuer, H. Bluhm and M. Pierobon, *J. Am. Chem. Soc.*, 1998, **120**, 12849-12859.
29. A. Gansäuer, T. Lauterbach, H. Bluhm and M. Noltemeyer, *Angew. Chem. Int. Ed.*, 1999, **38**, 2909-2910.
30. A. Gansäuer and H. Bluhm, *Chem. Commun.*, 1998, 2143-2144.
31. A. Gansäuer, *J. Org. Chem.*, 1998, **63**, 2070-2071.
32. A. Gansäuer, M. Moschioni and D. Bauer, *Eur. J. Org. Chem.*, 1998, **1998**, 1923-1927.
33. L. Moisan, C. Hardouin, B. Rousseau and E. Doris, *Tetrahedron Lett.*, 2002, **43**, 2013-2015.
34. A. F. Barrero, J. E. Oltra, J. M. Cuerva and A. Rosales, *J. Org. Chem.*, 2002, **67**, 2566-2571.
35. J. M. Cuerva, A. G. Campaña, J. Justicia, A. Rosales, J. L. Oller-López, R. Robles, D. J. Cárdenas, E. Buñuel and J. E. Oltra, *Angew. Chem. Int. Ed.*, 2006, **45**, 5522-5526.
36. A. Gansäuer, M. Behlendorf, A. Cangönül, C. Kube, J. M. Cuerva, J. Friedrich and M. van Gastel, *Angew. Chem. Int. Ed.*, 2012, **51**, 3266-3270.
37. H. R. Diéguez, A. López, V. Domingo, J. F. Arteaga, J. A. Dobado, M. M. Herrador, J. F. Quílez del Moral and A. F. Barrero, *J. Am. Chem. Soc.*, 2010, **132**, 254-259.
38. S. J. Blanksby and G. B. Ellison, *Acc. Chem. Res.*, 2003, **36**, 255-263.
39. V. B. Oyeyemi, J. A. Keith and E. A. Carter, *J. Phys. Chem. A*, 2014, **118**, 3039-3050.

40. C. Prieto, J. A. González Delgado, J. F. Arteaga, M. Jaraíz, J. L. López-Pérez and A. F. Barrero, *Org. Biomol. Chem.*, 2015, **13**, 3462-3469.
41. T. Suga, S. Shimazu and Y. Ukaji, *Org. Lett.*, 2018, **20**, 5389-5392.
42. Q. Lin, W. Tong, X.-Z. Shu and Y. Chen, *Org. Lett.*, 2022, **24**, 8459-8464.
43. B. Han, C. Ren, M. Jiang and L. Wu, *Angew. Chem. Int. Ed.*, 2022, **61**, e202209232.
44. K.-Y. Ye, T. McCallum and S. Lin, *J. Am. Chem. Soc.*, 2019, **141**, 9548-9554.
45. S. Das, D. Addis, S. Zhou, K. Junge and M. Beller, *J. Am. Chem. Soc.*, 2010, **132**, 1770-1771.
46. A. S. Wells, *Org. Process Res. Dev.*, 2010, **14**, 484-484.
47. S. C. Berk, K. A. Kreutzer and S. L. Buchwald, *J. Am. Chem. Soc.*, 1991, **113**, 5093-5095.
48. H. Li, Z. Yao, X. Wang, Y. Zhu and Y. Chen, *Energy Fuels*, 2022, **36**, 11745-11759.
49. X.-Q. Zhu, Y.-C. Liu and J.-P. Cheng, *J. Org. Chem.*, 1999, **64**, 8980-8981.
50. S. G. Ouellet, A. M. Walji and D. W. C. Macmillan, *Acc. Chem. Res.*, 2007, **40**, 1327-1339.
51. G. Li, R. Chen, L. Wu, Q. Fu, X. Zhang and Z. Tang, *Angew. Chem. Int. Ed.*, 2013, **52**, 8432-8436.
52. J. M. Blackwell, K. L. Foster, V. H. Beck and W. E. Piers, *J. Org. Chem.*, 1999, **64**, 4887-4892.
53. N. Sakai, K. Fujii, S. Nabeshima, R. Ikeda and T. Konakahara, *ChemComm.*, 2010, **46**, 3173-3175.
54. H.-J. Wang and Y. Fu, *J. Mol. Struct. Theochem*, 2009, **893**, 67-72.
55. K. Iwasaki, K. K. Wan, A. Oppedisano, S. W. M. Crossley and R. A. Shenvi, *J. Am. Chem. Soc.*, 2014, **136**, 1300-1303.
56. P. V. Kattamuri and J. G. West, *J. Am. Chem. Soc.*, 2020, **142**, 19316-19326.
57. S. W. M. Crossley, C. Obradors, R. M. Martinez and R. A. Shenvi, *Chem. Rev.*, 2016, **116**, 8912-9000.
58. C. Chatgililoglu, C. Ferreri, Y. Landais and V. I. Timokhin, *Chem. Rev.*, 2018, **118**, 6516-6572.
59. L. J. Donnelly, J.-C. Berthet and T. Cantat, *Angew. Chem. Int. Ed.*, 2022, **61**, e202206170.
60. S. L. Buchwald, *Chem. Eng. News*, 1993, **71**, 2-3.
61. R. J. Enemærke, G. H. Hjøllund, K. Daasbjerg and T. Skrydstrup, *C. R. Acad. Sci.*, 2001, **4**, 435-438.
62. D. Yeung, J. Penafiel, H. S. Zijlstra and J. S. McIndoe, *Inorg. Chem.*, 2018, **57**, 457-461.
63. M. L. H. Green and C. R. Lucas, *J. Chem. Soc., Dalton Trans.*, 1972, DOI: 10.1039/DT9720001000, 1000-1003.
64. R. J. Enemærke, J. Larsen, T. Skrydstrup and K. Daasbjerg, *J. Am. Chem. Soc.*, 2004, **126**, 7853-7864.
65. I. Vasil'eva, A. Naumova, A. Polyakov, T. Tyvina and N. Kozlova, *Zh. Prikl. Khim.*, 1990, **63**, 1879-1881.
66. J. J. Salzmänn, *Helv. Chim. Acta*, 1968, **51**, 526-529.
67. G. Englezou, K. Kortsens, A. A. C. Pacheco, R. Cavanagh, J. C. Lentz, E. Krumins, C. Sanders-Velez, S. M. Howdle, A. J. Nedoma and V. Taresco, *J. Polym. Sci.*, 2020, **58**, 1571-1581.
68. C. Kern, J. Selau and J. Streuff, *Chem. Eur. J.*, 2021, **27**, 6178-6182.
69. J. Guliński, H. Maciejewski, I. Dąbek and M. Zaborski, *Appl. Organomet. Chem.*, 2001, **15**, 649-657.
70. R. L. Halterman, K. P. C. Vollhardt, M. E. Welker, D. Blaeser and R. Boese, *J. Am. Chem. Soc.*, 1987, **109**, 8105-8107.
71. M. F. Sloan, A. S. Matlack and D. S. Breslow, *J. Am. Chem. Soc.*, 1963, **85**, 4014-4018.
72. E. Cesarotti, R. Ugo and H. B. Kagan, *Angew. Chem. Int. Ed.*, 1979, **18**, 779-780.
73. M. Ash and I. Ash, *Handbook of Green Chemicals*, Synapse Information Resources, 2004.
74. X. Shen, Q. Meng, Q. Mei, J. Xiang, H. Liu and B. Han, *Green Chem.*, 2020, **22**, 2191-2196.
75. M. Hassam, A. Taher, G. E. Arnott, I. R. Green and W. A. L. van Otterlo, *Chem. Rev.*, 2015, **115**, 5462-5569.
76. T. Wu, L. Valencia, T. Pfohl, B. Heck, G. Reiter, P. J. Lutz and R. Mülhaupt, *Macromolecules*, 2019, **52**, 4839-4846.
77. J. F. Harrod and S. S. Yun, *Organometallics*, 1987, **6**, 1381-1387.
78. R. Whetten and R. Sederoff, *Plant Cell*, 1995, **7**, 1001-1013.
79. C. W. Lahive, P. C. J. Kamer, C. S. Lancefield and P. J. Deuss, *ChemSusChem*, 2020, **13**, 4238-4265.

80. R. L. Wynn, *Gen. Dent.*, 1993, **41**, 27-29.
81. J. I. Perlmutter, L. T. Forbes, D. J. Krysan, K. Ebsworth-Mojica, J. M. Colquhoun, J. L. Wang, P. M. Dunman and D. P. Flaherty, *J. Med. Chem.*, 2014, **57**, 8540-8562.
82. Y. Liu, J. Gao, M. Peng, H. Meng, H. Ma, P. Cai, Y. Xu, Q. Zhao and G. Si, *Front. Pharmacol.*, 2018, **9**.
83. H. Xie, J. Guo, Y.-Q. Wang, K. Wang, P. Guo, P.-F. Su, X. Wang and X.-Z. Shu, *J. Am. Chem. Soc.*, 2020, **142**, 16787-16794.
84. L. R. Mills, J. J. Monteith, G. dos Passos Gomes, A. Aspuru-Guzik and S. A. L. Rousseaux, *J. Am. Chem. Soc.*, 2020, **142**, 13246-13254.
85. H. M. Walborsky, *Tetrahedron*, 1981, **37**, 1625-1651.
86. T. Suga, Y. Takahashi, C. Miki and Y. Ukaji, *Angew. Chem. Int. Ed.*, 2022, **61**, e202112533.
87. S. E. Stein, *National Institute of Standards and Technology*, 2008, **NIST Standard Reference Database User's Guide**.

## 7. Summary/Zusammenfassung

The deoxygenation reaction represents a useful transformation for both synthetic applications and industrial scale processes like the valorisation of biomass or the synthesis of bioactive compounds. In the first part of this thesis, some recently developed deoxygenation procedures of alcohols, carbonyls and other oxygen-containing substrates were presented while discussing their corresponding advantages and drawbacks. The methodologies which focused on the deoxygenation of alcohols were divided into two categories, direct and two-step deoxygenation procedures. Additionally, in this introductory section, the emergence of a new subcategory of the two-step procedures, which follow an oxidation-Wolff-Kischner reduction pathway was emphasized. Furthermore, the applicability of the deoxygenation procedures in biomass valorisation, especially lignin, was presented. In this section the structure of lignin was presented along with its potential to lead to the generation of biofuels and other industrially or commercially valuable compounds by applying various deoxygenation procedures on lignin was discussed. Subsequently, the hydrogen donating capabilities of formic acid, hydrosilanes and Hantzsch esters were considered, along several examples of reactions in which these were used as H-donors.

In the second section of the thesis, an overview of the literature on Pd-catalysed deoxygenations was made in order to better grasp the subtleties of these reactions/enhance the knowledge of these reactions' chemistry and to direct the effort of improving the optimization process of the Pd-catalysed transfer hydrogenolysis of benzylic alcohols procedure developed by Ciszek and Fleischer. The optimization started with a solvent screening and various loading experiments from which it was concluded that  $\text{CHCl}_3$  is a suitable solvent for this transformation and that higher amounts of formic acid and methanesulfonic acid facilitate the reaction. These experiments were followed by a ligand screening which further strengthened the hypothesis that dtbpx (**L1**) is the most suitable ligand and that the oxidized form of dtbpx (**L1-O<sub>2</sub>**) can have a stabilizing role on the catalytic active species. Additionally, the negative effect of the water content was proven.

In the third and fourth sections of this thesis, the development of new non-precious metal based deoxygenation procedures was attempted. During the development of these systems, the green chemistry principles were taken into account. First, a literature overview on various applications in which Co-pincer ligands complexes were utilized was presented. These literature reports supported the development of a Co-catalysed deoxygenation procedure by using various pincer ligands and formic acid as reducing agent. Moreover, solvent and additive screenings were conducted. Due to the unsatisfactory results of the Co-catalysed reaction, the suitability of a bimetallic catalytic system was tested. After analysing the available literature, a Co/Ti system was chosen for the deoxygenation of benzylic alcohols. Besides formic acid, hydrosilanes were also trailed as reductant. By using hydrosilanes as H-donor the catalytic system proved to be more efficient for the desired transformation compared to the Co-based system and after conducting the control reactions it was concluded that the Ti-based catalyst is solely able to facilitate the desired reaction. Besides hydrosilanes, the H-donor capabilities of Hantzsch esters were also tested in the Ti-catalysed methodology and although they proved to be very efficient for the generation of the desired products, the yields were lower compared to the Ti-hydrosilane system.

Consequently, multiple optimization reactions and screenings were conducted in order to optimize the Ti-catalysed deoxygenation method. These experiments showed that  $\text{Me}(\text{EtO})_2\text{SiH}$  was the optimal reducing agent for this transformation and that 1 equivalent of Mn was necessary to efficiently reduce  $\text{Cp}_2\text{TiCl}_2$  to  $\text{Cp}_2\text{TiCl}$ . Additionally, a prolonged activation and reaction time along



together with increased temperature and pressure inside the reaction vessel were beneficial for the desired transformation. Besides its suitability towards the deoxygenation of benzylic alcohols, this catalytic system proved to be efficient in the reduction of olefins, diols, carbonyls, esters and thioesters. Besides, sequential dehalogenation-deoxygenation and hydrogenation-deoxygenation reactions were successfully conducted. By applying this catalytic system for the reduction of lignin model substrates and lignin building blocks industrially valuable compounds were obtained, such as guaiacol and phenol.

Through radical scavenger and radical clock studies it was showed that this transformation follows a radical pathway. The deuteration experiments indicated that the hydrosilanes provide the hydrogen atom needed for the formation of a new C-H bond.

Although the results presented herein show, that the developed Ti-catalysed method for the cleavage of C-OH bonds is a a robust methodology viable for the deoxygenation at laboratory scale of a broad range of alcohols and other functional groups, more investigations should be conducted in order to enhance the selectivity of the procedure. Additionally, further optimization reactions should be conducted in order to the upscale the procedure.

Die Deoxygenierungsreaktion stellt eine nützliche Umwandlung sowohl für synthetische Anwendungen als auch für Verfahren im industriellen Maßstab dar, zum Beispiel für die Verwertung von Biomasse oder die Synthese bioaktiver Moleküle. Im ersten Teil dieser Arbeit wurden einige kürzlich entwickelte Verfahren zur Deoxygenierung von Alkoholen, Carbonylen und anderen sauerstoffhaltigen Substraten vorgestellt und ihre jeweiligen Vor- und Nachteile erörtert. Die Methoden, die sich auf die Deoxygenierung von Alkoholen konzentrierten, wurden in zwei Kategorien unterteilt: direkte und zweistufige Deoxygenierungen. Zusätzlich wurde in diesem einleitenden Abschnitt die Entstehung einer neuen Unterkategorie der zweistufigen Verfahren hervorgehoben, die einem Oxidations-Wolff-Kischner-Reduktionsweg folgen. Darüber hinaus wurde die Anwendbarkeit der Deoxygenierungsreaktionen bei der Verwertung von Biomasse, insbesondere von Lignin, vorgestellt. In diesem Abschnitt wurde die Struktur von Lignin vorgestellt und dessen Potenzial zur Erzeugung von Biokraftstoffen und anderen industriell oder kommerziell wertvollen Verbindungen durch die Anwendung verschiedener Desoxygenierungsmethoden erörtert. Anschließend wurden die Hydrierfähigkeiten von Ameisensäure, Hydrosilanen und Hantzsch-Estern sowie mehrere Beispiele von Reaktionen, bei denen diese als Wasserstoffdonoren eingesetzt wurden, betrachtet.

Im zweiten Abschnitt der Arbeit wurde ein Literaturüberblick zu Pd-katalysierten Desoxygenierungen gegeben, um die Feinheiten dieser Reaktionen besser zu verstehen bzw. das Wissen über diese Reaktionen zu erweitern. Des Weiteren wurden Bemühungen zur Verbesserung des Optimierungsprozesses des von Ciszek und Fleischer entwickelten Verfahrens der Pd-katalysierten Transferhydrogenolyse von Benzylalkoholen angestrebt. Die Optimierung begann mit einem Lösungsmittel-Screening und der Variation der Stöchiometrie. Dabei stellte sich heraus, dass  $\text{CHCl}_3$  ein geeignetes Lösungsmittel für diese Reaktion ist und dass höhere Mengen an Ameisensäure und Methansulfonsäure die Reaktion erleichtern. Auf diese Experimente folgte ein Ligandenscreening, das die Hypothese weiter untermauerte, dass dtbpx (**L1**) der am besten geeignete Ligand ist und dass die oxidierte Form von dtbpx (**L1-O<sub>2</sub>**) eine stabilisierende Rolle für die katalytisch aktive Spezies haben kann. Außerdem wurde der negative Einfluss des Wassergehalts nachgewiesen.

Im dritten und vierten Abschnitt dieser Arbeit wurde die Entwicklung von neuen, nicht edelmetallbasierter Deoxygenierungsverfahren untersucht. Bei der Entwicklung dieser Systeme wurden die Grundsätze der umweltfreundlichen Chemie berücksichtigt. Zunächst wurde ein Literaturüberblick über verschiedene Anwendungen gegeben, bei denen Co-Pincer-Liganden-Komplexe verwendet wurden. Diese Literaturberichte unterstützten die Entwicklung einer Co-katalysierten Deoxygenierungsmethode unter Verwendung verschiedener Pincer-Liganden und Ameisensäure als Reduktionsmittel. Außerdem wurden Lösungsmittel- und Additivscreenings durchgeführt. Aufgrund der unbefriedigenden Ergebnisse der Co-katalysierten Reaktion wurde die Eignung eines bimetallichen katalytischen Systems geprüft. Nach Analyse der verfügbaren Literatur wurde ein Co/Ti-System für die Desoxygenierung von Benzylalkoholen ausgewählt. Neben Ameisensäure wurden auch Hydrosilane als Reduktionsmittel verfolgt. Durch die Verwendung von Hydrosilanen als H-Donor erwies sich das katalytische System im Vergleich zum Co-basierten System als effizienter für die gewünschte Umwandlung, und nach Durchführung der Kontrollreaktionen wurde festgestellt, dass der Ti-basierte Katalysator allein in der Lage ist, die gewünschte Reaktion zu ermöglichen. Außer Hydrosilanen wurden auch die H-Donor-Fähigkeiten von Hantzsch-Estern in diesem Ti-katalysierten Protokoll getestet. Obwohl diese sich als sehr effizient für die Erzeugung der gewünschten Produkte erwiesen, waren die Ausbeuten im Vergleich zum Ti-Hydrosilan-System geringer.

Folglich wurden mehrere Optimierungsreaktionen und Screenings durchgeführt, um die Ti-katalysierte Deoxygenierungsmethode zu optimieren. Diese Experimente zeigten, dass  $\text{Me}(\text{EtO})_2\text{SiH}$  das optimale Reduktionsmittel für diese Umwandlung war und dass 1 Äquivalent Mn erforderlich war, um  $\text{Cp}_2\text{TiCl}_2$  effizient zu  $\text{Cp}_2\text{TiCl}$  zu reduzieren. Außerdem waren eine verlängerte Aktivierungs- und Reaktionszeit sowie eine erhöhte Temperatur und ein erhöhter Druck im Reaktionsgefäß für die gewünschte Umwandlung von Vorteil. Neben seiner Eignung für die Deoxygenierung von Benzylalkoholen erwies sich dieses Katalysatorsystem auch als effizient bei der Reduktion von Olefinen, Diolen, Carbonylen, Estern und Thioestern. Außerdem wurden sequenzielle Dehalogenierungs-Desoxygenierungs- und Hydrierungs-Desoxygenierungsreaktionen erfolgreich durchgeführt. Durch die Anwendung dieses katalytischen Systems für die Reduktion von Ligninmodellsubstraten und Ligninbausteinen wurden industriell wertvolle Verbindungen wie Guajakol und Phenol gewonnen.

Durch Radikalfänger- und Radikaluhrstudien wurde gezeigt, dass diese Umwandlung einem radikalischen Weg folgt. Die Deuterierungsexperimente deuteten darauf hin, dass die Hydrosilane das für die Bildung einer neuen C-H-Bindung benötigte Wasserstoffatom liefern.

Obwohl die hier vorgestellten Ergebnisse zeigen, dass die entwickelte Ti-katalysierte Methode zur Spaltung von C-OH-Bindungen eine robuste Methode ist, die für die Desoxygenierung eines breiten Spektrums von Alkoholen und anderen funktionellen Gruppen im Labormaßstab geeignet ist, sollten weitere Untersuchungen durchgeführt werden, um die Selektivität des Verfahrens zu verbessern. Außerdem sollten weitere Optimierungsreaktionen durchgeführt werden, um das Verfahren zu optimieren.

## 8. Experimental Part

### 8.1. General Information

Bis(cyclopentadienyl)titanium(IV) dichloride, was supplied by Sigma-Aldrich and was stored in the Glovebox (GS MEGA E-Line, Glovebox Systemtechnik). Mn dust (Mash 325) was obtained from Alfa Aesar and stored in the Glovebox. The silanes were supplied by Acros, Sigma-Aldrich and Alfa Aesar and stored under Ar in Schlenk tubes. The alcohols, aldehydes, ketones and all other chemicals used in the optimization and substrates screening, which were not synthesized, were purchased from TCI, Sigma-Aldrich, BLD Pharm, Fluorochem, Alfa Aesar and ABCR and used without any further purification. The dry and degassed solvents were stored under Ar over Molecular Sieves (3Å). All catalytical reactions were carried out under Ar atmosphere in under vacuum flame-dried Schlenk pressure tubes (maximum pressure 5 bar) bearing PTFE screw-caps.

### 8.2. Chromatography and Analytical Techniques

#### *Column chromatography and TLC*

Column chromatography was carried out manually using gravity flow under isocratic conditions. All the solvents used for chromatography were distilled prior to use. The silica gel (0.04–0.063 mm) was purchased from Machery&Nagel.

Thin-Layer Chromatography (TLC) was performed aluminum plates coated with silica gel 60 F254 (layer thickness: 0.2 mm) and analyzed under UV-light (254 nm) or stained with a potassium permanganate solution.

#### *Gas chromatography (GC)*

GC-FID analysis was carried out on an Agilent 7820A system with G4567A injector by using dry hydrogen as carrier gas and an Agilent 19091J-431 column (30 m, 320 µm, 0.25 µm). Two programs were used: heating from 50 °C to 280 °C with a 20 °C/min heating rate (**M<sub>FID1</sub>**) and heating from 35 °C to 280 °C with a 10 °C/min heating rate (**M<sub>FID2</sub>**).

The internal standard used for quantitative GC was *n*-pentadecane. The samples for the calibration lines used for determining the GC- yields were prepared by using defined amounts of substrate and internal standard. The obtained data was used to plot the ration of peak areas against the mass ratio and resulting slope, which is equivalent to the response factor (R), was used to quantify unknown samples by using following equation. y-Intercepts are not considered.

$$\frac{m(\text{substrate})}{m(\text{standard})} \times R = \frac{A(\text{substrate})}{A(\text{standard})}$$

GC-MS analysis was performed on an Agilent 7820A GC-system with G4513A injector coupled with an Agilent 5977B MSD by using hydrogen as carrier gas (Method: Heating from 50 °C to 280 °C with a 20 °C/min heating rate - **M<sub>MS1</sub>**), an Agilent 8890 GC-system with G4513A injector coupled with an Agilent 5977B MSD by using helium as carrier gas (Method: Heating from 40 °C to 300 °C with a 10 °C/min heating rate – **M<sub>MS2</sub>**) and Agilent 7820A GC-system with G4513A injector coupled with an Agilent 5977B MSD by using hydrogen as carrier gas (Method: Heating from 35 °C to 280 °C with a 10 °C/min heating rate - **M<sub>MS3</sub>**).

For the identification of non-isolated compounds the obtained GC-MS chromatograms (**Red**) were compared with the existing chromatograms in NIST GC-MS Database (**Blue**). As a quality

parameter Match Factor (MF) and Reverse Match Factor were considered (900 or greater - excellent match; 800–900 - a good match; 700–800 - fair match. Less than 600 - very poor match.)<sup>1</sup>

#### *Nuclear magnetic resonance (NMR) spectroscopy*

NMR spectra were recorded using a Bruker Avance 400 (<sup>1</sup>H: 400 MHz, <sup>13</sup>C: 101 MHz) or Bruker Avance 300 (<sup>1</sup>H: 300 MHz, <sup>13</sup>C: 75 MHz). All NMR measurements were performed at ambient temperature. Chemical shifts ( $\delta$ ) are reported in ppm (parts per million) relative to the residual NMR solvent signals (<sup>1</sup>H: CDCl<sub>3</sub>:  $\delta$  = 7.26 ppm, <sup>13</sup>C: CDCl<sub>3</sub>:  $\delta$  = 77.16). Coupling constants *J* are reported in Hz (Hertz) and the splitting patterns in <sup>1</sup>H NMR spectra are described as follows: s = singlet, bs = broad singlet, d = doublet, t = triplet, q = quartet, m = multiplet.

#### *Infrared spectroscopy*

FT-IR spectra were recorded using an Agilent Cary 630 FTIR.

### **8.3. General Experimental Procedures for Deoxygenation of Benzylic Alcohols**

#### *GP1. Pd-catalyzed deoxygenation procedure of benzylic alcohols developed during this thesis*

Palladium(II) bis(acetylacetonate) (3.05 mg, 0.01 mmol, 1.00 mol%) and dtbpx (21.0 mg, 0.05 mmol, 5.00 mol%) were added in a dry schlenk tube inside the glovebox. Dry chloroform (2 mL) and 1-phenylethanol (0.120 mL, 1.00 mmol, 1.00 equiv.) were added in the schlenk tube in argon counter stream and the reaction mixture was stirred for 2.5 h at room temperature. After this period methanesulfonic acid (0.013 mL, 0.20 mmol, 0.20 equiv.) was added and the resulting reaction mixture was stirred at room temperature for 30 min. Following these 30 min formic acid (0.19 mL, 10.0 mmol, 10.0 equiv.) was added and the reaction was stirred for 18 h at 100 °C. The palladium catalyst was quenched with Quadrasil. Yields were determined via quantitative GC-FID using n-pentadecane as internal standard.

#### *GP2. Ti/Co co-catalyzed deoxygenation of benzylic alcohols using disiloxane as reducing agent*

A flame-dried schlenk tube is charged with CoBr<sub>2</sub>•6H<sub>2</sub>O (26.2 mg, 0.12 mmol, 12.0 mol%) and heated under vacuum with the heat gun until colour change from purple to green is observed. After that it is charged with **L25** (40  $\mu$ L, 0.10 mmol, 10.0 mol%), Cp<sub>2</sub>TiCl<sub>2</sub> (24.9 mg, 0.10 mmol, 10.0 mol%) and Mn (27.5 mg, 0.50 mmol, 0.50 equiv.) in the glovebox. Afterwards the reaction vessel was taken out of the glovebox and 1-phenylethanol (0.120 mL, 1.00 mmol, 1.00 equiv.) and 3 mL dry THF are added. Subsequently, the reaction mixture is stirred for 30 min. at r.t. Thereafter TMDSO (0.53 mL, 3.00 mmol, 3.00 equiv.) was added and the reaction mixture was stirred over night at 80 °C. After this period the reaction mixture was cooled to r.t. and quenched with Lewatit TP207. The 0.1 mL sample from reaction mixture was diluted with 1.4 mL DCM and passed through a Celite, Alumina and MgSO<sub>4</sub> column. Yields were determined via quantitative GC-FID using n-pentadecane as internal standard.

#### *GP3. Ti-catalyzed deoxygenation of benzylic alcohols using Hantzsch esters as reduction agent*

A flame-dried inert Schlenk pressure tube was charged with Cp<sub>2</sub>TiCl<sub>2</sub> (37.3 mg, 0.15 mmol, 15 mol%) and Mn (54.9 mg, 1.00 mmol, 1.00 equiv.) in the glove box. Then, benzyl alcohol (0.104 mL, 1.00 mmol, 1.00 equiv.) and 2 mL THF were added outside the glovebox and the mixture was stirred for 2 h at 50 °C. Afterwards, Hantzsch ester (557 mg, 2.20 mmol, 2.20 equiv.) was added to the solution and the reaction was stirred for 18 h at 80 °C. After it cooled to room temperature, the crude reaction mixture was diluted with 3.5 mL ethyl acetate and 0.10 mL sample from the crude reaction mixture was further

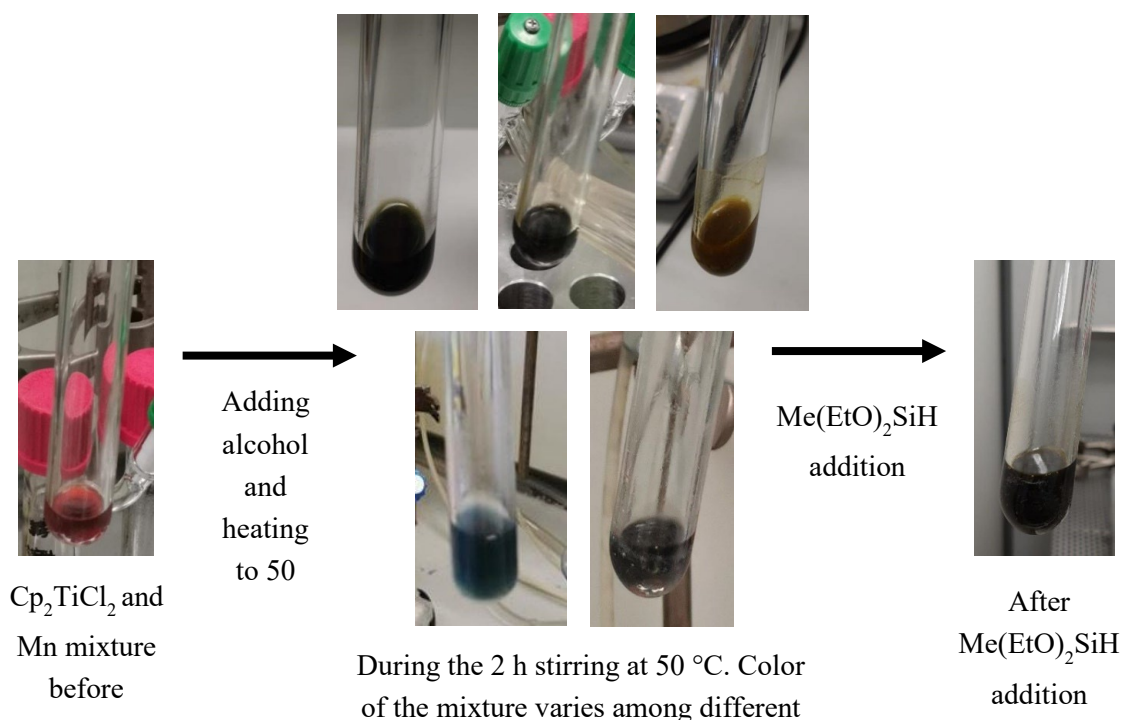
diluted with 1.4 mL DCM and passed through a Celite, Alumina and MgSO<sub>4</sub> column. The yields were determined via quantitative GC-FID using *n*-pentadecane as internal standard.

*GP4. Ti-catalyzed deoxygenation of benzylic alcohols using silanes as reduction agent*

A flame-dried Schlenk-tube equipped with a stirring bar was charged in the glovebox with Cp<sub>2</sub>TiCl<sub>2</sub> (24.9 mg, 0.10 mmol, 10.0 mol%) and Mn (54.9 mg, 1.00 mmol, 1.00 equiv.). Then, the vessel was taken out of the glovebox and the benzylic alcohol (1.00 mmol, 1.00 equiv.) was added to the mixture. The components were dissolved in 2 mL 2-MeTHF and stirred at 50 °C for 2.5 h. Diethoxymethylsilane (0.48 mL, 3.00 mmol, 3 equiv.) was added and the reaction was heated to 100 °C and stirred for 16h. After the completion of the reaction the mixture was cooled to 0 °C and quenched with Lewatit.

For NMR analysis: 1M HCl (5 mL) was added to the crude mixture and stirred for 24 h. Then, the reaction was extracted with DCM or EtOAc (3 × 10 mL) and the collected organic phases were washed with brine (3 × 10 mL), dried over Na<sub>2</sub>SO<sub>4</sub>, and filtered. The solvent was evaporated, and the crude product was purified by column chromatography (Solvent mixture stated for every reaction).

For GC-FID and GC-MS analysis: A 0.10 mL sample from the crude reaction mixture was diluted with 1.4 mL DCM and passed through a Celite, Alumina and MgSO<sub>4</sub> column. For analysis *via* GC-FID, *n*-pentadecane was used as internal standard.



#### 8.4. Other General Experimental Procedures

##### *GP5. Synthesis of benzylic alcohols*

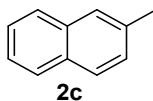
The benzylic alcohols were synthesized by reduction with NaBH<sub>4</sub> following a modified literature procedure.<sup>2</sup> In a 100 mL round bottom flask the respective aldehyde or ketone (5.00 mmol, 1.00 equiv.) was dissolved in methanol (10 mL) and cooled in an ice bath. Then, NaBH<sub>4</sub> (10.0 mmol, 2.00 equiv.) was added in portions. After the addition, the solution was allowed to warm to ambient temperature and was stirred until the completion of the reaction was confirmed by TLC. The solution was cooled in an ice bath and quenched with ice and water. Then, methanol was removed under reduced pressure and the mixture was extracted with DCM (3 × 10 mL). The collected organic phases were washed with brine (3 × 10 mL), dried over Na<sub>2</sub>SO<sub>4</sub> and filtered. The solvent was evaporated, and the respective alcohol was obtained and used without further purification except if otherwise stated.

##### *GP6. Synthesis of Hantzsch esters*

Following a modified literature procedure,<sup>3</sup> aldehyde (3.00 mmol, 1.00 equiv.), NH<sub>4</sub>OAc (2.25 mmol, 174 mg, 1.50 equiv.), ethyl acetoacetate (3.15 mmol, 0.40 mL, 2.10 equiv.) and 1.5 mL ethanol were mixed in a pressure tube and mixture was then stirred for 15 h at 85 °C. The reaction mixture was then cooled at room temperature and quenched with ice-cooled water. The aqueous phase was then extracted with ethyl acetate (3 × 5 mL) and the combined organic phases were washed with 5 mL thiosulfate solution, 5 mL water and then dried over Na<sub>2</sub>SO<sub>4</sub>. The solvent was evaporated in vacuo and the desire product was purification *via* recrystallization in EtOH/water.

## 8.5. Analytical Data for Isolated Deoxygenation Products

### 2-methylnaphthalene (2c)



According to **GP4**, 2-methylnaphthalene (**2c**) was synthesized from 2-Naphthalenemethanol (158 mg, 1.00 mmol, 1.00 equiv.), over 16 h. The product was isolated by column chromatography (Hexane/Ethyl acetate 4:1) and was afforded as a colorless solid (128 mg, 0.90 mmol, 90%, 95% determined by GC-FID). Analytical data was in accordance with the literature.<sup>4</sup>

$C_{11}H_{10}$  (142.20 g/mol)

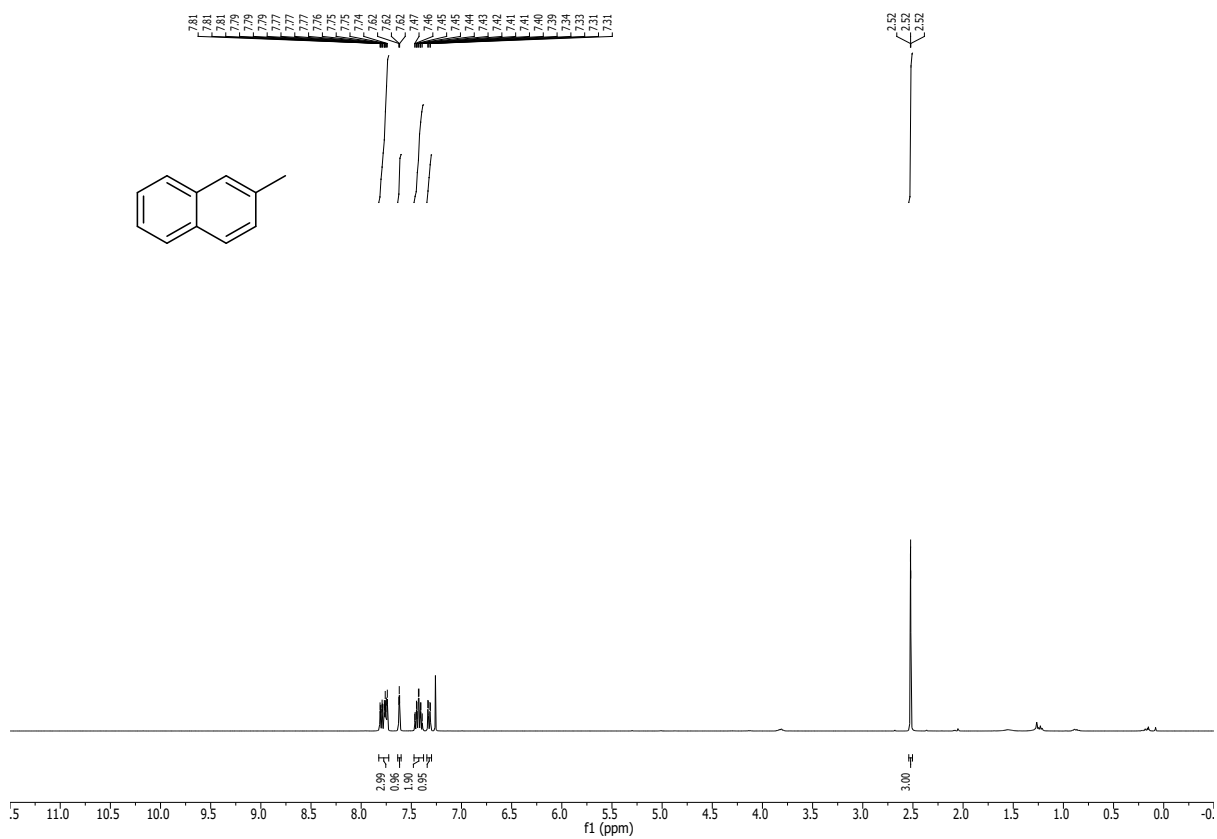
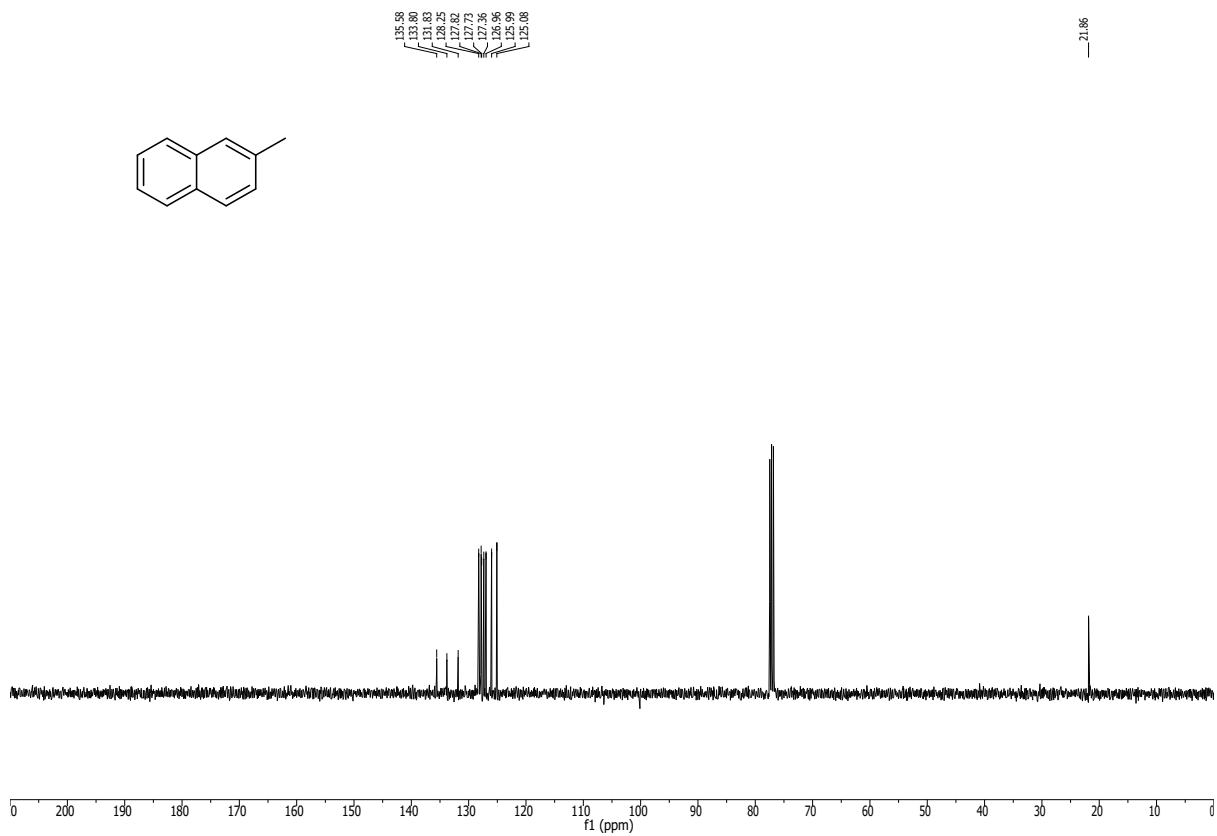
**R<sub>f</sub>**: 0.89 (4:1 Hex:EtOAc)

**<sup>1</sup>H-NMR** (400 MHz, Chloroform-d,  $\delta_H$ /ppm) 7.82 – 7.73 (m, 3H), 7.64 – 7.60 (m, 1H), 7.47 – 7.38 (m, 2H), 7.32 (dd,  $J = 8.4, 1.7$  Hz, 1H), 2.52 (s, 3H)

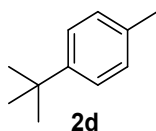
**<sup>13</sup>C-NMR** (100 MHz, CDCl<sub>3</sub>,  $\delta_C$ /ppm) 135.6, 133.8, 131.8, 128.3, 127.8, 127.7, 127.4, 126.9, 126.0, 125.1, 21.9.

**GC-MS** (EI): 142.1 (100, [M<sup>+</sup>]), 126.0 ([M<sup>+</sup>]-[CH<sub>3</sub>]), 115.0 ([M<sup>+</sup>]-[CH<sub>3</sub>]), 102.0 ([M<sup>+</sup>]-[CCHCH<sub>3</sub>])



$^1\text{H-NMR}$ : (400 MHz,  $\text{CDCl}_3$ ) of **2c** $^{13}\text{C-NMR}$ : (101 MHz,  $\text{CDCl}_3$ ) of **2c**

**1-(*tert*-butyl)-4-methylbenzene (2d)**



According to **GP4**, 1-(*tert*-butyl)-4-methylbenzene (**2d**) was synthesized from 4-*tert*-butylbenzyl alcohol (0.170 mL, 164 mg, 1.00 mmol, 1.00 equiv.), over 16 h. The product was isolated by column chromatography (Hexane/Ethyl acetate 4:1) and was afforded as a colorless oil (130 mg, 0.88 mmol, 88%, 92% determined by GC-FID). Analytical data was in accordance with the literature.<sup>5</sup>

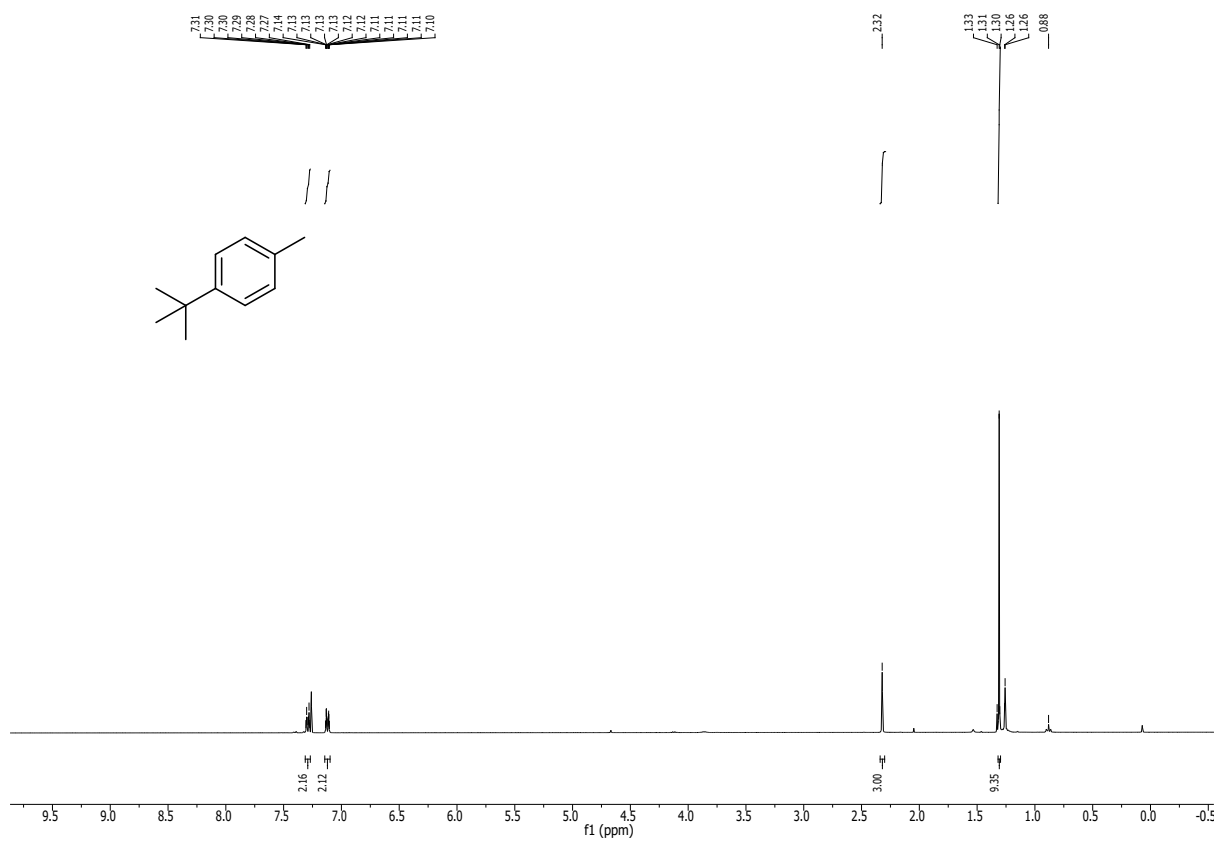
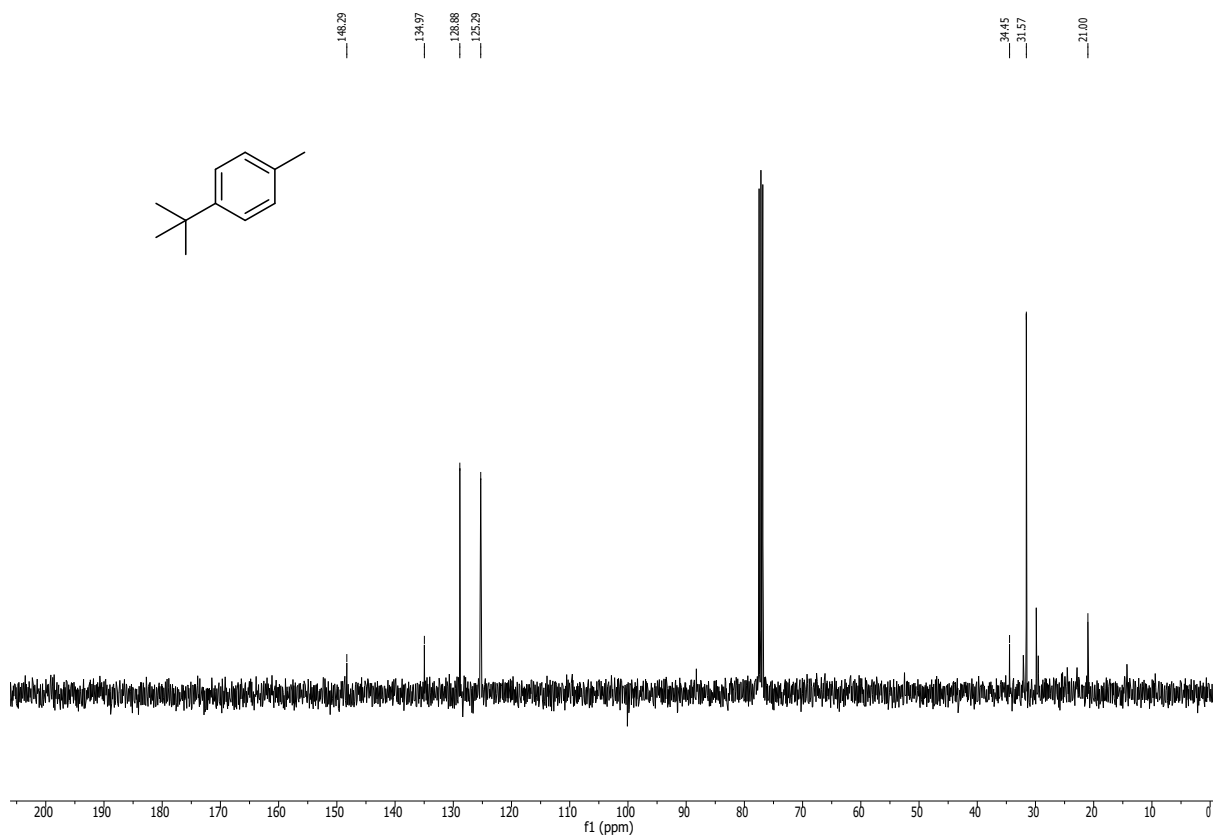
$C_{11}H_{16}$  (148.25 g/mol)

**R<sub>f</sub>**: 0.88 (4:1 Hex:EtOAc)

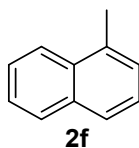
**<sup>1</sup>H-NMR** (400 MHz, CDCl<sub>3</sub>)  $\delta_H$ /ppm: 7.31 – 7.27 (m, 2H), 7.14 – 7.10 (m, 2H), 2.32 (s, 3H), 1.31 (s, 9H); Impurity – Pentadecane (internal standard)

**<sup>13</sup>C-NMR** (100 MHz, CDCl<sub>3</sub>)  $\delta_C$ /ppm: 148.3, 134.9, 128.9 (2), 125.3 (2), 34.5, 31.6, 21.0.

**GC-MS** (EI): 148.11 (100, [M<sup>+</sup>]), 133.12 ([M<sup>+</sup>]-[CH<sub>3</sub>•]), 115.05 ([M<sup>+</sup>]-2[CH<sub>3</sub>•]), 105.05 ([M<sup>+</sup>]-3[CH<sub>3</sub>•]), 93.07 ([M<sup>+</sup>]-3[CH<sub>3</sub>•]-[CH<sub>3</sub>•]), 91.07 ([M<sup>+</sup>]-[C<sub>4</sub>H<sub>9</sub>•]), 77.04 ([M<sup>+</sup>]-[C<sub>4</sub>H<sub>9</sub>•]-[CH<sub>3</sub>•])

$^1\text{H-NMR}$ : (400 MHz,  $\text{CDCl}_3$ ) of **2d** $^{13}\text{C-NMR}$ : (101 MHz,  $\text{CDCl}_3$ ) of **2d**

### 1-methylnaphthalene (**2f**)



According to **GP4**, 1-methylnaphthalene (**2f**) was synthesized from 1-naphthalenemethanol (158 mg, 1.00 mmol, 1.00 equiv.), over 16 h. The product was isolated by column chromatography (Hexane/Ethyl acetate 4:1) and was afforded as a colorless oil (134 mg, 0.94 mmol, 94%, 97% determined by GC-FID). Analytical data was in accordance with the literature.<sup>6</sup>

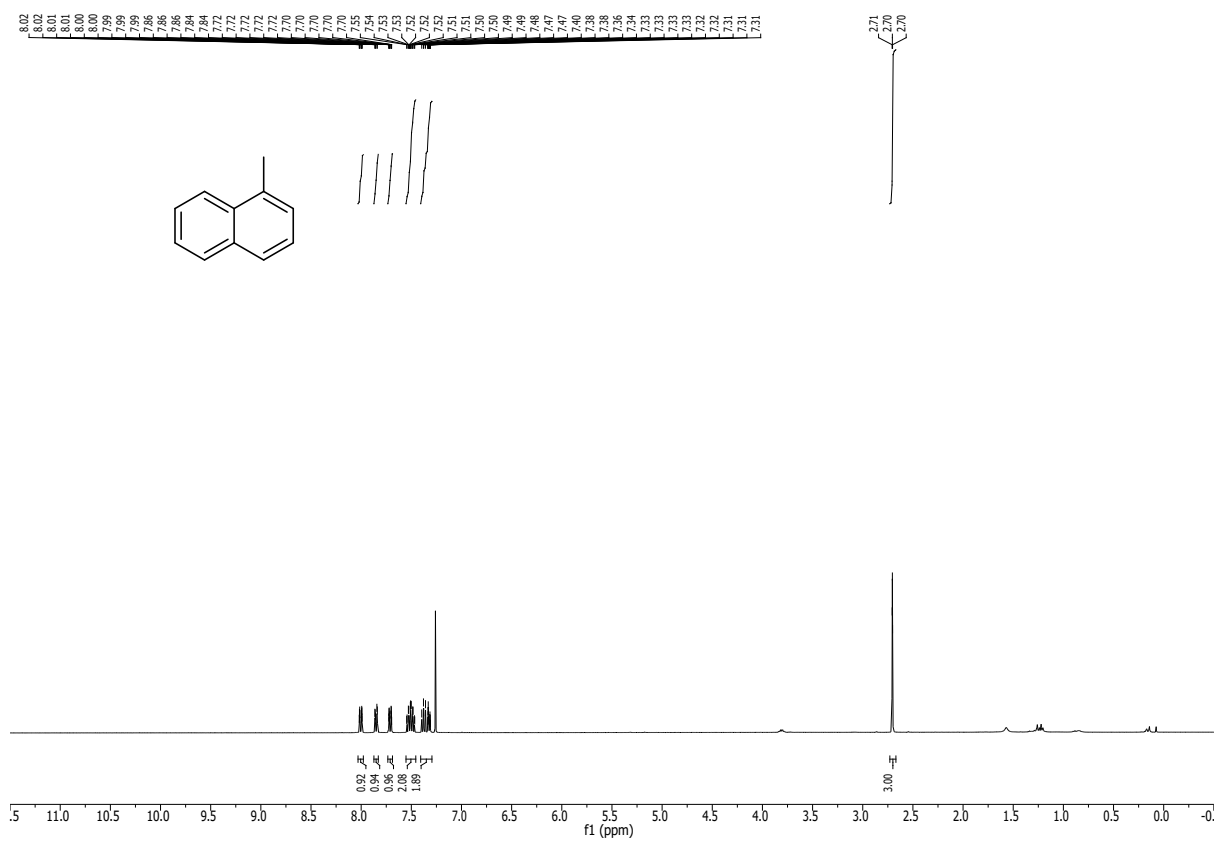
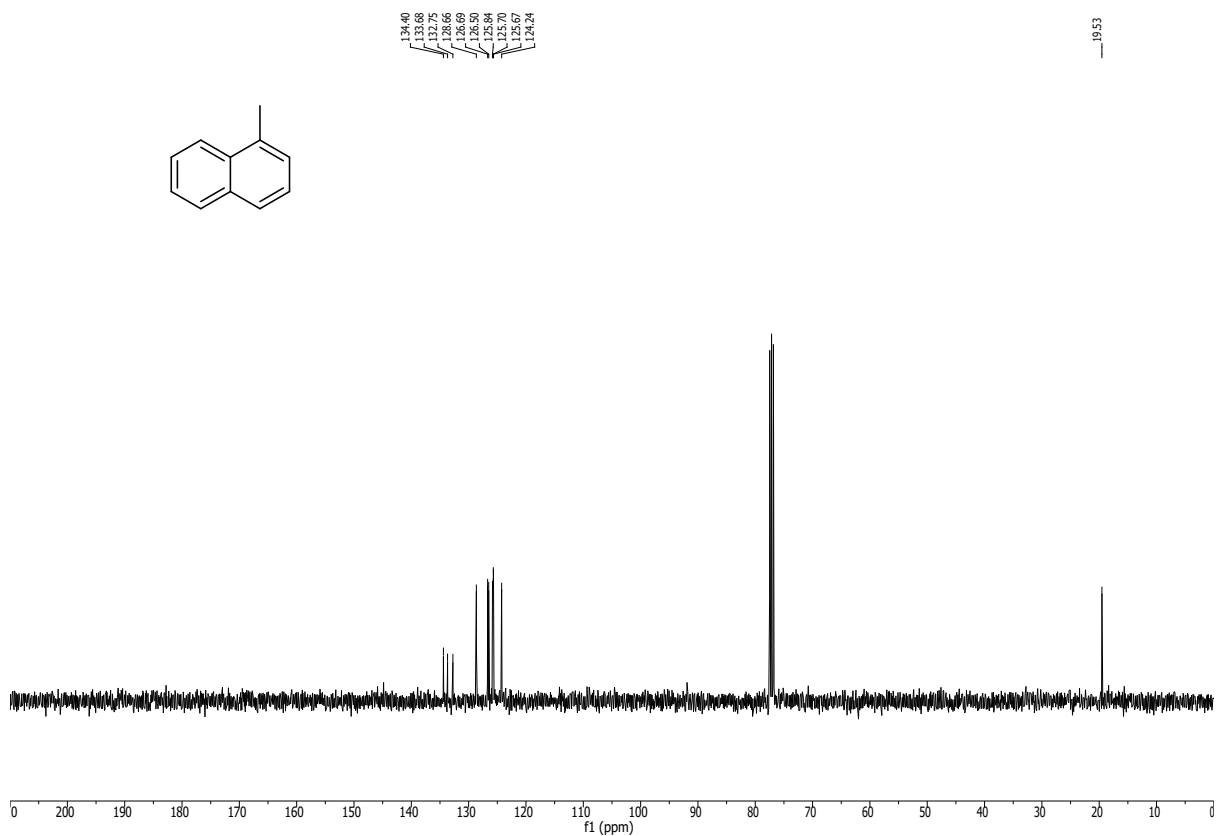
$C_{11}H_{10}$  (142.20 g/mol)

**R<sub>f</sub>**: 0.91 (4:1 Hex:EtOAc)

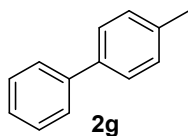
**<sup>1</sup>H-NMR** (400 MHz, Chloroform-d,  $\delta_H$ /ppm) 8.03 – 7.98 (m, 1H), 7.87 – 7.83 (m, 1H), 7.77 – 7.71 (m, 1H), 7.55 – 7.46 (m, 2H), 7.41 – 7.29 (m, 2H), 2.70 (s, 3H).

**<sup>13</sup>C-NMR** (100 MHz, CDCl<sub>3</sub>,  $\delta_C$ /ppm) 134.40, 133.7, 132.8, 128.7, 126.7, 126.5, 125.8, 125.7, 125.7, 124.2, 19.5.

**GC-MS** (EI): 142.1 (100, [M<sup>+</sup>]), 126.0 ([M<sup>+</sup>]-[CH<sub>3</sub>]), 115.0 ([M<sup>+</sup>]-[CH<sub>3</sub>]), 102.0 ([M<sup>+</sup>]-[CCHCH<sub>3</sub>])

$^1\text{H-NMR}$ : (400 MHz,  $\text{CDCl}_3$ ) of **2f** $^{13}\text{C-NMR}$ : (101 MHz,  $\text{CDCl}_3$ ) of **2f**

#### 4-methylbiphenyl (**2g**)



According to **GP4**, 1-methylnaphtalene (**2g**) was synthesized from 1,1-Biphenyl-4-methanol (184 mg, 1.00 mmol, 1.00 equiv.) over 16 h. The product was isolated by column chromatography (Hexane/Ethyl acetate 4:1) and was afforded as a colorless solid (138 mg, 0.82 mmol, 82%, 89% determined by GC-FID). Analytical data was in accordance with the literature.<sup>7</sup>

$C_{13}H_{12}$  (168.09 g/mol)

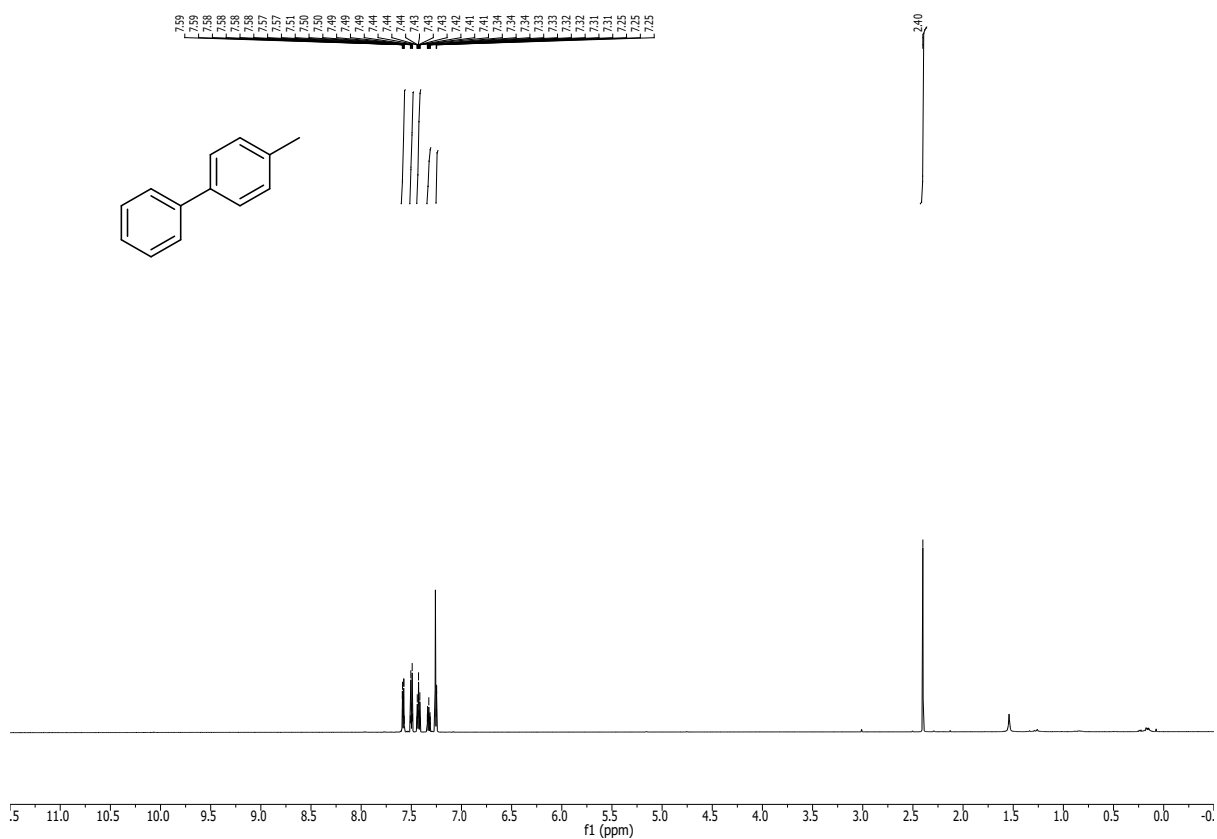
**R<sub>f</sub>**: 0.83 (4:1 Hex:EtOAc)

**<sup>1</sup>H-NMR** (400 MHz, CDCl<sub>3</sub>)  $\delta_H$ /ppm: 7.60 – 7.56 (m, 2H), 7.52 – 7.48 (m, 2H), 7.45 – 7.41 (m, 2H), 7.34 – 7.31 (m, 1H), 7.27-7,23 (m, 1H), 2.40 (s, 3H).

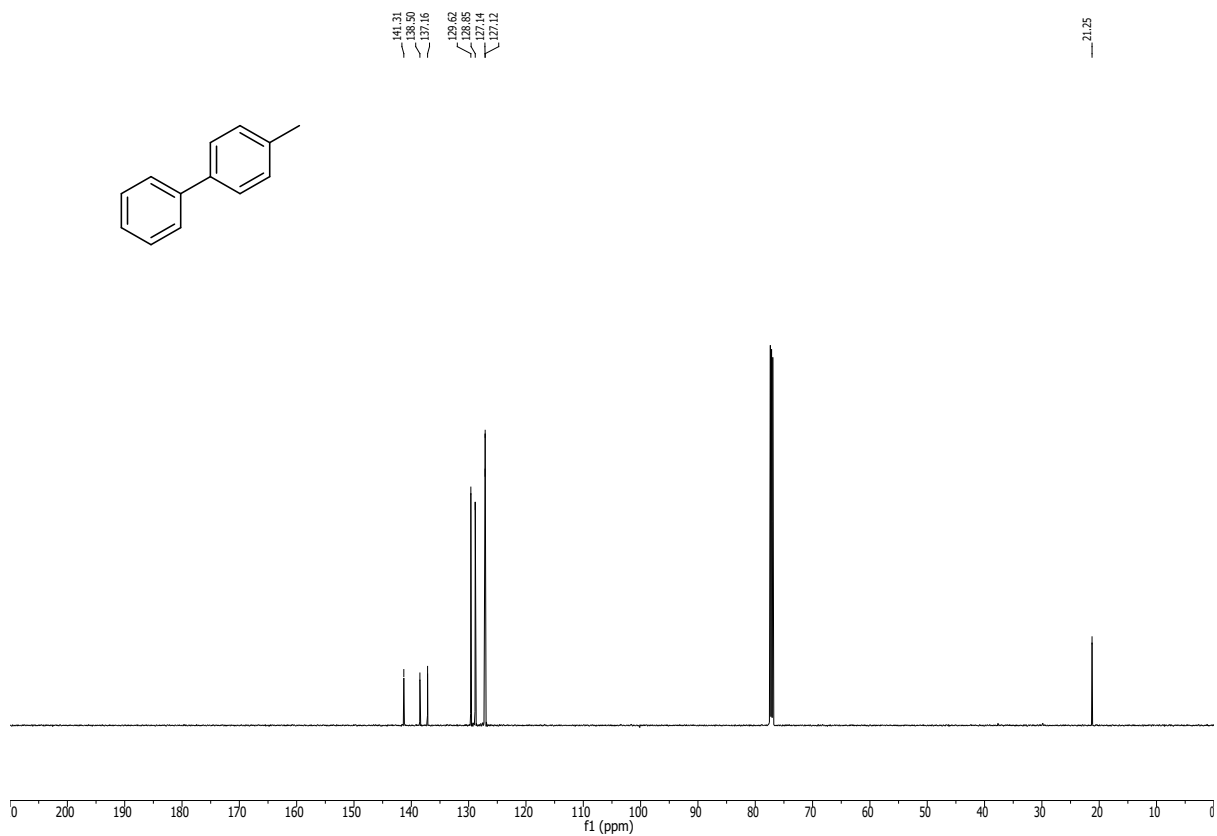
**<sup>13</sup>C-NMR** (100 MHz, CDCl<sub>3</sub>)  $\delta_C$ /ppm: 141.3, 138.5, 137.2, 129.6, 128.9, 127.1, 127.1, 21.3.

**GC-MS** (EI): 168.1 (100, [M<sup>+</sup>]), 152.1 (32, [M<sup>+</sup>]-[CH<sub>3</sub>•]), 91.0 (8, [M<sup>+</sup>]-[C<sub>6</sub>H<sub>5</sub>•])

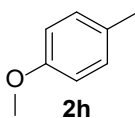
$^1\text{H-NMR}$ : (400 MHz,  $\text{CDCl}_3$ ) of **2g**



$^{13}\text{C-NMR}$ : (101 MHz,  $\text{CDCl}_3$ ) of **2g**



#### 4-methylanisole (**2h**)



According to **GP4**, 4-methylanisole (**2h**) was synthesized from 4-methoxybenzyl alcohol (0.127 mL, 138 mg, 1.00 mmol, 1.00 equiv.), over 16 h. The product was isolated by column chromatography (Hexane/Ethyl acetate 4:1) and was afforded as a colorless oil (56 mg, 0.46 mmol, 46%, 92% determined by GC-FID). Analytical data was in accordance with the literature.<sup>6</sup>

$C_8H_{10}O$  (122.07 g/mol)

**R<sub>f</sub>**: 0.74 (4:1 Hex:EtOAc)

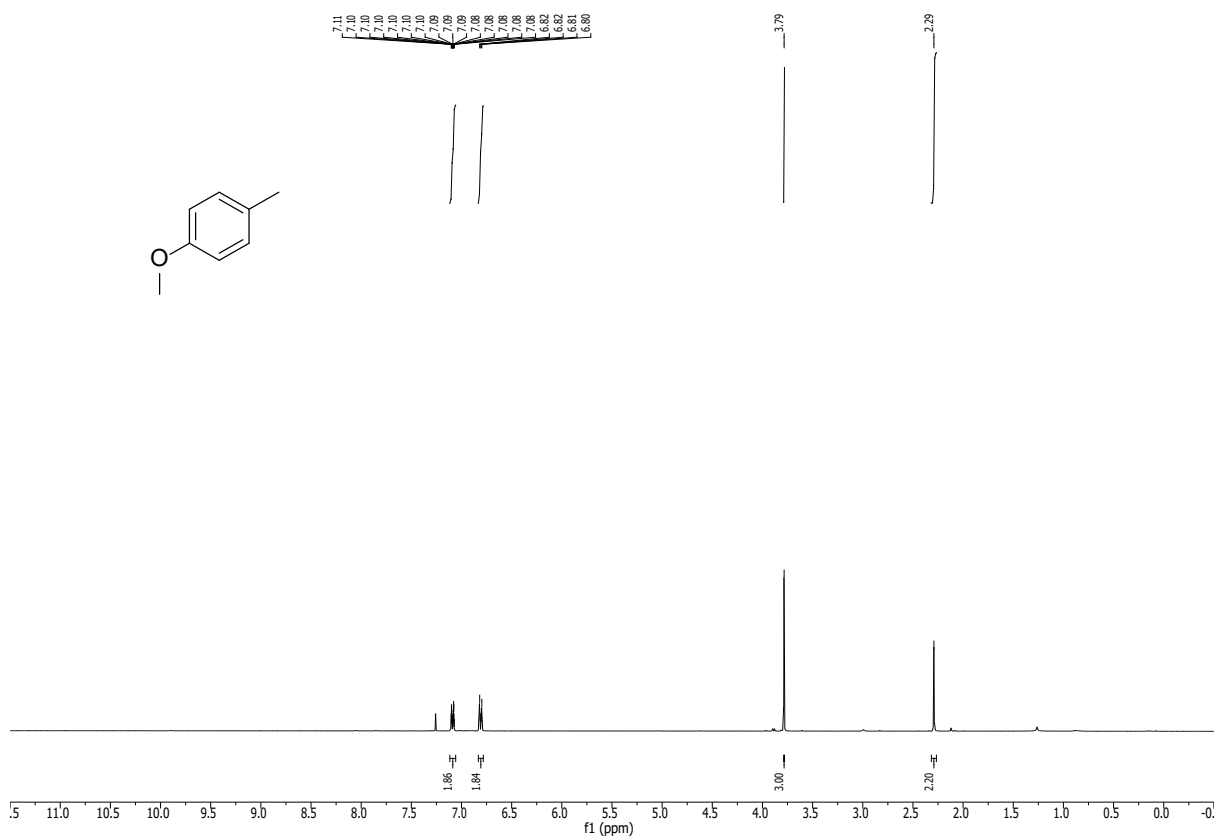
**<sup>1</sup>H-NMR** (400 MHz,  $CDCl_3$ )  $\delta_H$ /ppm: 7.13 – 7.04 (m, 2H), 6.85 – 6.76 (m, 2H), 3.78 (s, 3H), 2.29 (s, 3H).

**<sup>13</sup>C-NMR** (100 MHz,  $CDCl_3$ )  $\delta_C$ /ppm: 157.6, 130.0, 113.8, 55.4, 20.6.

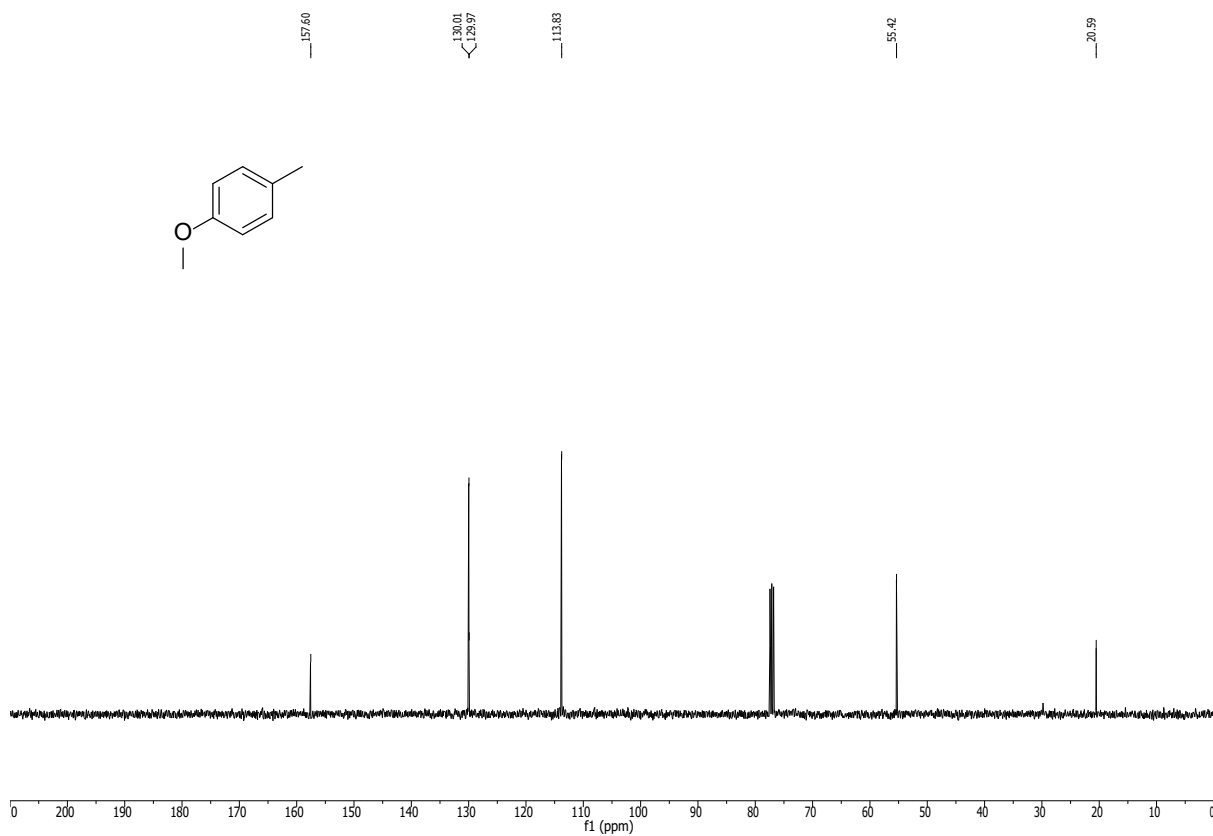
**GC-MS** (EI): 122.09 (100,  $[M^{+}]$ ), 107.05 ( $[M^{+}]-[CH_3^{\bullet}]$ ), 91.06 ( $[M^{+}]-[OCH_3^{\bullet}]$ ), 77.04 ( $[M^{+}]-[CH_3^{\bullet}]-[OCH_3^{\bullet}]$ )



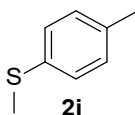
$^1\text{H-NMR}$ : (400 MHz,  $\text{CDCl}_3$ ) of **2h**



$^{13}\text{C-NMR}$ : (101 MHz,  $\text{CDCl}_3$ ) of **2h**



**1-methyl-4-methylsulfanylbenzene (2i)**



According to **GP4**, 1-methyl-4-methylsulfanylbenzene (**2i**) was synthesized from 4-(methylthio)benzyl alcohol (0.127 mL, 138 mg, 1.00 mmol, 1.00 equiv.) over 16 h. The product was isolated by column chromatography (Hexane/Ethyl acetate 98:2) and was afforded as a colorless solid (48 mg, 0.35 mmol, 35%, 48% determined by GC-FID). Analytical data was in accordance with the literature.<sup>8</sup>  
 $C_8H_{10}S$  (138.23 g/mol)

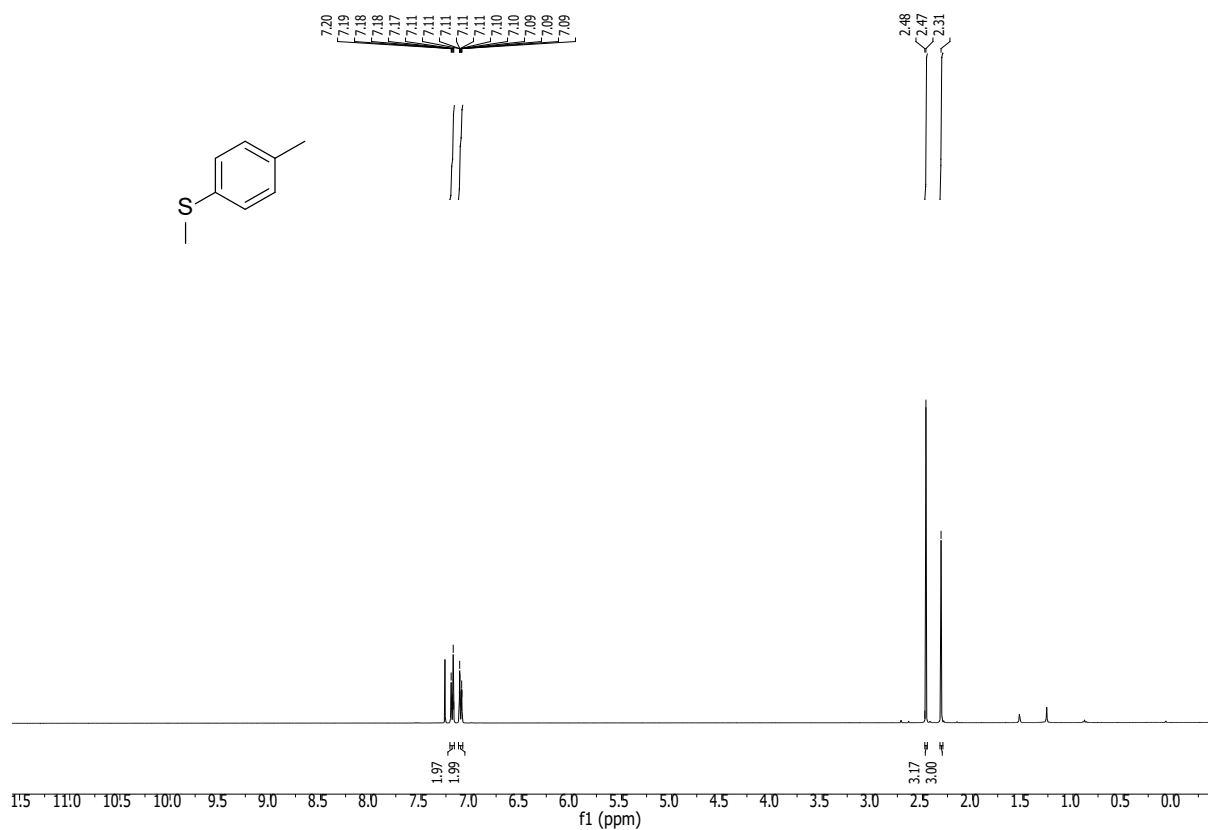
**R<sub>f</sub>**: 0.50 (98:2 Hex:EtOAc)

**<sup>1</sup>H-NMR**: (400 MHz,  $CDCl_3$ ):  $\delta$ /ppm = 7.20 – 7.17 (m, 2H), 7.11 – 7.09 (m, 2H), 2.46 (s, 3H), 2.31 (s, 3H)

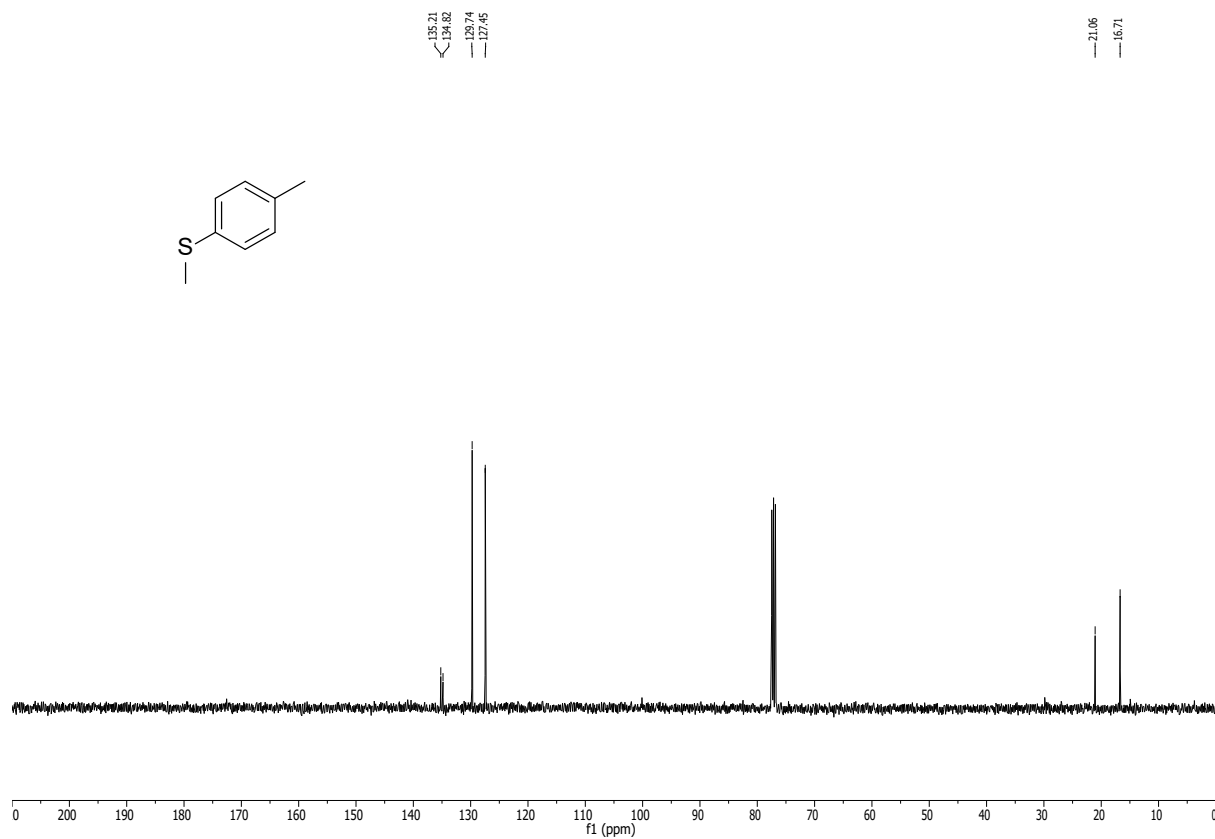
**<sup>13</sup>C-NMR**: (101 MHz,  $CDCl_3$ ):  $\delta$ /ppm = 135.2, 134.8, 129.7, 127.5, 21.1, 16.7.

**GC-MS**: (EI):  $m/z$  = 138.0 (100,  $[M^{+\cdot}]$ ), 123.0 (29,  $[M^{+\cdot}]-[CH_3^{\cdot}]$ ), 91.1 (60,  $[M^{+\cdot}]-[SCH_3^{\cdot}]$ )

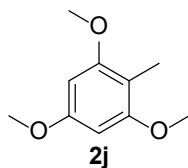
$^1\text{H-NMR}$ : (400 MHz,  $\text{CDCl}_3$ ) of **2i**



$^{13}\text{C-NMR}$ : (101 MHz,  $\text{CDCl}_3$ ) of **2i**



**1,2,3-trimethoxy-5-methylbenzene (2j)**



According to **GP4**, 1,3,5-trimethoxy-5-methylbenzene (**2j**) was synthesized from (2,4,6-trimethoxyphenyl)methanol (198 mg, 1.00 mmol, 1.00 equiv.) over 16 h. The product was isolated by column chromatography (Hexane/Ethyl acetate 98:2) and was afforded as a colorless solid (124 mg, 0.68 mmol, 68%, 73% determined by GC-FID). Analytical data was in accordance with the literature.<sup>9</sup> C<sub>10</sub>H<sub>14</sub>O<sub>3</sub> (182.22 g/mol)

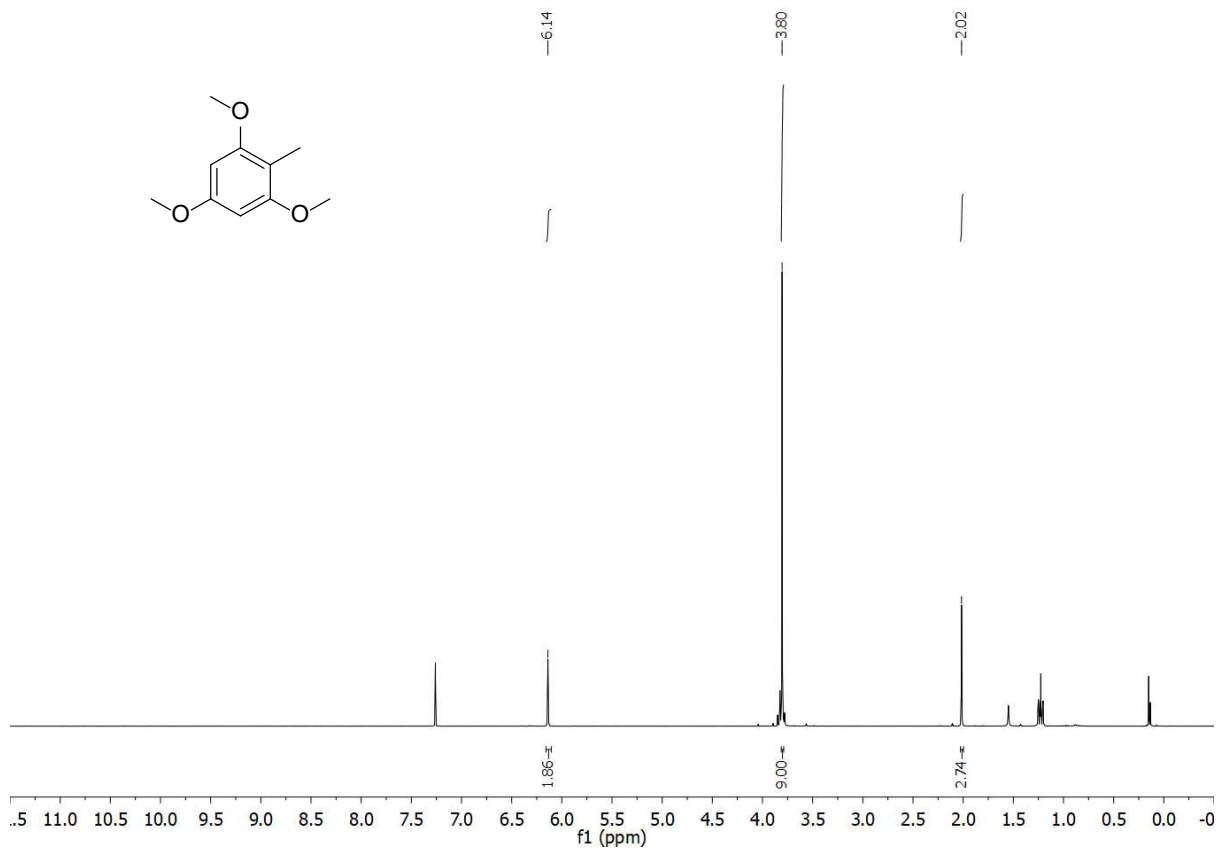
**R<sub>f</sub>**: 0.36 (98:2 Hex:EtOAc)

**<sup>1</sup>H-NMR**: (400 MHz, CDCl<sub>3</sub>): δ/ppm = 6.14 (s, 2H), 3.80 (s, 9H), 2.02 (s, 3H); Impurity – Ethyl acetate

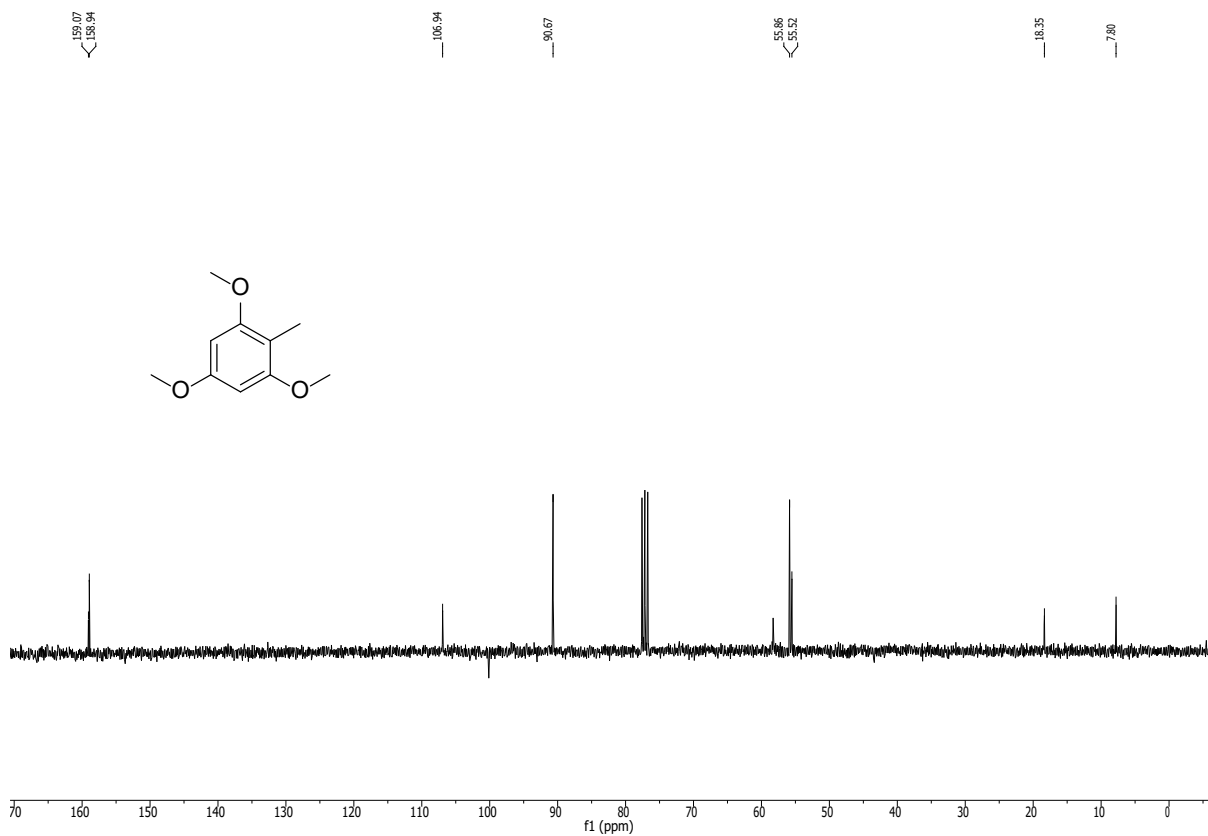
**<sup>13</sup>C-NMR**: (101 MHz, CDCl<sub>3</sub>): δ/ppm = 158.9, 106.9, 90.7, 58.3, 55.9, 18.4, 7.8.

**GC-MS**: (EI): m/z = 182.1 (100, [M<sup>+</sup>]), 167.1 (28, [M<sup>+</sup>]-[CH<sub>3</sub>•]), 151.1 (33, [M<sup>+</sup>]-[OCH<sub>3</sub>•])

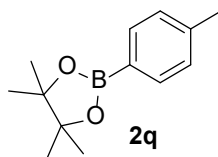
$^1\text{H-NMR}$ : (400 MHz,  $\text{CDCl}_3$ ) of **2j**



$^{13}\text{C-NMR}$ : (101 MHz,  $\text{CDCl}_3$ ) of **2j**



**4,4,5,5-tetramethyl-2-(4-methylphenyl)1,3,2-dioxaborolane (2q)**



According to **GP4**, 4,4,5,5-tetramethyl-2-(4-methylphenyl)1,3,2-dioxaborolane (**2q**) was synthesized from (4-(4,4,5,5-tetramethyl-1,3,2-dioxaborolan-2-yl)phenyl)methanol (234 mg, 1.00 mmol, 1.00 equiv.) over 16 h. The product was isolated by column chromatography (Hexane/Ethyl acetate 98:2) and was afforded as a colorless solid (205 mg, 0.94 mmol, 94%, 99% determined by GC-FID). Analytical data was in accordance with the literature.<sup>10</sup>

$C_{13}H_{19}BO_2$  (218.10 g/mol)

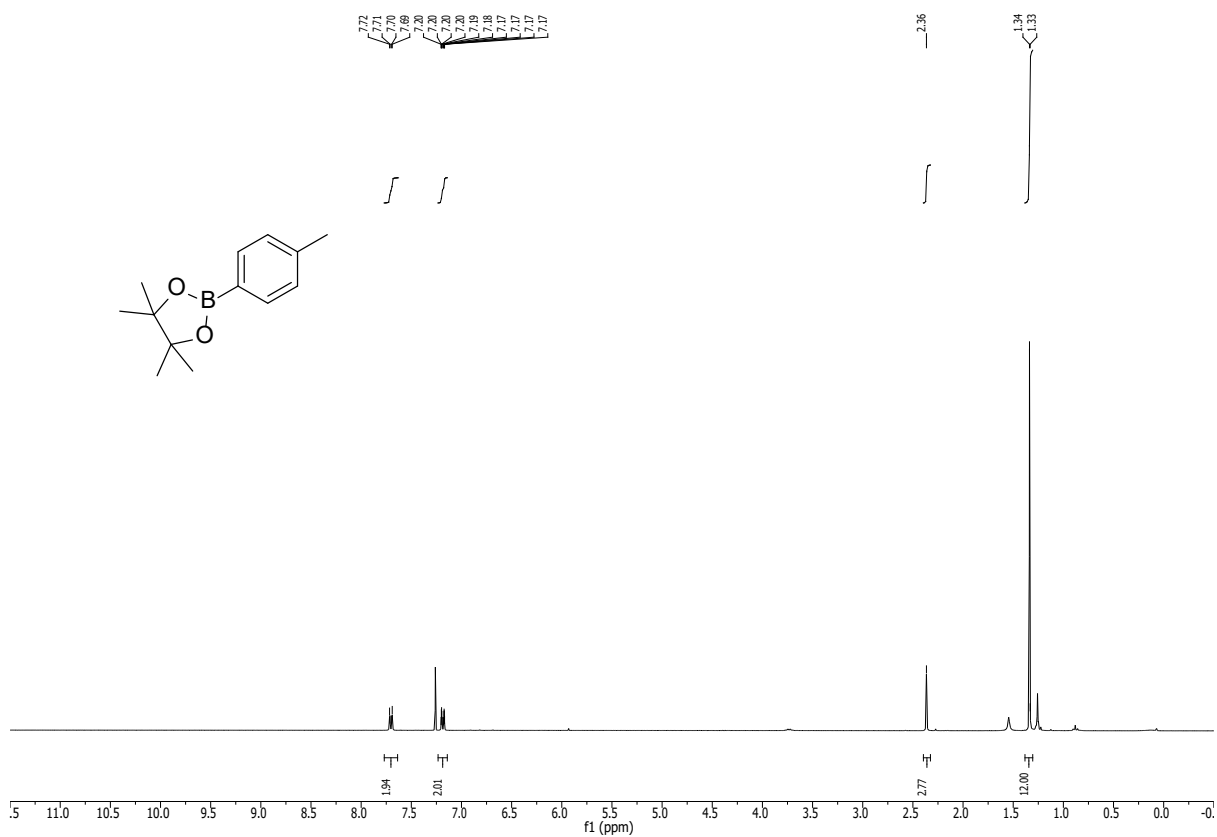
$R_f$ : 0.44 (98:2 Hex:EtOAc)

**<sup>1</sup>H-NMR**: (400 MHz,  $CDCl_3$ ):  $\delta$ /ppm = 7.70 (d,  $J = 7.5$  Hz 2H), 7.20 (d,  $J = 7.5$  Hz, 2H), 2.37 (s, 3H), 1.34 (s, 12H); Impurity – Pentadecane (internal standard)

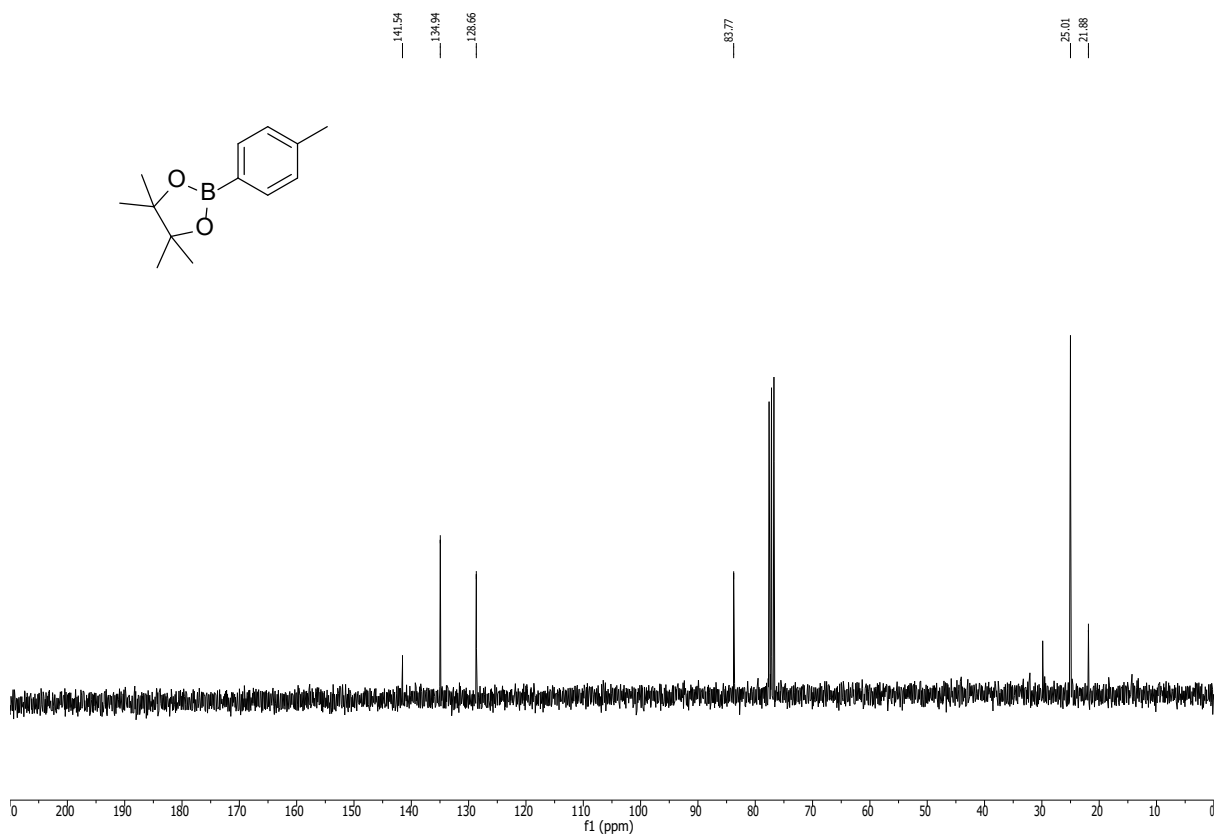
**<sup>13</sup>C-NMR**: (101 MHz,  $CDCl_3$ ):  $\delta$ /ppm = 141.5, 135.0, 128.7, 83.8, 29.9, 25.0, 21.9.

**GC-MS**: (EI):  $m/z$  = 218.2 (40,  $[M^+]$ ), 203.2 (52,  $[M^+]-[CH_3^+]$ ), 119.1 (100,  $[M^+]-[CH_3^+]-[C_2(CH_3)_4^+]$ ), 91.1 (20,  $[M^+]-[BO_2C_2(CH_3)_4^+]$ )

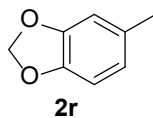
$^1\text{H-NMR}$ : (400 MHz,  $\text{CDCl}_3$ ) of **2q**



$^{13}\text{C-NMR}$ : (101 MHz,  $\text{CDCl}_3$ ) of **2q**



**5-methylbenzo[*d*][1,3]dioxole (2r)**



According to **GP4**, 5-methylbenzo[*d*][1,3]dioxole (**2r**) was synthesized from piperonyl alcohol (152 mg, 1.00 mmol, 1.00 equiv.) over 16 h. The product was isolated by column chromatography (Hexane/Ethyl acetate 98:2) and was afforded as a colorless oil (38 mg, 0.28 mmol, 28%, 94% determined by GC-FID). Analytical data was in accordance with the literature.<sup>11</sup>

$C_8H_8O_2$  (136.15 g/mol)

**R<sub>f</sub>**: 0.49 (98:2 Hex:EtOAc)

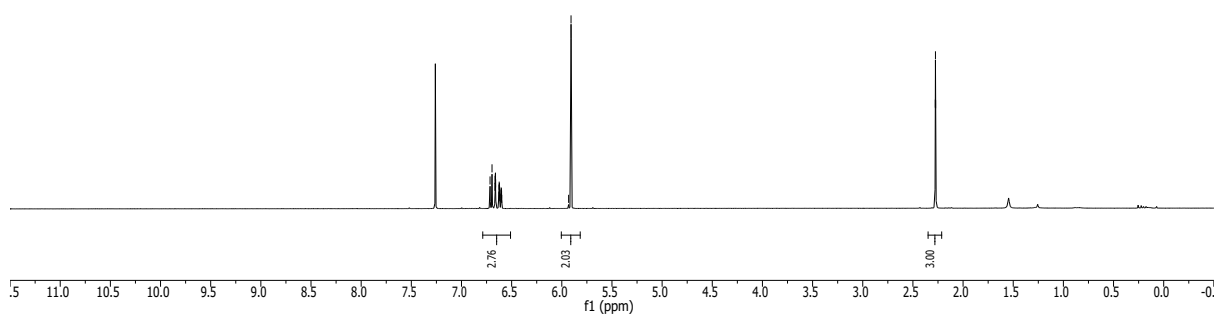
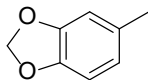
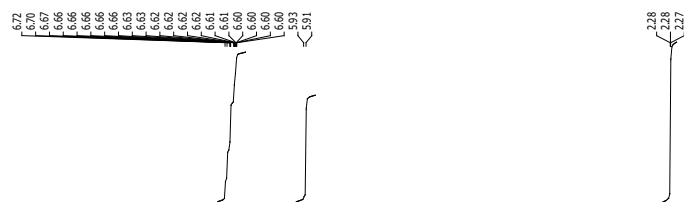
**<sup>1</sup>H-NMR**: (400 MHz, CDCl<sub>3</sub>):  $\delta$ /ppm = 6.72 – 6.70 (m, 1H), 6.67 – 6.66 (m, 1H), 6.63 – 6.60 (m, 1H), 5.91 (s, 2H), 2.28 (s, 3H)

**<sup>13</sup>C-NMR**: (101 MHz, CDCl<sub>3</sub>):  $\delta$ /ppm = 147.6, 131.4, 121.6, 109.7, 108.2, 100.8, 31.8, 21.3.

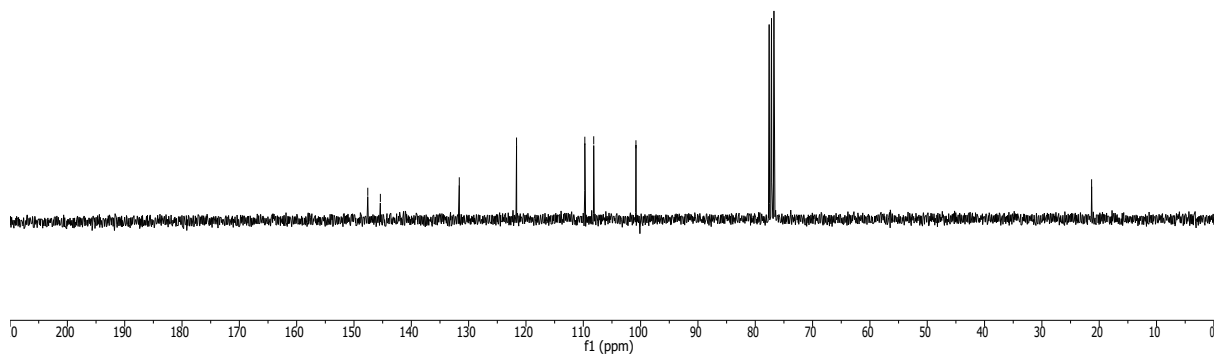
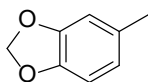
**GC-MS**: (EI):  $m/z$  = 136.0 (100, [M<sup>+</sup>]), 121.0 (3, [M<sup>+</sup>]-[CH<sub>3</sub>•]), 77.0 (45, [C<sub>6</sub>H<sub>5</sub>•])



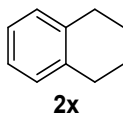
$^1\text{H-NMR}$ : (400 MHz,  $\text{CDCl}_3$ ) of **2r**



$^{13}\text{C-NMR}$ : (101 MHz,  $\text{CDCl}_3$ ) of **2r**



**1,2,3,4-tetrahydronaphthalene (2x)**



According to **GP4**, 1,2,3,4-tetrahydronaphthalene (**2x**) was synthesized from 1-Tetralol (0.136 mL, 148 mg, 1.00 mmol, 1.00 equiv.) over 16 h. The product was isolated by column chromatography (Hexane/Ethyl acetate 98:2) and was afforded as a colorless liquid (88 mg, 0.60 mmol, 60%, 86% determined by GC-FID). Analytical data was in accordance with the literature.<sup>12</sup>

$C_{10}H_{12}$  (132.21 g/mol)

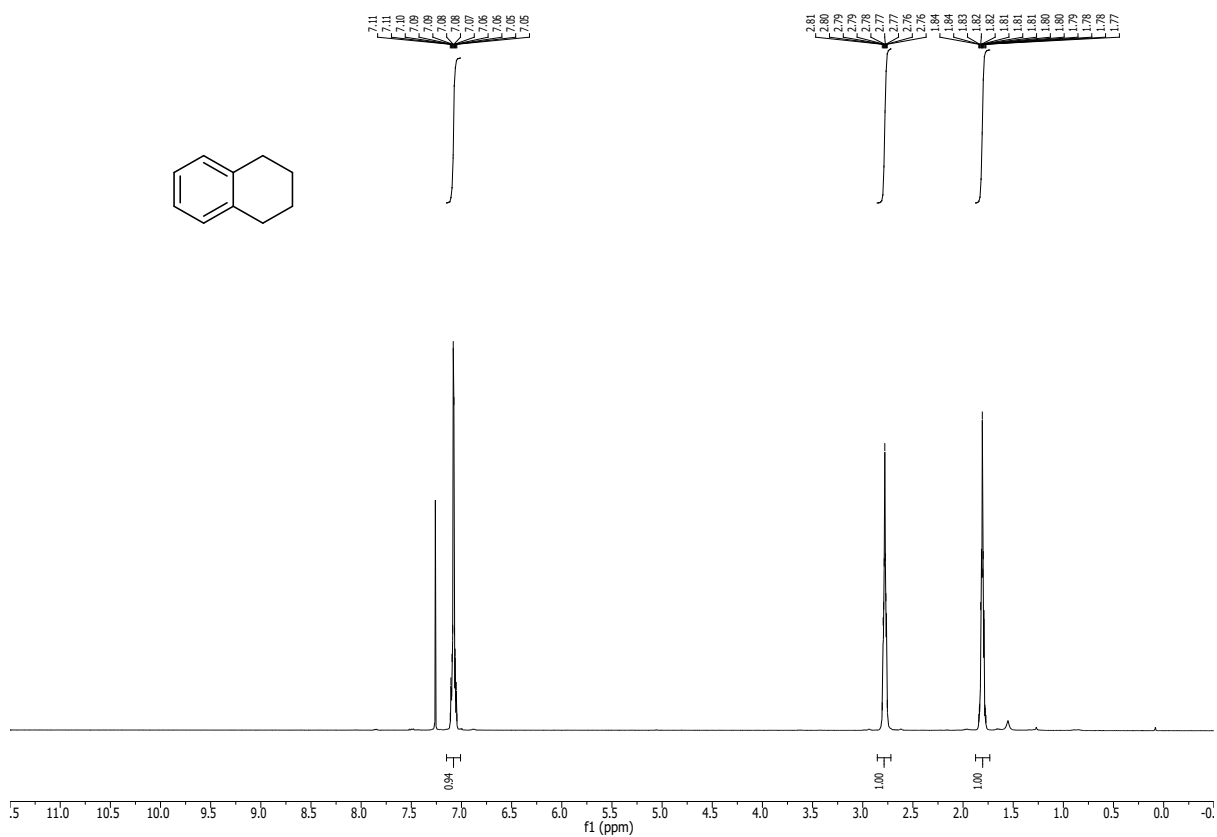
**R<sub>f</sub>**: 0.85 (98:2 Hex:EtOAc)

**<sup>1</sup>H-NMR**: (400 MHz, CDCl<sub>3</sub>):  $\delta$ /ppm = 7.09 – 7.06 (m, 4H), 2.78 (p,  $J$  = 3.9 Hz, 4H), 1.81 (p,  $J$  = 3.9 Hz, 4H)

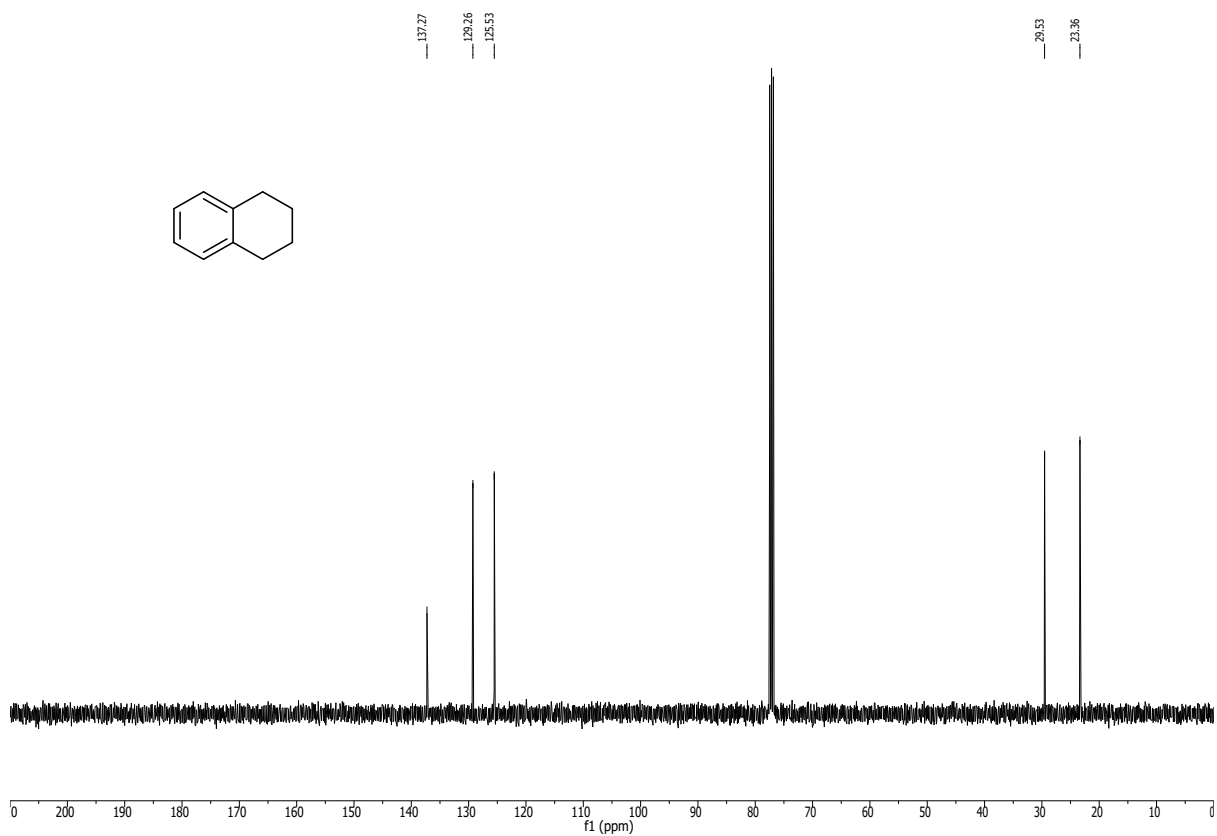
**<sup>13</sup>C-NMR**: (101 MHz, CDCl<sub>3</sub>):  $\delta$ /ppm = 137.3, 129.3, 125.5, 29.5, 23.3.

**GC-MS**: (EI):  $m/z$  = 132.1 (43, [M<sup>++</sup>]), 104.1 (100, [M<sup>++</sup>]-[C<sub>2</sub>H<sub>4</sub>]), 91.1 (40, [M<sup>++</sup>]-[C<sub>3</sub>H<sub>5</sub>])

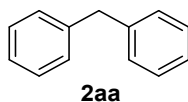
$^1\text{H-NMR}$ : (400 MHz,  $\text{CDCl}_3$ ) of **2x**



$^{13}\text{C-NMR}$ : (101 MHz,  $\text{CDCl}_3$ ) of **2x**



**diphenylmethane (2aa)**



According to **GP4**, diphenylmethane (**2aa**) was synthesized from benzhydrol (183 mg, 1.00 mmol, 1.00 equiv.) over 16 h. The product was isolated by column chromatography (Hexane/Ethyl acetate 98:2) and was afforded as a colorless oil (104 mg, 0.62 mmol, 62%, 75% by GC-FID). Analytical data was in accordance with the literature.<sup>13</sup>

$C_{13}H_{12}$  (168.26 g/mol)

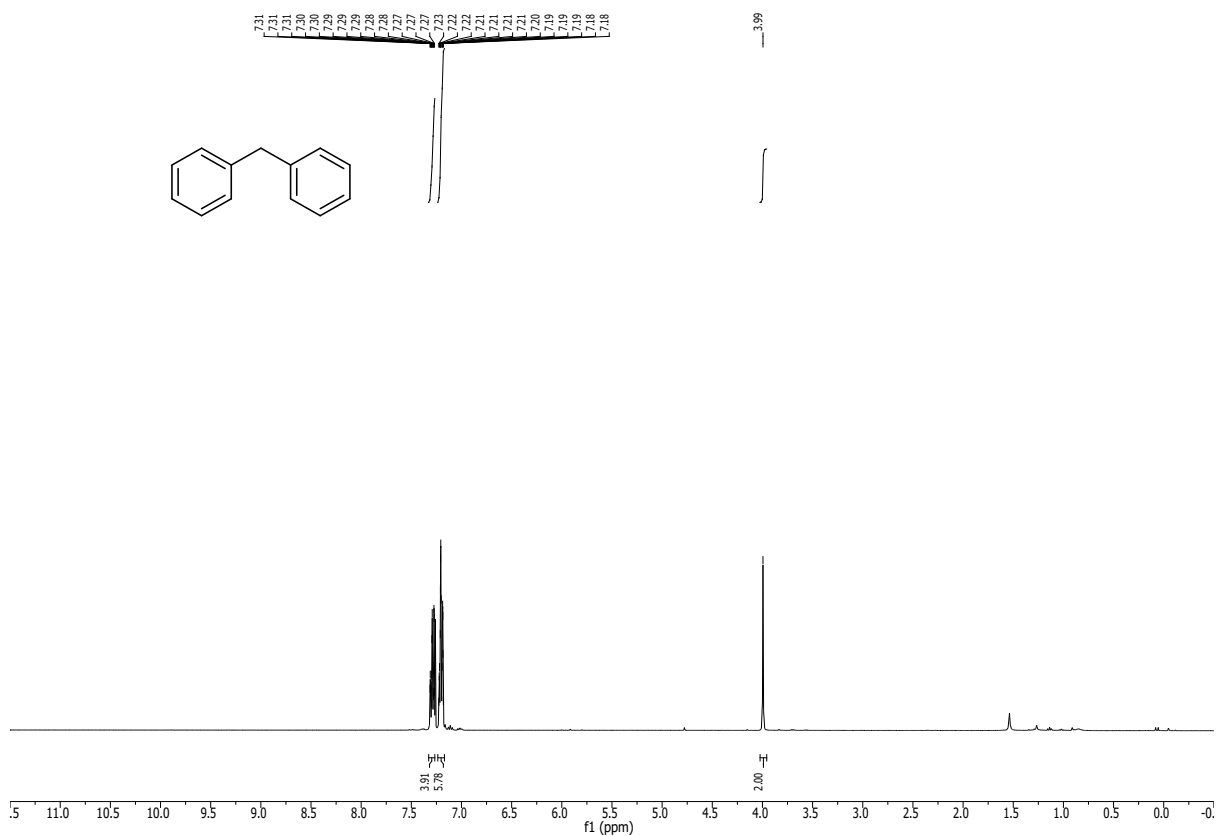
**R<sub>f</sub>**: 0.66 (98:2 Hex:EtOAc)

**<sup>1</sup>H-NMR**: (400 MHz, CDCl<sub>3</sub>):  $\delta$ /ppm = 7.31 – 7.27 (m, 4H), 7.22 – 7.19 (m, 6H), 3.99 (s, 2H)

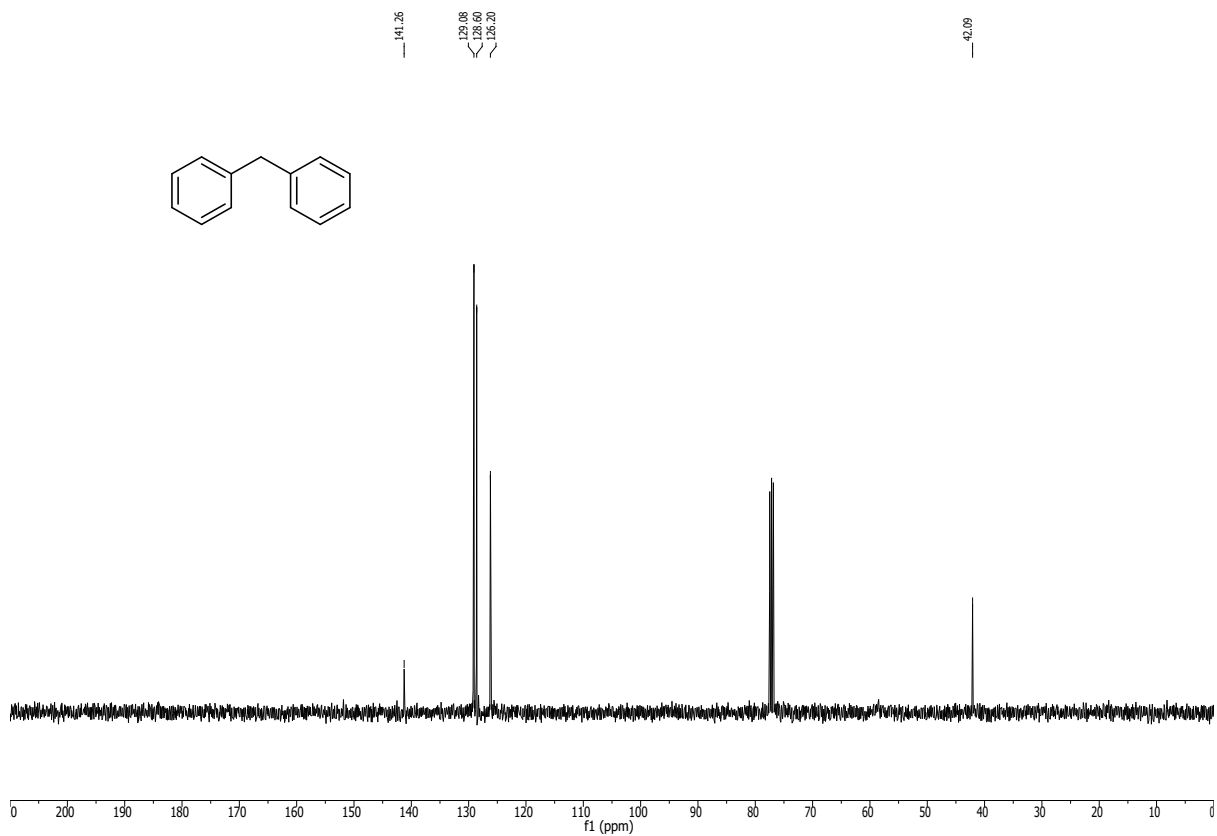
**<sup>13</sup>C-NMR**: (101 MHz, CDCl<sub>3</sub>):  $\delta$ /ppm = 141.3, 129.1, 128.6, 126.2, 42.1.

**GC-MS**: (EI):  $m/z$  = 168.1 (100, [M<sup>+</sup>]), 91.1 (29, [M<sup>+</sup>]-[C<sub>6</sub>H<sub>5</sub>•])

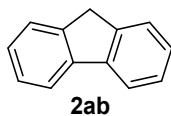
$^1\text{H-NMR}$ : (400 MHz,  $\text{CDCl}_3$ ) of **2aa**



$^{13}\text{C-NMR}$ : (101 MHz,  $\text{CDCl}_3$ ) of **2aa**



**9H-fluorene (2ab)**



According to **GP4**, 9H-fluorene (**2ab**) was synthesized from fluoren-9-ol (182 mg, 1.00 mmol, 1.00 equiv.) over 16 h. The product was isolated by column chromatography (Hexane/Ethyl acetate 98:2) and was afforded as a colorless solid (115 mg, 0.69 mmol, 69%, 88% determined by GC-FID). Analytical data was in accordance with the literature.<sup>14</sup>

C<sub>13</sub>H<sub>10</sub> (166.22 g/mol)

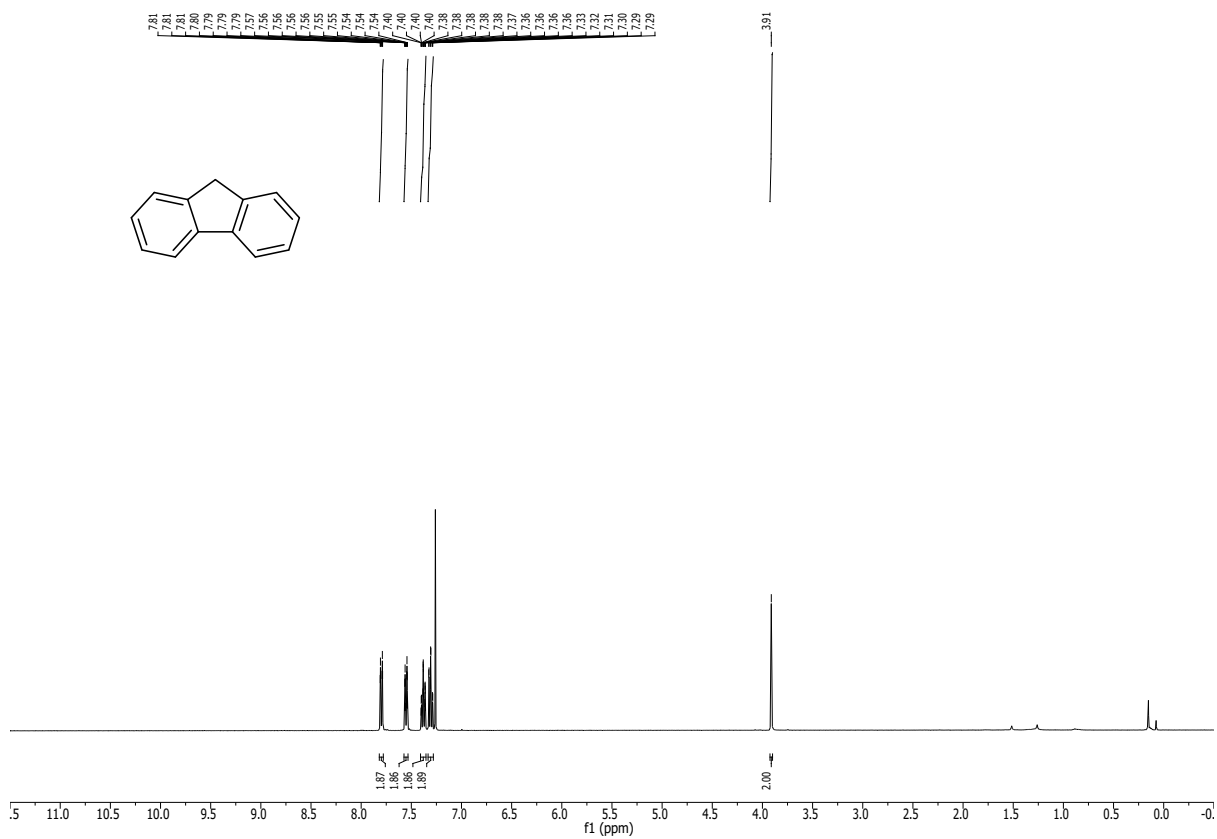
**R<sub>f</sub>**: 0.55 (98:2 Hex:EtOAc)

**<sup>1</sup>H-NMR**: (400 MHz, CDCl<sub>3</sub>): δ/ppm = 7.80 (d, J = 7.7 Hz, 2H), 7.55 (m, 2H), 7.41 – 7.35 (m, 2H), 7.32 – 7.28 (m, 2H), 3.91 (s, 2H).

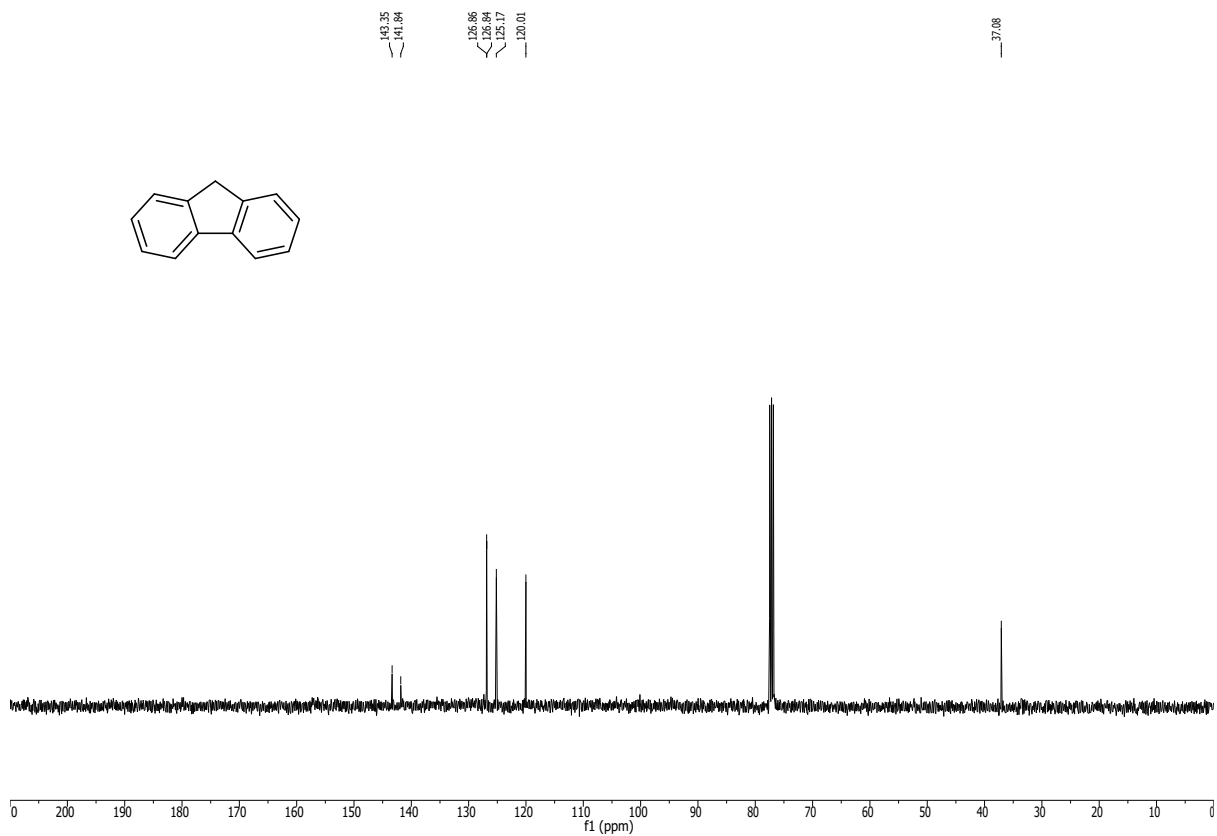
**<sup>13</sup>C-NMR**: (101 MHz, CDCl<sub>3</sub>): δ/ppm = 143.4, 141.8, 126.9, 126.8, 125.2, 120.0, 37.1.

**GC-MS**: (EI): m/z = 166.1 (100, [M<sup>+</sup>]), 165.1 (88, [M<sup>+</sup>]-[H<sup>+</sup>])

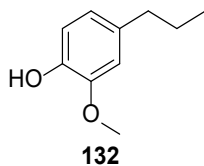
$^1\text{H-NMR}$ : (400 MHz,  $\text{CDCl}_3$ ) of **2ai**



$^{13}\text{C-NMR}$ : (101 MHz,  $\text{CDCl}_3$ ) of **2ai**



#### 4-Propylguaiacol (**132**)



According to **GP4**, 4-Propylguaiacol (**132**) was synthesized from coniferyl alcohol (180 mg, 1.00 mmol, 1.00 equiv.) over 16 h. The product was isolated by column chromatography (Hexane/Ethyl acetate 98:2) and was afforded as a colorless liquid (87 mg, 0.52 mmol, 52%, 76% determined by GC-FID). Analytical data was in accordance with the literature.<sup>15</sup>

$C_{10}H_{14}O_2$  (166.22 g/mol)

**R<sub>f</sub>**: 0.48 (98:2 Hex:EtOAc)

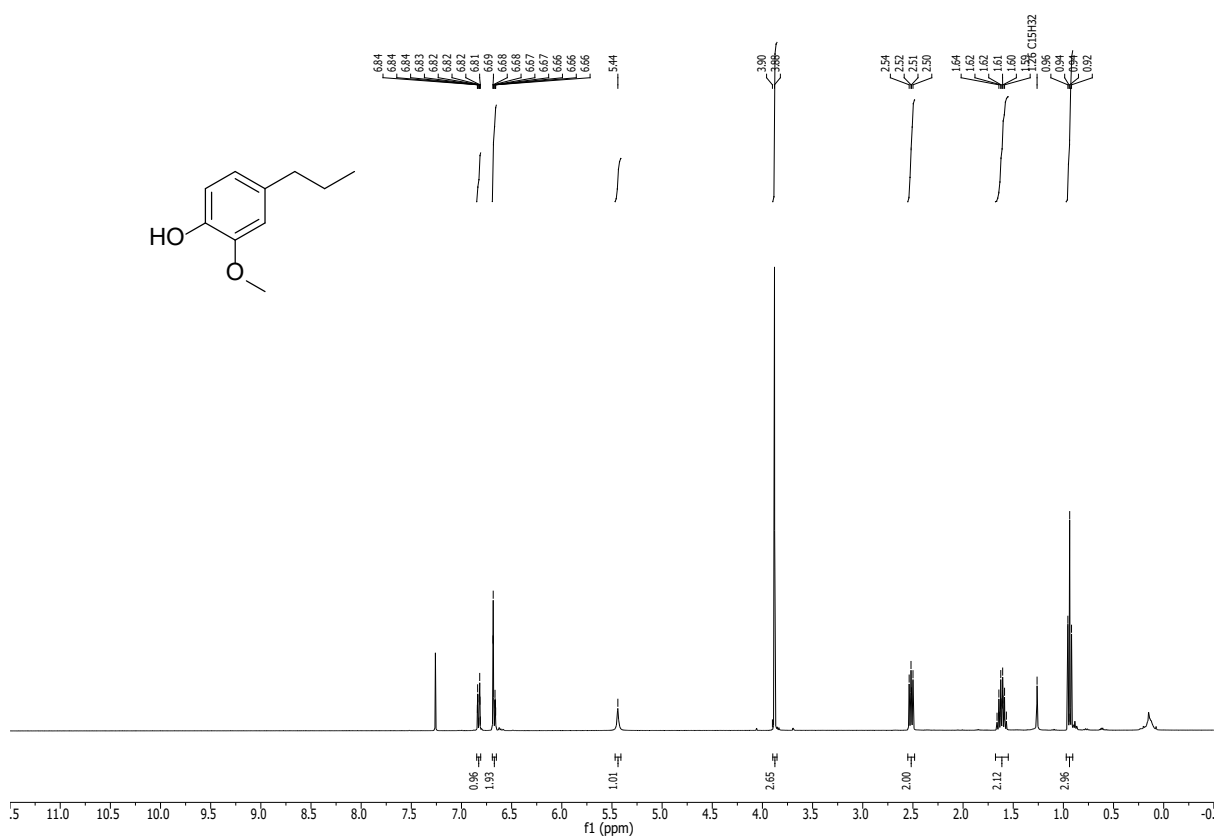
**<sup>1</sup>H-NMR**: (400 MHz,  $CDCl_3$ ):  $\delta$ /ppm = 6.83 (dd,  $J = 8.1, 0.9$  Hz, 1H), 6.68 (m, 2H), 5.44 (s, 1H), 3.88 (s, 3H), 2.52 (t,  $J = 7.3$ , 2H), 1.68 – 1.55 (m, 2H), 0.94 (t,  $J = 7.3$  Hz, 3H); (90% purity) Impurity – pentadecane

**<sup>13</sup>C-NMR**: (101 MHz,  $CDCl_3$ ):  $\delta$ /ppm = 146.4, 143.7, 134.8, 121.1, 114.2, 111.1, 56.0, 37.9, 25.0, 13.9.

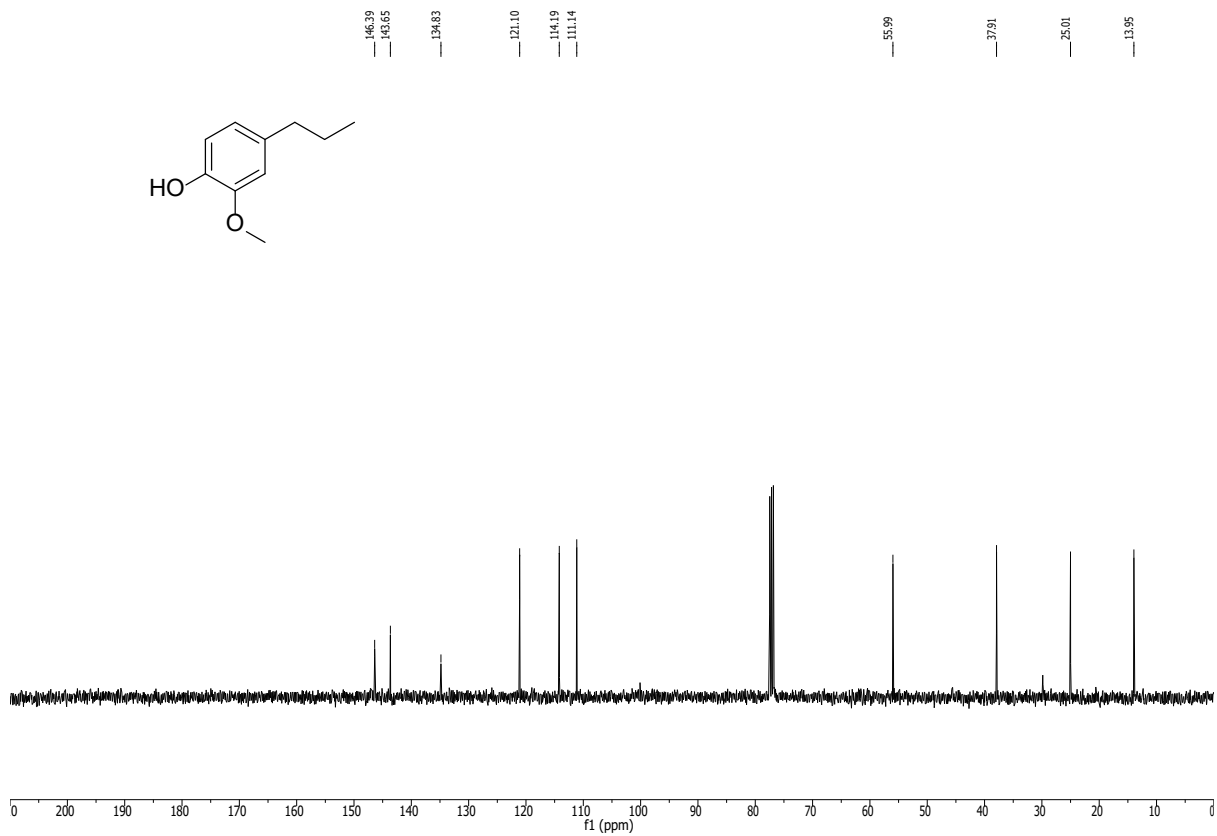
**GC-MS**: (EI):  $m/z = 166.1$  (32,  $[M^+]$ ),  $137.1$  (100,  $[M^+]-[C_2H_5^*]$ ),  $122.1$  (10,  $[M^+]-[C_3H_7^*]$ ),  $77.0$  (4,  $[C_6H_5^*]$ )



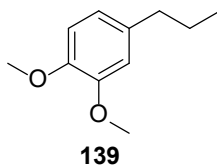
$^1\text{H-NMR}$ : (400 MHz,  $\text{CDCl}_3$ ) of **132**



$^{13}\text{C-NMR}$ : (100 MHz,  $\text{CDCl}_3$ ) of **132**



**1,2-dimethoxy-4-propylbenzene (139)**



According to lower scale **GP4** (0.75 equiv.) 1,2-dimethoxy-4-propylbenzene (**139**) was synthesized from adlerol (**138**)(250 mg, 0.75 mmol, 1.00 equiv.) over 16 h. The product was afforded as a colorless liquid (61 mg, 0.34 mmol, 45%, 67% determined by GC-FID). Analytical data was in accordance with the literature.<sup>16</sup>

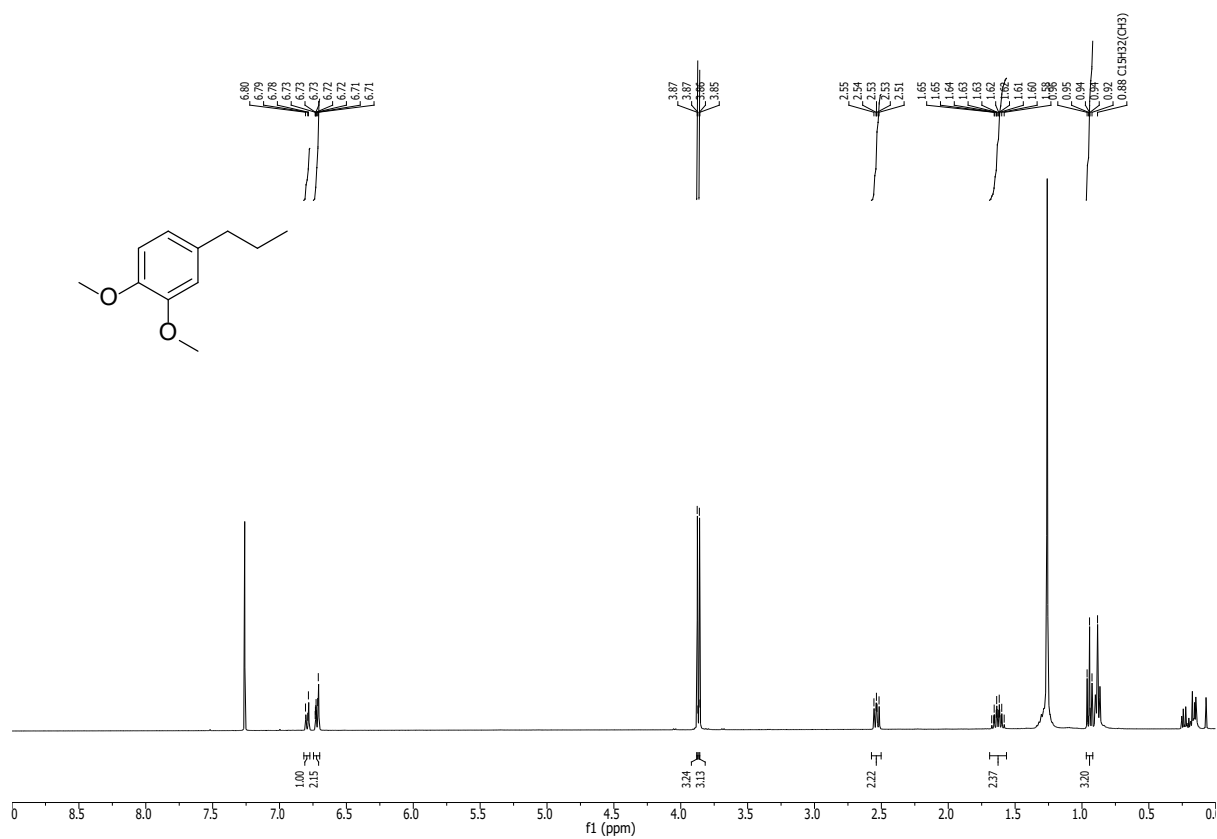
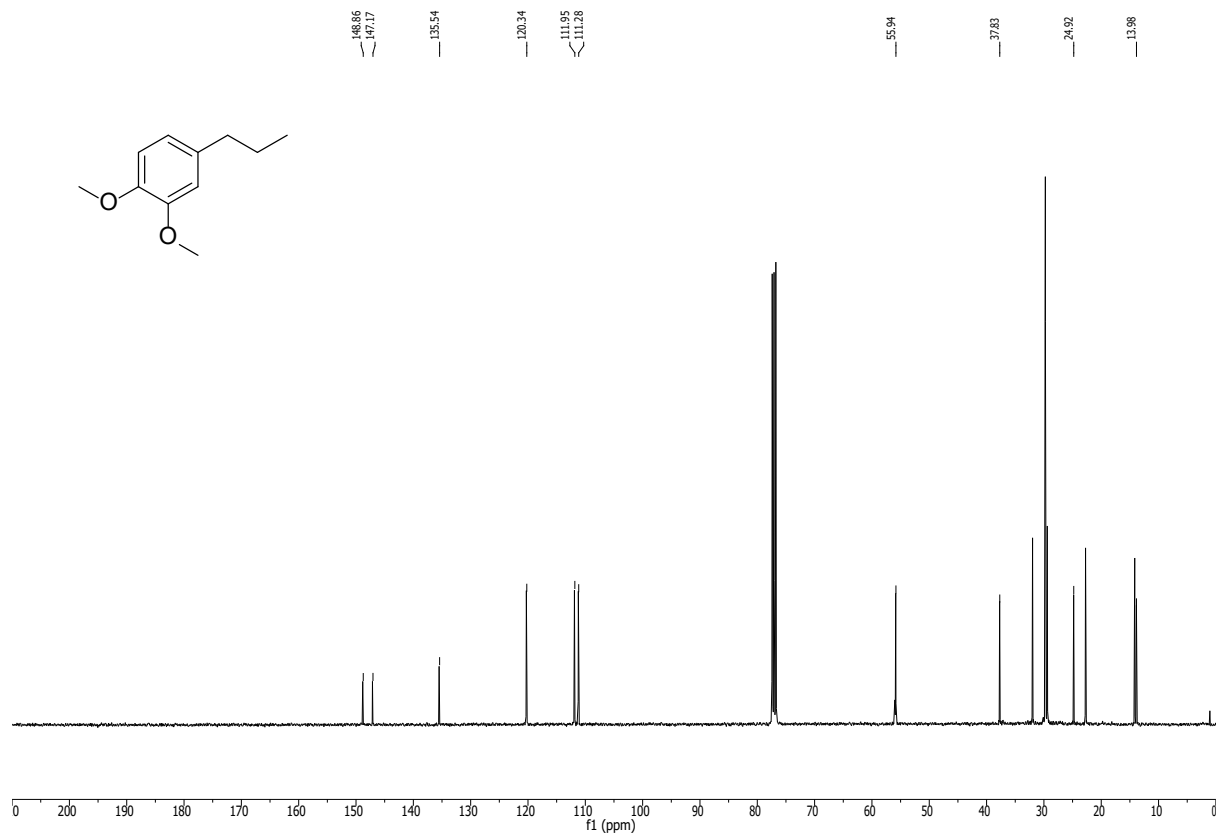
$C_{11}H_{16}O_2$  (180.25 g/mol)

**R<sub>f</sub>**: 0.76 (98:2 Hex:EtOAc)

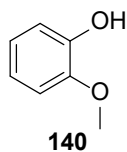
**<sup>1</sup>H-NMR**: (400 MHz, CDCl<sub>3</sub>):  $\delta$ /ppm = 6.79 (d, J = 8.7 Hz, 1H), 6.74 – 6.70 (m, 2H), 3.87 (s, 3H), 3.86 (s, 3H), 2.56 – 2.50 (m, 2H), 1.68 – 1.57 (m, 2H), 0.94 (t, J = 7.3 Hz, 3H) – 4:3 mixture product:pentadecane

**<sup>13</sup>C-NMR**: (101 MHz, CDCl<sub>3</sub>):  $\delta$ /ppm = 148.9, 147.2, 135.5, 120.3, 111.9, 111.3, 55.9, 37.8, 24.9, 13.9.

**GC-MS**: (EI): m/z = 180.1 (32, [M<sup>+</sup>]), 151.1 (100, [M<sup>+</sup>]-[C<sub>2</sub>H<sub>5</sub><sup>•</sup>]), 91 (19, [M<sup>+</sup>]-[CH<sub>3</sub> O<sup>•</sup>]-[C<sub>2</sub>H<sub>5</sub><sup>•</sup>]), 77.0 (21, [C<sub>6</sub>H<sub>5</sub><sup>•</sup>])

$^1\text{H-NMR}$ : (400 MHz,  $\text{CDCl}_3$ ) of **23** $^{13}\text{C-NMR}$ : (100 MHz,  $\text{CDCl}_3$ ) of **23**

**guaiacol (140)**



According to lower scale **GP4** (0.75 equiv.), guaiacol (**140**) was synthesized from adlerol (**138**) (250 mg, 0.75 mmol, 1.00 equiv.) over 16 h. The product was afforded as a colorless liquid (32 mg, 0.26 mmol, 34%, 41% determined by GC-FID). Analytical data was in accordance with the literature.<sup>17</sup> C<sub>7</sub>H<sub>8</sub>O<sub>2</sub> (124.14 g/mol)

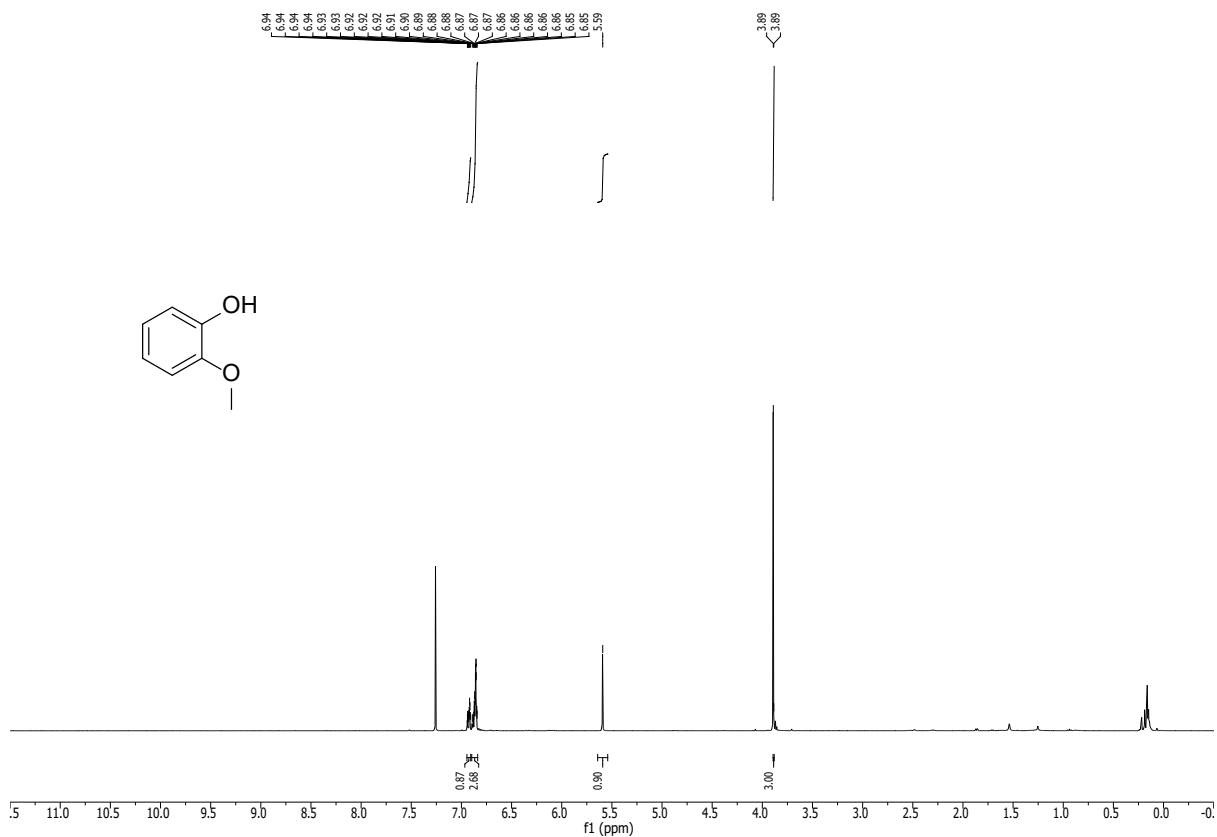
**R<sub>f</sub>**: 0.51 (98:2 Hex:EtOAc)

**<sup>1</sup>H-NMR**: (400 MHz, CDCl<sub>3</sub>): δ/ppm = 6.95 – 6.91 (m, 1H), 6.90 – 6.83 (m, 3H), 5.59 (s, 1H), 3.89 (s, 3H)

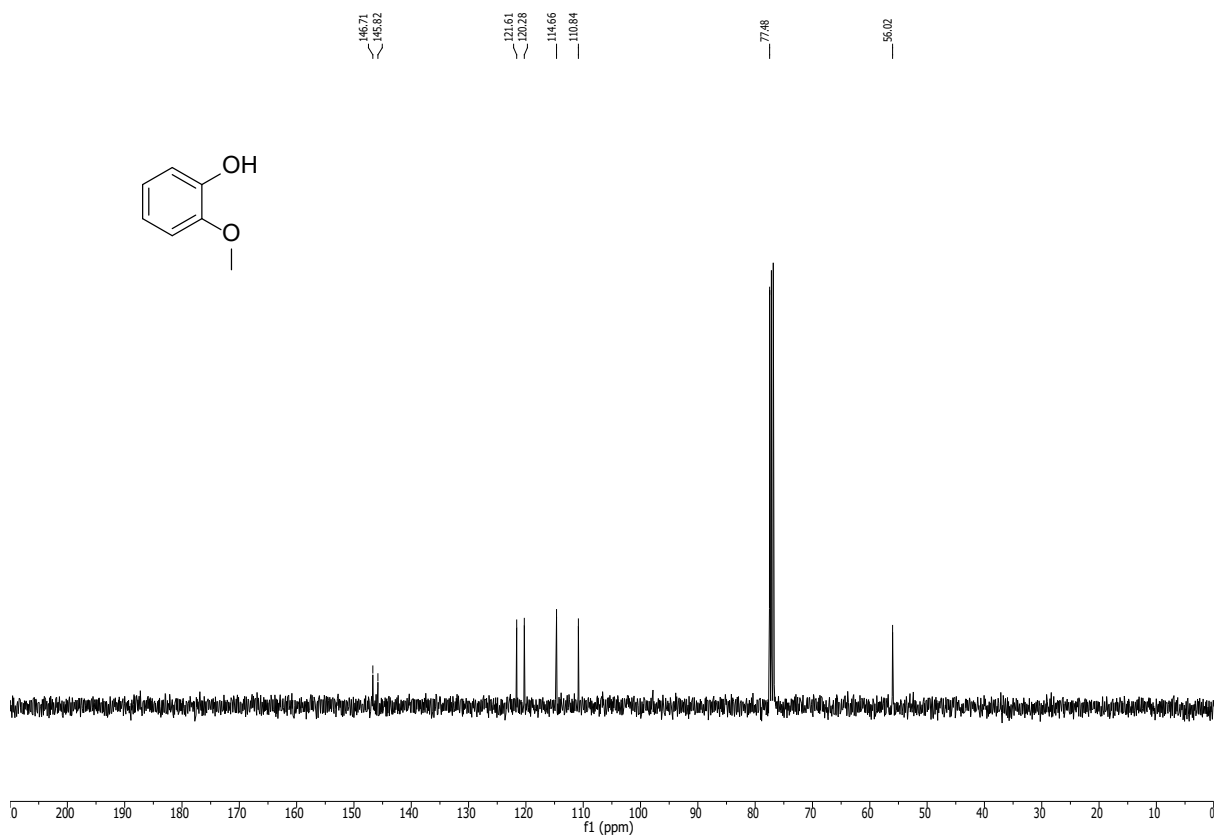
**<sup>13</sup>C-NMR**: (101 MHz, CDCl<sub>3</sub>): δ/ppm = 146.7, 145.8, 121.6, 120.3, 114.7, 110.8, 56.0.

**GC-MS**: (EI): m/z = 124.1 (29, [M<sup>+</sup>]), 109.1 (40, [M<sup>+</sup>]-[CH<sub>3</sub>•]), 81.1 (100, [M<sup>+</sup>]-)

$^1\text{H-NMR}$ : (400 MHz,  $\text{CDCl}_3$ ) of **140**

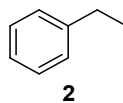


$^{13}\text{C-NMR}$ : (100 MHz,  $\text{CDCl}_3$ ) of **140**



## 8.6. Analytical Data for Non-isolated Deoxygenation Products

### ethylbenzene (2)

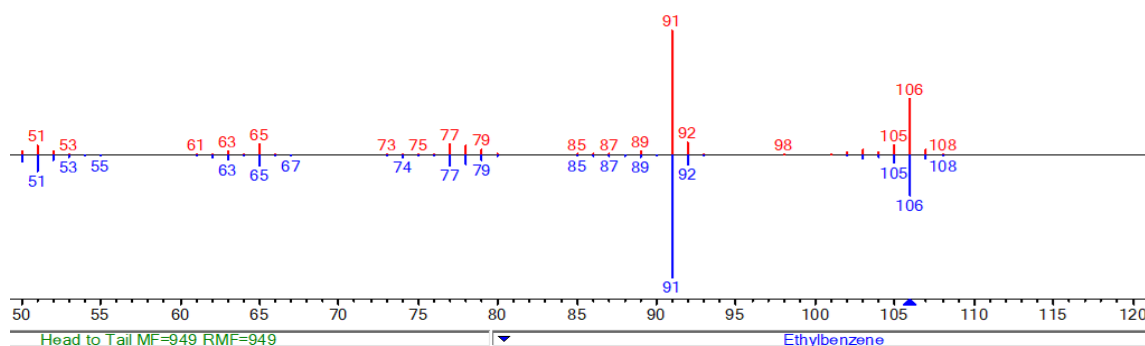


According to **GP4**, ethylbenzene (**2**) was synthesized from 1-phenylethanol (**4**) (0.120 mL, 122 mg, 1.00 mmol, 1.00 equiv.) and from styrene (0.115 mL, 104.1 mg, 1.00 mmol, 1.00 equiv.) over 16 h. The product was afforded in 78% (from 1-phenylethanol) and 72% (from styrene) yield determined by GC-FID.

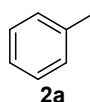
$C_8H_{10}$  (106.17 g/mol)

**GC-FID:**  $R_t = 3.582$  (**M<sub>FID1</sub>**)

**GC-MS:** (EI):  $m/z = 106.1$  (46,  $[M^+]$ ), 91.1 (100,  $[M^+]-[CH_3^+]$ ), 77.0 (10,  $[M^+]-[C_2H_5^+]$ );  $R_t = 6.985$  (**M<sub>MS2</sub>**)



### toluene (2a)

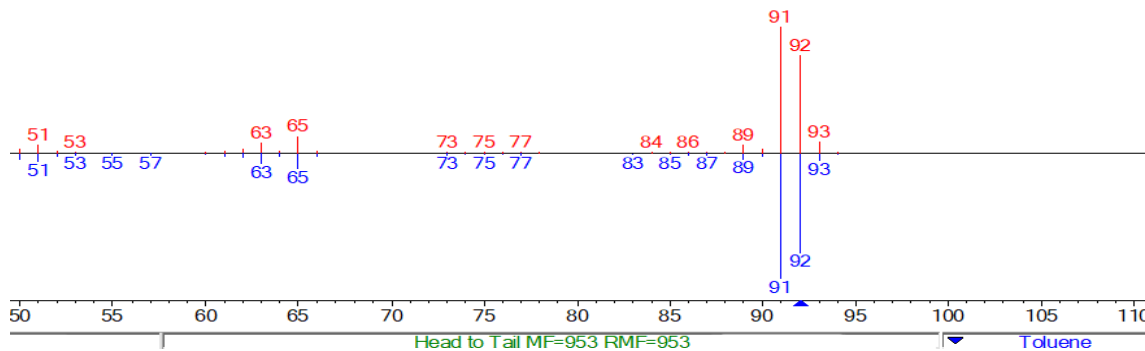


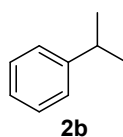
According to **GP4**, toluene (**2a**) was synthesized from benzyl alcohol (**4a**) (0.104 mL, 108 mg, 1.00 mmol, 1.00 equiv.) over 16 h. The product was afforded in 97% yield determined by GC-FID.

$C_7H_8$  (92.14 g/mol)

**GC-FID:**  $R_t = 3.052$  (**M<sub>FID1</sub>**);  $R_t = 4.254$  (**M<sub>FID2</sub>**)

**GC-MS:** (EI):  $m/z = 92.1$  (70,  $[M^+]$ ), 91.1 (100,  $[M^+]-[H^+]$ );  $R_t = 5.014$  (**M<sub>MS2</sub>**)



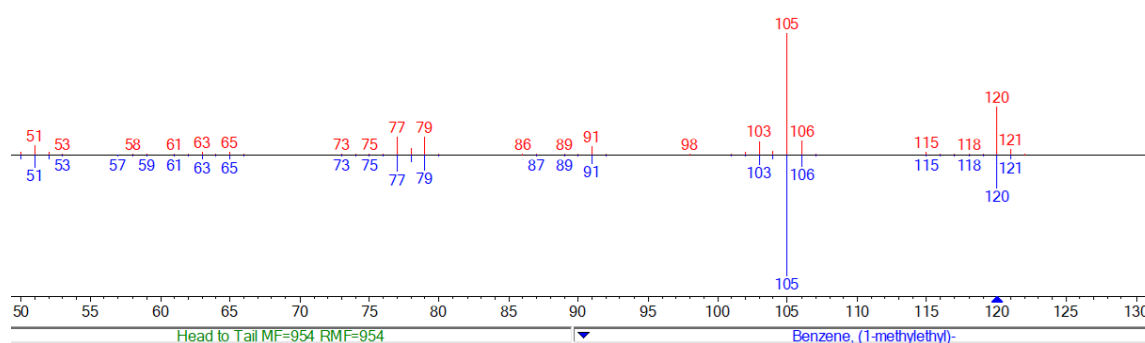
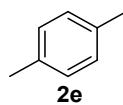
**cumene (2b)**

According to **GP4**, cumene (**2b**) was synthesized from 2-phenyl-2-propanol (**4b**) (0.140 mL, 136 mg, 1.00 mmol, 1.00 equiv.) over 16 h. The product was afforded in 19% yield determined by GC-FID.

$C_9H_{12}$  (120.09 g/mol)

**GC-FID:**  $R_t = 3.976$  (**M<sub>FID1</sub>**)

**GC-MS:** (EI):  $m/z = 120.1$  (39,  $[M^{+}]$ ), 105.1 (100,  $[M^{+}] - [C_2H_5^{\bullet}]$ ), 77.0 (15,  $[M^{+}] - [C_3H_7^{\bullet}]$ );  $R_t = 8.248$  (**M<sub>MS2</sub>**)

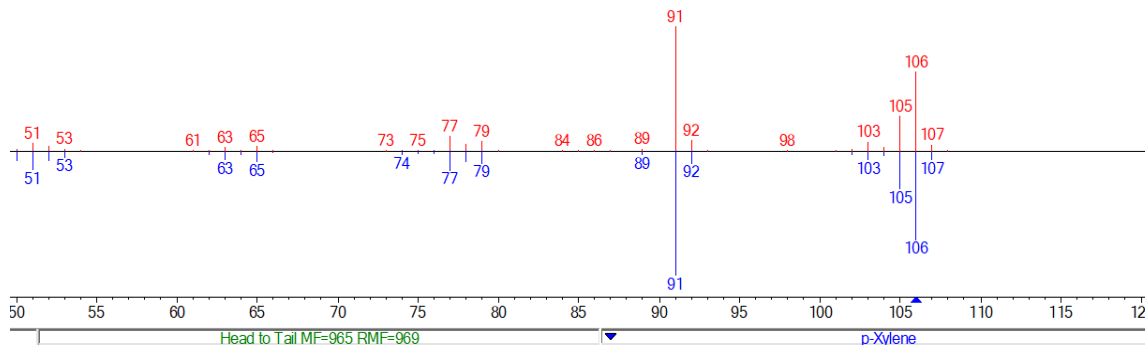
***p*-xylene (2e)**

According to **GP4**, *p*-xylene (**2e**) was synthesized from 4-methylbenzyl alcohol (**4e**) (0.120 mL, 122 mg, 1.00 mmol, 1.00 equiv.) over 16 h. The product was afforded in 95% yield determined by GC-FID.

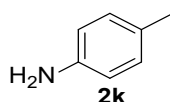
$C_8H_{10}$  (106.17 g/mol)

**GC-FID:**  $R_t = 3.617$  (**M<sub>FID1</sub>**)

**GC-MS:** (EI):  $m/z = 106.0$  (59,  $[M^{+}]$ ), 91.0 (100,  $[M^{+}] - [CH_3^{\bullet}]$ );  $R_t = 7.106$  (**M<sub>MS2</sub>**)



#### 4-methylaniline (2k)

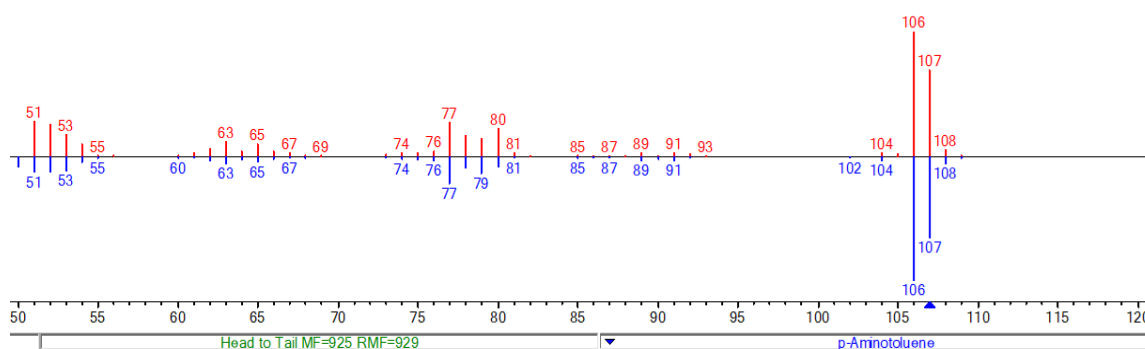


According to **GP4**, 4-methylaniline (**2k**) was synthesized from 4-aminobenzyl alcohol (**4k**) (123 mg, 1.00 mmol, 1.00 equiv.) over 16 h. The product was afforded in 60% yield determined by GC-FID.

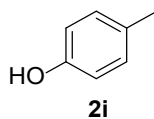
$C_7H_9N$  (107.16 g/mol)

**GC-FID:**  $R_t = 5.067$  (**M<sub>FID1</sub>**)

**GC-MS:** (EI):  $m/z = 107.0$  (70,  $[M^{++}]$ ), 106.0 [100,  $M^+$ ], 77.0 [26,  $M^{++}$ ];  $R_t = 3.362$  (**M<sub>MS1</sub>**)



#### *p*-cresol (2l)

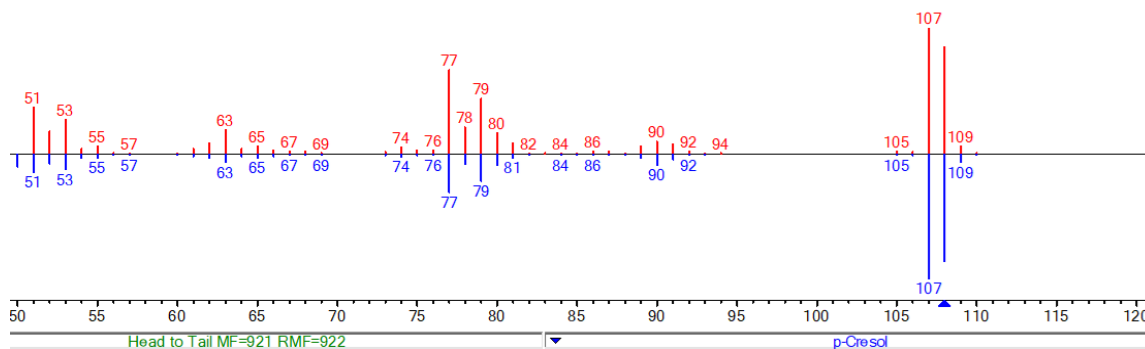


According to **GP4**, *p*-cresol (**2l**) was synthesized from 4-hydroxybenzyl alcohol (**4l**) (124 mg, 1.00 mmol, 1.00 equiv.) over 16 h. The product was afforded in 78% yield determined by GC-FID after workup with 1M HCl.

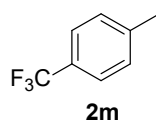
$C_7H_8O$  (108.14 g/mol)

**GC-FID:**  $R_t = 5.030$  (**M<sub>FID1</sub>**)

**GC-MS:** (EI):  $m/z = 108$  (86,  $[M^{++}]$ ), 107 (100,  $[M^+]-[H^+]$ ), 90 (11,  $[M^{++}]-[OH^+]$ ), 77.0 (66,  $[M^+]-[CH_3^+]$ );  $R_t = 3.316$  (**M<sub>MS1</sub>**)





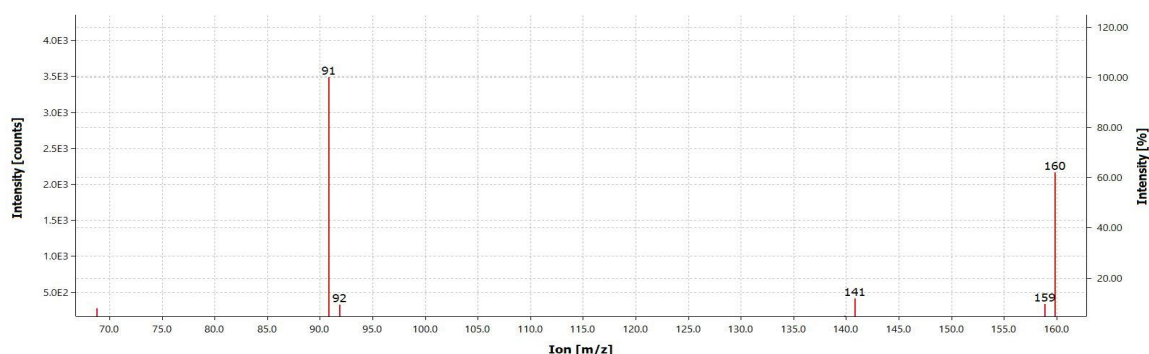
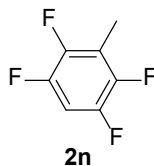
**1-methyl-4-(trifluoromethyl)benzene (2m)**

According to **GP4**, 1-methyl-4-(trifluoromethyl)benzene (**2m**) was synthesized from 4-(trifluoromethyl)benzenemethanol (**4m**) (0.137 mL, 176 mg, 1.00 mmol, 1.00 equiv.) over 16 h. The product was afforded in 86% yield determined by GC-FID.

$C_8H_7F_3$  (160.14 g/mol)

**GC-FID:**  $R_t = 3.279$  (**M<sub>FID1</sub>**)

**GC-MS:** (ED):  $m/z = 159.9$  (62,  $[M^{+}]$ ), 140.9 (12,  $[M^{+}]-[F^{\cdot}]$ ), 90.9 (100,  $[M^{+}]-[CF_3^{\cdot}]$ );  $R_t = 3.757$  (**M<sub>MS2</sub>**)

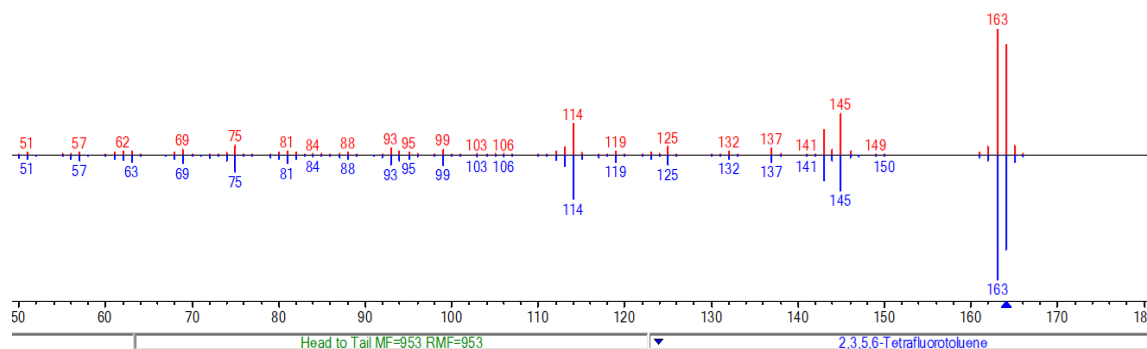
**1,2,4,5-tetrafluoro-3-methylbenzene (2n)**

According to **GP4**, 1,2,4,5-tetrafluoro-3-methylbenzene (**2n**) was synthesized from 2,3,5,6-tetrafluorobenzyl alcohol (**4n**) (0.120 mL, 180 mg, 1.00 mmol, 1.00 equiv.) over 16 h. The product was afforded in 95% yield determined by GC-FID.

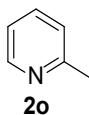
$C_8H_7F_4$  (164.02 g/mol)

**GC-FID:**  $R_t = 3.074$  (**M<sub>FID1</sub>**)

**GC-MS:** (ED):  $m/z = 164.0$  (88,  $[M^{+}]$ ), 163.0 (100,  $[M^{+}]-[H^{\cdot}]$ ), 145.0 (37,  $[M^{+}]-[F^{\cdot}]$ );  $R_t = 5.228$  (**M<sub>MS2</sub>**)



### 2-methylpyridine (2o)

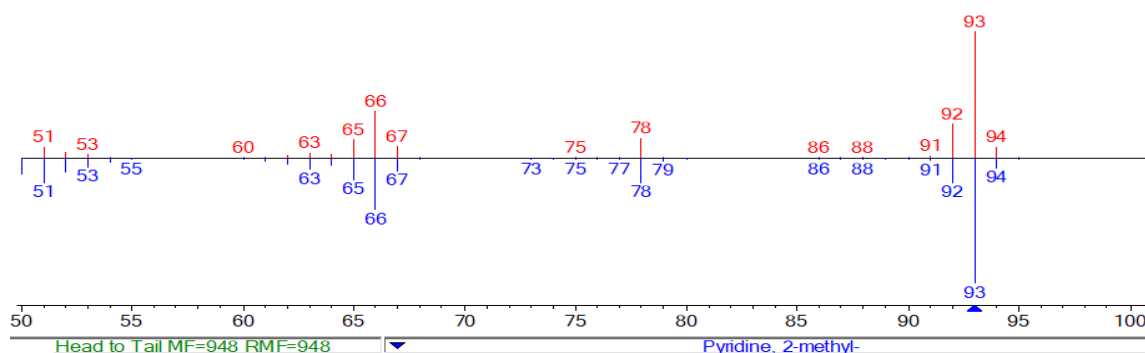


According to **GP4**, 2-methylpyridine (**2o**) was synthesized from pyridine-2-ylmethanol (**4o**) (0.096 mL, 109 mg, 1.00 mmol, 1.00 equiv.) over 16 h. The product was afforded in 37% yield determined by GC-FID.

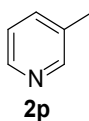
$C_6H_7N$  (93.13 g/mol)

**GC-FID:**  $R_t = 3.335$  (**M<sub>FID1</sub>**)

**GC-MS:** (EI):  $m/z = 93.0$  (100,  $[M^{++}]$ ), 78.0 (12,  $[M^+]-[CH_3^+]$ );  $R_t = 9.562$  (**M<sub>MS2</sub>**)



### 3-methylpyridine (2p)

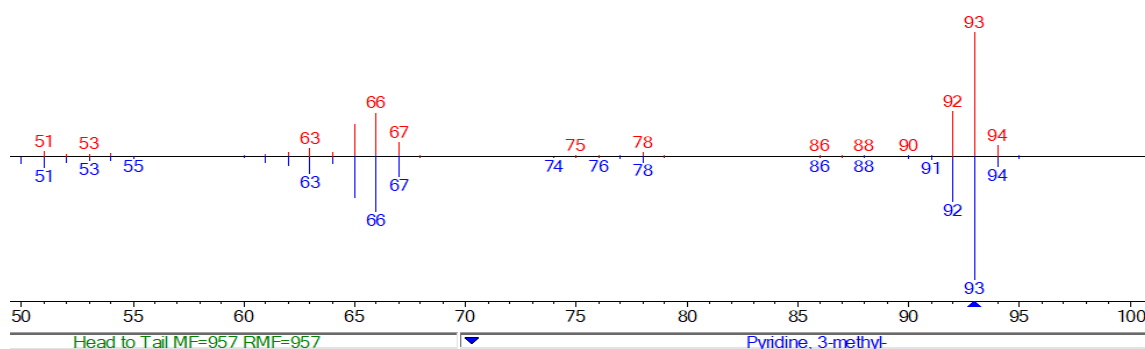


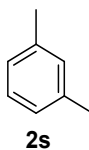
According to **GP4**, 3-methylpyridine (**2p**) was synthesized from pyridine-3-ylmethanol (**4p**) (0.097 mL, 109 mg, 1.00 mmol, 1.00 equiv.) over 16 h. The product was afforded in 37% yield determined by GC-FID.

$C_6H_7N$  (93.13 g/mol)

**GC-FID:**  $R_t = 3.551$  (**M<sub>FID1</sub>**)

**GC-MS:** (EI):  $m/z = 93.0$  (100,  $[M^{++}]$ ), 78.0 (3,  $[M^+]-[CH_3^+]$ );  $R_t = 9.847$  (**M<sub>MS2</sub>**)



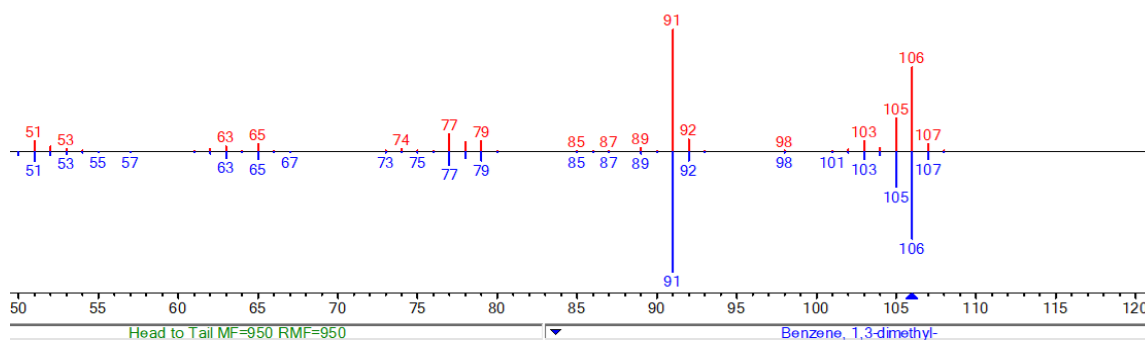
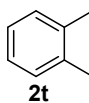
**m-xylene (2s)**

According to **GP4**, m-xylene (**2s**) was synthesized from 3-methylbenzyl alcohol (**4s**) (0.120 mL, 122 mg, 1.00 mmol, 1.00 equiv.) over 16 h. The product was afforded in 85% yield determined by GC-FID

$C_8H_{10}$  (106.17 g/mol)

**GC-FID:**  $R_t = 3,665$  (**M<sub>FID1</sub>**)

**GC-MS:** (EI):  $m/z = 106.0$  (56,  $[M^{++}]$ ), 91.0 (100,  $[M^+]-[CH_3^+]$ );  $R_t = 7.158$  (**M<sub>MS2</sub>**)

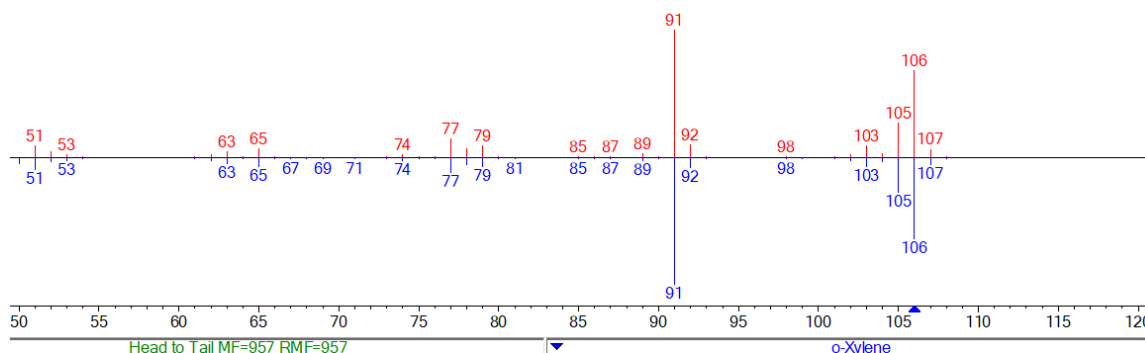
**o-xylene (2t)**

According to **GP4**, o-xylene (**2t**) was synthesized from 2-methylbenzyl alcohol (**4t**) (0.120 mL, 122 mg, 1.00 mmol, 1.00 equiv.) over 16 h. The product was afforded in 90% yield determined by GC-FID.

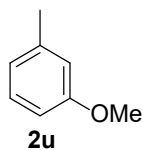
$C_8H_{10}$  (106.17 g/mol)

**GC-FID:**  $R_t = 3,790$  (**M<sub>FID1</sub>**)

**GC-MS:** (EI):  $m/z = 106.1$  (68,  $[M^{++}]$ ), 91.1 (100,  $[M^+]-[CH_3^+]$ );  $R_t = 7.635$  (**M<sub>MS2</sub>**)



### 3-methylanisole (2u)

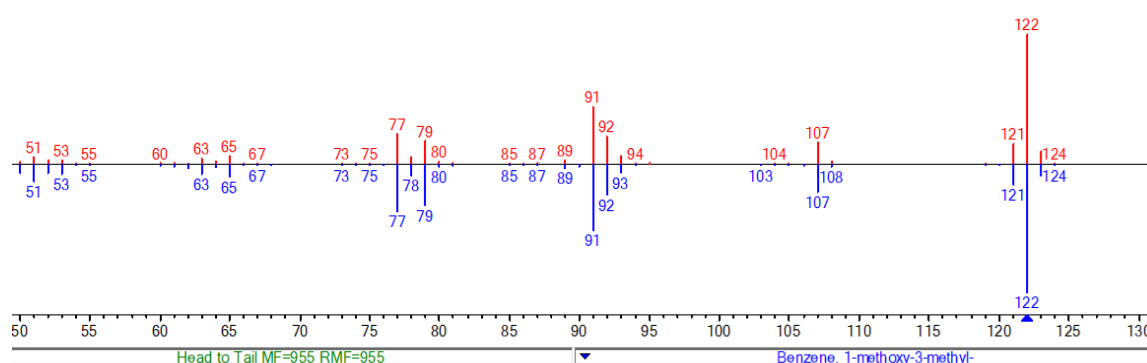


According to **GP4**, 3-methylanisole (**2u**) was synthesized from 3-methoxybenzyl alcohol (**4u**) (0.110 mL, 138 mg, 1 mmol, 1 equiv.) over 16 h. The product was afforded in 85% yield determined by GC-FID.

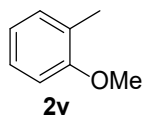
$C_8H_{10}O$  (122.07 g/mol)

**GC-FID:**  $R_t = 4.667$  (**M<sub>FID1</sub>**)

**GC-MS:** (EI):  $m/z = 122.1$  (100, [ $M^{+}$ ]), 107.0 (45, [ $M^{+}$ ]-[ $CH_3^{\cdot}$ ]), 91.0 (31, [ $M^{+}$ ]-[ $OCH_3^{\cdot}$ ]);  $R_t = 9.961$  (**M<sub>MS2</sub>**)



### 2-methylanisole (2v)

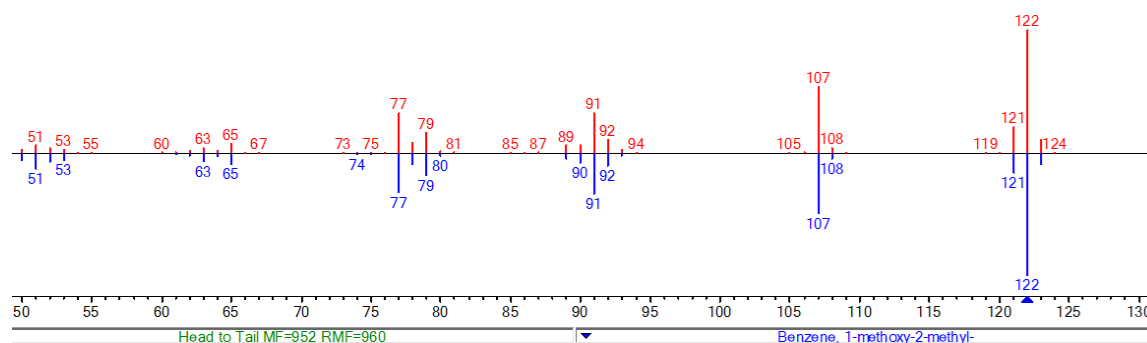


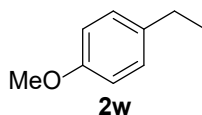
According to **GP4**, 2-methylanisole (**2v**) was synthesized from 2-methoxybenzyl alcohol (**4v**) (0.110 mL, 138 mg, 1.00 mmol, 1.00 equiv.) over 16 h. The product was afforded in 90% yield determined by GC-FID.

$C_8H_{10}O$  (122.07 g/mol)

**GC-FID:**  $R_t = 4.591$  (**M<sub>FID1</sub>**)

**GC-MS:** (EI):  $m/z = 122.1$  (100, [ $M^{+}$ ]), 107.0 (53, [ $M^{+}$ ]-[ $CH_3^{\cdot}$ ]), 91.0 (33, [ $M^{+}$ ]-[ $OCH_3^{\cdot}$ ]);  $R_t = 9.884$  (**M<sub>MS2</sub>**)



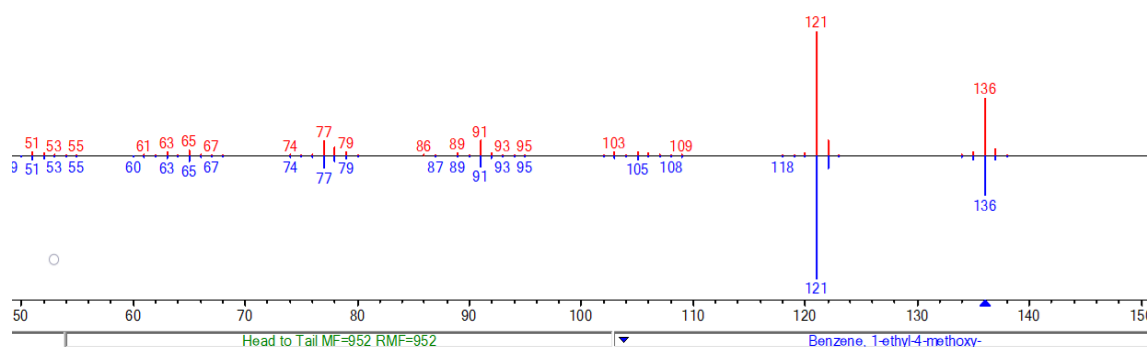
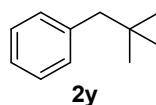
**1-ethyl-4-methoxybenzene (2w)**

According to **GP4**, 1-ethyl-4-methoxybenzene (**2w**) was synthesized from 1-(4-methoxyphenyl)ethanol (**4w**) (0.140 mL, 152 mg, 1.00 mmol, 1.00 equiv.) over 16 h. The product was afforded in 67% yield determined by GC-FID.

$C_9H_{12}O$  (122.07 g/mol)

**GC-FID:**  $R_t = 5.355$  (**M<sub>FID1</sub>**)

**GC-MS:** (EI):  $m/z = 136.1$  (42,  $[M^+]$ ), 121.1 (100,  $[M^+]-[CH_3^+]$ ), 77.0 (11,  $[M^+]-[OCH_3^+]$ );  $R_t = 11.616$  (**M<sub>MS2</sub>**)

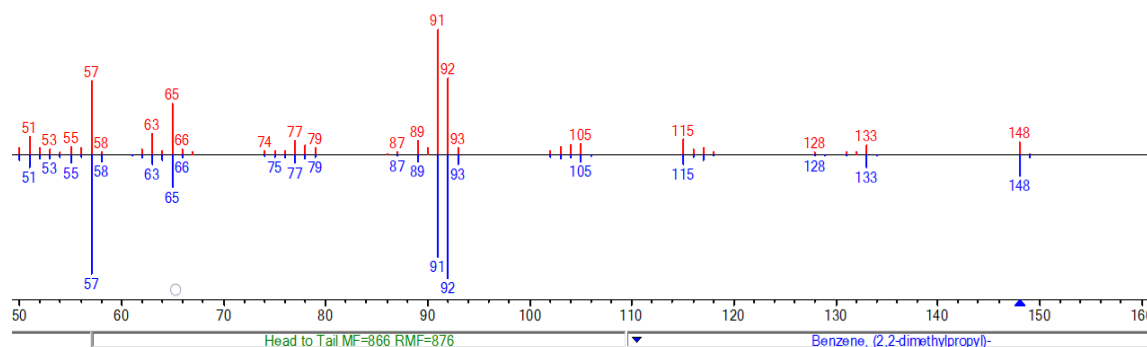
**2,2-dimethylpropylbenzene (2y)**

According to **GP4**, 2,2-dimethylpropylbenzene (**2y**) was synthesized from 2,2-dimethyl-1-phenylpropan-1-ol (**4y**) (164 mg, 1.00 mmol, 1.00 equiv.) over 16 h. The product was afforded in 23% yield determined by GC-FID.

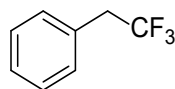
$C_{11}H_{16}$  (148.25 g/mol)

**GC-FID:**  $R_t = 4.963$  (**M<sub>FID1</sub>**)

**GC-MS:** (EI):  $m/z = 148.0$  (10,  $[M^+]$ ), 91.0 (100,  $[M^+]-[C(CH_3)_3^+]$ ), 77.0 (7,  $[M^+]-[C(CH_3)_3^+]-[CH_2^+]$ );  $R_t = 3.293$  (**M<sub>MS1</sub>**)



**2,2,2-trifluoroethylbenzene (2z)**



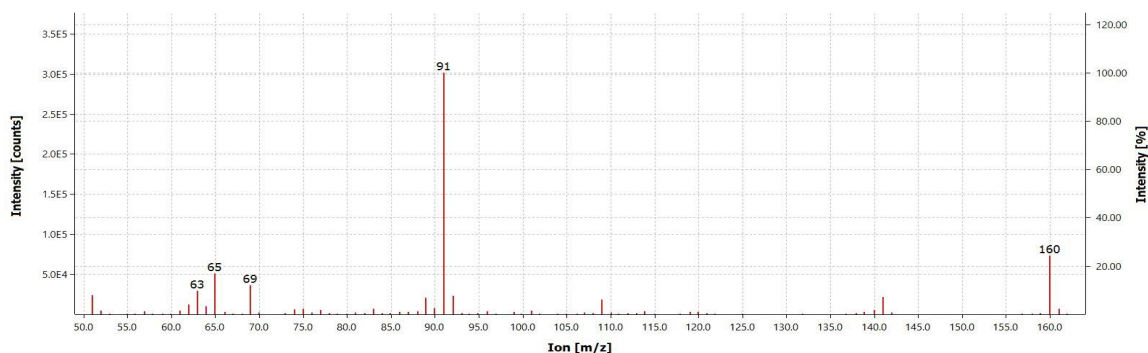
**2z**

According to **GP4**, 2,2,2-trifluoroethylbenzene (**2z**) was synthesized from 2,2,2-trifluoro-1-phenylethanol (**4z**) (176 mg, 1.00 mmol, 1.00 equiv.) over 16 h. The product was afforded in 31% yield determined by GC-FID.

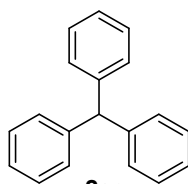
$C_8H_7F_3$  (160.14 g/mol)

**GC-FID:**  $R_t = 3.561$  (**M<sub>FID1</sub>**)

**GC-MS:** (EI):  $m/z = 160.0$  (23,  $[M^{+}]$ ), 141.0 (7,  $[M^{+}]-[F^{\bullet}]$ ), 91.0 (100,  $[M^{+}]-[CF_3^{\bullet}]$ );  $R_t = 4.237$  (**M<sub>MS3</sub>**)



**triphenylmethane (2ac)**



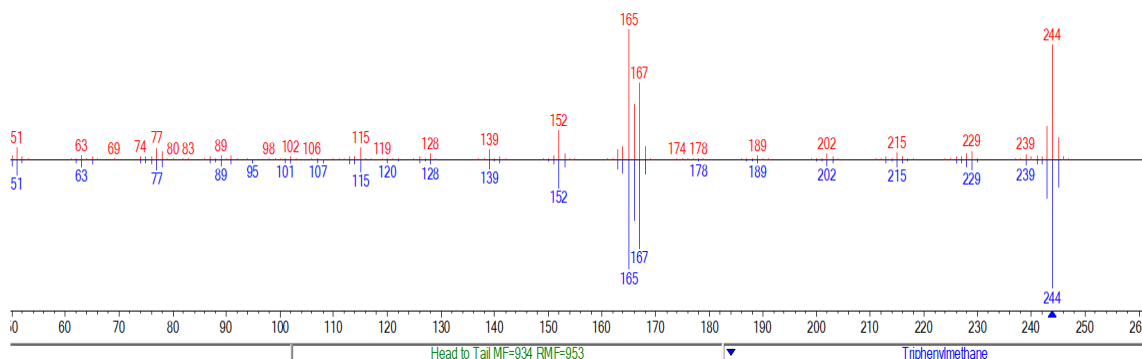
**2ac**

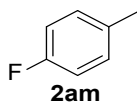
According to **GP4**, triphenylmethane (**2ac**) was synthesized from triphenylmethanol (**4ac**) (260 mg, 1.00 mmol, 1.00 equiv.) over 16 h. The product was afforded in 32% yield determined by GC-FID.

$C_{19}H_{16}$  (244.13 g/mol)

**GC-FID:**  $R_t = 10.681$  (**M<sub>FID1</sub>**)

**GC-MS:** (EI):  $m/z = 244.1$  (65,  $[M^{+}]$ ), 167.0 (58,  $[M^{+}]-[C_6H_5^{\bullet}]$ ), 165.0 (100,  $[M^{+}]-[C_6H_5^{\bullet}]-[H^{\bullet}]$ ), 77.0 (10,  $[M^{+}]-2[C_6H_5^{\bullet}]$ );  $R_t = 9.135$  (**M<sub>MS1</sub>**)



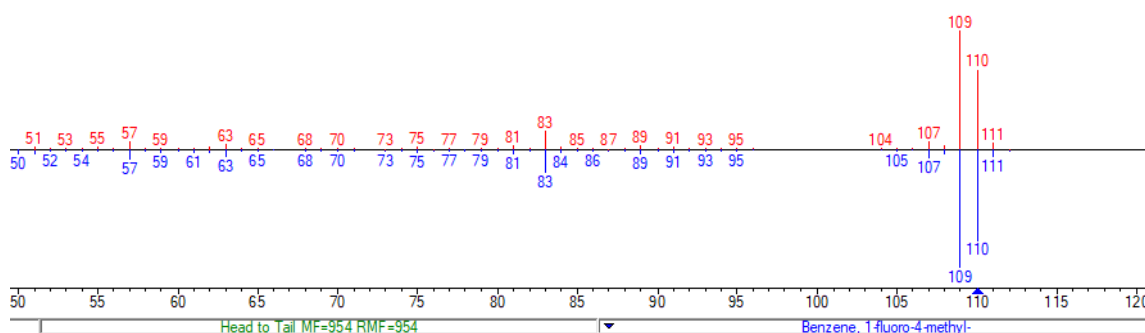
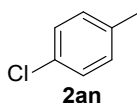
**4-fluorotoluene (2am)**

According to **GP4**, 4-fluorotoluene (**2am**) was synthesized from 4-fluorobenzyl alcohol (**4am**) (0.107 mL, 126 mg, 1.00 mmol, 1.00 equiv.) over 16 h. The product was afforded in 95% yield determined by GC-FID.

$C_7H_7F$  (110.13 g/mol)

**GC-FID:**  $R_t = 3.122$  (**M<sub>FID1</sub>**)

**GC-MS:** (EI):  $m/z = 110.0$  (63,  $[M^{++}]$ ), 109.1 [100,  $[M^+]-[H^+]$ ];  $R_t = 5.092$  (**M<sub>MS2</sub>**)

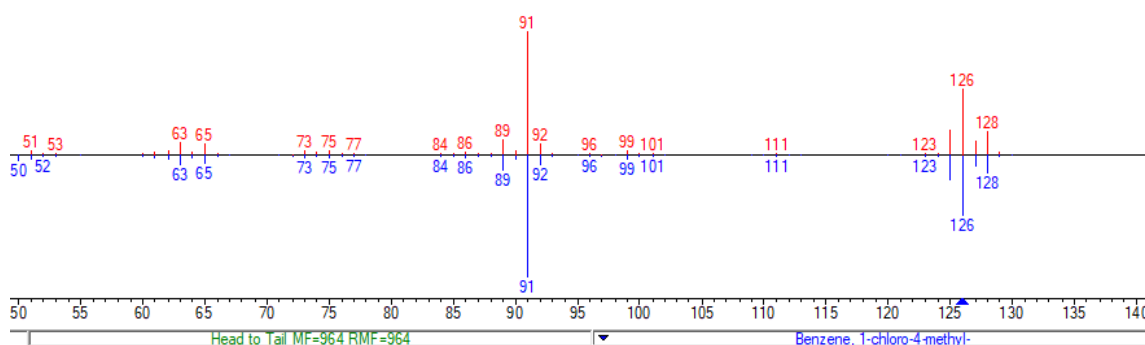
**4-chlorotoluene (2an)**

According to **GP4**, 4-chlorotoluene (**2an**) was synthesized from 4-chlorobenzyl alcohol (**4an**) (143 mg, 1.00 mmol, 1.00 equiv.) over 16 h. The product was afforded in 56% yield determined by GC-FID.

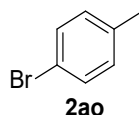
$C_7H_7Cl$  (126.58 g/mol)

**GC-FID:**  $R_t = 4.232$  (**M<sub>FID1</sub>**)

**GC-MS:** (EI):  $m/z = 128.0$  (17,  $[M^{++}]$ ), 126.0 [50,  $M^+$ ], 91.1 (100,  $[M^+]-[Cl^+]$ );  $R_t = 8.835$  (**M<sub>MS2</sub>**)



### 4-bromotoluene (2ao)

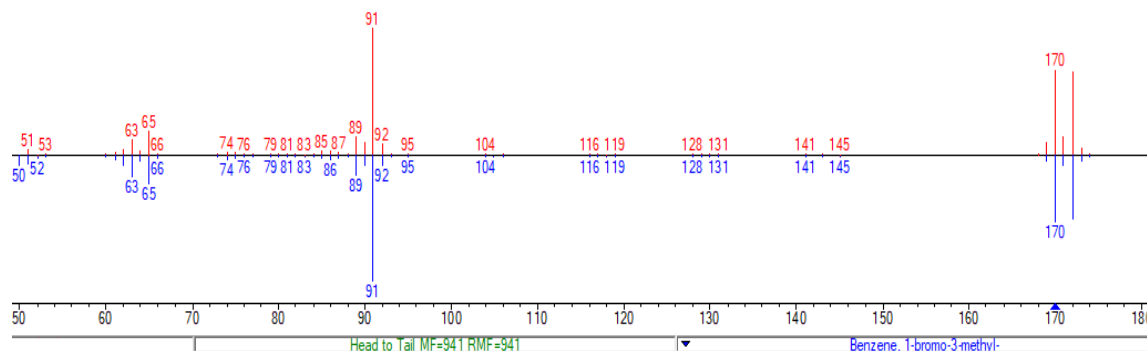


According to **GP4**, 4-bromotoluene (**2ao**) was synthesized from 4-bromobenzyl alcohol (**4ao**) (176 mg, 1.00 mmol, 1.00 equiv.) over 16 h. The product was afforded in 56% yield determined by GC-FID.

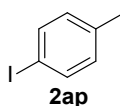
$C_7H_7Br$  (171.04 g/mol)

**GC-FID:**  $R_t = 4.873$  (**M<sub>FID1</sub>**)

**GC-MS:** (EI):  $m/z = 172.0$  (64,  $[M^{+}]$ ), 170.0 (63,  $[M^{+}]$ ), 91.1 (100,  $[M^{+}]-[Br^{\cdot}]$ );  $R_t = 10.458$  (**M<sub>MS2</sub>**)



### 4-iodotoluene (2ap)

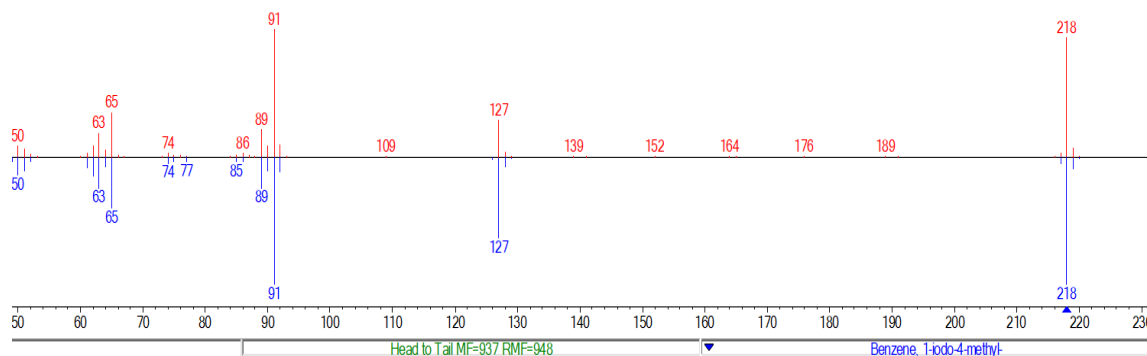


According to **GP4**, 4-iodotoluene (**2ap**) was synthesized from 4-iodobenzyl alcohol (**4ap**) (234 mg, 1.00 mmol, 1.00 equiv.) over 16 h. The product was afforded in 41% yield determined by GC-FID.

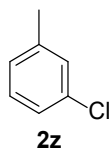
$C_7H_7I$  (218.04 g/mol)

**GC-FID:**  $R_t = 9.763$  (**M<sub>FID2</sub>**)

**GC-MS:** (EI):  $m/z = 217.9$  (93,  $[M^{+}]$ ), 126.8 [27,  $[I^{\cdot}]-[M^{+}]$ ], 91.0 (100,  $[M^{+}]-[I^{\cdot}]$ );  $R_t = 3.934$  (**M<sub>MS1</sub>**)





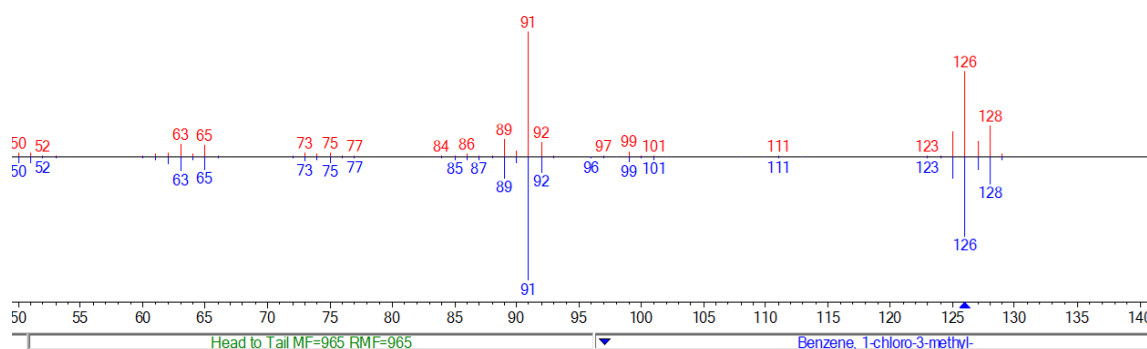
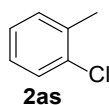
**1-chloro-3-methylbenzene (2ar)**

According to **GP4**, 1-chloro-3-methylbenzene (**2ar**) was synthesized from 3-chlorobenzyl alcohol (**4ar**) (1423 mg, 1.00 mmol, 1.00 equiv.) over 16 h. The product was afforded in 85% yield determined by GC-FID.

$C_7H_7Cl$  (126.58 g/mol)

**GC-FID:**  $R_t = 4.218$  (**M<sub>FID1</sub>**)

**GC-MS:** (EI):  $m/z = 128.0$  (19,  $[M^{++}]$ ), 126.0 [56,  $M^{+}$ ], 91.0 ( $[M^{++}]-[Cl^+]$ );  $R_t = 8.704$  (**M<sub>MS2</sub>**)

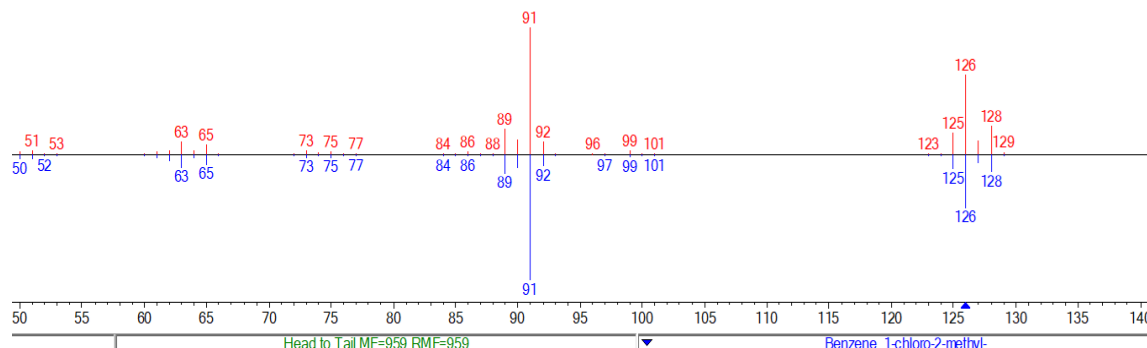
**1-chloro-2-methylbenzene (2as)**

According to **GP4**, 1-chloro-2-methylbenzene (**2as**) was synthesized from 2-chlorobenzyl alcohol (**4as**) (143 mg, 1.00 mmol, 1.00 equiv.) over 16 h. The product was afforded in 85% yield determined by GC-FID.

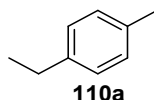
$C_7H_7Cl$  (126.58 g/mol)

**GC-FID:**  $R_t = 4.191$  (**M<sub>FID1</sub>**)

**GC-MS:** (EI):  $m/z = 128.0$  (16,  $[M^{++}]$ ), 126.0 (49,  $[M^{+}]$ ), 91.0 (100,  $[M^{++}]-[Cl^+]$ );  $R_t = 8.704$  (**M<sub>MS2</sub>**)



### 1-ethyl-4-methylbenzene (110a)

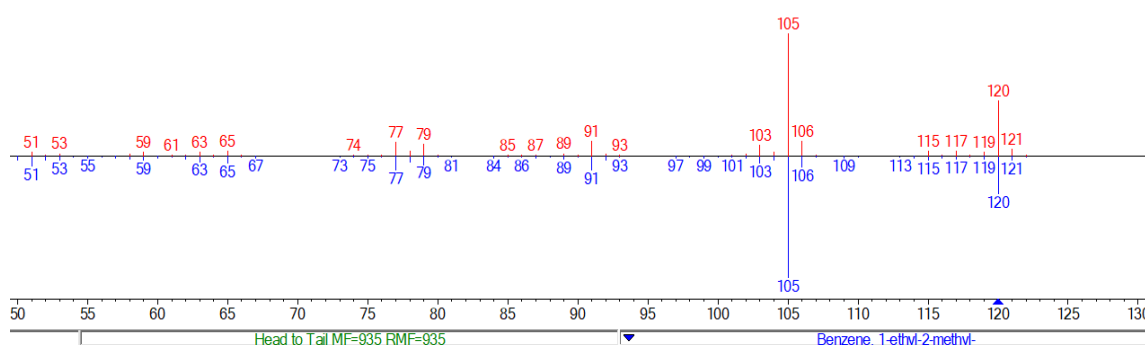


According to **GP4**, 1-ethyl-4-methylbenzene (**110a**) was synthesized from 4-vinylbenzyl alcohol (**109**) (0.130 mL, 134 mg, 1.00 mmol, 1.00 equiv.) and 4-ethynylbenzenemethanol (**111**) (0.122 mL, 132.2 mg, 1.00 mmol, 1.00 equiv.) over 16 h. The product was afforded in 45% (from 4-vinylbenzyl alcohol) and 15% (from 4-ethynylbenzenemethanol) yield determined by GC-FID.

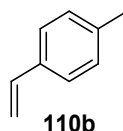
$C_9H_{12}$  (120.20 g/mol)

**GC-FID:**  $R_t = 4.220$  (**M<sub>FID1</sub>**)

**GC-MS:** (EI):  $m/z = 120.1$  (43,  $[M^{+}]$ ), 105.1 (100,  $[M^{+}]-[CH_3^{\cdot}]$ ), 91.0 (12,  $[M^{+}]-[C_2H_5^{\cdot}]$ ), 77.0 (9,  $[M^{+}]-[C_2H_5^{\cdot}]-[CH_3^{\cdot}]$ );  $R_t = 8.978$  (**M<sub>MS2</sub>**)



### 1-methyl-4-vinylbenzene

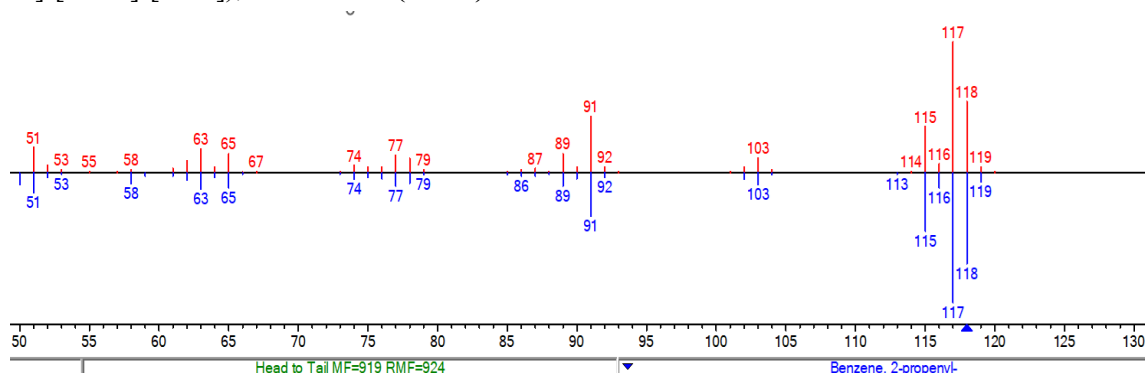


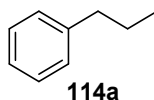
According to **GP4**, 1-methyl-4-vinylbenzene (**110b**) was synthesized from 4-vinylbenzyl alcohol (**109**) (0.130 mL, 134 mg, 1.00 mmol, 1.00 equiv.) and 4-ethynylbenzenemethanol (**111**) (0.122 mL, 132.2 mg, 1.00 mmol, 1.00 equiv.) over 16 h. The product was afforded in traces in both cases determined by GC-FID.

$C_9H_{10}$  (118.18 g/mol)

**GC-FID:**  $R_t = 4.645$  (**M<sub>FID1</sub>**)

**GC-MS:** (EI):  $m/z = 120.1$  (43,  $[M^{+}]$ ), 105.1 (100,  $[M^{+}]-[CH_3^{\cdot}]$ ), 91.0 (12,  $[M^{+}]-[C_2H_5^{\cdot}]$ ), 77.0 (9,  $[M^{+}]-[C_2H_5^{\cdot}]-[CH_3^{\cdot}]$ );  $R_t = 12.008$  (**M<sub>MS2</sub>**)



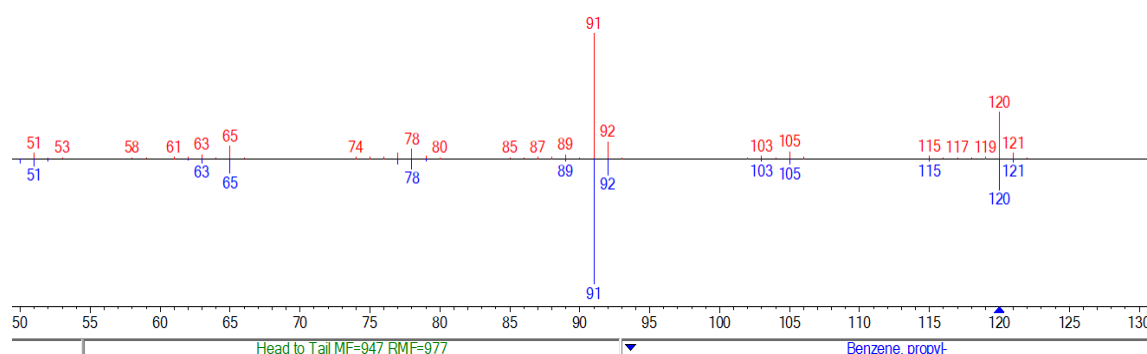
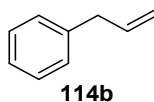
**Propylbenzene (114a)**

According to **GP2**, propylbenzene (**114a**) was synthesized from 1-phenyl-2-propen-1-ol (**113**) (0.131 mL, 134 mg, 1.00 mmol, 1.00 equiv.) and 1-phenyl-2-propyn-1-ol (**115**) (0.121 mL, 132.2 mg, 1.00 mmol, 1.00 equiv.) over 16 h. The product was afforded in 45% (from 1-phenyl-2-propen-1-ol) and 20% (from 1-phenyl-2-propyn-1-ol) yield determined by GC-FID.

$C_9H_{12}$  (120.20 g/mol)

**GC-FID:**  $R_t = 4.171$  (**M<sub>FID1</sub>**)

**GC-MS:** (EI):  $m/z = 120.1$  (37,  $[M^+]$ ), 105.1 (9,  $[M^+]-[C_2H_5^+]$ ), 91.0 (100,  $[M^+]-[C_2H_5^+]$ ), 78.0 (14,  $[M^+]-[C_3H_7^+]$ );  $R_t = 9.954$  (**M<sub>MS2</sub>**)

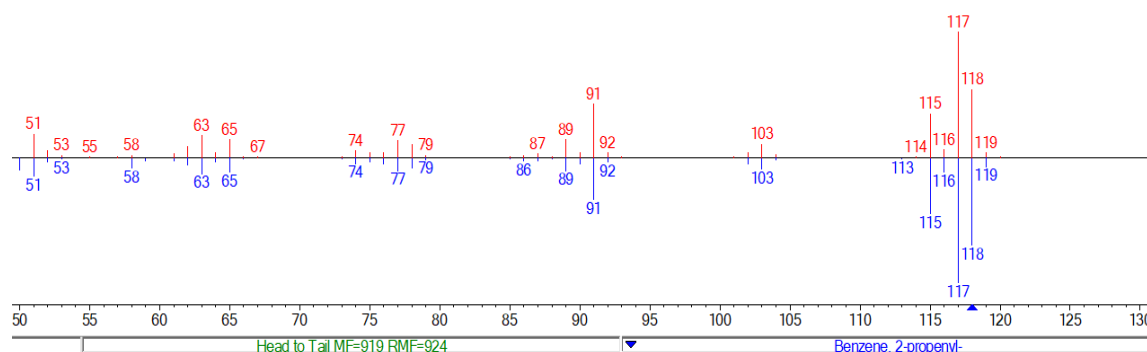
**Allylbenzene (114b)**

According to **GP4**, allylbenzene (**114b**) was synthesized from 1-phenyl-2-propen-1-ol (**113**) (0.131 mL, 134 mg, 1.00 mmol, 1.00 equiv.) and 1-phenyl-2-propyn-1-ol (**115**) (0.121 mL, 132.2 mg, 1.00 mmol, 1.00 equiv.) over 16 h. The product was afforded in 28% (from 1-phenyl-2-propen-1-ol) and 9% (from 1-phenyl-2-propyn-1-ol) yield determined by GC-FID.

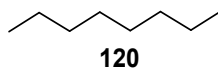
$C_9H_{10}$  (118.18 g/mol)

**GC-FID:**  $R_t = 4.657$  (**M<sub>FID1</sub>**)

**GC-MS:** (EI):  $m/z = 118.1$  (53,  $[M^+]$ ), 117.1 (100,  $[M^+]-[H^+]$ ), 105.1 (7,  $[M^+]-[CH^+]$ ), 91.0 (48,  $[M^+]-[C_2H_3^+]$ ), 77.0 (12,  $[M^+]-[C_3H_5^+]$ );  $R_t = 12.008$  (**M<sub>MS2</sub>**)



**n-octane (120)**

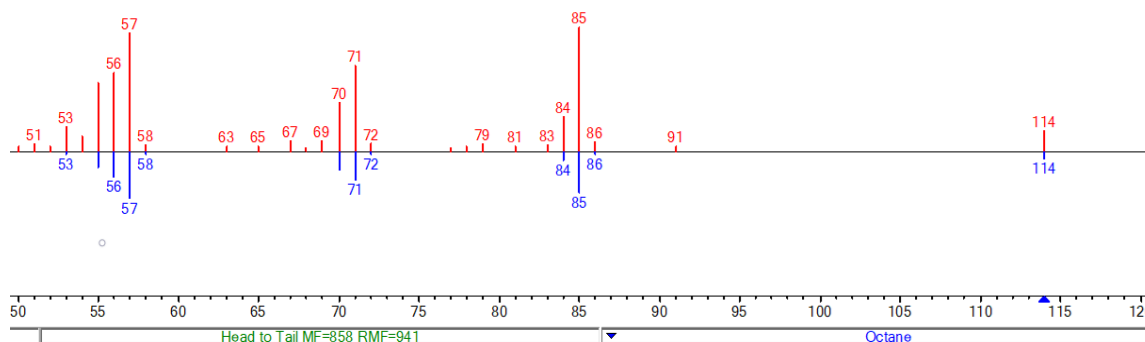


According to **GP4**, n-octane (**120**) was synthesized from 1-octene (**119**) (0.156 mL, 112 mg, 1.00 mmol, 1.00 equiv.) over 16 h. The product was afforded in 87% yield determined by GC-FID.

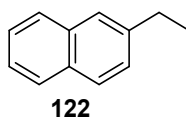
$C_8H_{18}$  (114.14 g/mol)

**GC-FID:**  $R_t = 3.172$  (**M<sub>FID1</sub>**)

**GC-MS:** (EI):  $m/z = 114.1$  (17,  $[M^{+}]$ ), 85.1 (100,  $[M^{+}]-[C_2H_5^{\bullet}]$ ); 71.1 (68,  $[M^{+}]-[C_3H_7^{\bullet}]$ ), 57.1 (95,  $[M^{+}]-[C_4H_9^{\bullet}]$ );  $R_t = 3.303$  (**M<sub>MS3</sub>**)



**2-ethylnaphthalene (122)**

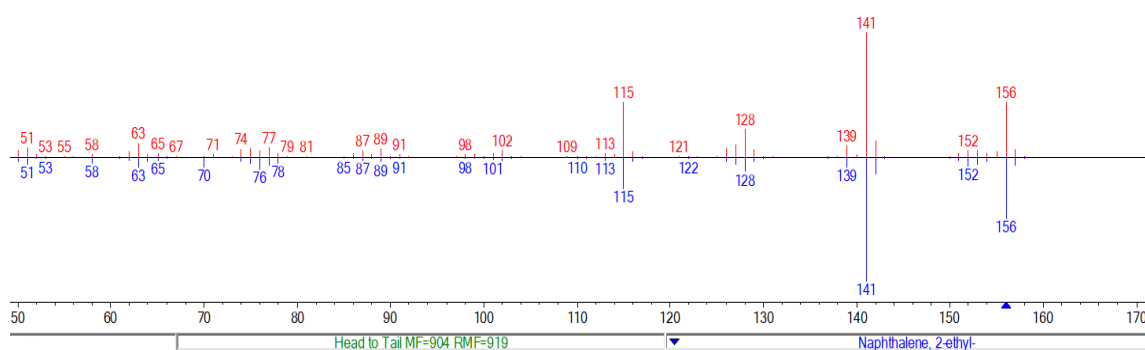


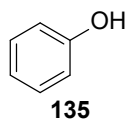
According to **GP2**, 2-ethylnaphthalene (**122**) was synthesized from 2-acetylnaphthalene (**121**) (170 mg, 1.00 mmol, 1.00 equiv.) over 16 h. The product was afforded in 91% yield determined by GC-FID.

$C_{12}H_{12}$  (156.09 g/mol)

**GC-FID:**  $R_t = 7.331$  (**M<sub>FID1</sub>**)

**GC-MS:** (EI):  $m/z = 156.1$  (100,  $[M^{+}]$ ), 141.0 (48,  $[M^{+}]-[CH_3^{\bullet}]$ );  $R_t = 5.651$  (**M<sub>MS1</sub>**)



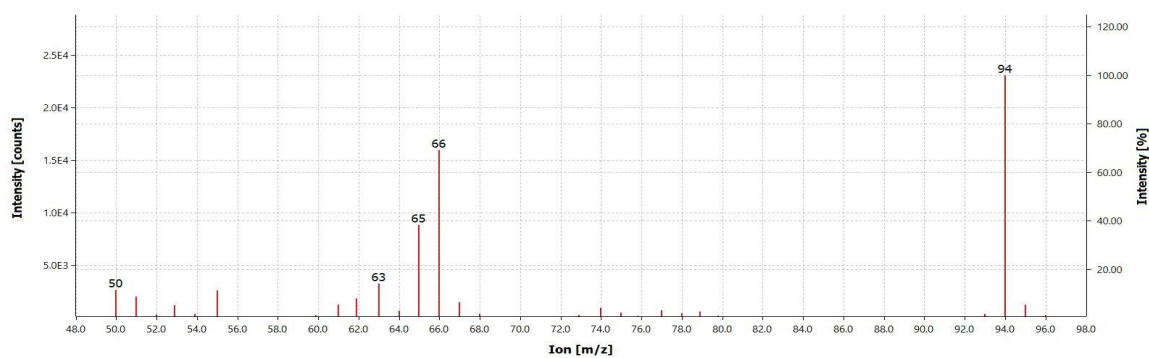
**phenol (135)**

According to **GP2**, phenol (**135**) was synthesized from  $\alpha$ -(Phenoxymethyl)benzenemethanol (**133**) (214 mg, 1.00 mmol, 1.00 equiv.) over 16 h. The product was afforded in 47% yield determined by GC-FID after workup with 1M HCl.

$C_6H_6O$  (94.11 g/mol)

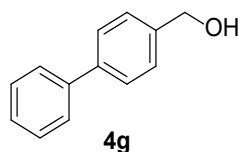
**GC-FID:**  $R_t = 4.335$  (**M<sub>FID1</sub>**)

**GC-MS:** (EI):  $m/z = 94$  (100,  $[M^{+}]$ ), 66 (64,  $[M^{+}] - [HO-C^{\bullet}]$ );  $R_t = 11.258$  (**M<sub>MS2</sub>**)



### 8.7. Analytical Data for Benzyl Alcohols

#### [1,1'-biphenyl]-4-methanol (**4g**)



According to **GP5**, [1,1'-biphenyl]-4-methanol (**4g**) was synthesized from [1,1'-biphenyl]-4-carboxaldehyde (911 mg, 5.00 mmol, 1.00 equiv.) and NaBH<sub>4</sub> (378 mg, 10.0 mmol, 2.00 equiv.) over 4 h. The product was afforded as a colorless solid (801 mg, 4.34 mmol, 87%). Analytical data was in accordance with the literature.<sup>18</sup>

C<sub>13</sub>H<sub>12</sub>O (184.09 g/mol)

R<sub>f</sub>: 0.42 (5:1 Hex:EtOAc)

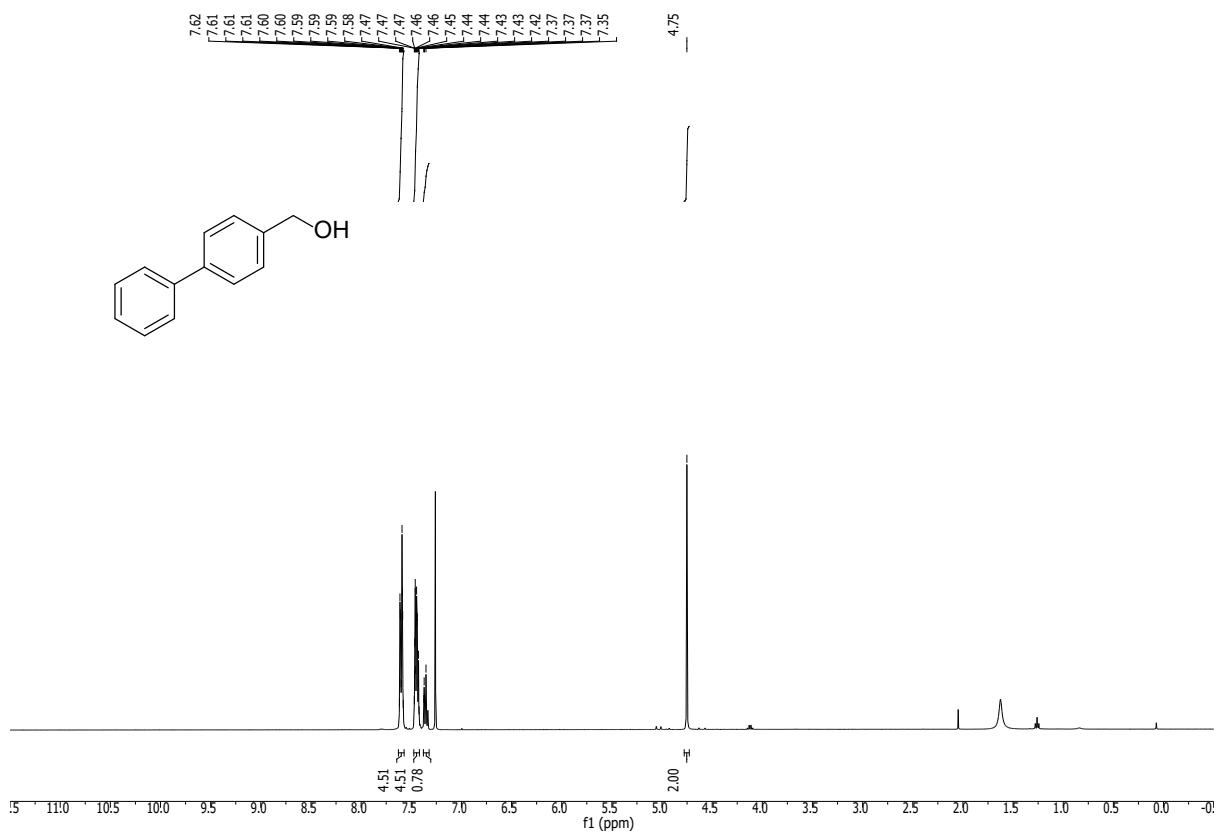
**<sup>1</sup>H-NMR:** (400 MHz, CDCl<sub>3</sub>): δ/ppm = 7.62 – 7.58 (m, 4H), 7.47 – 7.43 (m, 4H), 7.39 – 7.32 (m, 1H), 4.75 (s, 2H)

**<sup>13</sup>C-NMR:** (101 MHz, CDCl<sub>3</sub>): δ/ppm 140.9, 140.8, 140.0, 128.9, 127.6, 127.5, 127.5, 127.2, 65.3.

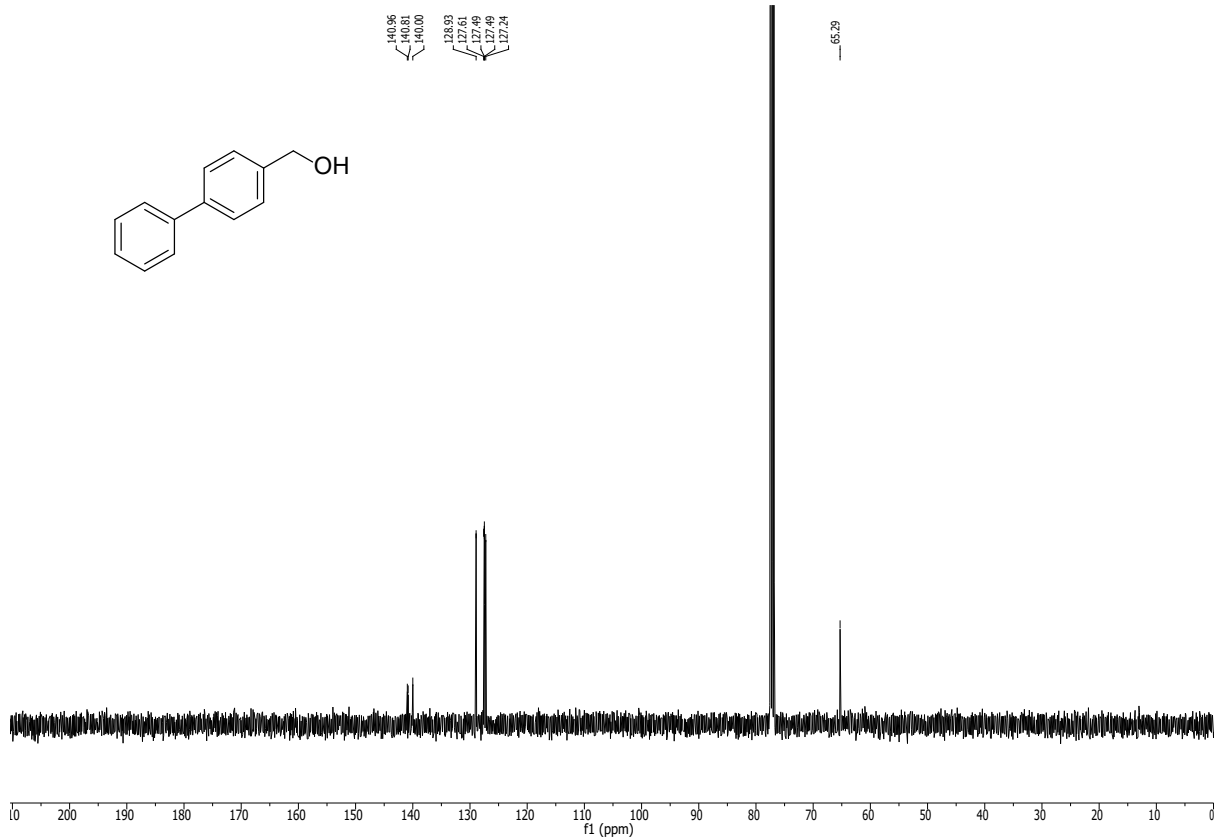
**GC-MS:** (EI): m/z = 184.1 (100, [M<sup>+</sup>]), [M<sup>+</sup>]-[OH<sup>+</sup>]), 167.1 (51, [M<sup>+</sup>]-[OH<sup>+</sup>]), 155.1 (66, [M<sup>+</sup>]-[OH<sup>+</sup>]-[CH<sub>2</sub><sup>+</sup>]), 77.1 (66, [C<sub>6</sub>H<sub>5</sub><sup>+</sup>])

**IR:** (ATR,  $\tilde{\nu}$ , [cm<sup>-1</sup>]): 3445 (w), 3426 (w), 2987 (m), 2837 (m), 1483 (m), 1373 (w), 1108 (m), 1046 (s), 991 (s), 816 (s), 749 (s), 708 (s), 673 (m)

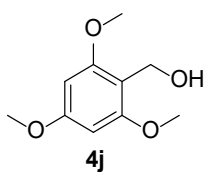
$^1\text{H-NMR}$ : (400 MHz,  $\text{CDCl}_3$ ) of **4g**



$^{13}\text{C-NMR}$ : (101 MHz,  $\text{CDCl}_3$ ) of **4g**



**(2,4,6-trimethoxyphenyl)methanol (4j)**



According to **GP5**, (2,4,6-trimethoxyphenyl)methanol (**4j**) was synthesized from 2,4,6-trimethoxybenzaldehyde (981 mg, 5.00 mmol, 1.00 equiv.) and NaBH<sub>4</sub> (378 mg, 10.0 mmol, 2.00 equiv.) over 5 h. The product was afforded as a colorless solid (809 mg, 4.08 mmol, 82%). Analytical data was in accordance with the literature.<sup>19</sup>

C<sub>10</sub>H<sub>14</sub>O<sub>4</sub> (198.22 g/mol)

R<sub>f</sub>: 0.42 (1:1 Hex:EtOAc)

**<sup>1</sup>H-NMR:** (400 MHz, CDCl<sub>3</sub>): δ/ppm = 6.13 (s, 2H), 4.70 (s, 2H), 3.82 (s, 6H), 3.81 (s, 3H), 2.22 (bs, 1H)

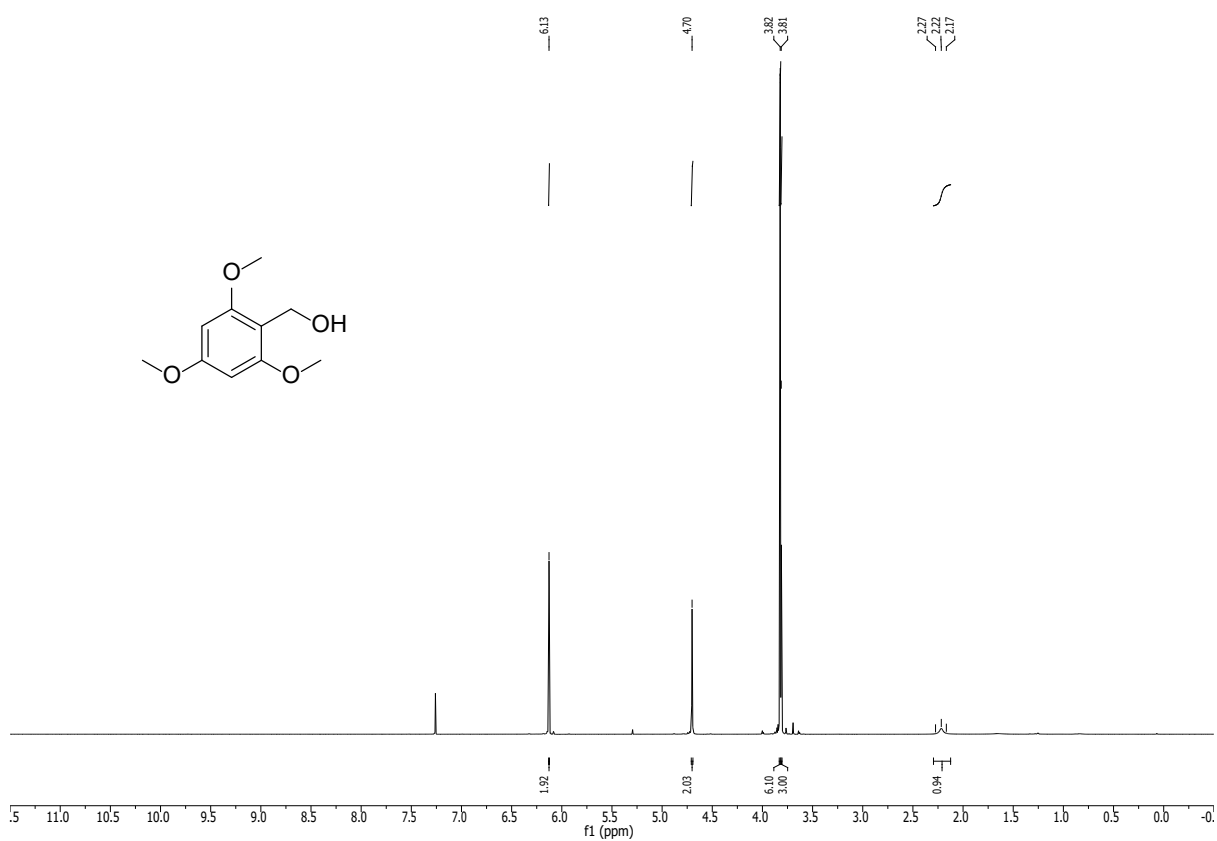
**<sup>13</sup>C-NMR:** (101 MHz, CDCl<sub>3</sub>): δ/ppm 161.1, 159.2, 109.9, 90.5, 55.7, 55.4, 54.4

**GC-MS:** (EI): m/z = 198.1 (82, [M<sup>+</sup>]), 181.1 (100, [M<sup>+</sup>]-[OH<sup>•</sup>]), 167.1 (25, [M<sup>+</sup>]-[OCH<sub>3</sub><sup>•</sup>]), 136.1 (24, [M<sup>+</sup>]-[OCH<sub>3</sub><sup>•</sup>]-[OCH<sub>3</sub><sup>•</sup>])

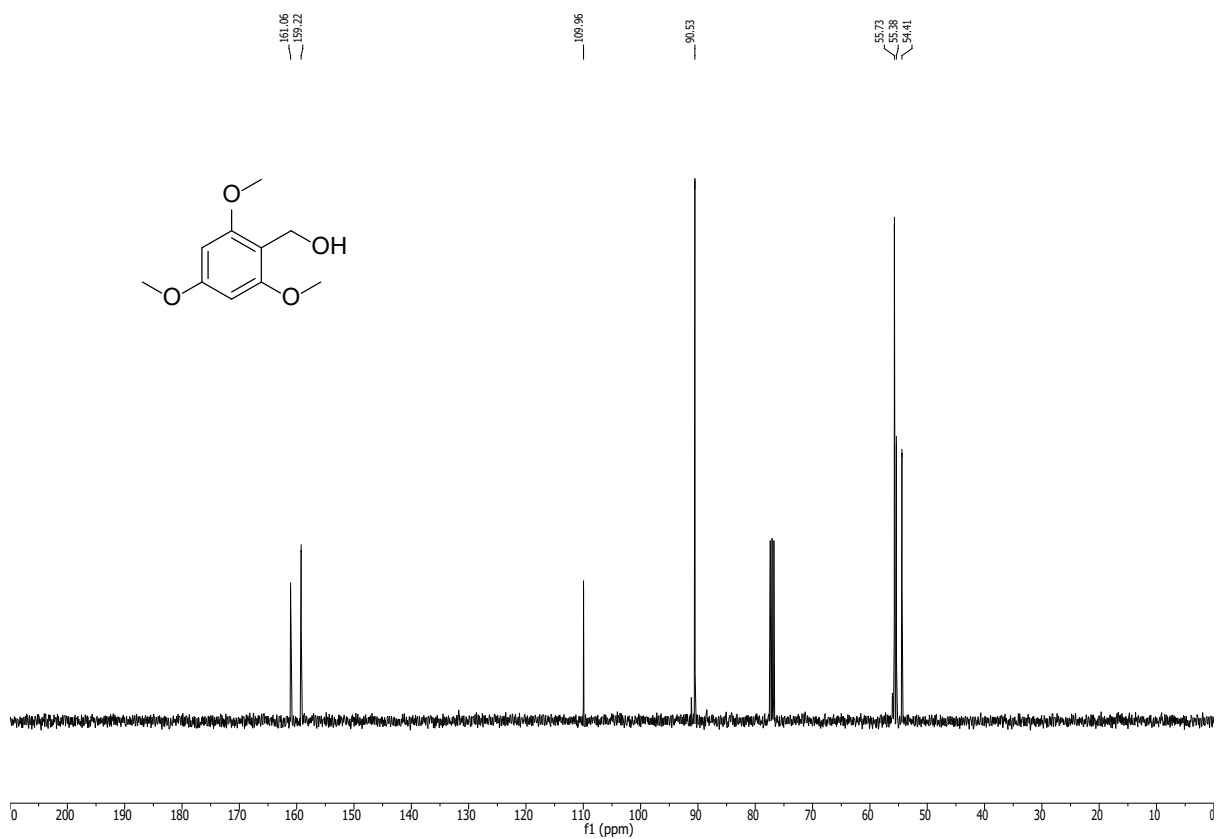
**IR:** (ATR,  $\tilde{\nu}$ , [cm<sup>-1</sup>]): 3444 (w), 2997 (w), 2937 (w), 2840 (w), 1592 (s), 1498 (m), 1454 (s), 1338 (w), 1200 (s), 1118 (s), 1036 (m), 992 (s), 947 (s), 813 (s), 731 (m)



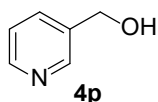
$^1\text{H-NMR}$ : (400 MHz,  $\text{CDCl}_3$ ) of **4j**



$^{13}\text{C-NMR}$ : (101 MHz,  $\text{CDCl}_3$ ) of **4j**



**pyridine-3-ylmethanol (4p)**



According to **GP5**, pyridine-3-ylmethanol (**4p**) was synthesized from 3-pyridinecarboxaldehyde (0.469 mL, 536 mg, 5.00 mmol, 1.00 equiv.) and NaBH<sub>4</sub> (378 mg, 10.0 mmol, 2.00 equiv.) over 16 h. The product was afforded as a colorless oil (213 mg, 1.95 mmol, 39%). Analytical data was in accordance with the literature.<sup>20</sup>

C<sub>6</sub>H<sub>7</sub>NO (109.13 g/mol)

**R<sub>f</sub>**: 0.19 (EtOAc)

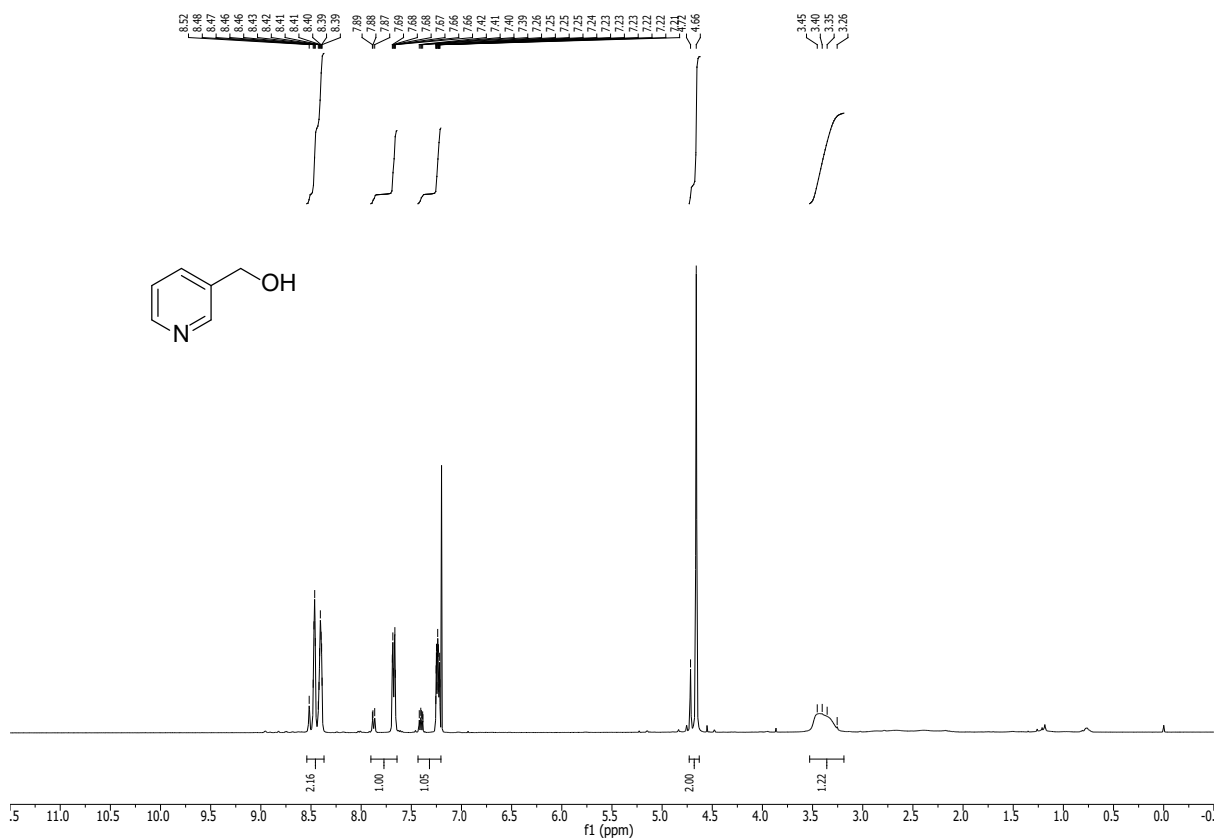
**<sup>1</sup>H-NMR**: (400 MHz, CDCl<sub>3</sub>): δ/ppm = 8.52 – 8.47 (m, 2H), 7.75 – 7.73 (m, 1H), 7.31 – 7.28 (m, 1H), 4.72 (s, 2H), 3.47 (bs, 1H)

**<sup>13</sup>C-NMR**: (101 MHz, CDCl<sub>3</sub>): δ/ppm = 148.6, 148.2, 135.3, 123.8, 124.2, 62.6

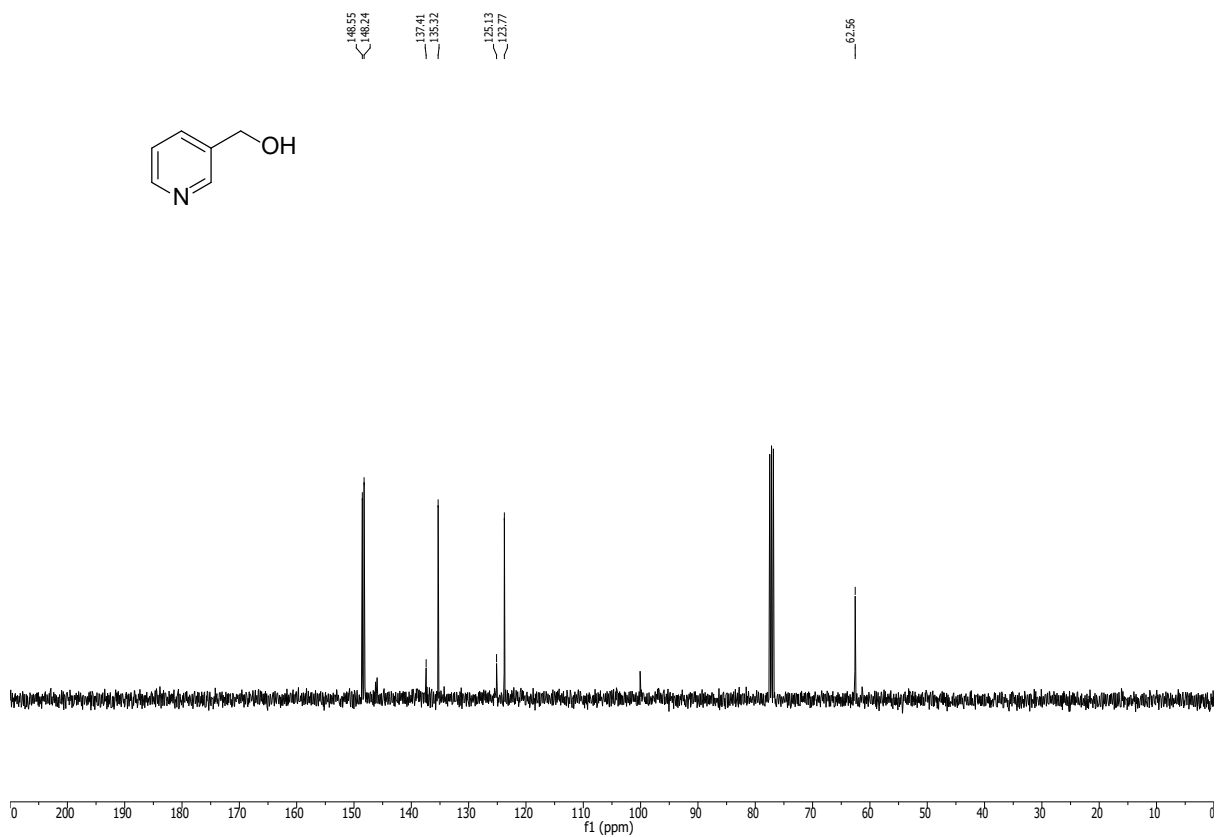
**GC-MS**: (EI): m/z = 109.0 (58, [M<sup>+</sup>]), 79.9 (100, [M<sup>+</sup>]-[OH<sup>-</sup>]-[CH<sub>2</sub><sup>+</sup>])

**IR**: (ATR,  $\tilde{\nu}$ , [cm<sup>-1</sup>]): 3206 (w), 2922 (w), 2855 (w), 1480 (w), 1424 (m), 1364 (w), 1126 (w), 1163 (w), 1215 (w), 1021 (s), 790 (s), 708 (s)

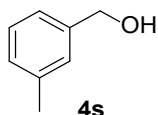
$^1\text{H-NMR}$ : (400 MHz,  $\text{CDCl}_3$ ) of **4p**



$^{13}\text{C-NMR}$ : (101 MHz,  $\text{CDCl}_3$ ) of **4p**



**(3-methylphenyl)methanol (4s)**



According to **GP5**, (3-methylphenyl)methanol (**4s**) was synthesized from 3-methylbenzaldehyde (0.590 mL, 601 mg, 5.00 mmol, 1.00 equiv.) and NaBH<sub>4</sub> (378 mg, 10.0 mmol, 2.00 equiv.) over 1.5 h. The product was afforded as a colorless oil (531 mg, 4.35 mmol, 87%). Analytical data was in accordance with the literature.<sup>21</sup>

C<sub>8</sub>H<sub>10</sub>O (122.17 g/mol)

**R<sub>f</sub>**: 0.25 (5:1 Hex:EtOAc)

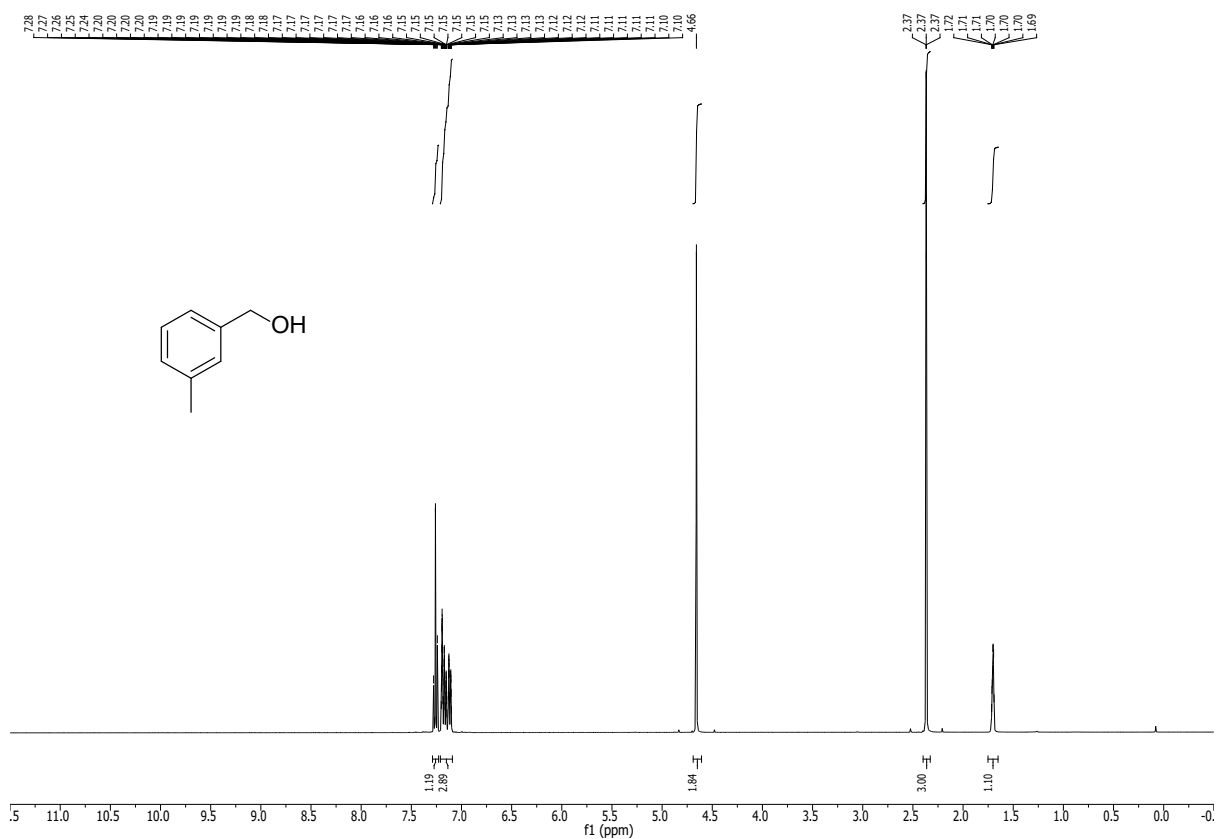
**<sup>1</sup>H-NMR**: (400 MHz, CDCl<sub>3</sub>): δ/ppm = 7.28 – 7.24 (m, 1H), 7.19 – 7.11 (m, 3H), 4.66 (s, 2H), 2.37 (s, 3H)

**<sup>13</sup>C-NMR**: (101 MHz, CDCl<sub>3</sub>): δ/ppm = 140.9, 138.4, 128.5, 127.9, 124.2, 65.6, 21.5.

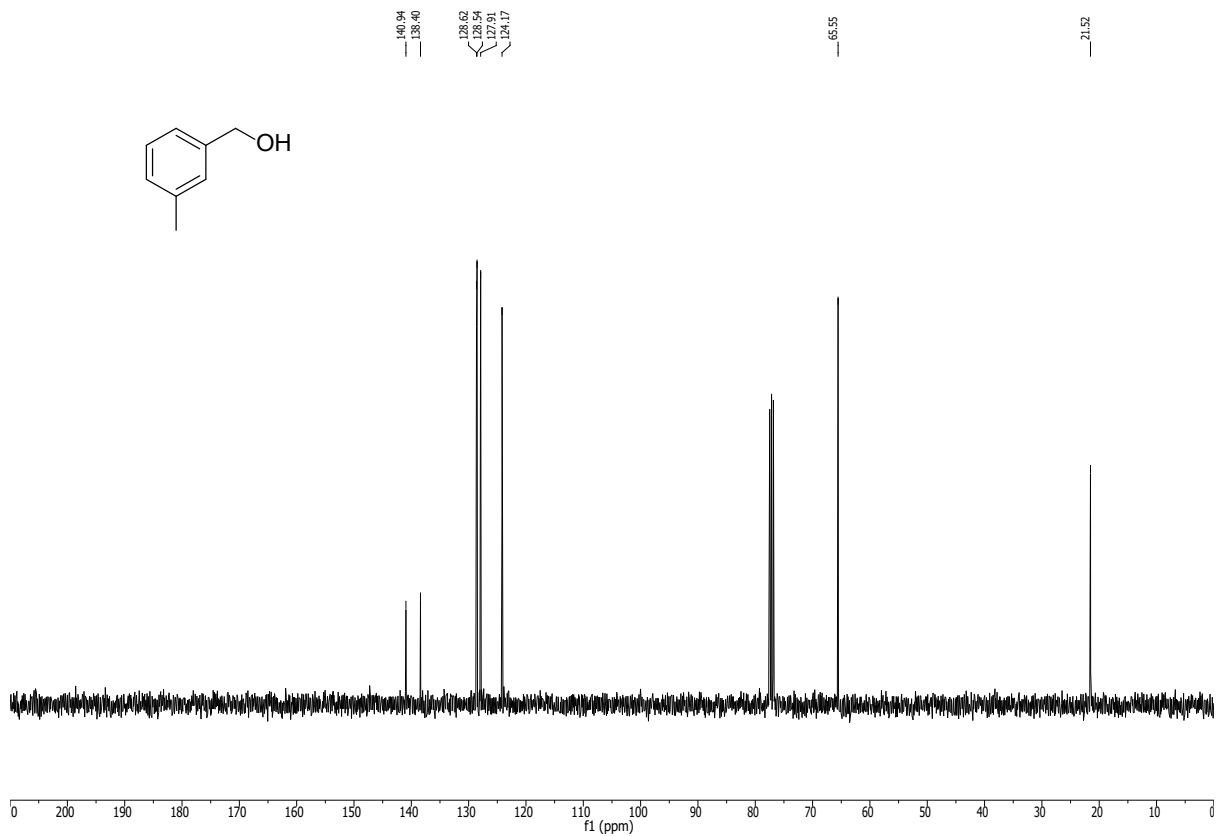
**GC-MS**: (EI): m/z = 122.0 (100, [M<sup>+</sup>]), 107.0 (71, [M<sup>+</sup>]-[CH<sub>3</sub>•]), 91.0 (55, [M<sup>+</sup>]-[CH<sub>3</sub>•]-[OH•])

**IR**: (ATR,  $\tilde{\nu}$ , [cm<sup>-1</sup>]): 3317 (w), 2919 (w), 2866 (w), 1487 (w), 1457 (w), 1156 (w), 1014 (w), 883 (w), 775 (s), 738 (s), 693 (s)

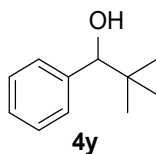
$^1\text{H-NMR}$ : (400 MHz,  $\text{CDCl}_3$ ) of **4s**



$^{13}\text{C-NMR}$ : (101 MHz,  $\text{CDCl}_3$ ) of **4s**



**2,2-dimethyl-1-phenylpropan-1-ol (4y)**



According to **GP5**, 2,2-dimethyl-1-phenylpropan-1-ol (**4y**) was synthesized from 2,2-dimethyl-1-phenyl-1-propanone (1.04 mL, 6.16 mmol, 1.00 equiv.) and NaBH<sub>4</sub> (466 mg, 12.3 mmol, 2.00 equiv.) over 3 h. The product was afforded as a colorless oil (836 mg, 5.09 mmol, 83%). Analytical data was in accordance with the literature.<sup>2</sup>

C<sub>11</sub>H<sub>16</sub>O (164.25 g/mol)

**R<sub>f</sub>**: 0.67 (5:1 Hex:EtOAc)

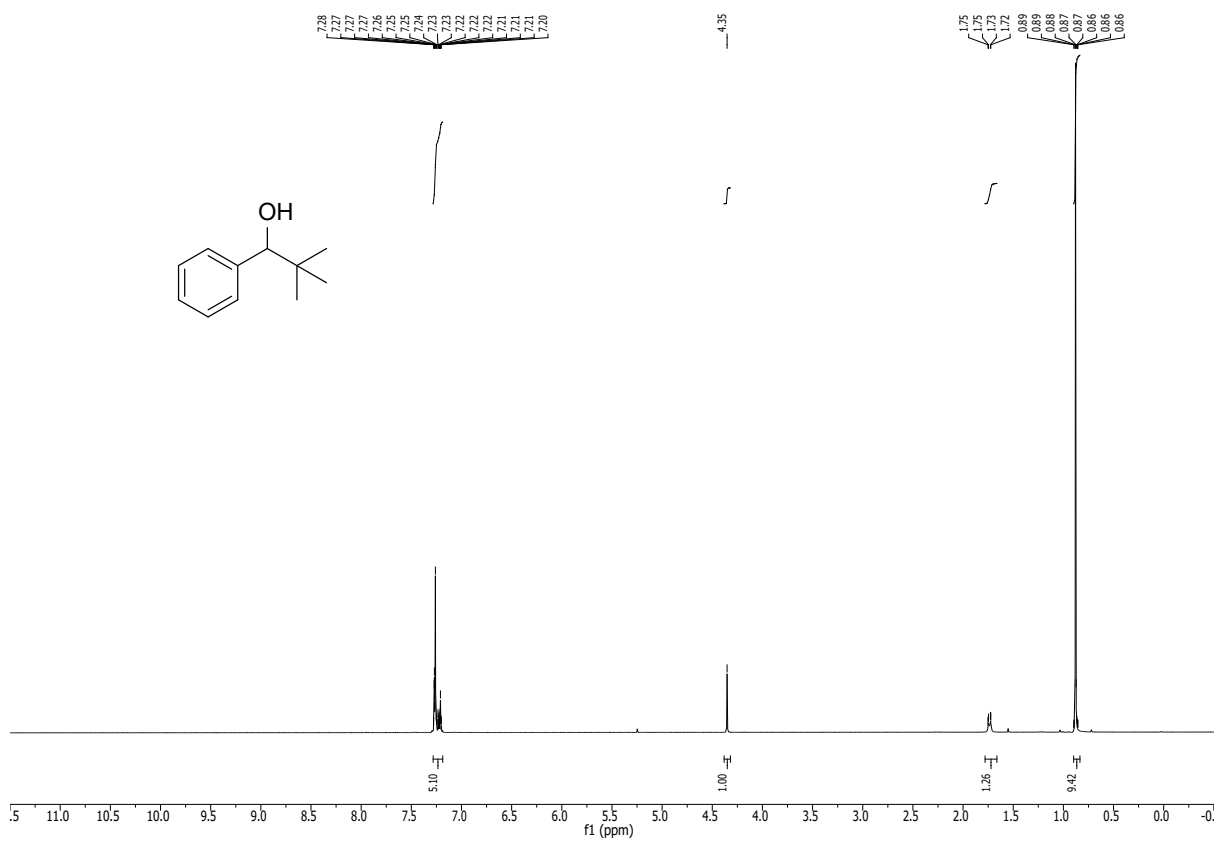
**<sup>1</sup>H-NMR**: (400 MHz, CDCl<sub>3</sub>): δ/ppm = 7.27 – 7.21 (m, 5H), 4.35 (s, 1H), 0.88 (s, 9H)

**<sup>13</sup>C-NMR**: (101 MHz, CDCl<sub>3</sub>): δ/ppm = 142.3, 127.8, 127.7, 127.4, 35.8, 26.1.

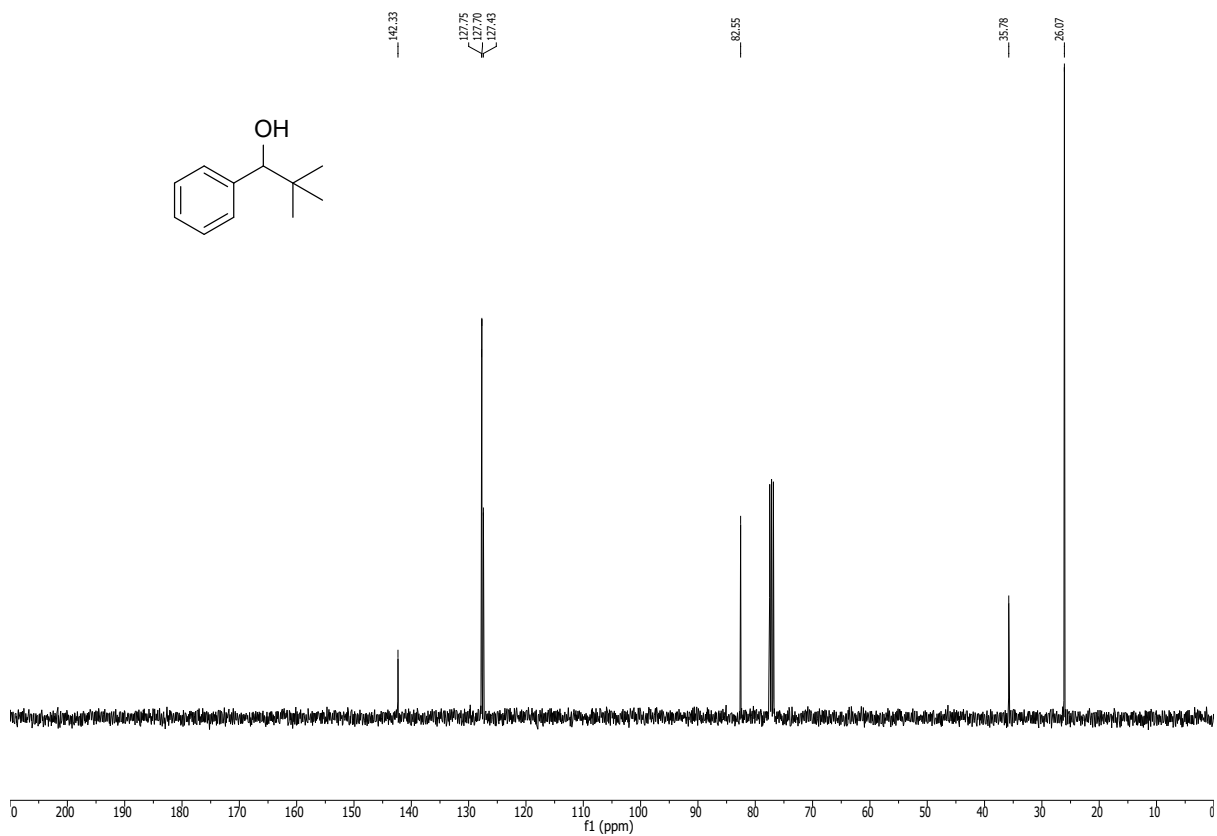
**GC-MS**: (EI): m/z = 164.1 (10, [M<sup>+</sup>]), 131.1 (31, [M<sup>+</sup>]-[OH<sup>+</sup>]-[CH<sub>3</sub><sup>+</sup>]) 107.1 (100, [M<sup>+</sup>]-[C(CH<sub>3</sub>)<sub>3</sub><sup>+</sup>]), 77.1 (39, [M<sup>+</sup>]-[C(CH<sub>3</sub>)<sub>3</sub><sup>+</sup>]-[CHOH<sup>+</sup>])

**IR**: (ATR,  $\tilde{\nu}$ , [cm<sup>-1</sup>]): 3440 (w), 2952 (m), 2904 (w), 2866 (w), 1480 (m), 1454 (m), 1364 (m), 1234 (w), 1178 (w), 1081 (w), 1044 (m), 1006 (s), 898 (w), 783 (w), 731 (s), 701 (s)

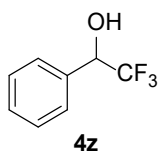
$^1\text{H-NMR}$ : (400 MHz,  $\text{CDCl}_3$ ) of **4y**



$^{13}\text{C-NMR}$ : (101 MHz,  $\text{CDCl}_3$ ) of **4y**



**2,2,2-trifluoro-1-phenylethanol (4z)**



According to **GP5**, 2,2,2-trifluoro-1-phenylethanol (**4y**) was synthesized from 2,2,2-trifluoro-1-phenylethanone (0.700 mL, 871 mg, 5.00 mmol, 1.00 equiv.) and NaBH<sub>4</sub> (378 mg, 10.0 mmol, 2.00 equiv.) over 17 h. The product was afforded as a colorless oil (838 mg, 4.76 mmol, 95%). Analytical data was in accordance with the literature.<sup>22</sup>

C<sub>8</sub>H<sub>7</sub>F<sub>3</sub>O (176.14 g/mol)

**R<sub>f</sub>**: 0.64 (5:1 Hex:EtOAc)

**<sup>1</sup>H-NMR**: (400 MHz, CDCl<sub>3</sub>): δ/ppm = 7.50 – 7.47 (m, 2H), 7.43 – 7.41 (m, 3H), 5.03 (q, *J* = 5.0 Hz, 1H), 2.56 (s, 1H)

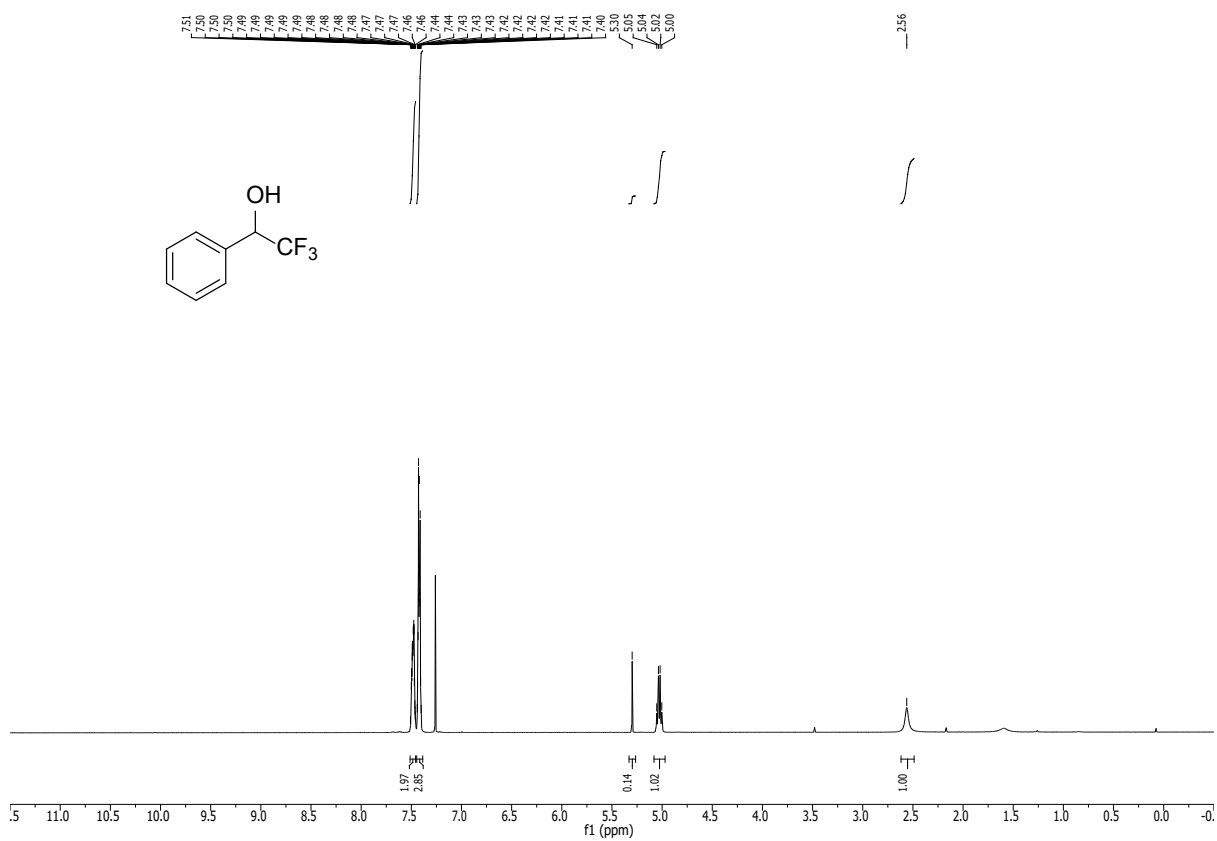
**<sup>13</sup>C-NMR**: (101 MHz, CDCl<sub>3</sub>): δ/ppm = 134.1, 129.7, 128.8, 127.6, 124.4 (q, *J* = 280 Hz), 72.9 (q, *J* = 31.6).

**GC-MS**: (EI): *m/z* = 176.0 (41, [M<sup>+</sup>]), 107.0 (100, [M<sup>+</sup>]-[CF<sub>3</sub>•]), 77.0 (72, [M<sup>+</sup>]-[CF<sub>3</sub>•]-[CHOH•])

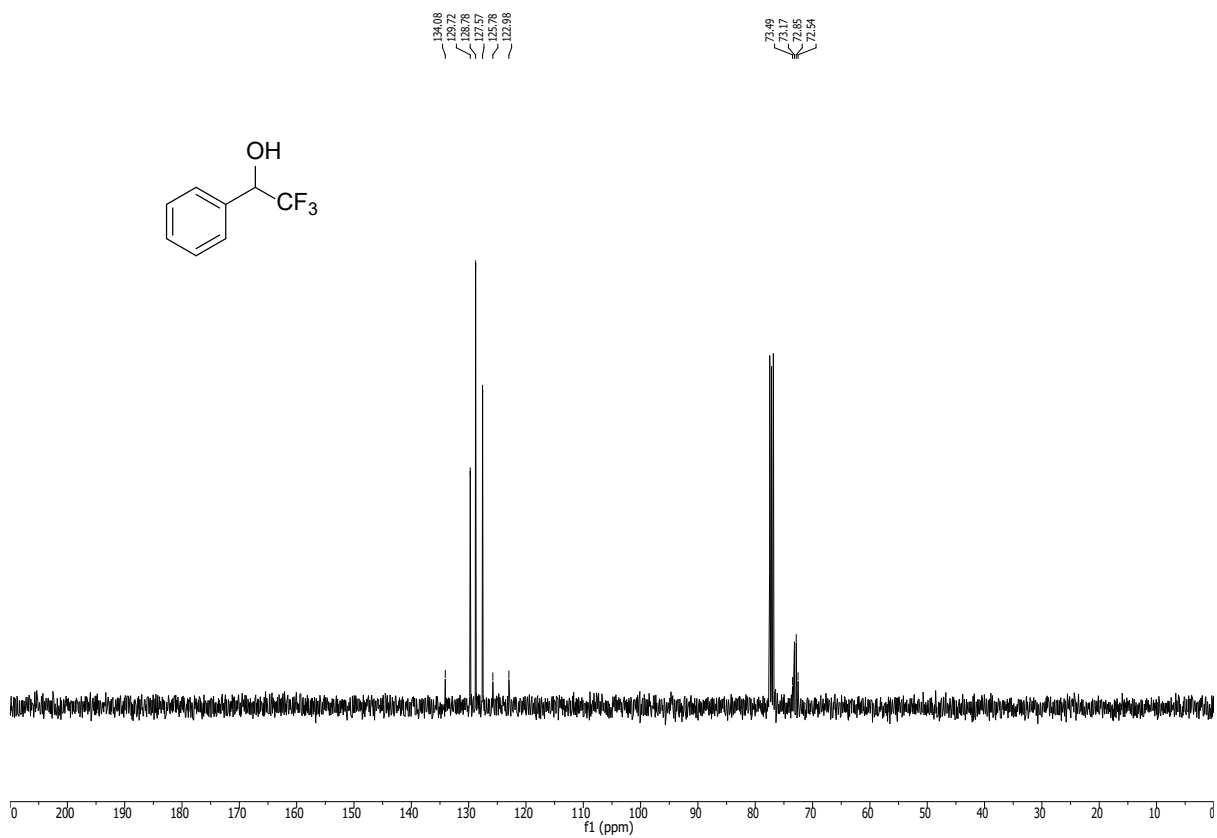
**IR**: (ATR,  $\tilde{\nu}$ , [cm<sup>-1</sup>]): 3384 (w), 1457 (w), 1357 (w), 1264 (m), 1167 (s), 1122 (s), 1059 (m), 865 (w), 835 (w), 760 (w), 701 (s)



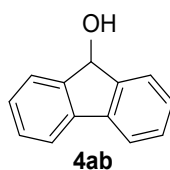
$^1\text{H-NMR}$ : (400 MHz,  $\text{CDCl}_3$ ) of **4z**



$^{13}\text{C-NMR}$ : (101 MHz,  $\text{CDCl}_3$ ) of **4z**



**9H-fluoren-9-ol (4ab)**



According to **GP5**, 9H-fluoren-9-ol (**4ab**) was synthesized from fluorenone (900 mg, 5.00 mmol, 1.00 equiv.) and NaBH<sub>4</sub> (378 mg, 10.0 mmol, 2.00 equiv.) over 17 h. The MeOH was removed through filtration instead of distillation. The product was afforded as a colorless solid (836 mg, 4.59 mmol, 92%). Analytical data was in accordance with the literature.<sup>23</sup>

C<sub>11</sub>H<sub>16</sub>O (182.22 g/mol)

R<sub>f</sub>: 0.45 (5:1 Hex:EtOAc)

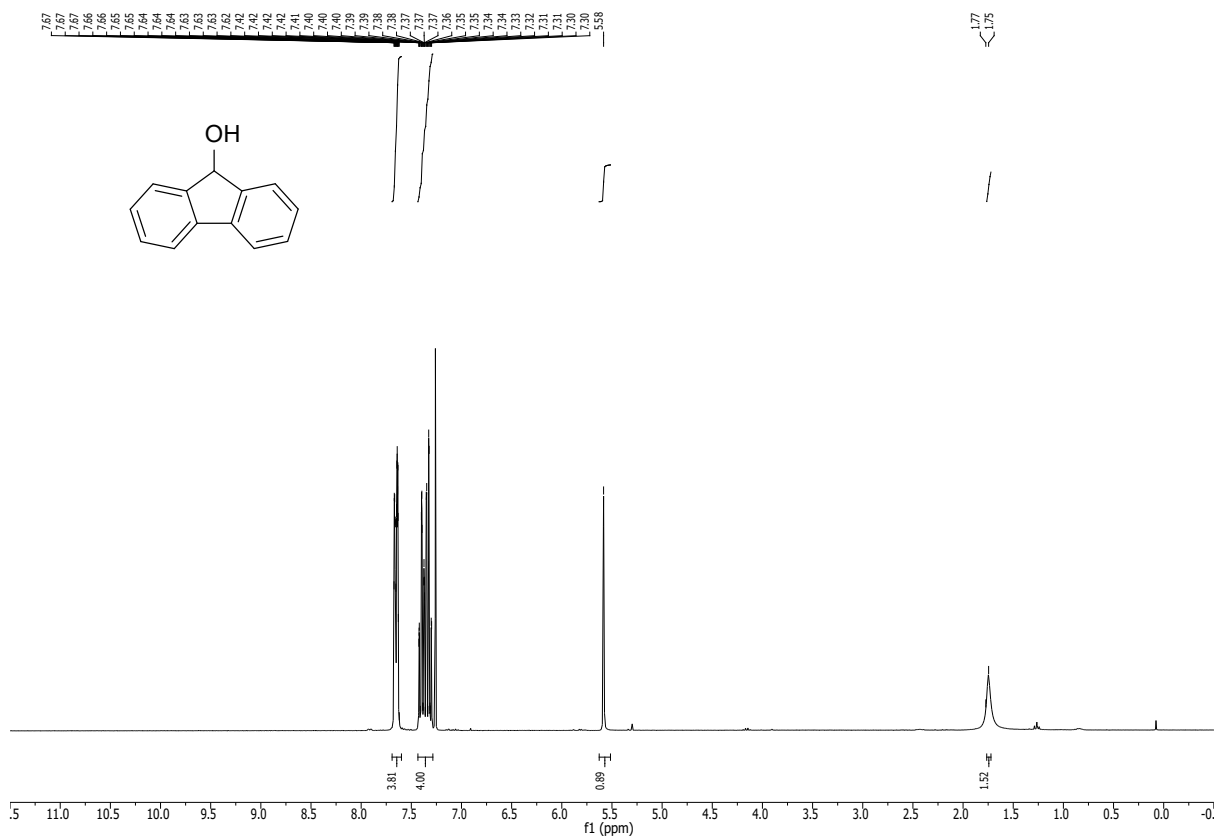
<sup>1</sup>H-NMR: (400 MHz, CDCl<sub>3</sub>): δ/ppm = 7.67 – 7.63 (m, 4H), 7.42 – 7.30 (m, 4H), 5.58 (s, 1H)

<sup>13</sup>C-NMR: (101 MHz, CDCl<sub>3</sub>): δ/ppm = 145.8, 140.2, 129.2, 128.0, 125.3, 120.1, 75.4.

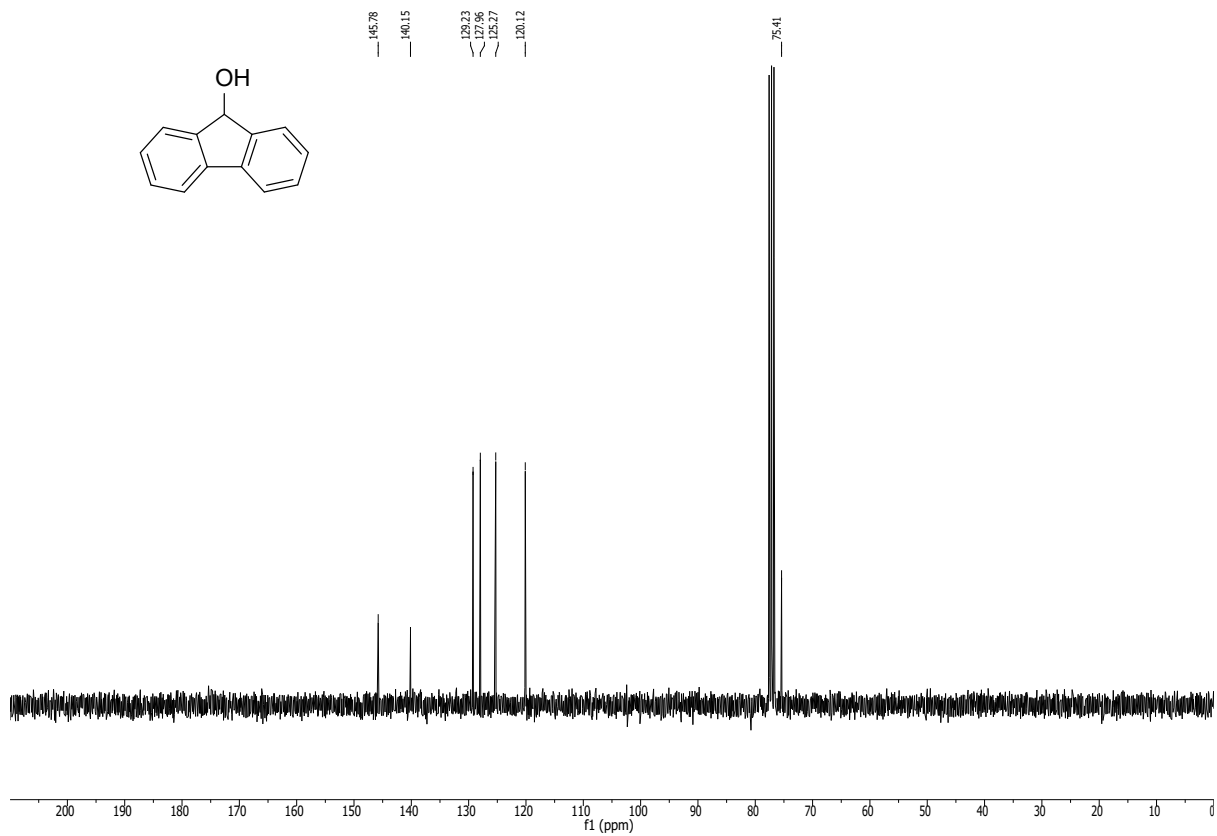
GC-MS: (EI): m/z = 182.1 (100, [M<sup>+</sup>]), 165.1 (47, [M<sup>+</sup>]-[OH<sup>+</sup>]), 152.1 (65, [M<sup>+</sup>]-[CHOH<sup>+</sup>]), 76.0 (16, [M<sup>+</sup>]-[CHOH<sup>+</sup>]-[C<sub>6</sub>H<sub>4</sub><sup>+</sup>])

IR: (ATR,  $\tilde{\nu}$ , [cm<sup>-1</sup>]): 3284 (m), 3064 (m), 3038 (m), 1450 (m), 1305 (m), 1185 (m), 1096 (w), 1021 (s), 943 (m), 846 (w), 764 (m), 734 (s), 671 (m)

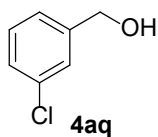
$^1\text{H-NMR}$ : (400 MHz,  $\text{CDCl}_3$ ) of **4ab**



$^{13}\text{C-NMR}$ : (101 MHz,  $\text{CDCl}_3$ ) of **4ab**



**(3-chlorophenyl)methanol (4aq)**



According to **GP5**, (3-chlorophenyl)methanol (**4aq**) was synthesized from 3-chlorobenzaldehyde (0.566 mL, 703 mg, 5.00 mmol, 1.00 equiv.) and NaBH<sub>4</sub> (378 mg, 10.0 mmol, 2.00 equiv.) over 2 h. The product was afforded as a colorless oil (692 mg, 4.85 mmol, 97%). Analytical data was in accordance with the literature.<sup>24</sup>

C<sub>8</sub>H<sub>7</sub>F<sub>3</sub>O (176.14 g/mol)

**R<sub>f</sub>**: 0.33 (5:1 Hex:EtOAc)

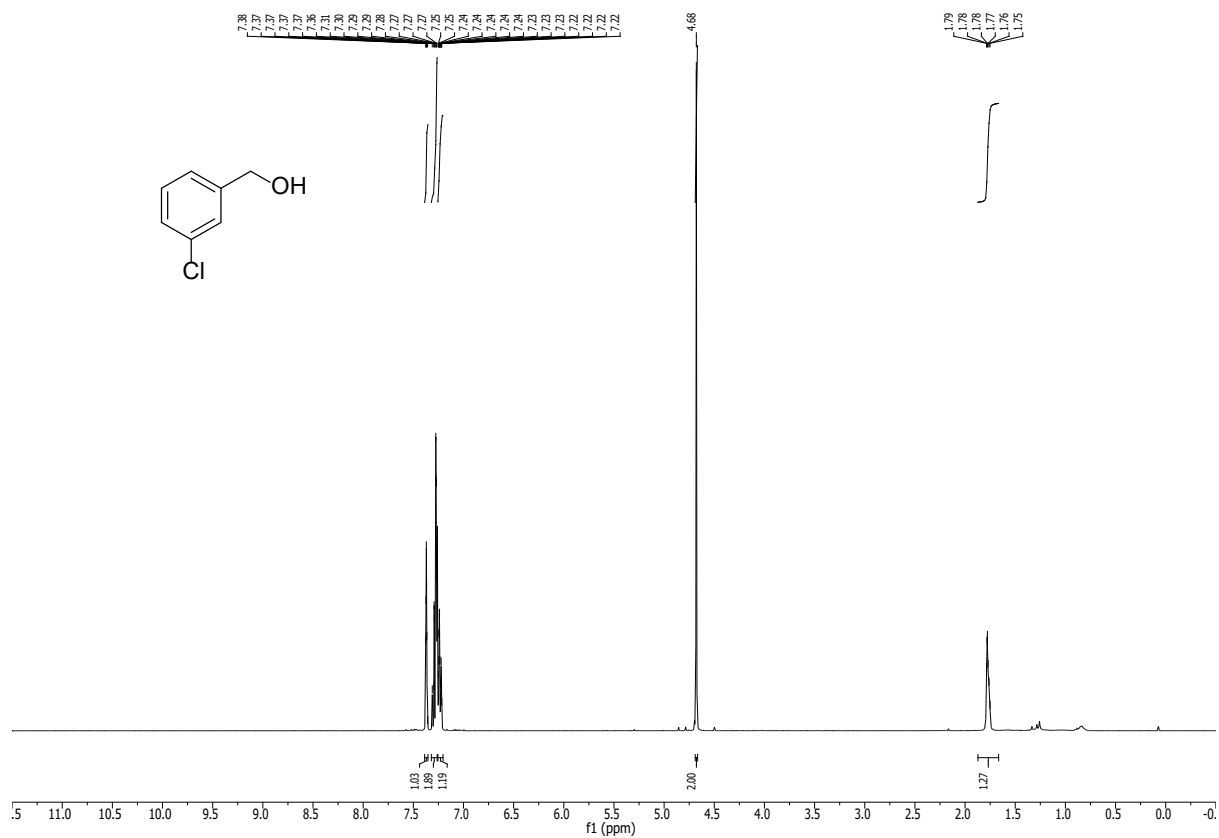
**<sup>1</sup>H-NMR**: (400 MHz, CDCl<sub>3</sub>): δ/ppm = 7.37 (s, 1H), 7.31 – 7.23 (m, 3H) 4.68 (s, 2H)

**<sup>13</sup>C-NMR**: (101 MHz, CDCl<sub>3</sub>): δ/ppm = 142.9, 134.6, 130.0, 127.9, 127.1, 125.0, 64.7.

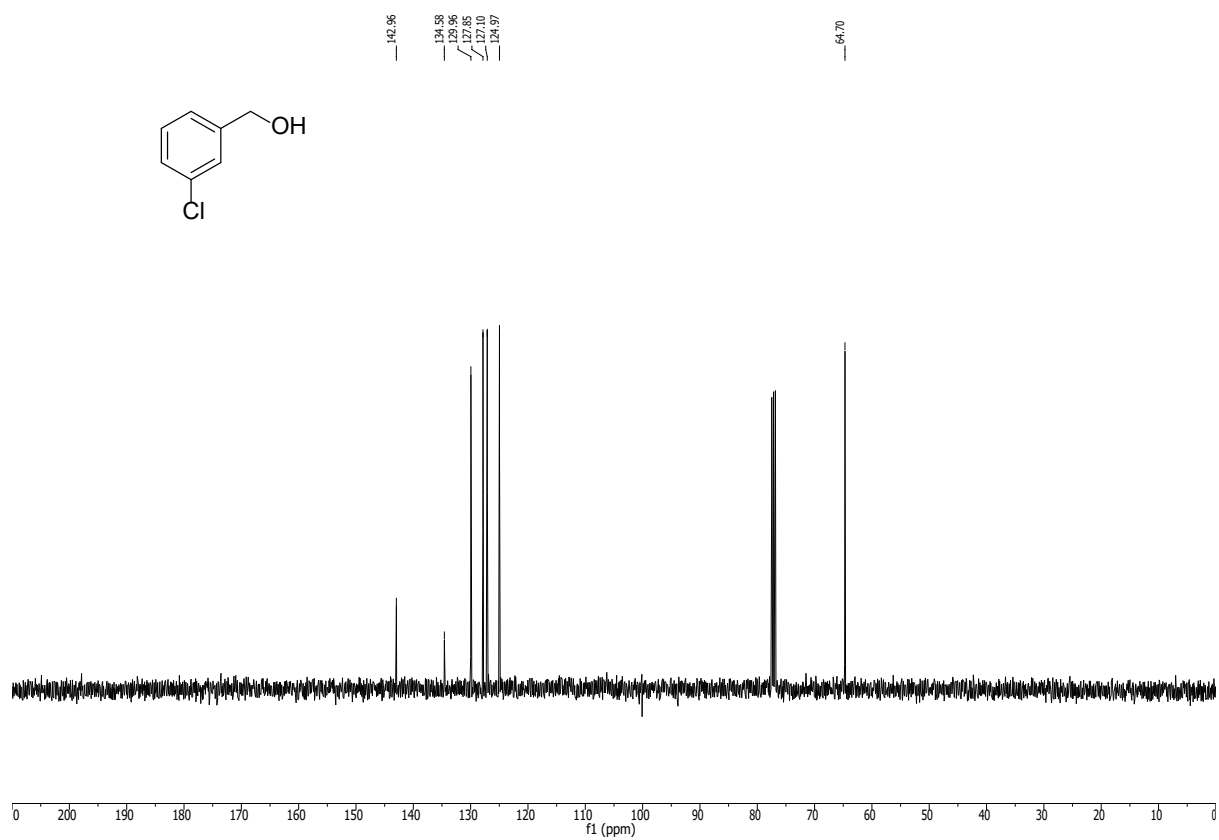
**GC-MS**: (EI): m/z = 142.0 (100, [M<sup>+</sup>]), 107.1 (100, [M<sup>+</sup>]-[Cl<sup>-</sup>])

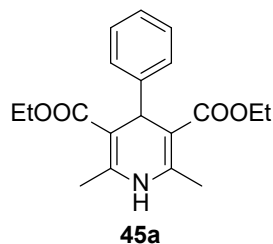
**IR**: (ATR,  $\tilde{\nu}$ , [cm<sup>-1</sup>]): 3288 (m), 2926 (w), 2874 (w), 1599 (w), 1476 (m), 1431 (m), 1360 (w), 1200 (m), 1096 (m), 1014 (s), 861 (m), 775 (s), 678 (s)

**<sup>1</sup>H-NMR**: (400 MHz, CDCl<sub>3</sub>) of **4aq**



<sup>13</sup>C-NMR: (101 MHz, CDCl<sub>3</sub>) of **4aq**



**8.8. Analytical Data for Synthesis of Hantzsch Esters****3,5-Diethyl-1,4-dihydro-4-phenyl-2,6-trimethyl-3,5-pyridinedicarboxylate (45a)**

According to **GP6**, **45a** was synthesized from benzaldehyde (0.300 mL, 318.4 mg, 3.00 mmol, 1.00 equiv.), NH<sub>4</sub>OAc (174 mg, 2.25 mmol, 1.50 equiv.), ethyl acetoacetate (0.400 mL, 409 mg, 3.15 mmol, 2.10 equiv.) in 1.5 mL ethanol over 15 h at 85 °C. After recrystallization out of hexane:water 1:1 the product was afforded as a yellow crystals (472 mg, 1.44 mmol, 48% yield). Analytical data was in accordance with the literature.<sup>25</sup>

C<sub>19</sub>H<sub>23</sub>NO<sub>4</sub> (329.40 g/mol)

**m.p.:** 150-156 °C

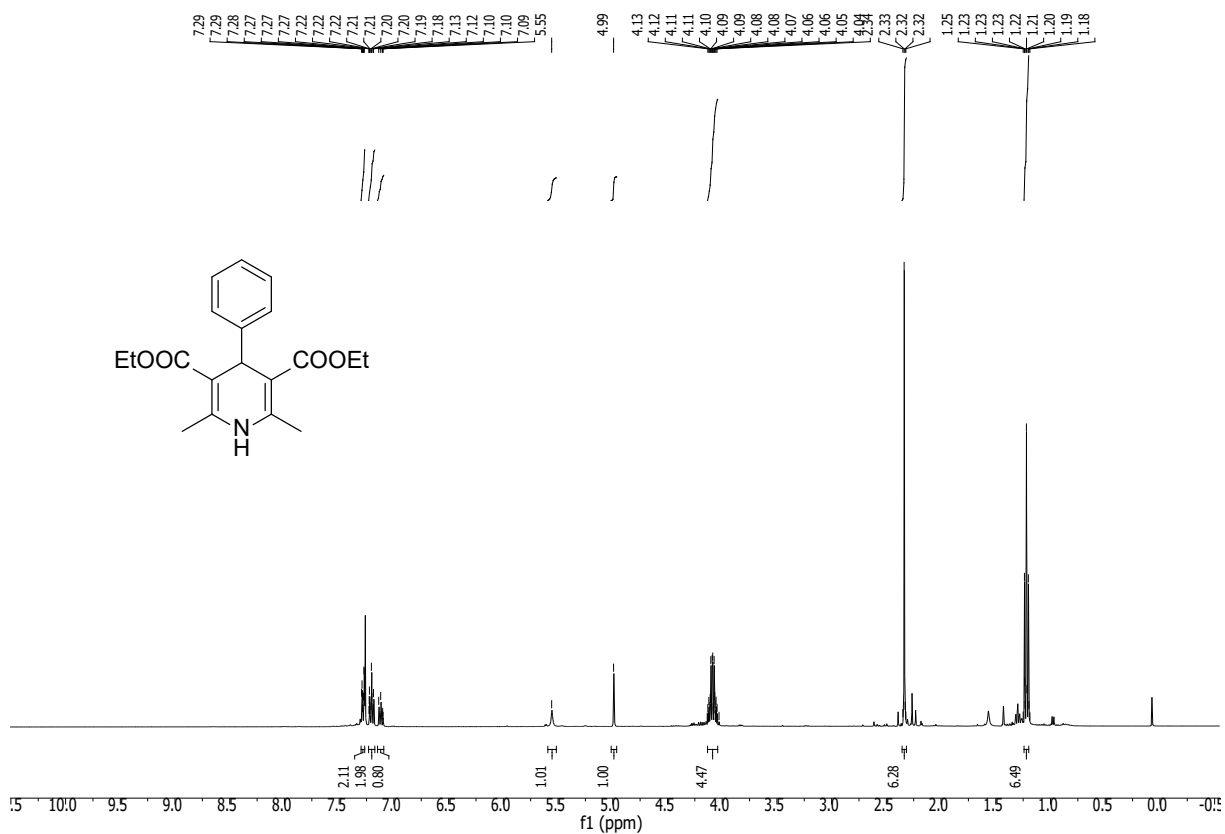
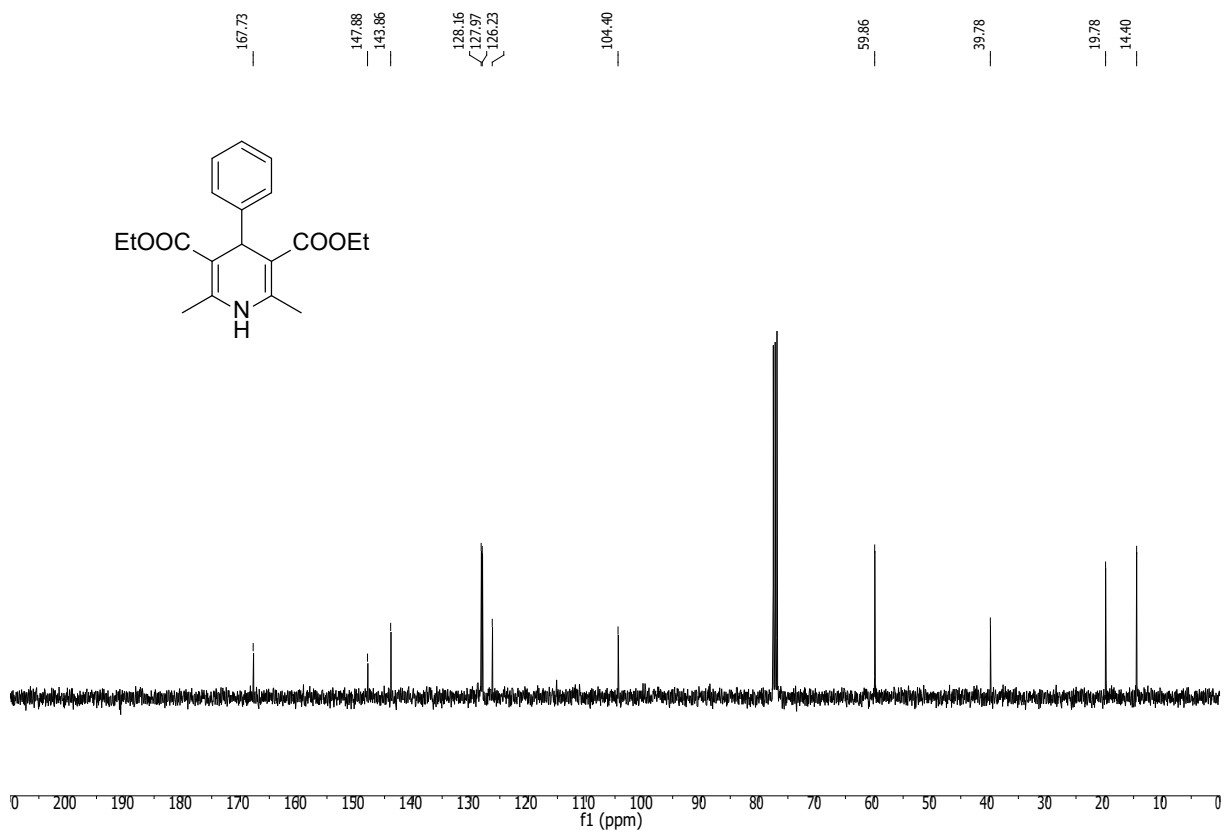
**R<sub>f</sub>:** 0.4 (hexane/ ethyl acetate 3:2)

**<sup>1</sup>H-NMR** (400 MHz, CDCl<sub>3</sub>) δ<sub>H</sub> (ppm): 7.30 – 7.26 (m, 2H), 7.23 – 7.17 (m, 2H), 7.15 – 7.09 (m, 1H), 5.55 (s, 1H), 4.99 (s, 1H), 4.08 (m, 4H), 2.33 (s, 6H), 1.22 (t, J = 7.1 Hz, 6H).

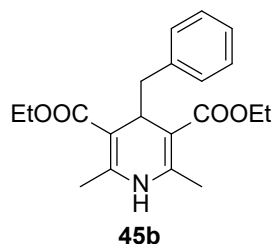
**<sup>13</sup>C-NMR** (101 MHz, CDCl<sub>3</sub>) δ<sub>C</sub> (ppm): 143.9, 128.2, 128.0, 126.2, 104.4, 77.5, 77.2, 76.8, 59.9, 39.8, 19.8, 14.4 .

**GC-MS** (EI, m/z): 253.1, 252.1, 224.1, 196.1, 196, 115, 105, 78, 77.1, 51.

**IR** (cm<sup>-1</sup>): 3339.7 (m), 2987.9 (w), 1684.8 (s), 1674.5 (s), 1487.2 (m), 1449.9 (m), 1371.7 (m), 1297.1 (s), 1244.9 (m), 1207.7 (s), 1121.9 (s), 1088.4 (s), 1047.4 (s), 1017.6 (s), 842.4 (m), 767.8 (s), 700.7 (s).

$^1\text{H-NMR}$ : (400 MHz,  $\text{CDCl}_3$ ) of **45a** $^{13}\text{C-NMR}$ : (101 MHz,  $\text{CDCl}_3$ ) of **45a**

**3,5-Diethyl-1,4-dihydro-2,6-dimethyl-4-benzyl-3,5-pyridinedicarboxylate (45b)**



According to **GP6**, **45b** was synthesized from phenylacetaldehyde (0.353 mL, 360 mg, 3.00 mmol, 1.00 equiv.), NH<sub>4</sub>OAc (174 mg, 2.25 mmol, 1.50 equiv.), ethyl acetoacetate (0.400 mL, 409 mg, 3.15 mmol, 2.10 equiv.) in 1.5 mL ethanol over 15 h at 85 °C. After recrystallization out of hexane:water 1:1 the product was afforded as a yellow crystals (420 mg, 1.23 mmol, 41% yield). Analytical data was in accordance with the literature.<sup>26</sup>

C<sub>20</sub>H<sub>25</sub>NO<sub>4</sub> (343.42 g/mol)

**m.p.:** 110-115 °C

**R<sub>f</sub>:** 0.23 (Hexane/ Ethyl acetate 3:2)

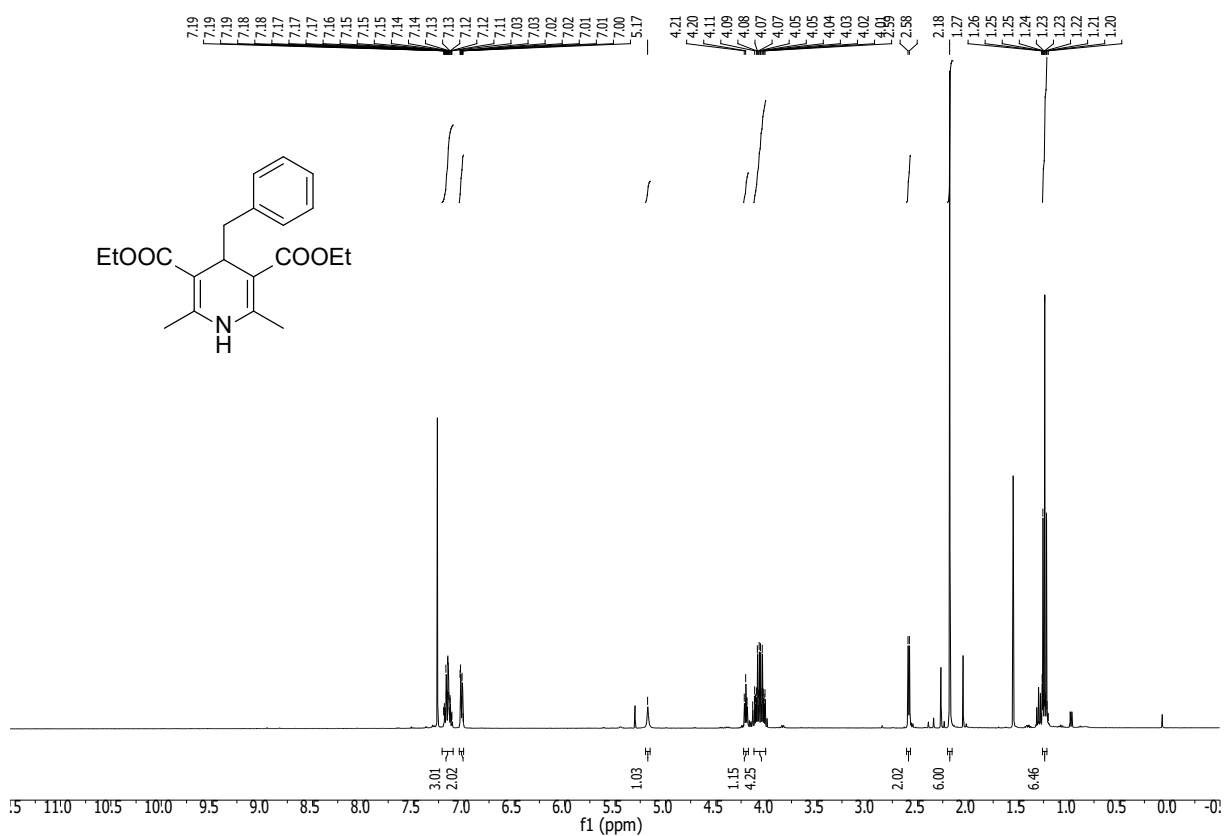
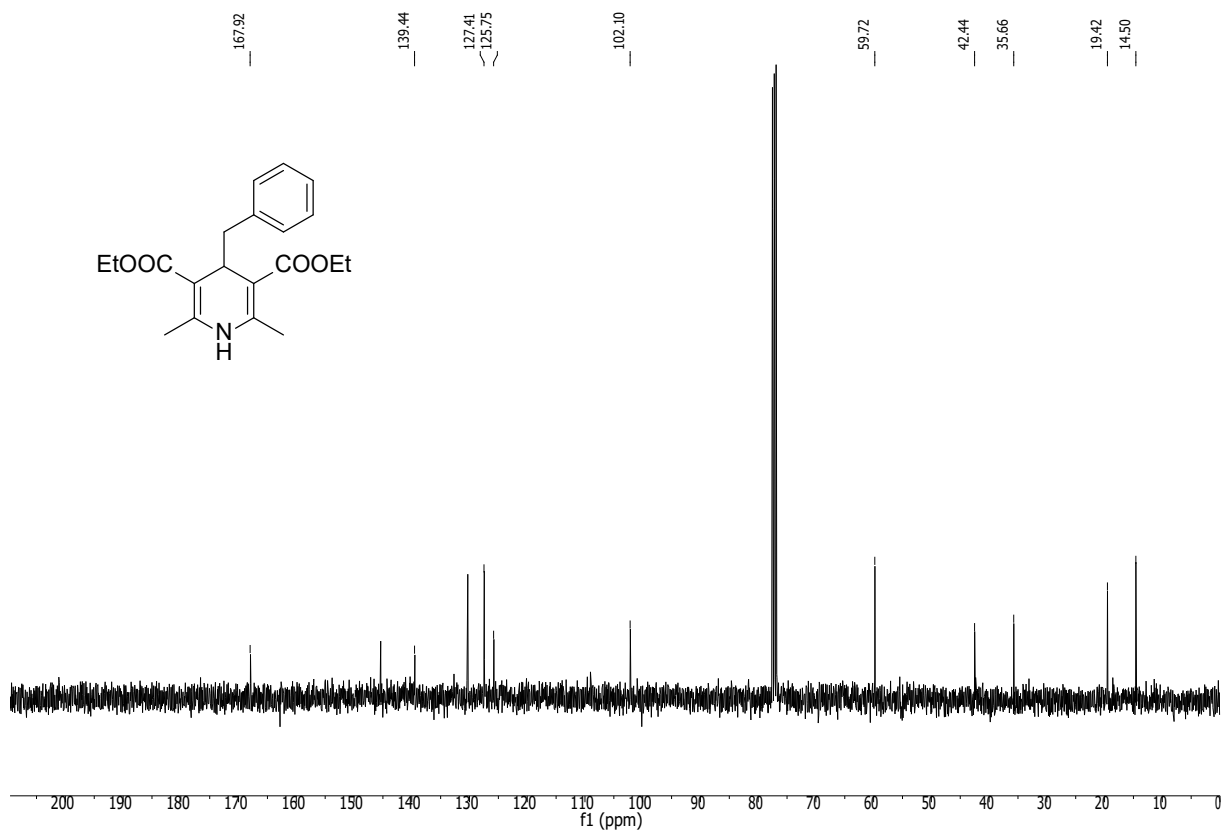
**<sup>1</sup>H-NMR** (400 MHz, CDCl<sub>3</sub>) δ<sub>H</sub> (ppm): 7.19-7.11 (m, 3H), 7.03-7.00 (m, 2H), 5.17 (s, 1H), 4.20 (t, 1H), 4.11-4.01 (m, 4H), 2.58 (d, 2H), 2.18 (s, 6H), 1.23 (s, 6H).

**<sup>13</sup>C-NMR** (101 MHz, CDCl<sub>3</sub>) δ<sub>C</sub> (ppm): 167.9, 139.4, 127.4, 125.8, 102.1, 59.7, 42.4, 35.7, 19.4, 14.5.

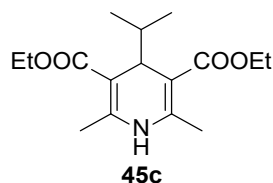
**GC-MS** (EI, m/z): 253.1, 252.1, 224.1, 196.1, 196.1, 179.1, 151.1, 150, 92, 91.1, 65.

**IR** (cm<sup>-1</sup>): 3339.2 (m); 2974.4 (w); 2933.4 (w); 2903.6 (w); 1692.2 (s); 1654.9 (s); 1476.0 (s); 1442.5 (m); 1367.9 (m); 1367.9 (m); 1323.2 (m); 1271.0 (m); 1207.7 (s); 1095.8 (s); 11051.1 (s); 864.7 (w); 823.7 (w); 775.3 (m); 719.4 (s).



$^1\text{H-NMR}$ : (400 MHz,  $\text{CDCl}_3$ ) of **45b** $^{13}\text{C-NMR}$ : (101 MHz,  $\text{CDCl}_3$ ) of **45b**

**3,5-Diethyl-1,4-dihydro-2,6-dimethyl-4-(1-methyl-ethyl)-3,5-pyridinedicarboxylate (45c)**



According to **GP6**, **45c** was synthesized from isobutyraldehyde (0.273 mL, 216.3 mg, 3.00 mmol, 1.00 equiv.),  $\text{NH}_4\text{OAc}$  (174 mg, 2.25 mmol, 1.50 equiv.), ethyl acetoacetate (0.400 mL, 409 mg, 3.15 mmol, 2.10 equiv.) in 1.5 mL ethanol over 15 h at 85 °C. After recrystallization out of hexane:water 1:1 the product was afforded as a yellow crystals (283 mg, 0.96 mmol, 32% yield). Analytical data was in accordance with the literature.<sup>26</sup>

$\text{C}_{16}\text{H}_{25}\text{NO}_4$  (295.38 g/mol)

**m.p.:** 100-103 °C

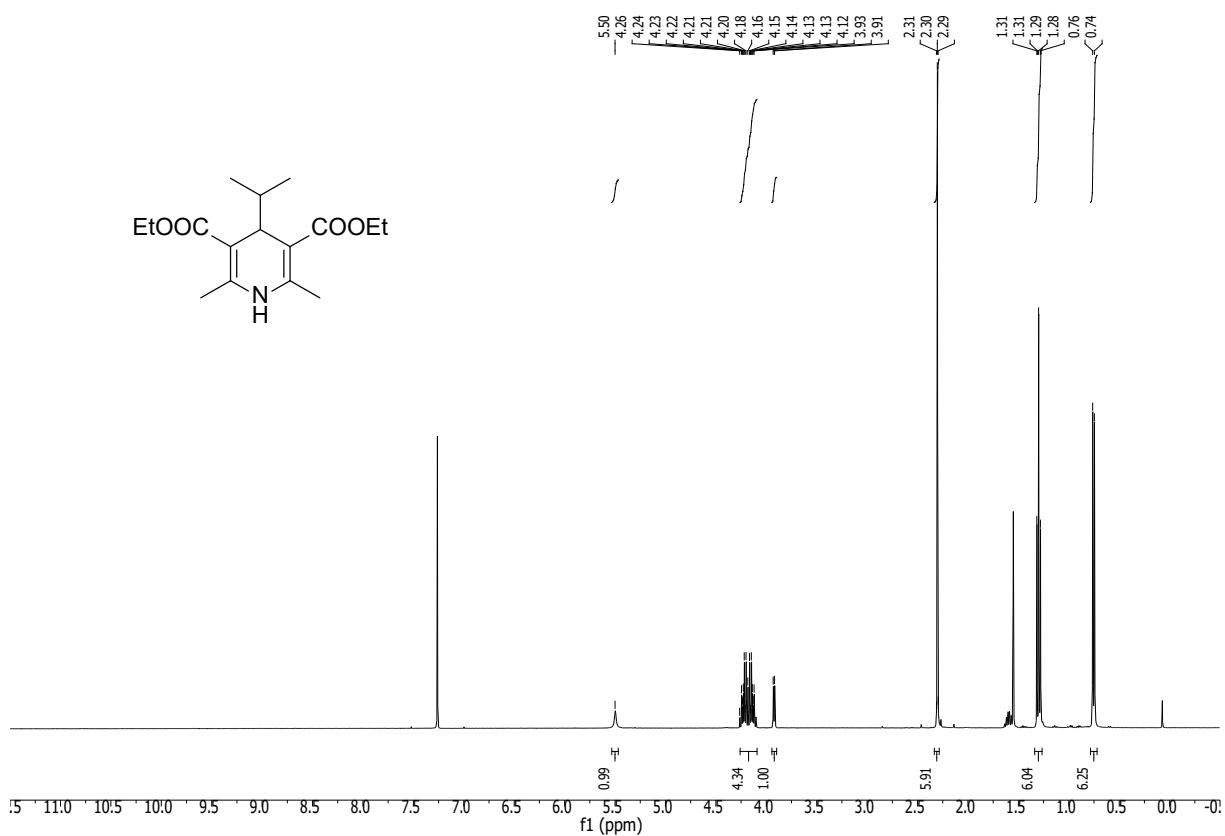
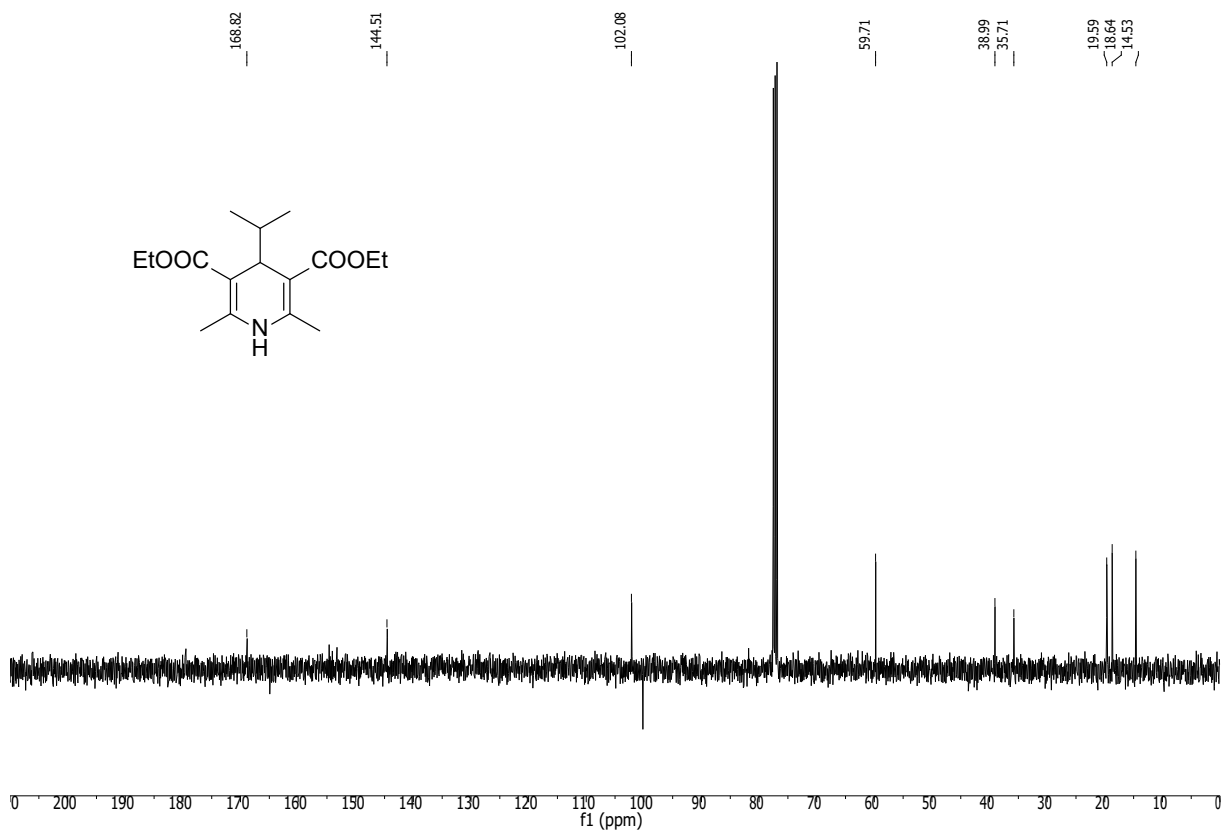
**R<sub>f</sub>:** 0.25 (Hexane/ Ethyl acetate 3:2)

**<sup>1</sup>H-NMR** (400 MHz,  $\text{CDCl}_3$ )  $\delta_{\text{H}}$  (ppm): 5.5 (s, 1H), 4.24-4.12 (m, 4H), 3.92 (d, 1H), 2.30 (s, 6H), 1.29 (t, 6H), 0.75 (d, 6H).

**<sup>13</sup>C-NMR** (101 MHz,  $\text{CDCl}_3$ )  $\delta_{\text{C}}$  (ppm): 168.8, 144.5, 102.1, 59.7, 39.0, 35.7, 19.6, 18.6, 14.5.

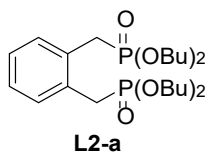
**GC-MS** (EI, m/z): 253.1, 252.1, 224.1, 196.1, 179.1, 178, 151, 150.1, 106.1.

**IR** ( $\text{cm}^{-1}$ ): 3339.7 (m); 2959.5 (w); 2899.9 (w); 1692.2 (m); 1647.5 (s); 1591.6 (m); 1483.5 (s); 1446.2 (m); 1364.2 (s); 1269.7 (m); 1252.4 (s); 1211.4 (s); 1177.8 (m); 1021.3 (s); 909.5 (m); 816.3 (s); 771.6 (m); 745.5 (m); 715.6 (m).

$^1\text{H-NMR}$ : (400 MHz,  $\text{CDCl}_3$ ) of **45c** $^{13}\text{C-NMR}$ : (101 MHz,  $\text{CDCl}_3$ ) of **45c**

## 8.9. Miscellaneous Products and Analytical Data

### Synthesis of tetrabutyl (1,2-Phenylenebis(methylene))bis(phosphonate) (L2-a)



According to the literature procedure,  $\alpha$ ,  $\alpha'$ -dibromo-*o*-xylene (2.64 g, 10.0 mmol, 1.00 equiv.) and tri(*n*-butyl)phosphite (10.8 mL, 40.0 mmol, 4.00 equiv.) were added in a flask under argon and stirred for 16 h at 120°C. After 16h the volatiles were distilled under vacuum resulting a yellow oil (4.70 g, 9.60 mmol, 96%). The obtained product was analyzed by  $^1\text{H}$ ,  $^{13}\text{C}$  and  $^{31}\text{P}$  NMR. Analytical data was in accordance with the literature.<sup>27</sup>

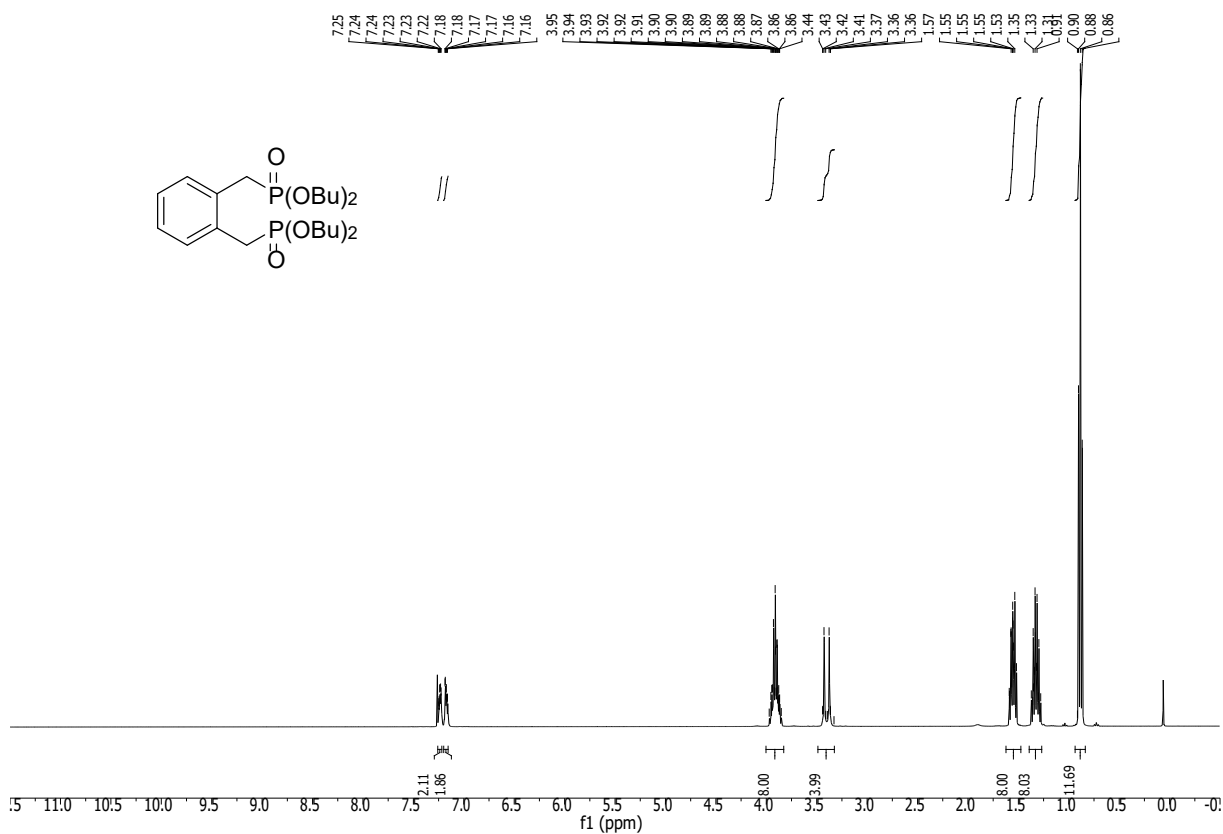
$\text{C}_{24}\text{H}_{44}\text{O}_6\text{P}_2$  (490.56 g/mol)

$^1\text{H-NMR}$  (400 MHz,  $\text{CDCl}_3$ )  $\delta_{\text{H}}$  (ppm): 7.25-7.16 (m, 4H), 3.95-3.86 (m, 8H), 3.40 (d, 4H), 1.57-1.53 (m, 8H), 1.35-1.31 (m, 8H), 0.88 (t, 12H)

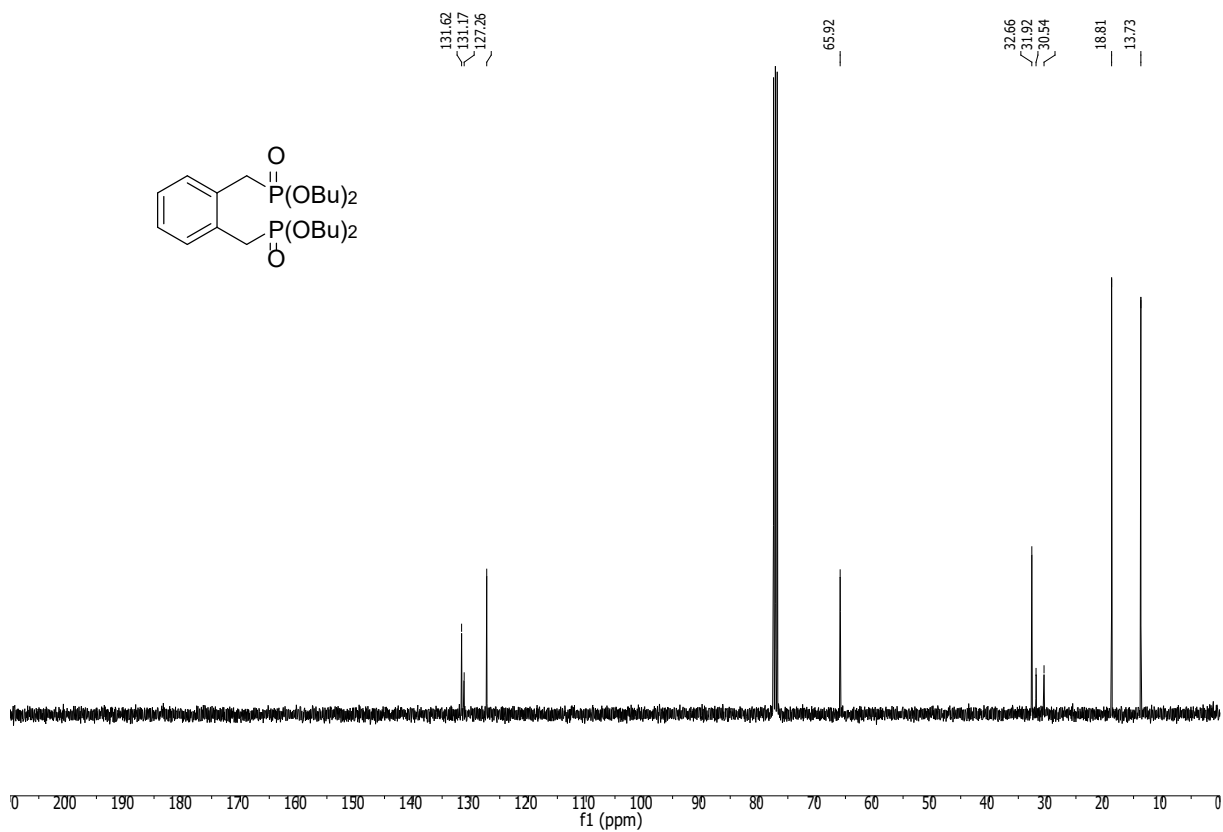
$^{13}\text{C-NMR}$  (101 MHz,  $\text{CDCl}_3$ )  $\delta_{\text{C}}$  (ppm): 131.6, 131.2, 127.3, 65.9, 32.7, 31.9, 18.8, 13.7

$^{31}\text{P-NMR}$  (162 MHz,  $\text{CDCl}_3$ )  $\delta_{\text{C}}$  (ppm): 26.72

$^1\text{H-NMR}$ : (400 MHz,  $\text{CDCl}_3$ ) of **L2-a**



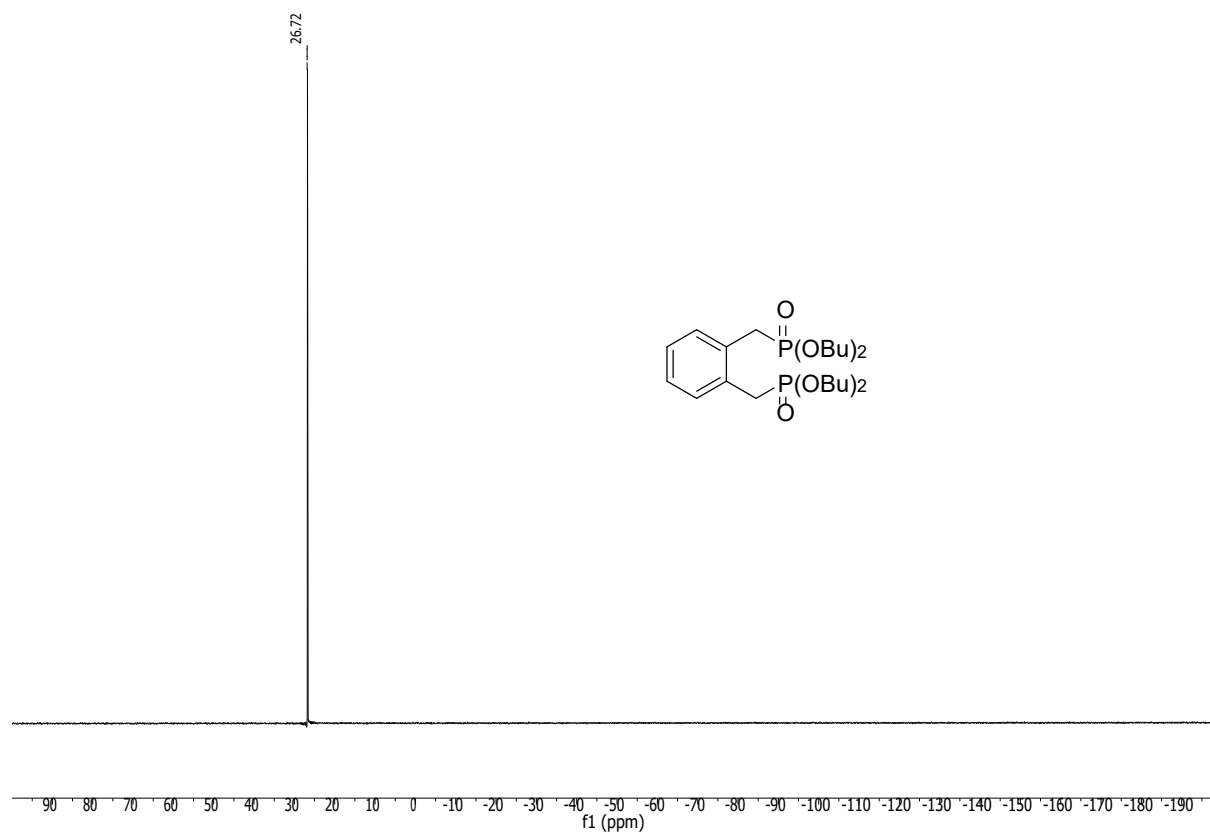
$^{13}\text{C-NMR}$ : (101 MHz,  $\text{CDCl}_3$ ) of **L2-a**

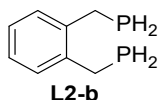


## Experimental section

---

$^{31}\text{P}$ -NMR: (161 MHz,  $\text{CDCl}_3$ ) of **L2-a**



**Synthesis of 1,2-Bis(phosphinomethyl)benzene (L2-b)**

According to the literature procedure, chlorotrimethylsilane (3.06 mL, 24.0 mmol, 4.00 equiv.) was added dropwise over a  $\text{LiAlH}_4$  (0.91 g, 24.0 mmol, 4.00 equiv.) suspension in THF (30 mL) at  $-78^\circ\text{C}$ . After the complete addition, the solution was heated to room temperature and stirred for 2h. After the 2h, the reaction mass was cooled to  $-50^\circ\text{C}$ , a tetrabutyl (1,2-phenylenebis(methylene))bis(phosphonate) (**L2-a**) (2.94 g, 6.00 mmol, 1.00 equiv) solution in THF (20 mL) was added dropwise. The resulted solution was heated to room temperature and stirred for 2h. The reaction was quenched by slow addition of deionzied, degassed water and 20% aq NaOH solution and dried over  $\text{MgSO}_4$  which was washed with THF (3x10 mL). The resulting oil was passed through a neutral alumina pulg and washed with  $\text{CHCl}_3$ . The resulted colorless oil was analyzed by  $^1\text{H}$ ,  $^{13}\text{C}$  and  $^{31}\text{P}$  NMR. Analytical data was in accordance with the literature.<sup>27</sup> (0.77 g, 4.52 mmol, 75% yield)

$\text{C}_8\text{H}_{12}\text{P}_2$  (170.13 g/mol)

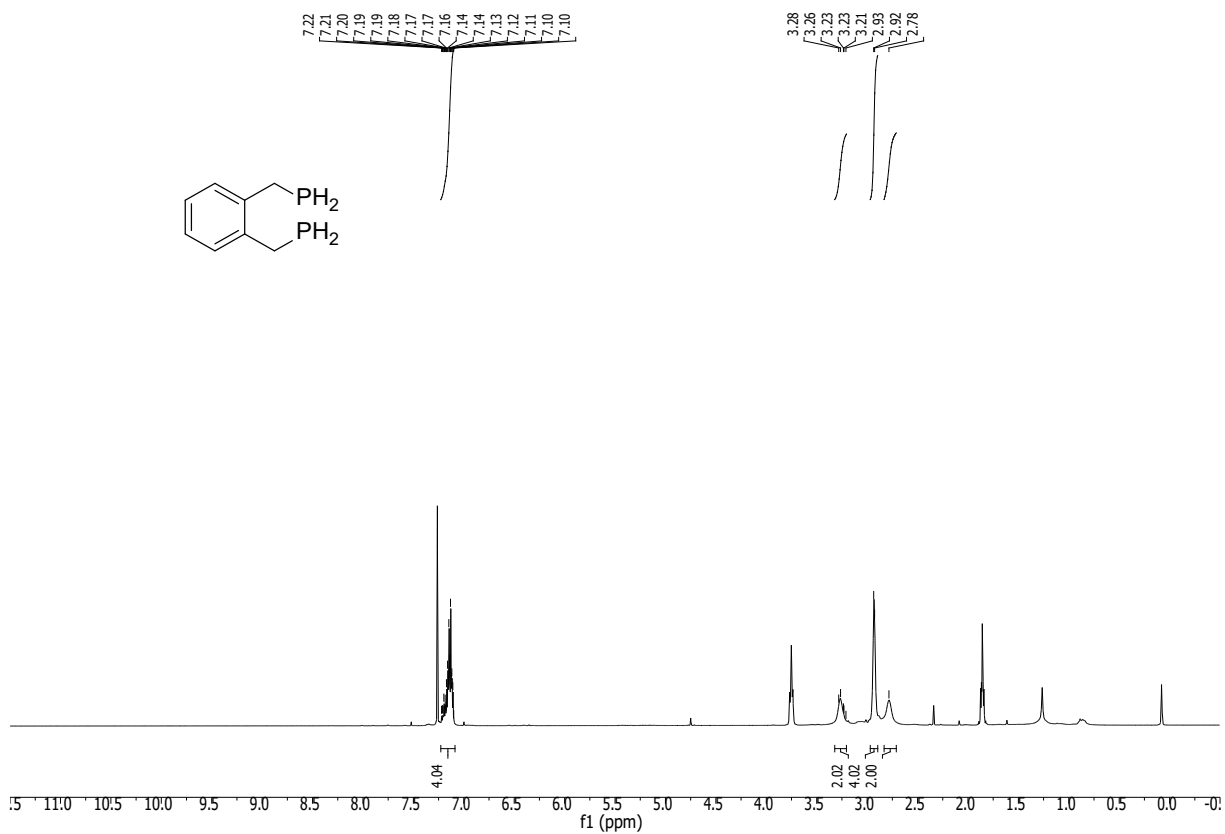
**$^1\text{H-NMR}$**  (400 MHz,  $\text{CDCl}_3$ )  $\delta_{\text{H}}$  (ppm): 7.22–7.10 (m, 4H), 3.03 (dt, 4H), 2.93–2.91 (m, 4H) and solvent impurities

**$^{13}\text{C-NMR}$**  (101 MHz,  $\text{CDCl}_3$ )  $\delta_{\text{C}}$  (ppm): 139.3 ,129.4 (m), 126.7, 18.0 and solvent impurities

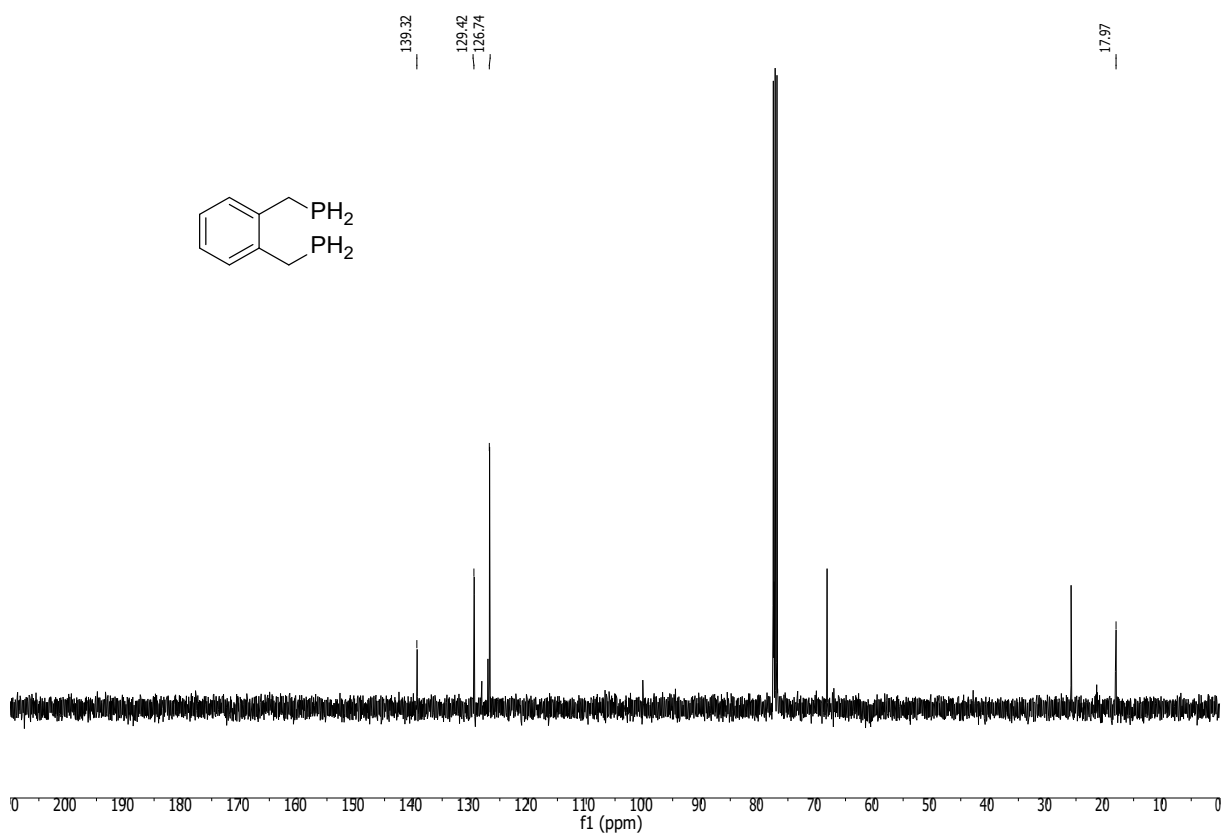
**$^{31}\text{P-NMR}$**  (161 MHz,  $\text{CDCl}_3$ )  $\delta_{\text{C}}$  (ppm): -125.5

## Experimental section

$^1\text{H-NMR}$ : (400 MHz,  $\text{CDCl}_3$ ) of **L2-b**

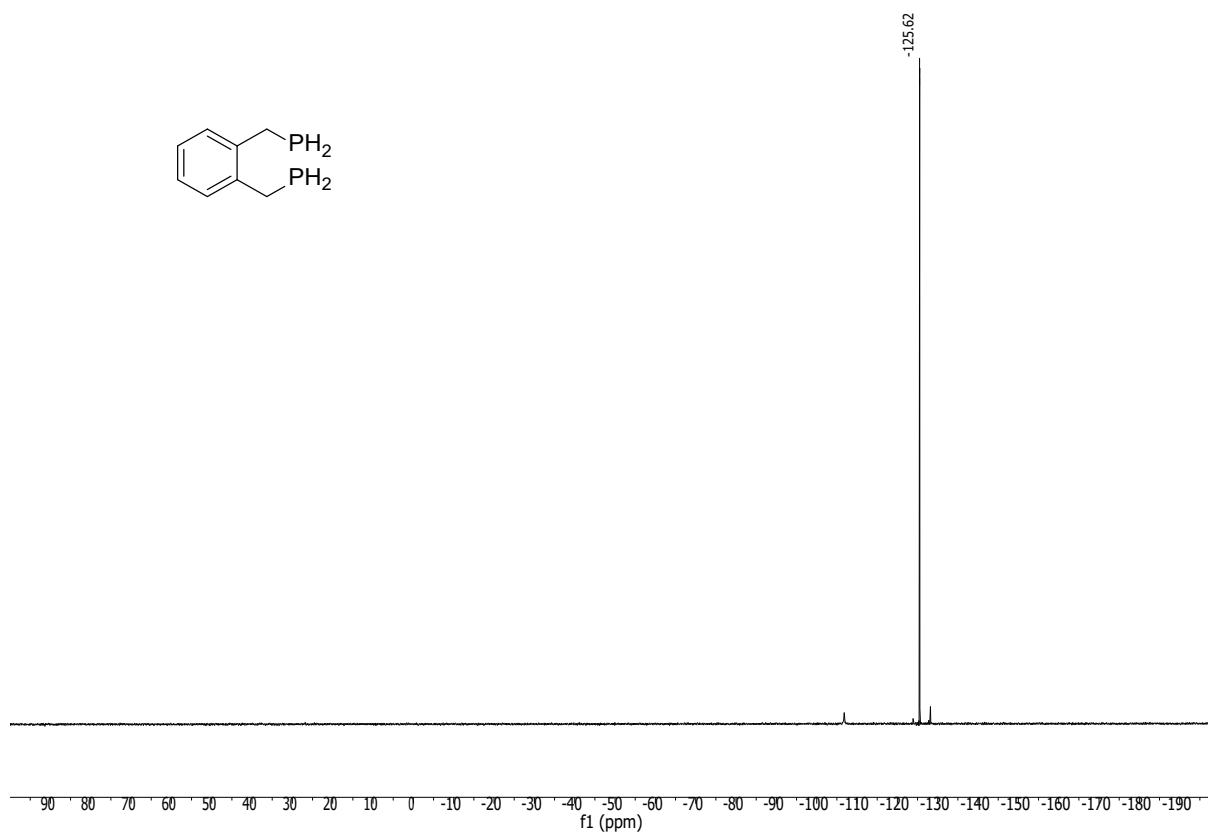
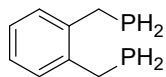


$^{13}\text{C-NMR}$ : (101 MHz,  $\text{CDCl}_3$ ) of **L2-b**

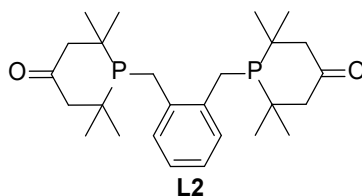




$^{31}\text{P}$ -NMR: (161 MHz,  $\text{CDCl}_3$ ) of **L2-b**



**Synthesis of 1,2-Bis(4-phosphorinone)xylene (L2)**

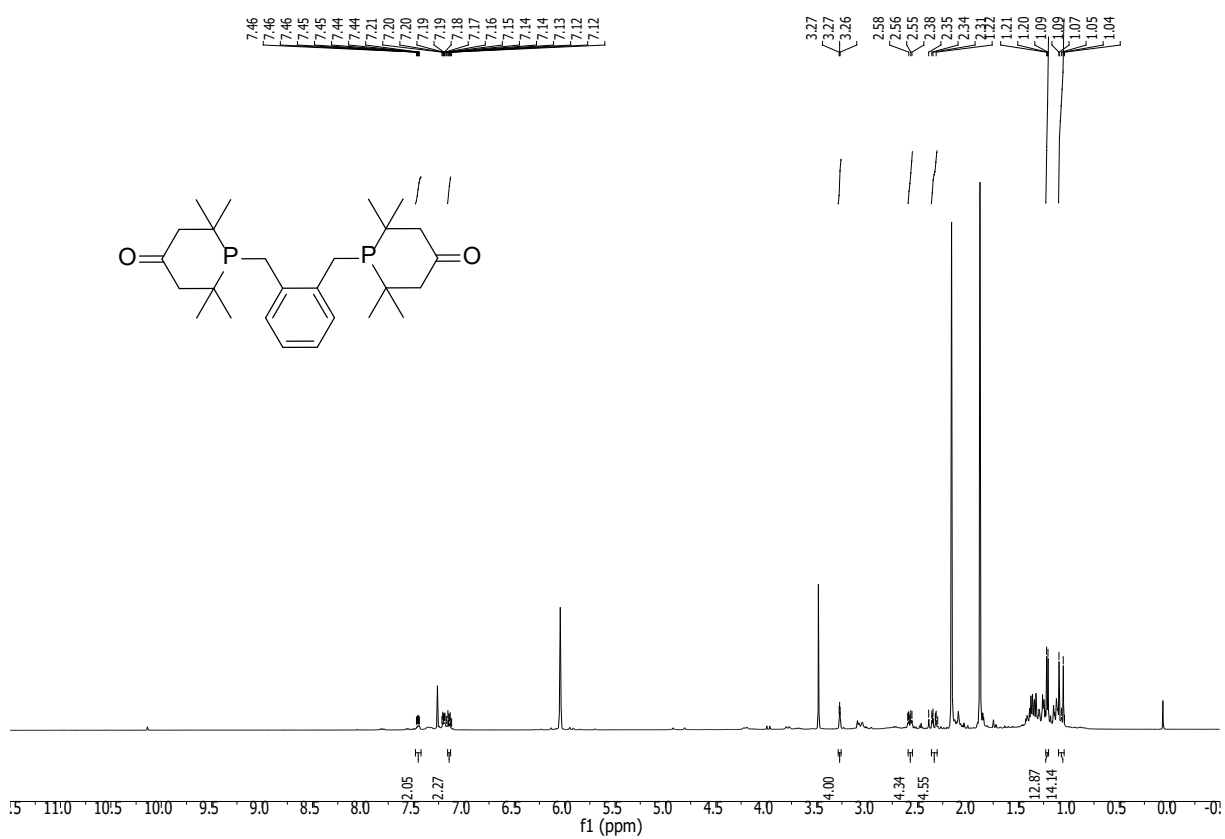


According to the literature procedure, 1,2-Bis(phosphinomethyl)benzene (0.77 g, 4.52 mmol, 1.00 equiv.) and phorone (1.55 g, 1.76 mL, 11.3 mmol, 2.50 equiv.) were added in a argon-filled flask and stirred for 22h at 120°C. The resulted oil was crystallized at 0°C and triturated with methanol for 16h. The solvent was distilled under vacuum and the brut resulted oil was analyzed by <sup>1</sup>H and <sup>31</sup>P NMR. Unfortunately, the purification attempts were unsuccessful, therefore the yield could not pe determined.  
 $C_8H_{12}P_2$  (170.13 g/mol)

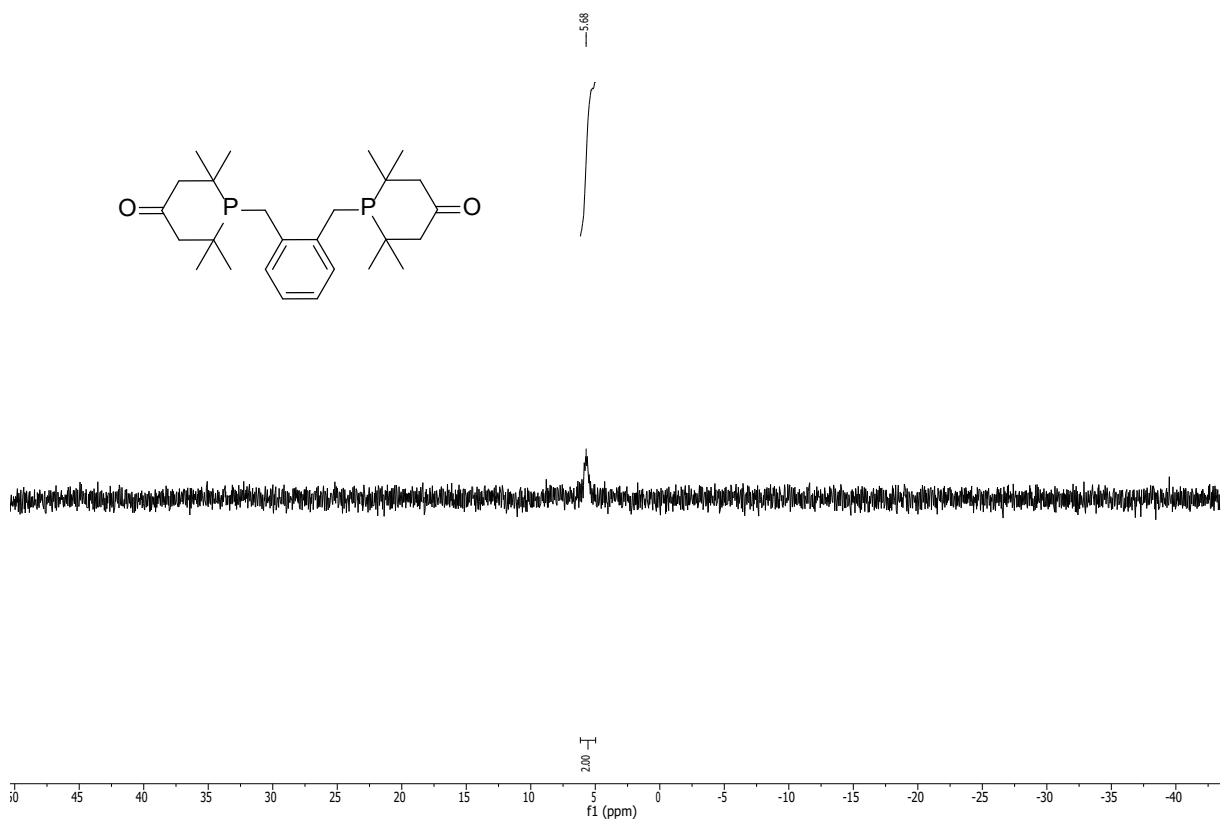
**<sup>1</sup>H-NMR** (400 MHz, CDCl<sub>3</sub>)  $\delta_H$  (ppm): 7.46–7.44 (m, 2H), 7.19–7.12 (m, 2H), 3.27–3.25 (m, 4H), 2.58–2.55 (m, 4H), 2.38–2.31 (m, 4H), 1.21 (d, 12H), 1.07 ppm (d, 12H)

**<sup>31</sup>P-NMR** (161 MHz, CDCl<sub>3</sub>)  $\delta_C$  (ppm): 5.66

$^1\text{H-NMR}$ : (400 MHz,  $\text{CDCl}_3$ ) of **L2**



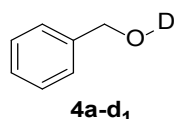
$^{31}\text{P-NMR}$ : (161 MHz,  $\text{CDCl}_3$ ) of **L2**



## Results of the mechanistic studies

### Synthesis of deuterated starting materials

#### Benzenemethanol-*d* (**4a-d<sub>1</sub>**)



In a round-bottom flask benzyl alcohol (**4a**) (1.04 mL, 1.08 g, 10.0 mmol) were dissolved in 10 mL D<sub>2</sub>O. The reaction was stirred under air at room temperature for 48 h. After the completion of the reaction, the mixture was extracted with ethyl acetate (3 × 10 mL) and the organic phases were washed with brine (3 × 10 mL), dried over Na<sub>2</sub>SO<sub>4</sub>, and filtered. The solvent was evaporated under reduced pressure yielding the product in quantitative yield without any further purification needed. Analytical data was in accordance with the literature.<sup>28</sup>

C<sub>7</sub>H<sub>7</sub>DO (109,06 g/mol)

**R<sub>f</sub>**: 0.27 (5:1 Hex:EtOAc)

**<sup>1</sup>H-NMR**: (700 MHz, CDCl<sub>3</sub>): δ/ppm = 7.38-7.36 (dd, *J* = 4.2, 1.1 Hz, 4H), 7.32 – 7.29 (m, 1H), 4.69 (s, 2H).

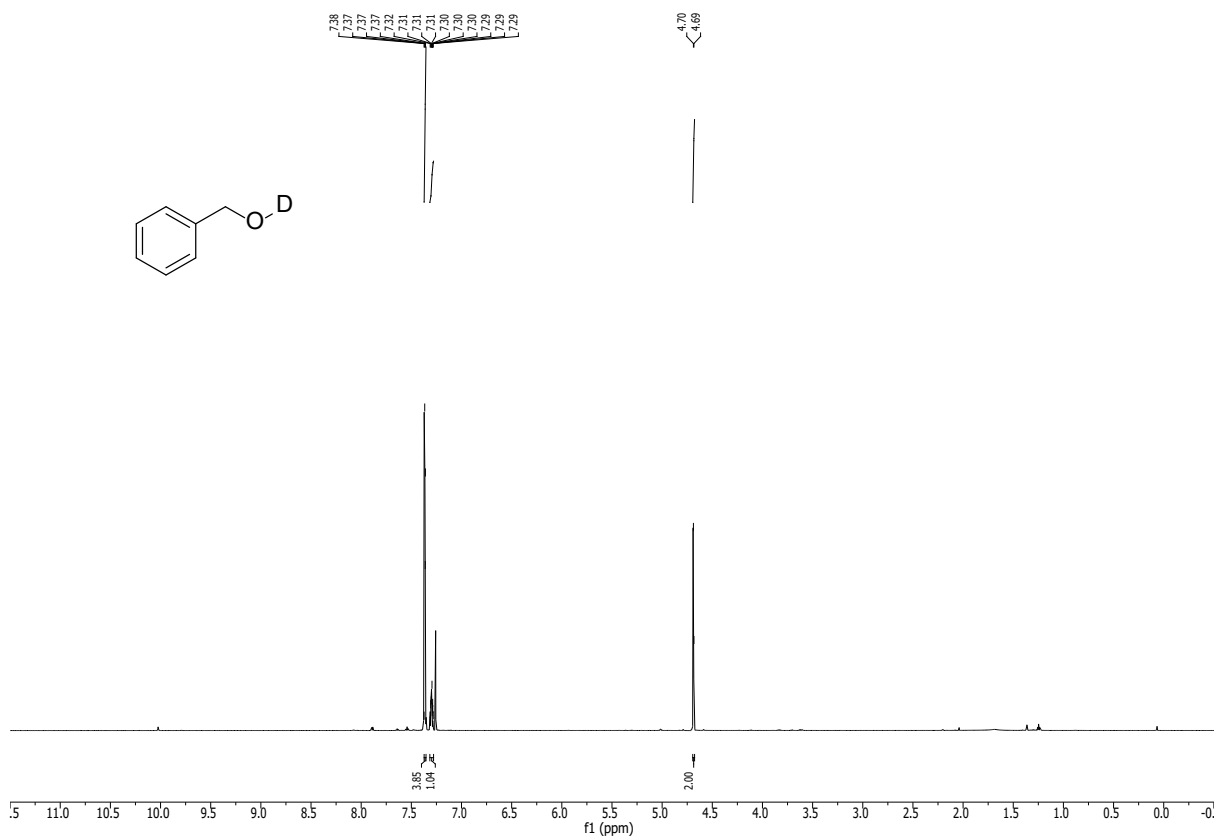
**<sup>2</sup>H-NMR**: (107 MHz, CDCl<sub>3</sub>): δ/ppm = 2.17 (bs)

**<sup>13</sup>C-NMR**: (101 MHz, CDCl<sub>3</sub>): δ/ppm = 140.9, 128.1, 127.8, 127.1, 65.5

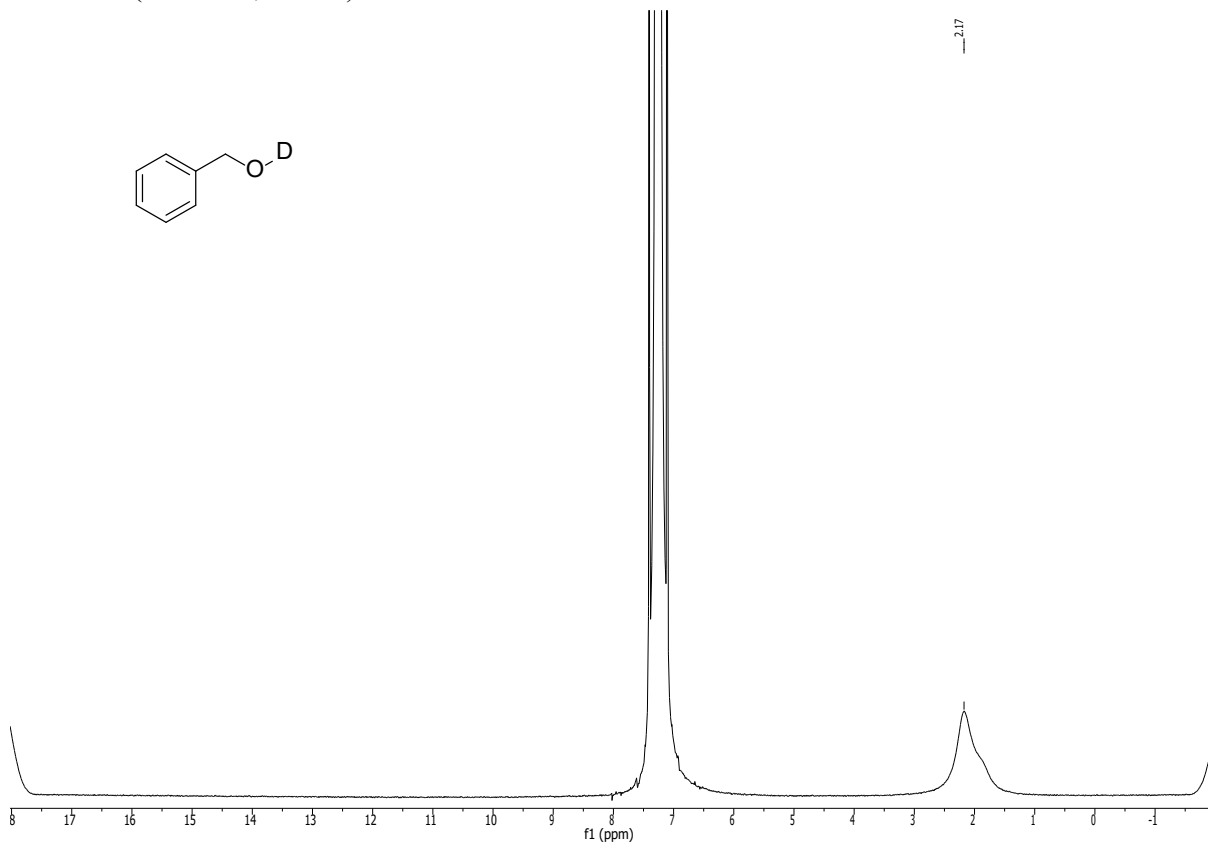
**GC-MS**: (EI): *m/z* = 109.1 (92, [M<sup>+</sup>]), 108.1 (100, [M<sup>+</sup>]-[H<sup>+</sup>]), 80.1 (71, [M<sup>+</sup>]-[<sup>•</sup>CH<sub>2</sub>-OD])

**IR**: (ATR,  $\tilde{\nu}$ , [cm<sup>-1</sup>]): 3326 (w), 3030 (w), 3030 (m), 2870 (m), 2467 (s), 1494 (m), 1453 (s), 1371 (s), 1207 (m), 1006 (s), 846 (m), 730 (s), 693 (s)

$^1\text{H-NMR}$ : (700 MHz,  $\text{CDCl}_3$ ) of **4a-d<sub>1</sub>**



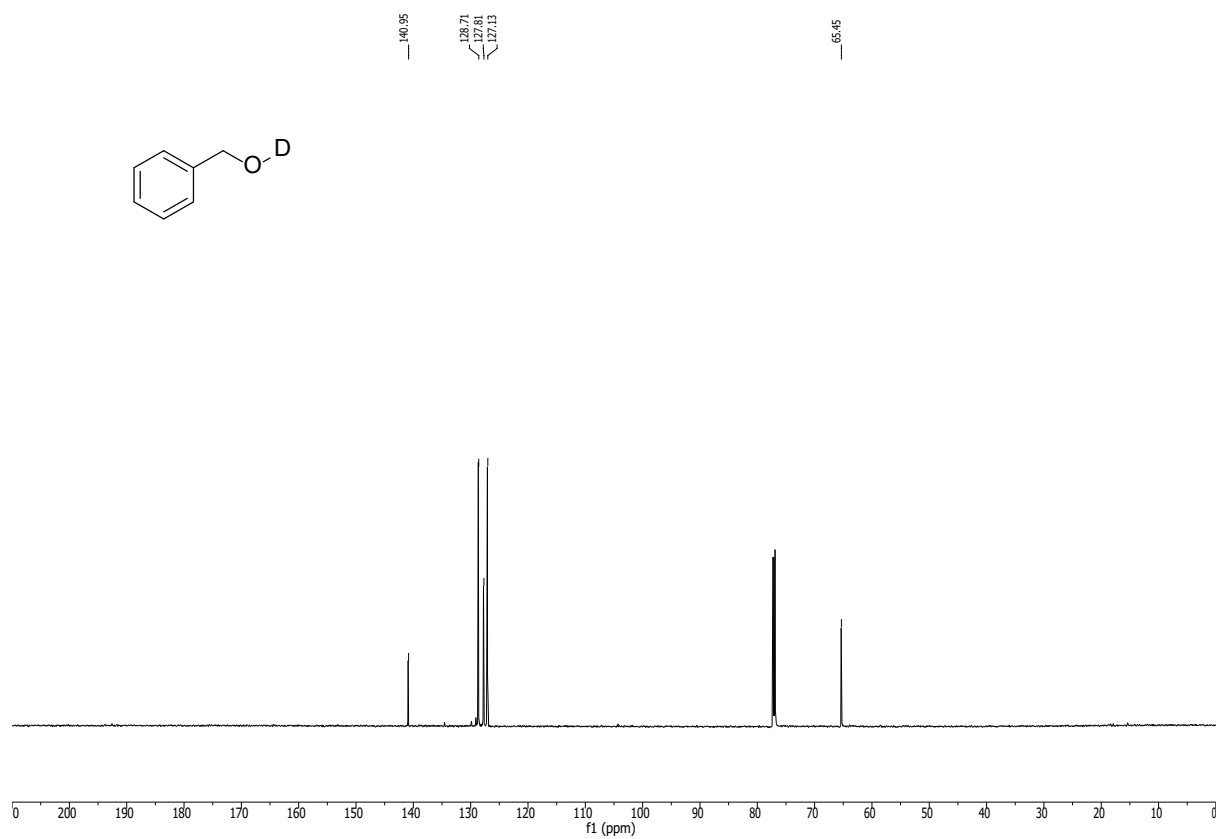
$^2\text{H-NMR}$ : (107 MHz,  $\text{CDCl}_3$ ) of **4a-d<sub>1</sub>**

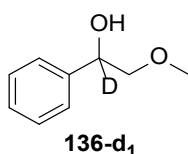


## Experimental section

---

$^{13}\text{C}$ -NMR: (101 MHz,  $\text{CDCl}_3$ ) of **4a-d<sub>1</sub>**



**2-methoxy-1-phenylethan-1-*d*-1-ol (136-*d*<sub>1</sub>)**

In a 100 mL round bottom flask 2-methoxy-1-phenylethanone (751 mg, 5.00 mmol, 1.00 equiv.) was dissolved in methanol-*d* (20 mL) and cooled in an ice bath. Then NaBD<sub>4</sub> (418 mg, 10.0 mmol, 2.00 equiv.) was added in portions. Upon complete addition the solution was allowed to warm to ambient temperature and was stirred until the completion of the reaction was confirmed by TLC. After 16 h the solution was cooled in an ice bath and quenched with ice and water. Then, methanol was removed under reduced pressure and the mixture was extracted with DCM (3 × 10 mL). The collected organic phases were washed with brine (3 × 10 mL), dried over Na<sub>2</sub>SO<sub>4</sub>, and filtered. The solvent was evaporated, and the respective alcohol was obtained and used without further purification. Analytical data was in accordance with the literature.<sup>29</sup>

C<sub>9</sub>H<sub>11</sub>DO<sub>2</sub> (153,2 g/mol)

**R<sub>f</sub>**: 0.23 (4:1 Hex:EtOAc)

**<sup>1</sup>H-NMR**: (700 MHz, CDCl<sub>3</sub>): δ/ppm 7.41 – 7.34 (m, 4H), 7.32 – 7.28 (m, 1H), 3.55 – 3.42 (m, 2H), 3.44 (s, 3H).

**<sup>2</sup>H-NMR**: (107 MHz, CDCl<sub>3</sub>): δ/ppm = 4.90 (s)

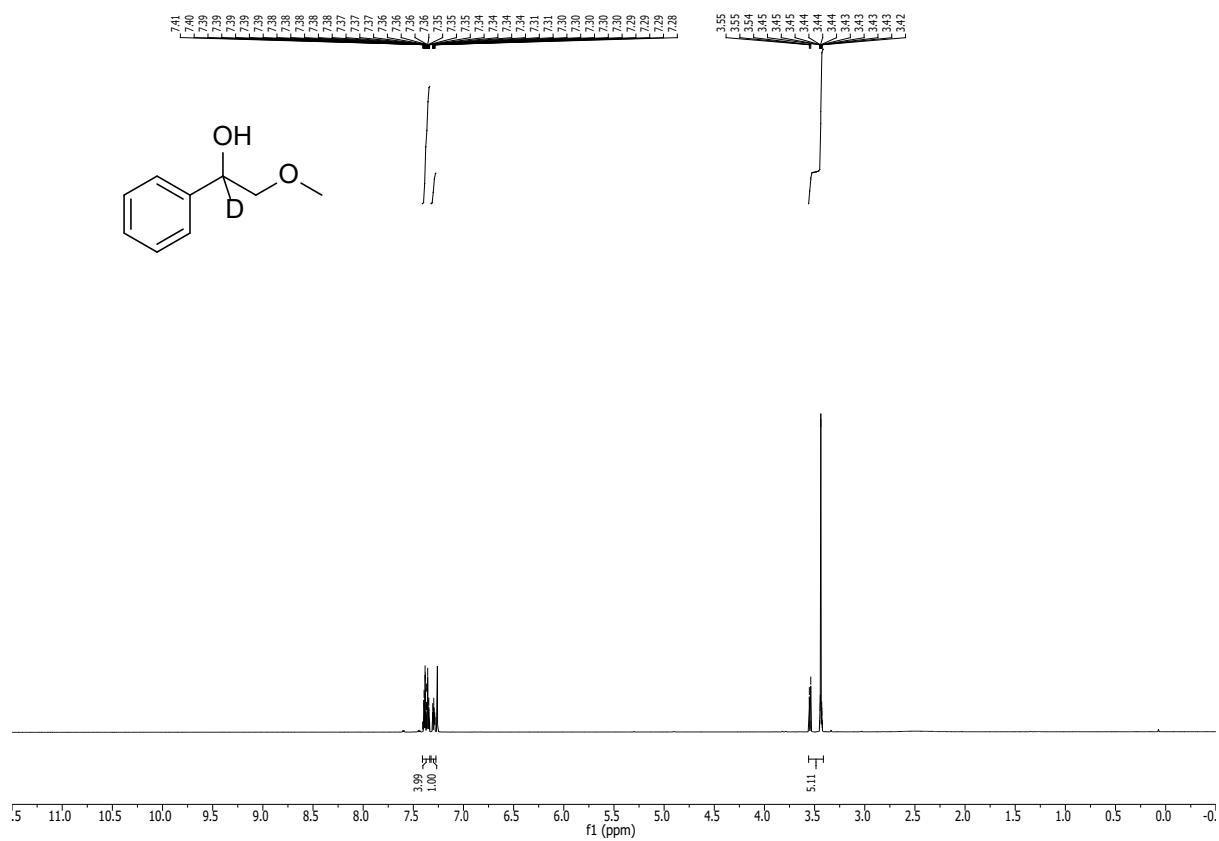
**<sup>13</sup>C-NMR**: (101 MHz, CDCl<sub>3</sub>): δ/ppm = 140.3, 128.5, 128.0, 126.3, 78.2, 72.2 (t, *J* = 22.2 Hz), 59.2.

**GC-MS**: (EI): *m/z* = 109.1 (92, [M<sup>+</sup>]-[H<sup>+</sup>]), 108.1 (100, [M<sup>+</sup>]-[C<sub>2</sub>H<sub>5</sub>O<sup>+</sup>]), 92.1 (71, [M<sup>+</sup>]-[C<sub>2</sub>H<sub>5</sub>O<sup>+</sup>]-[OH<sup>+</sup>])

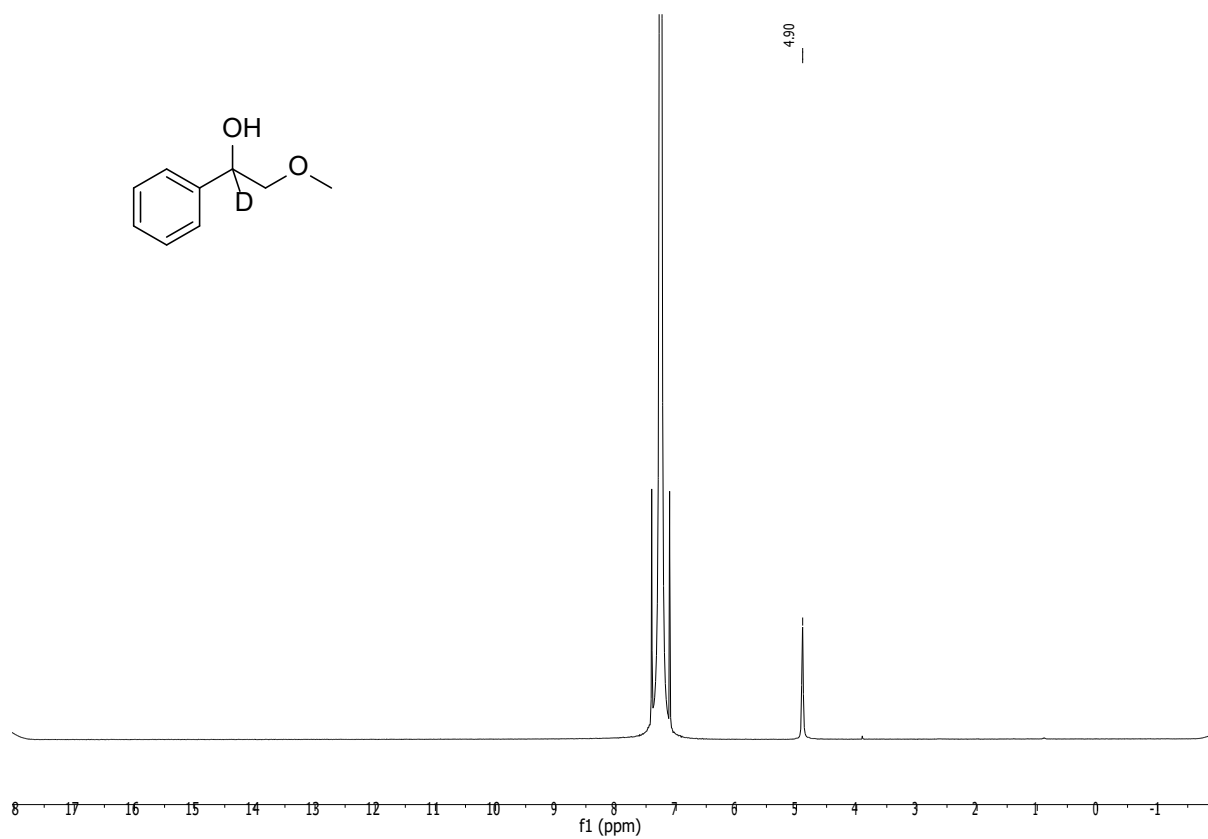
**IR**: (ATR,  $\tilde{\nu}$ , [cm<sup>-1</sup>]): 3421 (w), 2926 (w), 2885 (m), 2825 (w), 1490 (m), 1446 (s), 1196 (s), 1103 (s), 946 (s), 752 (s)

## Experimental section

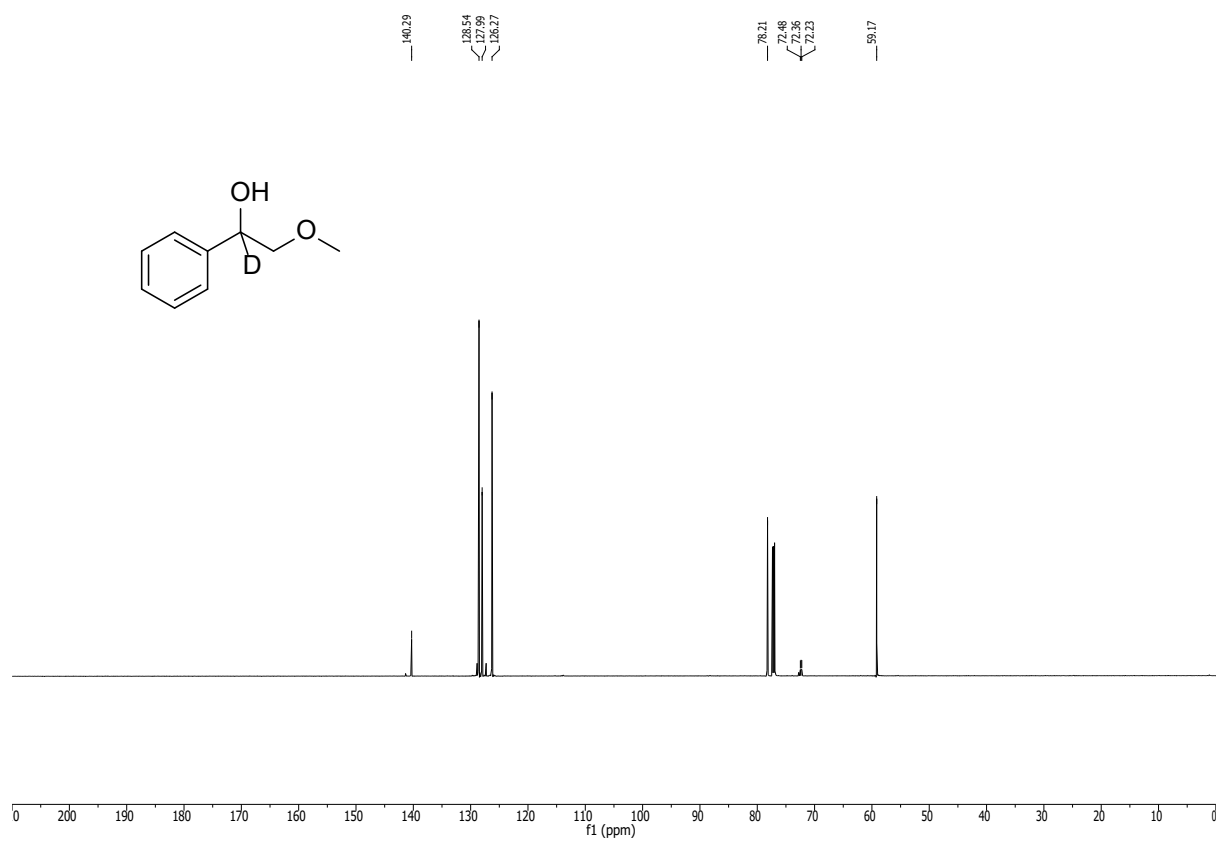
$^1\text{H-NMR}$ : (700 MHz,  $\text{CDCl}_3$ ) of **136-d<sub>1</sub>**

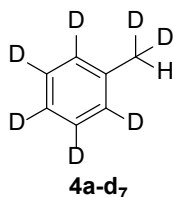


$^2\text{H-NMR}$ : (107 MHz,  $\text{CDCl}_3$ ) of **136-d<sub>1</sub>**





$^{13}\text{C}$ -NMR: (101 MHz,  $\text{CDCl}_3$ ) of **136-d<sub>1</sub>**

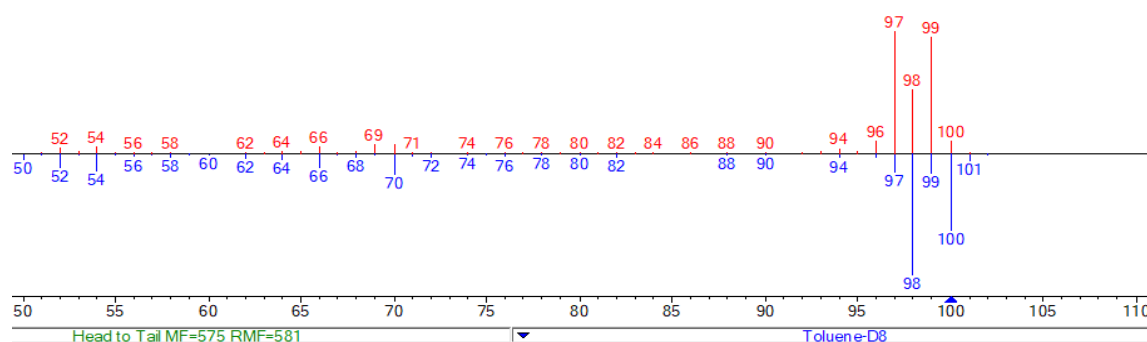
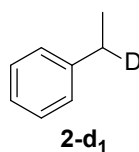
**1-(methyl-d<sub>2</sub>)benzene-2,3,4,5,6-d<sub>5</sub> (4a-d<sub>7</sub>)**


According to **GP4**, 1-(methyl-d<sub>2</sub>)benzene-2,3,4,5,6-d<sub>5</sub> (**4a-d<sub>7</sub>**) was synthesized from benzyl alcohol-d<sub>7</sub> (0.110 mL, 115 mg, 1.00 mmol, 1.00 equiv.) over 16 h. The product was afforded in 48% yield and 99% < D incorporation at the methyl group, both determined by GC-FID. The comparison with the literature available toluene-d<sub>8</sub> GC-MS chromatogram shows a very low matching factor.

C<sub>7</sub>HD<sub>7</sub> (99.11 g/mol)

**GC-FID:** R<sub>t</sub> = 4.213 (**M<sub>FID2</sub>**)

**GC-MS:** (EI): m/z = 100.1 (12, [M<sup>+</sup>]), 99.1 (100, [M<sup>+</sup>]-[C<sub>2</sub>H<sub>5</sub><sup>+</sup>]); 97.1 (98, [M<sup>+</sup>]-[C<sub>3</sub>H<sub>7</sub><sup>+</sup>]); R<sub>t</sub> = 4.750 (**M<sub>MS3</sub>**)

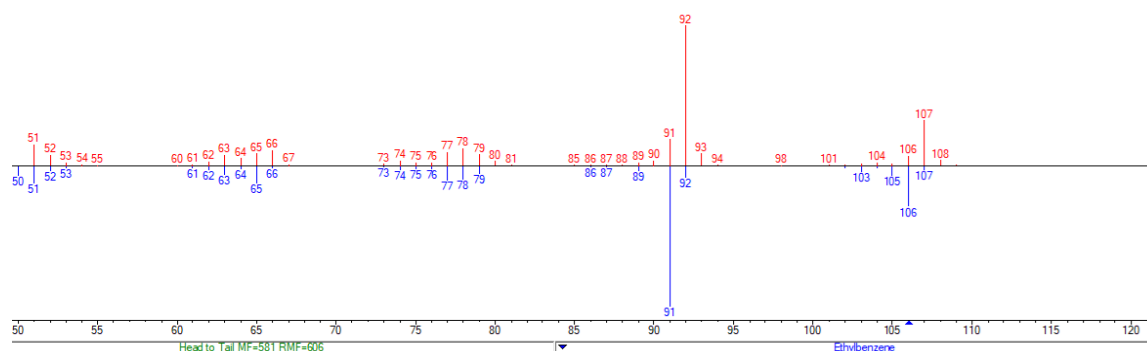

**(ethyl-1-d)benzene (2-d<sub>1</sub>)**


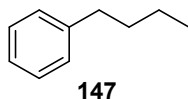
According to **GP4**, (ethyl-1-d)benzene (**2-d<sub>1</sub>**) was synthesized from benzyl alcohol-d<sub>7</sub> (0.141 mL, 153 mg, 1.00 mmol, 1.00 equiv.) over 16 h. The product was afforded in 77% yield and 99% < D incorporation at the methylene group, both determined by GC-FID. The comparison with the literature available ethyl benzene GC-MS chromatogram shows a very low matching factor.

C<sub>8</sub>H<sub>9</sub>D (107.17 g/mol)

**GC-FID:** R<sub>t</sub> = 3.328 (**M<sub>FID1</sub>**)

**GC-MS:** (EI): m/z = 107.1 (35, [M<sup>+</sup>]), 92.1 (100, [M<sup>+</sup>]-[CH<sub>3</sub><sup>+</sup>]); R<sub>t</sub> = 6.985 (**M<sub>MS2</sub>**)



**Radical clock reactions*****n*-Butylbenzene (147)**

*n*-Butylbenzene (**147**) was synthesized from  $\alpha$ -cyclopropylbenzyl alcohol (**146**) (0.130 mL, 148 mg, 1.00 mmol, 1.00 equiv.) over 16 h. The product was isolated by column chromatography (hexane/ethyl acetate 98:2) and was afforded as a colorless liquid (67 mg, 0.50 mmol, 50%, 69% determined by GC-FID). Analytical data was in accordance with the literature.<sup>30</sup>

C<sub>10</sub>H<sub>14</sub> (134.20 g/mol)

**R<sub>f</sub>**: 0.78 (98:2 Hex:EtOAc)

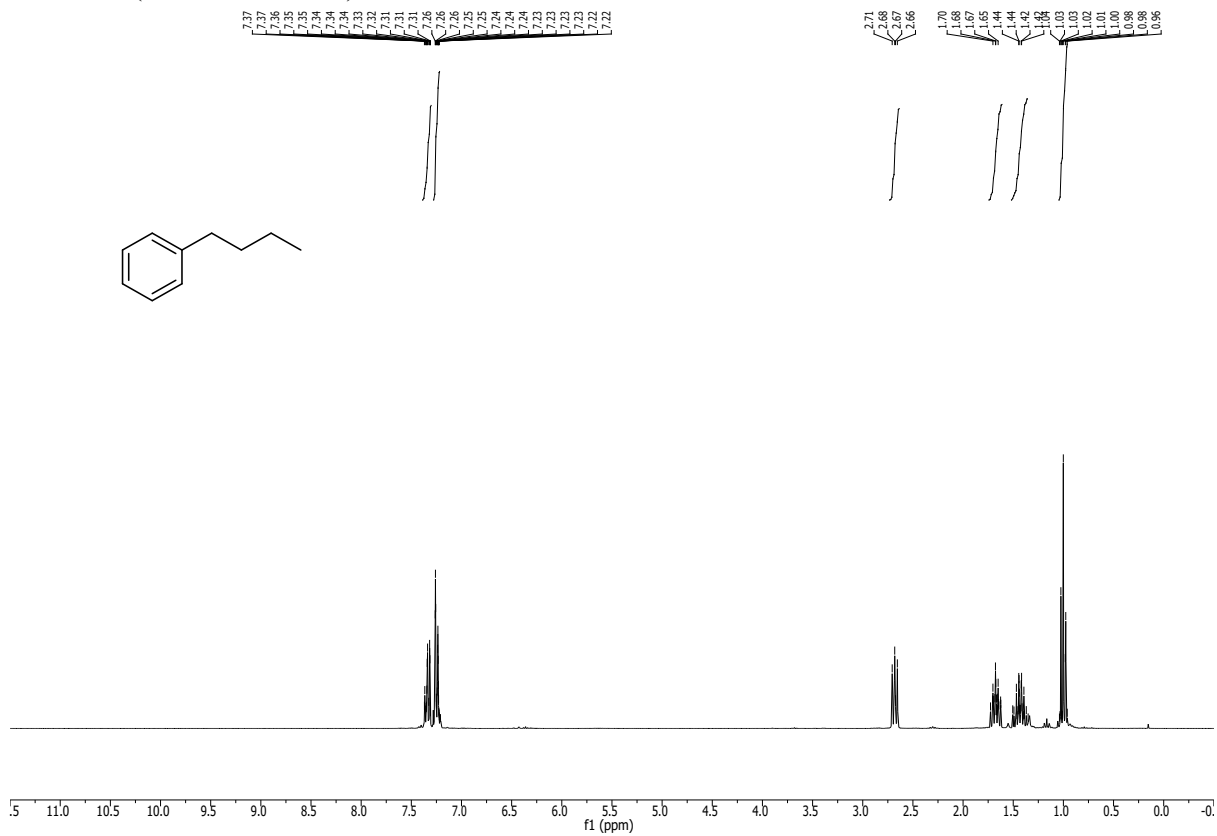
**<sup>1</sup>H-NMR**: (400 MHz, CDCl<sub>3</sub>):  $\delta$ /ppm 7.39 – 7.30 (m, 2H), 7.28 – 7.22 (m, 3H), 2.69 (t, J = 7.3 Hz, 2H), 1.70 – 1.62 (m, 2H), 1.44 – 1.36 (m, 2H), 0.99 (t, J = 7.3 Hz, 3H).

**<sup>13</sup>C-NMR**: (101 MHz, CDCl<sub>3</sub>):  $\delta$ /ppm = 143.0, 128.6, 128.4, 125.7, 35.8, 33.8, 22.5, 14.1.

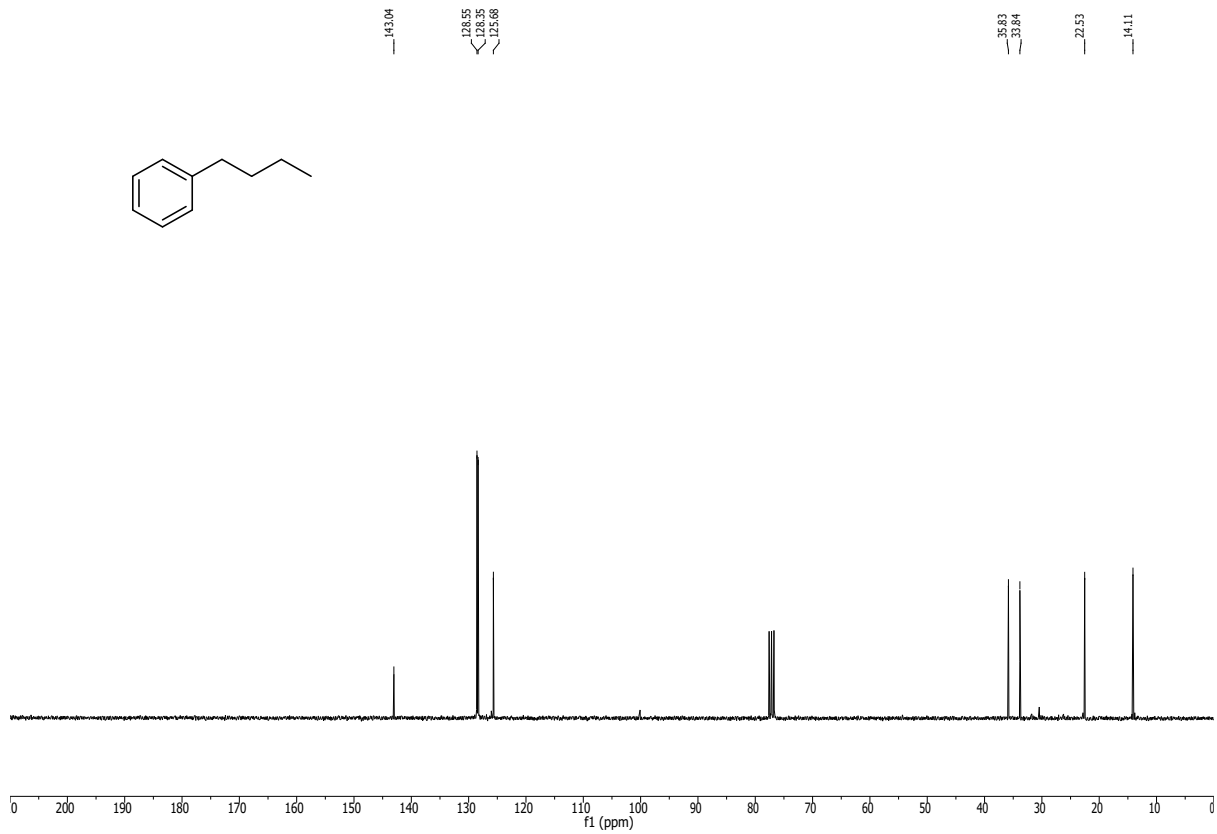
**GC-MS**: (EI):  $m/z$  = 133.9 (92, [M<sup>+</sup>]), 104.9 (100, [M<sup>+</sup>]-[C<sub>2</sub>H<sub>5</sub><sup>+</sup>]), 90.9 (71, [M<sup>+</sup>]-C<sub>3</sub>H<sub>7</sub><sup>+</sup>)

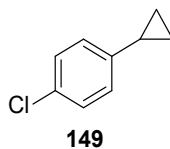
## Experimental section

$^1\text{H-NMR}$ : (400 MHz,  $\text{CDCl}_3$ ) of **147**



$^{13}\text{C-NMR}$ : (100 MHz,  $\text{CDCl}_3$ ) of **147**



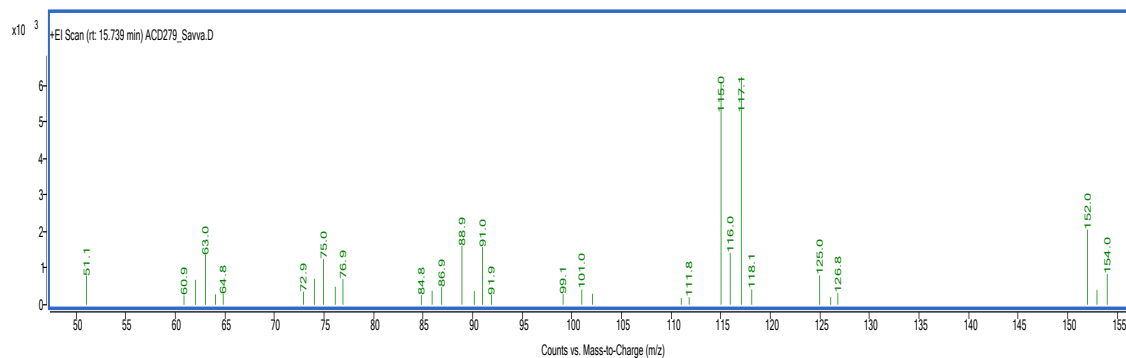
**1-chloro-4-cyclopropylbenzene (150)**

According to **GP4**, 1-chloro-4-cyclopropylbenzene (**150**) was synthesized from 1-(4-chlorophenyl)cyclopropanol (**149**) (168 mg, 1.00 mmol, 1.00 equiv.) over 16 h. The product was afforded in traces determined by GC-FID.

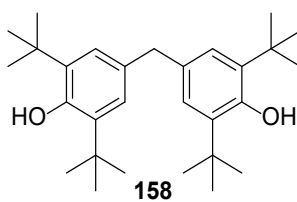
$C_8H_{18}$  (152.62 g/mol)

**GC-FID:**  $R_t = 8.469$  (**M<sub>FID1</sub>**)

**GC-MS:** (EI):  $m/z = 154.1$  (12,  $[M^{+}]$ ), 152.1 (37,  $[M^{+}]$ ); 117.1 (100,  $[M^{+}]-[Cl^{\cdot}]$ ), 115.1 (97,  $[M^{+}]-[Cl^{\cdot}]-2[H^{\cdot}]$ ), 111.8 (97,  $[M^{+}]-[C_3H_5^{\cdot}]$ );  $R_t = 15.739$  (**M<sub>MS3</sub>**)

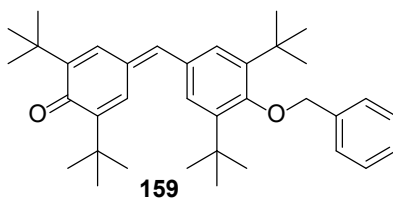
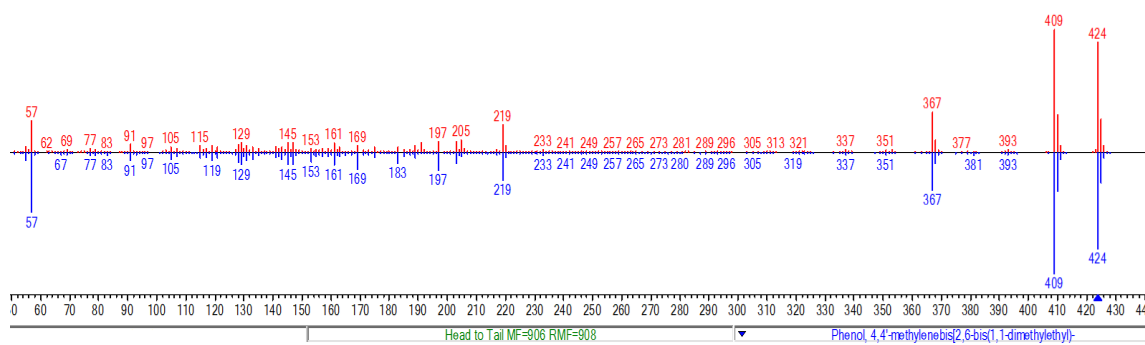


*Radical scavengers experiments – Galvinoxyl adducts*



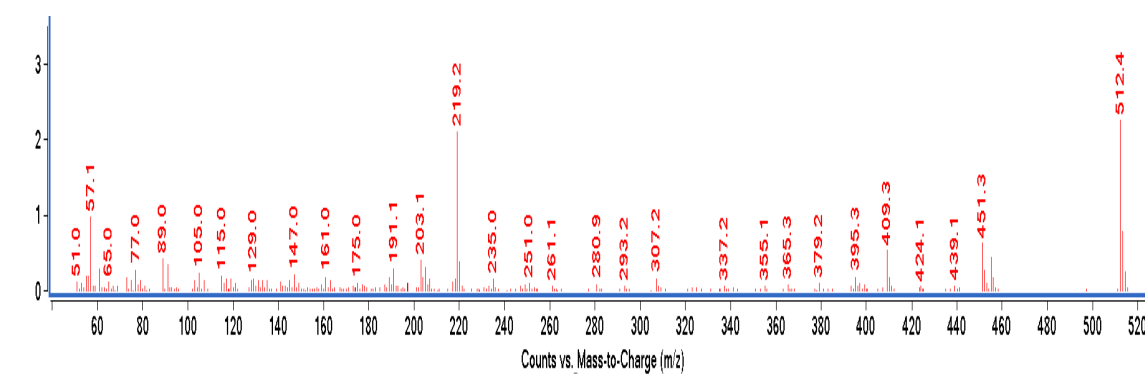
Exact Mass: 424.33

GC-MS (EI): 424.34



Exact Mass: 512.37

GC-MS (EI): 512.38

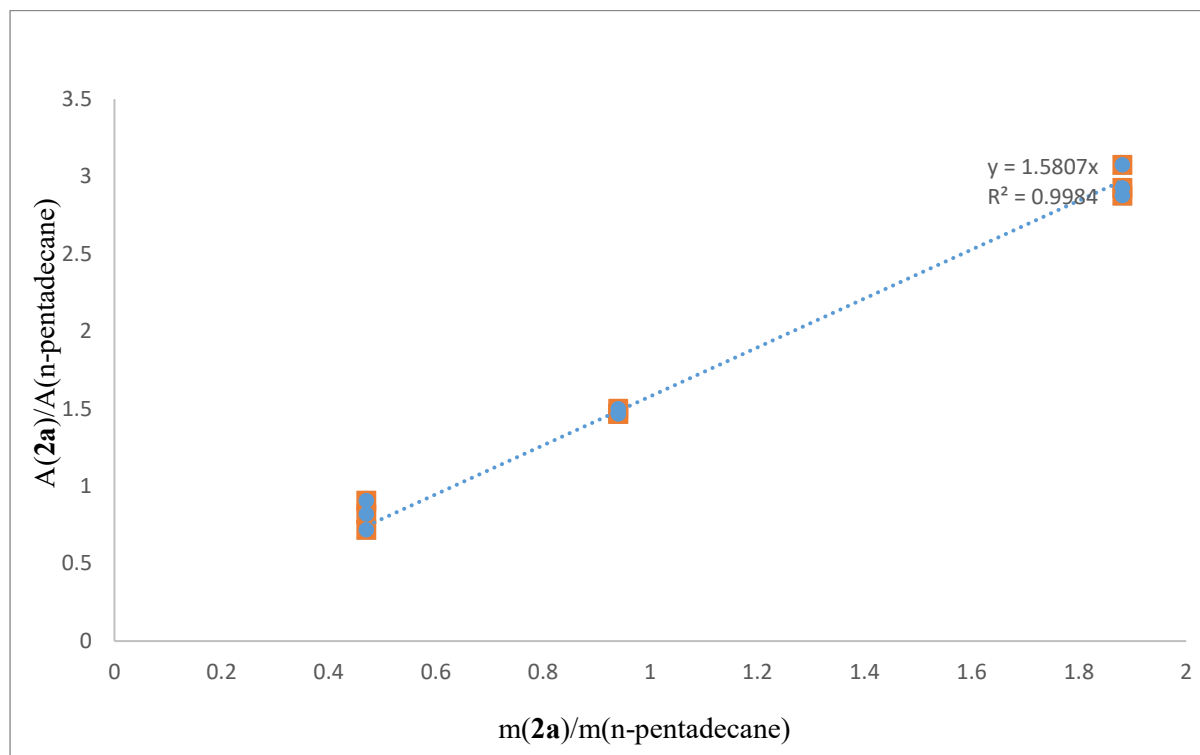


### 8.10. Calibration Data for GC-FID Analysis

GC calibration was performed by measuring samples with known amounts of analyte (here toluene) and internal standard (here n-pentadecane) (Table 8). Plotting of the area ratio of the two components versus the ratio of the respective masses leads to a calibration function which is used to calculate unknown amounts of analyte in samples taken from catalytic reactions.

Calibration line for toluene (**2a**)

Sample	Mass ( <b>2a</b> ) (mg)	Mass (n-pentadecane) (mg)	Area ( <b>2a</b> ) (pAs)	Area (n-pentadecane) (pAs)
1.1 Tol	1.5	3.19	7077	7800
1.2 Tol	1.5	3.19	7321	8924
1.3 Tol	1.5	3.19	6350	8848
2.1 Tol	3	3.19	12762	8703
2.2 Tol	3	3.19	13314	8875
2.3 Tol	3	3.19	13363	9093
3.1 Tol	4.5	3.19	25018	8697
3.2 Tol	4.5	3.19	26627	9100
3.3 Tol	4.5	3.19	26372	8578



**8.11. References**

1. S. E. Stein, *National Institute of Standards and Technology*, 2008, **NIST Standard Reference Database User's Guide**.
2. B. Ciszek and I. Fleischer, *Chem. Eur. J.*, 2018, **24**, 12259-12263.
3. S. M. Baghbanian, S. Khaksar, S. M. Vahdat, M. Farhang and M. Tajbakhsh, *Chinese Chemical Letters*, 2010, **21**, 563-567.
4. T. Suga, S. Shimazu and Y. Ukaji, *Org. Lett.*, 2018, **20**, 5389-5392.
5. M. P. Crockett, A. S. Wong, B. Li and J. A. Byers, *Angew. Chem. Int. Ed.*, 2020, **59**, 5392-5397.
6. G. Dilauro, A. Francesca Quivelli, P. Vitale, V. Capriati and F. M. Perna, *Angew. Chem. Int. Ed.*, 2019, **58**, 1799-1802.
7. W. Liu, J. Li, P. Querard and C.-J. Li, *J. Am. Chem. Soc.*, 2019, **141**, 6755-6764.
8. A. K. Clarke, A. Parkin, R. J. K. Taylor, W. P. Unsworth and J. A. Rossi-Ashton, *ACS Catal.*, 2020, **10**, 5814-5820.
9. T. de Haro and C. Nevado, *J. Am. Chem. Soc.*, 2010, **132**, 1512-1513.
10. H. D. S. Guerrand, L. D. Marciasini, M. Jousseau, M. Vaultier and M. Pucheault, *Eur. J. Chem.*, 2014, **20**, 5573-5579.
11. A. Tuley, Y.-S. Wang, X. Fang, Y. Kurra, Y. H. Rezenom and W. R. Liu, *Chem. Commun.*, 2014, **50**, 2673-2675.
12. S. G. Newman, L. Gu, C. Lesniak, G. Victor, F. Meschke, L. Abahmane and K. F. Jensen, *Green Chem.*, 2014, **16**, 176-180.
13. R. B. Bedford, N. J. Gower, M. F. Haddow, J. N. Harvey, J. Nunn, R. A. Okopie and R. F. Sankey, *Angew. Chem. Int. Ed.*, 2012, **51**, 5435-5438.
14. K. Morimoto, M. Itoh, K. Hirano, T. Satoh, Y. Shibata, K. Tanaka and M. Miura, *Angew. Chem. Int. Ed.*, 2012, **51**, 5359-5362.
15. A. T. Murray and Y. Surendranath, *ACS Catal.*, 2017, **7**, 3307-3312.
16. C.-T. Yang, Z.-Q. Zhang, Y.-C. Liu and L. Liu, *Angew. Chem. Int. Ed.*, 2011, **50**, 3904-3907.
17. Y. Mao, Y. Liu, Y. Hu, L. Wang, S. Zhang and W. Wang, *ACS Catal.*, 2018, **8**, 3016-3020.
18. S. Mao, Z. Chen, L. Wang, D. B. Khadka, M. Xin, P. Li and S.-Q. Zhang, *J. Org. Chem.*, 2019, **84**, 463-471.
19. S. Mavila, B. T. Worrell, H. R. Culver, T. M. Goldman, C. Wang, C.-H. Lim, D. W. Domaille, S. Pattanayak, M. K. McBride, C. B. Musgrave and C. N. Bowman, *J. Am. Chem. Soc.*, 2018, **140**, 13594-13598.
20. M. B. Widegren and M. L. Clarke, *Org. Lett.*, 2018, **20**, 2654-2658.
21. K. Kuciński and G. Hreczycho, *Green Chem.*, 2019, **21**, 1912-1915.
22. S. Elangovan, C. Topf, S. Fischer, H. Jiao, A. Spannenberg, W. Baumann, R. Ludwig, K. Junge and M. Beller, *J. Am. Chem. Soc.*, 2016, **138**, 8809-8814.
23. J. Wang, W. Wan, H. Jiang, Y. Gao, X. Jiang, H. Lin, W. Zhao and J. Hao, *Org. Lett.*, 2010, **12**, 3874-3877.
24. K. Zhu, M. P. Shaver and S. P. Thomas, *Eur. J. Org. Chem.*, 2015, **2015**, 2119-2123.
25. S. Rostamnia and A. Morsali, *RSC Advances*, 2014, **4**, 10514-10518.
26. Á. Gutiérrez-Bonet, J. C. Tellis, J. K. Matsui, B. A. Vara and G. A. Molander, *ACS Catal.*, 2016, **6**, 8004-8008.
27. J. D. Nobbs, C. H. Low, L. P. Stubbs, C. Wang, E. Drent and M. van Meurs, *Organometallics*, 2017, **36**, 391-398.
28. M. Utsunomiya, R. Kondo, T. Oshima, M. Safumi, T. Suzuki and Y. Obora, *Chem. Commun.*, 2021, **57**, 5139-5142.
29. T. A. Schmidt, B. Ciszek, P. Kathe and I. Fleischer, *Chem. Eur. J.*, 2020, **26**, 3641-3646.
30. J. H. Docherty, J. Peng, A. P. Dominey and S. P. Thomas, *Nat. Chem.*, 2017, **9**, 595-600.



## 9. Appendix

### 9.1. List of Abbreviations

<b>2-MeTHF</b>	2-methyltetrahydrofuran	<b>acac</b>	acetylacetonate
<b>AIBN</b>	azobisisobutyronitrile	<b>aq</b>	aqueous
<b>Ar</b>	aryl	<b>BDE</b>	bond dissociation energy
<b>BHT</b>	butylated hydroxytoluene	<b>BINOL</b>	1,1'-bi-2-naphthol
<b>B-M</b>	Barton-McCombie deoxygenation	<b>Bn</b>	benzyl
<b>bpx</b>	bis(phosphorinone)xylene	<b>Bz</b>	benzoyl
<b>C.S.</b>	conditions set	<b>CCB</b>	calcium channels blockers
<b>CCC</b>	C,C,C-tridentate Pincer ligand	<b>Cp</b>	cyclopentadienyl
<b>CzIPN</b>	1,2,3,5-tetrakis(carbazol-9-yl)- 4,6-dicyanobenzene, 2,4,5,6- tetrakis(9H-carbazol-9-yl) isophthalonitrile	<b>DCE</b>	1,2-dichloroethane
<b>DCE</b>	1,2-dichloroethane		
<b>DCM</b>	dichloromethane	<b>DCT</b>	dibenzo[a,e]cyclooctatetraene
<b>DDQ</b>	2,3-dichloro-5,6-dicyano-1,4- benzoquinone	<b>DFT</b>	density functional theory
<b>DG</b>	directing group	<b>DHP</b>	dihydropyridines
<b>DI</b>	deuterium incorporation	<b>Dmpe</b>	1,2-bis(dimethylphosphino)ethane
<b>DMSO</b>	dimethylsulfoxide	<b>DPAFIPN</b>	2,4,6-Tris(diphenylamino)-5- fluoroisophthalonitrile
<b>dppe</b>	1,2- bis(diphenylphosphino)ethane	<b>dppf</b>	1,1'- bis(diphenylphosphino)ferrocene
<b>dppm</b>	bis(diphenylphosphino)methane	<b>DTBMP</b>	2,6-di-tert-butyl-4-methylpyridine
<b>dtbpx</b>	$\alpha,\alpha'$ -bis(di-tert-butylphosphino)- ortho-xylene	<b>ee</b>	enantiomeric excess
<b>EPR</b>	electron paramagnetic resonance	<b>equiv</b>	equivalent
<b>Ery A</b>	erythromycin A	<b>ESR</b>	electron spin resonance spectroscopy
<b>ESR</b>	electron spin resonance spectroscopy	<b>Et</b>	ethyl
<b>FID</b>	flame ionization detector	<b>FT-IR</b>	fourier-transform infrared spectroscopy

<b>GC</b>	gas chromatography	<b>HA</b>	Brønsted acid
<b>HEH</b>	Hantzsch ester	<b>HFIP</b>	Hexafluoroisopropanol
<b>hν</b>	light	<b><i>i</i>Pr</b>	isopropyl
<b>ICy</b>	1,3-dicyclohexyl Imidazolium	<b>M</b>	molar
<b>LED</b>	light emitting diode	<b>Me</b>	methyl
<b>m.p.</b>	melting point	<b>M.S.</b>	molecular sieves
<b>GC-MS</b>	gas chromatography mass spectrometry	<b>NADH</b>	nicotinamide adenine dinucleotide
<b>Ms</b>	mesylate	<b>NIST</b>	National Institute of Standards and Technology
<b>NHC</b>	<i>N</i> -heterocyclic carbene	<b>NNP</b>	N,N,P-tridentate Pincer ligand
<b>NMR</b>	nuclear magnetic resonance	<b>Ph</b>	phenyl
<b>PET</b>	polyethylene terephthalate	<b>PMHS</b>	polymethylhydrosiloxane
<b>PLA</b>	polylactic acid	<b>POP</b>	P,O,P-tridentate Pincer ligand
<b>PNP</b>	P,N,P-tridentate Pincer ligand	<b>pyr</b>	pyridine
<b>PPP</b>	P,P,P-tridentate Pincer ligand	<b>TBAF</b>	tetra- <i>n</i> -butylammonium fluoride
<b>r.t.</b>	room temperature	<b><i>t</i>Bu</b>	<i>tert</i> -butyl
<b>TBHP</b>	<i>tert</i> -butyl hydroperoxide	<b>TEMPO</b>	(2,2,6,6-tetramethylpiperidin-1-yl)oxyl
<b>Temp.</b>	temperature	<b>Tf</b>	triflate
<b>TES</b>	triethylsilyl	<b>TfO</b>	triflate
<b>TFA</b>	trifluoroacetic acid	<b>TLC</b>	thin-layer chromatography
<b>THF</b>	tetrahydrofuran	<b>TMS</b>	tetramethylsilane
<b>TMDSO</b>	tetramethyldisiloxane	<b>TRIP</b>	3,3'-bis(2,4,6-triisopropylphenyl)-1,1'-binaphthyl-2,2'-diyl hydrogenphosphate
<b>TPP</b>	triphenylphosphine	<b>W-K</b>	Wolff-Kishner reduction
<b>w/w</b>	mass fraction	<b>wt%</b>	weight percent

## 9.2. Acknowledgements

First and foremost, I would like to express my sincere gratitude to my main supervisor, Prof. Dr. Ivana Fleischer, for welcoming me into her research group, for her invaluable advice, continued support, patience, and empathy during my PhD. The pleasant working environment she created, her thorough approach to research, the vast knowledge and experience in the field of chemistry which she always shared during this period is something that I admired and shaped my work. Just as important her thoughtful approach towards me is something that valued immensely, and I will forever cherish.

I want to express my appreciation to Prof. Dr. Florian Beuerle for accepting of being the second reviewer of my thesis and Prof. Dr. Doris Kunz and Prof. Dr. Martin Maier for agreeing to be members of the defence committee. Also, I am grateful to Prof. Stephanie Grond for her role as second supervisor my thesis as well as for advice and support.

Additionally, this endeavour would not have been possible without the financial support of the DFG and infrastructure of the University of Tübingen. I would like to offer a big thank you to Dr. Norbert Grzegorzec and the rest of the mass spectrometry department, as well as for to the whole NMR department for all the measurements and shared expertise during the course of my PhD. I am also grateful to the electronics department, the mechanics department and glassware department for their assistance and involvement during my PhD.

I extend my warm appreciation to all my former lab colleagues from the Fleischer Group: Dr. Marlene Bödl, Dr. Prasad Kathe, Dr. Valentin Geiger, Dr. Regina Oechsner, Anne Haupt, Savva Ponomarev, Robert Richter, for help in proofreading my thesis, and Ivo Lindenmaier. I am very grateful for the very good working environment, inspiring discussions but also for the late night talks. Additionally, I give special thanks to Dr. Prasad Kathe and Valentin Geiger for their scientific knowledge and to Anne Haupt for her friendship which expands beyond the lab and my time in Germany, academic input and for proofreading my thesis. Moreover, I want to thank my practicum students Christina Breitenstein, Khang Dam and Tim Heumesser and especially Jan Reger and Felix Vöhringer which helped me a lot with my work.

I am deeply grateful for to my parents, Adriana and Andrei-Gabriel, for their continued care during this period of my life and also for my future wife, Diana-Alexandra, for always being positive and for supporting me even in the hardest moments. I also want to thank my aunt and uncle, Mona and Csaba Roth for their support. On a personal note I would like to extend my sincere appreciation to Horia Duță and Raluca Andrei, for both helping me during my time in Germany, with the proofreading of the thesis but also for their friendship, constant backing and words of encouragement.